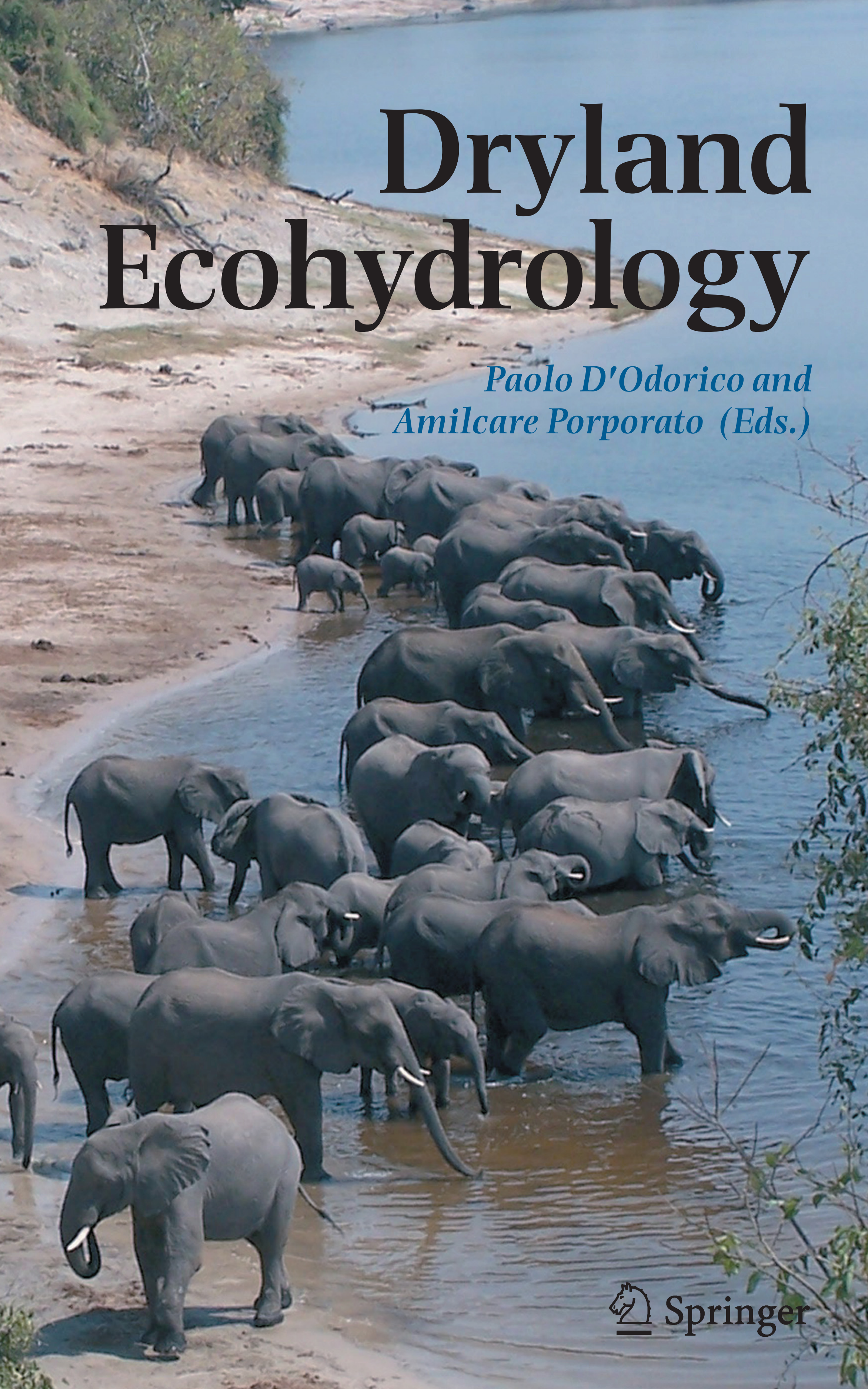

Dryland Ecohydrology

Paolo D'Odorico and
Amilcare Porporato (Eds.)

Springer

DRYLAND ECOHYDROLOGY

Dryland Ecohydrology

Edited by

PAOLO D'ODORICO
Department of Environmental Sciences,
University of Virginia, U.S.A.

and

AMILCARE PORPORATO
Department of Civil and Environmental Engineering,
Duke University, U.S.A.

Springer

A C.I.P. Catalogue record for this book is available from the Library of Congress.

ISBN-10 1-4020-4261-2 (PB)
ISBN-13 978-1-4020-4261-4 (PB)
ISBN-10 1-4020-4259-0 (HB)
ISBN-13 978-1-4020-4259-1 (HB)
ISBN-10 1-4020-4260-4 (e-book)
ISBN-13 978-1-4020-4260-7 (e-book)

Published by Springer,
P.O. Box 17, 3300 AA Dordrecht, The Netherlands.

www.springeronline.com

Printed on acid-free paper

Printed in the Netherlands.

Contents

PREFACE vii

1. Ecohydrology of Arid and Semiarid Ecosystems: An Introduction 1
Paolo D'Odorico and Amilcare Porporato

PART I: FUNDAMENTAL PROCESSES AND INTERACTIONS IN THE SOIL-CLIMATE-VEGETATION SYSTEM 11

2. Soil Physical Properties, Processes, and Associated Root-Soil Interactions 13
Jan W. Hopmans
3. Soil Moisture Dynamics in Water-Limited Ecosystems 31
Paolo D'Odorico and Amilcare Porporato
4. Ecophysiology of Plants in Dry Environments 47
Leonardo Lombardini
5. Soil Moisture Controls on Water Vapor and Carbon Fluxes in Semi-arid Regions 67
John D. Albertson, Christopher A. Williams, Todd M. Scanlon, and Nicola Montaldo
6. Interactions and Feedbacks between Climate and Dryland Vegetations 85
Yongkang Xue

PART II: HYDROGEOMORPHOLOGY OF ARID AND SEMIARID LANDSCAPES 107

7. Controls on Patterns of Soil Moisture in Arid and Semi-arid Systems 109
Rodger B. Grayson, Andrew W. Western, Jeffrey P. Walker, Durga D. Kandel, Justin F. Costelloe, and David J. Wilson
8. The History and Evolution of Desert Hydrology and Landforms: The Role of Climate Change 129
Andrew S. Goudie
9. Hydroclimatology of Wind Erosion in Arid and Semi-arid Environments 141
Wim M. Cornelis
10. Hydrological and Geomorphological Significance of Riparian Vegetation in Drylands 161
Carlo Camporeale, Paolo Perona, and Luca Ridolfi

PART III: ECOHYDROLOGIC CONTROLS ON NUTRIENT CYCLING 181

11. Modeling of Carbon and Nitrogen Cycling in Arid and Semiarid Ecosystems 183
Stafano Manzoni, Amilcare Porporato, and Paolo D'Odorico
12. Interactions of Water and Nitrogen on Primary Productivity across Spatial and Temporal Scales in Grassland and Shrubland Ecosystems 201
Howard E. Epstein, José M. Paruelo, Gervasio Pineiro, Ingrid C. Burke, William K. Lauenroth, and John E. Barrett
13. Interactions between Water Availability and Nutrient Cycling in Dry Tropical Forests 217
Larissa Read and Deborah Lawrence
14. Biogenic Emissions of Nitric Oxide and Nitrous Oxide from Arid and Semi-arid Land 233
Franz X. Meixner and Wen X. Yang

PART IV: DISTURBANCES AND PATTERNS IN ARID AND SEMIARID ECOSYSTEMS 257

15. Pattern and Process in Savanna Ecosystems 259
Kelly K. Caylor and Herman H. Shugart

16. Fire Regimes in Dryland Landscapes 283
Christelle Hély and Samuel Alleaume

17. Termites as Mediators of the Water Economy of Arid Savanna Ecosystems 303
J. Scott Turner

18. Understanding Global Desertification: Biophysical and Socioeconomic Dimensions of Hydrology 315
Fernando T. Maestre, James F. Reynolds, Elisabeth Huber-Sannwald, Jeff Herrick, and Mark Stafford Smith

CONTRIBUTORS 333

INDEX 337

Preface

This volume presents recent advances in the observation, understanding, and modeling of fundamental processes and feedback mechanisms occurring among climate, soil, and vegetation in dryland ecosystems. The goal is to provide scientists and students with a synthesis of new research approaches and recent results in the emerging field of Ecohydrology.

The focus on drylands is motivated by the strong coupling existing between ecological and hydrological processes in arid and semiarid environments. These ecosystems are highly sensitive to fluctuations in hydrologic conditions and, in turn, play an important role in affecting the regional water cycle.

The chapters collected in this book have been contributed by authors with different expertise, who work in several arid areas around the World. Mindful of the multidisciplinary and interdisciplinary nature of this effort, the authors of each chapter have included a broad and organic introduction with a sound review of the state of the art in the specific research area. At the same time, each chapter presents the most recent results and indicates future research directions in related subjects. The subdivision of the contributions in different topics tries to avoid overlap while preserving a wide coverage across disciplines. Each topic is covered in depth by field-experts, while cross-references to the other chapters indicate important connections to other related disciplines. It is hoped that this approach enhances both the breath and the depth of this synthesis of ecohydrological studies of arid and semiarid environments.

The book is structured more by ecosystem components and processes (e.g. soils, water budget, nutrient cycles, vegetation, etc.) than by ecosystem type (e.g. grassland, savanna, temperate forest, etc.), though - when necessary - some chapters focus on properties and processes characteristic of specific biomes. Such a structure is motivated by the very nature of this book which addresses not only ecologic dynamics but also a number of water-related processes which are not necessarily dependent on the ecosystem type. At the same time the analyses do not focus on a specific geographic region in that all authors have provided – when possible – a synthesis that goes beyond the presentation of region- or site-specific results.

We are indebted with several colleagues and friends, who have provided useful comments and suggestions. In particular, Ignacio Rodriguez-Iturbe (Princeton University) has pointed us to the field of Ecohydrology and has been an important source of inspiration. We thank him for his guidance and companionship. A number of colleagues around the world have reviewed the chapters contained in this volume. We refrain from going through this long list of referees to preserve their anonymity. The completion of this book has been possible thanks to the support from the DOE-Office of Science (Biological and Environmental Research Program) through NIGEC, Great Plains Regional Center (grant #DEFC02-03ER63613), NSF-Hydrology Program (grant #EAR-0236621), NSF-Geoscience Program (grant #EAR-0409305), USDA (Cooperative Agreement #2002-35102-11585), and NASA (grant #NNG-04-GM71G). We are also indebted with our institutions, the University of Virginia (Department of Environmental Sciences) and Duke University (Department of Civil and Environmental Engineering) for providing a high-quality academic environment that stimulates and inspires our work.

Charlottesville/Durham, April 26, 2005

Paolo D'Odorico and Amilcare Porporato

Chapter 1

ECOHYDROLOGY OF ARID AND SEMIARID ECOSYSTEMS: AN INTRODUCTION

Paolo D'ODORICO[1] and Amilcare PORPORATO[2]

[1]*Department of Environmental Sciences, University of Virginia, Charlottesville, VA 22904, USA*
e-mail: paolo@virginia.edu
[2]*Department of Civil and Environmental Engineering, Duke University, Durham NC 27708, USA*
e-mail: amilcare@duke.edu

1. Ecohydrology: Objectives and Challenges

Ecohydrology has been recently defined as "*the science, which seeks to describe the hydrologic mechanisms that underlie ecologic patterns and processes"* (Rodriguez-Iturbe, 2000; p. 1). This type of inquiry is fundamental to the understanding of the coupling existing between ecosystem dynamics and the water cycle, in particular in arid and semiarid environments, where water is an important limiting resource not only for its scarcity but also for its intermittency and unpredictable presence (Porporato and Rodriguez-Iturbe, 2002; Rodriguez-Iturbe and Porporato, 2005). The biogeoscience community has been recently trying to establish stronger connections between research in the physical and the natural sciences to provide a process-based understanding of the interactions existing between the hydrosphere and the biosphere. Thus, the research area at the border between hydrology and ecology is recently receiving a considerable attention. The term "Ecohydrology" itself, is becoming increasingly popular in the scientific literature. Nuttle (2002) provides a thorough analysis of this new and combined approach to hydrological and ecological studies: "*Eco-hydrology emerges as an engaging topic with multiple facets and deep roots in the history of hydrologic science*". It is "*the subdiscipline shared by the ecological and hydrological sciences that is concerned with the effects of hydrological processes on the distribution, structure, and function of ecosystems, and on the effects of the biotic processes on the elements of the water cycle.*" The same author notices that in this new context "*previously unrelated areas of scientific inquiry are now coming together.*" This approach is fundamental to the analysis of ecosystem dynamics, of their response to different hydrologic and climatic regimes as well as of their impact on regional and global climate. This book represents an effort exactly in this direction, in that it provides a background for a synthesis of new research approaches and recent results in the study of ecological and hydrological processes characteristic of arid environments.

The focus on drylands is motivated by their high sensitivity to daily, seasonal, and decadal perturbations in water availability. The analysis of how arid ecosystems respond to such perturbations is receiving increasing attention also due to the ecologic, climatic, and economic significance of most of the drylands around the world. This book addresses the impact of different hydrologic regimes on soil properties and processes, landforms, and spatial patterns of soil moisture. It shows what is the effect of these hydrologic conditions on the biosphere, in particular on plant physiology, nutrient cycles, plant competition, fire regime, and spatial patterns of vegetation. At the same time it is shown how changes in the biotic components of dryland ecosystems can affect the soil properties, the landscape, as well as the regional hydrology and climate. The book includes chapters on field studies, data analysis, interpretation of hydrologic and ecologic dynamics, and process-based modeling of ecosystem dynamics. In this chapter we briefly review some of the main eco-physiographic characteristics of dryland ecosystems.

P. D'Odorico and A. Porporato (eds.), Dryland Ecohydrology, 1–10.

2. Dryland Climates

Drylands are drought-prone areas of the world in which rainfall is less than the potential evapotranspiration for the whole year or for part of it, and conditions of either permanent or seasonal soil water deficit occur. The obvious features of the rainfall regime are the low precipitation amounts and the high variability and unpredictability of precipitation, which occurs in a discrete number of relatively infrequent events. Thus, dryland ecosystems are in general water-controlled "*with infrequent, discrete, and largely unpredictable water inputs*" (Noy-Meir, 1973, p. 26).

More than 40% of the continents is covered by drylands (e.g., Slaymaker and Spencer, 1998). These regions are mostly located (Figure 1) (1) in continental areas, away from marine sources of moisture; (2) in regions of persistent high pressure cells (i.e. between 20° and 40° latitude); (3) in rain shadow areas; (4) or along the western continental margins, where, due to the upwelling of deep oceanic water, low sea surface temperature causes high atmospheric stability (Slaymaker and Spencer, 1998).

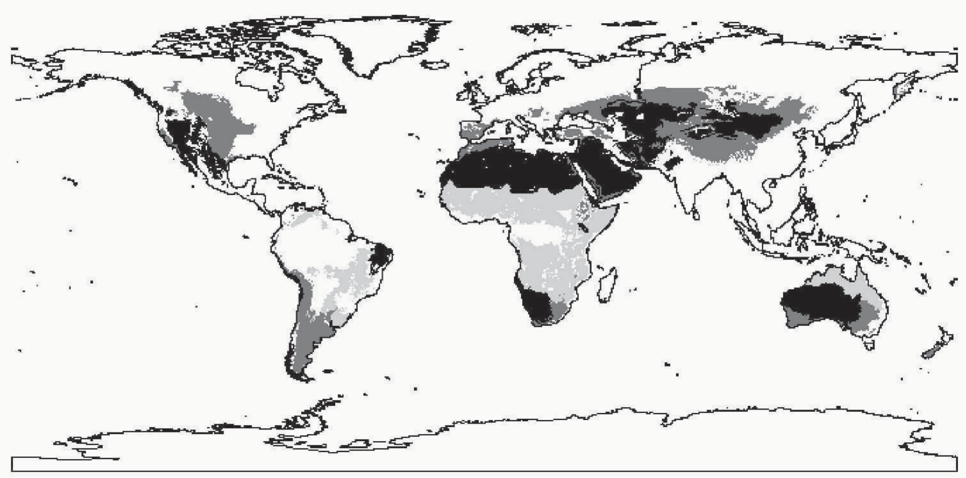

Figure 1. Map of the major drylands of the world classified as deserts (black), Mediterranean shrublands and mesic grasslands (in dark gray), and tropical savannas (light gray).

Annual precipitation is generally used to define four main dryland zones (e.g., Noy-Meir, 1973; Mainguet, 1994):

Extremely arid zones, with average annual rainfall below 60-100 mm, which is insufficient for dryland farming or livestock grazing;

Arid zones, with average annual rainfall between 100 mm and 150-250 mm and possible livestock grazing;

Semiarid zones, with average annual rainfall between 250 mm and 500-600 mm and possible cultivation of drought-resistant crops;

Dry sub-humid zones, with precipitation in the range from 600 mm to 1200 mm concentrated in one (or more) rainy seasons. Water deficit can be either seasonal or intermittent (Mainguet, 1994).

Other criteria for dryland classification are based on annual temperature or on the seasonality of precipitation. Mean annual temperature is used to distinguish *warm drylands*, which occur at low latitudes and altitudes (e.g., Northern Australia, Sahara, Sahel, Kalahari, and southwestern U.S.), from *cold drylands* (e.g. Central Asia and Central Chile). Drylands can be also divided into summer-rainfall and winter-rainfall regions. The timing of the rainy season is of foremost importance to the phenology of ephemeral and annual vegetation in the desert margins (see Section 4). In summer-rainfall drylands (e.g., the Sahel or the Kalahari) plant phenology is strongly dependent on precipitation (e.g., Larcher, 1995); both onset and length of the growing season are controlled by soil water availability (e.g., Noy-Meir, 1973). Vegetation resumes growth a few days or weeks after the beginning of the rainy season, while senescence occurs soon after the last storms of the season; ephemerals maintain no photosynthetic activity during the dry season, while perennials reduce photosynthetically active biomass by shedding leaves and rootlets in the surface soil layers. In winter-rainfall drylands (e.g. drylands with rainfall occurring in the cold season or cold deserts) bud burst and greening of vegetation is generally inhibited at low temperatures, despite the availability of soil moisture. Due to low evaporative losses, cold-season precipitation is stored in the ground and taken up by vegetation during the subsequent (dry) growing season. Thus, greening does not occur concurrently with moist surface conditions. Mediterranean regions, where the winters are cool, represent a particular case of winter-rainfall dryland in which growth is not completely inhibited by winter temperatures (Noy-Meir, 1973). Other types of dryland climates are characterized by two distinct rainy seasons (e.g. west Texas) and two associated germinations (Mott, 1972).

2.1 DROUGHT CONDITIONS

The classification of drylands on the basis of the rainfall regime provides a useful indication of their level of permanent or seasonal *aridity* through long-term average climatic variables. The concept of *drought* is instead used to characterize deviations from "normal" (i.e. long-term average) conditions. Droughts are generally defined as prolonged periods of below-normal water availability (Mainguet, 1994), which persist long enough to cause stress on water bodies, ecosystems, and societies. Thus droughts need to be studied with respect to their climatic, hydrologic, ecologic and human implications, including the feedbacks between climate and changes in land cover and use (Mainguet, 1994). To this end, four different types of droughts have been defined (American Meteorological Society, 1997): the meteorological, hydrological, agricultural, and societal droughts.

A number of indices have been developed and applied to quantify the severity and magnitude of aridity and drought conditions. Aridity indices are generally based on long-term average precipitation, available water, mean annual net radiation, or evapotranspiration. For example, the difference between precipitation and evapotranspiration, the ratio between potential and actual evapotranspiration (e.g., Thorntwaite, 1948), or between mean annual net radiation and the energy required to evaporate the total annual precipitation (Budyko, 1958; Lettau, 1969) can be used to characterize aridity. On the other hand drought indices should measure the departure from the long-term mean conditions. To this end, other indices are commonly used to characterize the meteorological, hydrological and agricultural droughts (Heim, 2002). The most common ones are the Palmer's indices (Palmer, 1965), i.e. the PDSI (Palmer Drought Severity Index) and the PHDI (Palmer Hydrological Drought Index) indices, which are calculated on the basis of a simplified soil water balance. However, neither these nor other drought indices can be considered as universal indicators, able to characterize completely drought occurrences and all their implications at any spatial and temporal scale (Heim, 2002).

2.1.1 Meteorological Drought

Droughts are often associated with anomalies in the regional and global climate, though they can be enhanced by changes in land cover and resource management. Meteorological droughts are periods in which precipitation is significantly below the long-term average at a certain location and time of the year. This definition is based only on rainfall statistics. Depending on the spatial extent of the region affected, droughts are usually classified as local, regional, and subcontinental (Mainguet, 1994).

The occurrence of meteorological droughts (i.e. departures from mean rainfall conditions) is usually strongly related to aridity (i.e. to mean rainfall conditions), in that the interannual rainfall variability is generally higher in the more arid regions, which are also the most sensitive to droughts. This fact is illustrated for example by the data in Table 1 (Nicholson, 1980; Porporato et al., 2003), showing changes in rainfall variability along two rainfall gradients in Northern and in Southern Africa: the stronger variability is associated with the most arid zones, suggesting a more frequent drought occurrence at the low end of these rainfall gradients.

In the case of Sahel, it has been reported (Lebarbe and Lebel, 1997) that most of the interannual variability of rainfall is due to changes in the number of rainstorms affecting a certain location in the course of the rainy season, more than to changes in the amount of rain yielded by each storm (or "storm depth"). Different results were found for savannas in southern Texas (D'Odorico et al., 2000) and in the Kalahari (Table 1, data from Porporato et al., 2003), where a strong variability was observed also in storm depth.

Table 1: Mean annual rainfall and coefficient of variation (CV) along two rainfall gradients (data from Nicholson, 1980 and Porporato et al., 2003). In the case of the Kalahari coefficients of variation are separately provided for the interannual variability of storm depth and storm frequency.

Zone	**Mean Annual Rainfall (mm)**	**CV (%)**	
Guinea-Sahel Transect			
Sahelo-Saharan	50-100	>50	
Sahelian	100-400	30-50	
Sudanian	400-1200	20-30	
Sudano-Guinean	1200-1600	15-20	
Kalahari Transect		*CV (%) (Storm Depth)*	*CV (%) (Storm Frequency)*
Vastrap	305	31	32
Sesheke	715	20	18
Mongu	942	17	16

2.1.2 Hydrological Drought

Hydrological droughts occur when the water level in lakes or rivers falls significantly below "normal" conditions for a certain location and time of the year. Thus, the hydrological drought is defined only on the basis of anomalies in storage or flow (generally base-flow) conditions in water bodies (e.g., Heim, 2002). Because these conditions depend also on water usage, evapotranspiration and infiltration, hydrological droughts are not necessarily a consequence only of meteorological conditions. Moreover, even when hydrological droughts are caused by below-average precipitation, there can be a significant delay in the response of water bodies to the climatic anomaly. In fact, fluctuations in lakes and rivers are indicators of changes in the rainfall regime integrated over the watershed area. Thus, the two types of drought (meteorological and hydrological), though related, are not necessarily concurrent. Mainguet (1994) discusses a number of cases of hydrological droughts through the analysis of multi-decadal records from Lake Victoria, Lake Chad and the Nile River. These hydrological droughts are shown to be associated with changes in weather patterns, soil type, land use and plant physiological characteristics (see Chapters 2-4).

Hydrological droughts are usually characterized (Yevjevich, 1967; Dracup et al., 1980) in terms of their duration, magnitude, severity, frequency, and spatial extent. With the exception of short-term seasonal events, droughts are defined as periods with below-average mean annual flow. Thus, drought duration is the number of consecutive years in which drought conditions persist, drought severity is the cumulative streamflow deficit observed throughout the event, while drought magnitude is the average streamflow deficit for the event duration (Heim, 2002).

2.1.3 Agricultural Drought

The agricultural drought is associated with the occurrence of low levels of plant available water, and the consequent reduction in agricultural production (Heim, 2002). This concept can be extended from agro- to natural ecosystems. In this case drought would be due to low levels of soil moisture and to the emergence of conditions of water stress in vegetation. In North America, Palmer's indices (1965) are generally used to characterize the severity of drought conditions. Ridolfi et al. (2000) and Porporato et al. (2001) have pointed out the importance of a probabilistic approach to plant water stress based on a statistical characterization (intensity, frequency and duration) of periods when plant activity is impaired by soil water deficit (see also Chapter 3). These types of drought are by definition associated only with soil moisture conditions occurring in the course of the growing season; thus, average root-zone seasonal soil moisture, as well as the duration and frequency of periods in which transpiration is limited by soil water availability can be taken as useful indicators of agricultural and ecosystem stress.

2.1.4 Societal Drought

This concept is closely related to the notion of agricultural drought: it occurs when the soil water deficit affects crop production to the point that there are significant economical losses with disruptive effects on the rural societies (e.g., Heim, 2002). This type of drought causes social and economical stress, which, in turn, is associated with famine and migratory fluxes. Societal drought is not necessarily just an effect of extreme agricultural droughts, in that it depends also on demographic changes, expansions of farming areas, and grazing pressure. The analysis of societal stress and of its interactions and feedbacks to dryland ecohydrology is beyond the scope of this book.

3. Dryland Soils

Soils of arid and semiarid regions are generally characterized by low soil water contents, high potential evapotranspiration and consequently relatively low rates of percolation and leaching, depending on the soil texture (e.g., Brady and Weil, 1996). Thus, water and nutrients partly remain available to vegetation in the root zone. The soil profile generally lacks of an E-horizon, while the processes of calcification and salinization accumulate within the soil column calcium carbonate, sodium chloride and other salts (e.g., Aber and Melillo, 1991). The typical soils (*Aridisol*) have a deep A-horizon and sustain tropical and temperate shrublands. Soils underlying grasslands and savannas have an A-horizon that is fairly well-mixed by animal activity and have a darker color, due to the more abundant organic material (melanization). This type of soil is classified as *Mollisol* and can be found both in tropical and temperate grasslands. It is not always clear what controls the predominance of either grasses or shrubs in arid and semiarid environments (see Section 4), though an important role seems to be played by rainfall regime, soil texture (Sala et al., 1997) and disturbances, such as climate fluctuations, grazing and fires (e.g., Aber and Melillo, 1991). Both Aridisols and Mollisols are characterized by very limited leaching and slow soil-forming processes. In areas with limited vegetation density these pedogenetic processes are mainly due to the physical weathering of the parent material by wind and water, while in grasslands and savannas soil formation is significantly contributed by biological processes.

Vegetation plays an important role in limiting water and wind erosion (Chapter 9); vegetation removal due to anthropogenic or natural disturbances is known for being one of the major causes of desertification (Chapter 18), i.e. of complex dynamics able to turn - even irreversibly - arid grasslands into deserts.

The seasonally dry tropics and subtropics are characterized by different soils, which are dry only in the course of the dry season. Thus, these soils (*Ultisols*) are significantly more humid than the Aridisols and Mollisols, and are consequently affected by severe weathering, leaching of iron and aluminum oxides and clays, which accumulate in the E horizon. Due to the higher moisture contents, soil formation and nutrient cycling are relatively fast, soils are nutrient-poor, and plant transpiration is limited by soil water availability only during the dry season (see Chapter 13).

4. Dryland Vegetation

The vegetation of arid and semiarid environments is in general well-adapted to conditions of water stress. Phenological and morphological adaptation to drought conditions, plant water relations and drought tolerance are among the attributes that are frequently used to group species into a few classes on the basis of their different access and use of the main limiting resource: water. This approach differs from more traditional classifications based only on morphology, evolutionary relationships, or plant genetics (Meanut et al., 1988).

Thus, dryland vegetation has been divided into a few major plant functional types - such as grasses, shrubs, forbs and succulents (Sala et al., 1997; Dodd and Lauenroth, 1997) - on the basis of their different water relations. According to this model the dominant vegetation type would result from its relative advantage in using available soil water stores (Noy-Meir, 1973): for example, grasses take up water from the surface soil layer and rely on relatively frequent and short pulses of soil moisture, while shrubs utilize water from deeper layers and rely on moisture that is available in infrequent and long-lived pulses. This classification would explain the dominance of a particular vegetation type on the basis of soil texture and seasonality of precipitation. In fact, these two environmental factors affect the amount and timing of water available at different depths (Sala et al., 1997). Grasses dominate drylands with continental climates, i.e. with rainy seasons occurring concurrently to the warm season. In these regions soil moisture is readily available to grasses during the growing season and grasses are in competitive advantage with respect to shrubs and trees. Deep-rooted perennials (e.g., shrubs and trees) dominate regions with a more Mediterranean climate, where the rainy season occurs in wintertime and, due to the low evaporative demand, rainfall is able to percolate to relatively deep layers. Thus, the overlapping between warm and wet seasons partly explains the dominance of different plant functional types. This analysis can be partly modified by the effect of soil texture, which affects the regime of soil moisture at different depths. For example, the presence of coarse-textured soils in continental regions allows for a relatively deep percolation of water in the course of the growing season, reducing the competitive advantage of grasses with respect to trees (Sala et al, 1997; Figure 2). This framework (Sala et al., 1997), which is based on the interplay of competitive advantages/disadvantages resulting from spatial and temporal niches of water availability, is coherent with Walter's observation (1971) that in tropical regions with summer rains and sandy soils, trees and grasses are found in ecological equilibrium (savannas). In these conditions the co-dominance of trees and grasses would be explained by the two-layer hypothesis (Walter, 1971) that grasses and trees compete for water at the surface, while woody plants have exclusive access to deep water. Even though the climate pattern would tend to favor grasses at the surface, the soil texture would allow trees to have a competitive advantage in the deeper layers, explaining the co-dominance of these two functional types.

Alternative theories have been recently formulated (Rodriguez-Iturbe et al., 1999), which explain the tree-grass coexistence on the basis of an optimality principle: for a given climate and soil texture, the most likely proportion of herbaceous and woody vegetation would be associated with the conditions of minimum ecosystem water stress. This and other theories (e.g., Schlesinger et al., 1990; Scholes and Archer, 1997) recognize the importance of the horizontal redistribution of of water and nutrients in the presence of heterogeneous vegetation cover. This concept has been recently incorporated in a more general framework (Breshears and Barnes, 1999) explaining the dominance and codominance of trees and grasses in semiarid landscapes on the basis of horizontal (e.g., Schelsinger et al., 1990) and vertical (e.g., Walter, 1971) heterogeneities in the distribution of soil moisture.

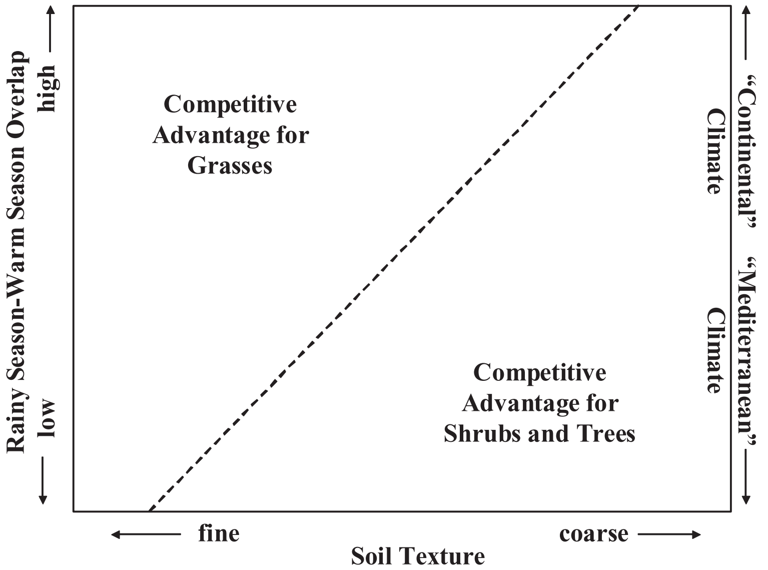

Figure 2. Conceptual model of the effect of climate and soil texture on dominant plant functional type (modified after Sala et al., 1997).

Southern African savannas are an example of how the soil geology may affect vegetation composition, nutrient cycling, and disturbance regime. By contrasting the ecohydrologic processes taking place on granitic and basaltic soils in Kruger National Park (S. Africa), Venter et al. (2003) showed how the clayey basaltic soils support a higher grass biomass than the granitic sandy soils. Due to the high water-holding capacity and the lower infiltration and leaching rates, the basaltic clayey soils retain moisture and nutrients at the surface, offering a competitive advantage to grasses (Figure 2). The typical vegetation in these nutrient-rich soils is an open savanna dominated by high-productivity C_4 perennial bunchgrasses (often exceeding 50 cm in height) and fine-leaf trees (*Acacias*). The high grass biomass characteristic of these soils results in high-intensity fires, which, in turn, prevent the establishment of denser woody vegetation (Venter et al., 2003). The nutrient-poor, granitic, sandy soils at Kruger are in general well-drained and with high rates of nutrient leaching (Scholes et al., 2003). Due to the low water retention, the soil surface is generally dry, and grasses are in competitive disadvantage with respect to woody vegetation (see Figure 2). As a consequence, these sites are dominated by short annual grasses (seldom taller than 50 cm) mixed with a dense vegetation of broad leaf woody plants (*Combretum* and *Terminalia*). The low grass productivity, combined with consequently low fuel loads and fire intensities explain the presence of dense bush savannas at these sites. Moving on the same granitic soils along a rainfall gradient (from 530 mm at Skukuza to 720 mm at Pretoriuskop) grass biomass and fire intensity are observed to increase (Venter et al., 2003). A similar combination of fine-leaved (*Acacia tortilis*) and broad-leaved (*Burkea africana*) vegetation sites can be found at the Nylsvley Nature Reserve (S. Africa), with the fine-leaved savanna having lower tree cover than the broad-leaved vegetation (Scholes and Walker, 1993). The different type of vegetation is associated with the soil nutrient content, with nutrient-rich soils supporting the fine-leaved savanna.

While Sala's model (1997) explains the dominance and co-dominance of different plant functional types on the basis of water relations, a more general analysis would account for the existence of other environmental controls able to determine vegetation types and structure. For example, south American savannas - also known as "*cerrados*" (e.g., Sarmiento, 1984) – generally grow on weathered infertile soils and in seasonally-dry sub-humid to humid climates. In this case tree-grass coexistence seems to be associated with nutrient rather than water limitations, as evidenced by the positive correlation found between soil fertility and tree cover across different types of cerrados (Kauffman et al., 1994). Nevertheless, climate exerts an important control on the vegetation structure through its influence on the fire regime. Thus, when water is not the only limiting resource, soil chemistry (in particular nutrients) and disturbances may explain the dominance of different vegetation types. This view supports other classifications of savanna ecosystems. For example, the Johnson-Tothill classification presented by Adams (1996) recognizes the existence of savannas in humid and sub-humid climates (Figure 3). While the existence of tropical savannas on sandy soils would be explained by water limitations, the occurrence of tropical savannas on fine-textured soils in floodplains and valley bottoms could be associated with nutrient limitations and disturbances.

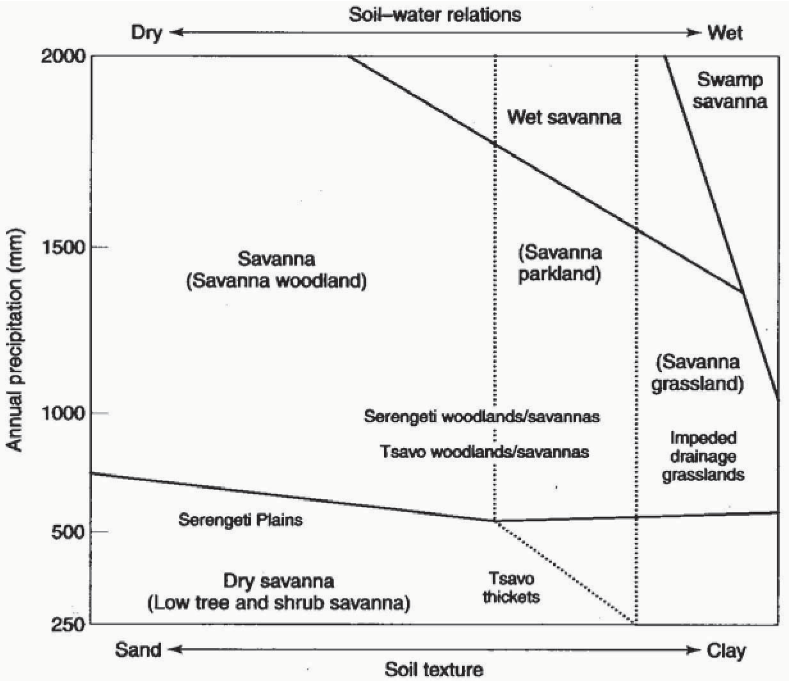

Figure 3. The Johnson-Tothill (1985) classification of tropical savannas (taken from Adams, 1996).

5. Multifaceted response of arid and semi-arid ecosystems

In summary, the dynamics of dryland ecosystems are complex and involve processes acting at different scales both in time and in space. These scales are dictated by a hierarchy of forcings and responses, from after-storm nutrient flushes, to plant competition, and community succession (e.g., Schwinning and Sala 2004; Austin et al. 2004). The unpredictable and pulsing nature of resource availability propagates through the complex ecosystem structure with many interactions and feedbacks and finally translates into a hierarchy of scales of ecosystem responses. The following chapters will describe the various interactions among the biotic and abiotic processes of dryland ecosystems (Figure 4), starting from basic processes in the soil-vegetation-climate system (Part I), to landscape-scale hydrologic and geomorphic processes (Part II), ecohydrologic controls on soil nutrient dynamics (Part III), and multiscale analyses of disturbances and patterns (Part IV).

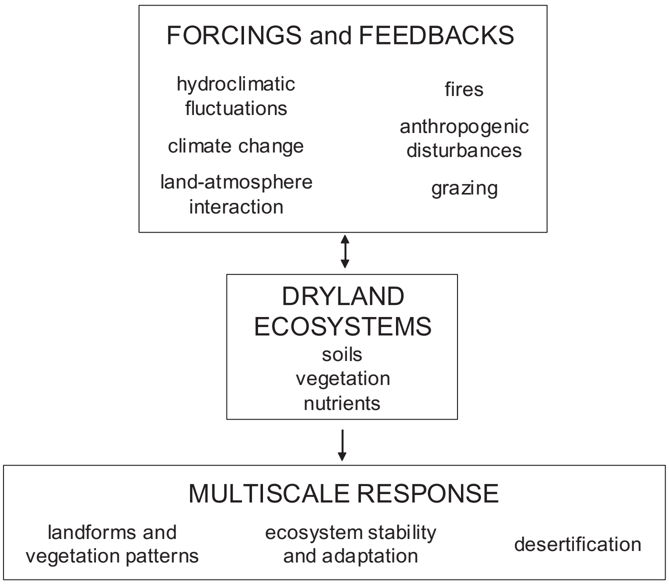

Figure 4. Interactions between biotic and abiotic processes in dryland ecosystems addressed in the following chapters of this book.

6. Acknowledgements

This research was funded by NSF (grants #EAR-0236621 and # EAR-0409305), DOE-NIGEC (Great Plains Regional Center, grant #DE-FC-02-03ER63613), USDA (Cooperative Agreement #2002-35102-11585), and NASA (grant #NNG-04-GM71G).

7. References

Aber J.D., and J.M. Melillo, (1991) Terrestrial Ecosystems, Saunders College Publishing, Philadelphia.

Adams, M.E. (1996). Savanna Environments. In W.M. Adams, A.S. Goudie, and A.R. Orme (Eds.), The Physical Geography of Africa, Oxford Univ. Press, Oxford, pp. 196-210.

American Meteorological Society (1997). Meteorological Drought-Policy Statement, Bull. Am. Meteorol. Soc., 78, 847-849.

Austin A.T., Yahdjian L., Stark J.M., Belnap J., Porporato A., Norton U., Ravetta D.A., and S.M. Schaeffer (2004). Water pulses and biogeochemical cycles in arid and semiarid ecosystems, Oecologia, 141: 221–235.

Brady N.C. and R.R. Weil (1996). The Nature and Properties of Soils, 11th ed.: Prentice Hall.

Breshears, D.D. and F.J. Barnes (1999). Interrelationships between plant functional types and soil moisture heterogeneity for semiarid landscapes within the grassland/forest continuum: a unified conceptual model, Landscape Ecology, 14, 465-478.

Budyko M.I. (1958). The Heat Balance of the Earth's Surface, U.S. Dept. of Commerce, Washington, D.C., 259 pp.

Dodd, M.B., and W.K. Lauenroth (1997). The influence of soil texture on the soil water dynamics and vegetation structure of a shortgrass steppe ecosystem, Plant Ecology, 133, 13-28.

D'Odorico, P., L. Ridolfi, A. Porporato and I. Rodriguez-Iturbe (2000). Preferential states of seasonal soil moisture: the impact of climate fluctuations, Water Resour. Res., 36(8). 2209-2219.

Dracup, J.A., K.S. Lee, and E.G. Paulson Jr. (1980). On the statistical characteristics of drought events, Water Resour. Res., 16, 289-296.

Heim, R.R. (2002). A review of twentieth-century drought indices used in the United States, Bull. Am. Meteorol. Soc., 83(8), 1149-1165.

Johnson R.W. and J.C. Tothill (1985). Definitions and broad geographic outline of savanna lands. In J.C. Tothill and J.G. Mott (Eds.), Ecology and Management of the World's Savannas, Commonwealth Agricultural Bureau, Canberra.

Kauffman, J.B., D.L. Cummings, et al. (1994). Relationships of Fire, Biomass and Nutrient Dynamics Along a Vegetation Gradient in the Brazilian Cerrado. Journal of Ecology, 82(3): 519-531.

Lebarbe, L and T. Lebel. (1997). Rainfall climatology of the HAPEX-Sahel region during the years 1950-1990, J. Hydrol., 189, 43-73, pp. 1-15.

Lettau, H. (1969). Evapotranspiration Climatonomy: 1. A new probabilistic approach to numerical prediction of monthly evapotranspiration, runoff, and soil moisture storage, Mon. Wea. Rev.97, 691-699.

Larcher, W. (1995). Physiological Plant Ecology, Springer, Berlin.

Mainguet, M. (1994). Desertification: Natural Background and Human Mismanagement, Springer-Verlag, Berlin.

Meanut, J-C, and I.R. Noble (1988). A functional classification of savanna plants. In B.H. Walker and J-C Meanut (Eds.) Responses of Savannas to Stress and Disturbance: Research Procedure and Experimental Design for Savanna Ecology and Management, pp. 8-11, International Union of Biological Sciences. Report 2., Paris.

Mott, J.J. (1972). Germination studies on some annual species from an arid region of Western Australia, J. Ecol., 60, 293-304.

Nicholson, S.E. (1980). The nature of rainfall fluctuations in subtropical west Africa, Mon. Weather Rev., 108, 473-487.

Noy-Meir, I. (1973). Desert Ecosystems: Environment and Producers, Ann. Rev. Ecol. Syst., 4, 25-51.

Nuttle W. (2002). Eco-hydrology's Past and Future, EOS, 83(19).

Palmer, W.C. (1965). Meteorological Drought, U.S. Weather Bureau Research Paper 45, 58 pp., Washington, D.C..

Porporato, A., F. Laio, L. Ridolfi, and I. Rodriguez-Iturbe (2001). Plants in water-controlled ecosystems: active role in hydrologic processes and response to water stress. III. Vegetation water stress. Adv. Water Resour., 24, 725–744.

Porporato A and I. Rodriguez-Iturbe (2002). Ecohydrology - a challenging multidisciplinary research perspective, Hydrol. Sci J., 47(5), 811-821.

Porporato, A., F. Laio, L. Ridolfi, K.K. Caylor, and I. Rodriguez-Iturbe (2003). Soil moisture and plant stress dynamics along the Kalahari precipitation gradient, J. Geophys Res., 108(D3), 4127, doi:10.1029/2002JD002448.

Ridolfi L., P. D'Odorico, A. Porporato, and I. Rodriguez-Iturbe (2000). Duration and frequency of water stress in vegetation: an analytical model, Water Resour. Res., 36(8), 2297-2307.

Rodriguez-Iturbe, I. and A. Porporato (2005). Ecohydrology of Water-Controlled Ecosystems: Soil Moisture and Plant Dynamics, Cambridge Univ. Press, Cambridge

Rodriguez-Iturbe, I. (2000)., Ecohydrology: A hydrologic perspective of climate-soil-vegetation dynamics, Water Resour. Res. 36(1), 3-9.

Rodriguez-Iturbe, I., P. D'Odorico, A. Porporato, and L. Ridolfi (1999). Tree-Grass coexistence in savannas: the role of spatial dynamics and climate fluctuations, Geophys. Res. Lett., 26(2), 247-250.

Sala, O.E., W.K. Lauenroth and R.A. Golluscio (1997). Plant functional types in temperate semi-arid regions. In T.M. Smith, H.H. Shugart, and F.I. Woodward (Eds.), Plant Functional Types, International Geosphere-Biosphere Programme Book Series 1, Cambridge University Press, pp 217-233.

Sarmiento, G. (1984). The Ecology of Neotropical Savannas, Harvard University Press, Cambridge.

Schlesinger, W.H., J.F. Reynolds, G.L. Cunnigham, L.F. Huenneke, W.M. Jarrell, R.A. Virginia, and W.G. Whitford (1990). Biological feedbacks in global desertification, Science, 247, 1043-1044.

Scholes, R.J., and B.H. Walker (1993). An African Savanna, Cambridge University Press, Cambridge.

Scholes, R.J. and S.R. Archer (1997). Tree-grass interactions in savannas, Ann. Rev. Ecol. Syst., 28, 517-544.

Scholes, M.C., R.J. Scholes, L.B. Otter, and A.J. Woghiren (2003). Biogeochemistry: the cycling of elements. In J. T. Du Toit, K.H. Rogers, and H.C. Biggs (Eds.), The Kruger Experience, Island Press, Washington, pp 130-148.

Schwinniing, S. and O. E. Sala (2004). Hierarchy of responses to resource pulses in arid and semi-arid ecosystems, Oecologia 141: 211–220.

Slaymaker, O. and T. Spencer (1998). Physical Geography and Global Environmental Change, Addison Wesley Longman, New York.

Thorntwaite, C.W. (1948). An approach toward a rational classification of climate, Geogr. Rev., 38, 55-94.

Yevjevich, V. (1967). An objective approach to definitions and investigations of continental hydrologic drought. Hydrology Paper 23, Colorado State University, Fort Collins, CO, 18 pp.

Venter, F.J., R.J. Scholes, and H.C. Eckhardt (2003). The abiotic template and its associated vegetation pattern. In J. T. Du Toit, K.H. Rogers, and H.C. Biggs (Eds.), The Kruger Experience, Island Press, Washington, pp. 81-129.

Walter, H. (1971). Ecology of Tropical and Subtropical Vegetation. Oliver and Boyd, Edinburgh.

PART I

FUNDAMENTAL PROCESSES AND INTERACTIONS IN THE SOIL-CLIMATE-VEGETATION SYSTEM

Water flow through the soil-plant-atmosphere continuum is regulated by a number of complex physical and biophysical processes, which act in conditions of mutual dependence. Important "top-down" controls on plant water uptake include hydrologic and climate conditions, which determine the rates of potential evapotranspiration, assimilation, and ecosystem productivity. On the other hand, through its interactions with the near-surface atmosphere, vegetation exerts a "bottom-up" control both on regional climate and hydrologic conditions. Almost all of the interactions in the soil-plant atmosphere system are mediated by soil moisture dynamics. Such a control is especially strong in arid and semi-arid regions where vegetation is subject to frequent water stress.

This first part starts with the analysis of fundamental processes controlling water flow in the root zone (Chapter 2), in the soil (Chapter 3), and through the plant xylem (Chapter 4). The physiology of vegetation under stress is analyzed in relation to factors controlling stress tolerance in plants (Chapter 4). The effects of soil moisture dynamics on water vapor fluxes, stomata regulation, and ecosystem productivity are discussed in Chapter 5. The last chapter of this section investigates the role played by dryland vegetation in land-atmosphere interactions and discusses how these interactions may lead to feedbacks between vegetation and precipitation.

Chapter 2

SOIL PHYSICAL PROPERTIES, PROCESSES AND ASSOCIATED ROOT-SOIL INTERACTIONS

Jan W. HOPMANS

Hydrology, Department of Land, Air and Water Resources, 123 Veihmeyer Hall, University of California, Davis, CA, 95616, USA – email:jwhopmans@ucdavis.edu

1. Introduction

The soil is the most upper part of the vadose zone, subject to fluctuations in water and chemical content by infiltration and leaching, water uptake by plant roots, and evaporation from the soil surface. It is the most dynamic, as changes occur at increasingly smaller time and spatial scales when moving from the groundwater towards the soil surface. Scientists are becoming increasingly aware that soils makeup a critically important component of the earth's biosphere, not only because of their food production function, but also as the safe-keeper of local, regional, and global environmental quality. For example, it is believed that management strategies in the unsaturated soil zone will offer the best opportunities for preventing or limiting pollution, or for remediation of ongoing pollution problems. Because chemical residence times in ground water aquifers can range from a few to thousands of years, pollution is often essentially irreversible. Prevention or remediation of soil and groundwater contamination starts, therefore, with proper management of the unsaturated zone. This includes the consideration of plants and trees.

The importance of root function in water and nutrient transport is becoming increasingly clear, as constraints on agricultural resources are imposed due to water limitations and environmental concerns. Favorable soil environmental conditions for plant and microbial growth allow for bioremediation of contamination by inorganic and organic chemicals. Microbial processes transform the parent chemical, thereby reducing its concentration, whereas plants can accumulate specific chemical species, e.g. through bioaccumulation of heavy metals in plant tissues. In addition, root water and nutrient uptake by plant and tree roots reduce leaching of water and salts below the rooting zone, thereby controlling percolation rates and the transport of dissolved chemicals to the groundwater.

In their recent review of root water and nutrient uptake modeling, Hopmans and Bristow (2002) concluded that progress in the basic understanding of transport processes in the soil-plant-atmosphere continuum (SPAC) has been slow, specifically regarding interfacial fluxes at the root-soil interface. They speculated that the so-called knowledge gap of plant responses to water and nutrient limitations is caused by the historical neglect of studies of below-ground processes. Consequently, water and nutrient uptake in plant growth and soil hydrological models are mostly described in an empirical way, often lacking a sound biophysical basis. This is unfortunate, as the exchange of water and nutrients is the unifying linkage between the plant root and surrounding soil environment. The simplified sink-approach is adequate for non-stressed plant growth conditions, and may work adequately for uniform soil conditions. However, it is clear that a different approach is needed if water and/or nutrient resources become limited. Increasingly, recommended irrigation water and soil management practices tactically allocate water and fertilizers, thereby maximizing their application efficiency and minimizing fertilizer losses through leaching towards the groundwater, so as to keep environmental effects of crop production within acceptable levels. We suggest that the effectiveness of such practices requires a thorough understanding of soil properties and

P. D'Odorico and A. Porporato (eds.), Dryland Ecohydrology, 13–29.

processes and associated plant-soil interactions in plant-stressed soil environmental conditions. This includes knowledge of the crops responses to the availability of spatially distributed soil water and plant-available nutrients, using a multi-dimensional modeling approach.

In the following, we first review soil physical properties and transport processes in soils. We then describe plant water and nutrient uptake modeling concepts in stressed soil environmental conditions, and conclude with a comprehensive modeling framework for the simulation of water and nutrient transport in soils.

2. Soil properties

Soils make up the upper part of the vadose zone where water flow occurs mostly under unsaturated conditions. The soil consists of a complex arrangement of mostly connected solid, liquid and gaseous phases, with the spatial distribution and geometrical arrangement of each phase, and the partitioning of solutes between phases, controlled by physical, chemical and biological processes. The unsaturated zone is bounded by the soil surface and merges with the groundwater in the capillary fringe. Water in the unsaturated soil matrix is held by capillary and adsorptive forces. Soils are subjected to fluctuations in water and chemical content by infiltration and leaching, water uptake by plant roots (transpiration) and evaporation from the soil surface. Water is a primary factor leading to soil formation from the weathering of parent material such as rock or transported deposits, with additional factors of climate, vegetation, topography, and parent material determining soil physical properties. The soil depth is controlled by the maximum rooting depth, generally within a few meters from the soil surface.

2.1. SOIL-WATER RETENTION

Unsaturated water flow is largely controlled by the physical arrangement of soil particles in relation to the water and air phases within the soil's pore space, as determined by pore size distribution and water-filled porosity or volumetric water content, θ (m^3 water /m^3 bulk soil). In addition to θ, the volume of water is sometimes defined by degree of saturation, $S_w = \theta/\theta_s$, or effective saturation (S_{ew}),

$$S_{ew} = \frac{\theta - \theta_r}{\theta_s - \theta_r} \tag{1}$$

where θ_s is the saturated soil water content and θ_r is the residual water content for which water is considered immobile.

In the Soil-Plant-Atmosphere-Continuum or SPAC, the driving force for water to flow is the gradient in total water potential (ψ_t). The total potential of bulk soil and plant water can be written as the sum of all possible component potentials, so that the total water potential (ψ_t) is equal to the sum of osmotic (ψ_o), matric (ψ_m), gravitational (ψ_g), and hydrostatic pressure potential (ψ_p). This additive property of water potential assumes that water is in thermal equilibrium and that physical barriers within SPAC behave as perfect semi-permeable membranes. Thus, contributions to the driving force for water flow may not only arise from gravity and matric forces, but may also include osmotic and pressure forces as well, such as in plant cells (see Chapter 4 for a detailed analysis of the components of water potential within plants). Whereas in physical chemistry the chemical potential of water is usually defined on a molar or mass basis, potential in soils is usually expressed with respect to a unit volume of water, thereby attaining units of pressure (Pa); or per unit weight of water, so that the potential represents the equivalent height of a column of water (m). The pressure head equivalent of the combined adsorptive and capillary forces in soils is defined as the matric pressure head, h_m. When expressed relative to the reference potential of free water, the water potential in unsaturated soils is negative (the soil-water potential is less than the water potential of water at atmospheric pressure). Hence, the matric potential decreases or becomes more negative as the soil water content decreases. In using head units for water potential, the total water potential (H) is defined as the sum of matric potential (h_m), gravitational potential (z), pressure potential (p) and osmotic potential (π), or

$$H = h_m + z + p + \pi \tag{2}$$

The measurement of the soil water matric potential *in situ* is difficult and is usually done by tensiometers in the range of matric head values larger (less negative) than –6.0 m. A tensiometer consists of a porous cup, usually ceramic, connected to a water-filled tube. The suction forces of the unsaturated soil draw water from the tensiometer into the soil until the water pressure inside the cup (at pressure smaller than atmospheric pressure) is equal to the pressure equivalent of the soil water matric potential just outside the cup. The water pressure in the tensiometer is usually measured by a vacuum gauge or pressure transducer. Other devices that are used to indirectly measure the soil water matric potential include buried porous blocks, from which either the electrical resistance or thermal conductivity is measured in situ, after coming into hydraulic equilibrium with the surrounding soil.

The soil-water retention function determines the relation between volume of water retained by soil matric or suction forces, as a function of θ, and is also known as the soil-water release or soil-water characteristic function. These suction forces increase as the size of the water-filled pores decreases, as may occur by drainage, water uptake by plant roots or soil evaporation. Since the matric forces are controlled by pore size distribution, specific surface area, and type of physico-chemical interactions at the solid-liquid interfaces, the soil water retention curve is soil-specific. It provides an estimate of the soil's capacity to hold water after free drainage, minimum soil water content available to the plant, and water availability for plants.

By way of the unique relationship between soil water matric head and the radius of curvature of the air-water interface, and using the analogy between capillary tubes and the irregular pores in porous media, a relationship can be derived between soil water matric head (h_m) and effective pore radius, r_e, or

$$\rho g h_m = \frac{2\sigma \cos\alpha}{r_e} \tag{3}$$

where σ and α are defined as the surface tension and wetting angle (of wetting fluid with solid surface), respectively, ρ is the density of water, and g is the acceleration due to gravity (9.8 m s^{-2}). As a result, the effective pore size distribution can be determined from the soil water retention curve in the region where matric forces dominate. Laboratory and field techniques to measure the soil water retention curve, and functional models to fit the measured soil water retention data, such as the van Genuchten (1980) and Brooks and Corey model, are described in Dane and Hopmans (2002) and Kosugi et al. (2002), respectively. An example of measured and fitted soil water retention data for two different soils is presented in Fig. 1 (Tuli and Hopmans, 2003).

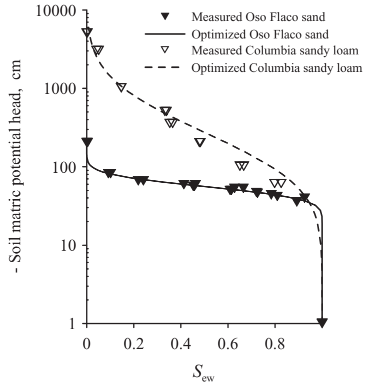

Figure 1. Measured (symbols) and fitted (lines) soil water retention data. (After Tuli and Hopmans, 2004).

2.2. UNSATURATED HYDRAULIC CONDUCTIVITY

The relation between the soil's unsaturated hydraulic conductivity, K, and volumetric water content, θ, is the second essential fundamental soil hydraulic property needed to describe water movement in the vadose zone. It is also a function of the water and soil matrix properties, and determines water infiltration and drainage rates, and is strongly affected by water content. It is defined by Darcy's equation, which relates the soil water flux density to the total driving force for flow, with K being the proportionality factor. Except for special circumstances, pneumatic and osmotic forces are irrelevant, so that the total driving force for water flow in soils is determined by the matric and gravitational forces, expressed by the total water potential gradient, $\Delta H/L$, where ΔH denotes the change in total head over the distance L, and $H = h_m + z$ (see Eq. (2)). For vertical flow, the application of Darcy's law yields the magnitude of water flow from the steady state flow equation:

$$J_w = -K(\theta)\left(\frac{\partial h_m}{\partial z} + 1\right) \tag{4}$$

where J_w is the Darcy water flux density ($L^3\ L^{-2}\ T^{-1}$), z is vertical position ($z > 0$, upwards, L), and $K(\theta)$ denotes the unsaturated hydraulic conductivity ($L\ T^{-1}$). A soil system is usually defined by the bulk soil, without consideration of the size and geometry of the individual flow channels or pores. Therefore, the hydraulic conductivity (K) describes the ability of the bulk soil to transmit water and is expressed by volume of water flowing per unit area of bulk soil per unit time. Functional models for unsaturated hydraulic conductivity are based on pore size distribution, pore geometry and connectivity, and require integration of soil water retention functions to obtain analytical expressions for the unsaturated hydraulic conductivity. The resulting expressions relate the relative hydraulic conductivity, K_r, defined as the ratio of the unsaturated hydraulic conductivity, K, and the saturated hydraulic conductivity, K_s, to the effective saturation, S_e, and can be written in the following generalized form (Kosugi et al., 2002)

$$K_r(S_e) = S_e^l \left[\frac{\int_0^{S_e} |h_m|^{-\eta}\, dS_e}{\int_0^1 |h_m|^{-\eta}\, dS_e} \right]^\gamma \tag{5}$$

where l and η are parameters related to the tortuosity and connectivity of the soil pores, and the value of the parameter γ is determined by the method of evaluating the effective pore radii. For values of $l = 0.5$, $\eta = 1.0$ and $\gamma = 2.0$, Eq. [5] reduces to the so-called Mualem (1976) model, that is routinely combined with the van Genuchten (1980) soil water retention model. The moisture-dependency is highly nonlinear, with a decrease in K of 4 to 5 or more orders of magnitude within field-representative changes in water content. Methods to measure the saturation dependency of the hydraulic conductivity are involved and time-consuming. A variety of methods are described in Dane and Topp (2002) and Dirksen (2001). Measurement errors are generally large, due to (1) the difficulty of flow measurements in the low water content range and (2) the dominant effect of large pores (macropores), cracks and fissures in the high water content range. An example of the unsaturated hydraulic conductivity for water, relative to its saturated values (K_{rw}), is presented in Fig. 2a, for the same two soils as in Fig. 1.

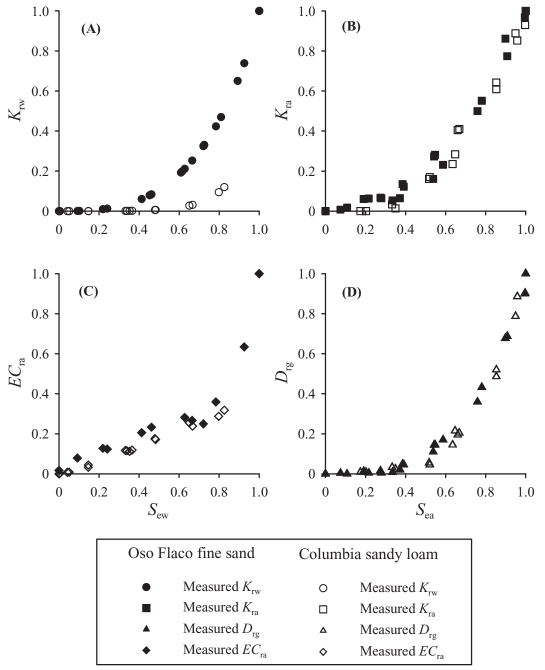

Figure 2. Measured relative hydraulic conductivity for water (K_{rw}), air conductivity (K_{ra}), gaseous diffusion (D_{rg}), and bulk soil electrical conductivity (EC_{rw}) as a function of degree of water (S_{ew}) and air (S_{ea}) saturation. (After Tuli and Hopmans, 2004).

The unsaturated hydraulic conductivity is related to the intrinsic soil permeability, $k(\mathrm{L}^2)$, by

$$K = \frac{\rho g k}{\mu} \tag{6}$$

where μ denotes the dynamic viscosity of water (F T L^{-2}). The usage of permeability instead of conductivity allows application of the flow equation to liquids other than water with different density and viscosity values.

This same Figure 2 also includes data for the saturation dependency of the relative air conductivity (K_{ra}), gaseous diffusion (D_{rg}) and bulk soil electrical conductivity (EC_{rw}). The gaseous phase transport parameters are typically determined to characterize soil gaseous transport, needed to determine the gaseous exchange of O_2, CO_2, N_2, and N_2O at the soil-atmosphere interface by root respiration and soil microbial processes (see Chapter 14). Bulk soil *EC* measurements, such as conducted by various EM and TDR methods, can be used to estimate soil solution concentration (Hendrickx et al., 2002).

3. Soil processes

3.1. MODELING OF SOIL WATER FLOW

Numerous studies have been published addressing different issues in the numerical modeling of unsaturated water flow using the Richards' equation. In short, the dynamic water flow equation is a combination of the steady-state Darcy expression and a mass balance formulation. Using various solution algorithms, the soil region of interest is discretized in finite-size elements, *i*, that can be 1, 2, or 3 dimensional, to solve for temporal changes in h_m, θ, or water flux, J_w, for each element or voxel *i* at any time *t*.

Most multi-dimensional soil water flow models use a finite-element, Picard time-iterative numerical scheme (Šimunek et al., 1999) to solve Richards' equation for soil water matric head h_m, or

$$\frac{\partial \theta}{\partial t} = \frac{\partial}{\partial x_i}\left[K\left(K_{ij}^A \frac{\partial h_m}{\partial x_j} + K_{i3}^A\right)\right] - S(x_j, h_m, \pi) \tag{7a}$$

where K_{ij}^A is the generic component of the dimensionless anisotropy tensor for the unsaturated conductivity (i, j = 1, 2, 3), x_i is the spatial coordinate, and S ($\mathrm{L}^3\mathrm{L}^{-3}\mathrm{T}^{-1}$) is the sink term, accounting for root water uptake. For isotropic conditions and one-dimensional vertical flow, it simplifies to:

$$\frac{\partial \theta}{\partial t} = \frac{\partial}{\partial z}\left[K(h_m)\frac{\partial h_m}{\partial z}\right] - S(z,t) \tag{7b}$$

Boundary conditions must be included to allow for specified soil water potentials or fluxes at all boundaries of the soil domain. Richards' equation is typically a highly nonlinear partial differential equation, and is therefore extremely difficult to solve numerically because of the largely nonlinear dependencies of both water content and unsaturated hydraulic conductivity on the soil water matric head. Both the soil water retention and unsaturated hydraulic conductivity relationships must be known a priori to solve the unsaturated water flow equation. Specifically, it will need the slope of the soil water retention curve, or water capacity $C(h_m)$, defined as $C(h_m) = d\theta / dh_m$.

3.2. MODELING OF SOLUTE TRANSPORT IN SOILS

As dissolved solutes move through the soils with the water, various physical, chemical and biological soil properties control their fate. In addition to diffusion and dispersion, fate and transport of chemicals in the subsurface is influenced by sorption to the solid phase and biological transformations. Both diffusion and dispersion of the transported chemical are a function of pore size distribution and water content. Mechanical or hydrodynamic dispersion is the result of water mixing within and between pores as a result of variations in pore water velocity. Increasing dispersivity values cause greater spreading of the chemical, thereby decreasing its peak concentration. Sorbed chemicals move through the vadose zone slower than non-interacting chemicals, and degree of sorption will largely depend on mineral type, specific surface area of the solid phase, and organic matter (OM) fraction. In addition, biogeochemical processes and radioactive decay affect contaminant concentration, such as by cation exchange, mineral precipitation and dissolution, complexation, oxidation-reduction reactions, and by microbial biodegradation and transformations. However, all these mechanisms depend on soil environmental conditions such as temperature, pH, water saturation, redox status, etc, and their soil spatial variations.

A general macroscopic transport model has been developed to solve the three-dimensional form of the convection-dispersion equation (CDE) for solute concentration c (ML^{-3}), as fully described in Šimunek et al. (1999), which solves for time-changes of nutrient concentration, c, and nutrient fluxes, J_s,

$$(\theta + \rho k)\frac{\partial c}{\partial t} = \frac{\partial}{\partial x_i}\left(\theta D_{ij}\frac{\partial c}{\partial x_j}\right) - J_{w,i}\frac{\partial c}{\partial x_i} - S' \tag{8a}$$

where ρ (M L^{-3}) is the soil bulk density, k (L^3 M^{-1}) is the linear adsorption coefficient, characterizing the adsorption of the specific nutrient to the soil's solid surface, thereby largely influencing the proportion of total ion content available for transport. D_{ij} (L^2 T^{-1}) is the generic component of the dispersion coefficient tensor, $J_{w,i}$ (L T^{-1}) is the Darcy water flux density component in the i-th direction, and S' (M L^{-3} T^{-1}) is the sink term to account for root nutrient uptake. The D-coefficient includes the ion-specific diffusion coefficient, which is highly dependent on water content. Many more rate constants can be added to the CDE, for example to allow for reactions of the solute in the dissolved or adsorbed phase, such as microbial degradation, volatilization and precipitation. Hence, the CDE allows for nutrient adsorption to the solid phase (left hand term), diffusion and dispersion, and mass flow (first and second terms on right hand of (8a), respectively) of the nutrient. The solution of Eq. (8a) yields the spatial and temporal distribution of nutrient concentration and fluxes at the same time resolution as Eqs. (7), when solved simultaneously. When simplified in the one-dimensional direction, z, the CDE is written as

$$\frac{\partial(\theta + \rho k)c}{\partial t} = \frac{\partial}{\partial z}\left(\theta D\frac{\partial c}{\partial z}\right) - \frac{\partial J_W c}{\partial z} - S' \tag{8b}$$

It must be pointed out that the solution of Eqs. (7) and (8) yields macroscopic quantities, i.e., values for matric potential, concentration or flux density denote voxel-representative values, with voxel sizes usually much larger than root diameter and root spacing. The integration of the flow and transport equations with plant growth includes its combination with plant water and nutrient uptake in multiple spatial dimensions. Accurate estimation of soil water and solute fluxes is especially challenging in arid climates, because of their orders of smaller magnitude than in agricultural settings.

In addition to movement of water and dissolved solutes, transport equations similar to Eqs. (7) and (8) can be written for soil gaseous and heat transport that include both diffusive and convective transport (Bear, 1972). All transport equations, including heat and gaseous transport, are usually solved simultaneously to ensure the incorporation of mutual interactions that may be especially relevant when including microbial and root respiration processes.

4. Coupled water and nutrient uptake

Water and nutrient transport towards plant roots can be mechanistically formulated by a set of coupled transport equations. At the *microscopic* level, the soil and root system can be simplified by a two-compartmental system, separated by a single effective semi-permeable membrane, separating the soil solution and apoplast from the cell solution or symplast. In this composite approach, steady state uptake rates of water (J_w) and nutrient (J_s) can be described by (Dalton et al., 1975):

$$J_w = L(\Delta h_m + \sigma \Delta \pi) \tag{9a}$$

and

$$J_s = \omega \Delta \pi + (1 - \sigma) C J_w + J^* \tag{9b}$$

where Δh_m and $\Delta \pi$ denote the matric and osmotic potential difference between the soil and xylem solution, respectively. The parameter σ denotes the effective reflection coefficient of all water-transporting root membranes combined between the soil and the xylem. The reflection coefficient value varies between zero and one. Its value is an indication of the effectiveness of the osmotic potential as a driving force for water flow into roots. Steudle et al. (1987) showed for maize roots that water uptake induced by matric pressure gradients is mainly apoplastic, whereas a major contribution to osmotic-induced uptake is the cell-to-cell or symplastic pathway. Equation (9b) defines root nutrient uptake by three different mechanisms. Firstly, transport is driven by concentration gradients (with ω denoting the effective diffusion coefficient), causing nutrient uptake by diffusion. Secondly, nutrients move into and through the root by mass transport, when dissolved in water. This mechanism is generally designated as the convective nutrient uptake component. It is computed from the product of nutrient concentration and water uptake rate. Thirdly, active uptake (J^*) occurs by nutrient flows against concentration or electrochemical gradients driven by specific energy-driven protein carriers and ion channels (Marschner, 1995). Most likely, nutrient uptake is dominantly by active uptake at low transpiration rates or low nutrient supplies, whereas passive uptake is likely favored at high transpiration rates or high soil nutrient concentrations (this concepts are applied to modeling plant nitrogen uptake in Chapter 11).

Although these steady state model types might be useful to simulate flow into roots, and for understanding of the coupled transport processes, they do not consider the dynamic interactions of plants with soil water and nutrients and are limited to one spatial dimension only. For example, roots can adjust their uptake patterns, thereby compensating for local stress conditions by enhanced or preferential uptake in other regions of the rooting zone with less stressful conditions. In this way, plants can temporarily deal with local stress. Dynamic root-soil interactions are prevalent during water infiltration and redistribution and fertigation, as soil water matric potential and solution concentration varies both spatially and temporally.

As an alternative, plant root water and nutrient uptake is simulated by a coupled dynamic approach, linking nutrient extraction to water uptake, controlled by the transient and locally-variable supply of water and nutrients to the roots. In the most general approach, the sink term S_i of Eq. (7a) for each soil compartment *i* of the root zone domain can be written as

$$S_i(t) = \alpha_i(h_m, \pi, t) RDF_i \, T_{pot}(t) \tag{10a}$$

where $T_{pot}(t)$ denotes the potential plant transpiration and RDF_i (L^{-1}) represents a multi-dimensional normalized root water uptake function, distributing water uptake according to the relative presence of roots. The localized stress response function $\alpha_i(h_m, \pi, t)$, accounts for the local influence of soil water osmotic and matric potential on root water uptake rate, with values between zero and one (no stress). The value of T_{pot} is solely defined by atmospheric conditions (evaporative demand), and needs to be corrected for soil evaporation (Allen, 2000). Thus, for non-stressed conditions, the extraction term for each soil compartment (S_i) is defined by $S_{max,i}$, where

$$S_{\max,i} = T_{pot} RDF_i \tag{10b}$$

The *RDF* could also be variable in time, as the active portions of plant roots grow and decay and new soil volumes are explored. For example, Clausnitzer and Hopmans (1994) characterized temporal changes in *RDF* using dynamic simulations of three-dimensional root-tip distribution.

Various empirical one-dimensional expressions have been developed to describe RDF_i, of which many are listed in Molz (1981), and Hoffman and van Genuchten (1983). Multi-dimensional root density distribution functions have recently been developed by Coelho and Or (1996) and Vrugt et al. (2001). For example, Vrugt et al (2001) introduced the following normalized three-dimensional root water uptake model

$$RDF_i = \frac{X_m Y_m \beta_i}{\int_0^{X_m} \int_0^{Y_m} \int_0^{Z_m} \beta_i \, dx\,dy\,dz} \tag{11a}$$

where

$$\beta_i = \left(1 - \frac{x_i}{X_m}\right)\left(1 - \frac{y_i}{Y_m}\right)\left(1 - \frac{z_i}{Z_m}\right) e^{-\left(\frac{p_x}{X_m}\left|x^* - x_i\right| + \frac{p_y}{Y_m}\left|y^* - y_i\right| + \frac{p_z}{Z_m}\left|z^* - z_i\right|\right)} \tag{11b}$$

and X_m, Y_m, and Z_m, denote maximum root exploration in directions of *x*, *y*, and *z*, respectively. With empirical parameters p_x, p_y, p_z, x^*, y^*, and z^*, this single expression was shown to simulate a wide variety of water-uptake patterns, with parameter values estimated using inverse modeling, minimizing residuals of spatially-distributed measured and simulated water content values.

Many different approached have been presented to define the stress response function $\alpha(h_m, \pi)$. In a comprehensive way, one can define a single crop water matric potential-salinity stress function, such as presented by Homae (1999), van Dam (1997), Shani and Dudly (2003), or van Genuchten (1987):

$$\alpha(h_m, \pi) = \frac{1}{1 + \left[\dfrac{\beta\, h_m + \pi}{\pi_{50}} \right]^3} \tag{12}$$

Equation (12) was used by Pang and Letey (1998), where β accounts for the differential response of the crop to matric and osmotic influences, and was set to the ratio of $h_{m,50}$ and π_{50}, designating the respective potentials at which potential plant transpiration is reduced by 50%.

Both water and nutrients enter the plant root freely through the apoplast, but their pathways and mechanisms of transport diverge when moving into the symplast. When addressing plant nutrient uptake, we must distinguish between the soil and plant root transport mechanisms, so that we can determine whether nutrient uptake is supply-controlled or demand-controlled. Demand-controlled nutrient uptake is regulated by plant parameters, such as defined by the potential nutrient uptake (S'_{pot}), whereas nutrient supply to the roots is controlled by soil nutrient transport as described by Eq. (8).

Excellent reviews on soil transport and uptake mechanisms of nutrients are presented in Barber (1984), Silberbush (1996), and Nye and Tinker (2000). Nutrient movement towards the root surface occurs by the parallel transport of convective flow ($J_{s,conv}$) and diffusion ($J_{s,dif}$). Nutrient transport by convection describes movement by the water as it moves through the soil towards the plant roots, as computed by solution of the Richards' Equation (7). High water flow rates, as for example induced by irrigation, will provide increased access of dissolved nutrients to the roots, whereas small water flow velocities tend to create depletion of nutrients near the roots. Although mass flow in general is not ion specific, differences in diffusion and adsorption coefficients between ions result in differences in soil transport rate and root supply between nutrients. Since nutrient uptake rates can be ion-specific, nutrient concentrations at the soil-root interface can be either accumulating or depleting.

In addition to soil transport, nutrient uptake is controlled by the spatial distribution of roots, as influenced by its architecture, morphology and presence of active sites of nutrient uptake, including root hairs. For nutrients that are immobile (e.g. phosphorus) or slowly mobile (ammonium), a root system must develop so that it has access to the nutrients, by increasing their exploration volume. Alternatively, the roots may increase their exploitation power for the specific nutrient by local adaptation of the rooting system, allowing for increased uptake efficiency of the nutrient. In the case of non-adsorbing nutrients, nutrient uptake is solely controlled by mass flow, as is the case of nitrate-nitrogen, which is hardly adsorbed by the soil. When considering the many complications and soil-root-nutrient interactions, the predictive ability of these supply-limiting mechanistic nutrient uptake models have been remarkably good. It therefore suggests that there is a reasonable level of understanding of the dominant physical and chemical processes of nutrient transport in soils.

Macroscopic models of nutrient uptake for a whole rooting system, use a macroscopic sink term *S'*, which predicts nutrient uptake for each soil element *i*,

$$S'_i = RDF_i J_{solute,i} \tag{13a}$$

where RDF_i ($L^2\ L^{-3}$) now denotes the multi-dimensional distribution of root nutrient uptake area per unit bulk soil volume within volume element *i*, and $J_{s,i}$ defines the local nutrient uptake per unit root area within root zone element *i* ($M\ L^{-2}\ T^{-1}$). The total nutrient uptake can be computed from integration of Eq. (13a) over the whole rooting zone. Nutrient uptake by plants may be simulated analogously to root water uptake, with total nutrient uptake controlled by plant nutrient demand or potential plant uptake, S'_{pot}. The plant nutrient demand, expressed in mass of specific nutrient required per unit mass dry matter produced, can be computed from the nutrient use efficiency using known values of the biomass produced per unit nutrient taken up. Tables with nutrient consumption rates for elements such as N, P and K for various crops as a function of time are listed in Bar-Yosef (1999).

Total actual nutrient uptake must be distributed across the rooting zone according to the spatial distribution of nutrient supply rate and root uptake sites. In addition to the presence of roots, it has also been demonstrated that plant root growth responds to local variations in nutrient supply. For example, as was experimentally determined by Drew and Saker (1975), localized proliferation of root growth can occur if part of the rooting zone is supplied with an enhanced supply of nitrate, with other soil environmental conditions non-limiting. The local high concentration of nitrate was able to offset the limited nutrient supply available to other parts of the rooting system. Simulation models, such as that presented by Pang and Letey (1999), provide mechanisms for enhanced plant nutrient uptake to compensate for local nutrient deficiencies. In addition, their root uptake model included the nutrient stress function, $\gamma(c_i)$, which was assigned a value of one, if the ratio of potential nutrient uptake rate and potential ET (defined as c^*) was larger than c_i, and values were smaller than one and equal to c_i/c, if $c_i<c$, so that

$$S_i^{'} = \gamma(c)RDF_i S_{pot}^{'} \tag{13b}$$

The nutrient stress factor then characterizes the effect of plant nutrient stress on crop biomass production.

Rather than by describing nutrient uptake by a single macroscopic mechanism, an alternative formulation may include both passive and active pathways, acting in parallel, with likely enhanced passive uptake for high-transpiration conditions, and active uptake dominating when passive nutrient uptake is not meeting plant nutrient demand. Such a mechanistic description by partitioning between passive (P) and active (A) nutrient uptake was first described by Somma et al. (1998). This was achieved by defining total root nitrate uptake for each volume element i by $S_i^{'} = P_i + A_i$ [$ML^{-3}T^{-1}$], where $P_i = S_i c_{i.}$ If $P > S_{pot}^{'}$, one may assume nutrient uptake is by passive uptake only ($A = 0$ for all i), so that $S^{'} = S_{pot}^{'}$ and $S_i^{'} = S_i c_i$. Alternatively, if $P < S_{pot}^{'}$ then one may define $A_{pot} = (S_{pot}^{'} - P)$ and $A_i = RDF_i A_{pot}$. Reduced active uptake (if $A_i > A_i^*$) is controlled by the Michaelis-Menten value of active uptake, A_i^*, as computed from

$$A_i^* = \left(\frac{J_{max} c_i}{K_m + c_i} + \chi \right) \tag{14a}$$

where J_{max} ($ML^{-2}T^{-1}$) is the maximum nutrient uptake rate, K_m (ML^{-3}) the Michaelis-Menten constant, and χ (LT^{-1}) allows for a first-order rate coefficient, simulating linear/diffusive uptake component. When integrated over the whole rooting zone, the reduced active uptake term is equal to A_{pot}^*, so that the active nutrient uptake for root zone element i can be defined by:

$$A_i^{'} = \gamma(c_i)\, RDFA_i\, A_{pot}^* \tag{14b}$$

where $\gamma(c_i) = A_i^* / A_i$ and *RDFA*$_i$ defines the spatial distribution function of active nutrient uptake sites, which is not necessarily equal to *RDF*$_i$. In this approach, the spatial distribution of *RDFA* can be determined from nitrate uptake experiments in nutrient-stressed conditions. However, in general, little is known about the relative magnitudes of the partitioning between passive and active uptake and spatial distribution of nutrient uptake sites. However, it is expected that it is plant and ion specific, whereas relative magnitudes may depend on nutrient and water availability and plant nutrient demand or deficit. Functional relationships of γ (x,y,z,t) can be developed, from measurements and simulations of multi-dimensional soil solution nitrate concentration and water content, optimizing root water and nutrient uptake parameters including their partitioning between passive and active uptake. Through minimization of the differences between measured and simulated water content and nitrate concentrations, the fractions of passive and active nitrate uptake to total nitrogen uptake, and the influence of water stress on active uptake can be determined.

5. Comprehensive example

In order to improve plant growth simulation models under stressed soil conditions, a comprehensive approach must be developed to allow for analysis of the influence of multi-dimensional distribution of root water and nutrient uptake sites within the root zone on plant growth and soil flow and transport processes. As an example, the interactions of root water uptake and soil moisture and their spatial variations within the root zone of a kiwifruit vine was demonstrated in Green and Clothier (1995). It was shown experimentally that following irrigation, preferential uptake of water shifted to the wetter parts of the soil within periods of days, away from the deeper drier parts of the root zone. Upon rewetting, plant roots recovered and showed enhanced activity by new root growth. A similar shifting of root water uptake patterns was observed by Andreu et al. (1997), using three-dimensional soil water content measurements around a drip-irrigated almond tree. The water and chemical trapping mechanisms by roots were illustrated in Clothier and Green (1997), designating roots as ‘the big movers of water and chemical in soil’. Their works shows that the overall functioning of the plant and its transpiration is controlled by the complicated variations in root water uptake rates along supply-active root segments within the whole root system. The challenge then is to integrate local uptake variations to total plant uptake, which requires better understanding of the link between root architecture and morphology, and the functioning of root water and nutrient uptake. Also, the extent and shape of the rooting system and their changes with time play a major role in determining uptake patterns. The coupling of water flow with nutrient transport is needed to simulate plant response to stresses in water, nutrients and salinity, and to predict the space and time distribution of soil water and nutrient concentrations as controlled by concomitant root uptake mechanisms.

The most comprehensive, dynamic multi-dimensional soil crop growth model to date was developed Clausnitzer and Hopmans (1994) and Somma et al. (1998), and is extensively described in Somma et al. (1997), linking a three-dimensional transient soil water flow and nutrient transport to root growth. Root water uptake was computed as a function of soil water matric and osmotic potential, whereas root nutrient uptake was calculated as a result of both passive and active uptake mechanisms. Root water and nutrient uptakes were computed at the same time and space scales, and were dynamically controlled by root and soil parameters in both unstressed and stressed conditions (soil resistance, temperature, water and nutrient stress). The final result was a transient model for the simultaneous dynamic simulation of water and solute transport, root growth, and root water and nutrient uptake in three dimensions. The model includes formulation of interactions between plant growth and nutrient concentration, thus providing a tool for studying the dynamic relationships between changing soil-water, nutrient status, temperature, and root activity. The essential components of the soil-crop model are presented in Fig. 3.

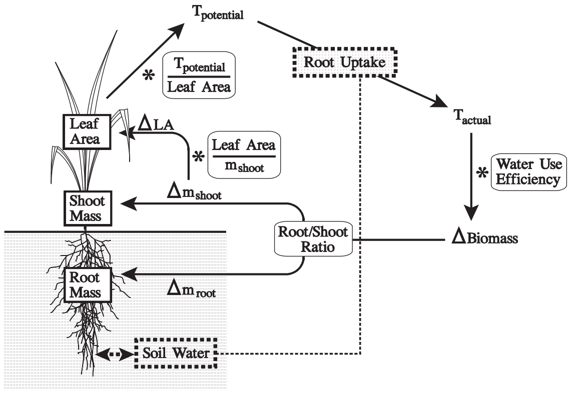

Figure 3. Concept diagram of comprehensive SPAC Modeling. (After Clausnitzer and Hopmans, 1994).

The convection-dispersion equation used for the simulation of nutrient transport was considered in its comprehensive form, thus allowing a realistic description of nutrient fate in the soil domain. Soil-water uptake was computed as a function of matric and osmotic potential, whereas absorption of nutrients by the roots was calculated as a result of passive and active uptake mechanisms. Uptake and respiration activities varied along the root axis and among roots as a result of root age. Genotype-specific and environment-dependent root growth processes such as soil moisture, nutrient concentration and soil temperature, were included using empirical functions. In concept, the modeling approach followed the requirement that plant transpiration and assimilation are directly coupled through a water use efficiency term. The root and soil parameters of root length, surface area, age, soil water content, temperature, and nutrient concentration were computed within priori-selected volume elements (*i*) at any desired temporal resolution. In order to solve the flow and transport equations (7) and (8), the soil domain was discretisized into a rectangular grid of finite elements, each defined by 8 nodes, with the element size defining the spatial resolution of the soil environment. Root growth, architecture, and age was simulated starting from a germinating seed that 'grows' at user-defined time intervals with new segments added to the apex of each growing root. The flow and transport model was integrated with the root growth model (Fig. 4), allowing soil-plant root interactions through water and nutrient uptake as a function of root properties (size and age) and soil properties (water content and nutrient concentration). Moreover, soil water content, resistance, nutrient concentration, and temperature affected root growth and architecture directly. The model tracks each segment by recording its topological position within the root system, and its spatial location within the model domain, as well as its age, mass and surface area.

Root growth was simulated as a function of mechanical soil strength, soil temperature and solute concentration. Root axes were generated at user-defined times. Branching time and spacing were described by user-defined functions of root age and branching order. A root growth impedance factor was calculated for each growing root apex as a function of the local soil strength, nutrient and temperature conditions and time, to reduce the length of the growing segment from its potential (unimpeded) value. The impedance factor varied linearly between zero and unity (unimpeded growth). Consequently, root growth rates were unaffected by nutrient availability, as long as the latter are maintained within an optimal concentration range. Because the optimal range and minimum and maximum concentration are both genotype- and nutrient-specific, nutrient-concentration effects were simulated using a piecewise linear impedance function, varying linearly between zero and unity (optimal concentration range). In a similar manner, other impedance functions were defined to simulate effects of soil strength and soil temperature on local root growth.

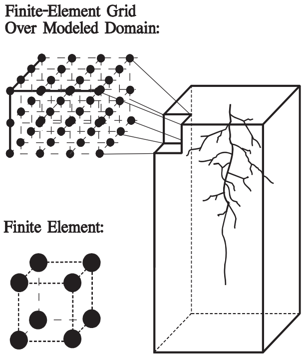

Figure 4. Discretization of soil-plant root domain. (After Clausnitzer and Hopmans, 1994).

To demonstrate the possible interactive processes that can be simulated with this type of approach, Fig. 5 shows the model-computed effects of soil strength and water content on root growth as presented in Clausnitzer and Hopmans (1994). Because higher soil water contents reduce soil strength, simulated roots tended to grow towards the wetter soil regions. In addition, the reduced mechanical impedance resulted in faster root elongation rates. Combined, these two factors resulted in enhanced root growth towards the irrigation emitters in Fig. 5. The simulated results agree with field studies showing a general decrease in root density with increasing distance from trickle emitters (Earl and Jury, 1977).

Another example demonstrates the possible influence of NO_3-N concentration on root growth in Fig. 6, which was taken from Somma et al. (1998), assuming passive nitrate uptake only. Both water and NO_3-N were supplied through a dripper, at the soil surface. Figures 6a and 6b show the simulated root system grown under non-limiting and deficient NO_3-N supply, respectively, at the end of a 25-day growth period. In both cases the soil-water content was such that soil strength did not limit root growth. Root density is presented to the left of each root system; with the NO_3-N concentration profile shown on the right. In the example of Figure 6a, NO_3-N was applied continuously with the irrigation water throughout the growth period (non-limiting N case). The predicted N-concentration was higher in the upper part of the soil domain. Similarly, the predicted root density decreased with increasing depth. In Figure 6b, NO_3-N was applied only during a limited time interval at the beginning of the growth period (deficient N case), with the total amount applied equal to the non-limiting case. Once N application stopped, the subsequent irrigations by the dripper moved the N plume downwards, causing a greater root density in the central part of the root zone where the NO_3-N content was higher. The downward movement of the N plume promoted root development at increasing depth, but resulted in a smaller average root density than for the nonlimiting-N case. Complementary simulations that included water and nutrient uptake, for both the nonlimiting and N-limited case also showed clearly the concomitant leaching of nitrate for the N-limited case. This was caused by the single early nitrate application that limited nutrient availability and potential nutrient uptake in the subsequent growing period.

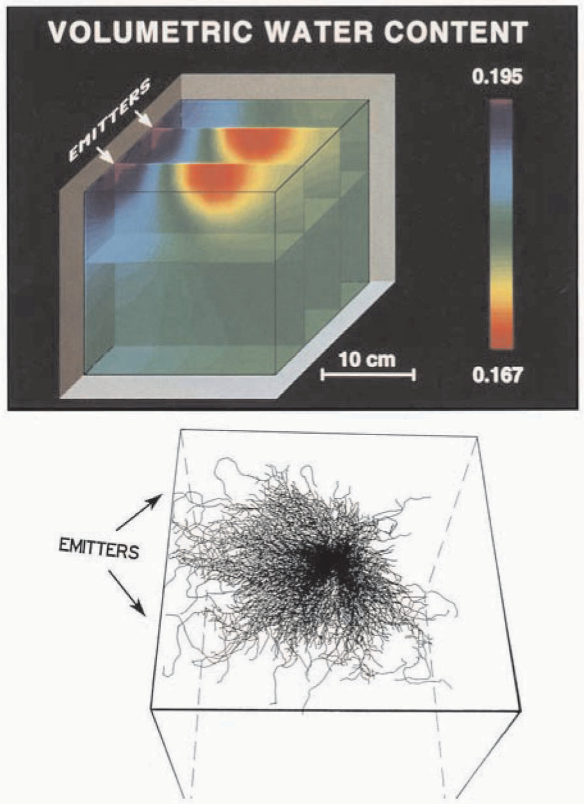

Figure 5. Simulated effect of water content on root growth. (After Clausnitzer and Hopmans, 1994).

6. Summary

An improved understanding of natural ecosystems and sustainable agricultural systems justifies the increasing need for combining soil knowledge with plant expertise, in particular as related to root development and functioning. This is especially the case for stressed soil conditions when water and plant nutrients become limiting, as is the case in dry ecosystems and sustainable irrigated agriculture. This includes knowledge of the plant's responses to the availability of spatially-distributed soil water and plant-available nutrients.

Although many models have been developed to simulate root growth and its interactions with soil water and nutrients, most of these are limited to one spatial dimension, and assume steady state flow of water. Alternatively, it is suggested to characterize root water and nutrient uptake by a coupled dynamic approach, linking nutrient extraction to water uptake, controlled by the transient and locally-variable supply of water and nutrients to the roots. Although much more complicated, this coupled multi-dimensional and mechanistic transport approach of water and nutrients is necessary if we intend to progress our understanding and ability to improve predictive capabilities of plant growth models in stressed soil conditions.

However, this approach is limited as it requires much more additional soil and plant parameters that can be obtained only from dedicated experiments (see e.g. the integration of experiments and modeling presented by Vrugt et al. (2001).

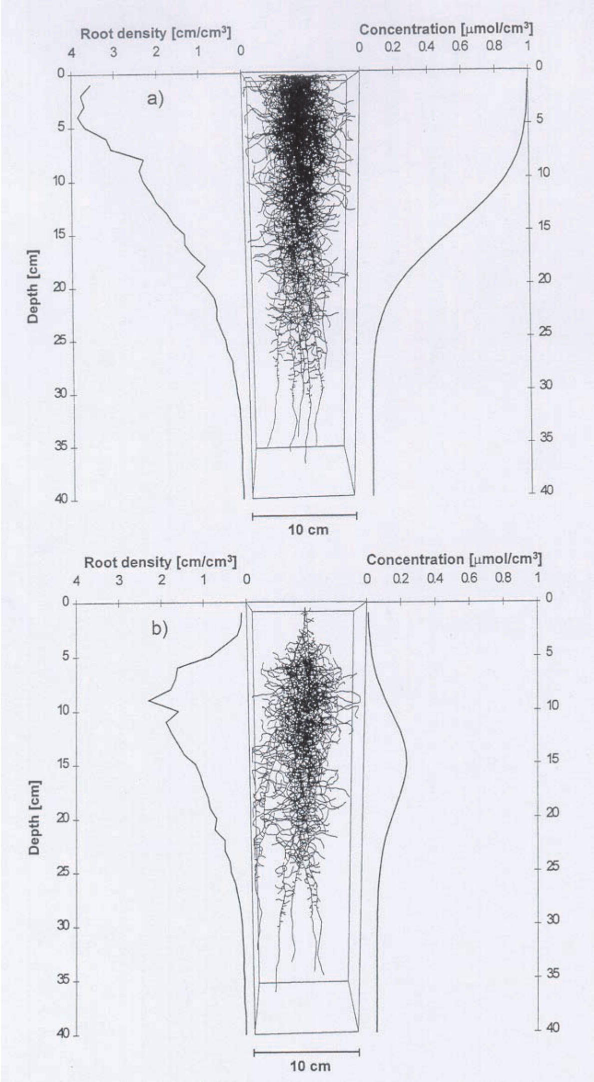

Figure 6. Simulated response of NO_3-N concentration on root growth for nitrate nonlimiting (a) and deficient (b) conditions. (After Somma et al, 1999).

7. References

Allen, R.G., L.S. Pereira, D. Raes, and M. Smith. (1998). “Crop evaporation. Guidelines for computing crop water requirements.” FAO Irrigation and Drainage Papers 56. FAO, Rome.

Andreu, L., J.W. Hopmans and L.J. Schwankl. (1997). Spatial and temporal distribution of soil water balance for a drip-irrigated almond tree. Agricultural Water Management 35, 123- 146.

Barber, D.A. (1984). “Soil nutrient bioavailability.” Wiley. New York

Bar-Yosef, B. (1999). Advances in Fertigation. Advances in Agronomy 65,1-75.

Bear, J. 1972. Dynamics of fluids in porous media. Dover Publications, Inc. New York.

Clausnitzer, V. and J.W. Hopmans.(1994). Simultaneous modeling of transient three-dimensional root growth and soil water flow. Plant and Soil 164, 299-314.

Clothier, B.E. and S.R. Green. (1997). Roots: The big movers of water and chemical in soil. Soil Science 162, 534-543

Coelho, F.E. and D. Or. (1996). A Parametric model for two-dimensional water uptake intensity by corn roots under drip irrigation. Soil. Sci. Soc Am. J. 60, 1039-1049.

Dalton, F.N., P.A.C. Raats and W.R. Gardner. (1975). Simultaneous uptake of water and solutes by plant roots. Agronomy Journal 67, 334-339.

Dane, J.H., and G.C. Topp. (2002). Methods of Soil Analysis. Part 4. Physical Methods. (Eds.). Soil Science Society of America Book Series No. 5. Madison, Wisconsin.

Dane, J.H., and J.W. Hopmans. (2002). Soil Water Retention and Storage - Introduction. IN: Methods of Soil Analysis. Part 4. Physical Methods. (J.H. Dane and G.C. Topp, Eds.). Soil Science Society of America Book Series No. 5. Madison, Wisconsin. Pages 671-674.

Dirksen, C. (2001). Unsaturated hydraulic conductivity. IN: Soil and Environmental Analysis. (Eds. K.A. Smith and C.E. Mullins)., Marcel Dekker, Inc. New York. Pages. 141-238.

Drew, M.C., and L.R. Saker. (1975). Nutrient supply and the growth of the seminal root system in barley. II. Localized, compensatory increases in lateral root growth and rates of nitrate uptake when nitrate supply is restricted to only part of the root system. J. Exp. Bot. 26, 79-90.

Earl, K.D., and W.A. Jury. (1977). Water movement in bare and cropped soil under isolated trickle emitters. II. Analysis of cropped soil experiments. Soil Sci. Soc. Amer. J. 41, 856-861.

Green, S.R., and B.E. Clothier. (1995). Root water uptake by kiwifruit vines following partial wetting of the root zone. Plant and Soil 173, 317-328.

Hendrickx, J.M.H., B. Das, D.L. Corwin, J.M. Wraith, and R.G. Kachanoski.(2002). Indirect measurement of solute concentration. IN: Methods of Soil Analysis. Part 4. Physical Methods. (J.H. Dane and G.C. Topp, Eds.). Soil Science Society of America Book Series No. 5. Madison, Wisconsin . Pages 1274-1305.

Hoffman, G. and M.Th. Van Genuchten. (1983). Soil properties and efficient water use: Water management of salinity control. In “Limitations for efficient crop production.” (H.M. Taylor, W.R. Jordan, and T.R. Sinclair, Eds.). pp. 73-86. ASA Inc. 677 South Segoe Road, Madison, WI 53711 USA.

Homae, M. (1999). “Root water uptake under non-uniform transient salinity and water stress.” PhD-Thesis Agricultural University Wageningen, the Netherlands.

Hopmans, J.W., and K.L. Bristow. (2002). Current capabilities and future needs of root water and nutrient uptake modeling. Advances in Agronomy. Volume 77, 104-175.

Kosugi, K., J.W. Hopmans and J.H. Dane. (2002). Water Retention and Storage - Parametric Models. IN: Methods of Soil Analysis. Part 4. Physical Methods. (J.H. Dane and G.C. Topp, Eds.). Soil Science Society of America Book Series No. 5. Madison, Wisconsin. Pages 739-758.

Marschner, H. (1995). “Mineral Nutrition of higher plants.” Second Edition. Academic Press.

Molz. F.J. (1981). Models of water transport in the soil-plant system: A review. *Water Resour. Res*. **17,** 245-1260.

Mualem, Y. (1976). A new model for predicting the hydraulicconductivity of unsaturated porous media. Wter Resour. Res. 12, 513-522.

Nye, P.H. and P.B. Tinker. (2000). Solute movement in the Rhizophere (Topics in sustainable agronomy). Oxford University Press, Second Edition.

Pang, X.P., and J. Letey. 1998. Development and evaluation of ENVIRO-GRO, an integrated, water, salinity, and nitrogen model. Soil Sci. Soc. Amer. J. 62:1418-1427.

Shani, U, and L.M. Dudley. (2003). Modeling water uptake by roots under water and salt stress. Vadose Zone Journal. In Press.

Silberbush, M. (1996). Simulation of ion uptake from the soil. In ”Plants Roots, the Hidden Half. Second Edition.”, (Y. Waisel, A. Eshel and U. Kafkafi. ,Eds.). pp. 643-658. Marcel Dekker, Inc. New York.

Šimunek, J., M. Šejna and M.Th. Van Genuchten. (1999). “The HYDRUS-2D software package for simulating two-dimensonal movement of water, heat, and multiple solutes in variable saturated media.” Version 2.0, IGWMC-TPS-53, International Ground Water Modeling Center, Colorado School of Mines, Golden, Colorado.

Somma, F., V. Clausnitzer, and J.W. Hopmans. (1998). Modeling of transient three-dimensional soil water and solute transport with root growth and water and nutrient uptake. *Plant and Soil*. **202**, 281-293.

Somma. F., V. Clausnitzer and J.W. Hopmans. (1997). “An algorithm for three-dimensional simultaneous modeling of root growth, transient soil water flow, and transport and uptake.” V. 2.1. Land, Air and Water Resources Paper No. 100034, Univ. of California, Davis.

Steudle, E., R. Oren and E-D. Schulze. (1987). Water transport in Maize Roots. *Plant Physiol*. **84**, 1220-1232.

Tuli, A.M., and J.W. Hopmans. (2003). Effect of degree of saturation on transport coefficients in disturbed soils. European Journal of Soil Science. 55:147-164.

Van Dam, J.C., J. Huygen, J.G. Wesseling, R.A. Feddes, P. Kabat, R.E.V. van Walsum, P. Groenendijk, and C.A. van Diepen. (1997). “Theory of SWAP version 2.0.” SC-DLO, Wageningen Agricultural University, Report 71, Department of Water Resources. The Netherlands.

Van Genuchten, M.Th. (1980). A closed-form equation for predicting the hydraulic conductivity of unsaturated soils. Soil Sci. Soc. Am. J. 44, 892-898.

Van Genuchten, M.Th. (1987). “A numerical model for water and solute movement in and below the root zone.” Research Report No 121, U.S. Salinity Lab, ARS USDA, Riverside, CA.

Vrugt, J.A., M.T. van Wijk, J.W. Hopmans, and J. Simunek. (2001). One, two, and three- dimensional root water uptake functions for transient modeling. Water Resour. Res. 37, 2457-2470.

Chapter 3

SOIL MOISTURE DYNAMICS IN WATER-LIMITED ECOSYSTEMS

Paolo D'ODORICO[1] and Amilcare PORPORATO[2]

[1]*Department of Environmental Sciences, University of Virginia, Charlottesville, VA 22904, USA*
e-mail: paolo@virginia.edu
[2]*Department of Civil and Environmental Engineering, Duke University, Durham NC 27708, USA*
e-mail: amilcare@duke.edu

1. Introduction

The main control exerted by hydrological processes on vegetation in water-limited ecosystems is through the soil water content, which, in turn, results from complex interactions between precipitation, infiltration, evaporation, transpiration, and soil drainage. Most of these processes are state-dependent, in that their rates are functions of the soil water content.

A number of eco-hydrological processes in water-limited ecosystems depend on the soil water content. Soil moisture dynamics affect the occurrence, duration and intensity of periods of water stress in vegetation (Hale and Orchutt, 1987; Smith and Griffiths, 1993; Porporato et al., 2001), with important effects on plant cell turgidity, stomatal conductance, and, in turn, on photosynthesis, carbon assimilation and ecosystem net primary productivity (see Chapter 4). The control of soil moisture on canopy conductance is also of foremost importance in modulating the heat and water vapor fluxes from terrestrial vegetation to the near-surface atmosphere, with important consequences for the moisture content and stability of the atmospheric boundary layer and consequent feedbacks to precipitation and the water cycle (Chapters 5 and 6). Soil moisture exerts an important control also on nutrient cycling (e.g., Linn and Doran, 1984, Skopp et al., 1990; Parton et al., 1998; Porporato et al., 2003), due to its effects on microbial activity, nitrogen leaching and nutrient uptake, as explained in Chapters 11 and 14. Other surface processes affected by the soil water content, include infiltration, runoff, soil erosion and dust emission from dryland landscapes (see Chapter 9).

The study of all these processes and of the impact of possible scenarios of climate variability and change, requires the analysis and modelling of soil moisture dynamics. To this end, a number of models have been developed by different authors to simulate the spatial and temporal patterns of soil moisture in the root zone. This chapter will focus on the temporal dynamics, while Chapter 7 discusses the topography-driven spatial variability of soil moisture.

2. Types of soil moisture models

Soil moisture dynamics are usually studied through a soil water budget accounting for the main inputs and outputs of soil water, namely rainfall infiltration, evapotranspiration, and drainage. The complexity of these models depends on the different levels of detail used in the representation of these fluxes, as well as in the number of soil layers used in the calculation of the soil water storage (Table 1).

A number of models have been developed by crop scientists, agro-meteorologists, and hydrometeorologists to calculate soil water content and evapotranspiration by coupling the soil water budget with the surface energy balance. Some of these models require the simultaneous solution of the water and energy balance equations to determine at the same time evapotranspiration rates and soil water contents. This class of agro-hydrological (e.g., Jones and Kiniry, 1986; Evett and Lascano, 1993; Daamen and Simmonds, 1994) and land surface models (e.g., Sellers et al., 1986; Dickinson et al., 1986) generally requires the measurement of several

P. D'Odorico and A. Porporato (eds.), Dryland Ecohydrology, 31–46.

micrometeorological and hydrological variables. In most applications, only limited information is available on vegetation canopy (e.g., the leaf area index, LAI) and a "two layer-two source" approach (e.g., Daamen, 1997; Xue et al, 1996) is often used to model evaporation from soil and leaf surfaces. A major problem in this modeling approach is in properly accounting for both the partitioning of the incident energy between vegetation and soil, and the to possible interactions between soil evaporation and transpiration. In other cases further complexity is added by including a multilayer representation of vegetation canopies (e.g., Norman, 1979; Chen, 1984; Baldocchi and Meyers, 1998).

Table 1: A classification of soil moisture models on the basis of different approaches used in the representation of soil, evapotranspiration, vegetation canopies, infiltration, and precipitation.

Soil	**Multilayer** (e.g., Evett and Lascano, 1993; Sellers et al., 1986; Dickinson et al., 1986; Xue et al., 1996; Daamen and Simmonds, 1994; Parton et al., 1998; Hopmans, 2002; Feddes et al., 2001; Guswa et al., 2002)
	Single Layer (e.g., Budyko, 1958; Rodriguez-Iturbe et al., 1991; 1999; Milly, 1993; Laio et al., 2001a)
Evapotranspiration	**Potential evapotranspiration approach** (e.g., Lai and Katul, 2000; Sellers et al., 1986; Dickinson et al., 1986; Milly, 1993; Rodriguez-Iturbe et al., 1999a; Laio et al., 2001a; Guswa et al., 2002)
	Simultaneous solution of energy and water balance equations (e.g., Evett and Lascano, 1993; Daamen and Simmonds, 1994; Daamen, 1997)
Canopy/Evaporating Surfaces	**1-layer ("big leaf")** with no account for soil evaporation (e.g., Milly, 1993; Rodriguez-Iturbe et al., 1999a; Lai and Katul, 2000; Guswa et al., 2002).
	2-layers: soil and a 1-layer canopy (e.g., Xue et al., 1991; 1996; Daamen and Simmonds, 1994; Evett and Lascano, 1993; Laio et al., 2001a).
	Multi-layer/multi-crop (e.g., Norman, 1979; Chen, 1984; Sellers et al., 1986; Dickinson et al., 1986; Baldocchi and Meyers, 1998).
Infiltration	**Integration of Richards equations** (Sellers et al., 1986; Dickinson et al., 1986; Xue et al., 1996; Evett and Lascano, 1993; Daamen and Simmonds, 1994; Hopmans, 2002; Feddes et al., 2001; Lai and Katul, 2000; Guswa et al., 2002)
	Conceptual model for single layer (Milly, 1993; Rodriguez-Iturbe et al., 1999a; Laio et al, 2001a) or multi-layer soil (e.g., Parton et al., 1998)
Rainfall	**Deterministic/data records** (e.g., Evett and Lascano, 1993; Daamen and Simmonds, 1994)
	Stochastic (e.g., Eagleson et al., 1978a; Milly, 1993; Rodriguez-Iturbe et al., 1999a; Laio et al., 2001a)

Other models (e.g., Lai and Katul, 2000), instead of solving simultaneously the energy and water balance equations, use the concept of potential evapotranspiration, E_p, and express the total (actual) evaporative fluxes, E_{act}, as the by-product between E_p and a function of soil moisture, $f(\tau)$, accounting for the reduction in evapotranspiration due to stomata resistance in conditions of limited soil water availability (e.g., Chapter 4),

$$E_{act}=f(\tau)\,E_p, \tag{1}$$

In equation (1) τ is the volumetric soil moisture, i.e. the ratio between water and void volumes in a soil sample. By definition, the rate of potential evapotranspiration does not depend on τ and can be calculated either with an energy balance or with a combination method, such as the Penman-Brutsaert model (e.g., Katul and Parlange, 1992). Thus, the solution of the energy balance (or of the combination) equation occurs independently of the integration of the soil moisture balance, allowing for significant simplifications in the numerical algorithms. The function, f(τ), represents the effect of soil moisture on canopy (and soil) resistance and is usually expressed either through empirical parameterizations (e.g., Jarvis, 1976; Jones, 1992), or through process-based models of the plant physiological response to water stress (e.g., Gao et al., 2002; Daly et al., 2003). More details on the modeling of f(τ) are provided in Section 3.1.

The soil water balance is usually expressed (e.g., Feddes et al., 2001; Lai and Katul, 2000; Guswa et al., 2002) by a one-dimensional (in the z-direction, with *z* being positive downward) mass-conservation equation for the root zone

$$\frac{\partial \theta(z,t)}{\partial t} = -\frac{\partial q(z,t)}{\partial z} - u(z,t) \tag{2}$$

where *q* is the unsaturated Darcian flux (Richards, 1931) associated with rainfall infiltration and *u* is the water uptaken by plant roots. *u(z)* is related to the actual rate of transpiration using, for instance, root distribution (or density) functions (e.g., Feddes et al., 2001; Hopmans et al., 2002), as explained in Chapter 2. Regardless of the particular method used in the calculations of the actual rates of evapotranspiration, root water uptake depends on soil moisture. Similarly, the infiltration rate is state-dependent, in that it can be expressed as

$$q = -K(\theta)\left[1 + \frac{\partial \psi(\theta)}{\partial z}\right] \tag{3}$$

with *K* (hydraulic conductivity) and | (soil water potential) being both non-linear functions of soil moisture. Appropriate boundary conditions need to be specified at the soil surface to account for soil evaporation and rainfall infiltration, and at the bottom to account for deep infiltration (e.g., Evett and Lascano, 1993). However, because this approach can be at times somewhat cumbersome, simplified models are often used in ecohydrology to calculate the soil water content. More details on the solution of the complete equations (2) and (3) are provided in Chapter (2). A number of analytical solutions of the non-linear infiltration equations are also available; a review can be found in Smith et al. (2002). Here we focus on simplified approaches to soil moisture modeling, involving some approximations in the representation of infiltration, runoff and evapotranspiration.

3. Processes affecting soil moisture dynamics

3.1. EVAPOTRANSPIRATION

The process of evapotranspiration includes soil evaporation, transpiration from the plant stomata, and evaporation of precipitation fractions intercepted by canopy and litter. Chapter 5 describes the dependence of evapotranspiration on solar irradiance, vapor pressure deficit, and wind speed, and explains how the atmospheric evaporative demand varies with these parameters. In arid and semiarid environments evapotranspiration is often limited by soil water availability more than by evaporative demand. Thus, any soil water balance model should include an adequate representation of the dependence of evapotranspiration on soil moisture, for instance, through the function f(τ) (see equation (1)). This function would parameterize the effect of stomata regulation described in Chapter 4.

Thornthwaite and Mather (1955) and Budyko (1958) expressed f(τ) using a piecewise linear function (Figure 1A). According to this model evapotranspiration occurs at a maximum (potential) rate for soil moisture values above a critical level, τ^*, and decreases with τ for $\tau<\tau^*$. This approach is often used in general circulation (e.g., Eagleson, 1982) and ecohydrological (Rodriguez-Iturbe et al., 1999a; Rodriguez-Iturbe and Porporato, 2005) models. In the past, some authors expressed τ^* and a fraction of the moisture content at field capacity (e.g., Eagleson, 1982) while it is now understood (Rodriguez-Iturbe et al., 1999b; Laio et al., 2001a) that τ^* depends not only on soil hydraulic properties but also on vegetation characteristics. It can also be observed that the Thornthwaite-Budyko model is unrealistic for low moisture contents, as it assumes that evapotranspiration becomes zero when the soil is completely dry. Stomatal conductance and transpiration are commonly found to become zero already at the so-called permanent wilting point, τ_{w}. In the crop science literature τ_{w} is usually taken as the soil water content corresponding to –1.5 MPa of soil matric potential (i.e., $|_{\mathrm{w}}$=-1.5 MPa). However, dryland vegetation is often found to wilt at water potentials much smaller than –1.5 MPa (e.g., Richter, 1976, pp. 47-49). Thus, in general, τ_{w} and τ^* depend both on soil texture and vegetation types, as different plants have different strategies to respond to water stress (Chapter 4).

Different models have been suggested to express the function f(τ) in equation (1) (Jarvis et al, 1976; Eagleson et al., 1982; Rodriguez-Iturbe et al., 1999a; Laio et al., 2001a; Daly et al., 2003). Laio et al. (2001a) used a piecewise continuous function (Figure 1B) accounting for soil moisture controls both on transpiration and soil evaporation

$$f(\theta)=\begin{cases} 1 & (\theta^* < \theta < n) \\ \dfrac{\theta-\theta_w}{\theta^*-\theta_w}\left(1-\dfrac{E_{evap}}{E_p}\right)+\dfrac{E_{evap}}{E_p} & (\theta_w < \theta < \theta^*) \\ \dfrac{E_{evap}}{E_p}\dfrac{\theta-\theta_h}{\theta_w-\theta_h} & (\theta_h < \theta < \theta_w) \\ 0 & (0 < \theta < \theta_h) \end{cases}, \qquad (4)$$

with n being the soil porosity and E_{evap} soil evaporation. This model assumes that no soil evaporation occurs below the hygroscopic point, τ_{h}, and that for $\tau_{\mathrm{h}} < \tau < \tau_{\mathrm{w}}$ soil moisture losses are due only to soil evaporation. Equation (4) will be applied in Sections 4 and 5 to as the evapotranspiration components of a stochastic model of soil moisture.

This section has discussed only possible parameterizations of the effect of soil moisture on the rate of evapotranspiration through stomata regulation. However, the physiological mechanisms controlling stomatal conductance and plant water relations in arid and semiarid ecosystems are more complex (see Chapter 4) and involve a number of other environmental and physiological variables. Plants may close their stomata not only to reduce the transpiration rates in water stress conditions, but also to control the assimilation rates in response to changes is light, enzyme, and CO_2 concentrations (Farquar et al., 1980). Equations (1) and (4) fail to account for the biochemical control on stomatal conductance. On the other hand, commonly used photosynthesis models (e.g., Ball et al., 1987; Collatz et al., 1991) do not account for soil moisture limitations. A unifying, process-based modelling framework can be found in Daly et al. (2003) and Katul et al. (2003), while more empirical approaches - frequently implemented in land surface models (e.g., Xue et al., 1996) - use Jarvis' (1976) formulation to account both for plant hydraulics and biochemical controls on stomatal conductance.

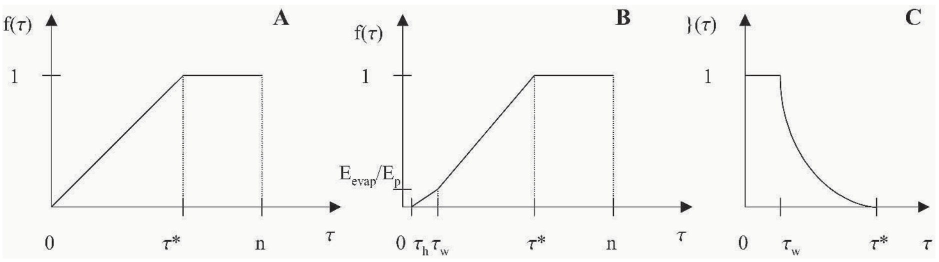

Figure 1. Dependence of evapotranspiration on soil moisture according (A) the Thorntwaite-Budyko model, and (B) the model by Laio et al. (2001a). The (static) stress function (equation (5), Porporato et al., 2001).

3.1.1. Water Stress in Vegetation

The soil moisture levels τ^* and τ_w are indicative of conditions of incipient and severe vegetation water stress, respectively. Thus, models of soil moisture dynamics have been used (e.g., Rodriguez-Iturbe et al., 1999b,c) to determine the impact of different climate, soil and vegetation characteristics on plant water stress. A water stress function, }, was suggested by Rodriguez-Iturbe et al. (1999b) to quantify this impact (Figure 1C). Plants are assumed to be unstressed when soil moisture exceeds τ^*, while the stress is maximum at the wilting point

$$\zeta(\theta) = \left(\frac{\theta^* - \theta}{\theta^* - \theta_w} \right)^q \qquad (\theta < \theta^*) \ , \tag{5}$$

and}(τ)=0 when $\tau > \tau^*$. A similar formulation was suggested by Sellers et al. (1986) in terms of leaf water potential. The exponent q in equation (5) accounts for the non linear response of vegetation to water deficit. Chapter 4 provides more details on the non-linear physiological processes controlling vegetation response to water deficit. Equation (5), expressing the stress level associated with a certain moisture content, τ, has been defined as "static stress" (Porporato et al., 2001) because it does not provide any information on the overall effect of the temporal dynamics of soil moisture on vegetation. Section 4.1.2 will discuss a stochastic approach to account for the frequency, duration, and intensity of water stress, based on a definition of a suitable "dynamic stress".

3.2. INFILTRATION AND RUNOFF

Infiltration is the water flux from the surface into the ground. It depends on rainfall rates and soil hydraulic properties, and can be calculated as $I=-q(z=0)$, with q given by equation (3) for $z=0$. As water infiltrates into the ground, surface soil moisture increases, leading to changes both in hydraulic conductivity and in water potential gradients. If the rainfall rate is greater than the saturated hydraulic conductivity, after some time the surface soil layer reaches saturation, water potential gradients at the surface tend to zero, and the maximum infiltration rate – known as infiltration capacity, I_c – tends to the saturated hydraulic conductivity, K_s (see equation (3)). Thus, the soil infiltration capacity decreases with time and tends asymptotically to K_s (Figure 2, white square boxes). I_c can be calculated with a number of analytical models as a function of the soil hydraulic properties (Green and Ampt 1911; Philip, 1957; 1969; Smith and Parlange 1978; See also Eagleson, 2002, p.176, and Smith et al., 2002, for a review).

Thus, if the rainfall rate exceeds the infiltration capacity, once the surface layer reaches saturation, infiltration is equal to I_c, and the rainfall excess generates runoff. This mechanism of runoff production is known as "Hortonian runoff" or "infiltration excess runoff" (Horton, 1933). Conversely, if the soil surface is fairly permeable and the rainfall is less than K_s, the precipitation rate is smaller than the infiltration capacity and no infiltration-excess runoff is generated. However, when a relatively shallow soil is underlain by an impervious surface (e.g., a bedrock, a clay layer, or the water table), only a limited amount of water can be stored in the soil and runoff may be generated by "saturation excess" (Dunne and Black, 1970; Dunne, 1978). While Hortonian runoff is observed in watersheds with low soil infiltration capacity, saturation-excess is typical of areas with limited soil storage capacity.

In a review of a number of case studies around the world, Dunne (1978) concluded that Hortonian runoff is typical of some arid and semiarid regions with thin vegetation cover, and of catchments disturbed by overgrazing or agriculture. Conversely, in regions with relatively dense vegetation saturation-excess is the dominant mechanism of runoff generation. Subsequent studies have confirmed that vegetation density plays an important role in determining the dominant mechanism of surface runoff production. Casenave and Valentin (1992) studied the ability of soils to generate infiltration-excess surface runoff and classified a number of tropical soils on the basis of vegetation cover, surface crusting, and other soil hydraulic properties. As expected, runoff was found to increase with decreasing vegetation densities and in the presence of soil crusting. Field studies have also shown that, due to the strong spatial heterogeneity of soil surface characteristics, the spatial patterns of overland flow are in general not uniform. Moreover, in areas with poor drainage networks, surface runoff collects into pools or "water holes", contributing to the spatial heterogeneity of surface moisture.

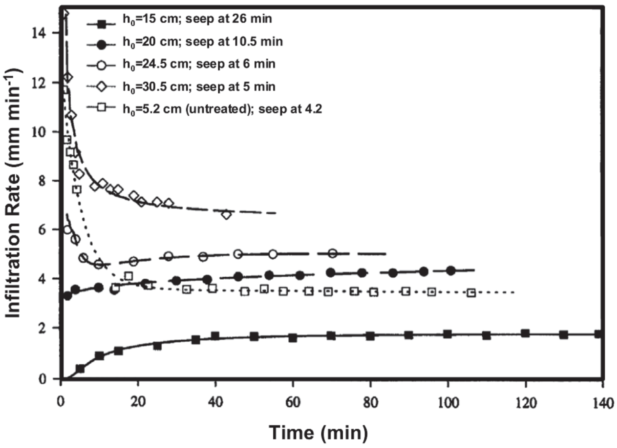

Figure 2. Infiltration rate as a function of time for untreated soils (white square boxes) and for soils treated with hydrophobic substances (see Section 3.3 for more details on hydrophobicity). The water-entry pressure head of the hydrophobic soil was h_p=| $_p$/γ_w=8.4 *cm and different depths,* h_0, *of ponding water were used. Taken from Letey (2001), published with permission from John Wiley & Sons* (©*John Wiley & Sons*).

3.3. EFFECTS OF DISTURBANCES ON INFILTRATION AND RUNOFF

3.3.1. The effect of logging and wood harvesting

A number of studies on watersheds around the world have shown how the removal of vegetation increases the water yield. Bosch and Hewlett (1982) reviewed 94 catchment studies on the effect of deforestation and forest harvesting on surface runoff: the removal of forest vegetation was found to consistently increase runoff, due to the loss of soil infiltration capacity and to the lower fraction of annual precipitation evapotranspired by vegetation (soil evaporation is usually smaller than plant transpiration). The effects of forest harvesting on runoff tend to last for several years in semiarid environments, due to the slow rates of forest regeneration. Both the plantation of commercial timber vegetation (afforestation) and the natural regrowth of forests after clearcut (reforestation) have effects that are opposite to deforestation: soil infiltration capacity increases due to the growth of roots and forest floor (see Table 2). Moreover evapotranspiration increases, due to canopy and litter interception, and to the ability of trees to tap deeper water.

The effect of savanna, grassland, and shrubland vegetation on infiltration and runoff has also been studied by several authors (e.g., Mainguet, 1999) who showed how vegetation removal resulting from overgrazing and poor land management decreases soil infiltration capacity and increases soil erosion.

Table 2: Infiltration capacity with different vegetation covers (data from Lull, 1964).

Surface cover	**I_c (mm h^{-1})**
Undisturbed forest floor	60
Forest floor without litter and humus	49
Yearly burned forest floor	40
Pasture	29

3.3.2. The impact of fires

The effect of fires on infiltration (Table 2), runoff, and water yield has important hydrologic implications (Krammer and DeBano, 1965). The post-fire increase in runoff and soil erosion was initially attributed to loss of infiltration capacity due to rainsplash and soil compaction. In addition, fires were believed to decrease surface soil permeability by clogging the soil pores with ashy particles (DeBano, 2000). Krammer and DeBano (1965) and DeBano (1966) showed that the decrease in infiltration capacity subsequent to fire is in large part associated with water repellency developed by the fire at the soil surface or at shallow depths. Organic compounds of chaparral and other vegetation types are volatilized by the fire and transported downwards into the soil by the strong temperature gradients existing through the soil profile. These gases condensate at a certain depth (of only a few centimeters), developing a hydrophopic coating around the soil particles (e.g., DeBano, 2000). This effect depends on the fire regime (Chapter 16), in particular on fire temperature, as repellency is observed (e.g., DeBano, 2000; Doerr et al., 2000) to develop neither with relatively low (e.g., $T<175\ ^{o}$C) nor with high temperatures ($T>300\ ^{o}$C). The organic compounds released by the fire affect the physical-chemical properties of the grain surfaces: in particular, the contact angle, ϖ, formed by the air-water interface with the soil grains becomes greater than 90^{o}, causing a positive capillary pressure head, $|_{p}$, in correspondence to the hydrophobic layer[1] (e.g., Letey, 2001). Thus a water drop reaching a water repellent surface is not drawn into that surface but sets on it. However, after some time water infiltrates through the hydrophobic layer, presumably due to a decay of the organic coating of the soil grains. This explains (see equation (3)) why in the presence of soil hydrophobicity infiltration capacity increases through time (Figure 2), while in wettable soils (section 2.1) both theory and observations suggest a decrease in infiltration capacity (Letey, 2001).

Thus, fire occurrences have important ecohydrological implications because the increase in runoff an of the associated erosion of the soil surface redistribute water and nutrients (e.g., Schlesinger et al., 1990) while the heterogeneity of burnt areas partly contributes to the emergence of patchy patterns of vegetation. A more thorough analysis of vegetation patterns and fire regimes can be found in Chapters 15 and 16.

3.4. VERTICAL REDISTRIBUTION OF SOIL MOISTURE BY TREE ROOTS

The physiological processes controlling water flow through the soil-plant-atmosphere continuum described in Chapter 4 suggest that transpiration is the main process of water loss by vegetation. However, some evidence exists that at night, when the stomata are closed, the root system may offer a preferential pathway for water flow through the soil column and contribute to the transfer of moisture between different soil layers (Burgess et al., 1998). For example, in rainless periods - when most of the root-zone soil moisture is concentrated in deep soil layers - roots may transfer water from the deep soil and release it in the dry shallow layers. Known as “hydraulic lift” (Richards and Caldwell, 1987), this effect is driven by water potential gradients between different parts of the soil profile. The occurrence of hydraulic lift has been documented for a number of different species and ecosystems (Caldwell et al., 1998, Richards and Caldwell, 1987; Burgess et. al., 1998; Horton and Hart, 1998; Ludwig et. al., 2002). The ecohydrological significance of this phenomenon in arid and semiarid ecosystems is due to its positive impact on neighboring shallow rooted species, as well as to the possible enhancement of plant nutrient uptake from nutrient-rich shallow soil layers (Caldwell and Richards, 1989; Dawson, 1993).

The opposite process has been also observed: soon after rain, when the soil surface is moister than the deep soil, night-time downward fluxes (probably due to soil water potential gradients) can occur through the root system of some species (Burgess et al., 1998; Schulze et al.,

---

[1] In fact, using the pore-capillary tube analogy, the water-entry pressure in the capillary tube is $|_{p}=-2\varphi\cos\varpi/(r\upsilon g)$, with φ being the surface tension of water, r the capillary tube radius, υ the water density, and g the gravitational acceleration.

1998; Smith et al, 1999). By means of this "reverse flow" (or "downward siphoning") trees and shrubs can subtract water and nutrients from the reach of shallow-rooted species.

4. Simplified models of soil moisture dynamics

One of the simplest models of soil water balance considers only one layer of soil (e.g., Budyko, 1958) and provides estimates of depth-average soil moisture through the equation (e.g., Rodriguez-Iturbe et al., 1999a)

$$Z_r \frac{d\theta}{dt} = I(\theta, t) - E(\theta) - L(\theta) \cdot \tag{6}$$

with Z_r being the depth of the root zone, I the rainfall infiltration, E the rate of evapotranspiration, and L the rate of drainage at the bottom of the soil layer. Rainfall infiltration is generally assumed to occur instantaneously and to be limited only by soil storage capacity. Thus, rainfall infiltration is equal either to the storm depth or to the soil storage capacity, $(n\text{-}\tau)Z_r$, whichever is less. Losses of water from the control volume are due to evapotranspiration and deep drainage. Evapotranspiration is generally calculated with equation (1), with a suitable function, $f(\tau)$, expressing the effect of soil moisture limitation (e.g., equation (4)). Drainage losses, $L(\tau)$, are assumed to be zero when soil moisture is below the so-called field capacity, τ_{fc}, representing the maximum moisture content at which water can be retained within the ground against gravity drainage. When $\tau > \tau_{fc}$ $L(\tau)$ can be expressed as equal to the (unsaturated) hydraulic conductivity, which in turn is a function of soil moisture (Chapter 2). For instance the following function has been used by Laio et al. (2001a)

$$L(\theta) = \frac{K_s}{e^{\frac{\beta}{n}(n-\theta_{fc})} - 1} \left[e^{\frac{\beta}{n}(\theta-\theta_{fc})} - 1 \right] \qquad (\theta_{fc} < \theta \leq n) \tag{7}$$

with K_s being the saturated hydraulic conductivity and ϵ a parameter depending on soil texture.

This model, sometimes referred to as "bucket model", has been widely used to determine surface boundary conditions in atmospheric models (Budyko, 1958), to study the feedbacks between the soil surface and the near-surface atmosphere (e.g., Rodriguez-Iturbe et al., 1991; 1998; Porporato et al., 2000; D'Odorico and Porporato, 2004), as well as in ecohydrological models of plant available water at the daily time scale (Rodriguez-Iturbe et al., 1999a,b,c).

The main limitation of this model is due to the use of only one soil layer. This approach does not allow for a calculation of the time needed by water to infiltrate to relatively deep soil layers and could lead to unrealistic soil moisture estimates at subdaily time scales. However, the comparison with the results of a more complex model based on the integration of Richards equation (1931) has shown (Guswa et al. (2002)) that that the two models provide similar results at the daily time scale. This is particularly true when roots are assumed to be able to extract more water from wet portions of the root zone to compensate for the lower uptake from the drier parts of the soil column. In some cases the single-layer ("bucket") model has been modified by adding multiple layers. A simplified multilayer model of the water balance uses equation (1) for each layer, considering as main moisture input to the lower layers the drainage from the overlying soil (Parton et al., 1998). Studies at relatively short (subdaily) time scales or in deep soils still require the numerical integration of Richards' (1931) equation through the soil profile (see Chapter 2).

4.1. A STOCHASTIC APPROACH

4.1.1. Probability distribution of soil moisture

In many ecohydrological applications the intermittent and unpredictable stochastic nature of rainfall occurrences and amounts suggests using a probabilistic approach in the modeling and characterization of precipitation and soil moisture regimes (Eagleson, 1978b). While several stochastic models of precipitation have been developed in the last few decades (e.g., Todorovic and Woolhiser, 1975; Eagleson, 1978a), the stochastic modeling of soil moisture is much more recent and, to date, only a few probabilistic models of soil water dynamics have been studied in detail, providing analytical solutions of the stochastic soil water balance equation (Rodriguez-Iturbe et al., 1999a; Laio et al. 2001a). These models use the simplified framework described in Section 3, where the soil water balance is expressed by equation (6). Losses due to evapotranspiration and drainage are modeled as deterministic functions of soil moisture (i.e., equations (4) and (7), respectively), while precipitation is expressed as a sequence of Poissonian occurrences of rate (e.g., Eagleson et al., 1978a), with each rainfall event having a random depth with exponential distribution of mean δ. Thus the rainfall regime is characterized by the two parameters, o and δ, representing the average storm frequency and depth. Eagleson (2002) calculated these parameters for a number of locations across the continental U.S. The decomposition of the rainfall regime into a sequence of storm events separated by intersorm periods is of foremost importance to the modeling of soil moisture because the timescales of variability of the soil water content are in general of only a few days, depending on depth, soil texture, and climate. Moreover the effect of climate change on the rainfall regime can be manifested (e.g., Knapp et al., 2002) either in changes in the number of storms occurring during the rainy season (i.e., of o) or in the their size (i.e., of δ). The effect of these changes on the soil water balance in dryland ecosystems is discussed in Section 4.1.3.

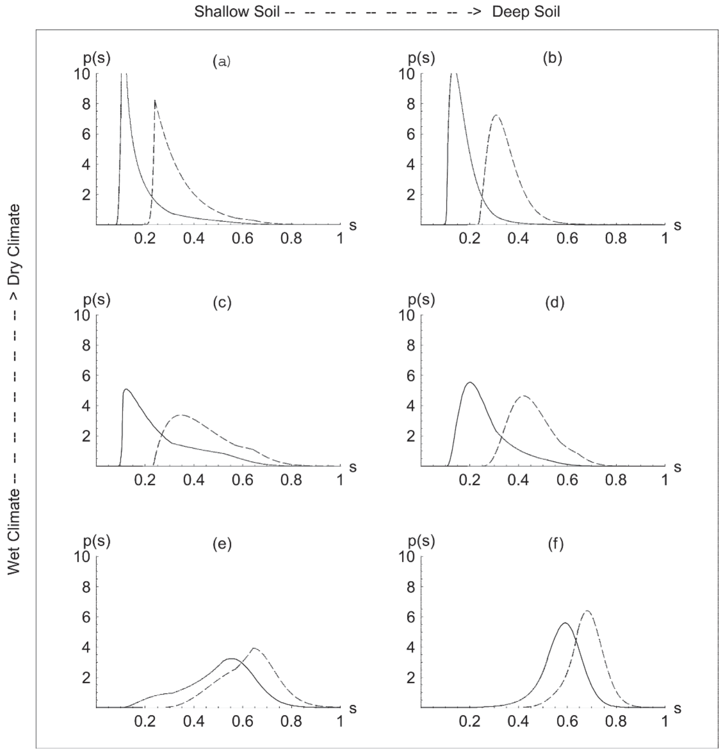

Figure 3. Examples of pdf's of soil moisture for different type of soil, soil depth, and mean rainfall rate. Continuous lines refer to loamy sand, dashed lines to loam. Left panels correspond to rooting depth of 30 cm, right panel to 90 cm. Top, center, and bottom graphs have a mean rainfall rate λ of 0.1, 0.2, and 0.5 d^{-1} respectively. Common parameters to all graphs are α=1.5 cm, and E_{max}=0.45 cm/d. After Laio et al. (2001).

The stochastic soil water balance studied by Rodriguez-Iturbe et al. (1999a) and Laio et al. (2001a) assumes that evapotranspiration changes are due only to soil moisture fluctuations, while E_p and E_{evap} are constant. This assumption is plausible for a fairly steady summer season, as long as equation (6) is considered at daily (or longer) time scales and diurnal fluctuations in potential evapotranspiration are ingored.

When rainfall infiltration is modeled as a stochastic process, equation (6) becomes a stochastic differential equation and its solution provides the probability density function of soil moisture as a function of rainfall, vegetation and soil parameters. Analytical solutions of the stochastic soil water balance equations were determined by Milly (1993; 2001), Rodriguez-Iturbe et al. (1999a), and Laio et al. (2001a). Figure 3 shows an example of probability distributions of relative soil moisture, s ($s=\tau/n$), for different soil and precipitation parameters. As the rainfall parameters, o (average storm frequency) and δ (average storm depth), increase, the probability distribution of soil moisture shifts towards wetter conditions. Moreover, coarser soils are consistently found to be drier than fine-texture soils, while the soil depth is found to affect the variance of soil moisture fluctuations, with the shallow soils having broader probability distributions of soil moisture. Information on the probability distribution of soil moisture is of foremost importance in ecohydrology, in that it allows, for instance, the estimation of the probability that vegetation is under stress during the growing season, as discussed in the following sections.

4.1.2. Duration and frequency of water stress in vegetation

The probabilistic framework presented in Section 4.1 has been used to calculate the level-crossing statistics of soil moisture. In particular, analytical expressions have been obtained to calculate (Ridolfi et al., 2000a; Porporato et al., 2001) the average duration and frequency of temporal intervals in which soil moisture is below a given critical level. In particular, these statistics were studied with respect to soil moisture levels of incipient (τ^*) and severe water stress (τ_{w}) and interesting non-linearities were found in the dependence on soil climate, and vegetation parameters.

These results were used by Porporato et al. (2001) to characterize the stress conditions associated with different regimes of soil moisture: a "dynamical water stress" function was defined as an indicator of the overall stress of vegetation throughout the growing season

$$\overline{\chi} = \begin{cases} \left(\dfrac{\overline{\zeta}'\overline{T}_{\theta*}}{kT_{seas}} \right)^{1/\sqrt{n_{\theta*}}} & \mathit{if} \quad \overline{\zeta}'\overline{T}_{\theta*} < kT_{seas} \\ 1 \quad \mathit{otherwise} \end{cases} \tag{8}$$

where T_{seas} is the growing season length, $\overline{T}_{\theta*}$, is the average length of an excursion below τ^*, $\mathrm{n}_{\tau*}$ is the number of intervals with $\tau<\tau^*$, and $\overline{\zeta'}$ is the average value of the static stress, }, (equation (5)) conditioned to } being greater than zero. The theoretical considerations justifying this formulation of the stress function can be found in Porporato et al. (2001) along with the analytical expressions of the dynamical stress as a function of plant, soil, and rainfall parameters. An example of the application of plant dynamic stress is presented in the following section.

4.1.3. The inverse texture effect.

The framework presented in the previous sections allows for the investigation of the effect of soil properties and rainfall regime on vegetation water stress. In particular, Laio et al. (2001b), used the concept of dynamic water stress to study the suitability of different soil textures to the growth of vegetation under different rainfall regimes. This approach allowed these authors to explain the "inverse soil texture effect" introduced by Noy-Meir (1973, p. 37), that "the same vegetation can occur at lower rainfall on coarse soils than it does on fine ones. The balance point between the advantage of coarser texture and its disadvantage occurs somewhere between 300 and 500 mm rainfall". Thus different combinations of climate and soil properties can lead to similar soil moisture regimes and explain the existence of the same vegetation with lower seasonal precipitation on coarser soils.

As an example of the inverse texture effect Laio et al (2001b) applied their stochastic soil moisture and water stress models to the shortgrass steppe in north-central Colorado. The recruitment patterns of *Bouteloua gracilis*, the dominant species in this steppe, is significantly affected by soil texture (Lauenroth et al., 1994). The dynamic water stress, $\overline{\chi}$, was used to express the combined effect on vegetation of static stress, and duration and frequency of water stress periods. Figure 4 shows the dynamic stress calculated for different combinations of soil textures in the USDA soil texture triangle. In the case of figure 4a the climate is relatively dry and the lowest stress is associated with coarse textures, suggesting a better fitness of *B. gracilis* on sandy soils. Conversely, in the case of a relatively wet climate, the same shortgrass would perform better in a fine soil. Laio et al. (2001b) showed also that in this area the point at which coarse soils become better than fine soils corresponds to an annual rainfall of about 370 mm, in agreement with the range of values indicated by Noy-Meir (1973). A similar study was proposed by Fernandez-Illescas et al. (2001) for different combinations of rainfall and vegetation conditions in savannas sites in southern Texas.

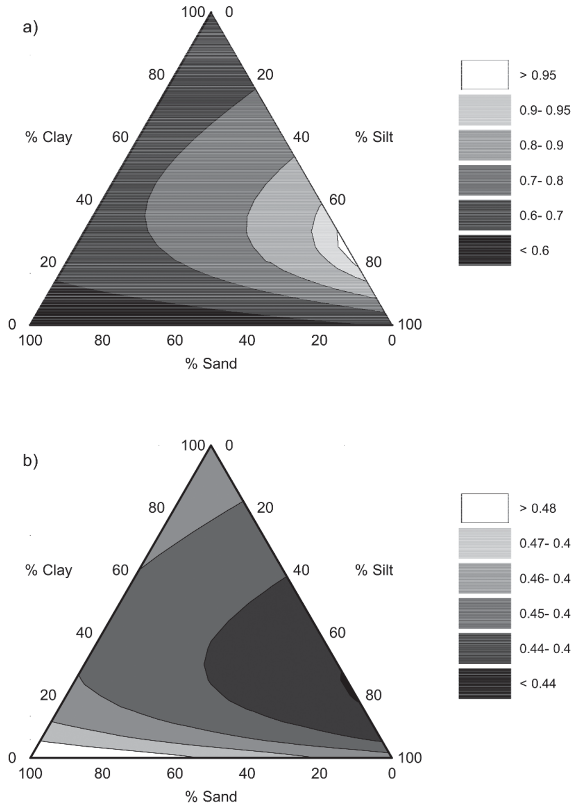

Figure 4. Dynamic water stress on the soil texture triangle for Bouteloua gracilis (a) under a relatively dry climate, α*=0.576 cm and* λ*=0.17* d^{-1}*; and (b) under a relatively wet climate,* α*=0.674 cm and* λ*=0.28* d^{-1}*. After Laio et al. (2001).*

4.1.4. The effect of interannual climate fluctuations

Climate variability affects terrestrial vegetation both through changes in temperature and rainfall regimes. In the case of arid and semiarid ecosystems in warm regions, changes in rainfall patterns are expected to have the most important effects on vegetation. These effects can be quantified by studying how soil moisture dynamics would change under different rainfall scenarios. This type of analysis was carried out by Rodriguez-Iturbe et al. (1999a) and Laio et al. (2001a) in a sensitivity analysis of their models with respect to the rainfall parameters (Figure 3).

However, the assessment of the effect of interannual climate fluctuations on vegetation is a different problem. In addition to the effect of daily hydrologic fluctuations, arid and semiarid regions are also characterized by strong year-to-year rainfall variability (Chapter 1), due anomalies in the large-scale atmospheric circulation. For example, in these regions differences in only a few rainstorm occurrences in course of the rainy season may significantly affect the total annual rainfall. D'Odorico et al. (2000) and Ridolfi et al. (2000b) studied the effect of climate fluctuations on average soil moisture, $\iota\,\theta\,|$ (or $\iota\,s\,|$), as well as on the duration, $T_{\tau*}$, and number, $n_{\tau*}$, of water stress periods during the growing season. Interannual fluctuations of the rainfall regime were modeled as fluctuations in the rainfall parameters, o (average storm frequency), and δ (average storm depth), in the stochastic soil moisture model of Section 4.1.1. Thus, o and δ were treated as random variables and their distributions were determined through the analysis of several decades of daily precipitation records (e.g., Figure 5). Each growing season was characterized by different rainfall parameters sampled from these distributions and the soil moisture statistics ($\iota\,\theta\,|$, $T_{\tau*}$, and $N_{\tau*}$) were calculated. The probability distributions of average seasonal soil moisture, stress duration and frequency were then calculated as derived probability density functions of the distributions of o and δ.

With this framework it was possible to address the important question of whether the non-linearities embedded in the soil moisture dynamics would enhance or damp fluctuations in the rainfall regime. By comparing the coefficient of variation (standard deviation/mean) of $T_{\tau*}$ with those of o and δ, Ridolfi et al. (2000b) were able to show that in most cases these nonlinearities enhance the interannual fluctuation of water stress, and hence the effect of disturbance exerted by climate fluctuations on arid and semiarid ecosystems.

The probability distributions of average seasonal soil moisture were calculated by D'Odorico et al. (2000) for different soil types and rainfall fluctuation parameters. Figure 6 shows an example of probability distribution or average seasonal soil moisture (in terms of relative soil moisture, $s = \theta/n$): a well defined bimodality exists with relatively strong rainfall fluctuations, while it disappears when the fluctuations become weaker. Thus, for some values of the coefficient of variation of o and δ, these distributions may exhibit bimodal behavior, suggesting that the system tends to select two preferential states and to switch between them due to the interannual fluctuations in rainfall parameters. The two preferential states correspond to "dry" and "wet" average seasonal soil moisture conditions. The implications of the emergence of bimodal behavior is of foremost importance for ecosystem dynamics because it implies that the system is more likely to be found in two states that are far form the long-term average, while the long-term average conditions occur with the lowest probability. Moreover, the bimodal behavior enhances the likelihood of occurrence of dry conditions and the effect of disturbance of climate fluctuations on terrestrial ecosystems.

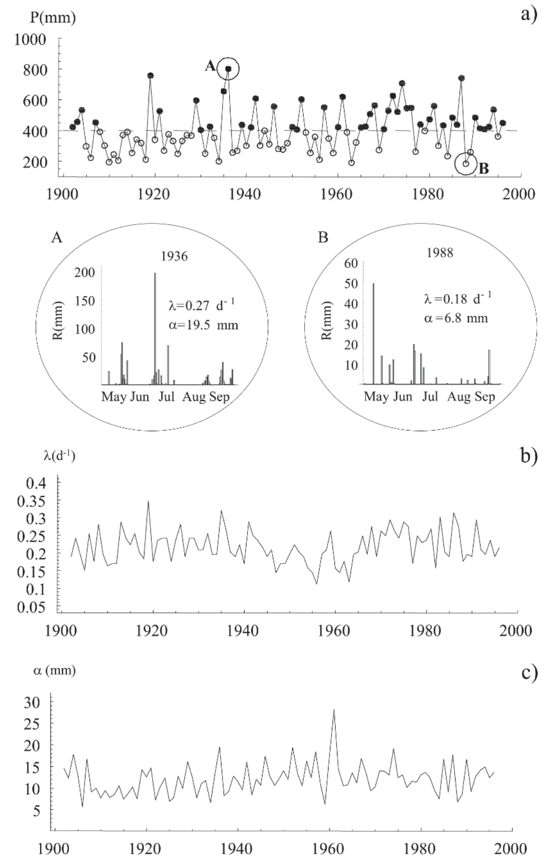

Figure 5. Analysis of the rainfall regime during the growing season at Luling (Texas) based on daily precipitation data: (a) time series of total seasonal rain (May 1^{st}-Sept. 30^{th}. (b) Time series of the estimated rate of storm arrivals, λ. (c) Time series of the average storm depth, α. After D'Odorico et al. (2000a).

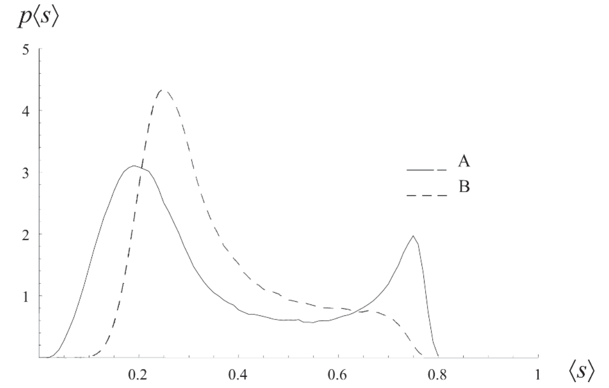

Figure 6. Probability density function of the average soil moisture during the growing season. The parameters for soil and vegetation are as follows: n=0.43; Z_r=1.40 m; K_s=9.5 10^{-6} m/s; s_1=0.8; s^*=0.36; E_{max}=3.2 mm/day. The rainfall is characterized by $\langle\alpha\rangle$=12.4 mm/storm and $\langle\lambda\rangle$=0.21 d^{-1}, with coefficients of variation: (A) $CV[\alpha]$=0.45; $CV[\lambda]$=0.23. (B) $CV[\alpha]$=0.22; $CV[\lambda]$=0.11. After D'Odorico et al. (2000).

5. Acknowledgements

This research was funded by NSF (grants #EAR-0236621 and # EAR-0409305), DOE-NIGEC (Great Plains Regional Center, grant #DE-FC-02-03ER63613), USDA (Cooperative Agreement #2002-35102-11585), and NASA (grant #NNG-04-GM71G).

6. References

Baldocchi, D., and T. Meyers, (1998). On using eco-physiological, micrometeorological and biogeochemical theory to evaluate carbon dioxide, water vapor and trace gas fluxes over vegetation: a perspective. Agric. For. Meteorol., 90(1-2), 1-25.

Ball, J.T., Woodrow, I.E., Berry, J.A. (1987). A model predicting stomatal conductance and its contribution to the control of photosynthesis under different environmental conditions. In J. Biggins (Ed.), Progress in Photosynthesis Research, Martinus-Nijhoff Publishers, Dordrecht, The Netherlands, pp. 221-224.

Bosch, J. M., and J. D. Hewlett (1982). A review of catchment experiments to determine the effect of vegetation changes in water yield and evapotranspiration, J. Hydrol. 55, 3-23.

Budyko, M.I. (1958). Heat balance of the earth's surface. U.S. Weather Bureau, Washington, D.C.

Burgess, S.S.O., Adams, M.A., Turner, N.C., Ong, C.K. (1998). The redistribution of soil water by tree roots, Oecologia, 115, 306-311.

Caldwell, M.M. and J.H. Richards (1989). Hydraulic lift water efflux from upper roots improves effectiveness of water uptake by deep roots, Oecologia, 79, 1-5.

Caldwell, M.M., T.E. Dawson, and J.H. Richards (1998). Hydraulic lift: consequences of water efflux from the roots of plants. Oecologia, 131, 151-161.

CasenaveA. and C. Valentin (1992). A runoff capability classification system based on surface feature criteria in semiarid areas of West Africa, J. Hydrol., 130, 231-249.

Chen, J. (1984). Uncoupled multi-layer model for transfer of latent and sensible heat flux densities from vegetation, Boundary Layer Meteorol., 28, 213-225.

Collatz, G.J., Ball, J.T., Grivet C., Berry J.A. (1991). Physiological and environmental regulation of stomatal conductance, photosynthesis and transpiration: a model that includes a laminar boundary layer, Agric. For. Meteorol. 54, 107-136.

Daamen, C.C. and L.P. Simmonds (1994). Soil, water, energy, and transpiration – a numerical modelof water and energy fluxes in soil profiles and sparse canopies, Department of Soil Science, University of Reading.

Daamen, C.C. (1997). Two-source model of surface fluxes for millet fields in Niger, Agric. For. Meteorol., 83, 205-230.

Dawson, T.E. (1993). Water sources of plants determined from xylem-water isotopic composition: perspectives on plant competition, distribution, and water relations, in J.R. Ehleringer, A.E. Hall, and G.D. Farquhar, G.D. (Eds.) Stable Isotopes and Plant Carbon/Water Relations, Academic Press, pp. 465–496.

DeBano, L.F. (1966). Formation of non-wettable soils involves heat transfer mechanism, USDA Forest Service Research Note PSW-132, 8pp.

DeBano, L.F. (2000). The role of fire and soil heating on water repellency in wildland environments: a review, J. Hydrol., 231, 195-206.

Dickinson R.E., A. Henderson-Sellers, PJ Kennedy, MF Wilson (1986). Biosphere-atmosphere transfer scheme (BATS) for the NCAR community climate model. NCAR Technical Note TN-275 + STR, 69 pp.

D'Odorico, P., L. Ridolfi, A. Porporato and I. Rodriguez-Iturbe (2000). Preferential states of seasonal soil moisture: the impact of climate fluctuations, Water Resour. Res., 36(8). 2209-2219.

D'Odorico P., and A. Porporato (2004). Preferential states in soil moisture and climate dynamics. Proc. Natnl. Acad. Sci. U.S.A, 101: 8848-8851, 10.1073/pnas.0401428101.

Doerr, S.H., R.A. Shakesby, and R.P.D. Walsh (2000). Soil water repellency: its causes, characteristics and hydrogeomorphological significance, Earth Sci. Rev., 51, 33-65.

Dunne, T and R.D. Black (1970). An experimental investigation of runoff prediction in permeable soils, Water Resour. Res., 6(2), 478-490.

Dunne, T. (1978). Field studies of hillsope flow processes, in M.J. Kirkby (Ed.) Hillslope Hydrology, J. Wiley& Sons, New York, pp. 227-293.

Eagleson, PS. (1978a). Climate, soil, and vegetation: The distribution of annual precipitation derived from observed storm sequences, Water Resour. Res. 14(5), 713-721.

Eagleson, PS. (1978b). Climate, soil, and vegetation: A simplified model of soil moisture movement in the liquid phase, Water Resour. Res. 14(5), 722-731.

Eagleson, PS., (1982). Land surface processes in atmospheric general circulation models, Cambridge University Press, Cambridge, UK.

Evett, S.R. and R.J. Lascano (1993). ENWATBAL.BAS: a mechanistic evapotranspiration model written in compiled BASIC, Agron. J., 85(3), 763-772.

Farquhar, G.D., von Caemmerer S., Berry J.A. (1980). A biochemical model of photosynthetic CO_2 assimilation in leaves of C_3 species. Planta 149, 78-90.

Feddes R.A., H. Hoff, M. Bruen, T. Dawson, P. de Rosnay, P. Dirmeyer, R. B. Jackson, P. Kabat, A. Kleidon, A., Lilly, and A. J. Pitman (2001). Modeling root-water uptake in hydrological and climate models, Bull. Am. Met. Soc., 82(12), 2797-2809.

Fernandez-Illescas CP, A. Porporato, F. Laio, and I. Rodriguez-Iturbe (2001). The ecohydrological role of soil texture in a water-limited ecosystem, Water Resour. Res., 37 (12): 2863-2872.

Gao, Q., P. Zhao, X. Zeng, X. Cai, and W. Shen (2002). A model of stomatal conductance to quantify the relationship between leaf transpiration, microclimate and soil water stress, Plant, Cell and Environment, 25, 1373-1381.

Green W.H. and C.A. Ampt (1911). Studies on soil physics, I. The flow of water and air though soils. J. Agric. Sci., 4, 1-24.

Guswa, A.J., M.A. Celia, and I. Rodriguez-Iturbe (2002). Models of soil moisture dynamics in ecohydrology: A comparative study, Water Resour. Res., 38 (9): Art. No. 1166.

Hale, M. G. and D. M. Orchutt (1987). The Physiology of Plants Under Stress, J. Wiley & Sons, New York.

Hopmans, J.W., and K.L.Bristow (2002). Current capabilities and future needs of root and nutrient uptake modeling, Advances in Agronomy, 77, 104-175.

Horton, R.E. (1033). The role of infiltration in the hydrologic cycle, Trans. Am. Geophys. U., 14, 446-460.

Horton, J.L., S.C. Hart (1998). Hydraulic lift: a potentially important ecosystem process. Tree 13 (6), 232-235.

Jarvis, P.G. (1976). The interpretation of the variations in leaf water potentialand stomatal conductance found in canopies in the field, Phil. Trans. R. Soc. Lond. B 273, 593-610.

Jones, H.G. (1992). Plants and microclimate, Cambridge University Press, 428 pp., Cambridge.

Jones, C.A. and J.R. Kiniry (1986). CERES-Maize: A Simulation Model of Maize Growth and Development, Texas A&M University Press, 194 pp.

Knapp, A. K., P. A. Fay, J. M. Blair, S. L. Collins, M. D. Smith, J. D. Carlisle, C. W. Harper, B. T. Danner, M. S. Lett, and J. K. McCarron (2002). Rainfall variability, carbon cycling and plant species diversity in a mesic grassland, Science, 298, 2202-2205.

Katul, G.G., and M.B. Parlange (1992). A Penman-Brutsaert model for wet surface evaporation, Water. Resour. Res., 28(1), 121-126.

Katul, G.G., R. Leuning and R. Oren (2003). Relationship between plant hydraulic and biochemical properties derived from a steady-state coupled water and carbon transport model, Plant, Cell and Environment, 26, 339-350.

Krammers, J.S. and L.F. DeBano (1965). Soil wettability: a neglected factor in watershed management, Water Resour. Res., 1, 283-286.

Lai, C-T, and G. Katul (2000). The dynamic role of root-water uptake in coupling potential and actual transpiration, Adv. Water Resour., 23, 427-439.

Laio F., A. Porporato, L., Ridolfi, and I. Rodriguez-Iturbe (2001a). Plants in water-controlled ecosystems: Active role in hydrological processes and response to water stress: II Probabilistic soil moisture dynamics, Adv. Water Res., 24 (7), 707-723.

Laio F., A. Porporato, C. P., Fernandez-Illescas, and I. Rodriguez-Iturbe (2001b). Plants in water-controlled ecosystems: Active role in hydrological processes and response to water stress: IV Discussion of real cases, Adv. Water Res., 24 (7), 745-762.

Lauenroth, W.K., O.E. Sala, D.P. Coffin, and T.B. Kirchner (1994). The importance of soil water recruitment of Bouteloua gracilis in the shortgrass steppe, Ecol. Appl., 4(4), 741-749.

Letey, J. (2001). Causes and consequences of fire-induced soil water repellency, Hydrol. Process., 15, 2867-2875.

Linn, D.M., and J. W. Doran (1984). Effect of water-filled pore space on carbon dioxide and nitrous oxide production in tilled and nontilled soils, Soil Science Society of America Journal, 48, 1267–1272.

Ludwig, F., T.E. Dawson, H., Kroon, F., Berendse, and H. H. T., Prins, (2002). Hydraulic lift in Acacia tortolis trees on and East African savanna. Oecologia 134, 293-300.

Lull, H.W. (1964). Ecological and silvicultural aspects. In V.T. Chow (Ed.), Handbook of applied hydrology, McGraw-Hill, New York, pp. 1 (6) 6-30.

M. Mainguet and M. Mainquet (1999). Aridity: Droughts and Human Development, Springer.

Milly, P.C.D. (1993). An analytic solution of the stochastic storage problem applicable to soil water. Water Resour. Res., 29, 3755-3758.

Milly, P.C.D. (2001). A minimalist probabilistic description of root-zone soil water, Water Resour. Res., 37(3), 457-463.

Norman, J.M. (1979). Modelling the complete canopy crop. In B. Barfield and J. Gerber (Eds.), Modifications of the aerial environment of crops, ASAE, St. Joseph, MI, pp. 249-277.

Noy-Meir, I. (1973). Desert ecosystems: environment and producers, Ann. Rev. Ecol. Systemat., 4, 25-51.

Parton, W.L., M. Hartman, D., Ojima, and D. Schimel (1998). DAYCENT and its land surface submodel: description and testing, Global and Planetary Change, 19: 35-48.

Peugeot C.M. Eteves, S. Galle, J.L. Rajot, and J. P. Vandervaere (1997). Runoff generation processes: results and analysis of field data collected at the East Central Supersite of the HAPEX-Sahel experiment, J. Hydrol., 188-189, 179-202.

Philip, J. R. (1975). Numerical solution of equations of the diffusion type with diffusivity concentrationdependent. Austral. J. Phys., 10, 29-42.

Philip, J. R. (1969). Theory of infiltration. In V. T. Chow, Advances in hydroscience, 5: 215-296. Academic Press, New York.

Porporato, A., P. D'Odorico, L. Ridolfi, and I. Rodriguez-Iturbe (2000). A spatial model for soil-atmosphere interaction: Model construction and linear stability analysis. Journal of Hydrometeorology 1:61-74.

Porporato, A., F. Laio, L., Ridolfi, and I. Rodriguez-Iturbe (2001)., Plants in water-controlled ecosystems: Active role in hydrological processes and response to water stress. III: Vegetation water stress. Adv. Water Resour., 24: 725-744.

Porporato, A, P. D'Odorico, F., Laio, and I. Rodriguez-Iturbe (2003). Soil moisture controls on the nitrogen cycle I: Modeling scheme, Adv. Water Res., 26, 45-58.

Richards L.A. (1931). Capillary conduction of liquids through porous medium, Physics (1), 318-333.

Richards, J.H. and M.M. Caldwell (1987). Hydraulic lift: substantial nocturnal water transport between soil layers by Artemisia tridentata roots. Oecologia 73, 486–489.

Richter, H. (1976). The water status in plants: Experimental evidence. In O.L. Lage, L. Kappen, and E-D Schulze (Eds.), Water and Plant Life: Problems and Modern Approaches, Springer-Verlag Berlin.

Ridolfi, L., P. D’Odorico, A. Porporato and I. Rodriguez-Iturbe (2000a). Duration and frequency of water stress in vegetation: an analytical model, Water Resour. Res., 36(8), 2297-2307.

Ridolfi, L., P. D’Odorico, A. Porporato and I. Rodriguez-Iturbe (2000b). Impact of climate variability on the vegetation water stress, J. Geophys. Res. (Atmospheres), 105(D14), 18013-18025.

Rodriguez-Iturbe, I., D. Entekhabi, and R. L. Bras (1991). Nonlinear dynamics of soil moisture at climate scales: 1. Stochastic analysis. Water Resour. Res., 27(8): 1899-1906.

Rodriguez-Iturbe, I, P. D’Odorico and A. Rinaldo (1998). A possible self-organizing dynamics for land-atmosphere interactions, J. Geophys. Res., 103(D18), 23,071-23,077.

Rodriguez-Iturbe, I., A. Porporato, L., Ridolfi, V., Isham, and D.R. Cox (1999a). Water balance at a point: the role of climate, soil and vegetation. Proc. R. Soc. Lond. A, 455, 3789-3809.

Rodriguez-Iturbe, I, P. D’Odorico, A. Porporato and L. Ridolfi (1999b). Tree-Grass coexistence in savannas: the role of spatial dynamics and climate fluctuations, Geophys. Res. Lett., 26(2), 247-250.

Rodriguez-Iturbe, I., P. D’Odorico, A. Porporato and L. Ridolfi (1999c). On the spatial and temporal links between vegetation, climate and soil moisture, Water Resour. Res., 35(12), 3709-3722.

Schulze E.D., M.M. Caldwell, J. Canadell, H.A. Mooney, R.B. Jackson, D. Parson, R. Scholes, O.E. Sala, and P. Timborn (1998). Downward flux of water through roots (i.e. inverse hydraulic lift) in dry Kalahari sands, Oecologia, 115, 460-462.

Sellers, P.J., Y. Mintz, Y.C. Sud, and A. Delcher (1986). A simple biosphere model (SiB) for use with general circulation models, J Atmos. Sci., 43, 505-531.

Skopp, J., M.D. Jawson, and J.W. Doran (1990). Steady-state aerobic microbial activity as a function of soil water content, Soil Sci. Soc. Am. J., 54, 1619-1625.

Smith, J.A.C., and H. Griffiths (1993). Water deficits: plant responses from cell to community, Bios, Oxford.

Smith, D.M., N.A. Jackson, J.M. Roberts, and C.K. Ong (1999). Reverse flow of sap in tree roots and downward siphoning of water by Grevillea robusta, Functional Ecology 12, 256-264.

Smith, R.E. and J-Y Parlange (1978). A parameter-efficient hydrologic infiltration model, Water Resour. Res., 14(3), 533-538.

Smith R.E., K.R.J. Smettem, P. Broadbridge, and D.A. Woolhiser (2002). Infiltration Theory for hydrologic applications, American Geophysical Union, Washington, D.C.

Thornthwaite, C. W., and J. R. Mather (1955). The water balance. In: Publications in Climatology, Drexel Institute of Technology, 8(1), 1-104.

Todorovic, P. and D.A. Woolhiser (1975). A stochastic model of n-day precipitation, J. Appl. Meteorol., 14, 17-24.

Xue, Y., P.J. Sellers, J.L. Kinter, and J. Shukla (1991). A simplified biosphere model for global climate studies, J. Clim., 4, 345-364.

Xue, Y., F.J. Zeng, and C.A. Schlosser (1996). SSib and its sensitivity to soil properties – a case study using HAPEX-Mobilhi data, Global and Planetary Change., 13, 183-194.

Chapter 4

ECOPHYSIOLOGY OF PLANTS IN DRY ENVIRONMENTS

Leonardo LOMBARDINI

Department of Horticultural Sciences, Texas A&M University, TAMU 2133, College Station, TX 77843, USA - e-mail: l-lombardini@tamu.edu

1. Introduction

Drought is a meteorological term which indicates a long period when there is not enough rain for the successful growing of crops or replenishment of water supplies. The expression *water stress* is frequently used to indicate the complex series of effects that are triggered in plants by drought. The term *drought stress* is more appropriate to specify when the stress status occurs only over a long period of time. However, because it is often difficult to separate the two phenomena, the definitions of water stress, drought stress and water deficit are frequently used interchangeably. Drought leads to water deficit in the soil and plant tissues, which in turn alters physiological processes and can have ultimate consequences for growth, development and survival of plants. Among the many biochemical and developmental processes that are affected by water stress, decrease of photosynthesis (Bradford and Hsiao, 1982; Flore and Lakso, 1989; Hsiao, 1973), changes in water relations (Brough et al., 1986; Olien and Lakso, 1986), reduction of both cell division and expansion (Hsiao and Acevedo, 1974), abscisic acid (ABA) synthesis (Davies and Zhang, 1991; Zeevaart and Creelman, 1988), and accumulation of sugars (Wang et al., 1995; Wang and Stutte, 1992) play a fundamental role in reducing productivity.

The concept of stress cannot be separated from that of *stress tolerance* (sometimes indicated with the less appropriate term of *stress resistance*), which is the plant's ability to survive in an unfavorable environment. Such ability can derive either from *adaptation* or *acclimation* to the stress condition. Both terms indicate an increase in tolerance and are sometimes erroneously used interchangeably. The difference is in the cause of the increased tolerance: in acclimated plants it is the result of a previous stress condition, while in adapted plants the tolerance is fixed in the genome and arises from selection processes that have occurred over many generations.

On the basis of their mechanisms of adaptation to soil water availability and their water requirements, plants are classified into three general groups. *Hydrophytes* require abundant water supply and flourish where water is almost always present. *Mesophytes* are plants adapted to moist, well-drained conditions (such as most crop plants), whereas *xerophytes* can survive prolonged dry soil conditions. Xerophytes are divided into three categories, *drought avoiders* (ephemerals), *drought resistors* and *drought endurers*. Drought avoiders are annual plants that complete their life cycle during wet periods and survive the dry season as seeds. Usually they are small in size, have high root to shoot ratios and do not need to develop morphological or anatomical adaptations to drought. Drought resistors avoid drought, either by using water conservatively and saving most of the water absorbed by the roots (*water savers*), or by developing structures/mechanisms that allow the uptake of considerable amounts of water and maintain high transpiration rates (*water spenders*). Examples of water savers are succulent plants, such as cacti and agave, which store large volumes of water in fleshy organs (leaves, stem, and roots). These plants have developed numerous adaptations to reduce water loss such as thick cuticles, small leaf size, leaf hairs, sunken stomata, etc. palms and mesquite trees (*Prosopis* sp.) are examples of water spenders, because they use considerable amounts of water. Such water amounts are supplied by the deep or widespread roots, which allow them to explore large volumes of soils. *Drought endurers* are those plants that, due to a series of adaptive mechanisms, can tolerate dehydration, sometime for very

P. D'Odorico and A. Porporato (eds.), Dryland Ecohydrology, 47–65.

long periods. Mosses, resurrection plant (*Selaginella lepidophylla*), some desert grasses, and sagebrush are examples of drought endurers.

In the present chapter, some of the typical responses of plants to water deficit conditions will be reviewed, with particular attention to the responses taking place in the vegetative tissue of higher plants. Other processes, such as flower and fruit production, seed germination and stress at cellular level will be discussed here only marginally. The present review also includes other types of plant stress frequently associated with drought, such as high temperature and salinity. The last part of the chapter will cover some of the main mechanisms that plants have evolved to cope with these unfavorable conditions. A modeling approach to water stress and its relations with soil moisture dynamics is given in Chapter 3.

2. Water relations

Water makes up between 85 and 90% of the fresh weight of most living herbaceous plants. In higher plants, water is absorbed by roots from soil and then moved to the shoots and leaves through the xylem vessels. The driving force for this movement is the pressure gradients developed by root pressure and by transpiration, which is in turn driven mainly by the difference in water vapor concentration between the leaf and the surrounding air.

The water status of plant tissues, soil, and atmosphere is commonly measured in terms of water potential (Ψ or Ψ_w), which is defined as the free energy per unit volume of water (J m^{-3}). Since energy per unit volume and pressure have the same dimensions, plant and soil water potentials are conventionally expressed in pressure units, such as the pascal (Pa), which is the common measurement unit for water potential (see also Chapter 2). Since the free energy of water is influenced by concentration of dissolved solutes, pressure and gravity, the water potential of a solution can be expressed as the sum of the following components:

$$\Psi = \Psi_0 + \Psi_s + \Psi_p + \Psi_g + \Psi_m + \Psi_v \qquad (1)$$

Ψ_0 is the reference potential of pure (no dissolved solutes), free (free of adsorptive forces) water at a specified temperature at sea level exposed to an atmospheric pressure of 101,325 Pa. This component can be ignored, as long as the others are accounted for. Ψ_s is the solute component which indicates that pure water will flow from where the solute potential is higher (i.e., dilute solutions) to where it is lower (i.e., concentrated solutions). Ψ_s is very frequently written as Ψ_π, which is called osmotic potential. Ψ_p is the pressure component which specifies that water under pressure has a higher potential to do work. Ψ_g is the gravitational component. Ψ_m denotes the effects of matric forces on the water potential and Ψ_v is the potential due to humidity (water vapor). Despite the many components of water potential, most of them are rather small in cells (and there is little difference in gravitational potential between a cell and the surrounding environment). Consequently, Eq. (1) can be simplified, to a good approximation, to just the sum of solute and pressure potentials:

$$\Psi = \Psi_s + \Psi_p \qquad (2)$$

Because of the complexity of plant and soil water relations, it is not possible to identify a unique index that is indicative of the degree of water deficit to which a plant is subjected. However, leaf or stem Ψ, is probably the most frequently used indicator of plant stress because it accounts for the effects of evaporative demands, the availability of water in the soil, and the hydraulic fluxes within the soil-plant-atmosphere continuum (Andrews et al., 1992). By using Ψ as a stress indicator, water deficit is quantified in terms of the extent to which tissue water content falls below that at full turgor, which is regarded as the optimum water content for growth and development.

Another frequently used indicator of plant water status is relative water content (RWC), which is the water content (on a percentage basis) relative to the water content of the same tissue at full turgor. Clearly, RWC is related to Ψ of the same tissue, although it is affected by stages of growth and by modifications induced by the environment. One disadvantage of using RWC as an indicator of stress is that it is rather insensitive to changes in plant water status when water deficit is not severe.

Even in conditions of adequate soil water supply, nearly all plants are exposed to some degree of water deficit conditions throughout their lives. Whenever the quantity of water loss via transpiration is greater than the amount absorbed by the roots, water in the xylem tissues is subject to a negative pressure (tension). Such a situation occurs regularly during the day, with more or less intensity, and is a function of the environment and of the physiological condition of the plant. Due to genetic variability and the influence of the environment, it is difficult to indicate which thresholds of water potential can be used to indicate levels of water stress. Nevertheless, three degrees of water deficit conditions of a typical mesophyte have been defined (Hsiao, 1973). According to this classification, a plant experiences mild stress when its cellular Ψ is greater than -0.5 MPa, moderate stress when Ψ is between -0.5 and -1.5 MPa and severe stress when Ψ_{cell} is below -1.5 MPa (Hsiao, 1973).

Hydraulic conductivity is a measure of the capability of a medium (in plant physiology, a cell membrane, a tissue, xylem elements, etc.) to transmit water. It is expressed as volume of water per unit area of medium per unit time per unit driving force (i.e., $m^3\ m^{-2}\ s^{-1}\ MPa^{-1}$). The loss of hydraulic conductivity experienced by the xylem plays an important role in reducing drought tolerance (Tyree and Sperry, 1989). When the xylem pressure becomes very negative, the column of water that moves in the xylem breaks and becomes air-filled, a phenomenon which is referred to as *cavitation* or embolism (Tyree and Zimmerman, 2002). Consequently, once a xylem vessel element cavitates, the water movement from the roots to the leaves is interrupted and hydraulic conductivity decreases markedly (Vilagrosa et al., 2003). The threshold value of xylem pressure for cavitation is usually defined by the species, as well as the anatomical characteristics of the xylem vessels, such as diameter (Sperry and Tyree, 1988). For example, poplar vessels cavitates at -1.6 MPa whereas those of juniper have a threshold of -3.5 MPa (Lambers et al., 1998). Many species subjected to water deficit have been found to operate very close to the point of cavitation. An effective control of stomatal aperture is important not only to regulate plant water losses, but also to reduce the risk of cavitation by maintaining xylem pressure within a safe range (Jones and Sutherland, 1991). Research conducted on Mediterranean species suggests that a higher resistance to cavitation might contribute to a higher tolerance to water deficit (Pockman and Sperry, 2000). Cavitation is also responsible for a decrease in gas exchange, and in particular of transpiration rate, thus affecting the amount of water that is absorbed by the roots (Cochard et al., 2002; Salleo et al., 2000).

Soil characteristics such as texture can influence plant water relations, thus superimposing on the influence of climate on plant productivity and diversity (see Chapters 2 and 3). When eight shrub species of the Great Basin desert of North America were compared, large differences in plant water relations occurred between sites of similar climate and topography, but with very different soil texture (Sperry and Hacke, 2002). Stem Ψ and vulnerability to cavitation were in fact lower in plants growing in finer-textured (loam) soils loamy versus soils characterized by larger pore spaces (sandy). Rooting depths also tended to be shallower at the loam site. The greater cavitation resistance measured in plants growing in loam soils is likely an adaptation to enhance the water extraction capability of a root system growing in a soil often characterized by lower Ψ. Roots of desert shrubs exposed to soil drought experience more cavitation than stems, suggesting that the root system represents the more limiting component to xylem transport (Kolb and Sperry, 1999; Sperry and Hacke, 2002). This could also represent an advanced evolutionary strategy of enduring or permitting cavitation in a few replaceable roots but preventing it in the stems. Thus, the damage caused by cavitation in roots is not as severe or long lasting as that caused by stem xylem cavitation. Variation in cavitation resistance within the root system has been observed both spatially and temporally (Hacke et al., 2000; Sperry and Ikeda, 1997). Some desert shrubs are mostly active during the early part of the growing season when soil moisture is more available from rain showers before shedding their leaves and starting a period of drought dormancy. Such drought-deciduous plants appear to have shallow root systems and greater cavitation resistance indicating an enhanced ability to capture water from the upper soil profiles (Sperry and Hacke, 2002). Species differences with respect to cavitation resistance also reflect differences in xylem anatomy and function as well as trade-offs between conductance and safety (Lambers et al., 1998). Although smaller xylem elements can minimize the chances of cavitation, they are also less efficient in hydraulic conductivity.

3. Growth and development

The initial effect of water deficit stress is loss of turgor, with a concomitant reduction in the rate of cell expansion and ultimately, decreased cell size, leaf expansion, stem elongation, seed/fruit size and yield. As water deficit stress develops, competition for water within the plant may occur with the outcome depending upon the stage of growth. Usually, those tissues that are actively growing take precedence over older tissues. Meristems may constitute strong hydraulic sinks because cell division and biosynthesis of new cell materials such as proteins increase the matric potential (lower Ψ) and establish a strong gradient for water movement to the meristematic tissue. Mesophyll and other photosynthetic tissues are also actively competing for water during mild stress because of the synthesis of new solutes which takes place there. Water may also be directed towards storage organs (e.g., tubers, rhizomes) and other sites where the number of solutes increase, for example due to hydrolysis of starch or other polysaccharides.

The primary effect caused by water deficit conditions on plants is a loss of turgor, which causes reduction in cell size and is accompanied by a reduction in leaf expansion and shoot extension. Reduction in leaf area has the advantage of decreasing the surface area for transpirational water loss. However, a smaller leaf area has the secondary effect of reducing light absorption and photosynthesis.

Under mild to severe water stress conditions, cell structure can be disrupted by dehydration. When the osmotic pressure of a solution is increased above that of the cells, the protoplast starts shrinking, and the plasma membrane separates from the wall protoplast (plasmolysis). This phenomenon mainly occurs in cells that are in contact with solution, such as in epidermal strips, or in root cells of intact plants grown in hydroponics (Munns, 2002). Plasmolysis is unlikely to occur in nature, except in severe conditions, but can be easily induced in the laboratory by immersing a plant cell in a very concentrated solution. Jones (1992) suggested that plasmolysis is rare in normal aerial tissues because it is the cell wall – not the plasma membrane – which supports the negative tensions. The capillary forces at the air-water interface in the cell wall microcapillaries would prevent them from draining and hence plasmolyzing. In the event that plasmolysis does occur, disruption of compartmentation may follow, with the concomitant release of lipases, hydrolases and other enzymes that destroy membranes and other substrates that are normally protected by isolation in compartments. Chloroplasts are also destroyed when they come in contact with vacuolar sap. The capacity to recover from this type of damage varies with the species and represents one of the resistance mechanisms initiated by plants to survive drought. Despite the degree of resistance, all plants have a ‘point of no return’ beyond which recovery is not possible and rehydration may actually aggravate the damage.

Water stress is particularly deleterious to development of reproductive organs. Flowers and fruits have a low frequency of stomata; hence, the driving force for water movement into stomata is smaller compared to leaves. Adequate water supply is, therefore, critically important during reproductive development, as nearly all phases from gamete production to anthesis and seed/fruit expansion are sensitive to water deficits. Water stress during gametogenesis or anthesis can lead to infertility and seed/fruit abortion. During a mild stress, rapidly transpiring and photosynthesizing leaves can become stronger sinks for water than fruits because of increasing solute accumulation (photoassimilates) in the former. Leaf solute accumulation lowers leaf Ψ, creating a strong gradient for water movement towards them and in severe cases water may actually be resorbed from fruits, thereby inhibiting fruit and seed enlargement.

4. Water deficit stress perception and signaling

Roots are able to detect the early stages of soil drying and many of the shoot responses to soil drying occur before any detectable change in the leaf water status. Although loss of turgor and wilting are the first visible symptoms of soil water availability, there is evidence that a change in water status does not always play the main role in the regulation of plant responses to drought (Davies and Zhang, 1991). In fact, it is now well established that the term water stress does not refer only to situations where water relation parameters are altered. From several studies it has emerged that soil water status, leaf water relations and plant responses are not always correlated (Davies and Zhang, 1991). For these reasons, leaf Ψ is not always representative of ongoing water stress conditions, although it is the most commonly used indicator of shoot water status. Other leaf variables, such as growth rate and stomatal conductance (g_s, reciprocal of the resistance to CO_2 and water vapor transfer between the atmosphere and the internal tissue of the leaf imposed by the stomata), may be more useful indicators of incipient water deficit than water potential or other more commonly used variables. Change in growth and development of plants growing in drying soils can in fact occur even when shoot water relations are not affected. Frequently, depression of gas exchange and of stomatal conductance are detectable at moderate leaf water deficits or even before leaf water status is influenced (Jones et al., 1985).

If changes in water potential are not always involved, plants must have a different type of signal which must communicate the information to the shoot and trigger its responses. Such a signaling system must not be directly associated with a reduction in the flux of water to the shoots and with the change in leaf water status but it has to be responsible for changes in stomatal behavior, leaf initiation and expansion, etc. Tan et al. (1981) reported that tomato plants that had 25% of the root system watered, showed only 20% reduction in transpiration. The authors suggested that tomato roots could adjust their relative absorption capacity for water uptake in response to the transpirational demand.

The ability to regulate stomatal behavior is of vital importance especially for plants growing in water limiting conditions. Consequently, the signaling mechanism allows plants to sense water availability in the soil and promptly develop a response by regulating stomatal aperture, water consumption and adjust leaf water status. When the first indirect pieces of evidence of such signaling system were formulated, scientists needed to find if such a system indeed existed, whether it was composed by just one or more mechanisms, and what its nature was (chemical, electrical, etc.).

Split-root studies have been used to simulate the heterogeneity in the field and study the effects of differential irrigation in herbaceous plants (Williams et al., 1991; Zhang and Kirkham, 1995). Water uptake by one part of the root systems has been shown to be mostly dependent on the localized soil water potential. However, the relationship between soil water potential and water uptake may be affected by variations of the soil water status in other parts of the root system (Simonneau and Habib, 1994). Split root experiments have been widely conducted on plants with commercial importance, such as apple (Gowing et al., 1990), peach (Simonneau and Habib, 1994), grapes (Stoll et al., 2000), sunflower (Masia et al., 1994), barley (Farrar and Minchin, 1991), etc. When apple trees were grown with their root system split between two containers (Gowing et al., 1990), and irrigation was applied only to one container over a three-week period, leaf area was reduced by approximately 50%, due to reduction of both leaf expansion rate and leaf initiation. These responses were obtained even though half of the root system received optimal supply of water and shoot and leaf water status was not affected. It was concluded that leaf initiation and expansion were somehow inhibited by a signal originated in the dry portion of the root system. Results of the split-root experiments reported above suggest that signaling between roots and shoots must be of a "positive" nature, which means that it is activated by the increase of a substance capable of eliciting a certain physiological response. Although "negative" signals (i.e., substances synthesized in the roots whose transport is completely stopped) have been considered, it is unlikely that they play a key role in the physiological and morphological changes induced by water stress. In order for such substances to be effective, leaves should be sensitive to minor changes in their concentration from very low levels to zero, which is very unlikely to occur (Davies and Zhang, 1991).

Split-root systems are not just experimental tools to study root-to-shoot signaling systems in plants; they are a way to simulate the heterogeneity of soil systems and in particular water availability in the soil. The larger a plant is, the greater the probability that its root system will grow into zones where water is readily available (e.g., deeper in the soil profile) and in others where water is scarce (e.g., more superficial layers). Although there is little information available on water relation profiles along the roots, studies conducted using split-root systems suggest that even if only a few roots are exposed to drying soil, a signal may be generated and translocated to the shoots and leaves. The intensity of such a signal would obviously increase when more and more roots are subjected to dehydration until a threshold is reached and a response is triggered in the canopy. Heterogeneity in plant root systems may be influenced also by size, class, characteristics, age, etc. of the single roots. Zhang and Davies (1989) reported for example that secondary and tertiary roots of maize are much less effective in maintaining tissue turgor when soil dries.

Among the possible chemical signals that may be involved in perception of developing water stress (cytokinins, pH, ion concentrations, etc.), ABA is the most likely (Davies and Zhang, 1991). ABA has long been known to increase considerably in leaves of plants subjected to drought. The marked increase is a consequence of the biosynthesis of this hormone, rather than of a release from storage forms present in the leaves (Dorffling, 1972). There is in fact a considerable body of evidence showing that leaves are not the only source of ABA and that ABA is also synthesized in roots (Cornish and Zeevaart, 1985; Davies and Zhang, 1991). The synthesis of ABA takes place in the root apices, in the non-growing regions, and in the cortex as well in the stele. When roots "sense" the reduction of soil water potential, they start producing ABA, which is then sent to the leaves via xylem flow, thereby functioning as a long distance signaling molecule. It is now widely accepted that stomatal conductance is controlled by the soil water status via ABA. The exact mechanism of action of ABA and its role on stomatal closure is still unclear although we do know that ABA induces efflux of anions and cations from the vacuole to the cytoplasm of guard cells, thus causing their loss of turgor and reduction of stomatal aperture (MacRobbie, 1997). It is not clear, however, if such reaction is caused by changes in ABA concentration in the leaves, by variations of its rate of delivery to the guard cells, or by other reasons, such as ABA-driven fluctuations in xylem pH.

Although leaf water status is often not considered as influencing the response of stomata to ABA, a few studies (Schurr et al., 1992; Tardieu and Davies, 1993; Tardieu et al., 1992) have reported that leaf water potential might have an indirect role in the regulation of the stomatal conductance, via a modification of the stomatal sensitivity to ABA. Moreover, a lower response of the conductance of ABA was observed when water potential was maintained high by pressurizing the root system (Schurr et al., 1992). Another study conducted on sunflower (Gollan et al., 1986) showed that, when leaf water potential and turgor do decline, stomatal conductance can be more closely related to the water status of the soil than to that of the leaves. In contrast to these assumptions, when ABA was removed from the sap of water-stressed wheat, the anti-transpirant activity was still present, which suggested that ABA could not be the only stress signal acting from roots to shoots (Munns and King, 1988).

Among the other types of signals that have been considered, ion and pH gradients may play a role in root-to-shoot communication. It has been reported that the pH of the xylem increase in response to drying soil (Davies and Zhang, 1991). The role of a higher pH could be to favor ABA distribution in the leaves. The variables involved in stomatal regulation are typically distinguished between those involved in the mechanics of stomatal movements and those implicated in the signals triggering these movements (Zeiger et al., 1987). Recently, however, other physiological variables have been proposed. These variables, such as whole-plant hydraulic resistance, soil resistance, root resistance, etc. may affect the hydraulic characteristics of the sap pathway and consequently induce stomatal closure (Cochard et al., 2002).

5. Gas exchange

Stomatal opening/closure provides an important mechanism for plants to regulate movement of gases into or out of leaves. Stomata occupy only about 1 % of the leaf surface area and, in most dicotyledonous plants, they are more numerous on the abaxial leaf surfaces compared to adaxial surfaces, with a stomatal frequency of 50-300 stomata per mm^2 being more representative for the abaxial leaf surface of most leaves (Nobel, 1999). In contrast, most monocotyledonous plants have approximately equal distribution of stomata on both sides of the leaf. In plants, transpiration (E) is the loss of water that occurs through stomata as the CO_2 needed for photosynthesis is absorbed from the atmosphere. Transpiration is a function of the hydrostatic pressure gradient and of the evaporative demand of the surrounding environment. This evaporative demand depends on the net radiation absorbed by leaves and on the drying power of the air (Nobel, 1999). Existence of a hydrostatic pressure gradient between roots and leaves drives water movement in plants from the soil into roots and ultimately to the atmosphere through leaf transpiration. Although transpiration serves a useful purpose of tissue cooling, excessive transpirational water loss can lead to soil water depletion and tissue dehydration. Stomata can be regulated in response to soil water status (e.g., via ABA) and other environmental cues such as vapor pressure deficit (VPD) and control water loss accordingly. Leaves continuously need to find a compromise between minimizing transpirational water loss and maximizing CO_2 uptake and photosynthesis. Stomata are the ultimate controllers of this delicate balance.

In the previous sections we have seen how water stress influences stomatal aperture, either directly, with the turgor loss of stomatal guard cells (hydropassive closure), or indirectly, with production of ABA or other inhibitory substances (hydroactive closure). In either case, stomatal closure induces a decline in carbon assimilation, with physiological and morphological consequences in both the vegetative and reproductive growth and development. Due to differences in molecular structure and diffusional properties of CO_2 and water, partial stomatal often limits transpiration more than it does CO_2 uptake. Stomatal conductance is in fact only part of the limitation on inward diffusion of CO_2, whereas it is the major limitation on outward diffusion of water vapor (Parkhurst, 1994). Some xerophytes have sunken stomata, an adaptation which increases the resistance to water vapor loss by transpiration. Other adaptations to regulate movement of gases into or out of leaves include small leaf size, thicker cuticles, pubescence, and glaucousness. The differential influence of stomatal closure on CO_2 uptake and water loss has important effects on water use efficiency (WUE). Leaf-level WUE refers to the ratio of photosynthesis (A) to transpiration, whereas WUE of productivity refers to the ratio between biomass accumulation and water used during production of that biomass. Since A and E are both affected by g_s, plant WUE, therefore, also depends on g_s and on factors influencing g_s such as the leaf-air vapor pressure difference (LA VPD, or the difference between the leaf's intercellular air spaces and the bulk air). Temperature also has a pronounced effect on plant WUE, since it affects LA VPD (Lambers et al., 1998).

Of special interest to life in dry environments is the fact that WUE is closely related to the carbon isotope (^{12}C or ^{13}C) composition of plant tissues. The C isotopic composition of plant tissues provides an integrated measure of the photosynthetic WUE during the time when the tissue C was assimilated. Plants tend to discriminate against the heavier C isotope, depending on processes such as diffusion or carboxylation (see Farquhar et al., 1989 for a detailed review). High g_s or low A often lead to large discrimination (Δ) against the heavier isotope (^{13}C), resulting in a lower ^{13}C isotope composition ($\delta^{13}C$) in plant tissues. The consistently close positive correlation between $\delta^{13}C$ and WUE has led researchers to propose using $\delta^{13}C$ as a screening index in breeding for high WUE (Hubick and Farquhar, 1987; Meinzer et al., 1990). This follows from ample experimental evidence showing that genotypes which perform best under dry environments (i.e. high WUE) also have higher $\delta^{13}C$ in their tissues than plants from mesic environments (Smedley et al., 1991).

Most plants (except for CAM plants; see section 7.2.1) keep their stomata closed at night. This allows them to recover from a mild stress thanks to water absorption that continues from the available water supply in the soil. At night, however, water movement is not driven by the negative pressure generated in the xylem by transpiration, because, with stomata being close, transpiration does not take place. In this case, the driving force is caused by the solutes actively accumulated in the xylem sap. Such accumulation induces a decrease in Ψ_s, and thus in Ψ, which drives water movement from the more diluted soil solution to the more concentrated root xylem. Such movement is generally enough to build up a positive hydrostatic pressure (usually between 0.05 and 0.5 MPa) in the xylem which is utilized to rehydrate tissues and repair cavitation.

6. Other stresses associated with drought

Understanding the physiology of plants exposed to environmental stresses can be particularly challenging when the responses derive from different factors. For this reason, in order to better understand the physiological responses of plants to drought, most experiments have been conducted in laboratory, under controlled conditions, with the attempt to maintain non-limiting conditions for all environmental factors except for limiting water availability. In natural habitats, however, such conditions are rare, and it is more common for two or more factors to play a role concurrently to the plant responses. In nature, locations that are subjected to frequent drought periods are frequently associated with levels of irradiance well above the rates required to saturate the photosynthetic processes. High air and soil temperatures are also frequently linked to dry environments, due to the presence of high irradiance levels, low air and soil moisture levels. At the same time, dry environments are often exposed to increasing cellular or soil concentrations of ions or molecules, which, singly or in combination, can cause inhibition of metabolism or physiology (toxicity effects). Such interactions among environmental constraints force plants react to their environment with very complex adaptive responses which influence growth and developmental processes. What follows is a brief review of some of the abiotic plant stresses that are commonly associated with water stress.

6.1. HIGH TEMPERATURE STRESS

The association between drought and high temperature stress is often so close that it is difficult to distinguish the effects of either stress on plant growth and development. In addition, adaptive mechanisms to drought can be truly effective only if they lead to tolerance or avoidance of both stress conditions. The main reason why the two unfavorable conditions are so tangled in nature is because the stress caused by high temperatures is a frequent consequence of limiting soil water availability and of the drought-induced reduction in stomatal aperture. As observed before, when water supply in the soil becomes limiting, ABA is synthesized in the roots and translocated to the leaves where stomatal closure is induced. Although stomatal closure has the advantage of preventing excessive water losses, it also reduces carbon assimilation and induces the cessation of transpirational cooling. The reduction in transpiration causes a rapid rise in leaf temperature (5 ºC and more above air temperature in bright light near midday), which can induce serious damage to the leaves and, if maintained for prolonged period, lead to the death of the plant. The precise temperature threshold for damage to leaves is usually above 45 ºC but it is function of several factors, such as species, growing temperature, potential prehardening conditions, environmental factors, etc. Well-hydrated plants can maintain the temperature of their tissues at values close to those of the surrounding air as long as they possess mechanisms to dissipate the heat generated by solar radiation. Plant tissues dissipate heat through three main mechanisms: heat convection, emission of long-wave (infrared) radiation and transpirational cooling. Of the three methods, transpiration is the most effective and, typically, half of the net heat input generated in a leaf by sunlight is dissipated by transpiration (Nobel, 1999). Transpiration dissipates heat because energy is required to break the bonds that hold the molecules of water together in the liquid phase. Consequently, water molecules which leave the walls of the mesophyll cells and are released into the atmosphere have a higher energy than those which are left behind in the leaf tissues. When the plant is well watered, transpiration rate is maximal and the leaf temperature is close to air temperature. On the other hand, when water deficit increases, stomatal aperture and transpiration are reduced and solar energy is no longer dissipated as latent heat for water evaporation, but rather converted into heat, which increases leaf temperature. This explains why, during hot summer days and when the soil water content becomes limiting, leaf temperature becomes higher than air temperature. Inversely, plants receiving an adequate amount of water through their roots have cooler leaves than those that are drought stressed. A relatively new method for the evaluation of plant water status can in fact be the measurement of leaf and canopy temperatures, and the difference between canopy and air temperature can be a tool to detect plant moisture stress (Jackson, 1982) and predict the potential yield of a crop (Tanner, 1963).

Cooling is not the only function of transpiration and water movement in the xylem elements. Water movement from root to shoot is the main avenue for nutrient movement and when transpiration rate decreases, so does nutrient distribution. Nutrient deficiency, however, is seldom a primary impairment for the growth and development of stressed plants because of the reduced metabolism during the unfavorable conditions.

In general, photosynthesis is one of the first processes to be affected by high temperatures. In particular, the chemical nature of the chloroplasts seems to be the reason for the high sensitivity of the electron transport of photosystem II (PS II) to high temperature values. The viscosity of the lipids forming thylakoid membrane changes in fact rapidly when leaf reaches temperatures between 45 and 55 ºC, which corresponds to the range within which severe damage to the leaves occurs in almost all plants. At high temperature, there is also decrease in the strength of hydrogen bonds and electrostatic interactions between polar groups of proteins. Consequently, protein structure and functionality are modified with consequences on permeability, biochemistry, etc.

High temperatures affect carbon metabolism not only by reducing photosynthesis but also by accelerating carbon losses. Although both processes are inhibited by high temperatures, the optimal range for respiration in response to temperature is broader than that for photosynthesis. Consequently, as temperature rises, photosynthesis decreases before respiration does. When temperature rises above the temperature compensation point (the temperature value at which the amount of CO_2 released by respiration equals the amount of fixed CO_2), more CO_2 is used as substrate for respiration than what photosynthesis can fix into carbohydrates.

Photorespiration is another process which causes the loss of CO_2 and which is affected by temperatures. Photorespiration occurs when rubisco (ribulose-1,5-bisphosphate carboxylase/oxygenase), the main enzyme involved in carbon assimilation, reacts with oxygen and, instead of producing two molecules of 3-phosphoglycerate, like it does when it reacts with CO_2, it originates 2-phosphoglycolate and 3-phosphoglycerate, thereby decreasing the efficiency of photosynthesis. As temperature increases, the concentration ratio of CO_2 to O_2 decreases and photorespiration rate increases more relative to the photosynthesis rate. Photosynthesis and photorespiration occur simultaneously, with loss of CO_2 from those same cells that are fixing CO_2 by the Calvin cycle. This effect is also enhanced by the kinetic properties of rubisco, which has a higher affinity for O_2 at higher temperature (Ku and Edwards, 1978).

6.2. FIRE

Fire is the most extreme case of high temperature stress. Wildfires are often very destructive and are often facilitated by prolonged drought events which create fuel (dead plant material) for such fires. Although wildfires are more often associated with human intervention, they are frequently caused by natural events such as volcanic eruptions and lightning strikes. Wildfires are more common in those regions characterized by a dry season, but can take place practically anywhere in particularly dry years (see Chapter 16).

The type of damage inflicted to plants by fire depends on the temperatures generated in proximity of soil, trunk and canopy. Temperatures are determined by the amount of heat released per unit area which is function of the amount of combustible present per unit area, of the type of combustible (dead wood, conifer needles, etc.), and of environmental factors, such as wind, which help dissipate the heat away from the source. The threshold temperature for plant survival is 60-70 ºC, which is a much lower range than the values reached by wildfires near the soil surface (100-150 ºC). Most living tissues are thus killed by fire, although the time of exposure to the fire has an influence on the extent of damage as well. Most of the seeds present in the superficial layers of the soil are also killed by the fire. However, frequently dormant seeds present at deeper layers can survive and their germination can actually be stimulated by the fire.

Destructive as fires may be in many dryland environments, they also serve a useful function as being a catalyst for regeneration. Fire plays an important role in accelerating nutrient cycles and their availability to plants. Many non-volatile elements (such as K, P, Ca, etc.) can become more rapidly available after the passage of fire, when they get concentrated in the surface ashes. However, most of the nitrogen present in plants is lost to the atmosphere during fires.

Several plant communities have characteristics that indicate strategies for survival against this sometime devastating environmental feature. Such characteristics include seed dispersal (e.g., *Pinus* spp.) and removal of dormancy triggered by high temperature, trunks protected by thick and fire-repellant bark (e.g., *Quercus suber*), rapid sprouting of new vegetative tissues from epicormic buds (e.g., *Eucalyptus*, *Myrtus*), bulbs, rhizomes, etc. to replaces the tissues damaged by fire. Typical fire-adapted communities include the Mediterranean *maquis*, the Californian *chaparral*, the Australian *kwongan*, and the South African *fynbos*.

6.3. HIGH IRRADIANCE

Areas that are exposed to drought are frequently characterized by cloudless sky, low relative humidity, and scarce vegetation. In such conditions, solar radiation can reach very high levels because less light is intercepted by clouds, water molecules present in the atmosphere or vegetation. For most plants, solar radiation is not only the primary source of energy for photosynthesis, but also acts as a stimulus regulating many growth and developmental processes (e.g., flowering). The direct thermal effects (warming) of solar radiation also allow many metabolic processes to proceed optimally. The thermal effects of solar radiation also help drive evapotranspiration and ultimately water shortages if replenishment from rain and irrigation are inadequate. However, solar radiation can also cause injury and damage, for instance through mutagenesis and through excessive absorption by plants. Very high irradiances can damage the photosynthetic system or leaves in which photosynthetic metabolism has been inhibited by other processes such as water stress or extreme temperatures. Shade-adapted plants are most susceptible to excessive irradiances. Damage can be a result of photooxydation, where bleaching of chlorophyll occurs, or photoinhibition, where no bleaching occurs. Photoinhibition has been defined as the reversible decrease in photosynthetic capacity induced by the exposure of photosynthetic tissues to high fluxes of photosynthetically active radiation (PAR, 400-700 nm) (Ort, 2001). The decrease in efficiency results largely from changes in photosystem II (PSII), and in particular the D1 protein, although photoinhibition of photosystem I (PSI) has also been reported in some species (Terashima et al., 1994). When excess light hits the protein D1, the excess quanta produced during the light reaction are transferred to the reaction centers instead of being disposed of as heat or fluorescence. This increases the amount of reducing power by creating singlet oxygen or free radicals, which easily damage or destroy the D1 protein itself. If a receptor for this reducing power is present, then the damage can be alleviated. Consequently, the damaged D1 protein has to be removed and replaced with a newly synthesized molecule. If the conditions leading to photoinhibition are persistent during the growing season, the damage can be significant. Photoinhibition can in fact cause decrease in both quantum efficiency and maximum photosynthetic activity. It has been estimated that in natural willow populations the daily depression in carbon assimilation induced by photoinhibition accounts for reduction in biomass of up to 10% (Long et al., 1994). Photoinhibition can be probed by measuring photosynthetic electron transport as oxygen exchange or chlorophyll *a* fluorescence, both of which reflect the electron transfer through the two photosystems (Bolhar-Nordenkampf and Oquist, 1993). Such measurements have shown strong correlations between photoinhibition and the inactivation of the D1 reaction center polypeptide of PS II which binds plastoquinone Q_B (Long et al., 1994). Plants have evolved a variety of mechanisms to avoid high-irradiation damage, for example, leaf movements (heliotropisms), developing highly reflective surfaces (e.g. pubescence), or rapid resynthesis of damaged, plastid pigments and proteins.

C_3 plants, especially those that are more shade-tolerant or more adapted to shady conditions, are more vulnerable to photoinhibition when they are suddenly exposed to high radiation levels. Conversely, sun-adapted plants and plants with C_4 metabolism are less susceptible to this harmful process. Photoinhibition is more common when high radiation levels follow periods characterized by low temperatures. Plant populations living in deserts or at high altitudes, where such climatic conditions are more frequent, are thus more exposed to photoinhibition. In these environments, the depression in photosynthetic rates is even more detrimental due to the limited resources that are available for plant growth.

6.4. SALINITY

Areas exposed to drought are characterized by high soil and plant evaporation rates which lead to depletion of water reserves not replenished by the scarce or absent precipitations. When evaporation exceeds precipitation, soil moisture decreases and salts become more concentrated in the rootzone. Salt accumulation in the soil is a phenomenon that has great repercussions on plant physiology and influence plant communities. Accumulation of salts in the environment induces two types of stresses in plants. First, accumulation of dissolved solutes reduces soil osmotic potential, which lowers the soil water potential (see Chapter 2). This affects the general water balance because plants have to develop an even lower water potential to maintain a downhill potential gradient between roots and soil to preserve water and nutrient uptake. The other consequence of accumulation of salts is the toxic effect caused by high concentration of ions both in the soil and at cellular level. Based on these differences, Levitt (1980) distinguished between salt and ion stresses. Salt stress was defined as the condition of a plant exposed to a salt concentration high enough to lower water potential by 0.05-0.1 MPa; ion stress occurs when the total ion concentration is not high, but the stress is induced by one particular species of ion which can result toxic to plants.

The extent of adaptation varies greatly among species and certain plants have evolved mechanisms for dealing with these stresses. Plants that thrive in the presence of high levels of salts and can complete their reproductive cycle are called *halophytes*, and are usually native to saline soils. *Salt-tolerant* are defined as those plants which are well adapted to high levels of salt. *Non-halophytes* (sometimes called less correctly *glycophytes*, "sweet plants") are plants that show toxicity symptoms even at relatively low levels of salt. Another classification distinguishes between plants that tolerate high sodium levels (*natrophilic* plants) and plants are affected by very low levels of soil sodium content (*natrophobic*). Distinction is also made between plants that can live in soil with high calcium content (i.e., in conditions of high pH soil), called *calcicole*, and plants that are more adapted to soil with less calcium content (low pH), known as *calcifuge*.

When referring to the effects of salts in the soil, *sodicity* indicates high concentration of sodium in the soil, whereas *salinity* refers to a high concentration of total salts. The two concepts are often related because soils with a high concentration of salts often have high sodium content. However, the opposite is not always true.

Although there are similarities between the low soil water potential conditions induced by drought and by excess salt content, there are differences in the mechanisms of adaptation initiated by plants (Munns, 2002). During soil desiccation the amount of water available to plants keeps decreasing with time, thus creating ever-decreasing water potentials and continuous renewal of adaptation strategies, such as osmotic adjustment. Conversely, in saline environments, water is usually available and the concentration of salts remains more or less stable, thus creating low, constant water potential conditions.

7. Mechanisms of adaptation

Water stress is not limited to plants living in environments characterized by low soil moisture content. Typically, even well-irrigated plants experience moderate water deficit conditions sometime during the day. This occurs because the evaporative demand, transpiration and evaporation are high and water movement within plants is relatively slow. Consequenctly, xylem tension increases with the intensity of the stress. Compared to other environmental stresses, such as hypoxia or temperature stresses, drought can take several days, sometime weeks, before it becomes severe enough to affect plant growth. Consequently, if the dehydration process of a plant cell or tissue is sufficiently slow, plants can develop changes in physiological and developmental processes to respond to the unfavorable conditions.

If the water stress condition continues for a prolonged period, however, plants may die of desiccation, unless mechanisms of resistance are initiated. Two main types of mechanism can help reduce the stress condition: 1) prevention or reduction of water loss in certain tissues or organs or 2) increase in rates of absorption and translocation of water. While the first type is usually activated as a quick response to the unfavorable conditions, the second type of reaction typically required anatomical/ morphological adaptations and are thus more efficient for prolonged stresses.

7.1. MORPHOLOGICAL ADAPTATIONS TO WATER STRESS

Most species that have evolved in environments where drought events occur more or less frequently have developed mechanisms of adaptation that enable them to avoid the hottest period of the year. It is quite common for many annual species, such as *Camissonia claviformis*, a drought avoider species native to the Death Valley, California, to complete their reproductive life during the cooler months. A few perennial species, such as in *Euphorbia dendroides*, a Mediterranean shrub, keep their leaves during winter and/or spring and abscise them with the onset of the hot season.

Other species can accurately control leaf angle and leaf folding in order to keep their leaves either parallel (paraheliotropic sun tracking) or perpendicular (diaheliotropic sun tracking) to the direct sunrays. Species with paraheliotropic sun tracking minimize the interception of solar radiation thus maintaining lower temperature. On the other hand, plants with diaheliotropic sun tracking maximize their interception and therefore carbon assimilation, which enables them to grow rapidly during the favorable conditions (e.g., after rainfall). Increasing the fraction of light that is reflected before it can be absorbed is another method for plants to ensure survival during high temperature stress. In environments with intense solar radiation and high temperatures, it is very frequent for leaves and other organs to be covered with reflective hairs and waxes. Such barriers reduce the amount of energy reaching the vital portions of the plants and decrease the need of evaporative cooling. An example of this type of adaptation can be found in the California desert brittlebush, *Encelia farinosa*, which has green, nearly hairless leaves in winter and develops more pubescent, silvery leaves only when this desert shrub begins to experience water stress during the spring. The new leaves are highly reflective and absorb less than 60% of the intercepted PAR, versus approximately 85% absorption of the non-pubescent leaf type (Ehleringer and Bjorkman, 1978).

As mentioned above, convection of excess heat is another mechanism allowing leaves to dissipate part of the energy derived from interception of solar radiation. Morphological features, such as small, dissected leaves, can reduce boundary layer resistance (r_b), which is the portion of resistance of the transpiration pathway which is caused by the layer of unstirred air surrounding the leaf surface and through which water vapor must diffuse before reaching the turbulent air of the atmosphere. There is a direct relationship between r_b and the thickness of the boundary layer δ, which depends on the wind speed u and leaf size d as

$$\delta \propto \sqrt{\frac{d}{u}}\,. \tag{3}$$

Consequently, under the same wind conditions, the larger a leaf is, the thicker is δ. With a thick δ, the r_b can be so large that, when the air surrounding the leaf is very still, the layer of unstirred air can be the primary obstacle to transpiration, and therefore to transpirational cooling. This explains why species, such as mesquite, adapted to hot environments, usually have small leaves or dissected leaves with very small leaflets.

Phenological adaptations are often accompanied by modifications at cellular level. Oleander (*Nerium oleander*) is a species native to the Mediterranean basin and very resistant to drought and high temperatures. In this species, a thick cuticle contributes to the reduction of water losses while an increased degree of saturation of fatty acids in membrane lipids makes the membrane less fluid, thus increasing the plant's resistance to high temperatures (Raison et al., 1982).

Conditions of water deficit decrease stomatal aperture and consequently carbon assimilation. Growth of all organs is thus reduced in drought condition. As a result, a reduction in root growth would be expected when the soil water potential declines. Nevertheless, several studies have reported an increase in the proportion of photoassimilates allocated in the root system, associated with water deficit conditions (Buwalda and Lenz, 1992; Hsiao and Jing, 1987). If the stress is not too extreme, plants can maintain root growth in order to increase the absorbing surface and explore bigger soil volume, with consequent increase in the root to shoot ratio. The allocation of photoassimilates for root growth could be interpreted as an investment for following unfavorable periods (Buwalda and Lenz, 1992). This adaptation mechanism is part of what Brouwer (1983) defined as 'functional equilibrium', by which plants respond to a decrease in above-ground resources with increased allocation to shoots, whereas they respond to a decrease in below-ground resources with increased allocation to roots.

7.2. PHYSIOLOGICAL ADAPTATIONS TO WATER STRESS

Loss of turgor induced by drought triggers physiological and biochemical adjustments that are as important for turgor maintenance as morphological adaptations. The importance of elastic and osmotic adjustments for plant resistance to water stress have been highlighted (Schulte and Henry, 1992). *Elastic adjustment* includes physical modifications in the cells, which make them more elastic, thereby facilitating tissue shrinkage during dehydration. *Osmotic adjustment*, or osmoregulation, is defined as the active accumulation of solutes inside the cell, with the consequent lowering of Ψ_s. This mechanism helps maintaining turgor and water absorption even at low tissue water potentials and prevents mechanical damages to plasma membranes. For mesophytes, the decrease in Ψ_s is usually between 0.2 and 0.8 MPa, but it can be greater in plants adapted to extremely dry conditions. The solutes that are most typically involved in this mechanism are small inorganic ions (mainly K^+), amino acids, organic acids and sugars. They are accumulated preferentially in the vacuoles, in order not to interfere with the structure and functioning of cytosolic enzymes. High solute concentrations can contribute to a greater capacity for turgor maintenance, but the contribution of electrolytes to osmotic adjustment is usually relatively low, if compared with other solutes. Inorganic ions can be toxic and disruptive to organelles, enzymes, and membrane-bound processes, whereas organic ions may serve as more compatible solutes, being tolerated at high concentrations in the cytoplasm (Ahmad et al., 1979; Bieleski, 1982). *Osmolytes* (also referred to as compatible solutes or osmoprotectants) are low molecular weight organic compounds that can be safely synthesized and accumulated in the cytoplasm without interfering with enzyme functions. Many are the plants and bacteria that synthesize osmolytes in response to environmental stresses (Tarczynski et al., 1993). Their main function is to maintain a water potential equilibrium within the cell when solutes are actively accumulated in the vacuole to increase the cell tolerance against abiotic stresses (Tarczynski et al., 1993). The level of many osmolytes increases in fact during the stress and declines when the stress is relieved. Examples of osmolytes are sugar alcohols (sorbitol and mannitol are the two most common ones), the amino acid proline, and glycinebetaine, a quaternary amine. In many species belonging to the *Rosaceae* family, sorbitol is the primary product of photosynthesis and the most actively translocated form of carbohydrate. In apple leaves it has been found to accumulate during drought stress (Bieleski, 1982) and perhaps this compatible solute plays a role in lowering leaf osmotic potential. However, not enough research has been conducted on young leaves, root and stems to determine its importance (Wang et al., 1995). In certain trees, such as apple, mature leaves seem to be able to adjust osmotically, whereas young leaves and tips seem not to be able to do this. The opposite seems to occur in peach, where immature leaves indicate osmotic adjustment and mature leaves do not (Wang et al., 1995). Osmotic adjustment in drought-stressed roots was observed by Ranney et al. (1991) for cherry trees. Numerous results have been obtained on experiments conducted on transgenic tobacco plants where the gene for mannitol was inserted (Tarczynski et al., 1993). Naturally, tobacco is not a mannitol-producer, but transformed plants produced mannitol (up to a maximum concentration of 100 mM) and seemed more tolerant to salinity stress. Genetically modified plants were also able to produce new growth and new leaves, when exposed for 30 days to 250 mM NaCl. There are no assumptions on how accumulation of intracellular mannitol may lead to new growth. The maintained production of roots and leaves, rather than a reallocation of resources, could explain the increased height and weight in transgenic plants (Tarczynski et al., 1993). Trehalose, a non-reducing disaccharide of glucose, is an osmoprotectant which plays an important role in stress protection in a large variety of organisms ranging from bacteria and fungi to invertebrate animals by effectively stabilizing dehydrated enzymes and lipid membranes, thereby protecting biological structures from damage during desiccation. During severe dehydration trehalose can act as a substitute for water, thus maintaining the native folding and biological activity of proteins, and preventing denaturation and aggregation. Despite the wide distribution of trehalose in microorganisms and invertebrates, trehalose had until recently only been found in a few plant species, notably highly desiccation-tolerant, resurrection plants (club mosses *Selaginella lepidophylla* and the angiosperm *Myrothamnus flabellifolius),* so named because of their unique ability to fully recover from a state of almost complete loss of water (Goddijn and van Dun, 1999). These resurrection plants can accumulate trehalose at levels approaching 1% of dry weight under non-stress conditions, whereas the majority of plants do not appear to accumulate easily-detectable amounts of trehalose. However, genes that encode enzymes of trehalose synthesis, i.e., trehalose-6-phosphate synthase (TPS) and trehalose-6-phosphate phosphatase (TPP), have been recently identified in a number of plants. Transgenic rice and tobacco plants expressing these genes have been shown to exhibit increased drought tolerance (Garg et al., 2002; Pilon-Smits et al., 1998).

As indicated in Figure 1, osmotic adjustment is not one of the first responses to water stress; instead, it follows loss of turgor, stomatal closure and reduction in carbon assimilation rate. However, the role of such mechanism is significant. Leaves that can adjust osmotically can in fact maintain turgor, thus maintaining cell elongation, growth and stomatal aperture at lower water potentials. Osmotic adjustment is a phenomenon that is not limited to leaves. Root cells can accumulate solutes actively into their vacuoles as well. It seems however that the magnitude of the adjustment is smaller in root cells than in leaf cells. The role of osmotic adjustment is the same in root and in leaf cells: reduce Ψ_s to favor water uptake from the surrounding cells (or from the soil, in case of root cells) in order to maintain turgor, cell extension and tissue growth.

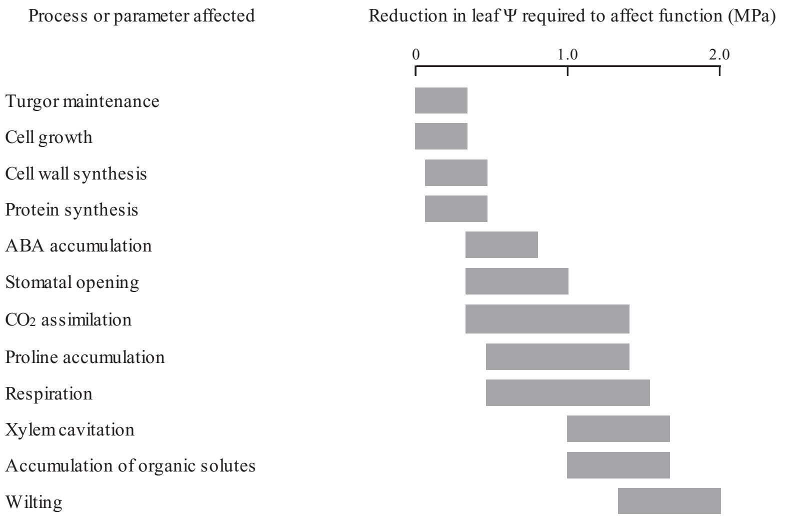

Figure 1. Responses of mesophytic plants to reduction of soil water availability. The horizontal bars indicate the range of lowering of leaf water potential at which symptoms first appear (Modified from Hsiao, 1973).

7.2.1. C_4 and CAM species

Some plant species have developed distinctive modes of photosynthesis, which confer them higher water-use efficiency, thus reducing water needs and increasing their resistance to more arid environments. The group of plants known as C_4 includes over 8000 species of angiosperms, both monocotyledons and dicotyledons, distributed among 16 different families. A prime example of C_4 plants is given by Gramineae of warmer regions like sugarcane, maize or tropical grasses. C_4 plants are so called because the first stable intermediates of photosynthesis present in their leaves are the four-carbon acids malate and aspartate (all other plants are known as C_3 because 3-phosphoglycerate is the first intermediate of the Calvin cycle). The primary carboxylation process in C_4 plants is not catalyzed by rubisco, as in C_3 plants, but by phosphoenolpyruvate (PEP) carboxylase. The C_4 photosynthesis is made possible by peculiar cells that are present in the leaves. A typical leaf of C_4 plants is in fact anatomically different from that of a C_3 plant. While all chloroplast-containing cells (mesophyll cells) in a C_3 leaf have similar structure, the leaf of a C_4 plants has two distinct cell types containing chloroplasts: mesophyll and bundle sheath cells (this particular structure is sometime referred to as Kranz anatomy, from the German word for wreath). After the C_4 acid is formed in the mesophyll cell, it is shuttled to the bundle sheath cells where decarboxylation of the C_4 acid takes place. The CO_2 released is then fixed by rubisco and converted into carbohydrate by the Calvin cycle, just like in C_3 plants. This mechanism allows the creation of a high concentration of CO_2 at the carboxylation site of rubisco, which facilitates carboxylation. In addition, the fact that rubisco is kept in the bundle sheath cells (i.e., not in direct contact with the external atmosphere) results in the elimination of photorespiration. The C_4 cycle is considered a direct adaptation to dry environments because it helps overcome the harmful effects of high temperature on photosynthesis. The suppression of photorespiration, combined with the high affinity that PEP carboxylase has for its substrate (HCO_3^-), enables C_4 plants to maintain photosynthetic and water use efficiencies equal or greater than those of C_3 plants. This allows them to live longer when subjected to water deficit conditions. However, if the stress is prolonged, they too eventually undergo severe damage and death from causes other than starvation.

While C_4 plants separate spatially PEP-carboxylation from rubisco-carboxylation, another group of plants, called CAM (crassulacean acid metabolism) plants, have the two carboxylation processes occurring in the same leaf cell but temporally separated. Plants with CAM photosynthesis have evolved in particularly dry environments and are usually considered as water savers. CAM metabolism was first researched in the 1800's in the Crassulaceae (Crassula, Sedum, Kalanchoe, etc.) family, hence its name. However, we now know that such metabolism is not exclusive to the Crassulaceae family, but it is present in more than 20,000 species of plants. Other families with CAM photosynthesis include Euphorbiaceae, Agavaceae, Cactaceae, and Orchidaceae. The peculiarity of CAM plants is that they can store considerable amounts of water in their shoots by keeping their stomata closed during the hot, dry days and fixing CO_2 during the cool, desert nights, when transpirative forces are lower. As in C_4 plants, the key enzyme for such a process is PEP carboxylase, located in the cytosol, which fixes CO_2 at night to form malate, a four-carbon organic acid, which is temporarily stored in the vacuole. During the day, the stored malate is transported to the chloroplasts where it gets decarboxylated, and the released CO_2 is fixed by rubisco in the Calvin cycle. Thanks to this mechanism, CAM plants have a better WUE than non-CAM plants (C_3) and can reduce water losses by 75-90% (Taiz and Zaiger, 2002).

The common ice plant (*Mesembryanthemum crystallinum*), a plant native to the Namibian Desert, South Africa, is capable of switching from C_3 to CAM metabolism. Such a transition occurs as young plants in their natural habitat experience drought and increasing salinity as the season progresses. This phenomenon could be based on changes in the external conditions alone but indications suggest the shift in metabolism is also part of the plant's developmental program (Cushman and Borland, 2002). *Mesembryanthemum crystallinum* has provided many clues about the mechanisms employed by stress-tolerant plants to survive extreme conditions. A variant of the CAM mechanism, called *CAM-idling*, allows certain CAM plants (or parts of them) to survive for prolonged periods of time with their stomata constantly closed thus losing extremely small amounts of water. Such a phenomenon is possible because the CO_2 that is released by respiration is fixed again into malate by PEP carboxylase. CAM-idling is in most cases the mechanism that allows portions of cacti or other succulents to survive for long periods (up to several months) after detachment from the plant.

8. Conclusions

During the last two- three decades, some of the most relevant concepts in water stress have been highlighted. We now know for example that root signals exert a somewhat dynamic control over stomatal behavior, although the exact modes of action are still extensively being investigated. Current evidence indicates that these signals are chemical in nature, but the potential role of signals of different nature (pH and ion gradients, action potentials, etc.) should not be overlooked, as these types of signals have important roles in the responses of plants to other stresses (e.g., cold, wounding, attack of pathogens) and in systemic acquired resistance.

Despite the progress obtained in this area of plant science, our understanding of the mechanisms of adaptation is insufficient to predict a plant's response and how these mechanisms may be interacting and integrating. One of the biggest obstacles derives from the fact that it is very difficult to separate the effects of different interrelated stress factors. In addition, we are still not able to assess the importance of one particular physiological or morphological adaptation relative to another.

The capacity that plants have to adjust to the environment is one of their most important attributes. Such ability is fundamental because it permits plants to colonize the most diverse environments. The immense variability of plant responses, however, makes it often difficult to generalize and categorize the different plant responses. This chapter has attempted to provide an overview of some the typical morphological and physiological mechanisms of adaptation to water stress and to evaluate their importance in the light of plant survival. With water becoming increasingly scarce, it will be extremely valuable to extend our knowledge on water stress physiology. The areas subjected to drought and high temperature conditions are increasing alarmingly. Ecosystems are disappearing due to climate change and diversion of natural waters to human activities. Water has always been one of the major constraints for crop production and ecosystem dynamics (see Chapter 3, 5, 18). The combined expertise of ecologists, breeders, plant physiologists, hydrologists, and biometeorologists is now more than ever before important to better understand these adaptive mechanisms and to select for improved stress tolerance in crop plants.

9. References

Ahmad, I., F. Larher, and G.R. Stewart. 1979. Sorbitol, a compatible osmotic solute in *Plantago maritima*. New Phytol. 82:671-678.

Andrews, P.K., D.J. Chalmers, and M. Moremong. 1992. Canopy-air temperature differences and soil water as predictors of water stress of apple trees grown in a humid, temperate climate. J. Amer. Soc. Hort. Sci. 117:453-458.

Bieleski, R.L. 1982. Sugar alcohols in plants. Encycl. Plant Physiol. 13A:158-192.

Bolhar-Nordenkampf, H.R. and G. Oquist. 1993. Chlorophyll fluorescence as a tool in photosynthesis research, p. 193-206. In: D.O. Hall, J.M.O. Scurlock, H.R. Bohlar-Nordenkampf, R.C. Leegood, and S.P. Long (eds.). Photosynthesis and production in a changing environment: a field and laboratory manual. Chapman & Hall, London.

Bradford, K.J. and T.C. Hsiao. 1982. Physiological responses to moderate water stress. Encycl. Plant Physiol. 12B:263-324.

Brough, D.W., H.G. Jones, and J. Grace. 1986. Diurnal changes in water content of the stems of apple trees, as influenced by irrigation. Plant Cell Environ. 9:1-7.

Brouwer, R. 1983. Functional equilibrium - Sense or nonsense. Netherlands Journal of Agricultural Science 31:335-348.

Buwalda, J.G. and F. Lenz. 1992. Effects of cropping, nutrition and water supply on accumulation and distribution of biomass and nutrients for apple trees on 'M9' root systems. Physiol. Plant. 84:21-28.

Cochard, H., L. Coll, X. Le Roux, and T. Ameglio. 2002. Unraveling the effects of plant hydraulics on stomatal closure during water stress in walnut. Plant Physiol. 128:282-290.

Cornish, K. and J.A.D. Zeevaart. 1985. Abscisic acid accumulation by roots of *Xanthium strumarium* L. and *Lycopersicon esculentum* Mill. in relation to water stress. Plant Physiol. 79:653-658.

Cushman, J.C. and A.M. Borland. 2002. Induction of Crassulacean acid metabolism by water limitation. Plant Cell Environ 25:295-310.

Davies, W.J. and J. Zhang. 1991. Root signals and the regulation of growth and development of plants in drying soil. Annu. Rev. Plant. Physiol. Mol. Biol. 42:55-76.

Dorffling, K. 1972. Recent advances in abscisic acid research, p. 281-295. In: H. Kaldeway and G. Vardar (eds.). Hormonal regulation in plant growth and development. Verlag Chemie, Weinheim.

Ehleringer, J.R. and O. Bjorkman. 1978. Pubescence and leaf spectral characteristics in a desert shrub, *Encelia farinosa*. Oecologia 36:151-162.

Farrar, J.F. and P.E.H. Minchin. 1991. Carbon partitioning in split root systems of barley: relation to metabolism. J. Exp. Bot. 42:1261-1269.

Flore, J.A. and A.N. Lakso. 1989. Environmental and physiological regulation of photosynthesis in fruit crops. Hortic. Rev. 11:111-157.

Garg, A.K., J.K. Kim, T.G. Owens, A.P. Ranwala, Y. Do Choi, L.V. Kochian, and R.J. Wu. 2002. Trehalose accumulation in rice plants confers high tolerance levels to different abiotic stresses. Proc. Natl. Acad. Sci. USA 99:15898-15903.

Goddijn, O.J.M. and K. van Dun. 1999. Trehalose metabolism in plants. Trends Plant. Sci. 4:315-319.

Gollan, T., J.B. Passioura, and R. Munns. 1986. Soil water status affects the stomatal conductance of fully turgid wheat and sunflower leaves. Aust. J. Plant Physiol. 13:459-464.

Gowing, D.J.G., W.J. Davies, and H.G. Jones. 1990. A positive root-sourced signal as an indicator of soil drying in apple, *Malus x domestica* Borkh. J. Exp. Bot. 41:1535-1540.

Hacke, U.G., J.S. Sperry, B.E. Ewers, D.S. Ellsworth, K.V.R. Schafer, and R. Oren. 2000. Influence of soil porosity on water use in *Pinus taeda*. Oecologia 124:495-505.

Hsiao, T.C. 1973. Plant responses to water stress. Annu. Rev. Plant. Physiol. 24:519-570.

Hsiao, T.C. and E. Acevedo. 1974. Plant responses to water deficits, water-use efficiency, and drought resistance. Agric. Meteorol. 14:59-84.

Hsiao, T.C. and J.H. Jing. 1987. Leaf and root expansive growth in response to water deficits, p. 180-192. In: D.J. Cosgrove and D.P. Knievel (eds.). Physiology of cell expansion during plant growth. The Pennsylvania State Univ.

Hubick, K.T. and G.D. Farquhar. 1987. Carbon isotope discrimination - selecting for water-use efficiency. Aust. Cotton Grow. 8:66-68.

Jackson, R.D. 1982. Canopy temperature and crop water stress, p. 43-85. In: D. Hillel (ed.). Advances in Irrigation. Academic Press. Inc., New York.

Jones, H.G. 1992. Plants and microclimate: a quantitative approach to environmental plant physiology. Cambridge University Press, Cambridge, England.

Jones, H.G., A.N. Lakso, and J.P. Syvertsen. 1985. Physiological control of water status in temperate and subtropical fruit trees. Hortic. Rev. 7:301-344.

Jones, H.G. and R.A. Sutherland. 1991. Stomatal control of xylem embolism. Plant Cell Environ. 14:607-612.

Kolb, K.J. and J.S. Sperry. 1999. Transport constraints on water use by the Great Basin shrub, *Artemisia tridentata*. Plant Cell Environ. 22:925-935.

Ku, S.B. and G.E. Edwards. 1978. Oxygen inhibition of photosynthesis .III. Temperature-dependence of quantum yield and its relation to O_2/CO_2 solubility ratio. Planta 140:1-6.

Lambers, H., F.S. Chapin III, and T.L. Pons. 1998. Plant physiological ecology. Springer-Verlag, New York.

Levitt, J. 1980. Responses of plants to environmental stresses. vol. 1. Academic Press, New York, NY.

Long, S.P., S. Humphries, and P.G. Falkowski. 1994. Photoinhibition of photosynthesis in nature. Annu. Rev. Plant. Physiol. Mol. Biol. 45:633-662.

MacRobbie, E. 1997. Signalling in guard cells and regulation of ion channel activity. J. Exp. Bot. 48:515-528.

Masia, A., A. Pitacco, L. Braggio, and C. Giulivo. 1994. Hormonal responses to partial drying of the root system of *Helianthus annuus*. J. Exp. Bot. 270:69-76.

Meinzer, F.C., G. Goldstein, and D.A. Grantz. 1990. Carbon isotope discrimination in coffee genotypes grown under limited water-supply. Plant Physiol. 92:130-135.

Munns, R. 2002. Comparative physiology of salt and water stress. Plant Cell Environ. 25:239-250.

Munns, R. and R.W. King. 1988. Abscisic acid is not the only stomatal inhibitor in the transpiration stream of wheat plants. Plant Physiol. 88:703-708.

Nobel, P.S. 1999. Physicochemical and environmental plant physiology. Academic Press, San Diego, CA.

Olien, W.C. and A.N. Lakso. 1986. Effect of rootstock on apple (*Malus domestica*) tree water relations. Physiol. Plant. 67:421-430.

Ort, D.R. 2001. When there is too much light. Plant Physiol. 125:29-32.

Parkhurst, D.F. 1994. Diffusion of CO_2 and other gases inside leaves. New Phytol. 126:449-479.

Pilon-Smits, E.A.H., N. Terry, T. Sears, H. Kim, A. Zayed, S.B. Hwang, K. van Dun, E. Voogd, T.C. Verwoerd, R. Krutwagen, and O.J.M. Goddijn. 1998. Trehalose-producing transgenic tobacco plants show improved growth performance under drought stress. J. Plant Physiol. 152:525-532.

Pockman, W.T. and J.S. Sperry. 2000. Vulnerability to xylem cavitation and the distribution of Sonoran desert vegetation. Am. J. Bot. 87:1287-1299.

Raison, J.K., C.S. Pike, and J.A. Berry. 1982. Growth temperature-induced alterations in the thermotropic properties of *Nerium oleander* membrane lipids. Plant Physiol. 70:215-218.

Ranney, T.G., N.L. Bassuk, and T.H. Whitlow. 1991. Osmotic adjustment and solute constituents in leaves and roots of water-stressed cherry (Prunus) trees. J. Amer. Soc. Hort. Sci. 116:684-688.

Salleo, S., A. Nardini, F. Pitt, and M.A. Lo Gullo. 2000. Xylem cavitation and hydraulic control of stomatal conductance in Laurel (*Laurus nobilis* L.). Plant Cell Environ 23:71-79.

Schulte, P.J. and L.T. Henry. 1992. Pressure-volume analysis of tissue water relations parameters for individual fascicles of loblolly pine (*Pinus taeda* L.). Tree Physiol. 10:381-389.

Schurr, U., T. Gollan, and E.-D. Schulze. 1992. Stomatal response to drying soil in relation to changes in the xylem sap composition of *Helianthus annuus*. II. Stomatal sensitivity to abscisic acid imported from the xylem sap. Plant Cell Environ. 15:561-567.

Simonneau, T. and R. Habib. 1994. Water uptake regulation in peach trees with split-root systems. Plant Cell Environ. 17:379-388.

Smedley, M.P., T.E. Dawson, J.P. Comstock, L.A. Donovan, D.E. Sherrill, C.S. Cook, and J.R. Ehleringer. 1991. Seasonal carbon isotope discrimination in a grassland community. Oecologia 85:314-320.

Sperry, J.S. and U.G. Hacke. 2002. Desert shrub water relations with respect to soil characteristics and plant functional type. Funct. Ecol. 16:367-378.

Sperry, J.S. and T. Ikeda. 1997. Xylem cavitation in roots and stems of Douglas fir and white fir. Tree Physiol. 17:275-280.

Sperry, J.S. and M.T. Tyree. 1988. Mechanism of water stress-induced xylem embolism. Plant Physiol. 88:581-587.

Stoll, M., B. Loveys, and P. Dry. 2000. Hormonal changes induced by partial rootzone drying of irrigated grapevine. J. Exp. Bot. 51:1627-1634.

Taiz, L. and E. Zaiger. 2002. Plant physiology. Sinauer Associates, Inc., Sunderland, MA.

Tan, C.S., A. Cornelisse, and B.R. Buttery. 1981. Transpiration, stomatal conductance, and photosynthesis of tomato plants with various proportions of root system supplied with water Varieties. J. Amer. Soc. Hort. Sci. 106:147-151.

Tanner, C.B. 1963. Plant temperature. Agron. J. 55:210-211.

Tarczynski, M.C., R.G. Jensen, and H.J. Bohnert. 1993. Stress protection of transgenic plants tobacco by production of the osmolyte mannitol. Science 259:508-510.

Tardieu, F. and W.J. Davies. 1993. Integration of hydraulic and chemical signalling in the control of stomatal conductance and water status of droughted plants. Plant Cell Environ. 16:341-349.

Tardieu, F., J. Zhang, and W.J. Davies. 1992. What information is conveyed by an ABA signal from maize roots in drying field soil? Plant Cell Environ. 15:185-191.

Terashima, I., S. Funayama, and K. Sonoike. 1994. The site of photoinhibition in leaves of *Cucumis sativus* L. at low temperatures is photosystem I, not photosystem II. Planta 193:300-306.

Tyree, M.T. and J.S. Sperry. 1989. Vulnerability of xylem to cavitation and embolism. Annu. Rev. Plant. Physiol. Mol. Biol. 40:19-36.

Tyree, M.Y. and M.H. Zimmerman. 2002. Xylem structure and the ascent of sap. Springer-Verlag, Berlin.

Vilagrosa, A., J. Bellot, V.R. Vallejo, and E. Gil-Pelegrin. 2003. Cavitation, stomatal conductance, and leaf dieback in seedlings of two co-occurring Mediterranean shrubs during an intense drought. J. Exp. Bot. 54:2015-2024.

Wang, Z., B. Quebedeaux, and G.W. Stutte. 1995. Osmotic adjustment: effect of water stress on carbohydrates in leaves, stems and roots of apple. Aust. J. Plant Physiol. 22:747-754.

Wang, Z.C. and G.W. Stutte. 1992. The role of carbohydrates in active osmotic adjustment in apple under water stress. J. Amer. Soc. Hort. Sci. 117:816-823.

Williams, J.H.H., P.E.H. Minchin, and J.F. Farrar. 1991. Carbon partitioning in split root systems of barley: The effect of osmotica. J. Exp. Bot. 42:453-460.

Wyn-Jones, R.G. and J. Gorham. 1983. Osmoregulation in plant cells, mathematical models. Encycl. Plant Physiol. 12C:35-58.

Zeevaart, J.A.D. and R.A. Creelman. 1988. Metabolism and physiology of abscisic acid. Annu. Rev. Plant. Physiol. Mol. Biol. 39:439-473.

Zeiger, E., G.D. Farquhar, and I.R. Cowan. 1987. Stomatal function. Stanford University Press, CA.

Zhang, J. and W.J. Davies. 1989. Abscisic acid produced in dehydrating roots may enable the plant to measure the water status of the soil. Plant Cell Environ. 12:73-81.

Zhang, J. and M.B. Kirkham. 1995. Water relations of water-stressed, split-root C4 (*Sorghum bicolor*; Poaceae) and C3 (*Helianthus annuus*; Asteraceae) plants. Am. J. Bot. 82:1220-1229.

Chapter 5

SOIL MOISTURE CONTROLS ON WATER VAPOR AND CARBON FLUXES IN SEMI-ARID REGIONS

John D. ALBERTSON[1], Christopher A. WILLIAMS[2], Todd M. SCANLON[3], Nicola MONTALDO[4]

[1]Department of Civil and Environmental Engineering, Duke University, Box 90287, Durham, NC, 27708, USA - e-mail: john.albertson@duke.edu
[2]Natural Resource Ecology Laboratory, Colorado State University, Campus Delivery 1499, Fort Collins CO, 80523, USA - e-mail: caw@nrel.colostate.edu
[3]Department of Environmental Sciences, University of Virginia, Box 400123, Charlottesville VA 22904, USA – e-mail: tms2v@virginia.edu
[4]Dipartimento di Ingegneria Idraulica, Ambientale, Infrastrutture viarie, e del Rilevamento, Politecnico di Milano, Piazza Leonardo da Vinci, 32, I-20133 Milano MI, ITALY, - e-mail: Nicola.Montaldo@polimi.it

1. Introduction

In this chapter we focus on savannas as a representative semi-arid, or dry-land, cover type. Savannas cover some 20% of the global land mass, including 40% of Africa (Scholes and Walker 1993). The term "Savanna" is defined by a co-existence of herbaceous and woody vegetation (often referred to as grass and trees, for simplicity) that is largely due to the limited nature of water availability (but also reflecting the imprints of fire and herbivory). In fact, as a type, the savanna is largely unique in the strength of contrast in the important characteristics between its two dominant vegetation types (Scholes and Walker, 1993). Savannas have a significant role in global net primary productivity, second only to tropical forests (Atjay et al. 1987). In contrast to tropical forests, however, these water limited systems exhibit dramatic changes in their structure (e.g. grass and tree densities) and function (e.g. water and carbon fluxes) in response to typical seasonal, inter-annual, ENSO, and decadal precipitation variability (Scanlon and Albertson 2003a). As for the southern African savannas, as an example, the anticipated decreases in regional rainfall (10-20%) and continued increases in population put the global and regional services of these savannas in jeopardy (IPCC 1992; Moleele and Mainah, 2003).

Changes in both the structure and the function of these savannas have the potential for large-scale impacts on peoples' livelihoods as well as on the global water, energy, and carbon cycles. This potential, coupled with an inadequate understanding of savanna dynamics, is responsible for the current concentration of research efforts on these systems. Savanna research is broadly guided by questions regarding either: (1) the structural co-existence of the grasses and the trees, or (2) the functional behaviour of these systems with respect to water and carbon cycling. In this chapter we address the functional aspects of savannas, while noting that the function, when integrated in time, forms the basis to describe structural aspects, such as the relative densities of grasses and trees on the landscape. In other words, if we understand adequately the function of a system, then we can predict the future state of that system. Such an understanding, formulated mathematically, provides the basis for studying the system dynamics, including characteristics such as stability and resilience (e.g. Walker et al. 1981, Walker and Langridge, 1997, Carpenter et al. 2001, Anderies et al. 2002, Folke et al. 2002, Walker et al. 2002; Whitford, 2002).

In this chapter we draw from past efforts in an attempt to identify a parsimonious representation of controls on energy, water, and carbon cycling in savannas. In particular, we seek a form that balances the need for simplicity for incorporation in a wide range of models -

P. D'Odorico and A. Porporato (eds.), Dryland Ecohydrology, 67–83.

from analytical treatment of stochastic point-process studies (Chapter 3) to distributed applications in general circulation models (e.g. Chapter 6; Bonan, 1998; Bounoua et al., 2002) - with the need to maintain fidelity to the essential underlying mechanisms, such as those reviewed in the preceding chapter (Lombardini, this volume).

2. Background and Theoretical Framework

In this section we summarize the principles governing fluxes and balances of energy, water, and carbon at the land surface. We adopt a framework that is suited to savannas, in general, and is consistent with the guiding philosophy described in the preceding paragraph.

All vertical fluxes and conservation equations are presented on a per m^2 basis. We focus on a representative description of the landscape that is at least at the field-scale (i.e. > 10^3 m^2). Since it is expected that such a parcel of land may be comprised of patches of trees, grasses, and bare soil (three functionally unique components, with contrasting fluxes and states), we therefore describe the land cover in terms of the three fractional cover components of Figure 1. As fractional covers, the following identity holds:

$$1 = f_w + f_g + f_s \tag{1}$$

We now present conservation equations and fluxes, using the index *i* to reflect either *w*, *g*, or *s*.

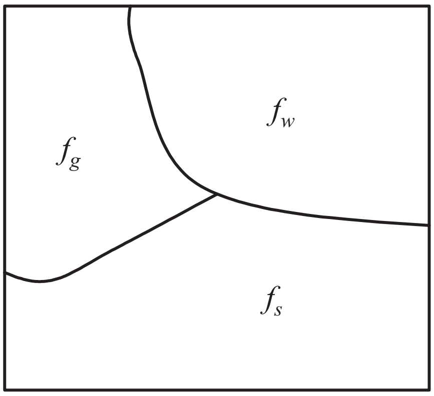

Figure 1. Decomposition of landscape into three fractional cover components, representing the fractions of the landscape covered by woody vegetation (f_w), grass (f_g), and bare soil (f_s).

2.1 SURFACE ENERGY, WATER, AND CARBON BALANCES

The states of energy, water, and carbon at the land surface are all governed by the conservation laws of energy and mass. The skin temperature of the ith component evolves *quickly* to affect a balance between the surface energy fluxes

$$\frac{dT_{si}}{dt} = \frac{1}{C_i}\left(R_{ni} - G_i - H_i - LE_i\right) \tag{2}$$

where T_{si} is the skin temperature, C_i [J m^{-2} ^{o}K^{-1}] is a surface heat capacity, R_{ni} the net radiation, G_i the heat flux into the soil, H_i the sensible heat flux into the atmosphere, and LE_i the latent heat flux into the atmosphere (Brutsaert, 1982).

An important assumption in what follows is that the roots of both grass and trees have access horizontally to all three components of the landscape (hence, there is no *i*-distinction for the soil moisture states). However, since tree roots tend to have access to water much deeper into the soil than grass roots (Williams and Albertson, 2004) we consider two separate layers of soil for the water balance. The moisture states of the shallow and deeper soil layers adjust to the vertical hydrological fluxes (see also Chapter 2), as

$$\frac{d\theta_1}{dt} = \frac{1}{d_1}\left(I - E_s f_s - T_g f_g - T_{w1} f_w - D_{1,2}\right) \tag{3a}$$

$$\frac{d\theta_2}{dt} = \frac{1}{d_2}\left(D_{1,2} - T_{w2} f_w - D_{2,\infty}\right) \tag{3b}$$

where θ_1 and θ_2 represent the volumetric soil moisture contents of the shallow (thickness d_1) and deep (thickness d_2) root zones, I is the surface infiltration rate, E_s the bare soil evaporation rate [mm hr^{-1}], T_g is the grass transpiration rate, T_{w1} is the portion of the tree transpiration rate taken from the shallow root zone, $D_{1,2}$ is the flux of water between the two root zones, T_{w2} is the portion of the tree transpiration rate taken from the deep root zone, and $D_{2,\infty}$ is the flux of water out of the bottom or the deep root zone. Note that the land surface fluxes that are tied to a particular cover type (i) are defined per unit area of that cover type and must, therefore, by scaled by f_i to account correctly for their fractional effect on the total area (c.f. Figure 1), since the moisture contents reflect the entire area.

Just as the surface temperature state reflects a short-time-scale integration of the surface energy fluxes, and the soil moisture states reflect medium-time-scale (~ up to inter-storm) integrations of the vertical hydrological fluxes, the biomass (stored carbon) states reflect slow integrations of surface CO_2 fluxes

$$\frac{dL_i}{dt} = Ph_i \Phi_i f_i - \Gamma_{L_i} L_i + \eta_i \tag{4a}$$

$$\frac{dS_i}{dt} = Ph_i \left(1 - \Phi_i\right) f_i - \Gamma_{S_i} S_i - \eta_i \tag{4a}$$

where L_i and S_i are the leaf and shoot biomass states for component i, respectively, Ph_i is the photosynthesis rate, Φ_i is the allocation rate of photosynthesis to leaf biomass, Γ_{Li} and Γ_{Si} are the respiration (maintenance plus growth) rate coefficients for the leaf and shoot pools, respectively, and η_i reflects the translocation of biomass from the shoot to the leaf pool (such as at spring leaf-out) and may be parameterized in terms of the prior year's biomass state. For more detail on vegetation dynamics modelling see Mougin et al., (1995), Chen et al. (1997), LoSeen et al. (1997), Calvet et al. (1998) Cayrol et al. (2000a,b), Nouvellon et al. (2000), and Williams and Albertson (2005). Note that the inclusion of the ith-type fractional cover (f_i) in (4) injects the necessary dependence of total field-scale photosynthesis on biomass, since f_i, is related to L_i (e.g. Williams and Albertson, 2005).

2.2 INTERSECTIONS OF THE MASS AND ENERGY BALANCES

The evaporation and transpiration rates in (3) correspond to the latent heat flux term in (2), following

$$\begin{aligned} LE_s &= \rho L_v E_s; \\ LE_g &= \rho L_v T_g; \\ LE_w &= \rho L_v \left(T_{w1} + T_{w2}\right); \end{aligned} \tag{5}$$

where ρ is the density of liquid water and L_v [energy/mass] is the latent heat of vaporization.

From a consideration of gas exchange through the stomatal pores of the leaves (see Figure 2) the transpiration rates of (3) are linked to the photosynthesis of (4). Applying integral forms of Fickian diffusion (Campbell and Norman, 1998) across the length of the pore we arrive at leaf-level expressions for water and carbon fluxes

$$Ph_i = g_c\left(c_a - c_*\right) \tag{6a}$$

$$T_i = g_w\left(e_* - e_a\right) \tag{6b}$$

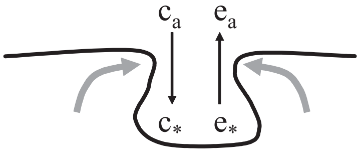

Figure 2. Schematic of a stomatal pore. CO_2 and H_2O are shown diffusing between the outer concentrations (c_a, e_a) and the internal concentrations (c_*, e_*); The curved gray arrows reflect stomatal control on conductance.

where c_a and c_* are the CO_2 concentrations outside and inside the leaf, respectively, and e_a and e_* are the water vapor pressures (i.e. concentrations) outside and inside the leaf, respectively,. (We note that while the field scale flux symbols (Ph_i and T_i) are used in (6a) and (6b), these equations are, in a strict sense, describing leaf level fluxes; however, for our demonstration purposes this is a useful and reasonable relaxation.) By noting that the conductance of CO_2 (g_c) is related to the conductance of water vapor (g_w) according to

$$g_c = \frac{MW_{H_20}}{MW_{CO_2}} g_w = 0.66 g_w \tag{7}$$

where the conductance is controlled by the plant guard cells (surrounding the opening of the stomata), predominantly in savannas to restrict water vapor loss during times of low soil moisture. Of course, this restriction works to limit CO_2 uptake as well, as shown by inverting (6b) for g_w and using this with (7) in (6a)

$$Ph_i = 0.66 g_w (c_a - c_*) = 0.66 \left(\frac{T_i}{e_* - e_a} \right) (c_a - c_*) \tag{8}$$

Hence, it is clear that Ph_i is fundamentally linked to T_i through the stomatal diffusion, with the ratio of CO_2 gain per unit water loss, typically referred to as the 'water use efficiency' (WUE), given by

$$WUE = \frac{Ph_i}{T_i} = 0.66 \left(\frac{c_a - c_*}{e_* - e_a} \right) \tag{9}$$

(provided the units are consistent.)

We progress now to present simple functional forms for a subset of the fluxes active in (2)-(4), as needed to support the examination of the central information cascade from rainfall through the budgets of water, energy and carbon in Section 2.4.

2.3 CONTROLS ON ENERGY, WATER, AND CARBON FLUXES

The net radiation (R_{ni}) is a weakly decreasing function of surface temperature (through the outgoing longwave radiation) and the soil and sensible heat fluxes (G_i and H_i) are strongly increasing functions of surface temperature, such that a positive imbalance on the right hand side of (2) acts to increase T_{si}, which in turn acts to quickly reduce R_{ni} and increase G_i and H_i such that T_{si} returns toward a quasi (dynamic) equilibrium (the opposite is true for negative imbalances in the energy fluxes). In the next section we will discuss the main source of imbalances.

As for the soil water balances, the infiltration (I) forcing comes simply from the stochastic input of precipitation minus any canopy interception and overland flow or ponding. The drainage rates are readily estimated from simplified forms of Darcy's law (e.g. Williams and Albertson, 2004). The evaporation and transpiration rates are taken to be moisture-limited fractions, $\beta_i(\theta)$, (Jacquemin and Noilhan 1990, Avissar and Pielke 1991, Mahfouf et al. 1996, Rodriguez-Iturbe et al. 1999b, Albertson and Kiely 2001; Williams and Albertson, 2004) of a potential evapotranspiration rate, PET_i, as

$$E_s = PET_s \beta_s \tag{10a}$$

$$T_g = PET_g \beta_g \tag{10b}$$

$$T_w = PET_w (\beta_{w1} \varepsilon_1 + \beta_{w2} (1 - \varepsilon_1)) \tag{10c}$$

where ε_1 is the fraction of tree roots located in the upper soil zone (i.e. active in (3a)). PET_i is estimated for simplicity here with the Priestley-Taylor (1972) formulation

$$PET_i = \alpha \frac{\Delta}{\Delta + \gamma} \frac{(R_{ni} - G_i)}{L_v} \tag{11}$$

where α (=1.26) accounts for large-scale advection and entrainment, γ is the psychrometric constant, and Δ is the slope of the saturation vapor pressure curve (Campbell and Norman 1998).

For bare soil, the β_s function has been expressed as a simple polynomial form of θ_1 (Parlange et al., 1999) or in some semi-arid region applications taken to be zero, since in these regions surface soil moistures are typically too low to support significant bare soil evaporation (Williams and Albertson, 2004). However, for transpiration the parameterizations of β_g and β_w are essential. The simplest of the various forms available is a piecewise linear function of soil moisture (e.g. Williams and Albertson, 2004)

$$\beta_g = \begin{cases} 0, & \text{for} \quad \theta_1 \le \theta_{g,wp} \\ \dfrac{\theta_1 - \theta_{g,wp}}{\theta_{g,\lim} - \theta_{g,wp}}, & \text{for} \quad \theta_{g,wp} < \theta_1 < \theta_{g,\lim} \\ 1, & \text{for} \quad \theta_1 \ge \theta_{g,\lim} \end{cases} \tag{12a}$$

$$\beta_{w1} = \begin{cases} 0, & \text{for} \quad \theta_1 \le \theta_{w,wp} \\ \dfrac{\theta_1 - \theta_{w,wp}}{\theta_{w,\lim} - \theta_{w,wp}}, & \text{for} \quad \theta_{w,wp} < \theta_1 < \theta_{w,\lim} \\ 1, & \text{for} \quad \theta_1 \ge \theta_{w,\lim} \end{cases} \tag{12b}$$

$$\beta_{w2} = \begin{cases} 0, & \text{for} \quad \theta_2 \le \theta_{w,wp} \\ \dfrac{\theta_2 - \theta_{w,wp}}{\theta_{w,\lim} - \theta_{w,wp}}, & \text{for} \quad \theta_{w,wp} < \theta_2 < \theta_{w,\lim} \\ 1, & \text{for} \quad \theta_2 \ge \theta_{w,\lim} \end{cases} \tag{12c}$$

where $\theta_{g,\lim}$ and $\theta_{w,\lim}$ are the soil moisture contents below which the grass and trees, respectively, experience a reduction in their transpiration rates with respect to the potential rates, and $\theta_{g,wp}$ and $\theta_{w,wp}$ are the soil moisture contents at which the grass and trees, respectively, wilt and thus experience a cessation of transpiration. These moisture limits vary according to the type of vegetation (e.g., Larcher, 1995; Eagleson, 2002) and are obtained by transforming limiting and wilting point water potentials (i.e. pressures) for savanna tree and grass plant functional types, PFTs, (Scholes and Walker 1993; Mahfouf et al. 1996; Rodriguez-Iturbe et al. 1999a,b,c, 2001) to corresponding soil moisture limits (with the Clapp and Hornberger (1978) relationships to relate potential to soil moisture with soil-specific parameters.)

The carbon balance is forced by photosynthesis, which, as shown in the previous section, is the flip side of the transpiration mechanism. From the ecological perspective photosynthesis is often computed using the biochemical principles of Farquhar et al. (1980), which essentially treats the rate as being driven by light and potentially reduced by other limiting factors. Our water-driven approach is similar, but markedly simpler in that soil moisture is taken to be the only (i.e. governing) limiting factor. Hence, we estimate photosynthesis as a function of transpiration using (9). The respiration rate can be modelled simply in terms of temperature, and the other parameters are available from the literature (e.g. Nouvellon et al., 2000; Cayrol et al., 2000a,b). The net carbon flux between the land and the atmosphere (F_c), also often called Net Ecosystem Exchange (*NEE*) of CO_2, reflects the net difference between photosynthetic uptake and respiration losses. Following micrometeorological convention, in our figures we plot F_c as negative when the net flux is toward the land (i.e. photosynthesis dominates) and positive when the net flux is toward the atmosphere (i.e. respiration dominates).

2.4 INFORMATION CASCADE THROUGH THE STATES AND FLUXES

Savannas are marked by strong temporal variability in their water and carbon fluxes. Before we progress to explore the results from recent field experiments it is instructive to summarize the main pathways by which the external forcings propagate through the states and fluxes described above.

During drought conditions, prior to a rainfall event, the moisture states are low and fairly static and surface temperatures are high. Upon arrival and infiltration of a rainfall pulse into (3a), θ_1 increases and excites some drainage ($D_{1,2}$) into θ_2. These elevated states of θ_1 and θ_2 lead to a rapid increase in evapotranspiration through the increase of the β_i terms. Through (5), this reflects a sharp increase in the latent heat flux, which reduces the surface temperature through (2), and ultimately reduces the sensible heat flux. And, finally, with the effect on photosynthesis, corresponding to that on transpiration through (8), the biomass density is excited in (4) – albeit slowly. Through time the evapotranspiration flux proceeds to deplete θ_1 and θ_2 and the system returns toward its pre-storm state. From this typical scenario it is clear that the energy balance and the water and carbon fluxes are all excited by precipitation through the first order control of soil moisture on T_i and Ph_i. It is with this in mind that we are promoting here a simple model of savanna function with respect to water and carbon fluxes, and now set forth to demonstrate its merit through an examination of field data.

3. Support from Field Experiments

In this chapter we seek to strike a balance between generality of the approach and demonstrating accuracy through comparison to actual field data. Hence, we focus on data from one of the more general settings available: The Kalahari Transect (KT) of southern Africa.

3.1 SETTING OF THE FIELD MEASUREMENTS

The KT spans a strong climatic gradient in southern Africa, from the arid south (<200 mm mean annual rainfall) to the humid north (>1000 mm mean annual rainfall), while remaining on a single soil type, the deep and widespread aeolian sands of the Kalahari basin (IGBP 1997). The vegetation ranges from grass dominated savannas in the south to Miombo woodland savannas in the north. The attributes of the KT make it a logical case study. The climate gradient is strong and persistent, the topography is flat and the variation in soil physical properties is minimal across the entire KT. Moreover, from a meteorological viewpoint, the absence of frequent frontal systems leads to simplified climatology in terms of describing seasonal variations in air temperature, relative humidity, and incident radiation. All things considered, this provides an excellent organizing framework to resolve the environmental controls on water-carbon-energy dynamics. And, as a canonical example of the semi-arid savanna, results from studies of the KT are readily transferable to other savannas, which cover close to one-half of Africa, Australia, and South America (Huntley and Walker, 1982), in addition to large regions in the US.

The field data presented in this chapter are derived from two separate experimental campaigns. The first campaign (Scanlon and Albertson, 2004) was conducted at four different sites along the KT in the wet (growing) season of 2000 (capturing spatial differences), and the second campaign (Williams and Albertson, 2004) was conducted over a longer period but only at one site (Ghanzi) toward the end of the wet season of 2002 (capturing temporal dynamics). The locations of the field sites are shown in Figure 3.

In each of the two campaigns eddy covariance instruments were installed on a tower that measured net mass and energy fluxes between the land and the atmosphere over a measurement footprint (e.g. Scanlon and Albertson, 2004). Sensible heat, latent heat, and CO_2 fluxes were measured with a triaxial sonic anemometer (CSAT-3, Campbell Scientific) in conjunction with an open path infrared CO_2/H_2O gas analyzer (Li-7500, Li-Cor). Eddy covariances (i.e. fluxes) were computed in half-hour averaging periods from 10 Hz data with appropriate data quality controls and adjustments (see Scanlon and Albertson, 2004). In addition, measurements were taken of short- and long-wave components of net radiation (CRN-1 radiometer), soil heat flux (HFT3, Campbell Scientific), air temperature and relative humidity (HMP45C, Campbell Scientific), soil moisture (CS615, Campbell Scientific) at several depths, and radiometric skin temperature (IRTS-P, Apogee Instruments), in addition to other ancillary measurements, all of which are described by Scanlon and Albertson (2004) and Williams and Albertson (2004).

In the 2000 wet season campaign measurements were conducted from North to South along the KT (Figure 3). One set of instruments was installed for the duration of the campaign at Mongu, Zambia while a second set was moved along the transect. The measurement periods were from 29 February through 10 March at Mongu, from 4-9 March at Maun, Botswana, from 10-13 March at ORC (near Ghanzi, Botswana), and 15-16 March at Tshane, Botswna (ending prematurely due to lightning). This campaign was designed to take a snapshot of how the function of the savanna vegetation differed spatially along the long-term aridity gradient. See Scanlon and Albertson (2004) for a description of the vegetation cover at the sites.

The 2002 wet season campaign took place on the Dqae Qare Reserve, near Ghanzi, Botswana from 5 March to 8 April 2002, near the end of the wet (growing) season. The goal of this campaign was to observe the response of the vegetation function to decreasing soil moisture availability. Fortuitously, a storm of 85 mm depth (~ 20% of the mean annual rainfall) occurred at the start of the campaign and no significant additions of rain occurred through the measurement (drydown) period, providing a clear view of the response of this savanna to increasing moisture limitation. Two sites were selected (less than 2 km apart) for intensive measurements, one with an herbaceous canopy composed primarily of grass (label as "Grass site" in Figures), and one with herbaceous vegetation mixed with a tree cover representative of the region (label as "Mixed site" in Figures).

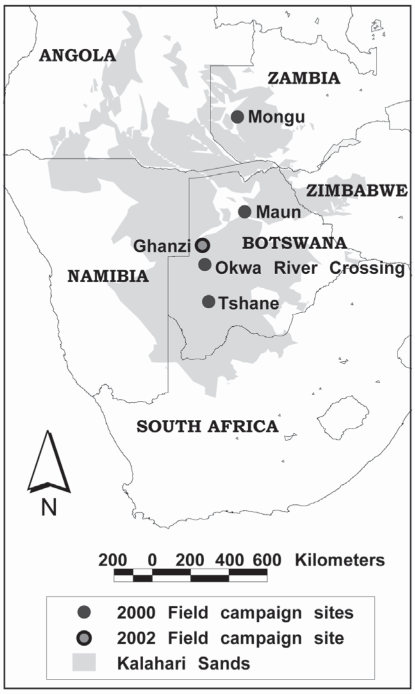

Figure 3. Measurement sites for the 2000 and 2002 wet season campaigns.

3.2 ENERGY BALANCE

Flux measurements derived from eddy correlation instruments are inherently 'field-scale' measures, reflecting the spatial integral of the land surface flux density over some so-called footprint on the landscape. Hence, in presenting results from the field experiments, the fluxes will not be explicitly tied to the individual cover components, but rather will reflect the following spatial aggregation

$$R_n = R_{nw} f_w + R_{ng} f_g + R_{ns} f_s \qquad (13a)$$

$$G = G_w f_w + G_g f_g + G_s f_s \qquad (13b)$$

$$H = H_w f_w + H_g f_g + H_s f_s \qquad (13c)$$

$$LE = LE_w f_w + LE_g f_g + LE_s f_s \qquad (13d)$$

$$ET = \frac{LE}{\rho L_v} = (T_{w1} + T_{w2}) f_w + T_g f_g + E_s f_s \qquad (13e)$$

Figure 4 presents data from the 2002 campaign to highlight how the soil moisture state impacts the surface energy balance. As the root zone of the soil dried (as shown here from day 75 to day 95), the transpiration (i.e. *LE*) was reduced dramatically from ~ 300 w/m^2 to less than 100 w/m^2; this reduction was compensated for by a concomitant increase in the surface temperature (lower left panel) as needed to increase the sensible heat flux (*H*) and the long wave outgoing radiation (as evidenced by the reduction in R_n).

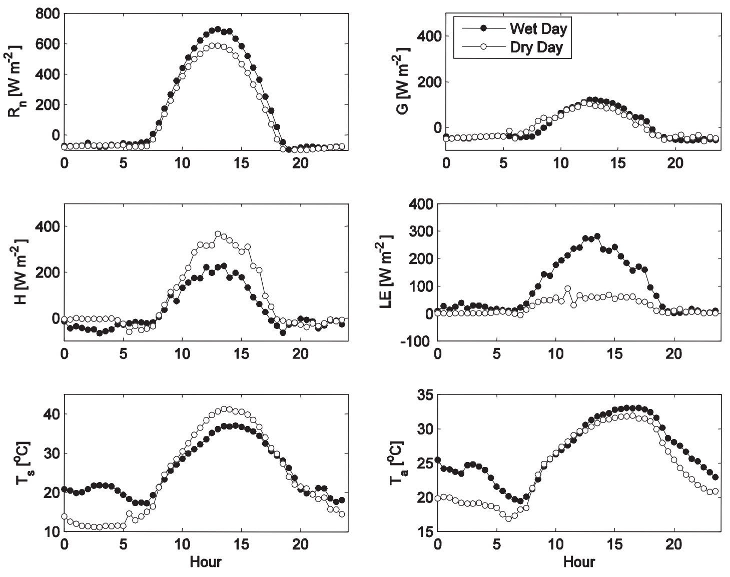

Figure 4. Energy balance contrasted for a wet day (DOY 75) and a dry day (DOY 95) for the data of the Mixed site described by Williams and Albertson (2004).

3.3 TRANSPIRATION RESPONSE TO SOIL DRYING

Here we explore the dynamics of the response of transpiration to soil moisture (also from the 2002 campaign). Figure 5 shows the decay of soil moisture (top 15 cm layer) over the drydown (in the top panel) with the resulting changes in mass and energy fluxes for the two sites. To focus on day-to-day changes we present fluxes that have been averaged between 0900 and 1600 hours and denote this averaging operation with angular brackets (<.>).

The first three days of the flux measurements were under significant cloud cover (>50% reduction in R_n), thus suppressing the fluxes. Other than this anomaly, it is clear that transpiration (i.e. *LE*) decreased monotonically through the drydown, and this decrease was matched by a corresponding decrease in the magnitude of the net carbon flux.

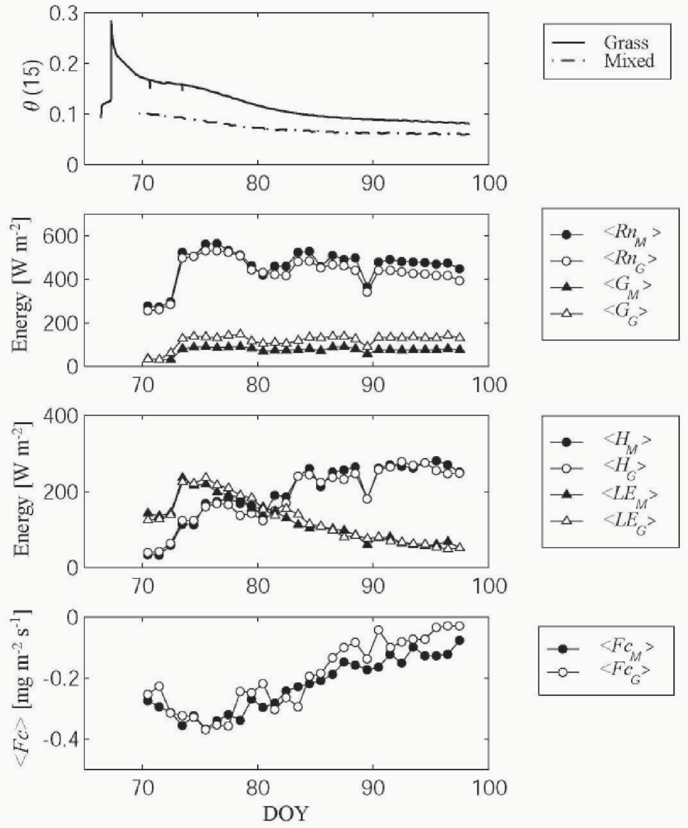

Figure 5. Time series of daily-averaged mass and energy fluxes through the drydown experiment of 2002. (From Williams and Albertson, 2004).

3.4 DEPENDENCE ON SOIL MOISTURE

The daytime transpiration fluxes (~ <*LE*>) presented in Figure 5 are not directly useful to define moisture limitation functions such as (12), but rather reflect a weighted aggregation across the fractional cover components (i.e. (1)) within the footprint.

We introduce and present in Figure 6 empirically defined field-scale soil moisture limitation functions, $\langle\beta\rangle = \langle ET\rangle / \langle PET\rangle$, for the two Ghanzi sites (see Chapter 3). Along with the data in Figure 6 we plot the piecewise linear soil moisture limitation function of (12) with critical and wilting point moisture contents obtained from literature values of trees and grasses representative of those present at the respective tower sites (Williams and Albertson, 2004 after Scholes and Walker, 1993). We note that a piecewise linear function appears to represent the data in a useful way, and that the literature values of the break points (which tend to be defined from leaf-level observations) in the function represent well the field-scale data. This is especially encouraging for our goal of identifying (with empirical support) a parsimonious model of water and carbon fluxes in savannas, in general. Furthermore, such a formulation submits itself to simple analytical treatment.

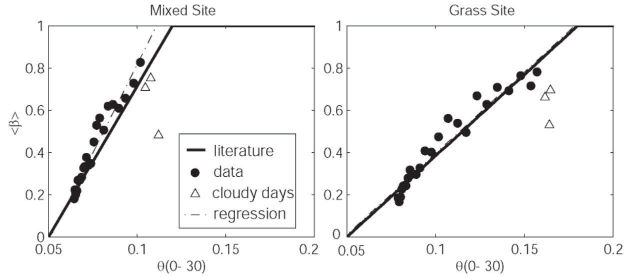

Figure 6. Field-scale observations of the ratio of <ET> to <PET> plotted against the volumetric soil moisture measured in the top 30 cm of the soil, for two towers at the Ghanzi site. (From Williams and Albertson, 2004).

3.5 ANALYTICAL TREATMENT OF INTERSTORM PERIODS

The horizontally-averaged water balance of a root zone is a first-order ordinary differential equation (ODE), c.f. (3). If we limit our focus to periods that begin some finite amount of time following rain events, then the infiltration and drainage terms will be small and, therefore, negligible in comparison to *ET*. And, furthermore if the moisture state remains below the critical value and above the wilting point as is common in semi-arid regions such as the KT and the moisture limitation function is linear in this range, then we arrive at a simple linear first-order ODE. Such an equation immediately presents an exponential time decay for the soil moisture state and, correspondingly, for *ET*,

$$ET_{daily}(t) = ET_o \exp\left[-\frac{PET_{daily}\ f_v\ \hat{t}}{d(\theta_{\mathrm{lim}} - \theta_{wp})}\right] \tag{14}$$

where ET_o is the daily evapotranspiration rate at the starting moisture content (i.e. initial condition to the solution), $f_v=f_w+f_g$, and θ_{lim} and θ_{wp} reflect field-scale aggregate values of the limiting and wilting moisture contents. Following such a list of simplifications a moment of scepticism is understandable - but hopefully it is quickly extinguished by the skill demonstrated in Figure (7). For details of the derivation and application see Williams and Albertson (2004).

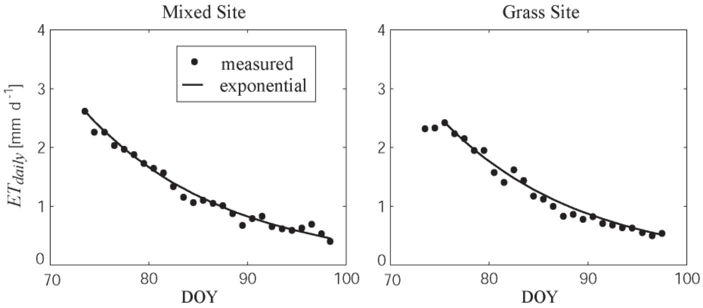

Figure 7. Field-scale observations of the decay of <ET> through time following a rainfall event for the Ghanzi site. (From Williams and Albertson, 2004).

3.6 WATER USE EFFICIENCY

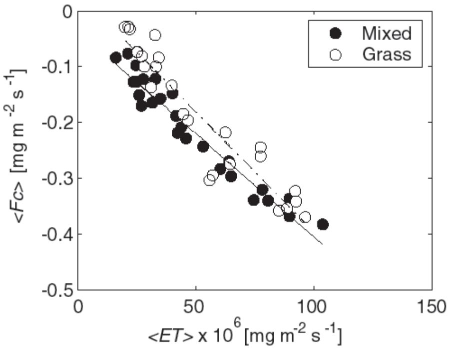

Figure 8 Field-scale observations of the relationship between NEE of CO2 (i.e. <Fc>) and <ET> for the Ghanzi site. (From Williams and Albertson, 2004).

Having established the simple and robust soil moisture dependence of evapotranspiration we proceed to explore the connection between carbon fluxes and water fluxes. As discussed in Section 2.2 the photosynthetic flux of CO_2 is related to the transpiration rate via the so-called water use efficiency, which is defined to be simply the ratio of carbon gained per unit of water lost. However, we are taking a bit of liberty to extend the use of this WUE to relate a measure of field-scale evapotranspiration to net carbon flux between the ecosystem and the atmosphere. The reasoning behind such an extension rests on the typical characteristics of savanna, those being low surface soil moisture and carbon contents that give rise to bare soil evaporation rates much lower than transpiration rates and heterotrophic (carbon) respiration rates that are low compared to photosynthesis rates during the growing season. The applicability of this approach is supported by the field-scale flux measurements as presented in Figure 8. The well-defined linear relationship between the water and carbon fluxes suggests not only that a WUE should be useful, but also that the value of the WUE (c.f. (9)) is relatively stable (constant) in time. The slight difference in the slopes relating F_c (as a field scale proxy for *Ph*) to ET (as a proxy for *T*) can be attributed to the difference in vegetation composition between the grass and mixed sites. It is important to note that C4 plants (such as many of the savanna grasses) tend to have lower values of c_* and hence higher values of WUE than C3 plants (such as the woody species) (e.g. Lecain et al. 2003). This is a likely explanation for the steeper relationship found at the site with a higher proportion of grass.

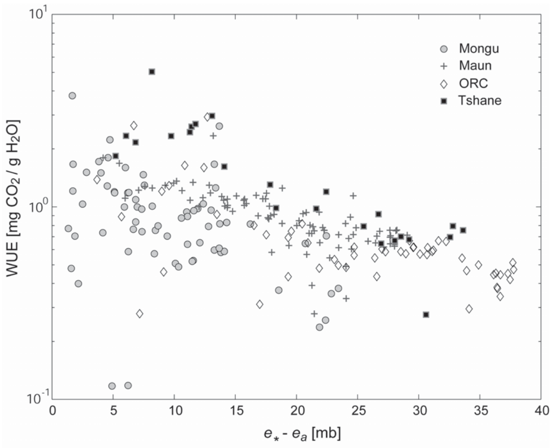

Figure 9. Field-scale measurements of WUE at the four sites shown in Figure 3 plotted against vapour pressure deficit (a measure of aridity at the vegetation-atmosphere interface). (From Scanlon and Albertson, 2004).

A further examination of the effect of land cover composition, in the sense of different PFTs is made with Figure 9. Here we present 30-minute average WUE data (which is inherently more variable than the daily-averaged WUE values presented above) collected from the four sites measured during the 2000 field campaign along the KT. The ratio of wood to grass tends to increase along the KT in the northerly direction (i.e. with increasing annual rainfall). The sites visited in the 2000 campaign from south (most arid) to north (least arid) were Tshane, ORC, Maun, and Mongu. Figure 9 shows that the WUE tends to decrease as the sites move from more to less arid, and therefore from more to less C4-grass coverage, for a given vapor pressure deficit (i.e. $e_* - e_a$ in

(9)). These findings demonstrate that a geographic (i.e. climatic) structure must be imprinted on the constant WUE to provide for a proper extension of water flux estimation into carbon flux estimation.

3.7 NET ECOSYSTEM EXCHANGE OF CARBON

The concept of a constant WUE (in a daily-averaged sense) is well suited for use with the analytical treatment of ET during the interstorm periods (c.f. Section 3.5). All that is required to predict a full evolution of daytime carbon flux through the interstorm period is to multiply (14) by the WUE constant (in this case, empirically defined from the data in Figure 8). We note an excellent agreement in Figure 10 between our field-scale measured daily carbon fluxes and those predicted by the combination of (14) and $F_c = WUE \cdot ET$. These results are encouraging, suggesting that: (i) field-scale ET in a savanna may be readily estimated by reducing a simple measure of PET by a linear function of soil moisture in the root zone, and (ii) field-scale net carbon fluxes may be linearly related to these ET fluxes through a temporally stable, but land cover-specific, water use efficiency.

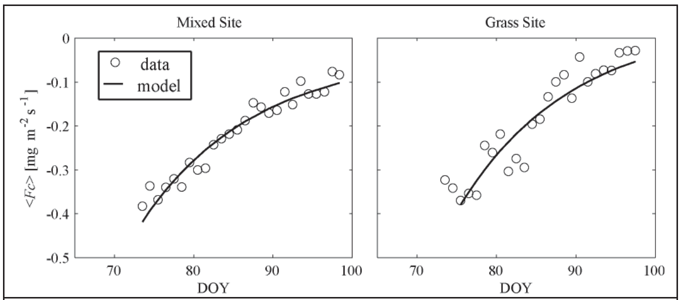

Figure 10. Field-scale observations of the decay of net CO_2 flux (i.e. $<F_c>$) following the rain event. Note that the model results are plotted with a solid line. These are for the Ghanzi site. (From Williams and Albertson, 2004).

3.8 OBSERVED CHANGE IN COMPOSITION ALONG AN ARIDITY GRADIENT

For estimation of water and carbon fluxes over larger geographical regions it is possible to use remotely sensed land cover data to identify the spatial distribution of grass and wood cover, since these two plant functional types have contrasting water use efficiencies and growth characteristics.

Scanlon et al. (2002) presented an approach to identify the geographic distribution of f_w and f_g from a combination of a remotely sensed greenness index (NDVI) dataset and a precipitation dataset. Basically, this approach makes use of historic NDVI and precipitation data along with the following heuristic argument to decompose an observed land-cover cover estimate (e.g., NDVI at some geographical location for a particular growing season) into its three components, f_w, f_g, and f_s: (i) woody vegetation cover has a high greenness (NDVI) and low sensitivity to interannual fluctuations in growing season rainfall totals, (ii) bare soil cover has a low greenness (NDVI) and a low sensitivity to interannual fluctuations in growing season rainfall totals, and (iii) grass cover has a moderate greenness (NDVI) and high sensitivity to interannual fluctuations in growing season rainfall totals. For brevity we refer the reader to Scanlon et al. (2002) for a full presentation of the details of the approach.

From the original case study along the KT we present results in Figure 11 that demonstrate the utility of this approach. Whereas in the dry year (1995) the fraction of grass cover is less than 5% all along the KT, the example wet year shows the fraction of grass ranging from 20% in the south (dry end) to > 40% in the middle to <10% in the north where the tree cover dominates. These results are directly useful for specifying the aggregate water use efficiency for any particular location along the climate gradient in any particular year.

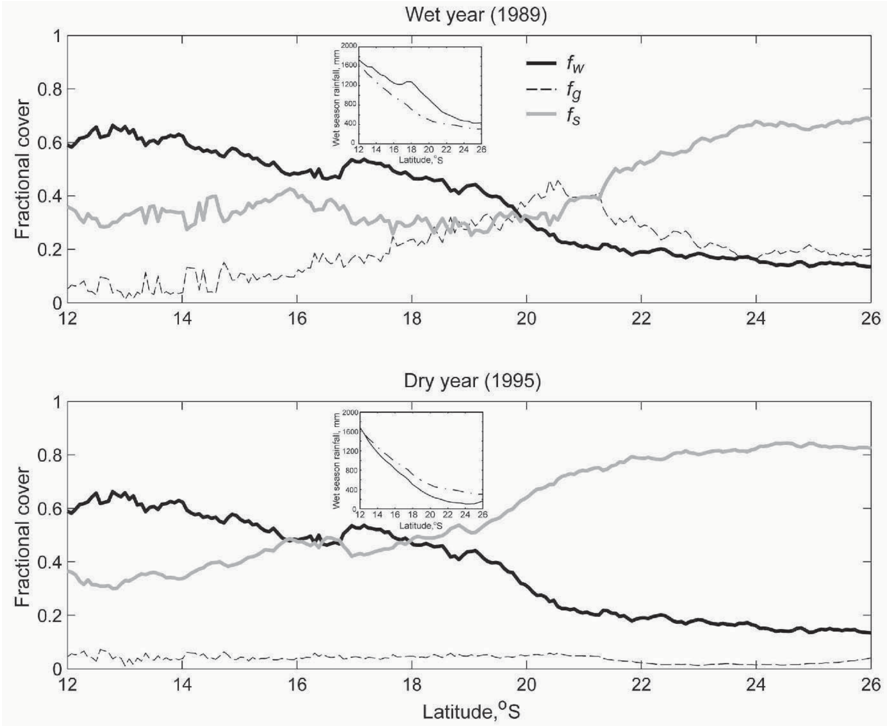

Wet year (1989)

Dry year (1995)

Fig 11. Demonstration of fractional cover estimation for contrasting wet and dry years along the KT. Note the variable nature of the grass fractional cover. The relationships between each year's precipitation distribution along the KT (solid line) and the climatological mean precipitation (dashed line) are shown in the insets. (From Scanlon et al., 2002).

3.9 PREDICTING CHANGES IN SAVANNA STRUCTURE

Our results demonstrate clearly how rainfall inputs to soil moisture stimulate temporal dynamics of plant water use and carbon exchange over interstorm periods. Now we briefly exhibit how knowledge of these functional responses can be employed for predicting changes in savanna vegetation structure. Daily growth and decay excite seasonal to interannual dynamics of leaf area and vegetation fractional cover as represented in (4). Equations 3 through 12 compile a field-scale savanna dynamics model that, when forced with daily meteorological conditions, can

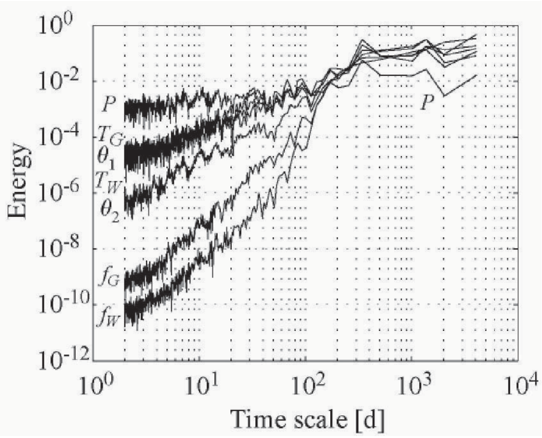

Figure 12. Spectral energy content of rainfall (P), grass and wood transpiration, shallow and deep soil moisture, and grass and wood fractional cover.

be used to simulate temporal dynamics of vegetation structure, as in Williams and Albertson (2005).

Inspecting results from a simulation spanning 1972 to 2000 reveals that energy cascades through the savanna ecohydrological system from rainfall, through daily fluxes, to structural adjustments with increasing spectral reddening (Figure 12). Thus, vegetation structure acts as a low-pass filter of rainfall fluctuations, further exemplified by the similarity between temporal traces of average annual fractional cover and a three-year moving average of annual rainfall (Figure 13). Grass cover is noticeably more responsive to annual rainfall fluctuations than is tree cover, owing to grass's relatively rapid colonization of bare ground in wet conditions and swift dieback with water stress. Thus, savanna's grass and wood functional components differ in the degree to which they modulate land-atmosphere exchanges at interannual timescales.

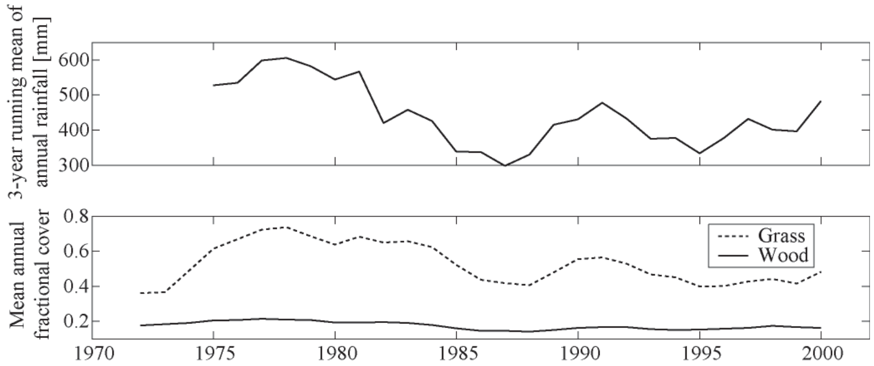

Figure 13. Time series of 3-year running mean annual rainfall and mean annual grass and wood fractional covers simulated with the model of Williams and Albertson (2005).

Changes to savanna structure through time can also be inferred from large-scale relationships between water availability and savanna composition, such as along the KT. As shown with simulation results in Figure 12, the timescales over which vegetation responds to variable climate are disparate for the particular functional forms. From an observation standpoint, satellite-derived woody fractional cover, f_w is highly correlated (spatially) with ground meteorological measurements of mean wet season rainfall ($R^2 = 0.94$) in the Kalahari region., whereas the savanna grass cover is strongly dynamic and its annual extent resonates with the amount of rainfall received in a given wet season. Models of grass growth and decay show that f_w and near-surface soil moisture are the two most important factors in controlling its annual extent (Scanlon et al., in press). The hydrological significance of the dynamic grass cover (e.g. Figure 12) is that it acts as a buffer against variability in wet season precipitation, and in doing so helps to maximize ecosystem water use. Mixed tree/grass savanna ecosystems are ideally suited to reach a dynamic equilibrium with respect to the use of a fluctuating limiting resource (water) by having functional components that respond to variability in rainfall over long timescales (woody vegetation) and short timescales (grasses) (Scanlon et al., in press). If disturbance factors such as grazing and fire are induced into the system, the efficiency of the coupling between the savanna vegetation and climate is reduced, and the altered structure can result in enhanced drainage and transport of nutrients from the root zone.

4. Conclusion

In response to observed and anticipated changes in both climate and human land use pressures there is a heightened realization of the importance to understand mechanistically how savanna vegetation structure and function respond to the dynamics of these external forcings. The potential savanna changes are likely to translate directly into both regional (livelihoods of local residents) and global (water, energy, and carbon cycle) impacts.

A simple, yet robust formulation was presented that captures the central information cascade from rainfall inputs through the water, energy, and carbon budgets. The approach was examined through the use of field data collected along the Kalahari Transect of southern Africa. By studying these interactions across such a dramatic climate gradient (i.e. the KT) we develop a confidence that the results should apply in a general sense to a wide array of savanna settings.

The field results, when analysed in the context of the proposed framework, are encouraging, suggesting that: (i) field-scale ET in a savanna may be readily estimated by reducing a simple measure of PET by a linear function of soil moisture in the root zone, and (ii) field-scale net carbon fluxes may be linear related to these ET fluxes through a temporally stable, but land cover-specific, water use efficiency. Beyond the field data, the use of remotely sensed land cover data along with rainfall data demonstrated the ability to estimate the spatial and temporal distribution of the different PFTs as needed to prescribe appropriately the water limitation function and the water use efficiency. And, finally, it was shown how an integration of the carbon fluxes into biomass changes can extend calculations of savanna function through time to present an evolving picture of the savanna structure. Not included here, but important nonetheless, is that grazing pressures and fire must be considered in (4) for long time scale predictions of savanna structural dynamics.

5. Acknowledgement

This material is based upon work supported by the National Science Foundation under grant 0243598 and by the Office of Science (BER), U.S. Department of Energy, Cooperative Agreement DE-FC02-03ER63613.

6. References

Albertson, J. D., and G. Kiely. 2001. On the structure of soil moisture time series in the context of land surface models. Journal of Hydrology 243:101-119.

Anderies, J. M., M. A. Janssen, and B. H. Walker. 2002. Grazing management, resilience, and the dynamics of a fire-driven rangeland system. Ecosystems 5:23-44.

Atjay, G. L., P. Ketner, and P. Duvigneaud. 1987. Terrestrial primary production and phytomass. Pages 129-181 in B. B. e. al., editor. The Global Carbon Cycle. SCOPE 13, John Wiley, New York.

Avissar, R., and R. A. Pielke. 1991. The impact of plant stomatal control on mesoscale atmospheric circulations. Agricultural and Forest Meteorology 54:353-372.

Bonan, G. 1998. The Land Surface Climatology of the NCAR Land Surface Model Coupled to the NCAR Community Climate Model. Journal of Climate, 11, 1307-1326.

Bounoua, L., R. DeFries, G. J. Collatz, P. Sellers, H. Khan, 2002. Effects of Land Cover Conversion on Surface Climate, Climatic Change, 52(1-2), 29 – 64.

Brutsaert, W., 1982, Evaporation into the atmosphere, Kluwer Academic Publ., Dordrecht, Holland, p. 299.

Calvet J.C., Noilhan J., Roujean J.L., Bessemoulin P., Cabelguenne M., Olioso A., and J.P. Wigneron, 1998, An interactive vegetation SVAT model tested against data from six contrasting sites, Agr. Forest Meteorol., 92 (2), 73-95.

Campbell, G. S., and J. M. Norman. 1998. An Introduction to Environmental Biophysics, 2nd edition. Springer, New York.

Carpenter, S., B. Walker, J. M. Anderies, and N. Abel. 2001. From metaphor to measurement: Resilience of what to what? Ecosystems 4:765-781.

Cayrol P., Chehbouni A., Kergoat L., Dedieu G., Mordelet P., Nouvellon Y., 2000a, Grassland modeling and monitoring with SPOT-4 VEGETATION instrument during the 1997-1999 SALSA experiment, Agric. For. Meteorol., 105, 91-115.

Cayrol P, Kergoat L, Moulin S, Dedieu G, Chehbouni A., 2000b, Calibrating a coupled SVAT-vegetation growth model with remotely sensed reflectance and surface temperature - A case study for the HAPEX-Sahel grassland sites, J. Appl. Meteorol., 39 (12), 2452-2472.

Chen, J.L., and J.F.Reynolds, 1997, GePSi: A generic plant simulator based on object-oriented principles, Ecol. Model., 94 (1), 53-66.

Clapp, R. B., and G. M. Hornberger, 1978, Empirical Equations for Some Soil Hydraulic-Properties, Water Resour. Res., 14, 601-604.

Eagleson, P. S., 2002, Ecohydrology: Darwinian Expression of Vegetation Form and Function, Cambridge University Press, New York.

Farquar, G. D., von Caemmere, S., Berry, J. A., 1980, A biochemical model of phosynthesis CO2 assimilation in leaves of C3 species, Planta, 149, 78-90.

Huntley, B. J., and B. H. Walker. 1982. Characteristic Features of Tropical Savannas - Conclusion. Ecological Studies 42:657-660.

IGBP. 1997. IGBP Report 42: The Kalahari Transect: Research on Global Change and Sustainable

IPCC. 1992. IPCC First Assessment Overview and Policymaker Summaries and 1992 IPCC Supplement. IPCC, Geneva, Switzerland.

Jacquemin, B., and J. Noilhan. 1990. Sensitivity study and validation of a land surface parameterization using the HAPEX-MOBILHY data set. Boundary Layer Meteorology 52:93-134.

Larcher, W., 1995, Physiological Plant Ecology, Springer, 506 pp.

Lecain, D.R., J.A. Morgan, A.R. Mosier, and J.A. Nelson, 2003, Soil and plant water relations determine photosynthetic responses of C-3 and C-4 grasses in a semi-arid ecosystem under elevated CO_2, Annals of Botany 92 (1): 41-52.

Lombardini, L., This volume, Responses of plants growing in dry environments.

LoSeen, D., A. Chehbouni, E. Njoku, S. Saatchi, E. Mougin, and G. Monteny, 1997, An approach to couple vegetation functioning and soil-vegetation-atmosphere-transfer models for semiarid grasslands during the HAPEX-Sahel experiment, Agric. For. Meteorol., 83 (1-2), 49-74.

Mahfouf, J. H., C. Ciret, A. Ducharne, P. Irannejad, J. Noilhan, Y. Shao, P. Thornton, L. Xue, and Z.-L. Yang. 1996. Analysis of transpiration results from the RICE and PILPS Workshop. Global and Planetary Change 13:73-88.

Moleele, N. M. and J. Mainah, 2003, Resource use conflicts: the future of the Kalahari ecosystem, Journal of Arid Environments, 54: 405–423.

Mougin, E., D. Loseen, S. Rambal, A. Gaston, and P. Hiernaux, 1995, A regional sahelian grassland model to be coupled with multispectral satellite data .1. model description and validation, Remote Sens. Environ., 52 (3), 181-193.

Nouvellon Y, Rambal S, Lo Seen D, Moran MS, Lhomme JP, Begue A, Chehbouni AG, Kerr Y., 2000, Modelling of daily fluxes of water and carbon from shortgrass steppes, Agr. Forest. Meteorol., 100 (2-3), 137-153.

Parlange, M.B., J.D. Albertson, W.E. Eichinger, A.T. Cahill and T.J.Jackson, 1999, Evaporation: Use of fast response turbulence sensors, raman lidar and passive microwave remote sensing, in: Vadose Zone Hydrology: Cutting Across Disciplines, M.B. Parlange and JW Hopmans (eds.), Oxford University Press, 260-278.

Priestley, C. H. B., and R. J. Taylor. 1972. On the assessment of surface heat flux and evaporation using large-scale parameters. Monthly Weather Review 100:81-92.

Rodriguez-Iturbe, I., P. D'Odorico, A. Porporato, and L. Ridolfi. 1999a. On the spatial and temporal links between vegetation, climate, and soil moisture. Water Resources Research 35:3709-3722.

Rodriguez-Iturbe, I., P. D'Odorico, A. Porporato, and L. Ridolfi. 1999b. Tree-grass coexistence in savannas: The role of spatial dynamics and climate fluctuations. Geophysical Research Letters 26:247-250.

Rodriguez-Iturbe, I., A. Porporato, L. Ridolfi, V. Isham, and D. R. Cox. 1999c. Probabilistic modelling of water balance at a point: the role of climate, soil and vegetation. Proceedings of the Royal Society of London Series a-Mathematical Physical and Engineering Sciences 455:3789-3805.

Rodriguez-Iturbe, I., A. Porporato, F. Laio, and L. Ridolfi. 2001. Plants in water-controlled ecosystems: active role in hydrologic processes and response to water stress - I. Scope and general outline. Advances in Water Resources 24:695-705.

Scanlon, T. M., K. K. Caylor, S. Manfreda, S. A. Levin, and I. Rodriguez-Iturbe, Dynamic response of grass cover to rainfall variability: Implications for the function and persistence of savanna ecosystems, Advances in Water Resources, 28: 291-302.

Scanlon, T. M., and J. D. Albertson. 2004. Canopy scale measurements of CO2 and water vapor exchange along a precipitation gradient in southern Africa. Global Change Biology, 10 (3): 329-341.

Scanlon, T. M., and J. D. Albertson, 2003a. Inferred controls on tree/grass composition in a savanna ecosystem: combining 16 year NDVI data with a dynamic soil moisture model. Water Resources Research 39 (8): Art. No. 1224.

Scanlon, T. M., and J. D. Albertson, 2003b. Water availability and the spatial complexity of CO2, water, and energy fluxes over a heterogeneous sparse canopy. Journal of Hydrometeorology, 4 (5): 798-809.

Scanlon, T. M., J. D. Albertson, K. K. Caylor, and C. A. Williams. 2002. Determining land surface fractional cover from NDVI and rainfall time series for a savanna ecosystem. Remote Sensing of Environment 82:376-388.

Scholes, R. J., and S. R. Archer. 1997. Tree-grass interactions in savannas. Annual Review of Ecology and Systematics 28:517-544.

Scholes, R. J., and B. H. Walker. 1993. An African savanna: synthesis of the Nylsvley study. Cambridge University Press, Cambridge, UK.

Veenendaal, E.M., O. Kolle, J. Lloyd, 2004, Seasonal variation in energy fluxes and carbon dioxide exchange for a broad-leaved semi-arid savanna (Mopane woodland) in Southern Africa, Global Change Biology, 10 (3): 318-328.

Walker, B. H., D. Ludwig, C. S. Holling, and R. M. Peterman. 1981. Stability of semi-arid savanna grazing systems. Journal of Ecology 69:473-498.

Walker, B. H. and J. L. Langridge, 1997, Predicting savanna vegetation structure on the basis of plant available moisture (PAM) and plant available nutrients (PAN): a case study from Australia, J. Biogeogr., 24, 813-825.

Walker, B., S. Carpenter, J. Anderies, N. Abel, G. Cumming, M. Janssen, L. Lebel, J. Norberg, G. D. Peterson, and R. Pritchard. 2002. Resilience management in social-ecological systems: a working hypothesis for a participatory approach. Conservation Ecology 6:art. no.-14.

Walker, B. H., editor. 1987. Determinants of tropical savannas: presentations made by savanna researchers at a workshop in Harare, Zimbabwe, December 1985. ICSU Press for the International Union of Biological Sciences, Oxford.

Williams, C.A., and J.D. Albertson, 2004, Soil moisture controls on canopy-scale water and carbon fluxes in an African savanna, Water Resources Research, Vol. 40, W09302, 14pp.

Williams, C. A. and J. D. Albertson, 2005, Contrasting short- and long-time scale effects of vegetation dynamics on water and carbon fluxes in water-limited ecosystems, in review, Water Resources Research.

Chapter 6

INTERACTIONS AND FEEDBACKS BETWEEN CLIMATE AND DRYLAND VEGETATIONS

Yongkang XUE

Department of Geography, Department of Atmospheric and Oceanic Sciences, University of California, Los Angeles, 1255 Bunche Hall. Los Angeles, CA 90095-1524, USA - e-mail: yxue@geog.ucla.edu

1. Introduction

1.1. HISTORICAL BACKGROUND OF STUDIES OF FEEDBACK AND INTERACTIONS BETWEEN VEGETATION AND CLIMATE

Interactions and feedbacks between terrestrial ecosystem processes and climate mainly take effect through biophysical and biogeo-chemical processes and affect atmospheric circulation, regional water cycles and the carbon budget. In biophysical processes, the atmosphere and the land-surface exchange radiation, heat, and momentum fluxes, as well as water vapor. Biophysical feedbacks affect atmospheric conditions by modifying evaporation, runoff, energy partitioning between latent heat and sensible heat fluxes, and upward radiation fluxes. Biogeochemical processes affect climate by altering atmospheric composition and the atmospheric radiation balance, especially by modifying exchange of trace gases, such as carbon dioxide and aerosols, between terrestrial ecosystems and the atmosphere. Figure 1 is a schematic diagram showing the exchange processes between land and atmosphere. This chapter mainly focuses on biophysical feedback.

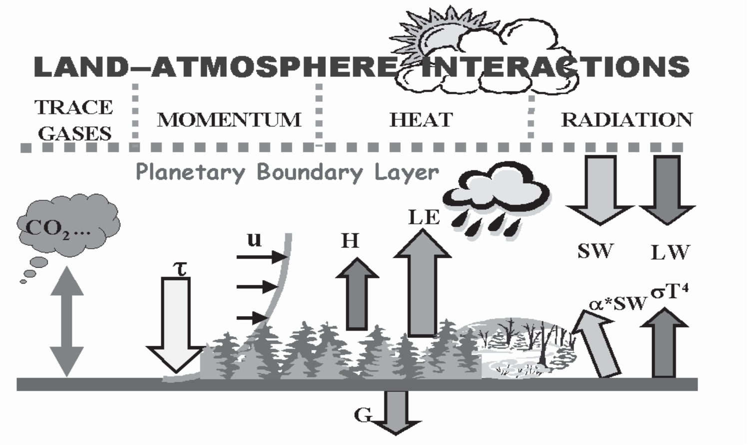

Figure 1. Schematic diagram of land/atmosphere interactions.

Although it is well recognized that climate exerts major control on the distribution of plant species and plant community composition, mainly through precipitation and temperature (e.g., Woodward, 1987; Mannion, 1997), the interactive effects, however, were largely ignored until the 1970s when more observational evidence and modeling results emerged to support such a notion. Charney (1975), motivated by unprecedented drought in semiarid Sahelian Africa during the late 1960s and the early 1970s, conducted the first biophysical feedback study using a 2-dimensional

P. D'Odorico and A. Porporato (eds.), Dryland Ecohydrology, 85–105.

simple atmospheric model. He noted, through the use of satellite data, that high albedo of the Sahara Desert contributed to a substantial radiative sink in that region and speculated that any changes in land-surface albedo due to anthropogenic effects would modify the radiation budget and then the atmospheric circulation and precipitation. His study showed that, by increasing the surface albedo over all of North Africa from 0.14 (a typical albedo for vegetation) to 0.35 (an albedo for desert) in the 2-dimensional atmospheric model, more short wave radiation was reflected back from the land-surface. This reduction in available energy contributed to a lower surface temperature and a loss of net radiative heating in the atmosphere, which produced sinking and drying of the air aloft and, therefore, a reduction of precipitation. Since less precipitation would reduce the soil moisture and therefore increase surface albedo, this albedo effect produces a positive feedback.

Another important biophysical feedback process involves the soil moisture. In a sensitivity experiment, Shukla and Mintz (1982) specified two initial soil moisture conditions globally in a general circulation model (GCM). In one experiment, the land-surface was saturated, and in another one, the land-surface was completely dry. Shukla and Mintz showed that, compared with the dry case, the wet surface condition created a substantially higher evaporation rate and then a higher precipitation rate over most parts of the world, which would further enhance the evaporation and produce a positive feedback. Meanwhile, the surface temperature became lower in the wet case because most of the net radiation was converted to latent heat flux.

In addition to albedo and soil moisture conditions, the role of surface roughness in biophysical feedbacks has also been explored. In a GCM sensitivity study (Sud et al., 1988), two surface roughness lengths were specified over land: one was 45 cm, a typical value for a vegetated surface, and another was 0.02 cm, a value for bare ground. It was found that lower surface roughness in the GCM reduced the surface stress and the momentum exchange, affecting the convergence of the horizontal water vapor transport in the boundary layer and reducing the precipitation. Lower precipitation could cause land degradation and further reduce the surface roughness length, also producing a positive feedback.

These three factors (albedo, soil moisture, and surface roughness length) were identified first and are still considered as among primary feedback mechanisms. However, the real atmosphere-biosphere interaction processes are very complex and involve more vegetation and soil properties. A comprehensive understanding of land-surface/atmosphere interaction can be obtained only when all major components that affect the surface energy and mass balance are considered. Encouraged by the discoveries from the early land/atmosphere studies, more complex biophysical models, such as the Biosphere-Atmosphere Transfer Scheme (BATS, Dickinson et al., 1986) and the Simple Biosphere Model (SiB, Sellers et al., 1986), have been developed since the early 1980s to understand the surface feedback mechanisms. Unlike previous land models, which regarded the land-surface properties that regulate the land/atmosphere interactions as separable parameters and therefore could be independently prescribed as boundary conditions with a GCM, these new generation models specify surface properties as mutually consistent properties and intend to model the major controlling biophysical processes with a consistent and coherent philosophy and strategy.

These biophysical models have first been applied to assess and evaluate the climate and hydrological impact of changes in land cover and land use because tropical forests and other vegetated surfaces in South America, Africa, and Southeast Asia are being severely deforested and desertified for agriculture and other purposes. Since complex land-surface schemes are coupled to GCMs, one can attempt to model in a realistic manner the changes at the surface and study the impact on climate. The first deforestation experiment was conducted by Dickinson and Henderson-Sellers in 1988. Since then, the experiments have been repeated with nearly all GCMs coupled to complex land-surface schemes (Nobre et al., 2004). In the meantime, the impact of desertification (See Chapter 18 for an extensive analysis of desertification processes) has also been investigated (e.g., Xue et al., 1990, 2004a). In this chapter, we will focus on the land/atmosphere interactions over drylands.

In addition to affecting the atmosphere through direct modification of water and energy balances over the land-surface, arid and semiarid regions contribute significant amounts of dust to the atmosphere. Chapter 9 discusses in detail the physical mechanisms controlling dust emissions from arid and semiarid landscapes. Mineral dust is a highly visible and persistent component of some drylands' (e.g., the Sahel's) climates (Nicholson, 2000). The dust can affect climate by scattering and absorbing solar radiation and by absorbing and emitting infrared radiation. Mineral dust aerosols have been largely ignored because it was thought that their scattering efficiency and concentrations were too low to have a substantial effect on climate. However, Li et al. (1996) have shown that, based on measurements of the light-scattering properties of North African dust that reached Barbados (13°15'N, 59°30'W) from 1984 to 1994, annual mean dust concentration is 16 times greater than that of non-sea-salt, and the dust's scattering contributes 56% of the total aerosol scattering coefficient of dust, non-sea-salt, and sea salt. However, whether dust would cause cooling or heating is a complex issue that depends on many factors and is not readily apparent from simple theoretical considerations (Nicholson, 2000).

The complex feedbacks are also manifested in the biophysical processes. Although all the biophysical hypotheses discussed above appear plausible, whether they occur in the real world and whether they are indeed important in climate processes needs to be tested using observational data. For instance, satellite data show that the changes in surface albedo in the Sahel region may range around 0.1 (Nicholson et al., 1998), not 0.23 as used by Charney (1975). Furthermore, the surface temperatures in areas associated with desertification are higher rather than lower, as Charney's study indicated (Ripley, 1976). These results imply that a feedback process in the Sahel caused by severe drought through albedo increase may not be a dominant factor or may not even have occurred.

1.2. IMPORTANT CHARACTERISTICS OF LAND/ATMOSPHERE INTERACTIONS IN SEMIARID REGIONS

Semiarid areas cover a substantial part of the Earth's land-surface (Figure 2), and the climate is variable but sufficient to sustain vegetation and human settlement (UNEP, 1992). As indicated in the last section, semiarid areas such as the Sahel have been hot spots in vegetation and climate interaction studies. The Sahel is a semiarid area located between the Sahara desert to the north and the savanna lands to the south (roughly between 10°N and 20°N) and extending from the Atlantic Ocean eastward to Ethiopia. It was the first region where the hypothesis on biophysical feedback was tested (Charney, 1975).

Several important factors make these semiarid areas sensitive to vegetation and climate interactions. Many semiarid areas, such as the Sahel and northern China, are located in transects from monsoon regions to inland arid regions (Figure 2). It should be noted that recent information shows that the semiarid area in China actually extends from Inner Mongolia to the southern part of the Tibetan Plateau (Fu, 1992), and Figure 2 underestimates the semiarid area in China (see Figure 3). The precipitation in these areas mainly relies on summer monsoons, but the monsoon rainfall normally exhibits very high interannual variability. For example, in East Asia, often the amplitude of the interannual variability can be as large as the mean state. The water supply is limited and variable. Any changes in the summer monsoon would have substantial impact on the regional climate and water supply.

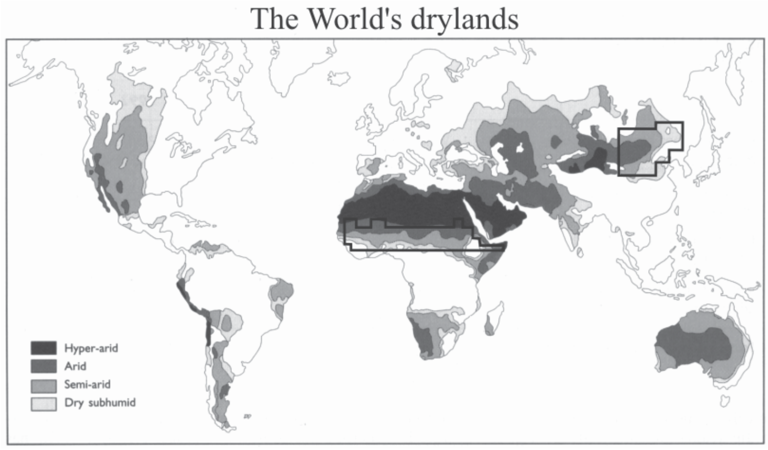

Figure 2. The world's drylands (after UNEP, 1992). The areas enclosed by the dark line are assigned degradation areas in numerical experiments discussed in the text.

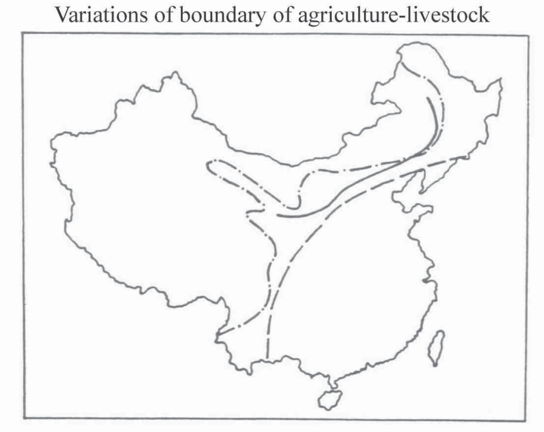

Figure 3. Changes of boundary of agriculture/livestock region since 1700 b.p. Dashed line is 1700-2100 b.p.; dotted and dashed line is 50 b.p.; solid line is 1980s. (Fu, 1992).

The boundaries of the semiarid areas are sensitive to natural climate variations as well as anthropogenic effects (Rasool, 1984; Fu, 1992). Figure 3 shows the changes of the southern boundary of the semiarid zone in China during the past 2000 years. The substantial northwestward shift of the boundary since 1700-2100 before present (b.p.) was mainly due to the development of agriculture. Because agricultural development strongly depends on water availability, the southern boundary of the semiarid region is consistent with the boundary of agriculture and livestock husbandry. The change between the 1940s and the 1980s might be due to increasing aridity (Fu, 1992) as well as land degradation (Zhu et al., 1988). Changes in boundaries of the semiarid area also occurred in the Sahel during the past million years (Rasool, 1984; Kutzbach et al., 1996). Studies have shown that the boundaries varied even during the past decades, but with quantitative disagreements (e.g., Tucker et al., 1991; Hulme and Kelly, 1993; Nicholson et al., 1998). These variations in boundaries indicate that the semiarid regions are vulnerable to climate variations.

Land degradation has occurred in the semiarid regions, such as the Sahel and East Asia, and has been reported in numerous documents (e.g., Dregne, 1983; Zhu et al., 1988; UNEP, 1992; Middleton, 1999; Goudie, 2000; Reynolds and Smith, 2002). In addition to natural processes (Chapter 8), anthropogenic effects due to population pressure play an important role in land degradation (see Chapter 18). These effects include over-exploitation of land resources by over-grazing, woodcutting, poor irrigation, and the destruction of woody vegetation. Soil can be eroded, salinized, or impoverished. Water can be lost through pollution or overuse. Improper land management may also result in wind and water erosion (Dregne, 1983; Zhu et al., 1988; Middleton, 1999; Goudie, 2000). Furthermore, the limited and variable water supply in semiarid regions leaves little margin for error. Nearly all drylands and their inhabitants are at constant risk from land degradation. For example, in northern China there are vast areas of desertification-prone land (about 158,000 km^2), and about 176,000 km^2 already became desertified during the 1980s. The desertified area has expanded at a rate of 1560 km^2 per year from the 1950s to the 1970s, associated with the population increase during that time. For example, the population density of Changhan O'bao, Yulin County, in northern China was 340 person km^{-2} in 1949, rising to 480 person km^{-2} during 1961-1963 and to 726 person km^{-2} during 1975-1977 (Zhu et al., 1988). The desertification there can be classified into three types: desertification of sandy steppes, reactivation of fixed dunes and encroachment of sand dunes. Table 1 shows the development of desertification in some regions of Inner Mongolia from the mid-1970s through the mid-1980s. Although the desertification extent was slightly reduced in two small regions, the total amount of desertified land has increased significantly. Several large areas (in Table 1) almost doubled their desertified area during these ten years.

Table 1: The development of desertification in Inner Mongolia (From Zhu et al., 1988).

Regions	Representative Region (km^2)	Desertified land in mid 1970		Desertified land in mid 1980		Period
		Area (km^2)	%	Area (km^2)	%	
Chahar	9,050	2848	31.5	5,992	66.1	1975-87
Ulanqab	46,660	2,031	4.4	4,055	8.7	1975-87
South	6,551	5,729	87.5	5,248	80.1	1977-86
Mid	2,709	1,270	46.9	1,152	42.5	1974-88
Mid Alxa	1,573	1,171	74.5	1,308	83.2	1974-84
West Alqa	16,200	3,480	21.5	5,955	36.8	1975-86
North	17,250	2,524	14.6	4,608	26.7	1975-87

Some semiarid regions, such as the Sahel, northern China, much of India, and South Africa, experience seasonal drought, where drought conditions prevail for part of the year but are balanced by a wet season (Kemp, 1994). If for some reason the rainy season is curtailed, the consequences could be devastating. It is not surprising that areas such as the Sahel have experienced the world's most spectacular and catastrophic droughts. Observational data show that only two regions of the world, the Sahel and East Asia, experienced significant droughts at continental scales during the 1980s (Xue and Fennessy, 2002). Since the late 1960s, a persistent drought in the Sahel has lasted for more than 30 years. Although rainfall was not as scarce in the 1990s as in the 1980s, it was still below the climatological average. Observations in China from 1951 to 1990 also reveal that, in general, the climate has been drying since the 1950s (Weng et al., 1999). Both southern and northern China have become increasingly dry from the 1950s to the 1980s, but rainfall has increased in central China, the Changjiang (Yangtze) River region. Thus, the rainfall anomaly has a negative-positive-negative (N-P-N) pattern. Because of the significant implications of such droughts in these highly populated areas, the possible causes of droughts, especially the contribution of land degradation, are much of the focus of land-atmosphere interaction studies (e.g., Charney, 1975; Laval and Picon, 1986; Kitoh et al., 1988; Xue and Shukla, 1993, 1996; Xue, 1996, 1997).

Another important aspect of semiarid areas is the transportation of significant amounts of dust produced in these areas to other regions (Chapter 9). For instance, the Sahara including the Sahelian area is a major source of dust in the troposphere. Between 100 and 400 million tons of dust every year are blown over the Atlantic and reach Barbados and Miami (Prospero et al., 1981). East Asian dust rises from the spring dust storms that originate in the arid Gobi Desert of Mongolia and China. It then travels a long distance by the westerlies and sometimes reaches North America (Tratt et al., 2001). The frequency of dust storms in East Asia has increased from an average of 5 times per year during the 1950s to around 23 times per year during the 1990s. Since such a large-scale phenomenon has an important influence on radiative transfer in the atmosphere and then the climate, it is imperative to understand the causes of the increase of dust storms and the consequences of their interactions with the climate.

2. Basic concepts

The land-surface acts as the lower boundary for the atmosphere and exchanges energy and mass with the atmosphere across the air-land interface. Although the interaction and feedback between vegetation and climate are very complex, as indicated in Section 1.1, and generally non-linear, these processes are all based on the water and energy balances at the surface. The net radiation at the land-surface is defined as follows:

$$\text{Net Radiation} = (1-\alpha)\, SW\downarrow + (LW\downarrow - \varepsilon\sigma T^4), \tag{1}$$

and it is partitioned into four components:

$$\text{Net Radiation} = (H + LE + Gsub + PH), \tag{2}$$

where α is surface albedo, $SW\downarrow$ is downward short wave radiation, $LW\downarrow$ is downward long wave radiation, ε is surface emissivity, σ is the Stefan-Boltzmann constant, T is surface temperature, H is sensible heat flux, LE is latent heat flux, Gsub is heat flux to or from soil, and PH is energy used for photosynthesis. The land-surface water balance may be written as:

$$\Delta G_w = P + I - E - R, \tag{3}$$

where ΔG_w is change of water storage at and below the surface, P is precipitation, I is irrigation, E is evapotranspiration, and R is runoff. Any changes in the components listed in equations (1)-(3) would affect the interactions between climate and vegetation. Among these components, PH is less than 1% of absorbed short wave radiation (Sellers, 1999). Gsub is a relatively small term when averaged over a day or longer, seldomly more than about 10% of net radiation. E and H, as well as their ratio, play a very important role in determining the surface water and energy balances.

The atmosphere influences vegetation through precipitations, temperature, water vapor, trace gasses, winds, and downward short wave and long wave radiation. The biosphere affects the atmosphere through surface albedo, surface temperature, and the partitioning of net radiation between sensible heat and latent heat fluxes, as well as partitioning of surface water into evaporation, soil moisture, and runoff. Surface resistances, which are controlled by vegetation structure and distribution, photosynthetic processes, and atmospheric and soil conditions, play a crucial role in the energy and water exchange across the interface.

Equations (1)-(3) provide the basis for vegetation and climate interaction, yet the real land-surface/climate interactions are complex and depend on many factors, such as the background atmospheric circulation, geographical locations, moisture source, etc. Even in some simple sensitivity studies, such as Shukla and Mintz' study (1982), in which the initial soil moisture in two cases was either completely dry or completely wet over global land-surfaces, the interaction was complex. Although the results in the dry case were generally dryer over most parts of the world, some places were wetter than in the wet case.

All three biophysical feedback studies (albedo, soil moisture, and surface roughness length) introduced in Section 1.1 show a positive feedback, but theoretically, negative feedback is also possible for these three effects depending upon the response in cloud cover. For example, high surface albedo causes lower net radiation and evaporation and then lowers precipitation. However, it also reduces cloud cover, which permits more solar radiation to reach the ground, which may compensate for the net radiation loss and produce higher evaporation and precipitation--a negative feedback. Similar negative feedback could occur for the changes in soil moisture and roughness length when the cloud effects become dominant. Nevertheless, thus far most feedback studies show that the positive feedback processes are dominant for these three factors.

Because of the complexity of interactions and feedback, there is no universal formula that enables explanation of every aspect in these processes. In this paper, we present several typical case studies related to arid and semiarid regions to facilitate understanding of the mechanisms in this field.

3. Models

Most feedback and interaction studies are normally conducted with coupled atmospheric GCM/land-surface models. The atmospheric GCMs mainly describe the movement of energy, momentum, and mass including different traces, as well as their conservation, in terms of basic flow dynamic and physical principles. They are designed to simulate the atmospheric climate. The physical processes in a GCM normally include radiative transfer, convective activities, cloud formation and cloud/radiation interactions, and heat and mass transfer in the planetary boundary layer and surface layer. The dynamics are governed by heating as well as the orography.

The models are divided into several vertical layers. At the surface, sea surface temperature (SST), sea and land ice, snow, vegetation, and soil are either prescribed or simulated by various parameterizations. For most land/atmosphere interaction studies, the surface processes are simulated by a variety of surface models with different degrees of complication. The following description of the coupling process in a coupled climate model is based on the Simplified Simple Biosphere Model (SSiB, Xue et al., 1991). For the numerical simulations, a world vegetation map, which specifies vegetation and soil types, is read into the coupled surface-atmosphere model to provide the land-surface conditions. Different vegetation and soil properties, including leaf area index (LAI), leaf reflectance, soil hydraulic conductivity, and surface roughness length, are defined for each vegetation type, and some vary with the month. These parameters plus solar zenith angle, snow cover, and soil moisture determine surface albedo, upward short wave radiation (SW, w m^{-2}) and the surface radiation budget.

With knowledge of the surface state and the atmospheric conditions at the lowest model level in the GCM, including temperature T_r (K), humidity Q_r (kg kg^{-1}), wind field U_r (m s^{-1}), and precipitation P (mm day^{-1}), the surface aerodynamic resistance r_a(s m^{-1}), stomatal resistance r_c(s m^{-1}), and soil resistance r_{soil}(s m^{-1}) can be calculated. These resistances are used to obtain the latent heat flux LE (w m^{-2}), sensible heat flux H (w m^{-2}), and momentum flux τ (kg m^{-2} s^{-1}). Meanwhile, the surface state variables, including soil wetness W_1, W_2, W_3 (the fraction of soil water content relative to saturation) for three soil layers, temperatures of the canopy T_c (K), near-surface soil layer T_{gs} (K), and deep-soil layer T_d (K), snow depth on the ground W_g (m), and intercepted water on the canopy W_c (m), are updated. Figure 4 is the process diagram for a coupled atmosphere-biosphere model. The solid lines indicate the atmospheric forcing and specified variables and parameters for SSiB. The dashed lines represent the effects from the surface to the atmosphere. For the sake of simplicity, secondary connections are omitted in the figure.

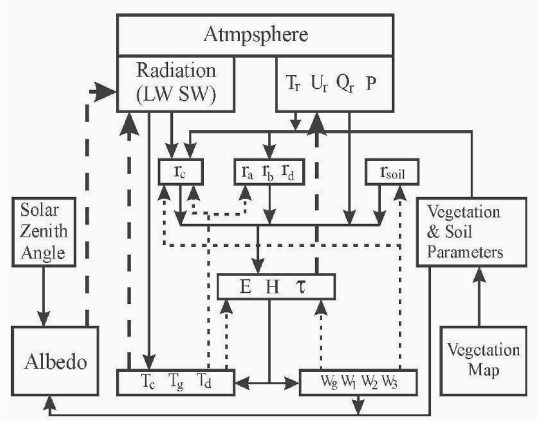

Figure 4. Computational flow diagram based on the SSiB. Symbols are defined in the text.

4. Biophysical feedback

4.1. REGIONAL CLIMATE AND CLIMATE ANOMALIES IN THE SAHEL AND EAST ASIA

Since the Sahel and East Asia both experienced significant continental scale anomalies in precipitation and land degradation during the 1980s, studies have been conducted to investigate the role of biophysical feedback in these anomalies. The Sahel is a bioclimatic zone of predominantly annual grasses with shrubs, trees, and drought-tolerant crops, receiving a mean annual rainfall of between 150 and 600 mm per year. Soils in this region are dominated by a sand sheet of varying depth, usually resulting in unstructured, free-draining soils with low nutrient content (Xue et al., 2004a).

The Sahel is characterized by the strong seasonality of the climate with a short rainy season (2-4 months) caused by the northward movement of the intertropical convergence zone (ITCZ) in the northern summer, which causes humid air from the Gulf of Guinea to undercut the dry north-easterly air. Rainfall in the Sahel is characterized by high spatial and temporal variability, both within and between seasons, and by a high north-south gradient in the region. Not only is year-to-year variability high, but also longer dryer or wetter periods may continue over a number of years. The summer climate is dominated by the West African monsoon system. The monsoon circulation is forced and maintained by thermal contrast between the continent and adjacent oceanic regions, and by latent heat released in the hydrological cycle. The continental-scale land mass and relatively flat orography (excluding the eastern Sahel) warrant that land-surface/atmosphere interactions play a major role in the regional climate and also make such interactions relatively easy to detect in model simulations.

In addition, investigations revealed that the temperature has increased in the Sahel during dry years (e.g., Schupelius, 1976). Observed temperature data, provided by the Oak Ridge National Laboratory (Vose et al., 1992), have also shown that the summer surface temperature over the Sahel region was greater by 1-2°C during the summers of the 1980s compared with the 1950s.

In East Asia, a semiarid zone extends from the southern part of the Tibetan plateau to the Inner Mongolian grasslands as indicated in Section 1.2 (Figures 2, 3). Meanwhile, the humid monsoon climate maintains a meridionally-oriented dense vegetation zone called the “green belt” to the east of the semiarid zone from tropical southeast Asia to sub-polar Siberia (Fu et al., 2003). Bordered by the Tibetan Plateau to the west, the Eurasian landmass to the northwest, and the vast Pacific Ocean to the south and east, East Asia has experienced one of the most pronounced monsoon climates of the globe for centuries. The regional climate in East Asia is dominated by summer and winter monsoon systems that consist of the Walker circulation going east-west and the cross-equatorial circulation going south-north (Webster et al., 1998). Due to the massiveness of the Eurasian continent, land-surface characteristics are also considered to play an important role in modulating the monsoon circulation and surface hydrology (Webster, 1987).

4.2. FEEDBACK STUDIES

Because of the significant land degradation in the Sahel (Dregne, 1983; Middleton, 1999), the feedback of land cover change has been the focus of most biophysical feedback studies on Sahelian climate change, especially on the causes of the unprecedented long-term drought. In this section, the results from our studies (Xue and Shukla, 1993, 1996; Xue, 1997; Clark et al., 2001) are briefly presented. In these studies, with a coupled Center for Ocean-Land-Atmosphere study (COLA) GCM/SSiB model, the land-surface conditions (i.e., the vegetation types) over the Sahel were changed to assess such interactions and to understand the mechanisms involved.

Table 2: Vegetation parameters for five vegetation types.

	Savannah	Grasslands	Shrubs with ground cover	Shrubs with bare soil	Desert
Mean surface albedo	0.20	0.23	0.20	0.28	0.32
Roughness length* (m)	0.95	0.08	0.25	0.06	0.01
LAI*	4.12	3.80	0.86	0.31	0
Greenness*	0.81	0.70	0.70	0.71	0
Minimum stomatal resistance (s/m)	282	117	1049	1049	N/A
Vegetation cover	0.3	0.9	0.1	0.1	0
Total depth of three soil layers (m)	3.5	1.50	1.5	1.5	0.49
Hydraulic conductivity of saturated soil (m/s)	0.2E-4	0.2E-4	0.176E-3	0.176E-3	0.176E-3
VSMC at the wilting level**	0.13	0.13	0.05	0.04	N/A

* *The numbers are for the means of June, July, and August.*

** *VSMC is the volumetric soil moisture content.*

Two model simulations were conducted: one has normal land cover conditions and another has degraded conditions over the Sahel. For land-surface degradation simulations, the normal vegetation types, savannah and shrubs with ground cover, in a Sahel-specified degradation area are changed to shrubs with bare soil that would result from land degradation (Figure 2), altering the prescribed vegetation and soil properties (Table 2). The selections of the degradation areas are based on the world vegetation map (UNEP, 1992).

To explore the impact of biophysical feedbacks in the Sahel, in particular land degradation, on seasonal climate variations and land-surface water balance, the coupled model has been integrated over several multi-year periods, using different initial atmospheric conditions. To separate the real climate signals from GCM model internal variability, ensemble means were used to present the model results. Climatological sea surface temperatures (SST) were used for all simulations as the lower atmospheric boundary conditions over the oceans. Therefore, the effects of the ocean are excluded when we determine the difference between these simulations. The ensemble means with climatological land-surface properties are labeled ‘C’ and those for land degradation simulation ‘D’ in this chapter.

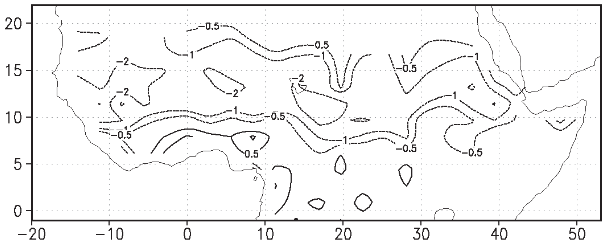
(a) observed JAS precipitation diff (80s – 50s) [mm/day]

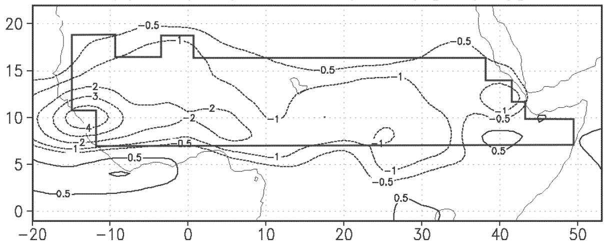
(b) JAS precipitation diff (D – C) [mm/day]

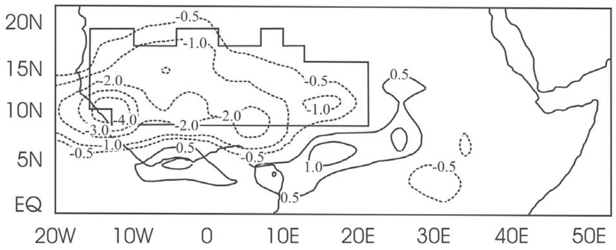
(c) JAS precipitation diff (D2 - C2) [mm/day]

Figure 5. JAS mean precipitation (mm day^{-1}). (a) Observed rainfall differences between 1980s and 1950s; (b) ensemble D minus ensemble C; (c) ensemble D2 minus ensemble C2 (Clack et al., 2001). The areas enclosed by the dark line are assigned desertification areas in numerical experiments.

The seasonal means of precipitation over a test area (from 9°N to 17°N and 15°W to 43°E), which includes most of the degraded area, and July-August-September (JAS) rainfall differences between experiments C and D are shown in Table 3 and Figure 5b, respectively. Table 3 shows that the model produced reasonable seasonal variation in precipitation climatology, which is crucial for credible studies of the impact of climate anomalies. Precipitation in JAS was reduced by 39 mm month^{-1}, close to the 45 mm month^{-1} observed reduction. The simulated spring precipitation anomalies were too high, compared to observed data. Latest observations indicate that the vegetation in this area starts growing in May (e.g., Gash et al., 1997), but model-specified vegetation grows in early spring. This inconsistency may cause the discrepancy in the model’s spring simulation.

The JAS rainfall is reduced in the degraded area, but increases slightly to the south. This dipole pattern is consistent with the observed pattern for climate anomalies (Figure 5a). The rainfall changes are significant at the 90% confidence level in most test areas. Charney’s hypothesis of biophysical feedback has been challenged because his albedo change has not been found in the real world and the cooling caused by high surface albedo is also not supported by observations (e.g., Ripley, 1976; Nicholson et al., 1998). The study presented here shows that the model is still able to produce a significant biophysical feedback even with the albedo change being about 0.1 (Table 3), which is much more in line with observed albedo change (Nicholson, 2002). Another challenge regards the changes in land degradation area. In early studies (e.g., Charney et al., 1977), the specified area changes were very large and arbitrary. However, if dramatic land-cover changes in that experiment had not produced substantial biophysical feedback in climate, any further investigations would have been in vain. In later studies (as presented in this chapter), the land cover changes were based on the world desertification map (UNEP, 1992). This map, however, may not accurately represent worldwide desertification (Nicholson, 2002). Since we may never know the exact extent and degree of real land degradation in the last fifty years, another set of tests was designed to investigate how the extent of specified land-surface changes may affect the results. Five subregions were degraded in turn: northern Sahel, southern Sahel, West Africa, East Africa, and the coastal area along the Gulf of Guinea (Clark et al., 2001). The results indicate that degradation in West African Sahel or southern Sahel alone was able to produce very significant reductions of rainfall. Figure 5c shows the results from the West African experiment. D2 minus C2 in the figure represents the difference between the simulations with desertification in West African and normal vegetation conditions.

The JAS surface air temperature is higher in the degraded simulation than in the control, consistent with the observed JAS temperature difference between the 1980s and the 1950s. In the test area, the simulated surface air temperature increases by 0.8 K, close to the observed increase over the same area, 1.1 K. The simulated soil moisture, surface runoff, and subsurface drainage also decrease, consistent with the reduction in rainfall.

Table 3: Seasonal mean precipitation (mm month^{-1}) over the test area.

Season	JFM	AMJ	JAS	OND
Observed climatology	4(3)	47(26)	155(143)	15(11)
Observed difference between 1980s and 1950s	-1(-1)	-7(-5)	-45(-43)	-6(-4)
Simulated precipitation in ensemble C	9	72	130	21
Difference between ensembles D and C	-6	-27	-39	-8

Note: The observational data are from S. Nicholson (1993) as well as M. Hulme (1992, in parentheses).

The relationship between land-surface degradation in the semiarid Mongolian and Inner Mongolian grasslands and the drought in East Asia has also been studied in numerical simulations with the coupled model (Xue, 1996). The vegetation in the degraded area in the COLA GCM was changed from grassland to bare soil (Figures 2, 6b). Six integrations over the East Asian summer monsoon period (from June 1 through August) were conducted, using different initial atmospheric conditions. The ensemble means with climatological land-surface properties are labeled ‘CA’ and those for land degradation simulation ‘DA’ in this chapter. The results indicate that degradation of the grassland could have a substantial impact on the regional climate and on some important features of the East Asian summer monsoon. In the degraded area and the region around it, a reduction in evaporation is accompanied by reduced rainfall and increased surface temperature, which is consistent with the observed rainfall reduction there. The studies of both regions show that the land-atmosphere interaction due to land degradation weakens the monsoonal flow. The area influenced by land cover change extends considerably beyond the semiarid area where degradation was specified.

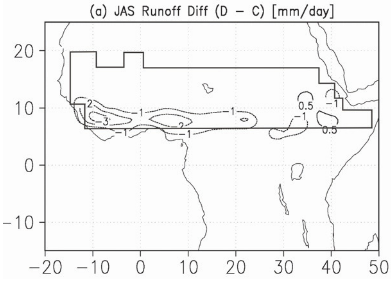

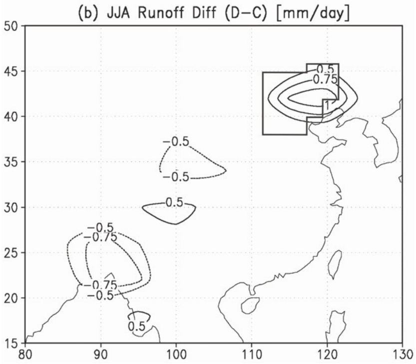

Figure 6. Runoff (mm day^{-1}*) (a) JAS ensemble D minus ensemble C; (b) JJA ensemble DA minus ensemble CA. The areas enclosed by the dark line are assigned desertification areas in numerical experiments.*

Land degradation has a substantial impact on runoff (Figure 6). The runoff was reduced in degraded and nearby areas in the Sahel case, but it was increased over the desertification area in the East Asian case. Outside the desertification area, the changes in runoff are simply in response to the precipitation variations. The simulation length caused the different responses in simulations. The Sahel simulations lasted for several years, and the runoff reached an equilibrium condition. Its reduction was a response to the reduction in precipitation. The East Asian simulations only lasted for three months, and the results show that when the soil became sandy, water holding capacity and evaporation were reduced, which led to the increase in runoff. At this transient stage, the surface soil and vegetation condition, not the precipitation reduction, was the dominant factor in influencing the runoff, which also appeared in the first year's simulation in the Sahel case.

4.3. MECHANISMS

The simulated biophysical feedbacks discussed in the last session are caused by the specified changes in land conditions, which affect the atmosphere mainly through modulating the hydrological processes and energy balance at the surface (see discussions in Section 2).

Table 4 lists the major differences between the degradation and control experiments in the test areas, which cover most degradation areas in the Sahel and East Asia. More short wave radiation is reflected from the surface as a result of the higher albedo that exists after land degradation, but this loss is partially diminished by the increased incoming short wave radiation due to less cloudiness in the drier atmosphere. The net long wave radiation is reduced because the decreased cloud cover and water vapor in the degradation simulations reduce incoming long wave radiation at the surface and the higher surface temperature increases outgoing long wave radiation (Table 4).

Table 4: Differences in energy and water balance between D and C over the Sahelian test area.

	Sahel		East Asia (JJA)
	JAS	Annual	
Latent heat flux at surface	-21	-14.5	-20
Sensible heat flux at surface	1	-10	-3
Net short wave flux at surface	-9	-15.3	-10
Net long wave flux at surface	-11	-9.3	-13
Cloud cover	-0.08	-0.058	-0.04
Outgoing long wave flux at top	10	6.8	-3.8
Precipitation	-39	-20.1	-17
Evaporation at surface	-24	-15.7	-21
Moisture flux convergence	-22	-5.5	-3
Runoff	-5	-2.5	0.2

* The units are W m^{-2} for fluxes; mm $month^{-1}$ for precipitation, evaporation, moisture flux convergence, and runoff; and no unit for cloud cover fraction.

** The test area for the Sahel covers an area from 9°N to 17°N and 15°W to 43°E.

** The test area for East Asia covers an area from 39°N to 48°N and 100°E to 120°E.

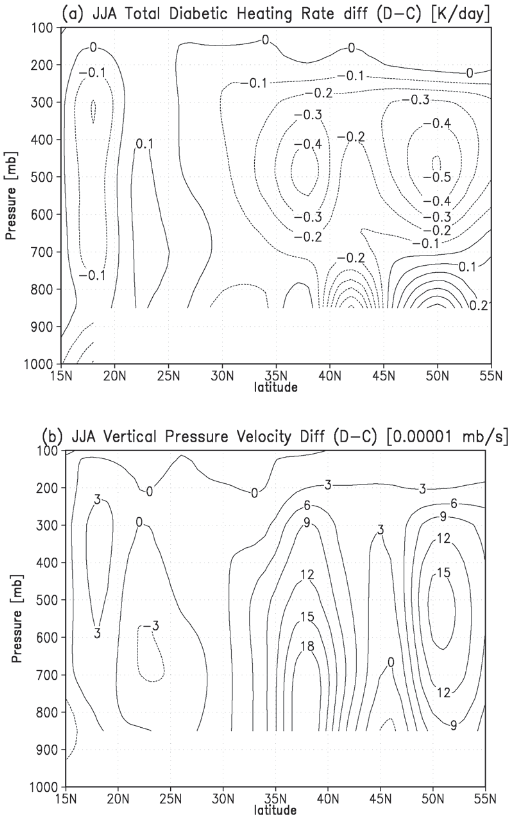

Figure 7. The JJA zonal differences averaged from 100°E to 115°E between ensembles DA and CA: (a) total diabatic heating rate (K day^{-1}); (b) vertical pressure velocity (10^{-5} hPa sec^{-1}).

Because of the lower net radiation at the surface, the total outgoing heat fluxes are also reduced to balance the energy budget. Lower LAI and higher stomatal resistance in the degradation simulations contribute to the substantially lower mean evaporations (Table 4). During the summer, sensible heat flux in the Sahel case even increases slightly to balance the dramatic reduction of latent heat flux at the surface.

Because of the large reduction in evaporation, less moisture is transferred to the atmosphere through the boundary layer. This results in less convection and lower atmospheric latent heating rates. Clear sky in the degradation case also contributes to the long wave radiation loss in the atmosphere (Table 4). However, the lower convective latent heating rate is responsible for more than 70% of the reduction in the total atmospheric diabatic heating rate in these experiments. Figure 7a shows the changes in heating rate from the East Asian study (Xue, 1996). The reduced total diabatic heating rate in the atmosphere is associated with relative subsidence (Figure 7b). Moisture is transported to the north by northward monsoonal flow (Figure 8a). The sinking motion weakens the monsoon flow (Figure 8b) and reduces moisture flux convergence. A similar change also occurs in the Sahel simulation (Xue, 1997). The maximum precipitation band shifts to the south and produces less rainfall in the Sahel and slightly higher precipitation to the south (Figure 5b). These changes further reduce the evaporation, producing a positive feedback. Changes in the radiative (due to changes in surface albedo) and other atmospheric heating rates have only a secondary effect on changes in the diabatic heating budget and the precipitation.

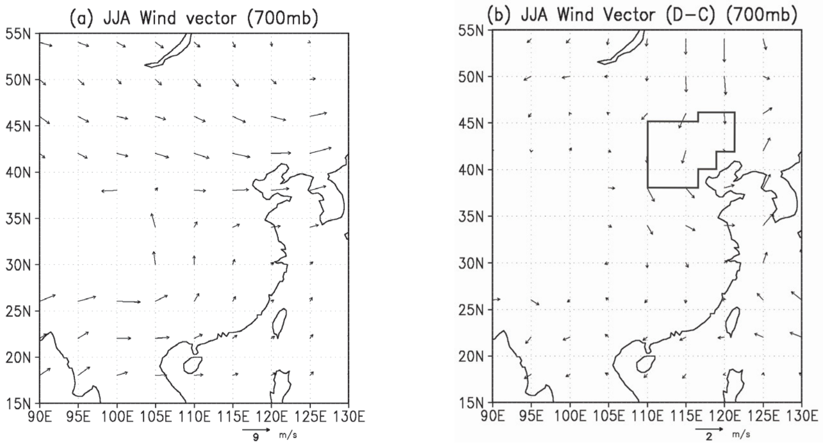

Figure 8. JJA wind vector (m s^{-1}). (a) ensemble CA; (b) ensemble DA minus ensemble CA.

4.4. PARAMETER EFFECTS

In early sensitivity studies, only one parameter (for example, albedo or initial soil moisture) was tested. Real atmosphere-biosphere interaction processes are much more complex and involve many more parameters and their complex interactions. In later studies such as those discussed in the last section, changes in vegetation types are used to investigate the feedbacks and interaction processes. A vegetation type includes many parameters. It is desirable to identify most important parameters and related processes as well as combinations of parameters in feedback and interaction processes. The effect of a single parameter on feedback is referred to as direct or first order, and the effect from a combination of several parameters, which includes interactions between them, is referred to as indirect or second order. The magnitudes of the direct and the indirect effects can be similar under certain circumstances, and often the directions of their effects can be opposite (Niyogi et al., 1999).

To resolve these direct and indirect effects explicitly, a Level-3 interaction analysis or a Response Surface Methodology (L3RSM) based approach can be efficiently designed (Niyogi et al., 1999). In this approach, a numerical model, SSiB, is used to conduct a set of experiments and generate a matrix of results (Niyogi et al., 2002). The selected vegetation and soil variables are altered in experiments and hence combinations of input conditions are developed. In employing the L3RSM analysis, the observational data from HAPEX-Sahel field measurements (Goutorbe et al., 1994) were used as forcing to drive SSiB (Niyogi et al., 2002). Six variables, soil wetness (*wet* in Figure 9), surface albedo (*alb*), minimum stomatal resistance (Rs_{min}), vegetative cover (*veg*), leaf area index (*LAI*), and atmospheric vapor pressure deficit (*vpd*), were systematically altered to “low,” “median,” and “high” values following a matrix approach to develop 48 different combinations. In studying the interactions and impact of the land-surface variables on evapotranspiration, the model outcome for evapotranspiration was then analyzed using a variety of graphical techniques to assess direct and indirect (first and second order) effects (Niyogi et al., 1999). Figure 9 is the Pareto-plot (Niyogi et al., 2002), which shows the importance of the input variables and their interactions in surface evapotranspiration in a decreasing order. The interactions are represented by terms such as *wet:veg* (which refers to the interaction between soil wetness and vegetation cover).

Figure 9 shows that the order of importance of direct effects in the Sahel is initial soil wetness, LAI, stomatal resistance, vegetal cover, albedo, and vapor pressure deficit. The results indicate that all the direct or first order effects are statistically significant. As such, direct effects dominate the Sahel evapotranspiration, and each of the surface variables independently controls the outcome. That is, surface components couple directly with the atmosphere *via* limited modulation from vegetation/bare ground interaction processes. Figure 9 demonstrates that there are only some significant interactions in the Sahel region, such as the triple interaction between stomatal resistance, LAI, and vegetal cover. In comparison, the mid-latitudinal case was dominated by second-order effects or interactive terms (Niyogi et al., 2002).

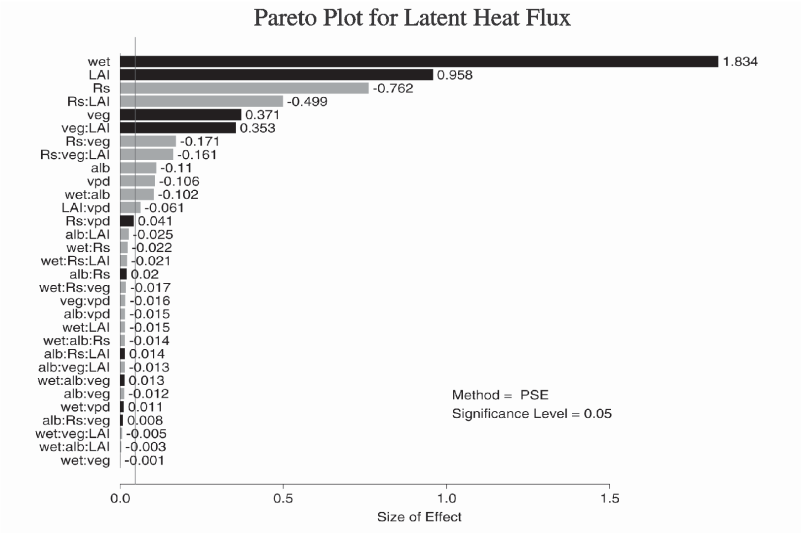

Figure 9. Pareto plot for HAPEX-Sahel latent heat flux. To the right of the vertical solid line, the effect is statistically significant. (Niyogi et al., 2002).

5. Two-way interactions

In the biophysical feedback studies described above, vegetation types were fixed and vegetation parameters were specified according to types and month during the period of model integration. For decadal to millennial scale studies, the response of land-surface conditions to environmental changes needs to be included. Although this type of study is still in the early stage, it already presents some interesting results.

Using a simple dynamic vegetation model, Zeng et al. (1999) showed that the interaction between vegetation, soil, and ocean components best reproduces observed decadal precipitation anomalies over the Sahel. In a run with soil moisture and vegetation fixed, precipitation showed little variability compared to the observed climatology of the last 50 years. A run with soil moisture feedback, but with the same imposed vegetation dynamics each year, improves interannual and decadal variability of precipitation somewhat. Allowing vegetation to respond to precipitation/soil moisture reproduced the best decadal variability of precipitation, with amplitude of the magnitude comparable to observations.

The role of vegetation/atmosphere feedback in North African climate in the early to middle Holocene is a focus of many paleoclimate studies, including the Paleoclimate Modeling Intercomparison Project (PMIP, Joussaume and Taylor, 2000). The climate in the Sahara during the early and middle Holocene was much wetter than today, as discussed in Chapter 8. GCM studies have shown that changes in Earth's orbital parameters enhanced the African monsoon but are not sufficient to explain the massive northward penetration as inferred from palaeorecords (Kutzbach, 1981). Several studies first replaced the Sahara Desert with vegetation in GCMs and found that surface modification enhanced the summer precipitation but not enough to sustain the expanded vegetation over the entire Sahara (Kutzbach et al., 1996; Texier et al., 2000). Using GCMs asynchronously coupled with vegetation models, several investigations studied vegetation and climate interactions in the early to mid Holocene. The results showed northward expansion of vegetation zones and enhanced precipitation in North Africa (Claussen and Gayler, 1997; Pollard et al., 1998; Texier et al., 1997). In asynchronous coupling, the GCM calculates a climate implied by a given land cover, and the vegetation model calculates the land cover implied by a given climate. This process is repeated until a mutual climate-vegetation equilibrium is reached. Because the asynchronous coupling technique is limited to the study of climate and vegetation equilibriums, a synchronously coupled climate and dynamic vegetation model (Foley et al., 1996), which explicitly models vegetation growth and competition, has also been used to explore the feedbacks (Doherty et al., 2000). Doherty et al.'s results are in general agreement with those of previously mentioned studies; that is, vegetation feedback substantially enhanced the northward shift of vegetation zones, further increased the peak rain intensity, and extended the rainy period. Nevertheless, there are also significant differences in detail among different model simulations--for instance, the extent of spatial northward expansion and spatial distributions.

In addition, studies have been conducted on multiple equilibrium vegetation statuses in West Africa. Claussen (1997) asynchronously coupled an equilibrium biogeography model (Prentice et al., 1992) to a GCM for a long-term climate study. It was found that starting from different initial conditions, the system came to multiple equilibrium states in climate/vegetation dynamics in Northern Africa. In the control simulation, the climatological vegetation distribution, based on the GCM and coupled vegetation model's 30-year simulation, was used for the initial vegetation condition. In the second simulation, the Sahara and Arabian and Indian deserts were replaced by xerophytic shrubs and savanna. Under present-day conditions of the Earth's orbital parameters and SST, two stable equilibria of vegetation patterns were possible from these two simulations. One solution from the control simulation corresponds to present-day sparse vegetation in the Sahel and desert in the Sahara (desert equilibrium), and the second solution yields savanna, which extends far into the western part of the Sahara (green equilibrium). Wang and Eltahir (1999) also confirmed that different initial vegetation conditions lead to different equilibrium vegetation-climate patterns with a zonally symmetric 2-dimensional regional atmospheric model synchronously coupled to a dynamic vegetation model (Foley et al., 1996). Using this model, they found that starting with desert covering all of West Africa, the vegetation at equilibrium varied from tall grass near the coast to short grass and desert northward. In contrast, starting with forest all over West Africa, the equilibrium vegetation consisted mostly of forests covering most of West Africa, with a much higher productivity and rainfall than the first case.

6. Dust effect

6.1. RELATIONSHIP BETWEEN DUST AND LAND DEGRADATION

Arid and semiarid regions are major sources of dust in the troposphere. Evidence has indicated that the location of the Saharan dust plume is subject to a seasonal shift following the ITCZ, which implies that a large portion of dust seems to originate from the Sahel. The transport of desert dust from Asia to the North Pacific atmosphere has also been well documented (e.g., Duce et al., 1980; Murayama et al., 2001). It rises from dust storms into the mid-troposphere by cold front and convection. The aerosol loading normally reaches a maximum each spring. In China, the dust is mainly concentrated in the troposphere lower than 5 km. It travels a long distance and sometimes reaches beyond the Pacific to North America.

Land degradation contributes significantly to the atmospheric dust load, as discussed in Chapter 9. For example, the highest dust production in the U.S. in the 1930s and the 1950s, known as the “dust bowl” was located over the areas where the soil was disrupted by cultivation (Middleton, 1999). Furthermore, in a study using a NASA three-dimensional tracer transport model, it was found that without the inclusion of anthro-pogenic dust sources, such as desertification, the model was not able to reproduce the seasonal shift of the Saharan dust plume over the Atlantic Ocean (Tegen and Fung, 1995). This model study suggested that the “disturbed” sources resulting in desertification-overgrazing, agricultural activities, and over-exploitation of vegetation might contribute about 30-50% of the total atmospheric dust loading.

The possible link between land degradation and dust can also be observed in the land degradation experiments described in the previous sections, even though there was no dust in the simulations. In the East Asian land degradation experiments, for example, the southerly wind and westerly wind in the degradation area increased about 1 m s^{-1} and 0.5 m s^{-1}, respectively. Dust clouds are normally formed when the friction from high surface wind speed (> 5 m/s) lifts loose dust particles into the atmospheric boundary layer (Gillette, 1978). The stronger wind in the simulation would help to produce more dust. Meanwhile, the enhanced westerly would help in transporting more dust to the Pacific Ocean (Figure 8b).

6.2. IMPACT OF THE ATMOSPHERIC DUST LOAD

Because the dust optical thickness can reach values of 0.6 to 1 (Rasool, 1984; Tegen and Fung, 1995), the radiative impact of desert dust can be expected to be significant in areas with high dust loading. Karyampudi and Carlson (1988) used a regional model to study two dust outbreaks. It was found that radiative heating by Saharan dust contributed to maintaining a warmer and deeper Saharan air layer over the ocean, which affected the midlevel easterly jet and convective precipitation.

Recently, another experiment has been conducted to test the climate response to soil dust aerosols using a NASA GCM with a mixed layer ocean model (Miller and Tegen, 1998). One case included a prescribed seasonal cycle of soil dust, and another case omitted it. The results show that soil dust both absorbs and reflects short wave radiation. Although some shortwave radiation is lost due to reflection, this amount is offset by upwelling long wave radiation, which is induced by the greenhouse effect caused by the dust particles. However, the average surface net radiation during the Northern Hemisphere (NH) summer is reduced by roughly 10 W m^{-2}. Because dust is concentrated near the dry arid and semiarid source regions, the reduced net radiation is mainly balanced by the reduction of surface sensible heat flux. The average upper-tropospheric temperature over the dust cloud increases by about 0.5° K during the NH summer, with a corresponding decrease at the surface, but this change is not uniform, as shown in Figure 10a. It is mostly located in the arid and semiarid regions in North America, the Sahara and Sahel, the Middle East, and Siberia. The precipitation is also reduced mainly in the tropical regions or the areas adjacent to the dust clouds (Figure 10b), such as the west coast of Africa and East Asia. Miller and Tegen (1998) attributed this to lower evaporation in response to the net radiation loss. Both reductions in evaporation and precipitation roughly equal one third of the reduction of net radiation.

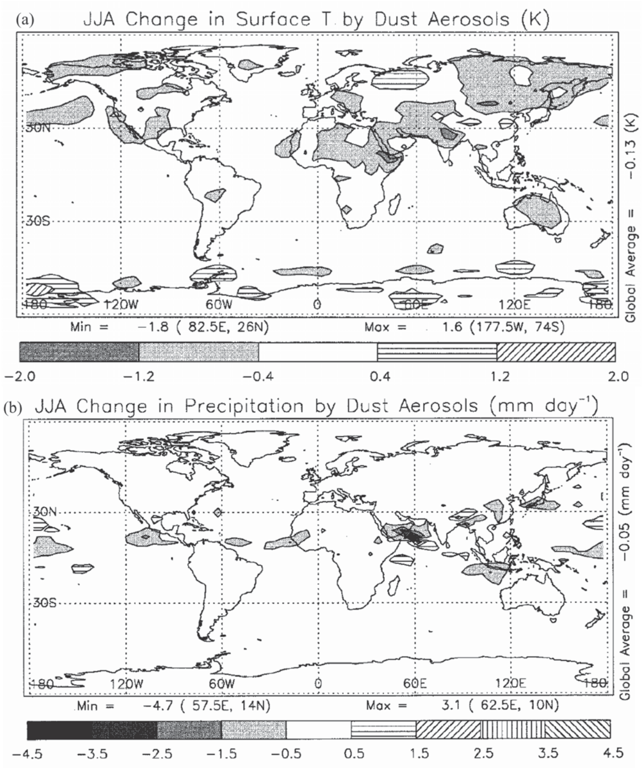

Figure 10. JJA changes by dust aerosols; (a) surface temperature (K); (b) precipitation (mm day^{-1}) (Miller and Tegen, 1998).

Miller and Tegen's study (1998) demonstrates that dust may contribute to climate anomaly in precipitation in the same direction as the biophysical feedback caused by land degradation, but may lessen surface warming due to land degradation. However, this study used fixed dust concentration and did not include biophysical feedback such as wind field change. Furthermore, the results in precipitation anomaly are very sensitive to the ocean conditions in the model (i.e., whether the ocean SST is specified or predicted). In other words, it depends on the extent to which the surface forcing is compensated by evaporation as opposed to dynamic ocean transports.

Nevertheless, this preliminary study demonstrates another promising direction in feedback and interaction between land and climate in arid and semiarid regions.

7. Discussion and conclusions

This chapter discusses the importance of arid and semiarid lands in land/atmosphere interactions and presents the principles and tools for interaction studies. In addition, studies of biophysical feedback in the Sahel and East Asia, two-way vegetation interaction in northern Africa, and dust effects are presented.

Biophysical feedback studies show that it is very likely that the land degradation in semiarid regions in the Sahel and Inner Mongolian and Mongolian grasslands contributes to the decadal climate anomalies in these regions. It appears that changes in the hydrological cycle at the surface and in the atmosphere, rather than the albedo/radiation interactions, are the major mechanisms that dominate the feedback processes in these two regions. The changes in local water balance of these two semiarid regions could have substantial impacts on atmospheric circulation beyond local disturbed regions, extending to much larger scales. Meanwhile, dust from arid and semiarid areas also has substantial effects on regional climate. It is likely to contribute to the precipitation anomalies in the same direction as the biophysical feedback but to lessen warming effects. Studies have identified North Africa as the region in the world where regional climate is probably most sensitive to land-surface processes.

However, the Earth environment is a complex system. Although the studies presented in this chapter emphasize the role of change in the hydrological cycle in regional climate anomalies, land interaction does not always dictate that more vegetation leads to more evaporation, which leads to more precipitation. Many factors, such as background atmospheric circulation, geographic locations, topographic situation, and temporal and spatial scales, affect the nature and controlling mechanisms of land/atmosphere interactions. A recent study (Xue et al., 2004b), reports that the sensible heat flux and the ratio of latent heat to sensible heat flux plays an important role in monsoon evolution and the formation of large-scale circulation during the early monsoon stage. Since this subject is out of the scope of this book, interested readers can find the discussions in the relevant literature.

Acknowledgement

Funding was provided by NSF grants EAR 9706403 and ATM-0097260. The author thanks Mr. Ratko Vasic and Mr. Dan Kahan for their assistance in preparation of this paper.

8. References

Charney, J. G., 1975: Dynamics of deserts and drought in the Sahel. Quart. J. Roy. Meteor. Soc., 101, 193-202.

Charney, J. G., W. K. Quirk, S.H. Chow, and J. Kornfield, 1977: A comparative study of the effects of albedo change on drought in semi-arid regions. J. Atmos. Sci., 34, 1366-1385.

Clark, D., Y. Xue, P. Valdes, R. Harding, 2001: Impact of land surface degradation over different subregions in Sahel on climate in tropical North Africa. J. Climate, 14, 1809-1822.

Claussen, M., 1997: Modeling biogeophysical feedback in the African and Indian monsoon region, Clim. Dynamics, 13, 247-257.

Claussen, M. and V. Gayler, 1997: The greening of the Sahara during the mid-Holocene: results of an interactive atmosphere-biome model. Global Ecology and Biogeography Letters, 6, 369-377.

Dickinson R.E., A. Henderson-Sellers, PJ Kennedy, MF Wilson, 1986: Biosphere-atmosphere transfer scheme (BATS) for the NCAR community climate model. NCAR Technical Note TN-275 + STR, 69 pp.

Dickinson R.E. and A. Henderson-Sellers , 1988: Modelling tropical deforestation: a study of GCM land-surface parameterizations. Q J Roy Meteor Soc, 114, 439–462

Doherty R., J. Kutzbach, J. Foley, and D. Pollard, 2000: Fully coupled climate/dynamical vegetation model simulations over North Africa during the mid-Holocene. Climate Dynamics, 16, 561-573.

Dregne, H. E., 1983: Desertification of arid Lands, 242 pp., Hardwood Academic Publications, New York.

Duce, R.A., C.K. Unni, B.J. Ray, M. Prospero, and J. T. Merrill, 1980: Long-range atmospheric transport of soil dust from Asia to the tropical North Pacific: temporal variability. Science, 209, 1522-1524.

Foley, J.A., I. C. Prentice, N. Ramankutty, S. Levis, D. Polard, S. Sitch, and A. Haxeltine, 1996: An integrated biosphere model of land surface processes, terrestrial carbon balance and vegetation dynamics. Global Biogeophysical Cycle, 10, 603-629.

Fu, C., 1992: Transitional climate zones and biome boundaries: a case study from China. In Landscape Boundaries. A. J. Hansen and F. d. Castri, eds., Springer-Verlag, New York, 394-402.

Fu, C., T. Yasunai, S. Lutkemeier, 2003: The Asian monsoon climate. in Vegetation, Water. Humans and the Climate, Eds, P. Kabat, M. Claussen et al. Springer. Heidelberg. 115-127.

Gash, J.H.C., P. Kabat, B.A. Monteny, M. Amadou, P. Pessemoulin, H. Billing, E.M. Blyth, H.A.R. deBruin, J.A. Elbers, T. Friborg, G. Harrison, C.J. Holwill, C.R. Lloyd, J.P. Lhomme, J.B. Moncrieff, D. Puech, H. Soegaard, J.D. Taupin, A. Tuzet, and A. Verhoef, 1997: The variability of evaporation during the HAPEX-Sahel intensive observation period. J. Hydrology. 188-189, 385-399.

Gillette, D., A, 1978: A wind tunnel simulation of the erosion of soil: Effect of soil texture, sandblasting, wind speed, and soil consolidation on dust production. Atmos. Environ., 12, 1735-1743.

Goudie, A.S., 2000: The Human Impact on the Natural Environment. The MIT Press, Cambridge, Massachusetts. 511 pp.

Goutorbe, J. P. et al., 1994: HAPEX-Sahel: a large-scale study of land-atmosphere interactions in the semiarid tropics. Ann. Geophys. 12, 53-64.

Hulme, M, 1992: A 1951-80 global land precipitation climatology for the evaluation of General Circulation Models. Climate Dyn., 7, 57-72.

Hulme, M and Kelly, P.M., 1993: Exploring the linkages between climate change and desertification Environment, 35, 4-11 & 39-45.

Joussaume, S., and K.E. Taylor, 2000: The Paleoclimate Modeling Intercomparison Project, in Paleoclimate Modelling Intercomparison Project (PMIP). Proceedings of the Third PMIP workshop., edited by P. Braconnot, pp. 9-25, WCRP, La Huardiere, Canada, 4-8 October, 1999.

Karyampudi, V. M. and T. N. Carlson, 1988: Analysis and numerical simulations of the Saharan air layer and its effect on easterly wave disturbances. J. of Atmos. Sci., 45, 3102-3136.

Kemp, D.D., 1994: Global Environmental Issues. Routledge, London. 224pp..

Kitoh, A., K. Yamazaki, and T. Tokioka, 1988: Influence of soil moisture and surface albedo changes over the African tropical rain forest on summer climate investigated with the MRI-GCM-I. J. Meteor. Soc. Japan, 66, 65-85.

Kutzbach, J.E., 1981: Monsoon climate of the early Holocene: climatic experiment using Earth's orbital parameters for 9000 years ago. Science, 214, 59-61.

Kutzbach, J.E., G. Bonan, J. Foley, S.P., Harrison, 1996: Vegetation and soil feedbacks on the response of the African monsoon to orbital forcing in the early to middle Holocene. Nature, 384, 623-626.

Laval, K., and L. Picon, 1986: Effect of a change of the surface albedo of the Sahel on climate. J. Atmos. Sci., 43, 2418-2429.

Li, X., M. D. Savoie, K. Voss, and J.M. Prospero, 1996: Dominance of mineral dust in aerosol light scattering in the North Atlantic trade winds. Nature, 380, 416-419.

Mannion, A. M., 1997: Vegetation in Applied Climatology, R. D. Thompson and A. Perry, eds. Routledge. London, 123-140.

Middleton, 1999: The Global Casino. Arnold. London. 370 pp.

Miller, R.L. and I. Tegen, 1998: Climate response to soil dust aerosols. J. Climate, 11, 3247-3267.

Murayama, T., N. Sugimoto, I. Uno, K. Kinoshita, et al., 2001: Ground-based network observation of Asian dust events of April 1998 in east Asia, J. Geophys. Res., 106, D16, 18345-18359.

Nicholson, S. E., C. J. Tucker, and M. B. Ba, 1998: Desertification, drought, and surface vegetation: an example from the West African Sahel. Bull. Amer. Meteorol. Soc., 79, 815-829.

Nicholson, S. E., 1993: An overview of African rainfall fluctuations of the last decade. J. Climate, 6, 1463-1466.

Nicholson, S. E., 2000: Land surface processes and Sahel climate. Review of Geophysics. 38, 117-139.

Nicholson, S. E., 2002: What are the key components of climate as a driver of desertification? In Global Desertification: Do Humans Cause Deserts? Reynolds, J.F., and D.M. Stafford Smith, eds. Dahlem University Press, Berlin, 41-58.

Niyogi, D., S. Raman, and K. Alapaty, 1999: Uncertainty in specification of surface characteristics, Part 2: Hierarchy of interaction explicit statistical analysis. Boundary-Layer Meteorology. 91, 341–366.

Niyogi, D., Y. Xue, and S. Raman, 2002: Hydrological feedback in land-atmosphere coupling: Comparison of a tropical and a mid-latitudinal regime. J. Hydrometeorology, 3, 39-56.

Nobre, C. A., M. A. Silva Dias, A. D. Culf, J. Polcher, J. H. C. Gash, J. A. Marengo, and R. Avissar, 2004: The Amazonian Climate in Vegetation, Water, Humans and the Climate. P. Kabat, M. Claussen et al. Eds. Springer. Heidelberg, 79-92.

Pollard, D., J. Bergengren, LM Stillwell-Soller, SL Thompson, 1998: Climate simulations for 10,000 and 600 years BP using the Genesis global climate model. Paleoclimates, 2, 183-218.

Prentice, I. C., W. Cramer, S.P. Harrison, R. Leemans, R.A. Monserud, and A.M. Solomon, 1992: A global biome model based on plant physiology and dominance, soil properties and climate. J. Biogeography. 19, 117-134.

Prospero, J. M., R.A.Glacuum, and R.T. Nees, 1981: Atmospheric transport of soil dust from Africa to South-America. Nature, 289, 570-572.

Rasool, S. I., 1984: On dynamics of deserts and climate. In The Global Climate, J.T. Houghton, ed. Cambridge University Press, 107-110.

Reynolds, J.F., and D.M. Stafford Smith, 2002: Global Desertification: Do Humans cause deserts? Dahlem University Press, Berlin, 437 pp.

Ripley, E.A., 1976: Drought in the Sahara: insufficient biogeophysical feedback? Science, 191, 100-101.

Schupelius, G. D., 1976: Monsoon rains over West Africa. Tellus, 28, 533.

Shukla, J., and Y. Mintz, 1982: Influence of land-surface evapotranspiration on the earth's climate. Science, 215, 1498-1501.

Sellers P.J., Y. Mintz, YC Sud, A. Dalcher, 1986: A simple biosphere model (SiB) for use with general circulation models. J Atmos Sci , 43:505–530.

Sellers P.J., 1999: Biophysical models of land surface processes. In Climate System Modeling, K. E. Trenberth, ed. Cambridge University Press, London, 451-490.

Sud, Y. C., J. Shukla, and Y. Mintz, 1988: Influence of land surface roughness on atmospheric circulation and rainfall: a sensitivity study with a general circulation model. J. Appl. Meteor., 27, 1036-1054.

Tegen, I., and I. Fung, 1995: Contribution to the atmospheric mineral aerosol load from land surface modification. J. Geophys. Res., 100, D9, 18707-18726.

Texier D, N. de Noblet, SP Harrison, A. Haxeltine, D. Jolly, S. Joussaume,, F. Laarif, IC. Prentice, P. Tarasov, 1997: Quantifying the role of biosphere-atmosphere feedbacks in climate change: coupled model simulations for 6000 years BP and comparison with paleodata for northern Eurasia and northern Africa. Clim Dynam 13:865–882.

Texier D, N. de Noblet, P. Braconnot, 2000: Sensitivity of the African and Asian monsoons to mid-Holocene insolation and data-inferred surface changes. J. Climate, 13, 164-181.

Tratt, D.M., R. J. Frouin, and D. L. Westphal, 2001: April 1998 Asian dust event: a southern California perspective. J. Geogphy. Res., 106, D16, 18,371-18379.

Tucker, C.J., H.E. Dregne, and W.W. Newcomb, 1991: Expansion and contraction of the Sahara desert from 1980 to 1990. Science, 253, 299-301.

UNEP, 1992: World atlas of desertification. Seven Oaks, Edward Arnold.

Vose, R.S., R. Keim, R. L. Schmoyer, T. R. Karl, P. M. Steuer, J. K. Eischeid, T. C. Peterson, 1992: The global historical climatology network: long-term monthly temperature, precipitation, sea level pressure, and station pressure data. ORNL/CDIAC-53, NDP-041, 189 pp.

Wang, G. and E.A.B. Eltahir, 1999: Biosphere-atmosphere interactions over West Africa. 2. Multiple Climate Equilibria. Q. J. R. Meteorol. Soc., 126, 1261-1280.

Webster, P.J., 1987: The elementary monsoons. Monsoons, J.F. Fein and P.L. Stephens, eds. John Wiley and Sons, 3-32.

Webster, P.J., V. Magana, T. N. Palmer, J. Shukla, R.A. Tomas, M. Yanai, and T. Yasunari, 1998: Monsoons: processes, predictability, and the prospects for prediction. J. Geophy. Res, 103, No. C7, 14,451-14,510.

Weng, H.Y., K.M. Lau, and Y. Xue, 1999: Long term variations of summer rainfall over China and its possible link to global sea-surface temperature variability. J. Meteor. Soc. of Japan, 4, 845-857.

Woodward, F. I,. 1987: Climate and Plant distribution, Cambridge University Press, Cambridge. 167 pp.

Xue, Y., K.-N. Liou, A. Kasahara, 1990: Investigation of the biogeophysical feedback on the African climate using a two-dimensional model. J. Climate, 3, 337-352.

Xue, Y., P. J. Sellers, J.L. Kinter III, and J. Shukla, 1991: A simplified biosphere model for global climate studies. J. Climate, 4, 345-364.

Xue, Y., and J. Shukla, 1993: The influence of land surface properties on Sahel climate. Part I: desertification. J. Climate, 6, 2232-2245.

Xue, Y., and J. Shukla, 1996: The influence of land surface properties on Sahel climate. Part II: afforestation. J. Climate, 9, 3260-3275.

Xue, Y., 1996: The Impact of desertification in the Mongolian and the Inner Mongolian grassland on the regional climate. J. Climate, 9, 2173-2189.

Xue, Y., 1997: Biosphere feedback on regional climate in tropical North Africa. Quart. J. Roy. Met. Soc, 123, B, 1483-1515.

Xue, Y., and M. D. Fennessy, 2002: Under what conditions does land cover change impact regional climate. In Global Desertification: Do Humans Cause Deserts? Reynolds, J.F., and D.M. Stafford Smith, eds. Dahlem University Press, Berlin, 59-74.

Xue, Y., R.W.A. Hutjes, R.J. Harding, M. Claussen, S. Prince, E. F. Lambin, S. J. Alan, P. Dirmeyer, 2004a: The Sahelian Climate (Chapter A5) in Vegetation, Water, Humans and the Climate, P. Kabat, M. Claussen et al., eds. Springer. Heidelberg, 59-77.

Xue, Y., H.-M. Juang, W. Li, S. Prince, R. DeFries, Y. Jiao, R. Vasic, 2004b: Role of land surface processes in monsoon development: Part I - East Asia and West Africa. J. Geophy. Res. 109, D03105, doi:10.1029/2003JD003556.

Zeng N, JD Neelin, K-M Lau, CJ Tucker, 1999: Enhancement of interdecadal climate variability in the Sahel by vegetation interaction. Science, 286,1537–1540

Zhu, Z., S. Liu, and X. Di, 1988: Desertification and Rehabilitation in China. Academic Press, Beijing, 126 pp.

PART II

HYDROGEOMORPHOLOGY OF ARID AND SEMIARID LANDSCAPES

Interactions between biotic and geomorphic processes determine important features of dryland ecosystems. On the one hand, a number of earth surface processes are affected by terrestrial vegetation. On the other hand, geophysical processes have a strong impact on plant ecosystems. In fact, soil formation results from interactions between biogenic and earth surface processes. Water and wind erosion is strongly controlled by the presence of vegetation, and, in turn, wind and water flows affect the availability of nutrients and water to terrestrial vegetation. Moreover, ecosystem processes and landforms concur in determining the spatial patterns of soil moisture, organic matter and nutrients.

This second part of the book provides a review of the main interactions between earth surface processes and ecosystem dynamics. Chapter 7 discusses the effect of topography on the spatial distribution of soil moisture at the landscape, regional and continental scales. Chapter 8 provides a thorough analysis of the relation between ecohydrological processes and recurrent features of arid landscapes under climate change conditions. Wind erosion dynamics are reviewed in Chapter 9 with a particular focus on hydrologic controls and ecological implications. Chapter 10 investigates the interactions between fluvial processes and riparian vegetation both in ephemeral and in perennial water courses.

Chapter 7

CONTROLS ON PATTERNS OF SOIL MOISTURE IN ARID AND SEMI-ARID SYSTEMS

Rodger B. GRAYSON, Andrew W. WESTERN, Jeffrey P. WALKER, Durga D. KANDEL, Justin F. COSTELLOE, and David J. WILSON

Department of Civil and Environmental Engineering and CRC for Catchment Hydrology, University of Melbourne, Victoria, Australia - e-mail: rodger@civenv.unimelb.edu.au

1. Introduction

Soil moisture is a major control on ecohydrological processes at both the storm event and seasonal scales. It influences the partitioning of precipitation into infiltration and runoff (Chapter 3), is a control on biogeochemical processes (Chapter 11) and is a control on evapotranspiration by limiting water availability to plants (Chapter 3), and so also affecting the partitioning of energy into latent and sensible heat (Chapter 5). In this way soil moisture is a link between the surface energy, water and biogeochemical cycles. In water limited systems such as the arid and semi-arid zones, soil moisture plays a major role in vegetation patterns and type of vegetation cover, and is consequently of primary importance to the ecosystems of these areas (Chapters 1, 15; Hupet and Vanclooster, 2002; Kim and Eltahir, 2004).

Figure 1a illustrates a typical one-dimensional conceptualisation of the soil profile and the fluxes that influence the soil moisture stored in the profile. The exchanges between the atmosphere and the soil (precipitation and evapotranspiration) dominate changes in soil moisture (eg. Wilson et al., 2004), with moisture being replenished by infiltration and depleted by soil evaporation and plant transpiration. The relative contribution of evaporation and transpiration depends on the vegetation cover, with transpiration dominating in well vegetated landscapes. Fluxes between the soil profile and groundwater (or deeper parts of the regolith) can be important in some contexts. Drainage from the soil profile is the primary source of recharge for many groundwater systems and capillary rise from shallow groundwater tables can be an important source of water replenishing the profile soil water store during drier periods. In arid and semi-arid environments, interaction with shallow groundwater systems is generally limited to floodplains (Chapter 10) and regionally low areas around lakes. It rarely occurs at the hillslope scale for any significant period of time.

Included on Figure 1a is a series of soil moisture profiles measured for a clay-loam soil on a hillslope in Victoria, Australia. Both the amount of soil moisture and its dynamics change with depth. In the upper 50 cm, soil moisture is strongly influenced by the fluxes between the active root zone and the atmosphere, and the moisture here is more variable than the moisture at depth. Surface soil moisture also responds more quickly and so has both short and long time-scale variability, while the moisture at depth is less responsive to short term variations in the fluxes across the soil–atmosphere interface. In arid systems, hillslope soil moisture at depth is typically very low, except following unusually large rain events during which episodic recharge may briefly occur.

Figure 1b illustrates a standard conceptualisation of a hillslope. The key difference between Figure 1a and 1b is that lateral flow may now act to redistribute water via both surface and subsurface flow pathways. For significant subsurface lateral drainage to occur the following conditions are necessary:

P. D'Odorico and A. Porporato (eds.), Dryland Ecohydrology, 109–127.

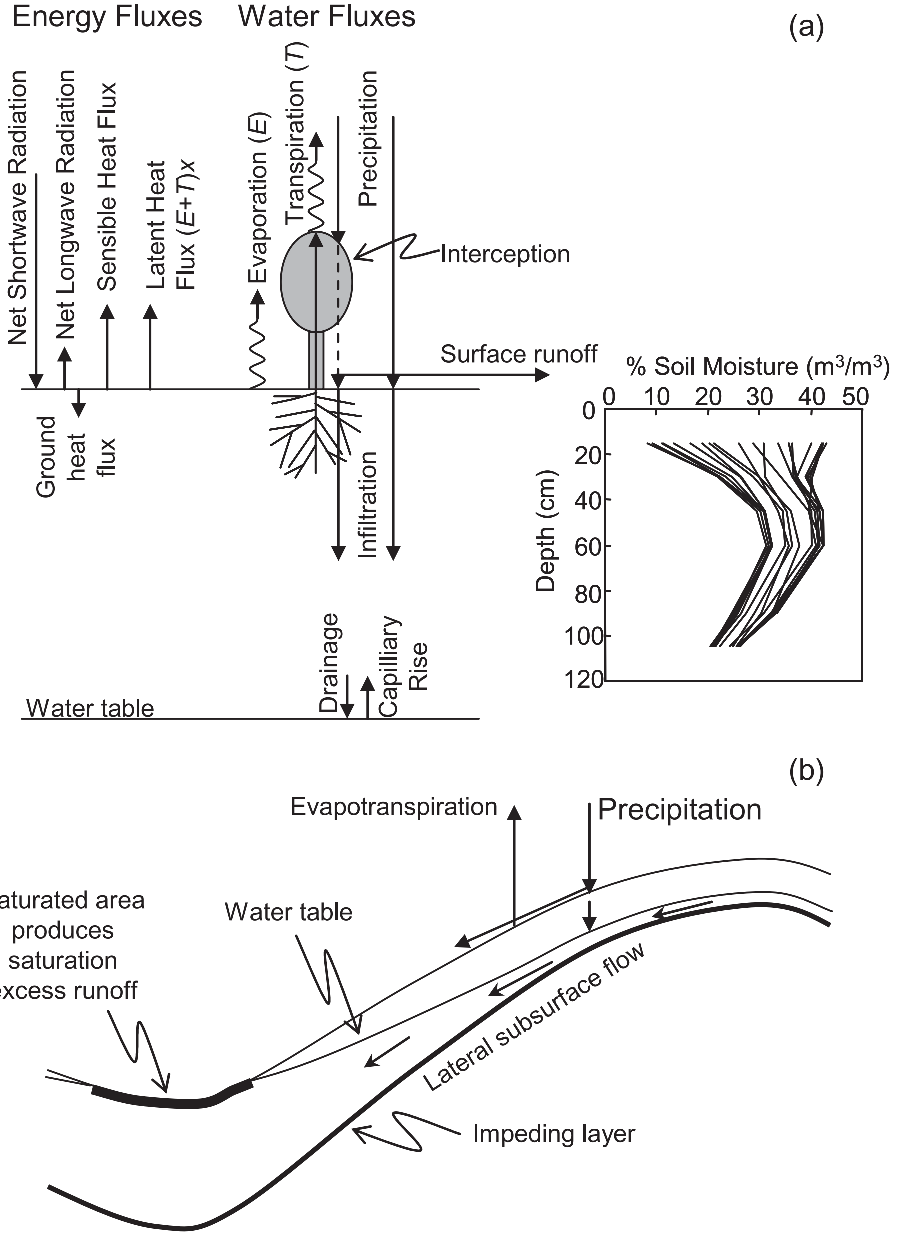

Figure1. a) A one-dimensional soil water balance. This is applicable where lateral flows are insignificant. The surface energy balance fluxes are also shown along with a time series of observed soil moisture profiles from the Tarrawarra Catchment. b) A two-dimensional conceptualisation of a hillslope where both subsurface and surface flow can redistribute precipitation and affect the local soil water balance. Source Western et al. (2002).

- Topographic relief with surface slopes greater than a few percent.
- An impeding layer in the soil profile limiting vertical drainage or anisotropy between vertical and horizontal hydraulic conductivities (Zavlasky and Sinai 1981).
- Sufficiently high moisture contents for periods long enough for flow to occur over significant distances.

In arid and semi-arid areas, the high moisture content conditions are present for only short periods following rainfall. Because there is a rapid decline in hydraulic conductivity or increase in resistance to flow as the soil dries (eg. Zaslavsky and Sinai, 1981), the distance over which lateral subsurface flow is important is very short, compared with wetter environments. However, high intensity rainfall can produce infiltration excess runoff, particularly from patches of (often unvegetated) soil (or rock) with low infiltration capacity, leading to wetter conditions down-slope due to run-on infiltration in patches of soil with higher infiltration capacity. Overland flow paths are also important over large scales because surface runoff is concentrated in topographic depressions and flood-flows overtopping river banks wet the floodplains (Figure 2). Thus the redistribution of water by surface flow paths is important over a range of scales from metres to thousands of kilometres.

These patterns of water movement can have important impacts on vegetation patterns. Water moving to areas of higher infiltration capacity or to small depressions on the hillslope encourages the growth of vegetation. This in turn enhances infiltration and hence increases soil water storage in these areas, thus supporting vegetation between rainfall events, thereby leading to a positive feedback between the vegetation, surface soil condition and hydrology (Chapter 5, this volume). In many arid areas, major streamflows are generated from many 100s or 1000s of km away, with the river acting as a conduit through the arid areas (see Chapter 10), replenishing soil moisture storages on the floodplains and river banks, supporting dense vigorous growth on the floodplain following flood events and supporting perennial riparian vegetation.

Topography is not the only influence on soil moisture in arid areas. Soil properties also affect soil moisture under both wet and dry conditions. The range in soil moisture is bounded at the upper end by the soil porosity and at the lower end by the wilting point (the value at which plants can no longer extract water and transpiration ceases) or residual soil moisture (the value at which the sun can no longer evaporate soil moisture; see Chapter 3). Soil properties also affect the amount of water held in the soil immediately following drainage after rainfall, commonly called the field capacity. These properties vary with soil type (texture and structure). Under extremely dry conditions, soil moisture patterns will be closely related to the pattern of wilting point, and hence be dominated by soil characteristics. Similarly, following rainfall and in the absence of lateral redistribution, soil moisture patterns will be dominated by the precipitation pattern, or if the soil becomes saturated, by the pattern of porosity or field capacity.

The notion of local and non-local controls on hillslope soil moisture patterns was introduced by Grayson et al. (1998). Non-local control occurs under wet conditions and is dominated by lateral water movement through both surface and subsurface paths, with catchment terrain leading to organisation of wet areas along drainage lines. Local control occurs under dry conditions and is dominated by vertical fluxes, with soil properties and only very local terrain (areas of high local convergence) influencing spatial patterns. The switch between these two was described in terms of the dominance of lateral over vertical water fluxes and vice versa. When evapotranspiration exceeds rainfall, the soil dries to the point where hydraulic conductivity is low and any rainfall essentially wets up the soil 'uniformly' and is subsequently evapotranspired before any significant lateral redistribution takes place. As evapotranspiration reduces and/or rainfall increases, areas of high local convergence become wet and runoff that is generated moves downslope, rapidly wetting up the drainage lines. In the wet to dry transitional period, a rapid increase in potential evapotranspiration causes drying of the soil and "shutting down" of lateral flow. Vertical fluxes dominate and the "dry" pattern is established. In arid and semi-arid regions, the local control exists during the vast majority of time, with non-local control occurring only immediately following rainfall at the hillslope scale. At the landscape and regional scale, the persistence of flows in rivers and across floodplains represents non-local control, but there is a sharp transition to local control outside the floodplains.

So in summary, soil moisture at a point is controlled by the balance between precipitation, evapotranspiration and lateral redistribution by surface and subsurface flow. These in turn are influenced by topography, soil properties and the patterns of vegetation. This chapter explores these various controls and influences through a series of examples from field and modelling studies in Australia. First we briefly introduce these studies and then separately discuss each of the controls and influences.

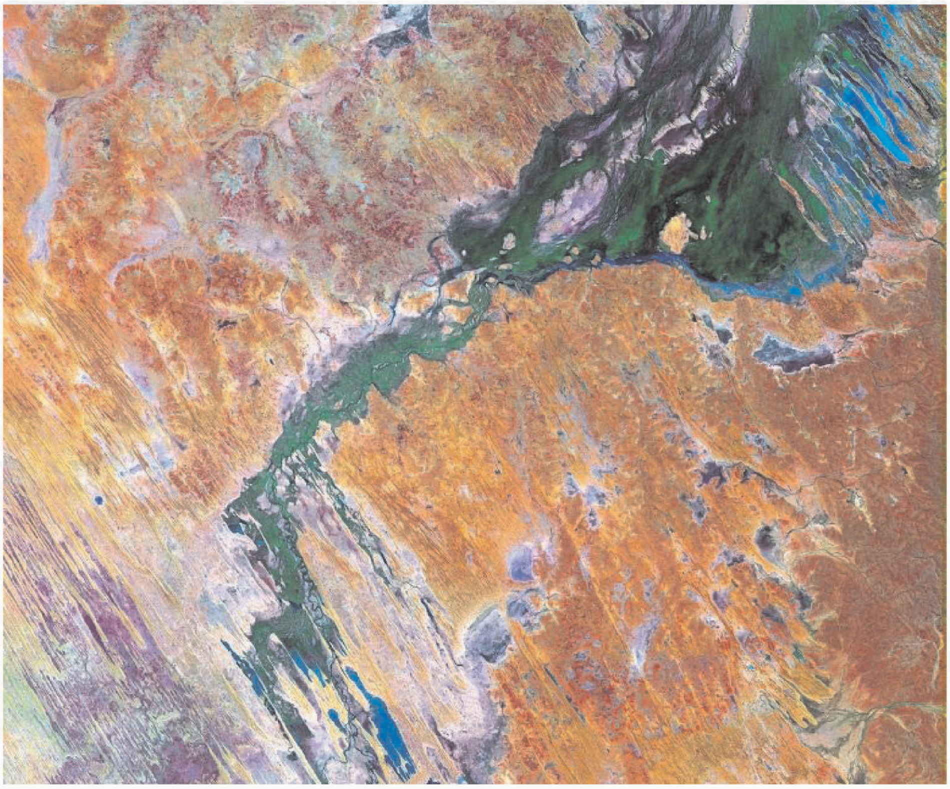

Figure 2. False colour Landsat image of the Goyder Lagoon region of the Diamantina/Warburton Rivers in the arid Lake Eyre basin (see Figure 3) showing a green flush in the floodplain and areas of local convergence following rainfall. Blue areas are a combination of flowing river water, floodwaters ponded in lakes and interdunal corridors and damp saline playas. Purple areas are dry floodplains and playas.

2. Overview of the field and modelling studies

Four studies will be used in the following discussion: i) several small temperate climate experimental catchments that experience summertime semi-arid conditions, ii) a large experimental catchment with climate ranging from humid to semi-arid and a range of landuses, iii) several catchments from the Lake Eyre Basin located in the Australian arid zone, and iv)

Australia-wide model simulated and satellite observed patterns of soil moisture in response to soils and vegetation.

The first is a series of field experiments on the temporal and spatial distribution of surface and shallow sub-surface soil moisture at hillslope to small catchment scale. These include the Tarrawarra (Western and Grayson, 1998) and Point Nepean (Wilson et al., 2004) catchments in South Eastern Australia (Figure 3). While these two Australian sites are located close to Melbourne, they have contrasting soil properties; Tarrawarra on silty clay loam and Point Nepean on sandy soil. Rainfall is quite uniform through the year but potential evapotranspiration (PET) rates change by almost an order of magnitude between summer and winter, leading to a monthly aridity index (PET/rainfall) varying between 0.2 in June and 2.9 in February (Western et al., 2004). The terrain is undulating with mean slopes of 8% at both sites. There is a difference in the geomorphology of these sites in that Tarrawarra is a fluvial landscape while the Point Nepean site is a dune field that retains its Aeolian morphology. In both these studies, soil moisture was measured using TDR instruments either in-situ or mounted on a small all-terrain vehicle, enabling spatial patterns to be measured over areas up to a square kilometre. These catchments are both in a temperate climatic zone, but the strong seasonal signal means that there are times of year when soil moisture controls are similar to those in semi-arid areas. These data will be used to indicate the relative importance of different sources of temporal and spatial variability in soil moisture.

The second study is at a much larger scale over the 80,000 km^2 Murrumbidgee River Basin (Figure 3). Although the headwaters of the basin lies within about 100 km of Australia's east coast, the basin lies to the west of the coastal divide and drains generally westward, discharging into the Murray-Darling River system. Most of the catchment is mixed rangeland and forest, with mean annual precipitation ranging from 1900 mm/yr in the east reducing to 320 mm/yr in the far west. There is a transect of ten soil moisture monitoring "sites" across the whole Murrumbidgee, measuring soil moisture profile and meteorological variables (Figure 3) (Western et al., 2002). On several occasions, mobile TDR equipment has been used to measure soil moisture in the top 30 cm over 10 km long transects near some of the ten Murrumbidgee sites. The data from this study will be used to highlight the effects of soil properties and changes in soil moisture behaviour over the large rainfall gradient.

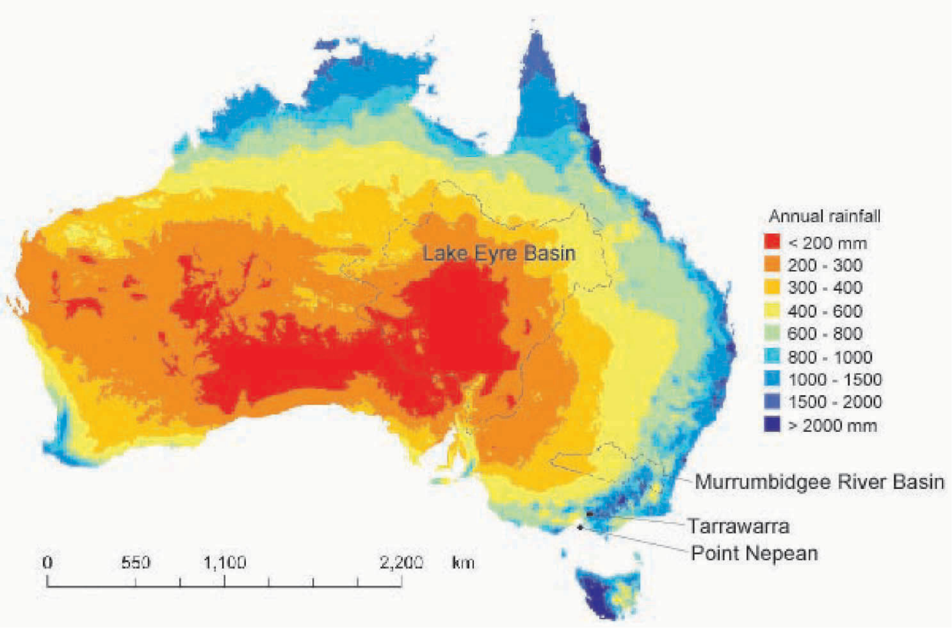

Figure 3. Location of Tarrawarra, Point Nepean, Murrumbidgee and Lake Eyre sites within Australia. The shading shows average annual precipitation across Australia, highlighting the Australian arid and semi-arid zones.

The third study focuses on the rivers and floodplains of the Lake Eyre Basin in the arid heart of Australia (Figure 3). Here we are working on the hydrological behaviour of sub-catchments ranging in size from 10,000 km^2 (in the Peake and Neales Rivers) to 160,000 km^2 (Diamantina River). Data from here are a combination of streamflow and groundwater monitoring along with observations of vegetation response to floods from satellite imagery (Figure 2). Rainfall-runoff modelling has also been undertaken on these catchments (Costelloe et al., in press) to provide key hydrological indicators to assist in ecological studies of the region. These data and model results are used to illustrate the dominance of large scale topography (river courses and floodplains) and the relative insignificance of hillslope scale topography on the soil moisture patterns in the arid zone.

The final study consists of a series of simulated and observed soil moisture patterns across the whole of Australia. The simulated patterns are based on results from a land-surface model (Koster et al., 2000) that incorporates topographic control as well as enabling soil and vegetation characteristics to be varied spatially. These simulations are all driven by the same forcing data (Walker et al., 2003), but vary in the level of detail provided on soil and vegetation properties. Comparison between the simulations provides some indication of the likely influence of soil and vegetation variability on soil moisture at the continental scale. In addition, the dominance of precipitation and effects of soil characteristics following rain can be observed. The observed soil moisture patterns are from the Scanning Multichannel Microwave Radiometer (SMMR) satellite (Owe et al., 2001).

3. Control by precipitation and climate

Soil moisture patterns are generally dominated by precipitation over a range of temporal scales and at larger spatial scales. We illustrate this at two very different scales using the data from the detailed field studies (Tarrawarra and Point Nepean) and the Australia-wide modelling.

Figure 4a shows the components of total temporal variance at each monitoring station at Tarrawarra (total variance 30-55% (m^3/m^3)^2) and Point Nepean (total variance 10-15% (m^3/m^3)^2) based on high resolution (30min) time series of root-zone soil moisture. The seasonal signal was identified in the time series, leaving a residual (representative of event scale variability), a component due to measurement error and a remaining "unexplained" component (see also Wilson et al., 2004).

Between 71 and 81 per cent of the temporal variance is explained by seasonal variance at Tarrawarra. In contrast, on the sandy soils of Point Nepean, seasonal variance explains only between 18 and 53 per cent of the overall temporal variance (Figure 4a). Variance in moisture content at the storm event-scale is more important to overall variance on the sandy soil. At Point Nepean, the average residual variance accounts for between 33 and 59 per cent of the temporal variance, while the highest was 24 per cent at Tarrawarra. This difference reflects differences in soil water storage capacity due to the soil texture differences. Very little of the temporal variance in soil moisture could not be explained by a combination of variance in the seasonal series, variance in the average residual series or by measurement error.

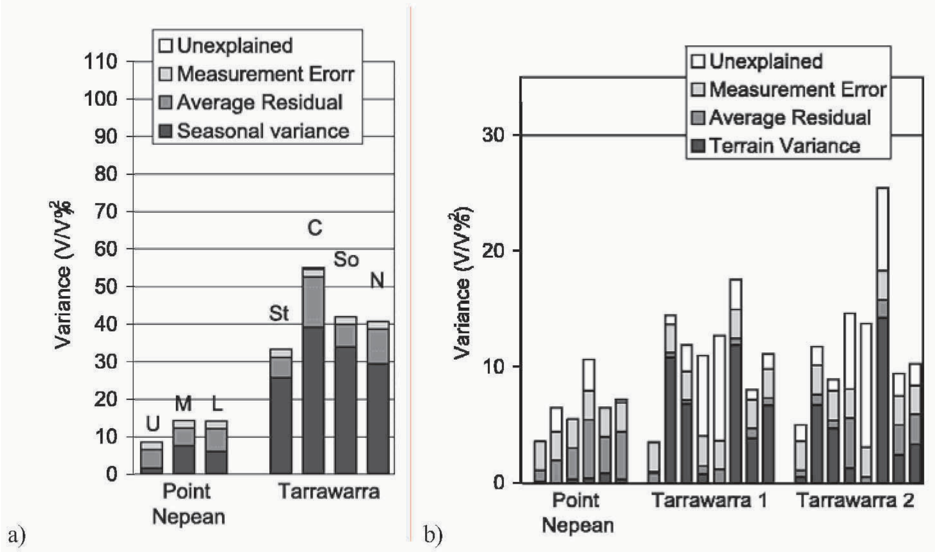

Figure 4. Classified a) temporal and b) spatial variance in soil moisture for Point Nepean and Tarrawarra field sites.

Compared to temporal variability, spatial variability, is relatively small (total variance <10-20%(m^3/m^3)^2 at Tarrawarra and <5-10%(m^3/m^3)^2 at Point Nepean). Measurements of the spatial distribution of soil moisture indicate that landscape related processes operating at a variety of scales control the distribution (see below) but that overall variance is much lower than temporal variance. The total spatial variance at each monitoring location is shown as the total column height in Figure 4b (sites are assessed individually whereas they are grouped in 4a). Using a similar approach as in 4a, a "terrain signal" was identified from the data via a multiple linear regression against static terrain parameters, the average spatial residual (as an analogue for static soils and vegetation effects) was also identified, as was a measurement error, leaving a small "unexplained variance" (Wilson et al., 2004).

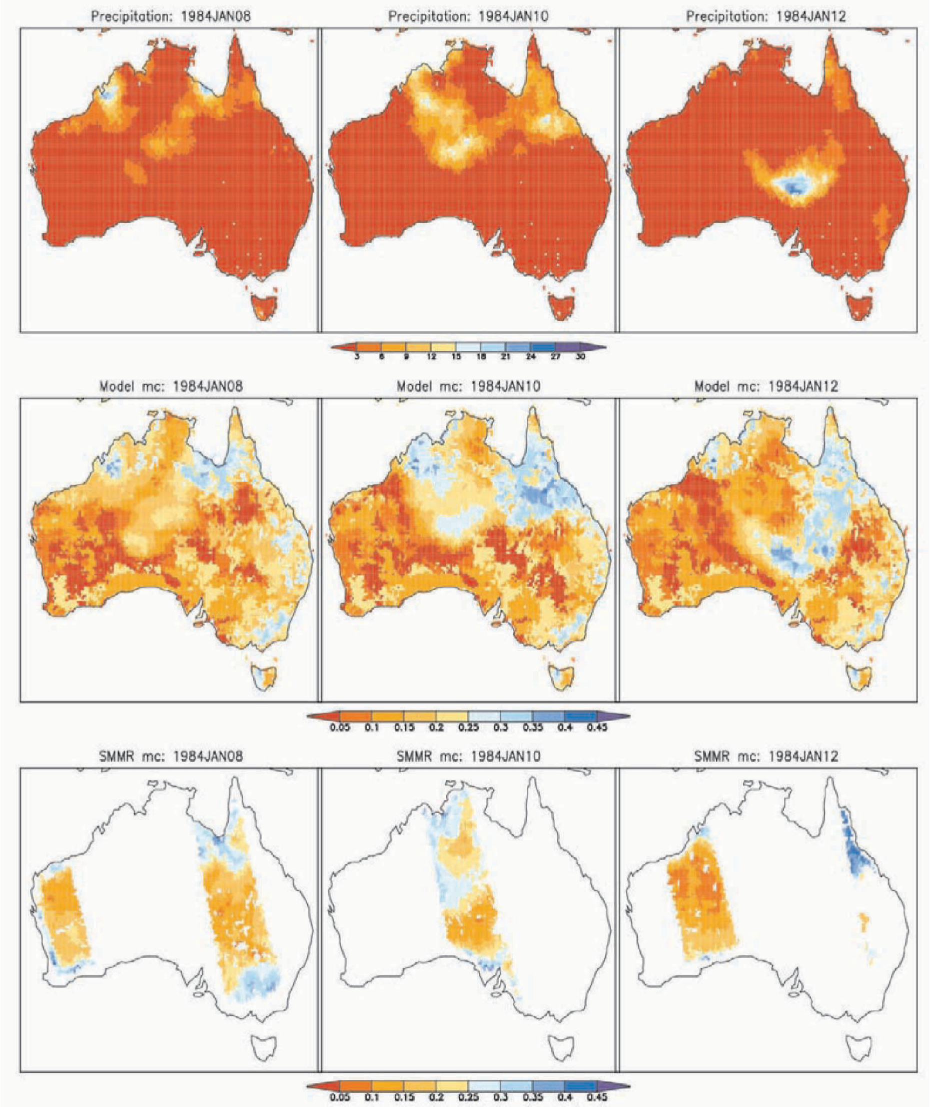

Figure 5. Pattern of near-surface soil moisture in response to precipitation: a synoptic front passing across Australia (columns 1 to 3) showing the rainfall field (top row), model derived near-surface soil moisture content (middle row) and remotely sensed surface soil moisture content by the Scanning Multichannel Microwave Radiometer (bottom row).

The clear message from Figure 4 is that at the small catchment scale, total variance in the temporal pattern of moisture content dominates over that in the spatial pattern, with temporal variance up to 10 times greater than spatial variance. Whether seasonal or event scale temporal effects are dominant depends on the storage characteristics of the soils and meteorological forcing pattern. Precipitation is also the dominant control on patterns in near-surface soil moisture content at much larger spatial scales. This is demonstrated in Figure 5 where a synoptic precipitation event can be seen passing across Australia, resulting in a closely matching pattern in surface soil moisture.

Both climatic and soil property variations are major controls on the spatial distribution of soil moisture at large scales. Figure 6 shows the soil moisture behaviour at the monitoring sites over the Murrumbidgee River Catchment. Figure 6a shows 10th, 25th, 50th, 75th and 90th percentiles of 0-30cm soil moisture. Clearly there are sites in the dry western half of the catchment that have low soil moisture (e.g. Balranald) and other sites that have consistently higher soil moisture (eg Hay). While there is some indication of a reduction in soil moisture in the semi-arid parts of the basin (west) compared with the humid (east) of the basin, this is disguised by soil type effects to a large degree. Figure 6b shows the same percentiles for reduced soil moisture, P, where $P = \frac{\theta - \theta_w}{\theta_f - \sigma_w}$ and θ is soil moisture, θ_w is the soil moisture at wilting point and θ_f is the soil moisture at field capacity. The wilting point and field capacity were inferred from the soil moisture time series. This normalisation removes the soil effect and shows the impact of climate on the spatial distribution more clearly.

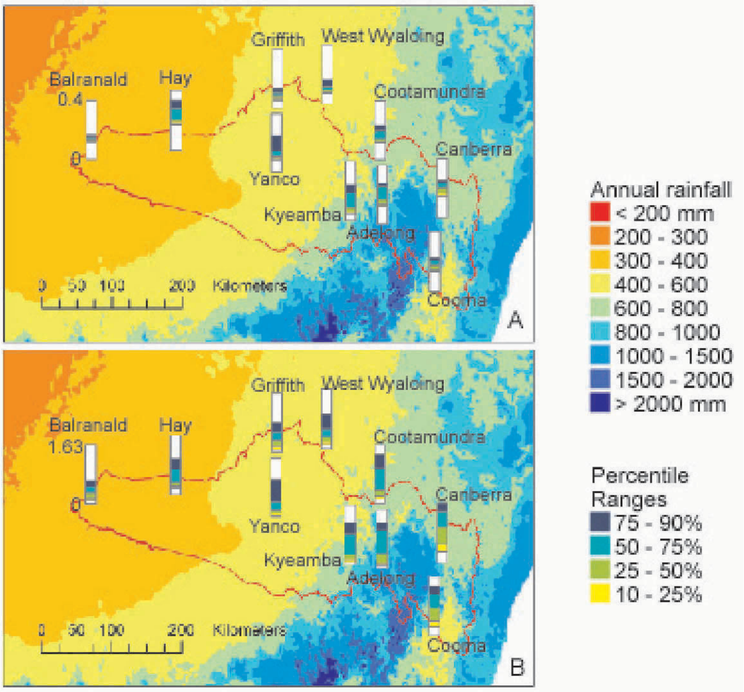

Figure 6. a) The temporal distribution of soil moisture. b) The temporal distribution of normalized soil moisture, P. In both maps, the columns are all drawn to the same scale (0 to 0.4 m^3/m^3) and the coloured bands represent the moisture contents corresponding to the percentile ranges given in the legend. The sites are located at the centre of the base of each column. The average annual precipitation is shown as the background pattern and the Murrumbidgee River Basin is outlined.

The typically low values of soil moisture in arid and semi-arid areas also influence the soil moisture profile behaviour. There is typically a large soil moisture deficit and thus a substantial amount of storage available in the upper part of the soil column that needs to be filled before drainage to the deeper soil layers occurs. This means that the deeper layers are typically dry and they respond episodically when rainfall events are sufficiently large to fill the storage available in the upper layer. Figure 7 shows the response of soil moisture in the 0-7cm, 0-30cm, 30-60cm and 60-90cm layers, along with rainfall for the period October 2001 to May 2004. This effect is clear here. In contrast in Adelong Creek, which is in the higher rainfall part of the Murrumbidgee basin, the soil moisture at depths responds seasonally and it is typically at or above field capacity during the wet part of the year. These results reinforce the point made earlier that where soil water storage is large (due to either more precipitation and in soils with higher storage capacity), seasonal timescales dominate temporal behaviour while where storage is limited or precipitation is low, the event scale is more important.

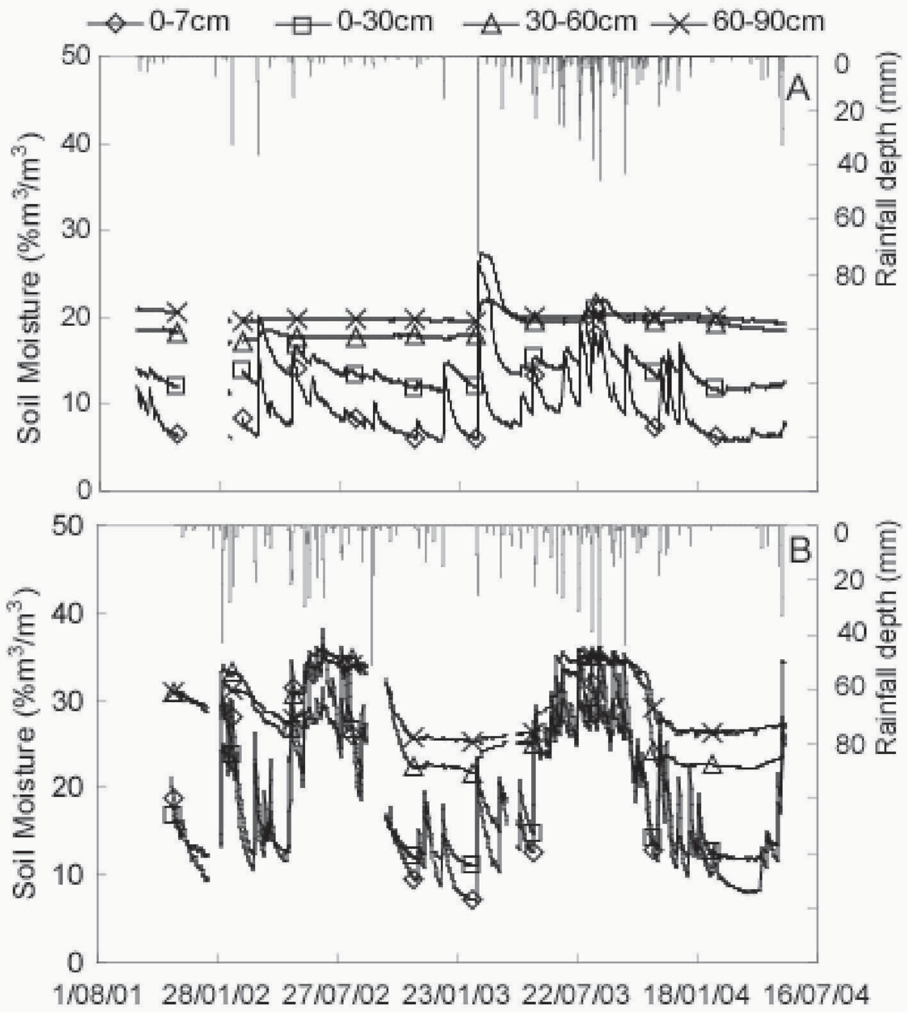

Figure 7. Observed soil moisture for four depths at a) Balarnald and b) Adelong (see Figure6).

4. Control due to topographic convergence and lateral movement

A number of empirical studies have examined the correlation between terrain properties and a measure of soil water storage status. Rarely has the percentage of variance explained exceeded 50% and at no sites has it consistently exceeded 50% (eg. Familglietti et al., 1998; Nyberg, 1996; Zaslavsky and Sinai, 1981; Moore et al., 1988; Ladson et al., 1992; Burt and Butcher, 1985; Moore and Thomson, 1996 and Jordan, 1994). At Tarrawarra we found that the explained variance ranged between 0 and 50% for individual terrain parameters and up to 61% under moderately wet conditions where lateral flow was active but saturated areas were confined to the drainage lines (see also Figure 4b).

At Tarrawarra the proportion of variance explained by topography is strongly related to the catchment wetness status. Figure 8 shows the proportion of spatial variation in 0-30 cm soil moisture explained by topography. Dry conditions at Tarrawarra are an analogue of the conditions found in arid and semi-arid landscapes for the vast majority of time in that soil moisture is close to wilting point. In these conditions there is essentially no relationship to terrain at the hillslope scale because there is no lateral redistribution of soil moisture. The results at Tarrawarra also show how it takes time for topographic redistribution to occur. The measurements on 14 February 1996 (mid summer) follow approximately 60 mm of rain in the preceding four days yet no topographic effects are evident and soil moisture is still low. As the catchment wets in autumn, the strength of the relationship with topography is much less than during the drying period the following spring, which follows an extended wet period.

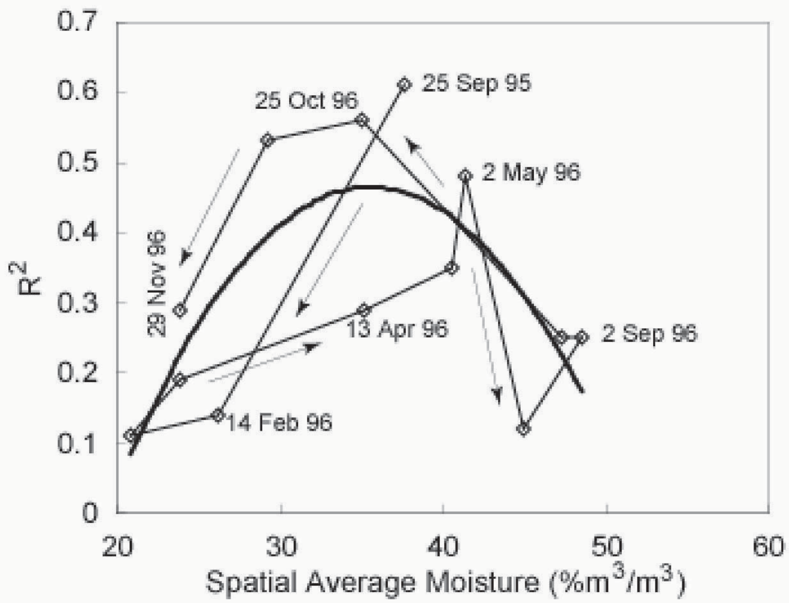

Figure 8. The proportion of spatial variance explained by multiple regression of soil moisture against the topographic wetness index and a potential solar radiation index and its relationship to catchment wetness (Western et al., 1999). The curved line shows a quadratic fit to the data and the arrows indicate the progression through time. Key dates of samples are shown.

In summary, at the hillslope scale, the topographic control on moisture content depends on overall wetness, being greatest when there is sufficient water for significant lateral redistribution, but not so much that everything is saturated (because porosity controls the moisture content then). In arid and semi-arid conditions, it is rare for lateral redistribution to be significant (i.e. the landscape is typically in the "dry" or "local control" state, Grayson et al., 1998). As illustrated in Figure 2, at very large scales, topographic control is represented by river and floodplain networks, but outside the immediate vicinity of the network, lateral redistribution is restricted to very short periods following heavy precipitation, where surface runoff processes dominate.

5. Control due to soils and vegetation

In the preceding examples, soils effects have been mentioned in relation to soil water storage and subsequent effects on temporal and spatial patterns. Soil texture, the amount of organic matter present and soil structure are all recognised to affect the moisture storage capacity of a soil. Soil texture, for example, influences moisture holding capacity, as fine textured soils retain water more effectively than sandy soils. The vegetation characteristics also have the potential to affect effective storage due to different rooting depths and effects on total evaporation.

In this section, we illustrate the relative importance of soil and vegetation effects, largely through the example of soil moisture simulations across Australia. The land surface model used for simulating soil moisture content across Australia uses spatially varying information on topography, soil properties, soil depth and vegetation type (Figure 9), and both spatially and temporally varying information on vegetation dynamics (Figure 10) through the leaf area index and fraction of vegetation that is actively transpiring or "green". In this application soil properties were defined by a set of characteristic soil properties for each soil texture type, and mapped according to the distribution in soil texture. Likewise the vegetation albedo and momentum parameters for evapotranspiration calculations were derived from a characteristic set of values for each vegetation type. Moreover, some of the soil moisture distribution timescale parameters used by the model are derived from the soil properties, soil depth and topographic data. Hence, specifying a uniform set of soil parameters for Australia additionally implies a uniform soil depth and topographic characteristics.

For a single day with minimal precipitation across the continent, Figure 11 shows the effect of spatially varying soil and vegetation parameters on root zone soil moisture compared with spatially uniform soil with spatially varying vegetation, spatially uniform vegetation with spatially varying soil, and soil and vegetation both spatially uniform. Figure 12 shows a summary of these three scenarios through the seasonally averaged root zone soil moisture residual from the spatially varying soil and vegetation parameter case for a single year.

Comparing Figures 11 and 12 to the patterns of 9 and 10 clearly show that, when precipitation effects are either minimal or averaged out, the soil parameters have the greatest impact on spatial soil moisture pattern, with the pattern in soil moisture residual closely matching the pattern in assumed soil texture. Vegetation makes only a minor contribution to the pattern of root zone soil moisture content. The importance of soil properties on observed soil moisture was also shown in Figure 6 for the Murrumbidgee River Basin sites. The dominance of soil properties over vegetation effects is consistent with modeling results from these sites (Richter et al., in press) and with the modeling results of Shao et al (1997). Apart from some minor influence of broadleaf evergreen trees, there is a poor match in the vegetation effect residual (Figures 11 and 12) with the vegetation type (Figures 9 and 10).

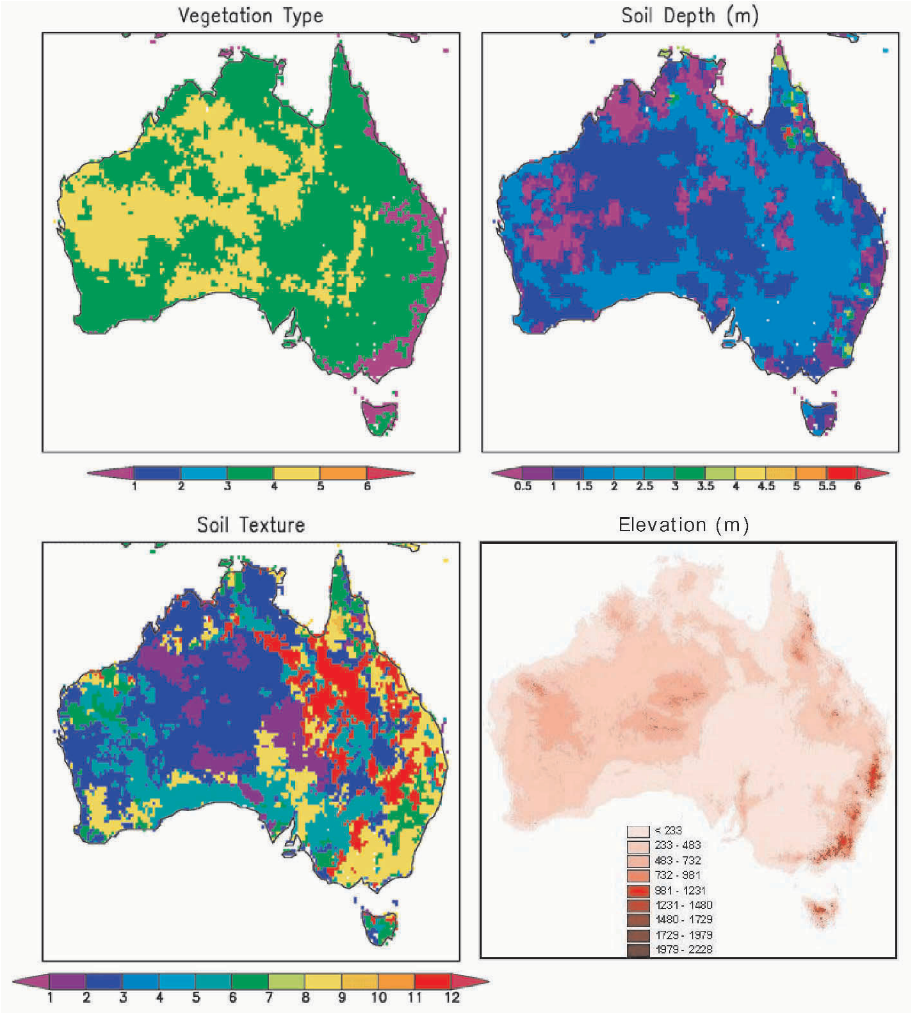

Figure 9. Static patterns underlying topographic, soils and vegetation parameters used by the land surface model. Vegetation albedo and momentum parameters were defined by vegetation type[1] *while soil hydraulic parameters were defined by soil texture*[2].

---

[1] **Vegetation/Land use type** 1. Broadleaf evergreen trees; 2. Broadleaf deciduous trees; 3. Needle-leaf trees; 4. Grass land; 5. Broadleaf shrubs; 6. Dwarf trees; 7. Bare soil

[2] **Soil texture class**:1. Sand; 2. Loamy sand; 3. Sandy loam; 4. Silt loam; 5. Silt; 6. Loam; 7. Sandy clay loam; 8. Silt clay loam; 9. Clay loam; 10. Sandy clay; 11. Silty clay; 12. Clay.

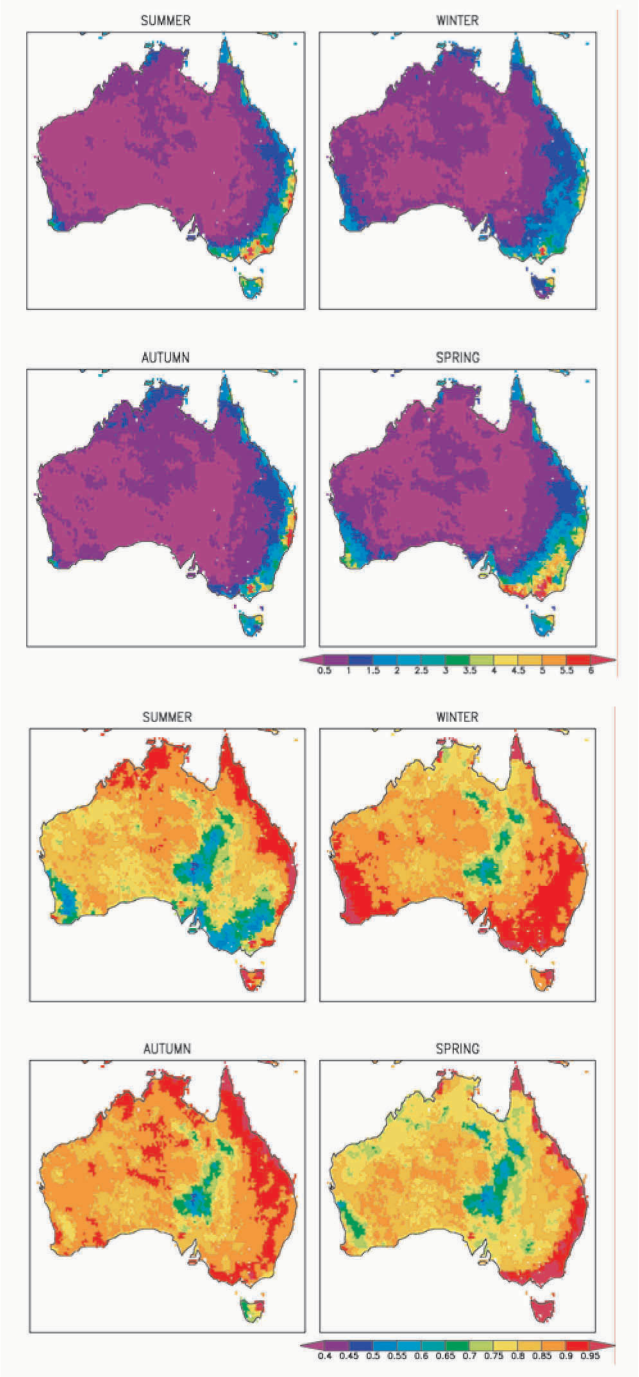

Fig 10: Dynamic patterns underlying the vegetation parameters used by the land surface model. Remotely sensed spatial and temporal variation in vegetation a) leaf area index and b) greenness. The seasonal data has been derived from monthly observations.

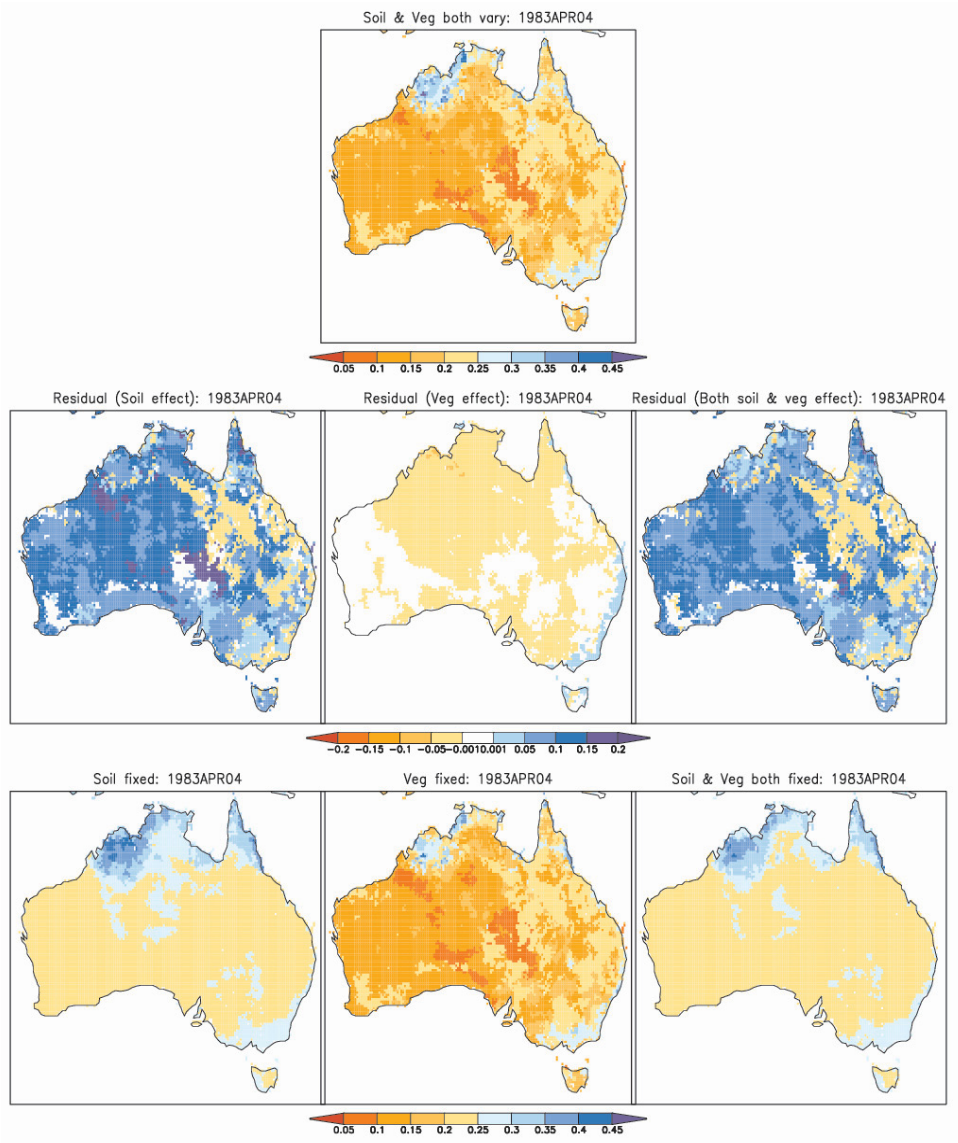

Figure 11. Patterns in root zone soil moisture resulting from patterns in vegetation, soils and topographic parameters used by the land surface model. The top row is model derived soil moisture with spatially varying parameters and bottom row is with one or more parameters fixed. The middle row is the residual when subtracting the bottom row from the top row. Results are for a single day where there is no rainfall.

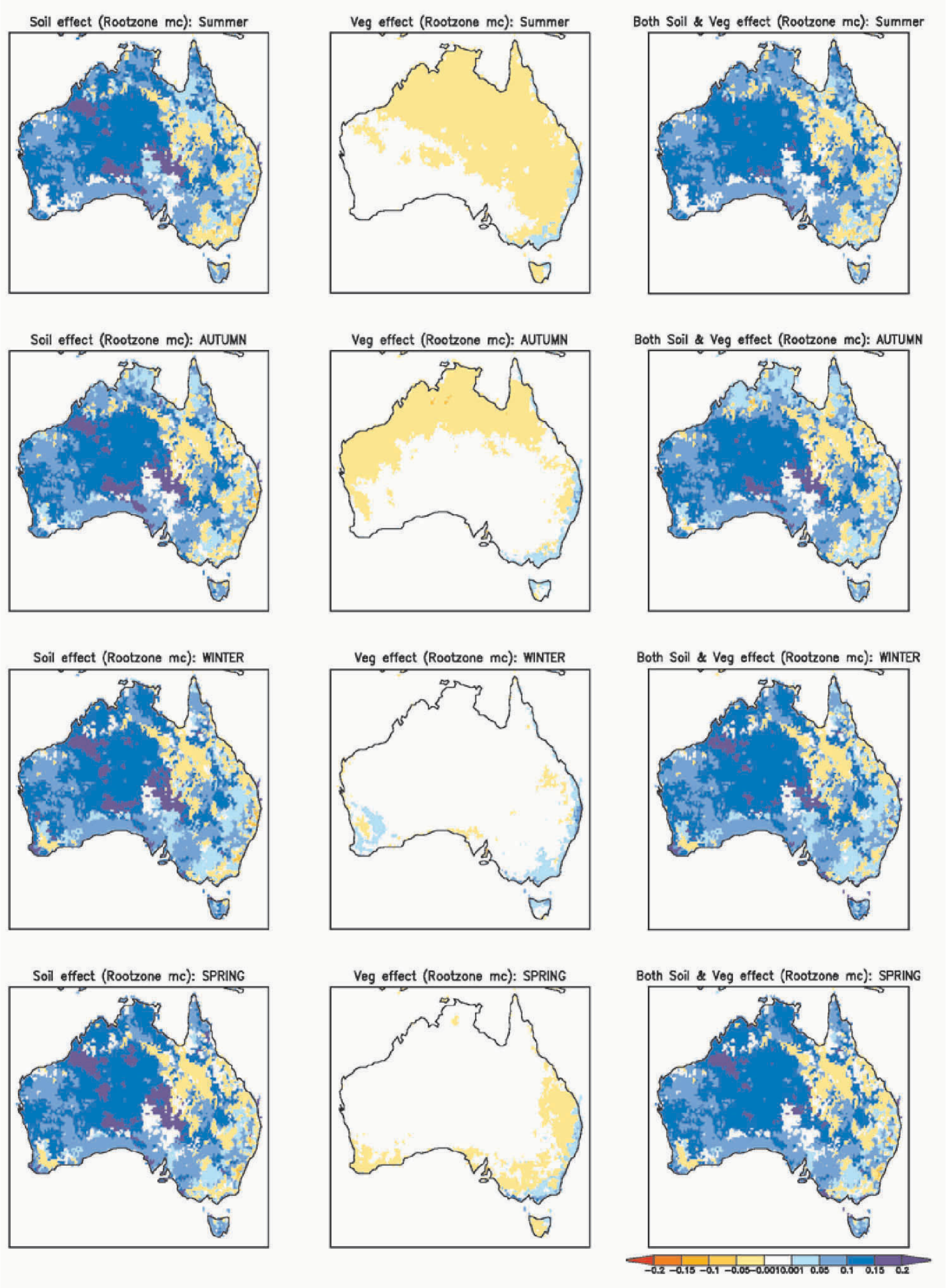

Figure 12. Seasonally averaged residuals of root zone soil moisture resulting from patterns in vegetation, soils and topographic parameters used by the land surface model.

Whether the simulations in Figures 11 and 12 represent reality is dependent on how well the maps of soil texture/type reflect differences in hydraulic characteristics, the maps of vegetation reflect spatio-temporal variation in important vegetation characteristics including canopy characteristics and rooting depth, and how well the model captures the functioning of the vegetation and soils. Wilson et al. (2004) show that over small areas such as Pt Nepean and Tarrawarra, there are static characteristics of the landscape that strongly affect soil moisture patterns (see "average residual" in Figure 4b), but are not well reflected in standard "soil type" maps. Houser et al. (2000) show a similar result for small catchments in the arid Walnut Gulch area.

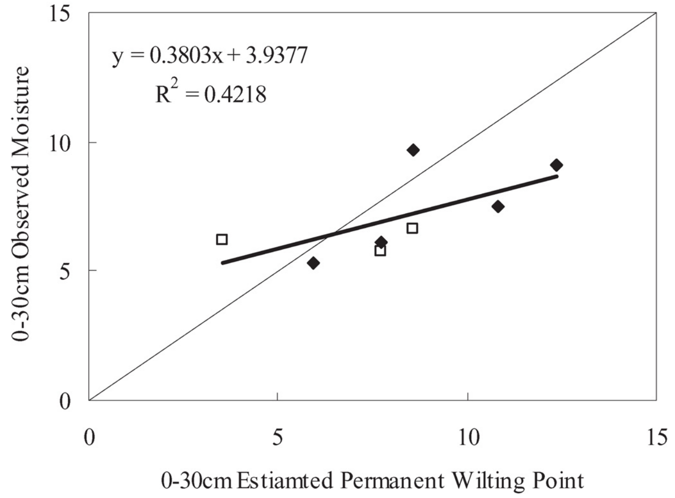

Figure 13. Estimated wilting point from soils mapping compared to observed moisture content during an extended drought period.

Nevertheless, at larger scales or where mapping has been particularly detailed, maps of soil texture/type can provide some indication of real controls on soil hydraulic behaviour. Figure 13 shows the relationship between wilting point as estimated from detailed soil mapping and as measured using TDR for five 1ha patches and for the soil types encountered along a 4 km transect across Kyeamba Creek (Murrumbidgee catchment). The observed data are averages of between 11 and 43 individual measurements within the one mapped soil unit. The measurements were taken after an extended period of drought. It can be seen here that the wilting point is related to the observed "dry-end" soil moisture where bare soil evaporation is likely to have reduced moisture contents at the surface to close to residual values due to the extended drought period.

These results (and other similar results across large areas) indicate that the general patterns reflected in Figures 11 and 12 are realistic, and while the absolute values may not be correct, the conclusions regarding the general influence of soils versus vegetation appear sound, at least in terms of soil moisture content. It is likely that if total water availability was considered, the importance of vegetation would increase.

6. Summary

In this chapter we have explored the various controls on soil moisture variability in time and space, using examples from field and modelling studies from small catchments to continental scales. It is shown that precipitation events are the dominant control on soil moisture in the semi-arid and arid zones. Where rainfall is higher and soil water storage capacity is greater, the seasonal signal of precipitation dominates temporal variability. As the environment becomes more arid and/or soil water storage is lower, event-scale variability becomes an increasing component of overall soil moisture variability.

Topographic effects are significant at the small catchment scale under wetter conditions, where there is opportunity for lateral subsurface flow, but under arid conditions, this effect occurs only at the very local scale. In arid areas, the dominant lateral redistribution process is surface runoff, where long-term wet regions are restricted to the major river and floodplain networks and thus affected by large-scale topography. At these scales, topography is a dominant control on moisture patterns, with floodplain inundation creating persistent wet areas throughout the arid zone (eg. Figure 2).

Soil effects are shown to be important because they affect the total storage capacity and the wet and dry limits of soil water content. Particularly under dry conditions where the residual water content is closely related to soil texture, patterns of soil moisture reflect patterns of soil texture. At the scales studied here, vegetation is shown to have a limited influence on soil moisture patterns. This is partly because of the interrelationship between climate, soils and vegetation distribution and partly because we are looking at soil moisture content rather than total water availability (where rooting depth becomes important).

7. References

Burt, T. P., and Butcher, D. P., Topographic controls of soil moisture distributions, *Journal of Soil Science, 36*, 469, 1985.

Costelloe JF, Grayson RB, McMahon TA, Argent RM. in press. Spatial and temporal variability of water salinity in an ephemeral, arid zone river, central Australia. *Hydrological Processes*.

Costelloe, J.F., Grayson, R.B., McMahon, T.A., In press. Modelling streamflow for use in ecological studies in a large arid zone river central Australia. *Hydrological Processes*, in press.

Famiglietti, J. S., Rudnicki, J. W., and Rodell, M., Variability in surface moisture content along a hillslope transect: Rattlesnake Hill, Texas, *Journal of Hydrology, 210*, 259, 1998.

Grayson, R.B. and Western, A.W., Towards areal estimation of soil water content from point measurements: time and space stability of mean response, *Journal of Hydrology*, *207*: 68-82, 1998.

Grayson, R.B., Western, A.W., Chiew F.H.S. and G. Blöschl, 1997. Preferred States in spatial soil moisture patterns: Local and nonlocal controls. Water Resources Research, 33(12):2897-2908.

Houser, P, Goodrich, D and Syed, K, 2000. Runoff, precipitation and soil moisture at Walnut Gulch, Chapter 6 in *Spatial Patterns in Catchment Hydrology - Observations and Modelling*, Ed. R.B. Grayson and G. Blöschl, Cambridge University Press. 404p.

Hupet, F., and M. Vanclooster 2002, Intraseasonal dynamics of soil moisture variability within a small agricultural maize cropped field, *J. Hydrol.,* 261(1– 4), 86–101.

Jordan, J. P., Spatial and temporal variability of stormflow generation processes on a Swiss catchment, *Journal of Hydrology, 152*, 357, 1994.

Kim, Y and E.A.B. Eltahir, 2004. Role of topography in facilitating coexistence of trees and grasses within savannas. *Water Resources Research. W07505, doi:10.1029/2003WR002578.*

Koster, R.D., M.J. Suarez, A. Ducharne, M. Stieglitz and P. Kumar, A catchment-based approach to modeling land surface processes in a GCM. Part 1: Model structure*, Journal of Geophysical Research,* 105, D20, 24809-24822, 2000.

Ladson, A. R., and Moore, I. D., Soil water prediction on the Konza Prairie by microwave remote sensing and topographic attributes, *Journal of Hydrology, 138*, 385, 1992.

Moore, R. D., and Thompson, J. C., Are water table variations in a shallow forest soil consistent with the TOPMODEL concept?, *Water Resources Research, 32*, 663, 1996.

Moore, I. D., Burch, G. J., and Mackenzie, D. H., Topographic effects on the distribution of surface soil water and the location of ephemeral gullies., *Transactions of the American Society of Agricultural Engineers, 31*, 1098, 1988.

Nyberg, L., Spatial variability of soil water content in the covered catchment at Gårdsjön, Sweden, *Hydrological Processes, 10*, 89, 1996.

Owe, M., R. deJeu and J.P. Walker, A methodology for surface soil moisture and vegetation optical depth retrieval using the microwave polarization difference index, *IEEE Transactions on Geoscience and Remote Sensing*, 39, 8, 1643-1654, 2001.

Richter, H., Western, A.W. and Chiew, F.H.S., in press. The Effect of Soil and Vegetation Parameters in the ECMWF Land Surface Scheme. Journal of Hydrometeorology.

Shao, Y., Leslie, L.M., Munro, R.K., Irannejad, P., Lyons, W.F., Morison, R., Short, D. and Wood, M.S., 1997. Soil moisture prediction over the Australian Continent. Meteorology and Atmospheric Physics, 63(3-4): 195-215.

Walker, J. P., Ursino, N., Grayson, R. B., and Houser, P. R., 2003. Australian Root Zone Soil Moisture: Assimilation of Remote Sensing Observations, In: D. Post (Ed.), *Proceedings of the International Congress on Modelling and Simulation (MODSIM).* Modelling and Simulation Society of Australia and New Zealand, Inc., Townsville, Australia, 14-17 July, 2003, 1:380-385.

Western, A.W. and R.B. Grayson, 1998. The Tarrawarra data set: Soil moisture patterns, soil characteristics and hydrological flux measurements. *Water Resources Research* 34(10):2765-2768.

Western, A.W., Richter, H., Chiew, F.H.S., Young, R.I., Mills, G., Grayson, R.B., Manton, M.and T.A. McMahon, 2002. Testing the Australian Bureau of Meteorology's Land Surface Scheme using Soil Moisture Observations from the Murrumbidgee Catchment. *Hydrology and Water Resources Symposium, July, 2002.*

Western, A. W., Zhou, S.-L., Grayson, R.B., McMahon, T.A., Blöschl, G., and Wilson, D.J., 2004. Spatial correlation of soil moisture in small catchments and its relationship to dominant spatial hydrological processes. Journal of Hydrology 286:113-134

Wilson, D.J. Western, A.W., and R.B. Grayson, 2004. Identifying and quantifying sources of variability in temporal and spatial soil moisture observations. *Water Resources Research*, VOL. 40, W02507, doi:10.1029/2003WR002306,

Wilson, D.J. Western, A.W., and R.B. Grayson, in press. A terrain and data-based method for generating the spatial distribution of soil moisture. *Advances in Water Resources.*

Zaslavsky, D. and Sinai, G. Surface hydrology: I - Explanation of phenomena. J. of the *ASCE Hyd. Div. HY1*:1-18. 1981

Chapter 8

THE HISTORY AND EVOLUTION OF DESERT HYDROLOGY AND LANDFORMS: THE ROLE OF CLIMATE CHANGE

Andrew S. GOUDIE

School of Geography and the Environment, University of Oxford, Mansfield Road, Oxford, OX1 3TB, United Kingdom - e-mail: Andrew.goudie@stx.ox.ac.uk

1. Introduction: Aridity

The purpose of this chapter is to describe the nature of the evidence that can be used to establish the nature of environmental conditions in deserts, and to demonstrate the changes that have occurred in their hydrology and geomorphology, particularly during the course of the last few millions of years.

Arid lands, which cover about a third of our land surface, occur in every continent (Goudie 2002). They have, predominantly because precipitation is low, a severe shortage of moisture. In some years they may even receive no rain at all. In some deserts aridity also results from high temperatures, which means that evaporation rates are also high (Mainguet 1999).

Aridity can be defined by the water balance concept. This is the relationship that exists between the inputs of water in precipitation (P), the losses arising from evaporation and transpiration (evapotranspiration) (E_t), and any changes that occur in storage (soil moisture, groundwater, etc.) In arid regions there is an overall deficit in the annual water balance, and the size of that deficit determines the degree of aridity. The actual amount of evapotranspiration (AE_t) that occurs varies according to whether there is available water to evaporate, so the concept of potential evapotranspiration (PE_t) has been devised. This is a measure of the evapotranspiration that could occur from a standardized surface never short of water. The volume of PE_t varies in response to four climatic factors: radiation, humidity, temperature, and wind. Thornthwaite (1948) developed a general aridity index based on PE_t:

when $P = PE_t$ throughout the year, the index is 0
when $P = 0$ throughout the year, the index is –100
when P greatly exceeds PE_t throughout the year, the index is +100

Areas with values below –40 are classified as arid, those between –20 and –40 as semi-arid, and those between 0 and –20 as sub-humid (Meigs 1953). The arid category can be subdivided into arid and extreme arid, with the latter being defined as the condition in any locality where at least 12 consecutive months without any rainfall have been recorded, and in which there is not a regular seasonal rainfall rhythm.

Extremely arid areas, such as the Atacama, Namib, inner Arabia and central and eastern Sahara, cover about 4 per cent of the earth's surface, arid about 15 per cent, and semi-arid about 14.6 per cent. In addition, deserts can be classified on the basis of their proximity to the oceans or their continentality. Coastal deserts, such as the Namib or the Atacama, have very different temperatures and humidities from those of continental interiors. They have modest daily and seasonal temperature ranges and are subject to fogs. They are also very dry. In addition to the coastal and inland deserts of middle and low latitudes there are also the cold polar deserts. The precipitation of the Arctic regions can be as low as 100 mm per year and at Vostok in Antarctica can be less than 50 mm.

P. D'Odorico and A. Porporato (eds.), Dryland Ecohydrology, 129–140.

2. Causes of aridity

Most deserts are dry because they occur where there is subsiding air, relative atmospheric stability and divergent air flows at low altitudes, associated with the presence of great high-pressure cells around latitude 30°. Such areas are infrequently subjected to precipitation-bearing disturbances and depressions either from the Intertropical Convergence Zone or from the belt of mid-latitude depressions associated with the circumpolar westerlies. The trade winds that blow across these zones cause evaporation, and because of the trade-wind inversion they are areas of subsidence and stability. These global tendencies are often reinforced by more local factors. Of these, *continentality* can be dominant and plays a part in the location and character of the deserts of areas like central Asia. The *rain-shadow* produced by mountains ranges can create arid areas in their lee, as in Patagonia, where the Andes have an influence. Other deserts are associated with cold currents offshore (e.g. Namib and the Atacama). Winds that do blow onshore tend to do so across cold currents (e.g. the Benguela and the Peruvian) and so are stable because they are cooled from beneath, and also have a relatively small moisture-bearing capacity. They reinforce the stability produced by the dominance of subsiding air.

3. Aridity indicators

There are three main categories of phenomena that indicate aridity: geomorphological, sedimentological and biological. These have demonstrated that aridity has both been greater and less than today and that aridity has shown frequent and substantial temporal changes.

Indicators of former higher precipitation levels (pluvials or lacustrals) include: high lake levels marked by ancient shorelines; expanses of fossil soils of humid type (e.g. laterites); spreads of spring-deposited *tufa*; river systems which are currently inactive and blocked by dune fields; and animal, plant and cultural remains in areas now too dry for their survival. The evidence for formerly drier conditions includes the presence of degraded, stable dunes in areas now too wet and vegetated for sand movement to occur.

4. Aeolian phenomena

Large tracts of dunes provide strong evidence of dryness. Chapter 9 discusses in detail the hydroclimatic controls on wind erosion and dust emission in arid landscapes. The existence of heavily vegetated, weathered, and degraded dunes indicates that there has been a shift towards greater humidity (Tchakerian 1999). There is, however, some dispute about the precise precipitation thresholds that control major dune development. Undoubtedly wind strength, which may have been greater during glacials, and the nature of the vegetation cover have to be considered, but systems of demonstrably inactive and stable dunes are today widespread in areas of relatively high precipitation (over 500 mm per annum) (e.g. the northern Kalahari, western India and northern Australia).

Studies where dunes are currently active suggest that vegetation only becomes effective in restricting dune movement in non-coastal areas where annual precipitation totals exceed about 100 to 300 mm. Dunes may also provide evidence for multiple periods of sand movement, because of the presence of palaeosols in them (Allchin *et al*. 1978). Moreover, comparison of modern winds and potential sandflows with those indicated by fixed dunes may suggest that there have been changes in wind directions and atmospheric circulation patterns. The interrelationships of dunes and rivers may indicate alternations of aeolian (dry) and fluvial (wet) conditions, as is made evident by consideration of the courses of some tropical rivers (e.g. Senegal, Niger, Fitzroy), which have in the past been ponded up or blocked by dunes.

Dunes (lunettes) developed from lake basins by deposition of material deflated from their beds on lee sides may indicate changing hydrological conditions, with dunes comprised of clay pellets and salts tending to form from desiccated saline surfaces, and those with a predominance of quartzose and sand-size material tending to form from lake beaches developed at times of higher lake levels (Bowler 1973).

Other aeolian features which have palaeoclimatic significance are loess sheets in areas like China and Central Asia. These result from deflation of silt from relatively unvegetated surfaces and its deposition downwind. Within loess profiles there may be multiple palaeosols which resulted from stabilization of land surfaces under vegetated conditions. A detailed treatment of the significance of such materials is provided by Pye and Sherwin (1999). Dating of loess in China has been used to establish the initiation of desert conditions in that area, possibly as a result of circulation changes produced by the uplift of the Tibetan Plateau.

5. Pluvial lakes

Pluvial lakes are bodies of water that accumulated in basins because of former greater moisture availability resulting from changes in temperature and/or precipitation. Their study developed in the second half of the nineteenth century. Jamieson (1863) drew attention to the former greater extent of the great saline lakes of Asia: The Caspian, Aral, Balkhash and Lop-Nor and Lartet (1865) pointed to the expansion of the Dead Sea. The term pluvial itself was first applied to an expanded lake by Hull (1885). A discussion of these early studies and their bibliographic details is given in Flint (1971). A major advance in the study of pluvial lakes came in the western USA with the work of Russell (1885) on Lake Lahontan and of Gilbert (1890) on Lake Bonneville. The Great Basin held some 80 pluvial lakes during the Pleistocene, and they occupied an area at least 11 times greater than the area they cover today. Lake Bonneville was roughly as big as present-day Lake Michigan, about 370m deep and covered 51, 640 km². Lake Lahontan was more complicated in form, covered 23, 000 km², and reached a depth of about 280m. It was nearly as extensive as present-day Lake Erie. River courses became integrated and lakes overflowed from one sub-basin to another. For example, the Mojave River drainage, the largest arid fluvial system in the Mojave Desert, fed at least four basins and their lakes: Lake Mojave (including present day Soda and Silver lakes), the Cronese basin and the Manix basin (which includes the Afton, Troy, Coyote and Harper sub-basins) (Tchakerian and Lancaster, 2001).

Much work has been done to date and correlate the fluctuations in lake levels. Smith and Street-Perrott (1983) demonstrated that many basins had particularly high stands during the period that spanned the Late Glacial Maximum, between about 25, 000 and 10, 000 years ago. More recently there have been studies of the longer term evolution of some of the basins, facilitated by the study of sediment cores, as for example from Owens Lake, the Bonneville Basin, Mono Lake, Searles Lake and Death Valley.

The high lake levels during the Last Glacial Maximum may have resulted from a combination of factors, including lower temperatures and evaporation rates, and reduced precipitation levels. Pacific storms associated with the southerly branch of the polar jet stream were deflected southwards compared to today.

Other pluvial lakes occurred in the Atacama and Altiplano of western South America (Lavenu *et al*., 1984). The morphological evidence for high lake stands is impressive and this is particularly true with regard to the presence of algal accumulations at high levels above the present saline crusts of depressions like Uyuni (Rouchy *et al*., 1996). There exists a great deal of confusion about climatic trends in this region, not least with respect to the situation at the Late Glacial Maximum and in the mid-Holocene (Placzek *et al*., 2001). Nonetheless, various estimates have been made of the degree of precipitation change that the high lake stands imply. Pluvial Laguna Lejíca, which was 15-25m higher than today at 13.5 to 11.3 Kyr BP and covered an area of 9-11km^2 compared to its present extent of 2km^2, had an annual rainfall of 400-500 mm, whereas today it has only around 200 mm. Pluvial Lake Tauca (which incorporates present Lake

Poopo, the Salar de Coipasa and the Salar de Uyuni and which had a high stillstand between 15 and 13.5 Kyr BP), had an annual rainfall of 600 mm compared with 200-400 mm today.

In the Sahara there are huge numbers of pluvial lakes both in the Chotts of Tunisia and Algeria, in Mali (Petit-Maire *et al*., 1999) and in the south (e.g. Mega-Chad). In the Western Desert of Egypt and the Sudan there are many closed depressions or playas, relict river systems, and abundant evidence of prehistoric human activity (Hoelzmann *et al*., 2001). Playa sediments indicate that they once contained substantial bodies of water, which attracted Neolithic settlers. Many of these sediments have now been radio-carbon dated and indicate the ubiquity of an early to mid-Holocene wet phase, which has often been termed the 'Neolithic pluvial'. A large lake, 'The West Nubian Palaeolake', formed in the far north west of Sudan, (Hoelzmann *et al*., 2001). It was especially extensive between 9500 and 4000 years BP, and may have covered as much as 7000km^2. If it was indeed that big, then a large amount of precipitation would have been needed to maintain it – possibly as much as 900 mm compared to the less than 15 mm it receives today. The Sahara may have largely disappeared during what has been called 'The Greening of Africa'.

In the Kalahari of southern Africa, Lake Palaeo-Makgadikgadi encompassed a substantial part of the Okavango Delta, parts of the Chobe-Zambezi confluence, the Caprivi Strip, and the Ngami, Mababe amd Makgadikgadi basins. It was over 50m deep and covered 120, 000km^2, vastly greater than the present area of Lake Victoria (68,800km^2). This makes Palaeo-Makgadikgadi second in size in Africa to Lake Chad at its Quaternary maximum. Its dating is, however, problematic (Thomas and Shaw, 1991) as is its source of water. Some of the water may have been derived when the now dry valleys of the Kalahari were active and much could have been derived from the Angolan Highlands via the Okavango. However, tectonic changes may have led to inputs from the Zambezi.

In the Middle East, expanded lakes occurred in the currently arid Rub-Al-Khali and in Anatolia (Roberts, 1983). In Central Asia the Aral-Caspian system also expanded. At several times during the late Pleistocene (Late Valdai) the level of the lake rose to around 0m (present global sea level) compared to –27m today and it inundated a huge area, particularly to its north. In the Early Valdai it was even more extensive, rising to about +50m above sea level, linking up to the Aral Sea, extending some 1300km up the Volga River from its present mouth and covering an area greater than 1.1 million km^2 (compared to 400, 000km^2 today). At its highest it may have overflowed into the Black Sea. In general, such transgressions have been associated with warming and large-scale influxes of melt-water (Mamedov, 1997), but they are also a feature of glacial phases when there was a decrease in evaporation and a blocking of groundwater by permafrost. Regressions occurred during interglacials and so, for example, in the Early Holocene the Caspian's level dropped to –50 to –60m.

Large pluvial lakes also occurred in the drylands and highlands of China and Tibet, where levels were high from 40, 000 to 25, 000 BP (Li and Zhu, 2001). Similarly the interior basins of Australia, including Lake Eyre, have shown major expansions and contractions, with high stands tending to occur in interglacials (Harrison and Dodson, 1993).

As can be seen from these regional examples, pluvial lakes were widespread (even in hyper-arid areas), reached enormous dimensions, and had different histories in different areas. Pluvials were not in phase in all regions and in both hemispheres (Spaulding, 1991). In general, however, dry conditions during and just after the Late Glacial Maximum and humid conditions during part of the Early to Mid Holocene appear to have been characteristic of tropical deserts, though not of the south-west USA (Street and Grove, 1983).

Changes in effective precipitation may also be reflected in the frequency and range of floods in desert rivers and in their load:discharge ratios (see Chapter 10 for interactions between rainfall regime and fluvial landforms). In particular, in sensitive piedmont zones, marked alternations may occur between deposition and erosion. Although phases of alluvial aggradation and entrenchment may be a response to precipitation changes, they can also result from tectonism, from changes in sediment supply resulting from the operation of such temperature-controlled processes as frost-shattering, or from the inherent instability of the fan surfaces themselves.

Less contentious are the remains of river systems in areas where under present conditions flow is either very localised or non-existent. For example, great wadi systems, traced by the presence of both palaeochannels and associated coarse gravels, occur in hyper-arid areas such as the southeastern Sahara (Pachur & Kröpelin 1987, Brookes 2001).

6. Karst, carbonate precipitates and groundwater

Solution of carbonate rocks to produce karstic phenomena (e.g. cave systems) requires water, and so may give some indication of past humidity. More importantly speleothems from caves often provide a record of environmental change that can be studied by sedimentological and isotopic means. Caves are also receptacles in which aeolian, slope and river sediments can accumulate.

Caves can also preserve the remains of small rodents and insectivores, many of which are the result of deposition of regurgitated pellet material by birds. These indicate environmental conditions both through their species composition and through the size of bones, which may be related to palaeotemperature (Avery, 1982).

Also significant for environmental reconstruction are limestone precipitates that occur on the margins of limestone areas in the form of tufas. These freshwater carbonates may contain floral and faunal remains, palaeosols, etc., which provide environmental information, and the tufas themselves may be indicative of formerly active groundwater and fluvial systems (Nicoll *et al* 2001). Notable examples occur in the Naukluft of Namibia and the Kharga oasis of Egypt.

The isotopic dating of groundwater has demonstrated when it was or was not being recharged. For example, Sonntag and collaborators (1980) have indicated that only limited recharge occurred in the Sahara during the last glacial maximum (20,000 – 14,000 BP), confirming that this was a period of relative aridity. Likewise many of the aquifers of Arabia are relicts from Late Pleistocene times.

7. Other geomorphological indicators

In some arid areas there are weathering crusts and palaeosols that exist outside what are considered to be their normal formative climatic ranges, and which are out of equilibrium with the present climate. Examples are the iron-rich or silica-rich duricrusts of the southern margins of the Sahara and in arid Central Australia. The presence of extensive relict frost screes has also been seen as having climatic significance, having been produced under colder, but probably moist, conditions. These are widespread in North Africa and the Middle East.

Elsewhere, slope deposits and mass movements provide evidence of changes in precipitation (Busche, 1998). For example, slumping along the escarpments of the plateaux of Colorado has been attributed to cooler and wetter conditions which caused shales to become saturated and unstable. In the Atacama ancient debris flow deposits have been used to reconstruct the history of El Niño flood events. Likewise, in southern and central Africa, there are sheets of colluvium (slope wash deposits), which have infilled old drainage lines, and which may have formed when steep slopes behind the pediments on which the colluvium was deposited were destabilized by vegetation sparsity under arid conditions, providing more sediment supply than could be removed by pediment and throughflowing stream systems (Price-Williams *et al.* 1982).

8. Fauna and flora

Pollen analysis (palynology) provides evidence of past vegetation and (by inference), climate conditions. Care has to be taken in assessing the significance of any pollen type which is produced in large quantities and which can also be preferentially transported and deposited over large distances by wind or other mechanisms. Nonetheless, there have been some notable studies of long climatic sequences developed from pollen studies (e.g. Ritchie and Haynes, 1987). Other evidence of past vegetation conditions is provided by scanning electron microscopic study of charcoal which can enable the identification of woody plants, sometimes to the species level. Moreover, stumps of trees such as acacia and fig in the Western Desert of Egypt and Sudan indicate the presence of Savanna in what is now a hyper-arid region.

In the southwestern USA there are middens that were accumulated by pack rats – rodents of the genus *Neotama*. These contain extensive plant debris, and those sheltered in caves or overhangs may remain intact for tens of thousands of years (Madsen *et al*. 2001).

Inferences of palaeoclimate may also be drawn from faunal remains and knowledge about their modern habitat preferences. For example, the relative proportions of grazers and browsers may indicate the importance of grassland or predominantly bushy vegetation respectively (Klein 1980).

9. Archaeological and historical evidence

The changing distributions and histories of human groups have been used to infer changes in the suitability of deserts for habitation. The absence of their artefacts has been used to infer increased aridity, while their existence in hyper-arid areas has been used to infer the existence of humid conditions. Considerable care needs to be exercised in attributing the rise and fall of particular cultures to climatic stimuli of this type, given the range of other factors (e.g. warfare, social collapse) that could be important, but there are some instances where the evidence is relatively unambiguous. For example, in the hyper-arid Libyan Desert of Egypt, where the rainfall is less than 1 mm per annum, artefactual materials occur in areas which are far too dry for human habitation today (Wendorf *et al.* 1976), and are often found in association with old spring deposits, drainage lines and small lake basins.

In historical times, attempts have been made to reconstruct African climates on the basis of famine and drought chronologies, and geographical and climatic descriptions in travellers' reports and diaries (Nicholson 1996). Likewise, there are records of El Niño fluctuations dating back to the sixteenth century AD in Peru (Ortlieb, 2000).

10. The ocean core evidence

One of the most important developments in environmental reconstruction since the 1950s has been the use of ocean cores. Information derived from them can cover millions of years, and has been less fragmented than most terrestrial evidence.

Ocean floors off the world's deserts have accumulated sediments derived by aeolian and fluvial inputs from neighbouring land (Sirocko & Lange 1991). These may be susceptible to relatively accurate dating, and record the relative importance of fluvial and aeolian inputs, the degree of weathering of river-borne feldspars, the pollen and phytolith rain, the salinity of the ocean or sea, the intensity of monsoonal winds and of upwelling activity (Prell *et al.* 1980) and the temperature of offshore waters recorded by oxygen isotope ratios in foraminiferal tests.

11. The antiquity of deserts

Although formerly many deserts were regarded as a result of Holocene (post-glacial) progressive desiccation, it is now clear that many of our present deserts are old (Goudie 2002). This applies particularly in the case of the Namib and the Atacama coastal deserts. Their climatic development was closely related to plate tectonics and sea-floor spreading in that the degree of aridity must have been largely controlled by the opening up of the seaways of the Southern Ocean, the location of Antarctica with respect to the South Pole, and the development of the offshore, cold Benguela and Peruvian currents. Arid conditions appear to have existed in the Namib for some tens of millions of years, as is made evident by the Tertiary Tsondab Sandstone – a lithified sand sea (Ward 1988) that underlies the current Namib erg. Likewise the Atacama of South America appears to have been predominantly arid since at least the late Eocene, with hyper-aridity since the middle to late Miocene. The uplift of the Andes during the Oligocene and early Miocene produced a rain-shadow effect while the development of cold Antarctic bottom waters and the Peruvian current at 15-13 million years ago created another crucial ingredient for aridification (Alonso *et al*. 1999).

In India and Australia, latitudinal shifts caused by sea-floor spreading and continental drift led to moist conditions during much of the Tertiary, but they entered latitudes where conditions were more arid in the late Tertiary. Isotopic studies in the Siwalik foothills of Pakistan illustrate increasing aridity in the late Miocene, where C3/C4 analyses show a change from a C3 (mainly forested) setting to a C4 (mainly grassland) setting at about 7 million years ago (Quade *et al*. 1989). In China, Miocene uplift and a resulting transformation of the monsoonal circulation caused aridification. The aeolian red clays and loess of China may have started to form around 7.2-8.5 million years ago (Qiang *et al.* 2001). Indeed it is possible that the uplift of mountains and plateaux in Tibet and North America may have caused a more general change in precipitation in the Late Miocene, as is made evident by the great expansion of C4 grasses in many parts of the world (Pagani *et al.* 1999).

With regard to the Sahara, sediment cores from the Atlantic contain dust-derived silt that indicates that a well-developed arid area, producing dust storms, existed in North Africa in the early Miocene, around 20 million years ago (Diester-Haass & Schrader 1979). It is possible that uplift of the Tibetan Plateau played a role in this by creating a strong counter-clockwise spiral of winds that drove hot, dry air out of the interior of Asia across Arabia and northern Africa (Ruddiman 2001, p. 388).

12. Pleistocene intensification of aridity

In many regions aridity intensified in the late Pliocene and Pleistocene. It became a prominent feature of the Sahara in the late Cenozoic, partly because of ocean cooling and partly because ice cap build up created a steeper temperature gradient between the Equator and the Poles. This led to an increase in trade-wind velocities and in their ability to mobilise dust and sand. deMenocal (1995) recognised an acceleration in dust loadings in ocean cores off the Sahara and Arabia after 2.8 Ma, and attributed this to decreased sea surface temperatures associated with the initiation of extensive Northern Hemisphere glaciation. Likewise, loess deposition accelerated in China after around 2.5 Ma ago (Ding *et al.* 1992). The study of sediments from the central North Pacific suggests that dust deposition became more important in the late Tertiary, accelerating greatly between 7 and 3 Ma (Leinen & Heath 1981), but it was around 2.5 Ma ago that there occurred the most dramatic increase in dust sedimentation.

13. Fluctuations within the Pleistocene

All deserts show the impact of Pleistocene climatic changes. They expanded from time to time, covering areas that are now heavily vegetated. As a consequence stabilised sand seas occur in areas where rainfall levels are currently in excess of 500-800 mm. Stabilised sand seas occur on the south side of the Sahara between Senegal and the Sudan, while in southern Africa the Mega-Kalahari extended as far north as the Congo basin. Relict dunes also occur in parts of South America, including the Llanos in the north and the Pampas in the south. The High Plains of America also have extensive areas of stabilised dunes, the most notable examples of which are the Nebraska sandhills. In North West India the dunes of the Mega-Thar can be traced from Rajasthan southwards into Gujarat and eastwards towards Delhi (Allchin *et al*, 1978), while in

Australia large linear dunes can be found in Kimberleys of the tropical north (Goudie *et al.,* 1993). Changes in the extent of sand seas may be the result of changes in precipitation, but it is also possible that high glacial trade wind velocities played a role (Ruddiman 1997) by increasing rates of sand transport. These higher wind velocities may also have had a marked influence on deflation and dust storm activity. There is clear evidence for dust fluxes into the oceans at the time of the Last Glacial Maximum being 2 to 4 times higher than at present (Grousset *et al.* 1998). Studies have also been made of wind-transported materials (including diatoms deflated from desiccated lakes) to plot wind strength changes over extended periods (e.g. Shi *et al.* 2001).

Conversely, at other times, as we have seen, large, freshwater lakes occupied the Altiplano basins of South America, the many depressions of the Basin and Range Province in the USA (notably Lahontan and Bonneville), the Aral-Caspian of Central Asia, the Chad-Bodélé depression in the Sahara, the Dead Sea in the Middle East and the Lake Eyre basin in Australia. Even in the hyper-arid heart of the Sahara and the Libyan deserts there are lake deposits, tufas, old drainage lines and other evidence of enhanced hydrological activity.

14. The Frequency of climatic change

In addition to being severe, Quaternary climatic changes in deserts were frequent. Dunes were repeatedly reactivated and stabilised, both in the Pleistocene and the Holocene, lakes rose and fell over short spans of time, and pulses of dust were deposited in the world's oceans. The frequency of change is indicated by high-resolution studies of ocean and lake cores and because of the increasing availability of high-resolution optical and thermal luminescence dates for dune sands and loess. The multiple glaciations and deglaciations of high latitudes, and the multiple fluctuations within them, all indicate the instability of Quaternary climates. They were all associated with major changes in the oceans, pressure systems and wind belts which in turn had an impact on deserts. Lake level fluctuations in arid basins may indicate short-lived fluctuations that correlate with Heinrich events (Benson *et al*. 1998) and Dansgaard-Oescheger cycles (Lin *et al.* 1998), while the Younger Dryas also seems to have its counterparts in arid regions (e.g. Zhou *et al*. 2001).

15. The context of change

Pluvials were neither in phase in all areas nor in both hemispheres (Spaulding 1991). In a mid-latitude location like the south-west of the USA (Smith and Street-Perrott, 1983), there was greatly increased effective moisture at the time of the Last Glacial Maximum, eighteen to twenty thousand years ago. This was partly caused by decreased evaporation, but also by an intensified zonal circulation and the equatorward displacement of mid-latitude westerlies and associated rain-bearing depressions, particularly in winter.

The tropics were much less influenced by the displaced full glacial westerlies. They experienced relatively dry conditions at that time, but subsequently experienced a major pluvial in the early to mid-Holocene (Grove and Goudie 1971). Under warmer Holocene conditions, monsoonal circulation was intensified, and in the Northern Hemisphere the Intertropical Convergence Zone would have shifted north, bringing rainfall into areas like West Africa, the Sudan, Ethiopia, Arabia and the Thar. The basis for this may have been increased summer solar insolation associated with the 23,000 year rhythm of orbital precession, for at around 9000 years BP Milankovitch-forcing led to Northern Hemisphere summers with almost 8 per cent more insolation than today (Kutzbach and Street-Perrott 1985). Higher insolation caused greater heating of the land, stronger convection, more inflow of moist air and a higher summer monsoonal rainfall. In contrast, weaker insolation maxima around 35,000 and 60,000 years ago would have created weaker monsoons (Ruddiman 2001).

Changes in insolation receipts at 9000 BP can help to explain the Northern Hemisphere low latitude pluvial, but they have less direct relevance to the Southern Hemisphere (Tyson and Preston-Whyte 2000). Also important in determining the spatial and temporal patterning of precipitation change are sea surface temperature conditions associated with the build-up and disintegration of the great ice-sheets (Shi *et al*. 2000; Rognon and Coudé-Gaussen 1996). In addition, changes in snow and ice cover over Asia, including Tibet and the Himalayas, could have had a major effect on the monsoon (Zonneveld *et al*. 1997).

The Holocene experienced abrupt and relatively brief climatic episodes, which caused dune mobilization in the American High Plains (Arbogast 1996) and alternations of pluvials and intense arid phases in tropical Africa. The Holocene in low latitudes was far from stable and it is possible that a climatic deterioration around 4,000 years ago could be involved in the near simultaneous collapse or eclipse of civilizations in Egypt, Mesopotamia, and Northwest India (Dalfes *et al*. 1997).

These brief events cannot be readily accounted for by orbital changes, so other mechanisms need to be considered, including changes in the thermohaline circulation in the oceans, or in land surface conditions (Gasse and van Campo 1994). Certainly the mechanisms causing changes in atmospheric circulation would have been both numerous and complex, and there will have been lagged responses (e.g. slow decay of ice-masses, gradual falls of groundwater, etc.). It is also apparent that there will have been differing hemispheric and regional responses to change (deMenocal and Rind 1993). For example, Arabia and Northeast Africa may have been especially sensitive to changes in North Atlantic sea surface temperatures, while monsoonal Asia have been especially affected by snow and ice conditions in the Himalayas and Tibetan Plateau.

16. Recent change

At the present day, deserts continue to change, sometimes as a result of climatic fluctuations like the run of droughts that has afflicted the West African Sahel over recent decades (see Chapter 6). The changing vegetation conditions in the Sahel, which have shown marked fluctuations since the mid- 1960s, have been mapped by Tucker *et al.* (1991). Interannual variability in the position of the southern boundary of the Sahara, as represented by the 200 mm isohyet, can be explained in large measure by changes in the North Atlantic Oscillation and the El Niño Southern Oscillation (ENSO) (Oba *et al* 2001). The drought also led to reductions in the flow of rivers like the Senegal and Niger, and to an increase in dust storm activity (Middleton, 1985). The extent of Lake Chad's water surface has also fluctuated dramatically (Nicholson 1996). It was particularly badly affected by the drought, which caused the lake surface area to fall from *c.* 25,000 km^2 in 1960 to just a tenth of that figure in the mid-1980s (Birkett, 2000).

We also know from recent centuries that ENSO fluctuations have had important consequences for such phenomena as droughts and dune reactivation (Forman *et al*. 2001), and through their effect on vegetation cover have had major impacts on slope stability and soil erosion (Viles and Goudie, 2003). Lake levels have responded to El Niño influences (Arpe *et* al. 1997), large floods have occurred, valleys have been trenched (Bull 1997), erosivity patterns have altered (D'Odorico *et* al. 2001), and landslides and debris flows have been generated (Grosjean *et al.* 1997). To that we need to add the increasing numbers of changes being wrought by human agency, changes that are often categorized as 'desertification' (Chapter 18): surface degradation, gully formation, ground subsidence, salinisation, bush encroachment and the like (Middleton and Thomas, 1997). In the future, global warming may increase the aridity of many drylands, leading to further geomorphological changes and placing further pressures on hydrological resources.

References

Allchin B., Goudie A.S. and Hegde K.T.M., (1978). The prehistory and palaeogeography of the Great Indian Desert. London, Academic Press.

Alonso R.N., Jordan T.E., Tubbutt K.T., and Vandervoort D.S., (1999). Giant evaporite belts of the Neogene central Andes. Geology 19, 401-4.

Arbogast A.F. (1996). Stratigraphic evidence for late-Holocene Aeolian sand mobilisation and soil formation in south-central Kansas, USA, Journal of Arid Environments, 34: 403-14.

Arpe K., Bengtsson L., Golitsyn G.S., Mokhov I.I. and Ettahir E.A.B. (1997). Connection between Caspian sea level variability and ENSO. Geophysical Research Letters 27, 2693-2696.

Avery D. M. (1982). Micromammals as palaeoenvironmental indicators and an interpretation of the late Quaternary in the Southern Cape Province, South Africa. Annals of the South African Museum 85, 183-374.

Benson L., Lund S. P., Burdett J. W., Kashgarian M., Rose T. P., Smoot J. P. and Schwartz M. (1998). Correlation of Late-Pleistocene Lake-Level oscillations in Mono Lake, California, with North Atlantic climate events, Quaternary Research, 49: 1-10.

Birkett C.M. (2000). Synergist remote sensing of Lake Chad: variability of basin inundation, Remote Sensing of Environment, 72: 218-36.

Bowler J. M. (1973). Clay dunes: their occurrence, formation and environmental significance, Earth-Science Reviews, 9: 315-38.

Brookes I. A. (2001b). Possible Miocene catastrophic flooding in Egypt's Western Desert, Journal of African Earth Sciences, 32: 325-33.

Bull W.B. (1997). Discontinuous ephemeral streams. Geomorphology 19, 227-276.

Busche D. (1998). Die Zentrale Sahara (Gotha: Justus Perthes Verlag).

Dalfes H. N., Kukla G., and Weiss H. (1997). (eds.), Third Millennium BC Climate Change and Old World Collapse (Berlin: Springer Verlag).

DeMenocal P. B. (1995). Plio-Pleistocene African climate, Science, 270: 53-9.

DeMenocal, P. B. and Rind D. (1993). Sensitivity of Asian and African Climate to variations in seasonal insolation, glacial ice cover, sea surface temperature and Asian orography, Journal of Geophysical Research, 98 (D4): 7265-87.

Diester-Haas L., and Schrader H. J. (1979). Neogene coastal upwelling history off north-west and south-west Africa, Marine Geology, 29: 39-53.

Ding Z., Rutter N., Han J. and Liu T., (1992). A coupled environmental system formed at about 2.5 Ma in East Asia. Palaeogeography, Palaeoclimatology, Palaeoecology 94, 223-242.

D'Odorico P., Yoo J.C. and Over T.M. (2001). An assessment of ENSO - induced patterns of rainfall erosivity in the southwestern United States. Journal of Climate 14, 4230-4242.

Flint R.F. 1971. Glacial and Quaternary Geology. New York: Yohn Wiley and Sons.

Forman S.L., Oglesby R. and Webb R.S. (2001). Temporal and spatial patterns of Holocene dune activity on the Great Plains of North America: megadroughts and climate links. Global and Planetary Change 29, 1-29.

Gasse F. and Van Campo E., (1994). Abrupt post-glacial climate events in west Africa and North Africa monsoon domains. Earth and Planetary Science Letters 126, 435-456.

Gilbert G.K. (1890). Lake Bonneville. U.S. Geological Survey Monograph 1.

Goudie, A.S. (2002). Great Warm Deserts of the World. Oxford: Oxford University Press.

Goudie A.S., Stokes S., Livingstone I., Bailiff I.K., and Allison R.J., (1993). Post-depositional modification of the linear sand ridges of the west Kimberley area of north-west Australia. Geographical Journal 159, 306-317.

Grosjean M, Núñez L, Castajena I and Messerli B. (1997). Mid-Holocene climate and culture change in the Atacama Desert, northern Chilie. Quaternary Research 48, 239-246.

Grousset F. E., Parra M., Bory JA., Martinez P., Bertrand P., Shimmield G. and Ellam R. M. (1998). Saharan wind regimes traced by the Sr-Nd Isotopic composition of subtropical Atlantic sediments: Last Glacial Maximum vs today, Quaternary Science Reviews, 17: 395:409.

Grove A.T. and Goudie A.S. (1971). Late Quaternary Lake Levels in the Rift Valley of Southern Ethiopia and elsewhere in Tropical Africa. Nature 234, 403-405.

Harrison S.P. and Dodson J. (1993). Climates of Australia and New Guinea since 18,000 yr B.P., in H.E.Wright, J.E.Kutzbach, T. Webb, W.F.Ruddiman, F.A.Street-Perrott and P.J.Bartlein (eds.) Global climates since the Last Glacial Maximum. Minneapolis: University of Minnesota Press, pp. 265-293.

Hoelzmann P., Keding B., Berke H., Kröpelin S. and Kruse H-J. (2001). Environmental change and archaeology: lake evolution and human occupation in the Eastern Sahara during the Holocene. Palaeogeography, Palaeoclimatology, Palaeoecology 169, 193-217.

Jamieson, T.F. (1863), On the parallel roads of Glen Roy and their place in the history of the glacial period, Quarterly Journal of Geological Society London, 19, 235-259.

Lartet, L. (1865), Sur la formation du basin de le mer morte ou lac asphaltine et sur les changements survenus dans nivau de ce lac. Comptes Rendus Academie des Sciences (Paris), 60, 796-800.

Klein R.G. (1980). Environmental and ecological implications of large mammals from Upper Pleistocene and Holocene sites in southern Africa. Annals of the South African Museum 81, 223-83.

Kutzbach J. and Street-Perrott F. A. (1985). Milankovitch forcing of fluctuations in the level of tropical lakes from 18 to 0 kyr BP, Nature, 317: 130-4.

Lavenu A., Fournier M and Sebrier M. (1984). Existence de deux nouveaux episodes lacustres quaternaires dans lAltiplano peruvo-bolivien. Cahiers ORSTOM, ser. Géologie 14, 103-114.

Leinen M. and Heath G.R. (1981). Sedimentary indicators of atmospheric activity in the northern hemisphere during the Cenozoic. Palaeogeography, Palaeoclimatalogy, Palaeoecology 36, 1-21.

Li B.Y. and Zhu L.P, (2001). "Greatest lake period" and its palaeo-environment on the Tibetan Plateau. Journal of Geographical Sciences (Acta Geographica Sinica) 11, 34-42.

Lin J.C., W.S. Broecker, S.R. Hemming, I. Haidas, R.F. Andreson, G.I. Smith, M. Kelley, and G. Bonani. (1998). A reassessment of U-Th and C_{14} ages for late glacial high-frequency hydrological events at Searles Lake, Calofornia. Quaternary Research, 49(1), 11-23.

Madsen D.B., Rhode D., Grayson D.K., Broughton J.M., Livingston S.D., Hunt J., Quade J., Schmitt D.N. and Shaver M.W. (2001). Late Quaternary environmental change in the Bonneville basin, western USA. Palaeogeography, Palaeoclimatology, Palaeoecology 167, 243-271.

Mainguet M. (1999). Aridity, Droughts and Human Development. Heidelberg: Springer.

Mamedov A.V. (1997). The Late Pleistocene-Holocene history of the Caspian Sea. Quaternary International 41/42, 161-166.

Meigs P. (1953). World distribution of arid and semi-arid homoclimate. UNESCO Arid Zone Research Series, 1, 203-209.

Middleton N.J. and Thomas, D.S.G. (1997). World atlas of desertification (2^{nd}. Edition). London:Arnold.

Middleton N.J. (1985). Effect of drought on dust production in the Sahel. Nature 316, 431-4.

Nicholson S.E. (1996). Environmental change within the historical period. In, W.M.Adams, A.S.Goudie and A.R.Orme (eds,) The Physical Geography of Africa. Oxford: Oxford University Press, pp. 60-87.

Nicoll K. (2001). Radiocarbon chronologies for prehistoric human occupation and hydroclimatic change in Egypt and northern Sudan. Geoarchaeology 16, 47-64.

Oba, G., E. Post, and N.C. Stenseth. (2001). Subsaharan desertification and productivity are linked to hemispheric climate variability, Global Change Biology, 7(3), 241.

Ortlieb L. (2000). The documented historical record of El Niño events in Peru: an update of the Quinn record (sixteenth thrugh nineteenth centuries). In Diaz H.F. and Markgraf V. (eds.) El Niño and the Southern Oscillation. Cambridge, pp. 207-295.

Pachur H.J. and Kröpelin S. (1987). Wadi Howar: Paleoclimatic evidence from an extinct river system in the southeastern Sahara. Science 237, 298-300.

Pagani M., Freeman K.H. and Arthur M.A. (1999). Late Miocene atmsopheric CO_2 concentrations and the expansion of C4 grasses. Science 285, 876-879.

Petit-Maire N., Burollet P.F., Ballais J-L., Fontugne M., Rosso J-C. and Lazaar A, (1999). Paléoclimats Holocènes du Sahara septentionale. Dépôts lacustres et terrasses alluviales en bordure du Grand Erg Oriental à l'extrême – Sud de la Tunisie. Comptes Rendus Académie des Sciences, Series 2, 312, 1661-1666.

Placzek C., Quade J. and Betancourt J.L. (2001). Holocene lake-level fluctuations of Lake Aricota, southern Peru. Quaternary Research 56, 181-190.

Prell, W. L., Hutson W.H., Williams D.F., Be A.W.H, Geitzenauer K., Molfino B. (1980). Surface circulation of the Indian Ocean during the last glacial maximun, approximately 18,000 BP. Quaternary Research 14, 309-36.

Price-Williams D., Watson A., Goudie A.S. (1982). Quaternary colluvial stratigraphy, archaeological sequences and palaeoenvironments in Swaziland, southern Africa. Geographical Journal 148, 50-67.

Pye K. and Sherwin D., (1999). Loess. In: A.S. Goudie, I. Livingstone and S. Stokes (eds.) Aeolian Environments, Sediments and Landforms. Chichester: Wiley, 214-238.

Qiang X.K., Li Z.X., Powell C.McA. and Zheng H.B. (2001). Magnetostratigraphic record of the Late Miocene onset of the East Asian monsoon, and Pliocene uplift of northern Tibet. Earth and Planetary Science Letters 187, 83-93.

Quade J., Cerling T.E. and Bowman J.R. (1989). Development of Asian monsoon revealed by marked ecological shift during the latest Miocene in northern Pakistan. Nature 342, 163-166.

Ritchie J.C. and Haynes C.V. (1987). Holocene vegetation zonation in the eastern Sahara, Nature, 330: 645-7.

Roberts N. (1983). Age, paleoenvironments, and climatic significance of late Pleistocene Konya Lake, Turkey. Quaternary Research 19, 154-71.

Rognon P. and Coudé-Gaussen G. (1996). Paleoclimates off Northwest Africa (28º - 35ºN) about 18,000 yr BP based on continental aeolian deposits. Quaternary Research 46, 118-126.

Rouchy J.M., Servant M., Fournier M. and Causse C. (1996). Extensive carbonate algal bioherms in upper Pleistocene saline lakes of the central Altiplano of Bolivia. Sedimentology 43, 973-993.

Ruddiman W.F. (1997). Tropical Atlantic terrigenous fluxes since 25,000 yrs B.P. Marine Geology 136, 189-207.

Ruddiman W.F. (2001). Earth's climate: Past and Future. New York: W.H.Freeman and Company.

Russell I.C. (1885). Geological history of lake Lahontan. U.S. Geological Survey Monograph 11.

Shi N., Schneider R., Beug H-J., and Dupont L.M., (2001). Southeast trade wind variations during the last 135 kyr: evidence from pollen spectra in eastern South Atlantic sediments. Earth and Planetary Science Letters 187, 311-321.

Sirocko F. & Lange H. (1991). Clay mineral accumulation rates in the Arabian Sea during the later Quaternary. Marine Geology 97, 105-19.

Smith G.I. and Street-Perrott F.A. (1983). Pluvial lakes of the western United States. In S.C. Porter (ed.) Late Quaternary Environments of the United States. Vol. 1, the Late Pleistocene. Longman : London 190-212.

Sonntag C., Thorweite R.J., Lohnert E.P., Junghans C., Munnick K.O., Klitzsch E., El Shazly E.M., Swailem F.M. (1980). Isotopic identification of Saharan groundwater – groundwater formation in the past. Palaeoecology of Africa 12, 159-71.

Spaulding W.G. (1991). Pluvial climatic episodes in North America and North Africa: types and correlation with global climate. Palaeogeography, Palaeoclimatology, Palaeoecology 84, 217-229.

Street F. A. and Grove A. T. (1979). Global maps of lake-level fluctuations since 30,000 yr BP, Quaternary Research, 12: 83-118.

Tchakerian V.P. (1999). Dune palaeoenvironments. In A.S. Goudie , I. Livingstone and S.Stokes (eds.) Aeolian Environments, Sediments and Landforms. Chichester : Wiley, pp. 261-292.

Tchakerian V.P. and Lancaster N. (2001). Late Quaternary arid/humid cycles in the Mojave Desert and Western Great Basin of North America. Quaternary Science Reviews (in press).

Thomas D.S.G. and Shaw P. (1991). The Kalahari Environment. Cambridge: Cambridge University Press.

Thornthwaite C.W. (1948). An approach towards a rational classification of climate. Geographical Review 38, 55-94.

Tucker C.J., Dregne H.E. and Newcomb W.W. (1991). Expansion and contraction of the Sahara Desert from (1980) to (1990). Science 253, 299-301.

Tyson P.D. and Preston-Whyte R.A. (2000). The Weather and Climate of Southern Africa. Cape Town: Oxford University Press.

Viles H.A. and Goudie A.S. (2003). Interdecadal, decadal and multidecadal scale climatic variability and geomorphology. Earth-Science Reviews 61, 105-131.

Ward J.D. (1988). Eolian, fluvial and pan (playa) facies of the Tertiary Tsondab Sandstone Formation in the Central Namib Desert, Namibia. Sedimentary Geology 55, 143-162.

Wendorf F., Schild R., Said R.,. Haynes C.V, Gautier A., Kobusiewicz P. (1976). The prehistory of the Egyptian Sahara. Science 193, 103-16.

Zhou W., Head M.J., An, Z., De Deckker P., Liu Z., Liu X., Li X., Donahue D., Jull A.J.T. and Beck W.W. (2001). Terrestrial evidence for a spatial structure of tropical-polar interconnections during the Younger Dryas episode. Earth and Planetary Science Letters 191, 231-239.

Zonneveld K.A.F., Ganssen G., Troelrma S., Versteegh G.J.M. and Visser H. (1997). Mechanisms forcing abrupt fluctuations of the Indian Ocean Summer Monsoon during the last deglaciation. Quaternary Science Reviews 16, 187-201.

Chapter 9

HYDROCLIMATOLOGY OF WIND EROSION IN ARID AND SEMI-ARID ENVIRMONMENTS

Wim M. CORNELIS

International Centre for Eremology, Department of Soil Management and Soil Care, Ghent University, Coupure links 653,B-9000 Ghent, Belgium - e-mail: wim.cornelis@UGent.be

1. Introduction

The wind has been active as an erosive agent throughout geological times in many parts of the world. It takes up soil from one place and deposits it in another. Outstanding examples are the extensive loess deposits along the Huanghe River (Yellow River) in China, and along the Missouri and Mississippi rivers in the USA. However, in recent years, wind erosion has become more active and more destructive on a global scale, due to the action of man, which is associated with a drastic growth of the world's population over the past century. This accelerated erosion has been caused by inadequate land management including, clearance of the natural vegetation, overgrazing and non-adapted agricultural practices leading to land degradation. In the 1930, a decreased precipitation coupled with intensive agricultural activities caused a dramatic increase in wind erosion in the Great Plains of the United States, resulting in the so-called Dust Bowl. Another example is the Mu Us region in North China with an annual precipitation of 400 mm, which was once grassland partially covered with forest, while now is one of the major sources of dust in the world as a result of overgrazing and agricultural practices.

On a continental scale wind erosion is mainly confined to the so-called drylands, which comprise arid, semiarid and dry sub-humid areas (see Figure 1) and where the following conditions frequently occur: a loose, dry, finely divided soil and a smooth land-surface devoid of a vegetative cover due to low precipitation, large fields, and strong winds (FAO, 1960). According to the GLASOD database (Global Soils Degradation Database), wind erosion accounts for 42% of the degraded area in these drylands (UNEP, 1997; see Table 1). This value, however, varies according to the aridity zone. In arid regions, wind erosion accounts for more than 60%, a figure that falls to 21% in dry subhumid areas. The proportion of drylands affected by wind erosion differs also from continent to continent. In Africa, the dominating form of soil degradation is wind erosion, whereas in other continents water erosion is the main cause of soil degradation.

In order to control wind erosion effectively, farmers should be supported by government policies. As Agnew and Warren (1990) noted: "Ultimately most of the practices that lead to the degradation of arid land can be traced not to the specific farmers, but to poorly conceived policies".

2. Effects of wind erosion

Concerning the damage resulting from wind erosion events, on-site as well as off-site effects occur. An important on-site effect is the sorting action of the wind that causes loss of the finer, lighter organic matter, silt, and clay fractions from the surface soil, leaving coarser, less productive material behind (Chepil, 1957; FAO, 1960; Chepil and Woodruff, 1963; Schmidt and Triplett, 1967; Knottnerus, 1985). During the progression of the erosion process, the particles that move in saltation are piled up in drifts over much of the eroded area. The abrasive action of these saltating particles causes a disintegration of the clods. The longer erosion continues, the greater is

P. D'Odorico and A. Porporato (eds.), Dryland Ecohydrology, 141–159.

the amount of drifted material accumulated in the vicinity of the eroded area and the lower is the subsequent velocity of the wind required to initiate erosion (Chepil, 1958a). The sorting action over many years – with a remaining soil more susceptible to wind erosion (Fryrear, 1969) – makes soils progressively coarser until nothing remains but infertile skeletal material forming shifting sand dunes and gravely pavements (Chepil, 1962; Lyles, 1975). As a result of the evanescence of the most fertile part of the soil, the land becomes less productive, leading to decreasing crop yields when this land is cultivated (Stallings, 1957). Growth and development of seedlings can be delayed with several weeks depending the severity of the injury and the crop type itself (Fryrear, 1969).

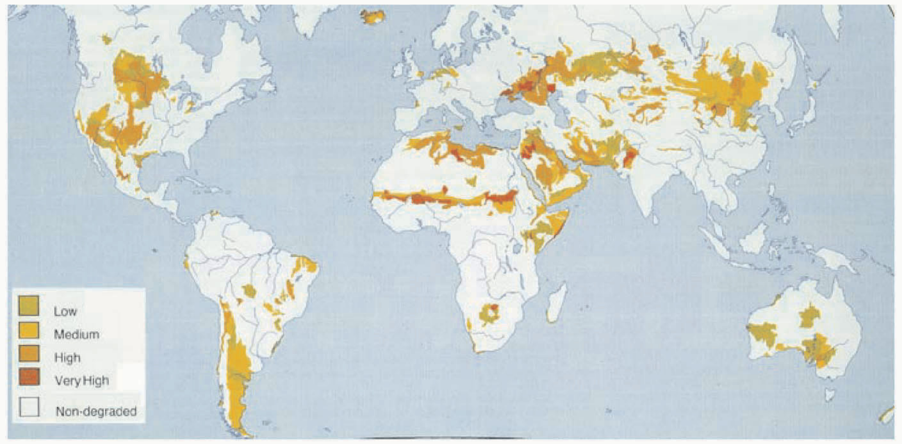

Figure 1. Degraded dryland area susceptible to wind erosion. Note that the white areas are non-degraded: the Sahara sand desert e.g. is not considered as being degraded (source: GLASOD; UNEP, 1997).

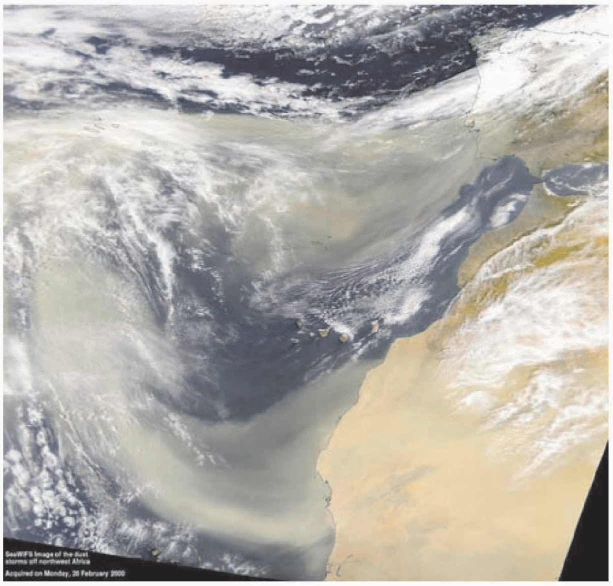

Figure 2. Satellite image of a dust storm originating in the Saharan desert on 26 February 2000. The image, from 28 February 2000, shows the dust cloud moving towards the Atlantic but then bending towards Europe (Provided by the SeaWiFS Project, NASA/Goddard Space Flight Center and ORBIMAGE).

Table 1. Soil degradation type by region in susceptible dryland area (10^6 ha) (source: GLASOD; UNEP, 1997).

	Dryland area susceptible to soil degradation by				
	Water erosion 10^6 ha	Wind erosion 10^6 ha	Chemical deterioration 10^6 ha	Physical deterioration 10^6 ha	*Total* 10^6 ha
Africa	119.1	159.9	26.5	13.9	*319.4*
Australia	69.6	16.0	0.6	1.2	*87.4*
Asia	157.5	153.2	50.2	9.6	*370.5*
Europe	48.1	38.6	4.1	8.6	*99.4*
North America	38.4	37.8	2.2	1.0	*79.4*
South America	34.7	26.9	17.0	0.4	*79.0*
Total	*467.4*	*432.4*	*100.7*	*34.7*	*1035.2*

Besides the lower productivity of the soil, plant seedlings are damaged physically resulting from the abrasive effects of blowing sand grains. Young plants can be cut off by the sandblasting effect. Leaves and stems are shredded or damaged by abrasion, reducing or delaying growth, or causing greater susceptibility to diseases. Roots can be exposed by removal of soil, and in some cases young plants are completely blown out of the soil or buried (FAO, 1960; Schmidt and Triplett, 1967; Knottnerus, 1985). Studies by Armbrust (1984) have shown that physical damage to wheat leaves caused a twofold or greater increase in leaf conductance. Where dust from blowing soil settles on plants, it impairs the plant's ability to use sunlight for photosynthesis (Nanney et al., 1993). Fully developed crops suffer less severely from the effect of soil movement than young emerging plants. Therefore, protection from erosive and abrasive winds in a semiarid environment may be needed most during early plant development (Banzhaf et al., 1992).

Wind erosion not only has direct effects, it also indirectly influences agriculture in that blowing soil permeates machinery and carries pesticides for long distances, removes fertilizers, increases the susceptibility of plants to certain types of stress including diseases, contributes to the transmission of some plant pathogens, causes respiratory ailments both to man and animals, fills drainage ditches and channels, and increases irrigation costs (FAO, 1960; Hayes, 1965; Duncan and Moldenhauer, 1968; Peerlkamp, 1970; Claflin et al., 1973; Fryrear and Downes, 1975; Wilson and Cooke, 1980; Knottnerus, 1985; Skidmore, 1986; Nanney et al., 1993).

Furthermore, wind erosion not only causes on-site problems. Significant off-site effects on a local scale are blockage of roads and railways, reduction of visibility, etc. (FAO, 1960; Duncan and Moldenhauer, 1968; Fryrear, 1969; Skidmore, 1986, 1989).

On a more global scale, wind erosion is a devastating environmental threat as the finest particles can be transported over hundreds of kilometres (Figure 2). Major sources of windblown dust are the arid and semi-arid areas where the soil is exposed seasonally to strong winds (Pye, 1987). Ephemeral river flood plains, dry lakes, coastal sabkhas, alluvial fans, and loess deposits strongly contribute to the production of windblown dust. Dust storms causing serious off-site environmental problems occur most frequently in the Arabian Peninsula, the Seistan Basin of Iran, the Indus Plain, former Soviet central Asia, the Tarim Basin of China and the Sahara (Goudie, 1983; Middleton et al., 1986). Studies by the U.S. Geological Survey have linked the decline of the coral reefs in the Caribbean to the increasing frequency and intensity of Saharan dust storms and sand storms. Saharan dust could also play a role in determining the frequency and intensity of hurricanes formed in the eastern Atlantic. Changes in dust emissions from arid and semi-arid areas may significantly affect the radiative budget in the sub-tropical regions and, hence, the atmospheric global circulation (Li et al., 1996). Aerosols directly affect the radiative budget by absorbing and reflecting solar radiation, which reduces the radiation reaching the Earth surface. Thus, due to the direct radiative forcing, aerosols cool up the Earth surface (e.g., Ramanathan et al., 2001; Kaufman et al., 2002). Indirectly, because dust particles act as cloud condensation nuclei (Rosenfeld et al., 2001), aerosols disrupt also cloud microphysical processes. In addition, the spread of foot and mouth disease in Western Europe and the asthma outbreaks in the Caribbean and the USA have been associated with desert storms in northern Africa (McKie, 2001). However, deposition of desert dust is also known for being an important source of nutrients in ecosystems located downwind of active regions of dust emission. A typical example is the supply of nutrients by Saharan dust to the tropical Atlantic sea floor and Amazon Basin (Swap et al., 1992).

.

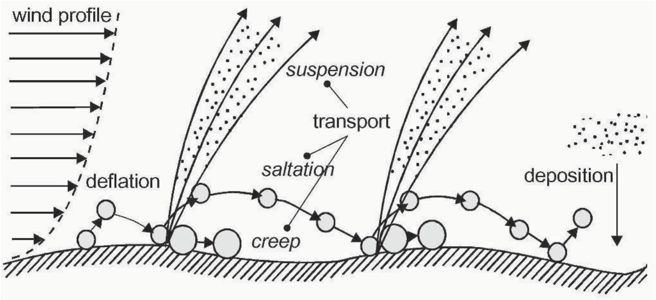

Figure 3. Schematic representation of the main phases involved in the wind-erosion process.

3. Wind-erosion processes

Wind erosion is the physical process of wind-induced movement of sediment. Three distinct phases are generally considered: (*i*) *deflation*, i.e. the blowing away of soil and sand particles by wind shear at the surface, (*ii*) their subsequent *transport* by wind through creep, saltation or suspension, and (*iii*) their *deposition* through dry and wet removal (Shao, 2000). These phases of the wind-erosion process are schematically depicted in Figure 3. Another wind-erosion process that is often considered is *abrasion*, i.e. the sandblasting of rocks, soil aggregates and crops by a sediment-laden air stream.

Aeolian transport of sediment has three distinct modes, depending primarily on the particle size (Bagnold, 1941) and the atmospheric flow conditions (Shao et al., 1996) (see Figure 3). Sand-sized particles of approximately 60-1000 µm move downwind over short distances and within the lower 1 m of the atmosphere (Cooke et al., 1993) by *saltation*. It is the initial type of transport of soil particles after they have been detached from the surface bed. Saltation is a jumping movement of particles caused by consecutive transfer of momentum of falling particles. Very small dust-sized particles (<60µm if from mineralogical origin) are transported in *suspension*. These particles can remain airborne for some time and can be transported over relatively long distances while dispersed beyond the atmospheric surface layer. This transport mode is primarily induced by bombardment of saltating sand-sized particles. Particles larger than 500 µm or less exposed particles may be pushed or rolled along the surface by the impact of saltating particles in what is know as *surface creep*. Although the distinction between sand and dust is set at 60 µm (Bagnold, 1941), a stricter, aerodynamic based classification can be considered. Shao et al. (1996) defined dust particles as those with a fall velocity smaller than 50% of the mean Langrangian vertical velocity for fluid elements. The fall velocity, which is a function of particle size, can be calculated from Malcolm and Raupach's equation (1991), whereas the vertical wind velocity is derived from the logarithmic law of Prandtl-von Kármán (1935).

4. Factors that influence wind-erosion

Wind-erosion processes are governed by many interacting factors that can be grouped into four categories:

- meteorological conditions, including wind shear, precipitation, evaporation, humidity and temperature;
- static soil characteristics such as particle size distribution and particle shape, and dynamic soil characteristics including near-surface soil-water status, aggregate size distribution, organic matter, and salt content;
- land-surface properties, such as roughness, coverage of vegetation and other non-erodible elements, crust formation, and fetch or field length;
- land-use practices, including cropping practices (crop types, residue, strip cropping, etc.), windbreaks and shelterbelts, soil-water management and tillage operations.

The wind shear is usually expressed as the erosivity, or the eroding capacity of the wind, and the static and dynamic soil properties as the erodibility or the soil's resistance to the wind.

Meteorological conditions. The erosivity of the wind is generally quantified by means of the shear (or friction) velocity u_*, which is a measure for the shear stress of the *wind*, and depends on the atmospheric conditions and the surface roughness. *Precipitation* and *evaporation* will primarily affect the soil-water status and are hence associated with the erodibility parameter. The erosivity of the rain, which can be expressed e.g. in terms of kinetic energy or momentum of the raindrops, and/or rainfall intensity, is generally not considered in wind erosion studies. However, Cornelis et al. (2004d,e) demonstrated that the contribution of splash-saltation due to wind-driven rains in the total sediment transport budget can be substantial during periods with relatively low wind velocities. The effects of *humidity* and *temperature* upon entrainment of particles by wind can be incorporated in the soil erodibility parameter (McKenna-Neuman, 2003).

Soil properties. The erodibility is generally expressed in terms of the threshold shear velocity u_{*t}, which is the minimal shear velocity required to initiate deflation of soil particles. In other words, for a given wind velocity and surface roughness, particles will be set in motion once the shear velocity u_* exceeds the threshold shear velocity u_{*t}. Because of the dynamic nature of the soil properties affecting the erodibility, u_{*t} needs to be considered as a time-variant parameter. Apart from the *particle-size distribution* and *aggregate-size distribution*, u_{*t} is primarily determined by the near-surface *water status* (Chepil, 1956; Belly, 1964; Bisal and Hsieh, 1966; Kawata and Tsuchiya, 1976; Azizov, 1977; Logie, 1982; Horikawa et al., 1982; Hotta et al., 1984; McKenna-Neumann and Nickling, 1989; Gregory and Darwish, 1990; Namikas and Sherman, 1995; Saleh and Fryrear, 1995; Chen et al., 1996; Shao et al., 1996; van Dijk et al., 1996; Fécan et al., 1999; Cornelis and Gabriels, 2003; Cornelis et al., 2004a,b,c). The abrasion of *aggregates,* due to bombardment of saltating particles during a wind erosion event, has been reported by Hagen (1991a) and Hagen et al. (1992). The role of *organic matter* upon entrainment of particles by wind has been described by e.g. de Vos (1996). Nickling and Ecclestone (1981) and Nickling (1984) demonstrated the effect of *soluble salts*, whereas Bradley at al. (1992) studied the effects of glycerol and soybean oil.

Land-surface properties. Soil-surface roughness, vegetation and non-erodible elements influence wind-erosion processes in that they not only determine the magnitude of the wind shear, but also trap material in transport. The soil-surface *roughness* or microrelief refers to the small-scale features produced by tillage ridges, clods, rocks, or other surface features, excluding vegetation or other large obstructions present on the soil (Zobeck et al., 2003). It can be expressed in terms of aerodynamic roughness length that can be determined from the well-known logarithmic law of Prandtl-von Kármán (1935). Tillage operations create oriented roughness or ridges and random roughness resulting in random orientation of soil aggregates and clods (Armbrust et al., 1964; Fryrear, 1984; Hagen, 1991b; Hagen and Armbrust, 1992; Zobeck, 1991a). As regards to *vegetation,* Hagen and Armbrust (1992) and Hagen (1996) related (standing or flat) biomass to threshold shear velocity and trapping flux. *Crusts* can be formed in unconsolidated soils by raindrop impact and are affected by soil aggregation and roughness (Zobeck and Popham, 1992) or they are due to cyanobacterial lichens (Marticorena et al., 1997a) and precipitation of soluble salts (Nickling, 1978; Pye, 1980; Gilette et al., 1980, 1982). These kinds of crusts are of great importance in arid and semi-arid areas and protect the soil against wind erosion unless they are disturbed by cattle, man, natural desiccation or abrasion (Marticorena et al., 1997a; Nickling and Gillies, 1989). Their effects on wind erosion have been measured by e.g. Zobeck (1991b), Hagen et al. (1992), Rice et al. (1996, 1997), Marticorena et al. (1997a), Sterk et al. (1999), Gomes et al. (2003) and Rajot et al. (2003). The *field length* finally is important as it determines the mass transport rate at a given distance from the upwind border of the field. The mass transport rate increases from zero (at the upwind field border) towards a critical maximum, which depends on the transport capacity of the wind, the soil erodibility and the aforementioned land-surface characteristics (Stout, 1990; Gilette et al., 1996).

Land-use practices. The land-use practices will influence the three other categories and are therefore useful as wind-erosion control measures when applied properly (see e.g. Chepil and Woodruff, 1963; Chepil et al., 1963; FAO, 1960; Schwab et al., 1993; Skidmore, 1986).

5. Wind-erosion modelling

5.1. WIND EROSIVITY AND SHEAR VELOCITY

When a fluid is flowing over a solid surface, the surface will experience a shear stress from the fluid. Due to the law of action and reaction, the fluid will experience a similar but opposite stress and will slow down. The reduction of the flow velocity, or in our case the wind velocity, is greatest near the surface boundary but decreases gradually with height above the surface. The fluid layer in which the wind velocity deviates from the free-stream wind velocity, i.e. the wind velocity that is not influenced by the solid surface, is called the boundary layer. Under neutral atmospheric conditions, the wind-velocity profile in the lower part of the boundary layer - where the shear stress is constant - can be described by the well-known law of Prandtl-von Kármán (1935)

$$u = \frac{u_*}{\kappa} \ln \frac{z}{z_0} \tag{1}$$

where u is the wind velocity (m s^{-1}) at height z (m), u_* is the shear velocity (m s^{-1}), κ is the von Kármán constant (≈ 0.4), and z_0 is the aerodynamic roughness length (m). If the surface contains large roughness elements with high cover density, a zero-plain displacement D (m), i.e. the vertical distance over which the logarithmic wind profile has been displaced, has to be accounted for. Equation (1) then becomes

$$u = \frac{u_*}{\kappa} \ln \frac{z - D}{z_0} \quad . \tag{2}$$

As a rule of thumb, D is about 0.7 times the height of the larger roughness elements.

The shear velocity is not a physical parameter in the strict sense, but is a measure for the shear stress with units of velocity

$$u_* = \sqrt{\frac{\tau_0}{\rho_f}} \tag{3}$$

where τ_0 is the (constant) shear stress in the inner zone of the boundary layer, and ρ_f is the fluid density (Mg m^{-3}). Both u_* and z_0 are generally determined from wind-velocity profiles using linear least-squares analysis.

Sometimes, the erosivity of the wind is expressed in terms of wind power, which is proportional to the shear velocity cubed. As will be demonstrated in section 5.4, it is the third power of u_* that determines the mass of windblown sediment.

Equations (1) and (2) define the instantaneous wind velocity as a function of height in a given direction. However, wind velocity and wind direction are variable in time and for modelling purposes, their distributions rather than their average values need to be considered. The importance of knowing wind direction relative to the orientation of fields and wind barriers is that it determines the wind travel distance from a non-eroding boundary, and hence it will determine the relative field length. It is further important in its relation to the orientation of row crops and some tillage operations (Skidmore and Tatarko, 1990).

The distribution of wind velocity at a given location is generally described by a cumulative Weibull distribution function (Skidmore and Tatarko, 1990; Shao et al., 1996). When eliminating the calm periods and normalizing the probability of wind in each wind velocity group to give a total of 1 for each of the 16 cardinal wind directions, the resulting Weibull distribution becomes

$$F(u) = F_0 + (1 - F_0)\left\{1 - \exp\left[-\left(\frac{u}{c}\right)^k\right]\right\} \tag{4}$$

where $F(u)$ is the probability that the wind velocity is less than u, F_0 is the probability of calm periods, c is the Weibull scale parameter (m s^{-1}), and k is the dimensionless Weibull shape parameter. Daily wind velocity and weather data in general for many locations throughout the world and for given periods were collected by the late Dr. Arlin Nicks and are available at http://hydrolab.arsusda.gov/nicks/nicks.htm. These data can be used to stochastically simulate weather (including wind direction and velocity) for longer or other periods using the climate generators (Nicks et al., 1987).

5.2 SOIL ERODIBILITY AND DEFLATION THRESHOLD SHEAR VELOCITY

5.2.1 Erodibility of dry sediments

The erodibility of the soil represents the retarding forces that must be overcome by the aerodynamic forces - represented by the wind erosivity or shear velocity - in order to initiate entrainment of sediment (or deflation). The retarding forces acting on dry particles are the gravitational force or particle weight, and the dry-bonding (interparticle) force (Cornelis et al., 2004a,c). The gravitational force is equal to the weight of the particle. The interparticle force is defined by the cohesion between individual particles. In the two-phase solid-air state, the dry-bonding force results from electrostatic bonding and van der Waals-bonding (Harnby, 1992; Cornelis and Gabriels, 2004). The retarding forces are hence determined by the static and dynamic soil properties. The aerodynamic forces include the horizontal drag force, the vertical lift force and the aerodynamic moment forces (Iversen and White, 1982; Cornelis and Gabriels, 2004), and are proportional to particle diameter and to the square of the shear velocity, the latter being equal to the threshold shear velocity at the instant of particle motion.

Solving the balance equation of moments associated with the aerodynamic and retarding forces that act on a particle at rest, leads to an expression for the threshold shear velocity - a parameter that can be used to quantify the soil erodibility -, which is generally defined by (Bagnold, 1941)

$$u_{*t} = A\sqrt{\frac{\rho_s - \rho_f}{\rho_f} g\, d} \tag{5}$$

where u_{*t} is the deflation threshold shear velocity, ρ_s is the particle density (Mg m^{-3}), g is the gravitational acceleration (m s^{-2}), and d is the particle diameter (m). When considering the aforementioned aerodynamic and retarding forces, Cornelis and Gabriels (2004) expressed the parameter A as

$$A = \sqrt{A_1 \left[1 + A_2 \frac{1}{\left(\rho_s - \rho_f \right) g \, d^2} \right]} \tag{6}$$

where A_1 and A_2 are model coefficients associated with respectively aerodynamic forces and interparticle forces between dry particles.

The threshold shear velocity thus not only depends on the soil characteristics, but also implicitly on the aerodynamic properties. Shao and Lu (2000), and Cornelis and Gabriels (2004) demonstrated, however, that for terrestrial conditions the aerodynamic properties are constant which implies the effect of a varying Reynolds number to be negligible. Using the wind-tunnel data of Iversen and White (1982) obtained from dry sediment experiments, Cornelis and Gabriels (2004) found $A_1 = 0.013$ and $A_2 = 1.7\ 10^{-4}$ N m^{-1}.

The threshold shear velocity as predicted from Eqs. (5) and (6) is applicable for soils with uniform and more or less spherical particles spread loosely over a bare and dry surface and hence they define the lower limit of u_{*t} for a given soil type (Shao and Lu, 2000). For multiple-sized soils, Shao et al. (1996) and Shao (2000) assumed that the dependence of the mass transport on u_* and u_{*t} for one particle-size range is not significantly altered by the presence of other particle sizes. The mass transport rate for a given soil can then be calculated by weighted integration of the mass transport rate for a given particle size multiplied by the particle-size distribution (see section 5.4.2.). In doing so, soil aggregates should be treated as individual particles with a density equal to their bulk density, and hence minimally-dispersed particle-size distributions - in which aggregates are not broken down - should be considered, rather than the granulometric composition of the soil (Cornelis and Gabriels, 2004).

Figure 4 shows the effect of particle diameter on the threshold shear velocity for sand grains (with $\rho_s = 2.65$ Mg m^{-3}) and sandy loam aggregates (or particles with $\rho_s = 1.47$ Mg m^{-3}) as predicted by the model of Cornelis and Gabriels (2004). It is clear that particles with sizes between 80 and 100 µm are most sensitive to deflation. For particles smaller than this range, u_{*t} increases with decreasing particle size. This is due to the interparticle cohesion that is becoming the dominant retarding force in that particle-size range. Bagnold (1941) further attributed this trend to the drag being more evenly distributed over the whole soil surface rather than being carried by the individual particles as they become larger. Particles cease to behave as isolated obstacles in the path of the fluid throwing off a chain of tiny eddies from their lee face as they become smaller than ca. 80 µm. However, as mentioned above, Shao and Lu (2000), and Cornelis and Gabriels (2004) showed that under terrestrial conditions, these aerodynamic effects are negligible compared to the effect of the interparticle cohesion. If particle size exceeds ca. 100 µm, particle weight becomes the dominant retarding force, and consequently, u_{*t} increases with increasing particle size.

5.2.2. The effect of near-surface water on the soil erodibility

To solve the moment balance of wetted sediments subjected to an airstream, the weight of the particle should theoretically be augmented with the mass of the water film attached to the particle. The interparticle cohesion force is now the sum of the dry and the wet bonding force. In the three-phase state solid-air-liquid, the wet-bonding forces between two particles are characterized by liquid-bridge bonding (capillary forces) and adsorbed-layer bonding (adhesion forces) (Cornelis et al., 2004a,c).

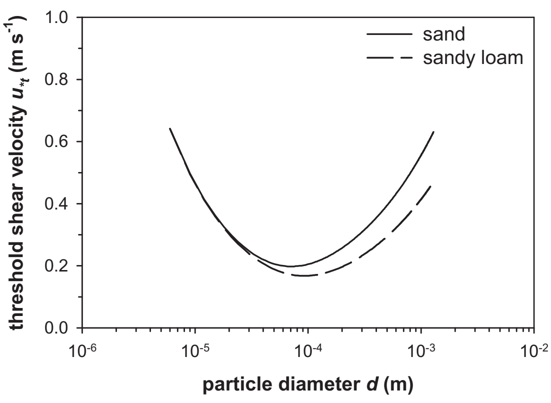

5.1.

Figure 4. Threshold shear velocity u_{*t} *as a function of particle diameter* d *for sand grains (with* ρ_s *= 2.65 Mg m*$^{-3}$*) and sandy loam aggregates (or particles with* ρ_s *= 1.47 Mg m*$^{-3}$*).*

In combining the model of Fisher (1926) for capillary forces with the Young-Laplace equation, Cornelis et al. (2003, 2004a,b) expressed the capillary force as a function of liquid surface tension squared, particle diameter squared and the inverse of capillary potential. They proposed a similar function for the adhesion forces in which the responsible potential is the potential generated by adsorptive forces instead of the capillary potential. This function was obtained by assuming the adsorbed-layer bonding to be equal to the tensile strength and hence excluding the term for the pressure deficiency associated with the effects of capillarity, which was introduced by Fisher (1926) as a correction to Haines' model (1925) for the tension due to the air-water interface. In expressing the total wet bonding force, equal weight was given to both the capillary force and the adsorptive force, and the interparticle force was written as a function of liquid surface tension squared, particle diameter squared and the inverse of matric potential.

Since determination of matric potential is a key limitation from a practical perspective (Namikas and Sherman, 1995), Cornelis et al. (2004a,b,c) related it to gravimetric water content w (see also Chapter 2). In literature, many functions are given to relate water content to matric potential ψ_m, such as the well-recognized models of Brooks and Corey (1964), Campbell (1974), van Genuchten (1980), and Kosugi (1994, 1997). These models are intended to describe the water retention curve over the whole range of water contents, but often give poor results at low water contents. According to Rossi and Nimmo (1994), the water content becomes approximately proportional to the logarithm of matric potential in the dry range of the water retention curve, where the above mentioned water retention models seem to be inappropriate. As an example, Figure 5 shows the water retention models of Brooks and Corey (1964), and Rossi and Nimmo (1994) which are fitted against water retention data of 300-500-µm sized sandy loam aggregates. Cornelis et al. (2004a,b,c) assumed therefore a logarithmic relation including the Ross et al. (1991) correction to force the model to converge to zero water content at oven dryness ($\psi_m \approx -10^3$ MPa). When considering data from Campbell and Shiozawa (1992) and Schofield (1935), Cornelis et al. (2004a,b,c) showed that such relation described the water retention curve very well at matric potentials that are of interest in the light of deflation of soil particles. Matric potential was then expressed as a function of water content including only one unknown parameter, viz. water content at -1.5 MPa, $w_{1.5}$.

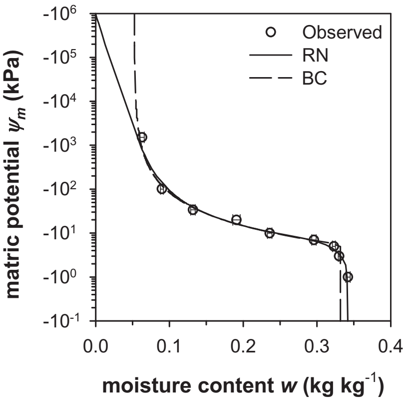

Figure 5. Observed water retention data of 300-500-μm sized sandy loam aggregates, and fitted water retention models of Brooks and Corey model (1964; BC), and Rossi and Nimmo (1994; RN).

Solving the moment balance equation for entrainment of wetted soil particles by wind, including the moments associated with the aforementioned forces, resulted in following equation for the parameter A in Eq. (5) (Cornelis et al., 2004a,b,c)

$$A = \sqrt{A_1 \left[1 + w + A_2 \frac{1}{\left(\rho_s - \rho_f\right) g\, d^2} \left(1 + A_3 \frac{\sigma^2 d}{\left|\psi_{md}\right| \mathrm{e}^{-6.5 \frac{w}{w_{1.5}}}} \right) \right]} \tag{7}$$

where A_3 is a model coefficient associated with the effects of soil water through capillary and adsorptive forces, σ is the surface tension of the liquid (N m^{-1}), ψ_{md} is the matric potential at oven dryness ($\approx -10^3$ MPa), w is the gravimetric water content (kg kg^{-1}), and $w_{1.5}$ the gravimetric water content at -1.5 MPa (kg kg^{-1}). Cornelis et al. (2004b) found through wind-tunnel experiments that $A_3 = 3\ 10^{14}$ N^{-1} m^{-1}. Figure 6 illustrates how the model of Cornelis et al. (2004a) predicts the effect of water content on the threshold shear velocity for sand particles and sandy loam aggregates with a mean particle size of 150 μm. Note that in computing u_{*t}, the particle density of the individual particles was considered to be equal to the bulk density in case of the sandy loam aggregates, which was 1.5 Mg m^{-3} (and equal to the density of quartz or 2.65 Mg m^{-3} in case of the sand particles). The water content at -1.5 MPa $w_{1.5}$ was determined on particles and aggregates with diameter ranging from 100 μm to 200 μm using a pressure chamber. Figure 6 shows that at low water contents, the increase in u_{*tw} with w is gradual. As w further increases, the threshold shear velocity reaches a very high value above which no particle entrainment can occur. The soil surface has to dry to a matrix potential below -1.5 MPa for deflation to take place.

5.2.3. Temporal changes of near-surface moisture and soil erodibility

As was pointed out in section 5.2., the wind needs to dry the surface layer of the soil until water content becomes smaller than the water content at -1.5 MPa matric potential. However, the near-surface water content is a dynamic soil property that will change temporally. These temporal changes are not only due to (i) a varying input of water and its subsequent infiltration and redistribution and to (ii) a changing evaporation rate and drying of the soil surface as such, but also to (iii) short term removal of the upper tiny sediment layer once dry enough under the given aerodynamic conditions.

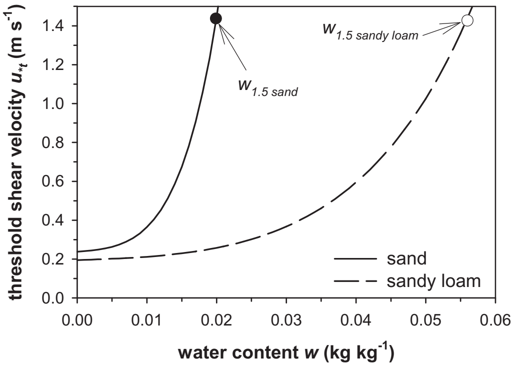

Figure 6. Threshold shear velocity u_{*t} *as a function of water content* w *for sand particles and sandy loam aggregates with a mean diameter of 150* μm.

With respect to input of water, the soil obtains it from many sources. In dryland areas, the primary origin for water is the atmosphere, where water is added by precipitation, or by condensation of water vapour directly on the surface. The atmosphere is also an important source in coastal areas, but substantial quantities of water are added by wave uprush, overwash, or water-level fluctuations associated with tides or surges. In fluvial systems, flood-water and the atmosphere are the sources (Namikas and Sherman, 1995). Further, runoff, lateral subsurface flow and capillary rise from the groundwater table can moisten the near-surface soil layer. Irrigation water can also be considered as a source of water. These input sources are of course variable in time and space (see Chapters 3, 7, and 10).

A soil that has received water from one of the above input sources will be subjected to evaporation and will hence dry out. The evaporation rate depends primarily on wind shear, relative humidity, temperature, and radiation (see e.g. the Penman-Monteith approach; Monteith, 1981), which are time variable as well. However, even if the evaporation rate remains constant, the near-surface water status will change as the soil dries out (the temporal variability of soil moisture and evapotranspiration is discussed in detail in Chapters 3 and 5).

Finally, deflation and subsequent transport of sediment as such, will also change the near-surface water content. Cornelis and Gabriels (2003) demonstrated through wind-tunnel experiments that, for a given shear velocity of the wind, particles will start to deflate as the uppermost surface layer dries out below a given water content - which can be computed from Eq. (5) in combination with Eq. (7) - and that subsequently, this tiny layer will be subjected to particle dislodgment. As a tiny but relatively dry layer has now been removed, the 'new' surface will have a higher water content compared with the layer removed. This 'new' surface thus has to dry out again before particle entrainment will occur. When dry enough to be blown away, a third surface layer with a higher water content will appear. This phenomenon will repeat itself, until u_* drops below the u_{*t} for the air-dry sediment. In Figure 7, the particle number rate i (impact counts per unit time), which was measured in 10-seconds intervals with a saltiphone (Spaan and van den Abeele, 1990) above a sample tray containing dune sand with a mean particle size of 250 µm and an initial water content equal to 0.040 kg kg^{-1}, is plotted against time t, for different shear velocities ranging from 0.46 to 0.77 m s^{-1}. The run time of the experiments was 2 minutes in which the shear velocity was held constant and the average water content at the end of the experiment was 0.021 kg kg^{-1}. Details about these and other experiments can be found in Cornelis and Gabriels (2003). Since the shear velocity was constant within each test run, the observed variation in particle number rate, which was most pronounced at high shear velocities, was attributed to the above-described phenomenon. The drop in water content between the beginning and the end of the experiment was due to evaporation.

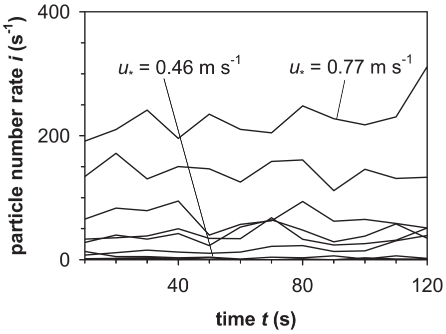

Figure 7. The particle number rate i as a function of time t for2-minute test runs. The runs were carried out on dune sand with an initial water content equal to 0.040 kg kg^{-1} *at shear velocities u*$_*$ *ranging from 0.46 to 0.77 m s*$^{-1}$ *(i.e. at u*$_*$ *equal to respectively 0.46, 0.49, 0.52, 0.55, 0.61, 0.71 and 0.77 m s*$^{-1}$*).*

The dynamics of a changing water status at the soil surface due to (i) and (ii) can be modeled with hydrological models. However, modeling the temporal changes in water status associated with (iii) is not reported in literature. This poses central questions for future research on hydrodynamics of wind erosion.

Shao et al. (1996) simulated the near-surface soil water in their wind-erosion assessment model by using the simple force-restore two-layer model of Deardorff (1977). Other methods are based on deterministic and stochastic models of the soil water balance (see Chapters 2, 3, and 7).

5.3. EFFECT OF SURFACE ROUGHNESS ON EROSIVITY AND ERODIBILITY

Non-erodible elements affect the erosivity or shear velocity in that they consume part of the fluid momentum. Given the conservation of momentum and hence a constant overall momentum or wind shear, the momentum to move fluid particles will be reduced accordingly. As a result, the shear velocity that will initiate particle motion becomes smaller. Non-erodible elements further cover part of the surface and thus protect it from the erosive energy.

The effect of roughness on the erosivity index can be quantified by using a drag-partitioning scheme, in which the drag is partitioned between the roughness elements and the erodible surface (Raupach et al., 1993). The overall shear velocity (which is e.g. measured at a nearby meteorological station) is reduced with a factor f_{eff}, if roughness elements are present at the field under investigation

$$u_*^s = f_{eff}\, u_* \tag{8}$$

where u_*^s is the small-scale shear velocity (m s^{-1}), which represents the shear stress that acts on the uncovered surface and that should exceed the threshold shear velocity to initiate particle motion. Marticorena and Bergametti (1995) suggested following expression for f_{eff}, which is based on an approach developed by Arya (1975)

$$f_{eff} = 1 - \frac{\ln\left(z_0 / z_{0s} \right)}{\ln\left[A_4 \left(x / z_{0s} \right) A_5 \right]} \tag{9}$$

where z_{0s} indicates the roughness length of the uncovered surface (m), x is the distance downstream of the roughness element (m), and A_4 and A_5 are dimensionless parameters equal to respectively 0.35 and 0.8 (Glaser, 1955). Performing various simulations with roughness lengths varying from 2.2 to 20 cm height, and spacing from a few to hundreds of centimeters, corresponding to a roughness density ranging from 0.001 to 0.2, Marticorena and Bergametti (1995) found f_{eff} not being very sensitive to x and suggested $x = 0.1$ m.

In calculating sediment transport using a sediment transport rate equation (see section 9.4), f_{eff} can also be incorporated into the threshold shear velocity rather than considering a reduction in shear velocity as in Eq. (8) (Marticorena and Bergametti, 1995; Marticorena et al., 1997a,b). The overall threshold shear velocity of a surface with non-erodible elements will hence increase with a factor $1/f_{eff}$ compared to the "smooth" situation

$$u_{*_t} = \frac{u_{*_t}^s}{f_{eff}} \tag{10}$$

where $u_{*_t}^s$ is the threshold shear of a surface without roughness elements and calculated from Eq. (5). Alternative approaches for the modelling of the effect of surface roughness on threshold velocity have been suggested by Raupach et al. (1993) and Crawley and Nickling (2003).

5.4. SEDIMENT MASS TRANSPORT RATE

5.4.1. Horizontal mass transport or saltation

The seminal work of Bagnold (1941) forms the basic theoretical background for most research on mass transport rates of sand-sized particles. He related the mass transport rate of sand that moves in saltation to the cube of the shear velocity. Owen (1964) extended Bagnold's model partitioning the overall fluid shear stress into the particle-borne shear stress and the airborne shear stress. With the overall shear stress equal to $\rho_f\, u_*^2$ (see Equation (3)), and assuming the airborne shear stress at the surface to approach $\rho_f\, u_{*_t}^2$ if saltation is at equilibrium, Owen (1964) suggested the particle-borne shear stress to be equal to $\rho_f \left(u_*^2 - u_{*_t}^2 \right)$. In the case of strong saltation, $u_*^2 >> u_{*_t}^2$ and at the surface, the particle-borne shear stress becomes much larger than the airborne shear stress. Finally, Owen (1964) presented the following equation for the saltation mass transport rate $\tilde{Q}_s$ (kg m^{-1} s^{-1}) of particles with diameter d_s (where the tilde denotes that Q applies to uniform particles of size d_s)

$$\begin{aligned} \tilde{Q}_s(d_s) &= 0 && \text{for } u_* < u_{*_t} \\ \tilde{Q}_s(d_s) &= C \frac{\rho_f}{g} u_* (u_*^2 - u_{*_t}^2) && \text{for } u_* \geq u_{*_t} \end{aligned} \tag{11}$$

where C is a dimensionless proportionality constant.

The total saltation mass transport rate for a given soil can then be calculated by weighted integration of the saltation mass transport rate $\tilde{Q}_s(d_s)$ for particle sizes d_s (m) in the sand-size range ($d_1 < d_s < d_2$) (Shao et al., 1996)

$$Q_s = \int_{d_l}^{d_2} \widetilde{Q}(d_s)\, p(d_s)\, \mathrm{d}d_s \tag{12}$$

where $p(d_s)$ is the minimally-dispersed particle-size distribution (i.e., the mass fraction of particles with diameters ranging between d and $d + \mathrm{d}d$), d_l is the particle diameter (m) marking the transition between dust and sand (d_l calculated from the particle fall velocity using e.g. Malcolm and Raupach's equation, 1991), and d_2 is the diameter (m) of the largest particles which can be transported under a given shear velocity.

5.4.2. Vertical mass transport or suspension

The dominant mechanism for entrainment of dust-sized particles in suspension is saltation bombardment. Under normal conditions, direct aerodynamic dislodgement is generally insignificant due to the relative importance of interparticle cohesion forces of dust-sized particles. The suspension mass transport rate $\widetilde{Q}_{su}(d_d, d_s)$ of dust particles of size d_d (m) induced by saltation bombardment of sand particles of size d_s is (Shao et al., 1996)

$$\widetilde{Q}_{su}(d_d, d_s) = \frac{2}{3}\frac{\rho_s}{\rho_f}\frac{\beta_b \gamma g}{u_{*t}^2}\widetilde{Q}_s(d_s) \tag{13}$$

where β_b is an empirical bombardment parameter (m) and γ is a dimensionless parameter depending on take-off and impact velocities of saltating particles. Equation (13) demonstrates that the the vertical mass transport rate is linearly related to the horizontal mass transport rate by a constant fraction, which was suggested by Marticorena and Bergametti (1995). They used an empirical function to relate that factor to clay content.

The total suspension mass transport Q_{su} of dust particles of all sizes ($0 < d_d < d_l$), induced by bombardment of sand particles of all sizes can be written as (Shao et al., 1996)

$$Q_{su} = \int_{d_l}^{d_2}\int_{0}^{d_l} \widetilde{Q}_{su}(d_d, d_s)\, p(d_d)\, p(d_s)\, \mathrm{d}d_d\, \mathrm{d}d_s \quad . \tag{14}$$

For more information on how to determine the model coefficients, the reader is referred to Shao et al. (1996).

5.4.3. Effect of field length

The mass transport rate as defined by Eq. (12) refers actually to the maximum capacity of the wind to carry soil material under the given conditions. However, in the case of an erodible field adjacent to a non-erodible field, the mass transport rate will increase with the windward distance in the field (and is zero at the upwind edge of the field). According to Stout (1990), the horizontal distribution of the mass transport rate is

$$\frac{\mathrm{d}Q(x)}{\mathrm{d}x} = \frac{2x}{s(x)^2}\left[Q_{max}(x) - Q(x)\right] \tag{15}$$

where x is the distance from the upwind edge of the field (m), Q_{max} is the maximum transport rate (kg m^{-1} s^{-1}), and s is a field length scaling factor. Equation (12) is the governing equation in RWEQ (Fryrear et al., 1998; see section 9.5.) and should be solved numerically.

5.5. WIND-EROSION PREDICTION MODELS

As outlined in the previous sections, numerous factors are involved in the wind-erosion process. These factors act in conditions of mutual interaction and their description requires the development of process-based models. These functional models can be empirical or physical, but essentially, most models developed to date are a combination of both approaches. What makes these models appealing is that they serve as (i) research tools allowing a better understanding of the processes and the interactions between the factors involved, (ii) decision-support tools for wind-erosion risk assessment and for scenario-analysis including the evaluation of wind-erosion control measures.

Widely used wind-erosion prediction models include the Wind-Erosion eQuation, WEQ (Woodruff and Siddoway, 1965; Skidmore et al., 1970), the Revised Wind-Erosion eQuation, RWEQ (Fryrear et al., 1998), the Wind-Erosion Prediction System, WEPS (Hagen, 1991c), the Erosion-Productivity Impact Calculator, EPIC (Williams, 1994), the Texas Erosion Analysis Model, TEAM (Singh et al., 1999), the Wind-Erosion Assessment Model, WEAM (Shao et al., 1996), the atmospheric dust cycle model (Marticorena and Bergametti, 1995; Marticorena et al., 1997b) and the WEELS (Wind Erosion on European Light Soils) model (Groβ and Bärring, 2003). The user must determine which model will produce the desired output with the available input data, and, if possible, calibrate and validate the model using field data.

6. Wind-erosion measuring and data-analysis methods

Accurate and reliable methods for measuring the quantity of windblown sediment and for the analysis of the hence obtained data are indispensable for assessment of soil loss through an erosion inventory, scientific erosion research, development and evaluation of erosion control technology, development of erosion prediction technology, allocation of conservation resources, and development of policies and regulations (Toy et al., 2002). It is an illusion to think that the role of measurements can be taken over by using erosion prediction technology. Measurements are needed to develop, calibrate and validate that technology (Stroosnijder, 2003).

For more information about measurement and data-analysis methods for field-scale wind erosion studies, the reader is referred to Fryrear et al. (1991) and Zobeck et al. (2003).

7. Wind-erosion control principles

Principles of reducing wind erosion have been defined by many authors (FAO, 1960; Skidmore, 1986; Nanney et al., 1993). The three basic methods to control wind erosion are (*i*) to reduce erosivity of the wind to a level below the threshold value that will initiate soil movement, (*ii*) to reduce the soil drift, and (*iii*) to reduce the erodibility of the soil. Based on these methods Chepil et al. (1961) defined the wind erosion control principles as (*i*) keep the soil firm and moist, (*ii*) create soil aggregates or clods large and stable enough so they cannot be moved or abraded by wind, (*iii*) roughen the surface to trap and protect the fine soil particles, (*iv*) cover with and preferably maintain vegetation or vegetative residues on the land, (*v*) narrow the width of fields at right angles to the prevailing wind direction, and (*vi*) reduce the velocity of wind near the ground by using barriers placed along the path of the wind.

These principles of control apply everywhere, but the relative utility of each varies with local climate, soil and land-use conditions. For example, on coarse textured soils, formation of stable clods is usually difficult, and control of erosion by either clod maintenance or roughening the surface is at best temporary. On finer textured soils effective control can be much more efficacious using these methods (FAO, 1960).

Usually not one but a combination of methods will be most effective and dependable on cultivated lands. For example, where erosion-susceptible crops are grown in sequence with resistant ones, planting in strips in combination with proper residue maintenance may be much more effective than either practice alone. Similarly, strip cropping in a small grain-fallow sequence is usually beneficial in combination with maintenance of surface residues (FAO, 1960).

In practice, the three basic wind erosion control principles as mentioned above, can be realised by controlling surface wind velocity and soil drift, and by controlling soil factors. This boils down to applying the following methods respectively: (*i*) vegetative measures (i.e., cultivating crops and crop residue management, cover crops, strip cropping, shelterbelts and windbreaks), tillage practices, and mechanical methods, and (*ii*) conservation of moisture to improve vegetative growth and conditioning of the surface soil to improve aggregation. Many methods, such as permanent grass and contouring, provide both types of control. In each, the height and spacing of obstructions, the breaking effect on the wind and the resistance of the soil to movement influence the degree of protection. Vegetation is generally the most effective means of wind erosion control. Cultivated crops reduce wind velocity and hold against the tractive force of the wind. Woody plants such as shrubs and trees, may be planted to reduce wind velocities over large areas. Wind erosion hazards often exist when fields are bare of growing crops. Cultural methods of control, though temporary, are effective under these conditions. Whenever possible cultural practices should be used before blowing starts, for wind erosion is easier to prevent than to arrest (Schwab et al., 1993). To cite Stallings (1957, p. 77): "wind erosion in some respects is like an epidemic disease. It must be controlled at its source before it gets out of hand entirely". In general, long periods of drought will obliterate the effects of cultural treatments. For a recent review on some popular wind-erosion control measures, I further refer to Nordstrom and Hotta (2004).

8. References

Agnew, C.T. and A. Warren (1990). Sand trap: agriculture not desert is the greatest threat to arid land. The Sciences, March/April, 14-19.

Armbrust, D.V. (1984). Wind and sandblast injury to field crops: effect of plant age. Agron. J., 76, 991-993.

Armbrust, D.V., W.S. Chepil, and F.H. Siddoway (1964). Effects of ridges on erosion of soil by wind. Proc. Soil Sci. Soc. Am., 28, 557-560.

Arya, S.PS.S. (1975). A drag partitioning theory for determining the large-scale roughness parameter and wind stress on Artic pack ice. J. Geophys. Res., 80, 3447-3454.

Azizov, A. (1977). Influence of soil moisture in the resistance of soil to wind erosion. Soviet Soil Sci., 1, 105-108.

Bagnold, R.A. (1941). The physics of blown sand and desert dunes. Chapman & Hall, London.

Banzhaf, J., D.E. Leihner, A. Buerkert, and P.G. Serafini (1992). Soil tillage and wind break effects on millet and cowpea: I. Wind speed, evaporation, and wind erosion. Agron. J., 84, 1056-1060.

Belly, P.Y. (1964). Sand movement by wind. Tech. Memo. 1. U.S. Army Corps of Engineers, Coastal Engineering Research Center, Washington D.C..

Bisal, F., and J. Hsieh (1966). Influence of moisture on erodibility of soil by wind. Soil Sci., 102, 143-146.

Bradley, N.W., J.M. Gregory and G.R. Wilson (1992). Wet-bonding chemical effects on threshold friction velocity. Pap. ASAE, 922515, St. Joseph MI.

Brooks, R.H., and A.T. Corey (1964). Hydraulic properties of porous media. Hydrology Paper 3, Colorado State Univ., Fort Collins, CO.

Campbell, G.S. (1974). A simple method for determining unsaturated conductivity from moisture retention data. Soil Sci., 117, 311-314.

Campbell, G.S., and S. Schiozawa (1992). Prediction of hydraulic properties of soils using particle size distribution and bulk density data. In: International workshop on indirect methods for estimating the hydraulic properties of unsatured soils. Univ. Calif. Press, Berkeley.

Chepil, W.S. (1956). Influence of moisture on erodibility of soil by wind. Soil Sci. Soc. Am. Proc., 20, 288-292.

Chepil, W.S. (1957). Sedimentary characteristics of dust storms: sorting of wind eroded soil material. Am. J. Sci., 255, 12-22.

Chepil, W.S. (1958a). Soil conditions that influence wind erosion. Tech. Bull. No. 1185.

Chepil, W.S., N.P. Woodruff, and F.H. Siddoway (1961). How to Control Soil Blowing. USDA Farmers Bull. No. 2169.

Chepil, W.S. (1962). Mechanics of wind erosion and significance as a sediment source. Presented at ARS-SCS Sedimentation Workshop, Panguitch, UT.

Chepil, W.S., and N.P. Woodruff (1963). The physics of wind erosion and its control. Adv. Agron., 15, 211-302.

Chen, W., Z. Dong, Z. Li and Z. Yang (1996). Wind tunnel test of the influence of moisture on the erodibility of loessial sandy loam soils by wind. J. Arid Environ., 34, 391-402.

Claflin, L.E., D.L. Stuteville, and D.V. Armbrust (1973). Windblown soil in the epidemiology of bacterial leaf spot of alfalfa and common blight of beans. Phytopathology, 63, 1417-1419.

Cooke, R., A. Warren, and A. Goudie (1993). Desert geomorphology. UCL Press, St. Ives.

Cornelis, W.M. and D. Gabriels (2003). The effect of surface moisture on the entrainment of dune sand by wind: an evaluation of selected models. Sedimentology. 50, 771-790.

Cornelis, W.M., D. Gabriels and R. Hartmann (2004a). A conceptual model to predict the deflation threshold shear velocity as affected by near-surface water content: 1. Theory. Soil Sci. Soc. Am. J.. 68, 1154-1161.

Cornelis, W.M., D. Gabriels and R. Hartmann (2004b). A conceptual model to predict the deflation threshold shear velocity as affected by near-surface water content: 2. Calibration and Verification. Soil Sci. Soc. Am. J.. 68, 1162-1168.

Cornelis, W.M., D. Gabriels and R. Hartmann (2004c). A parameterisation for the threshold shear velocity to initiate deflation of dry and wet sediment. Geomorphology. 59, 43-51.

Cornelis, W.M., G. Oltenfreiter, D. Gabriels and R. Hartmann (2004d). Splash-Saltation of Sand due to Wind-Driven Rain: Vertical Deposition Flux and Sediment Transport Rate. Soil Sci. Soc. Am. J.. 68: 32-40

Cornelis, W.M., G. Oltenfreiter, D. Gabriels and R. Hartmann (2004e). Splash-Saltation of Sand due to Wind-Driven Rain: Horizontal Flux and Sediment Transport Rate. Soil Sci. Soc. Am. J.. 68: 41-46.

Cornelis, W.M. and D. Gabriels (2004). A simple model for the prediction of the deflation threshold shear velocity of loose particles. Sedimentology, 51: 1-13.

Crawley, D.M. and W.G. Nickling (2003). Drag partition for regularly arrayed rough surfaces, *Boundary Layer Meteorology,* 107: 445-468.

Deardorff, J.W. (1977). Parameterization of ground-surface moisture-content for use in atmospheric prediction models. J. Applied Meteorology, 16, 1182-1185.

de Vos, J.A. (1996). Testing compost as an anti wind erosion agent in a wind tunnel. Soil Tech., 9, 209-221.

Duncan, E.R., and W.C. Moldenhauer (1968). Controlling Wind Erosion in Iowa. Iowa State Univ. Sci. Techn., Cooperative Extension Service. Pm-432.

FAO (1960). Soil erosion by wind and measures for its control. FAO Agricultural Development Paper 71, Rome.

Fécan, F., B. Marticorena, and G. Bergametti (1999). Parametrization of the increase of the aeolian erosion threshold wind friction velocity due to soil moisture for arid and semi-arid areas. Ann. Geophysicae, 17, 149-157.

Fisher, R.A. (1926). On the capillary forces in an ideal soil: correction of the formulae given by W.B. Haines. J. Agric. Sci., 16, 492-503.

Fryrear, D.W. (1969). Reducing wind erosion in the southern great plains. Texas Agricultural Experiment Station, MP-929.

Fryrear, D.W. (1984). Soil Ridges-Clods and Wind Erosion. Trans. Am. Soc. Agr. Eng., 27, 445-448.

Fryrear, D.W., and J.D. Downes (1975). Consider the Plant in Planning Wind Erosion Control Systems. Trans. ASAE, 18, 1070-1072.

Fryrear, D.W., J.E. Stout, L.J. Hagen and E.D. Vories (1991). Wind erosion - field measurement and analysis. Trans. ASAE., 34 , 155-160.

Fryrear, D.W., A. Saleh, J.D. Bilbro, H.M. Schomberg, J.E. Stout, and T.M. Zobeck (1998). Revised Wind Erosion Equation. Tech. Bull. No. 1. USDA-ARS, Big Spring, TX.

Gilette, D.A., J. Adams, A. Endo and D. Smith (1980). Threshold velocities for the input of soil particles into the air by desert soils. J. Geophys. Res., 85, 5621-5630.

Gilette, D.A., J. Adams, D. Muhs and R. Kihl (1982). Threshold friction velocities and rupture moduli for crusted desert soils for the input of soil particles in the air. J. Geophys. Res., 87, 9003-9015.

Gillette, D.A., G. Herbert, P.H. Stockton .and P.R. Owen (1996). Causes of the fetch effect in wind erosion. Earth Surf. Proc. Landf., 21, 641-659.

Glaser, A.H. (1955). The temperature above an airport runway on a hot day: Moist climate, Texas A&M Res. Foundation Contract AF (19(604)-977, Sci. Rep. 5.

Gomes L, J.L. Arrue, M.V. Lopez, G. Sterk, D. Richard, R. Gracia, M. Sabre, A. Gaudichet and J.P. Frangi (2003). Wind erosion in a semiarid agricultural area of Spain: the WELSONS project, Catena, 52, 235-256.

Goudie, A.S. (1983). Dust storms in space and time. Progress in Physical Geography, 7, 502-529.

Gregory, J.M., and M.M. Darwish (1990). Threshold friction velocity prediction considering water content. Pap. ASAE, 902562, St. Joseph MI.

Groβ, J. and L. Bärring (2003). Wind erosion in Europe: where and when. In: A. Warren (Ed.). Wind erosion on agricultural land in Europe. European Commission, Brussels.

Hagen, L.J. (1991a). Wind erosion mechanics - abrasion of aggregated soil. Trans. ASAE, 34, 831-837.

Hagen, L.J. (1991b). Wind erosion: emission rates and transport capapcities on rough surface. Pap. ASAE, 912082, St. Joseph MI.

Hagen, L.J. (1991c). A wind erosion prediction system to meet user needs. J. Soil Water Cons., 46, 106-111.

Hagen, L.J. (1996). Crop residue effects on aerodynamic processes and wind erosion. Theor. Applied Climatology, 54, 39-46.

Hagen, L.J. and D.V. Armbrust (1992). Aerodynamic roughness and saltation trapping efficiency of tillage ridges. Trans. ASAE, 35, 1179-1184.

Hagen L.J., E.L. Skidmore and A. Saleh (1992). Wind erosion - prediction of aggregate abrasion coefficients. Trans. ASAE, 35, 1847-1850.

Haines, W.B. (1925). Studies of the physical properties of soils. II. A note on the cohesion developed by capillary forces in an ideal soil. J. Agric. Sci., 15, 529-535.

Harnby, N. (1992). The mixing of cohesive powders. In: N. Harnby et al. (Eds.) Mixing in the process industries, 2nd Ed. Nienow, Butterworth-Heinemann Ltd, Oxford. pp. 79-98.

Hayes, B.A. (1965). Wind Erosion Equation Useful in Designing Northeastern Crop Protection. J. Soil Water Cons., 20, 153-155.

Horikawa, K., S. Hotta, and S. Kubota (1982). Experimental study of blown sand on a wetted sand surface. Coastal Eng. Japan, 25, 177-195.

Hotta, S., S. Kubota, S. Katori, and K. Horikawa (1984). Sand transport by wind on a wet sand surface. Proceedings of the 19th Coastal Engineering Conference, ASCE, New York, pp. 1263-1281.

Iversen, J.D., and B.R. White (1982). Saltation treshold on Earth, Mars and Venus. Sedimentology, 29, 111-119.

Kaufman, Y.J., D. Tanre' and O. Boucher (2002). A satellite view of aerosols in the climate system, Nature, 419, 215-223.

Kawata, Y., and Y. Tsuchiya (1976). Influence of water content on the threshold of sand movement and the rate of sand transport in blown sand. Proc. of JSCE, 249, 195-100.

Knottnerus, D.J.C. (1985). Verstuiven van grond. Inst. Bodemvruchtbaarheid, Haren. Nota 144.

Kosugi, K. (1994). Three-parameter lognormal distribution model for soil water retention. Water Resour. Res., 32, 891-901.

Kosugi, K. (1997). A new model to analyze water retention characteristics of forest soils based on soil pore-radius distribution. J. For. Res., 2, 1-8.

Li, X., H. Maring, D. Savoie, K. Voss and J.M. Prospero (1996). Dominance of mineral dust in aerosol light scattering in the North-Atlantic trade winds, Nature, 380, 416-419.

Logie, M. (1982). Influence of roughness elements and soil moisture on the resistance of sand to wind erosion. Catena, Suppl., 1, 161-174.

Lyles, L. (1975). Possible Effects of Wind Erosion on Soil Productivity. J. Soil Water Cons., 30, 279-283.

Malcolm, L.P., and M.R. Raupach (1991). Measurements in an air settling tube of the terminal velocity distribution of soil material. J. Geophys. Res., 96, 15275-15286.

Marticorena, B., and Bergametti, G. (1995). Modeling the atmospheric dust cycle: 1. Design of a soil-derived dust emission scheme. J. Geophys. Res., 100, 16,415-16,430.

Marticorena, B., G. Bergametti, D. Gillette and J. Belnap (1997a). Factors controlling threshold friction velocity in semiarid and arid areas of the United States. J. Geophys. Res., 102, 23277-23287.

Marticorena, B., G. Bergametti, B. Aumont, Y. Callot, C. N'Doumé, and M. Legrand (1997b). Modeling the atmospheric dust cycle: 2. Simulation of Saharan dust sources. J. Geophys. Res., 102, 4387-4404.

McKenna-Neuman, C., and W.G. Nickling (1989). A theoretical and wind tunnel investigation of the effect of capillary water on the entrainment of sediment by wind. Can. J. Soil Sci., 69, 79-96.

McKenna-Neuman, C.M. (2003). Effects of temperature and humidity upon the entrainment of sedimentary particles by wind. Boundary-Layer Meteorology, 108, 61-89.

McKie, R. (2001). Deadly dust 'brought foot and mouth here'. Guardian Unlimited Archive. 9 Sept. http://www.guardian.co.uk/archive/article/
0,4273,4253037,00.html

Middleton, N.J., A.S. Goudie and G.L. Wells (1986). The frequency and source areas of dust storms. *In*: W.G. Nickling (Ed.). Aeolian geomorphology. 237-259. Allen & Unwin, London.

Monteith, J.L. (1981). Evaporation and surface temperature. Quarterly J. Royal Soc., 107, 1-27.

Namikas, S.L., and D.J. Sherman (1995). A review of the effects of surface moisture content on aeolian sand transport. In: Desert Aeolian Processes. Ed. V.P. Tchakerian. Chapman & Hall, London. pp. 269-293.

Nanney, R.D., D.W. Fryrear, and T.M. Zobeck (1993). Wind Erosion Prediction and Control. Water Sci. Techn., 28, 3-5.

Nickling, W.G. (1978). Eolian sediment transport during dust storms: Slims River Valley, Yukon Territory. Can. J. Soil Sci., 15, 1069-1084.

Nickling, W.G. (1984). The stabilizing role of bonding agents on the entrainment of sediment by wind. Sedimentology, 31, 111-117.

Nickling, W.G., and M. Ecclestone (1981). The effects of soluble salts on the threshold shear velocity of fine sand. Sedimentology, 28, 505-510.

Nickling, W.G., and J.A. Gillies (1989). Emission of fine-grained particles from desert spoils. *In*: M. Leinen and M. Sarnthein (Eds.). Paleoclimatology and paleometeorology: modern and past patterns of global atmospheric transport. Kluwer, Amsterdam. 133-165.

Nicks, A.D., J.R. Williams, C.W. Richardson and L.J. Lane (1987). Generating climatic data for a water erosion prediction model. Pap. ASAE, 87-2541,. Joseph MI.

Nordstrom, K. and S. Hotta (2004). Wind erosion from cropland in the USA: a review of problems, solutions and prospects. Geoderma, 121, 157-167.

Owen, P.R. (1964). Saltation of uniform grains in air. J. Fluid Mech., 20, 225-242.

Peerlkamp, P.K. (1970). Grondverstuivingen en hun bestrijding. Jaarverslag 1970. Inst. Bodemvruchtbaarheid, Haren. pp. 74-86.

Prandtl, H. (1935). The mechanics of viscous fluids: aerodynamic theory. Julius Springer, Berlin.

Pye, K. (1980). Beach salcrete and eolian sand transport: evidence from North Queensland. J. Sediment. Petrology, 50, 257-261.

Pye, K. (1987). Aeolian dust and dust deposits. Academic Press, London.

Rajot, J.L., S.C. Alfaro, L. Gomes, A. Gaudichet (2003). Soil crusting on sandy soils and its influence on wind erosion. Catena, 53, 1-16.

Ramanathan, V., P.J. Crutzen, J.T. Kiehl, and D. Rosenfeld (2001). Aerosols, Climate, and the Hydrological Cycle, Science, 294, 2119-2124.

Raupach M.R., D.A. Gillette, J.F. Leys (1993). The effect of roughness elements on wind erosion threshold, *J. Geophys Res.*, 98(D2), 3023-3029.

Rice, M.A., B.B. Willetts and I.K. McEwan (1996). Wind erosion of crusted soil sediments. Earth Surf. Proc. Landf., 21, 279-293.

Rice, M.A., C.E. Mullins and I.K. McEwan (1997). An analysis of soil crust strength in relation to potential abrasion by saltating particles. Earth Surf. Proc. Landf., 22, 869-883.

Rosenfeld, D., Y. Rudich, and R. Lahav (2001). Desert dust suppressing precipitation: A possible desertification feedback loop, Proc.Natl. Acad. Sci. U.S.A.,98(11), 5975-5979.

Ross, P.J., J. Williams, and K.L. Bristow (1991). Equation for extending water-retention curves to dryness. Soil Sci. Soc. Am. J., 55, 923-927.

Rossi, C., and J.R. Nimmo (1994). Modeling of soil water retention from saturation to oven dryness. Water Resour. Res., 30, 701-708.

Saleh, A., and D.W. Fryrear (1995). Threshold wind velocities of wet soils as affected by wind blown sand. Soil Sci., 160, 304-309.

Schmidt, B.L., and G.B. Triplett (1967). Controlling Wind Erosion. Ohio Report, May-June. pp. 35-38.

Schofield, R.K. (1935). The pF of the water in soil. Trans. Int. Congr. Soil Sci. 3rd, II. pp. 38-48.

Schwab, G.O., D.D. Fangmeier, W.J. Elliot, and R.K. Frevert (1993). Wind Erosion and Control Practices. In: Soil and Water Conservation Engineering, John Wiley & Sons, Inc., New York.. 114-133.

Shao, Y. (2000). Physics and modelling of wind erosion. Atmospheric and oceanographic sciences library, 23, Kluwer Academic Publishers, Dordrecht.

Shao, Y., and H. Lu (2000). A simple expression for wind erosion threshold friction velocity. J. Geophys. Res., 105, 22,437-22,443.

Shao, Y., M.R., Raupach, and J.F. Leys (1996). A model for predicting aeolian sand drift and dust entrainment on scales from paddock to region. Aust. J. Soil Res., 34, 309-342.

Singh, U.B., Gregory, J.M. and Wilson, G.R. (1999). Texas Erosion Analysis Model: Theory and validation. In: Proceedings of Wind Erosion: An International Symposium/Workshop, Manhattan, KS. Manuscript on CD-Rom. 23 pp.

Skidmore, E.L. (1986). Wind erosion control. Clim. Change, 9, 209-218.

Skidmore, E.L. (1989). Wind erosion in stressed environments. USDA-ARS, Kansas Agric. Exp. Sta., 89-542-A.

Skidmore, E.L. and J. Tatarko (1990). Stochastic wind simulution for erosion modeling. Trans. ASAE, 33, 1893-1899.

Skidmore, E.L., P.S. Fisher, and N.P. Woodruff (1970). Wind Erosion Equation: Computer Solution and Application. Soil Sci. Soc. Am. Proc., 34, 931-935.

Spaan, W.P., and G.D. van den Abeele (1991). Wind borne particle measurements with acoustic sensors, Soil Technology, 4, 51-63.

Stallings, J.H. (1957). Soil Conservation. Prentice-Hall, Inc., Englewood Cliffs, New York.

Sterk, G., M.V. Lopez and J.L. Arrue (1999). Saltation transport on a silt loam soil in Northeast Spain. Land Degr. Developm., 10, 545-554.

Stout, J.E. (1990). Wind erosion within a simple field. Trans. ASAE, 33, 1597-1600.

Stroosnijder, L. (2003). Measurement of erosion: is it possible? *In*: D. Gabriels and W.M. Cornelis (Ed.). 25 years of assessment of erosion. Ghent University, Ghent.

Swap R., Garstang, Greco, S. (1992). Saharan dust in the Amazon Basin, Tellus, 44B, 133-149.

Toy, T.J., G.R. Foster and K.G. Renard (2002). Soil Erosion, Wiley.

UNEP (1997). World atlas of desertification. Arnold, London.

van Dijk, P.M., L. Stroosnijder, and J.L.M.P. de Lima (1996). The influence of rainfall on transport of beach sand by wind. Earth Surf. Proc. Landf., 21, 341-352.

van Genuchten, M. Th. (1980). A closed-form equation for predicting the hydraulic conductivity of unsaturated soils. Soil Sci. Soc. Am. J., 44, 892-898.

Williams, J.R. (1994). The EPIC model. USDA-ARS, Temple, TX.

Wilson, S.J., and R.U. Cooke (1980). Wind erosion. In: M.J. Kirkby, and R.P.C. Morgan. Soil Erosion. John Wiley & Sons, Chichester. pp. 217-251.

Woodruff, N.P., and F.H. Siddoway (1965). A Wind Erosion Equation. Soil Sci. Soc. Am. Proc., 29, 602-608.

Zobeck T.M. (1991a). Abrasion of crusted soils - influence of abrader flux and soil properties. Soil Sci. Soc. Am. J., 55, 1091-1097.

Zobeck T.M. (1991b). Soil properties affecting wind erosion. J. Soil Water Cons., 46, 112-118.

Zobeck, T.M. and T.W. Popham (1992). Influence of microrelief, aggregate size, and precipitation on soil crust properties. Trans. ASAE, 35, 487-492.

Zobeck, T.M., G. Sterk, R. Funk, J.L. Rajot, J.E. Stout, R.S. Van Pelt (2003). Measurement and data analysis methods for field-scale wind erosion studies and model validation. Earth Surf. Proc. Landf., 28, 1163-1188.

Chapter 10

HYDROLOGICAL AND GEOMORPHOLOGICAL SIGNIFICANCE OF RIPARIAN VEGETATION IN DRYLANDS

Carlo CAMPOREALE[1], Paolo PERONA[2], and Luca RIDOLFI[1]

[1]*Dipartimento di Idraulica, Trasporti ed Infrastrutture Civili, Politecnico di Torino, Corso Duca degli Abruzzi, 24, 10129, Turin, ITALY*
[2]*Institute of Hydromechanics and Water Resources Management, ETH Hönggerberg,W. Pauli Strasse 15, 8093, Zurich, SWITZERLAND - e-mail:perona@ihw.baug.ethz.ch*

1. Introduction

Drylands are regions encompassing hyper-arid, arid, semi-arid or sub-humid climatic conditions (see also, Chapter 1). They include cold and warm subtropical deserts, savannas, and the Mediterranean environments. Our focus is here on warm drylands, which are generally characterized by the existence of a well-defined dry season dominated by subtropical high pressure (Malanson, 1993), and a rainy season with average precipitation of less than 700 mm/year. Such regions cover approximately 50% of the continents, with about 20% of the world's population living in these areas (Le Houerou, 1982; Nanson et al., 2002). This explains the growing scientific interest in the study of drylands. Here we focus on the interactions between fluvial geomorphology and riparian vegetation. These interactions act at different spatial and temporal scales, suggesting the existence of an intrinsic and remarkable sensitivity of riparian ecosystems to hydrological and geomorphological modifications. Riparian ecosystems have often been affected by heavy anthropogenic disturbances, with great reductions in spatial extent (up to 80%, as in certain U.S.A. sites) with respect to presettlement times (Smith et al., 1991; Tooth, 2000a,b; Salinas et al., 2000; O'Connor, 2001; Pettit et al., 2001).

From a geomorphological point of view, vegetation near rivers can be classified as upland or riparian. Upland vegetation is present in those areas that do not belong to channels that are potentially still active. Despite its importance for a number of geomorphological processes (see for example, Malanson, 1993) upland vegetation will not be analysed in this chapter.

Riparian vegetation can be defined as an 'ecosystem adjacent to the river' (Malanson, 1993), that is, 'those plant communities which are restricted to the zone directly influenced by the stream' (Hancock et al., 1996). These characteristics suggest that differences between upland and riparian vegetation should be stronger in drylands than in humid areas (Smith et al., 1993). In fact, in semiarid and arid regions vegetation distribution and abundance is largely controlled by water availability in the nearby rivers. Thus, water availability is - fundamental to sustain the richness of species (Hancock et al., 1996) and explains why some species are only found within or close to river channels (Tooth and Nanson, 2000). Dryland rivers control the surrounding vegetation through manifold actions; for example, when the duration and intensity of flood events are not too destructive in relation to the ability of vegetation to withstand relatively infrequent submergence, floods provide debris, moisture and nutrients to the riparian soil. In this sense, short-term rainfall variability and the consequent runoff would be more important to vegetation dynamics than average long-term climatic parameters. These hydrological characteristics, along with several other environmental factors such as evapotranspiration, soil type, groundwater regime and land use, are relevant to grant the survival of the ecotone and to drive the related zonation of species (Hooke and Mant, 2002). In turn, riparian vegetation has been recognized to be fundamental in influencing the morphodynamics of equilibrium or non-equilibrium of the river, depending on the

P. D'Odorico and A. Porporato (eds.), Dryland Ecohydrology, 161–179.

different response to external forcing (see, for example, Wolman and Gerson, 1978; Carter Johnson et al., 1995; Tooth and Nanson, 2000; Hooke and Mant, 2002; Nanson et al., 2002). These dynamics are yet not completely clear though some features are being studied and understood. The interaction between riparian vegetation and river dynamics is still one of the key points: this interaction would explain the peculiarity of the geometries observed in drylands both in fluvial and in vegetation patterns suggesting the need to consider the two components, i.e. river and vegetation, as dynamically coupled.

The high variety of geomorphological and riparian vegetation characteristics existing in drylands suggests that there are no geomorphic features really unique to drylands (Smith et al., 1993; Tooth, 2000a; Nash, 2001; Nanson et al., 2002). This diversity of ecological landscapes may be due to the different impacts of climatic conditions on plant ecosystems. Thus, subhumid climates do not imply necessarily the lack of water deficit. For instance, Australia has a high annual rainfall, but the corresponding high evaporation rate makes it the world's driest continent (Nanson et al., 2002). In this sense, aridity can be further emphasized by seasonal factors (Puckridge et al., 2000; Tooth, 2000a; Nanson et al., 2002) and by significant infiltration into the alluvium, with high transmission losses and important effects on river flow conditions. These losses can, for example, lead to rapid downstream decline in mean and peak discharges per unit (contributing) area (McMahon, 1979; Nanson et al., 2002). Due to the consequent irregularity and intermittence in river flow, streams can be ephemeral and discontinuous leading to fluvial dynamics, which alternate between aggradation and degradation both in time and space (Bull, 1997). The occurrence of either one of these mechanisms depends on the interplay between sedimentation, erosion and water availability, and, in turn, determines the presence and the distribution of vegetation resulting from sporadic flooding. Along the same line, the ability of dryland rivers to adjust more rapidly to climatic changes than the whole landscape, suggests that in the short term the geomorphological characteristics of these water courses may reflect contemporary climatic conditions and changes. The complexity of the fluvial and ecological processes occurring in the river channel and in the riparian zone explains the difficulty in finding a few distinctive features of dryland rivers. In the following we will focus on to the main geomorphological characteristics of the river-vegetation interaction observed worldwide in arid and semiarid regions.

The present review is organized in the following manner. Section 2 conceptually frames the type of interactions between river and riparian vegetation with a focus on the two roles (passive and active) played bt vegetation in this interaction. The main hydrological and geomorphological characteristics of rivers in drylands are discussed in Section 3. A numerical investigation of the dynamics of meandering rivers in drylands is also presented. Section 4 is devoted to riparian vegetation and to its significance within the whole fluvial ecosystem. Finally, some conclusions are drawn in Section 5.

2. Characteristics of the interaction between river and riparian vegetation

An instructive way of introducing the subject discussed in this chapter, is by focusing on the reciprocal interaction between vegetation and river dynamics: on the one hand, the river provides water to the nearby riparian environment according its hydrological, hydraulic and geomorphological characteristics; on the other hand, vegetation uses water for life and growth, and significantly affects the hydraulic and geotechnical characteristics of bed and banks, with an impact on the river morphodynamics. In this sense, the role of riparian vegetation can be interpreted as passive or active (see, Figure 1). In the first case (i.e., the passive role), the biological activity of the vegetation is not considered and only the effect of vegetation morphological and mechanical characteristics on river dynamics is discussed. From this point of view vegetation merely affects roughness, hydraulic resistance, and bank erodibility in the same manner as any a-biotic element with the same mechanical and morphological characteristics. *Vice* *versa*, vegetation is considered to be an active element if its biological activity – e.g., birth, growth, and death - and ecological dynamics are able to interact with the fluvial processes leading to changes in the evolution of river patterns and, in turn, in the whole river-riparian vegetation system.

The investigation of the passive role of vegetation is the usual approach followed in hydraulic engineering, which led to important theoretical and applied results (see, for example Kouwen and Li, 1980; Masterman and Thorne, 1992; Darby, 1999; Millar, 2000; Graf, 2002). However, some difficulties still exist in quantifying and in modeling riparian vegetation. These difficulties are in particular related to (i) the evaluation of the geotechnical characteristics of river banks as well as of the erodibility of alluvial soils; (ii) the spatial and temporal regime of soil moisture and groundwater near the river; (iii) the effect of vegetation on the flooding of the overbanks, on the kinematics of overbank flow, and on the related processes of deposition and erosion; (iv) the role of chemical and biological filtering played by riparian vegetation in the exchange processes occurring between river and upland vegetation.

The concept of an active role emerges when vegetation is no longer considered as a static element in the river dynamics but instead its temporal and spatial dynamics are included in the bio-geomorphological evolution of the river-riparian vegetation system. Thus the riparian zone should be considered in all its biotic and abiotic components, as an ecosystem with spatial and temporal patterns of interactions with the hydrological and geomorphological river regime (see,

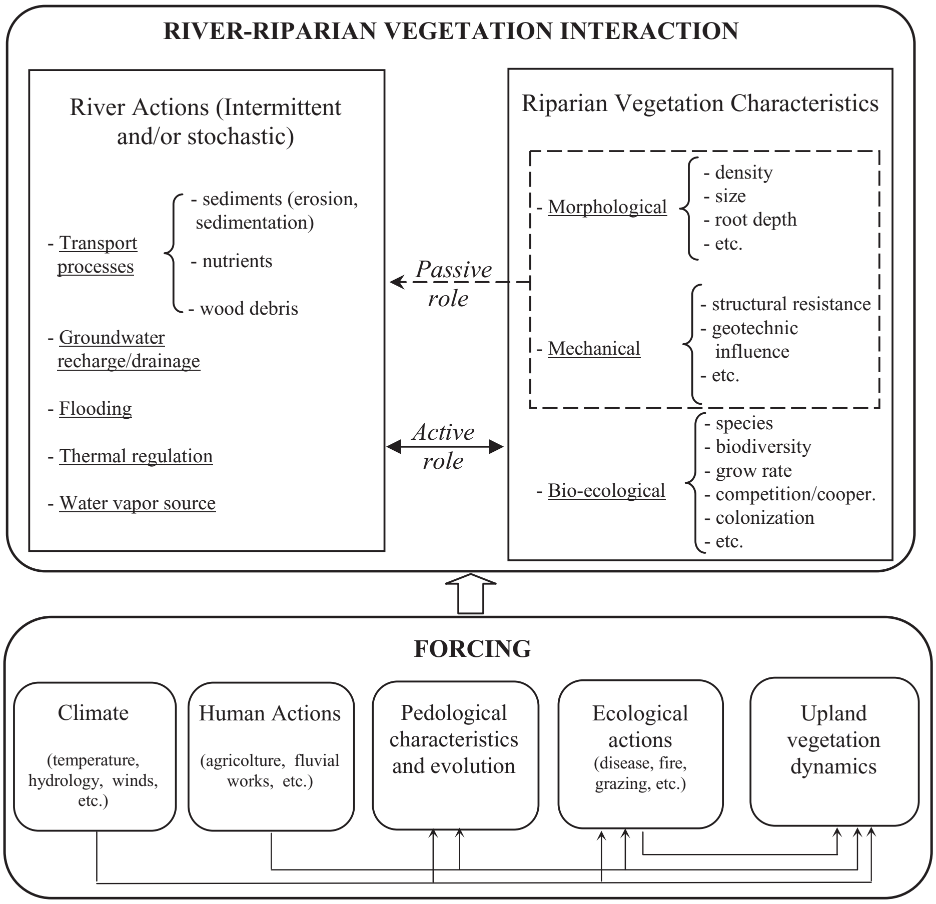

Figure 1. General scheme of the interactions between river and riparian vegetation.

Figure 1). It is important to observe that the temporal scales of river geometry evolution can be compared with those of the bio-ecological processes. Therefore, the geomorphological and vegetation dynamics are closely coupled. This coupling leads to linear and nonlinear dynamics, which may drive the river-vegetation system into an equilibrium state regulated by feedback mechanisms. Furthermore, the whole process can be subjected to the action of external forcings (see, Figure 1) able to add further complexity to the ecological and geomorphological patterns. Moreover, a number of processes listed in Figure 1 have both deterministic and stochastic components, which are able to lead to nontrivial behaviors in the evolution of the river-vegetation system (Perona et al., 2002).

It is worth remembering some of the requirements that seem to be fundamental to study the complex and fascinating picture that links river and riparian vegetation, namely: (i) an adequate selection and knowledge of the key variables involved in the phenomenon; (ii) the ability to quantitatively model the complex ecological mechanisms, such as plant recruitment, competition and cooperation intra- and inter- species, colonization of sites abandoned by the river during its planimetric evolution, water stress, and death of vegetation; (iii) to understand the influence of the hydrological and hydraulic characteristics of the river on such mechanisms, i.e. the influence of floods and the groundwater regime; (iv) to use a multidisciplinary approach with a cooperation of expertise in geomorphology, hydraulics, ecology, and bio-geography.

3. Main aspects of fluvial geomorphology in drylands

3.1. HYDROLOGY

The fluvial hydrology of drylands has been recently studied by a number of authors, leading to the production of a significant body of literature on this topic (see, for example, Graf, 1981; Farquharson et al., 1992; Knighton and Nanson, 1994; Thornes, 1994; Hooke and Mant, 2002; Lopez-Bermudez, 2002; Nanson et al., 2002) in spite of the difficulty in making both measurements (López-Bermudez et al., 2002) and mathematical models (Chebaane et al., 1995).

Rainfall regimes typical of arid and semiarid climates are characterized by either low and persistent or high and impulsive precipitation events, with an average annual rain of about 300-400 mm/year and the occurrence of strong isolated events. For example, sudden and intense rainfall events are responsible for the critical inundations observed in the Mediterranean regions in recent years, e.g. in Spain (López-Bermudez et al., 2002), and change in their statistical occurrence can be interpreted as a potential indicator of desertification processes (López-Bermudez et al., 2002).

The hydrological dynamics of dryland rivers are yet not clearly understood and only a few basic characteristics have been identified as being really unique to such rivers. These include: the high value of transmission losses due to both evaporation and infiltration (Hooke and Mant, 2002; Nanson et al., 2002); the downstream decrease of channel size (Figure 2a); the tendency of vegetation to colonize the river bed; the alluvial induration and lithification; the significant interactions between fluvial and aeolian processes when the river is adjacent to dunefields. Evaporation and rapid infiltration are responsible for slow and distributed water losses which may cause re-precipitation of minerals in solution (thus promoting the abovementioned effect of induration) and the consequent decrease both in peak discharge and flow volume in the downstream direction (Figure 2b). Extreme arid climatic conditions enhance transmission losses of ephemeral channels (Knighton and Nanson, 1994; Tooth, 2000b), with the consequent disappearance of some of these rivers along their course (Tooth, 2000a-b). This behavior is one of the peculiar aspects of dryland fluvial systems and it greatly influences the river-vegetation interaction (Nanson et al., 2002). In arid and semiarid regions runoff is generally dominated by Hortonian overland flow. This explains the occurrence of flash floods and the steep rising limbs of the flood hydrograph, with relatively high and frequent peak flow values (see, Knighton and

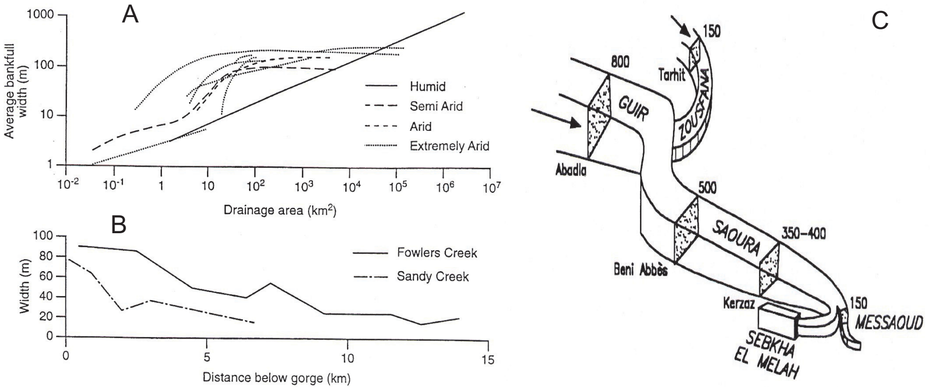

Figures 2. (a, b) Contrasting patterns in channel width along dryland channels (from Tooth, 2000b); (c) The downvalley decrease in the flood discharge (Guir-Saoura-Messaoud catchment, northwestern Sahara) (from Tooth, 2000a).

Nanson, 1997; Tooth, 2000a; Graf, 2002). Figure 3 shows as an example the flood magnitude (normalized with respect to the 2.33 yr discharge) in some dry regions of North America compared to humid European regions (Lewin, 1989; Farquharson, 1992; Knighton and Nanson, 1997).

Dryland hydrology has also a strong influence on the spatial development of river systems: a first important classification needs to be made between allogenic and endogenic rivers (Figure 4). Allogenic rivers (Figure 4a) generally have long mainstreams connecting several sub-basins; they can originate into humid and then cross semiarid, arid or even hyper arid regions. This type of river has a hydrological regime that is usually characterized by multiple intense or seasonal peaks and is likely to sustain perennial flow (Nanson et al., 2002). Endogenic rivers (Figure 4b), instead,

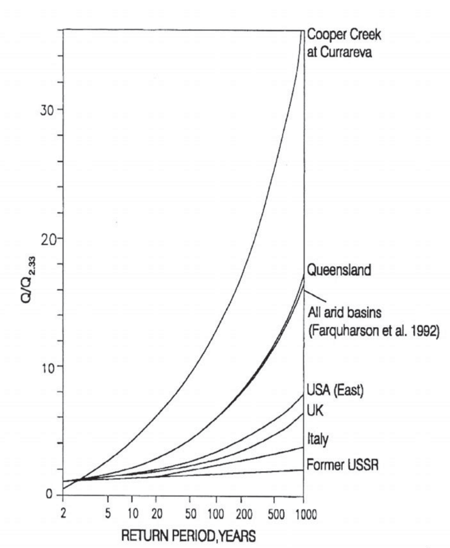

Figure 3. Regional flood frequency curve, illustrating the large increase in relative flood magnitude ($Q/Q_{2,33}$) that is characteristic of dryland regions compared to humid regions in Europe and North America (from Tooth, 2000a).

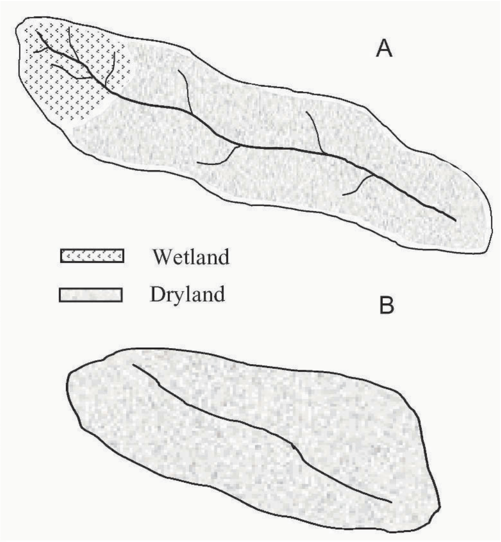

Figures 4. Scheme of allogenic (a) and endogenic (b) rivers in drylands. Because of the spatial scale, long dryland rivers belong mainly to the first category, whereas only the shorter ones are truly endogenic ephemeral or intermittent.

are short and belong to small single basins. Transmission losses are usually more pronounced for this kind of river configuration (Hooke and Mant, 2002) and the corresponding hydrological regime is usually characterized by flash floods or single peaks in the flood hydrograph, that are usually less intense and with short duration (Nanson et al., 2002).

An interesting hydrological feature regards the effects of different sediment stratigraphy on flood propagation. An interesting case observed in the extremely arid regions deals with the so-called 'red sedimentary unit' that is a continuous, compacted geological unit lying below the surficial non-cohesive alluvium (see, for example Schick, 1988; Lekach et al., 1998). In these cases, the presence of a superficial soil with high porosity and permeability hides a less permeable substrate (sub-alluvial bedrock), with the consequence that during the rare but intense rainfalls, infiltration is rapid in the first soil layer. Such a situation provides a variation to the alluvium-infiltration-flood problem and is the subject of recent discussions. Schick (1988) claimed that during inundation the wetting front is arrested by the substrate, thus giving rise to flood waves that travel on top of the saturated medium. This theory, however, has been criticized on the base of recent experiments that were conducted on a specific 'red sedimentary' site (in the Nahal Yael desert, Southern Negev, Israel), which seemed to indicate that downstream flow propagation does not necessarily requires that the medium is fully saturated (Lekach et al., 1998).

3.2. GEOMETRY

The geometry of dryland rivers is the result of the influence of hydrological and geomorphical processes, water-vegetation interaction and of the pedological characteristics of the planform. As dry regions are widely diffused throughout the world, allogenic and endogenic planforms show a large variety of landscape characteristics and slopes (for example, Mediterranean areas are mainly drained by steepland allogenic rivers and many landscapes are often shaped by the action of surface runoff water (Lopez-Bermudez et al., 2002)). This aspect explains the wide variety of geometries typical of these rivers, including braiding, meandering, anabranching or more complicated patterns, like waterholes and arroyos where the role of vegetation has been the subject of recent studies (Tooth and Nanson, 2000; Dunkerlay and Brown, 2002). In general, ephemeral channels are poorly defined, rather wide, shallow, and with low and indistinct banks (Hooke and Mant, 2002); this leads to configurations such as braiding (Graf, 1981; Clark and Davies, 1998; Tooth, 2000a, b; Nanson et al., 2002) or more confined shapes, but always with irregular patterns, such as anabranched reaches. Park (1977) and Wolman and Gerson (1978) showed that the channel width of several ephemeral channels varies nonlinearly in the downstream direction: both increasing (widening) and decreasing (narrowing) of channel width are commonly observed; this feature is in contrast to the widening generally exhibited by rivers in humid regions due to the presence of tributaries. Park (1977) calculated the values of the exponents of the power law models used to describe the scaling of width, mean depth and flow velocity with the river discharge. The numerical values of these exponents provided a first quantitative indication of the effects of both the discontinuous nature of the flow and of the high transmission losses. Such values reflect the widening and narrowing mechanisms observed along ephemeral streams: widening and narrowing occur at different time scales, ranging from hours (e.g. in the case of widening due to extreme floods), to decades (in the case of gradual narrowing associated with vegetation growth (Friedman and Lee, 2002)). Some examples exist of anabranched geometries that constitute an interesting case of mutual adaptation between river and vegetation. There are in fact some cases of streams forming sand ridges which can be colonized by vegetation and transformed into wide and vegetated islands or can give rise to deep anabranches, as in the case of the Marshall River in Australia (Wende and Nanson, 1998; Tooth and Nanson, 2000). A similar behavior is also observed in several ephemeral streams flowing across smooth valleys: these streams gradually form shallow discontinuous channels, which can also transform into arroyos (Bull, 1997). Similarly, waterholes – i.e., enlarged channel segments generated by particular concentrations of flow and by the consequent strong erosion – are also very important from an ecological point of view as they provide water to vegetation, while vegetation does not seem to have a direct influence on their formation (see, for example only a few of them being true alluvial meanders. This case is particular frequent in Mediterranean regions. The meandering geometry typical of dryland rivers has seldom been investigated, but it seems to show a lower sinuosity compared to that commonly observed in meandering rivers in humid regions (see for example Leopold and Wolman, 1960; Clark and Davies, 1998; Tooth, 2000a; , Knighton and Nanson (2000)).

Along with the aforementioned patterns, some examples of single-thread channels have also been recognized and recently documented by Tooth (2000a). He suggested that these channels can manifest either stability or instability. Stable channels can have inherited shape that comes from a past of more morphodynamic activity; in such cases the actual intrinsic stability is often associated with the presence of vegetation in the alluvium (Tooth, 2000b; Nanson et al., 2002). On the contrary, unstable channels can evolve forming series of meanders with Hooke and Mant, 2002). However, further quantitative analyses to assess the differences existing - both in the fluvial geometry and the evolutive dynamics – between rivers in dry and wet regions, still have to be investigated in detail. This fact motivated our numerical simulations presented in section 3.4.

3.3. TRANSPORT PROCESSES

Transport processes are very important for both the life of the fluvial ecotone and the planimetric evolution of the river. Most of the transport processes take place, in particular, during floods, with a significant movement of sediment load and debris (wood, waste, etc.) which modify the soil morphology and the chemical characteristics of the floodplain, thus influencing the soil moisture content as well as the quality of the water and nutrient cycling (Puckridge et al, 2000; Tooth, 2000a). In this context, it is important to observe that the amount of phosphorus, nitrogen and organic carbon in the soil, generally increases downstream and variations of such components tend to be positively correlated to the amount of silt (Jacobson et al., 2000). A positive trend in the soil salinity downstream has also been measured (Flügel, 1995; Jolly, 1996).

Dryland rivers appear to be much more efficient in bedload transport than rivers in humid zones with the same shear stress (Laronne and Reid, 1993). It has been estimated (see, for example, Langbein and Shumm (1958)) that for rivers of similar characteristics, sediment yields reach a maximum when the mean annual effective precipitation is between 250 mm and 350 mm. Sporadic inundation on dry terrain produces erosion both of the bank and of the bed so that scour material is mobilized and entrained continuously downstream (Tooth, 2000a-b). This mechanism, apart from being important for the successive remodelling of river reaches, seems to contribute significantly to increase the soil salinization of those sites where entrapment of sediments is facilitated (Jolly et al., 1993; Busch and Smith, 1995; Jacobson et al., 2000). In the transport processes, the differences with respect to humid regions have generally been attributed to the relative lack of armouring of rivers flowing in drylands (Laronne and Reid, 1993; Reid and Laronne, 1995; Reid et al., 1998).

3.4. A NUMERICAL MODEL FOR MEANDERING RIVERS IN DRYLANDS

In recent years, numerical models of meandering dynamics have been used to investigate some geometric characteristics of the long term evolution of rivers in humid regions (see, for example, Howard and Knudson, 1984; Sun et al., 1996; Stølum, 1996, Perona et al., 2002). To the authors' knowledge, similar simulations have never been made for drylands. In this paragraph, therefore, we present and briefly discuss a preliminary example of such meandering processes that could occur in sub-humid or semi arid areas. In particular, we focus on the morphodynamics of potentially unstable rivers where the influence of evaporative and infiltration rates is able to reduce the flow rate downstream giving rise to a spatially decreasing discharge $Q = Q(s)$, where s is the intrinsic coordinate along the river. This hydrological effect is expected to produce interesting differences from the typical patterns that can be observed in the humid regions, where flow rate is either uniform or increases in the downstream direction.

Different models of meandering evolution have been proposed in the past by several authors (Ikeda at al., 1981; Blondeaux and Seminara, 1985; Johannesson and Parker, 1989; Zolezzi and Seminara, 2002; Lancaster and Bras, 2002). Apart from the model by Johannesson and Parker (1989) and the detailed model by Zolezzi and Seminara (2002), the approach by Ikeda et al. (1981) is commonly used in the modelling of river meandering. Despite its simplicity, this model is based on a consistent, process-based analysis of the fluid dynamical processes – through the de Saint Venant equations for shallow steady turbulent flow in a sinuous channel - and it explains some of the main features of real meanders, including wavelength selection, elongation, deformation and downstream migration (Ikeda et al., 1981). Thus, the Ikeda model is used in this section because of its ability to model the main physical processes with only a limited numerical complexity.

From a mathematical point of view, because meandering rivers have the tendency to maintain a locally constant width in time (see, for example Camporeale et al., 2004), the river can be schematically represented as a curved line evolving onto a sloped plane; the points of this line migrate driven by the local velocity in direction normal to the curve (e.g., Perona et al., 2002). Complicated mechanisms such as bank collapsing, interaction with riparian vegetation, and temporal evolution of local erodibility, are not considered in the present simulations. The essential role of cutoffs is instead taken into account, while the effect of secondary currents in the river bends is considered by assuming a semi-theoretical relationship between the topography of the bed and the local curvature of the river centreline. The downstream reduction in discharge is modelled according to the exponential law $Q = Q_0 \operatorname{Exp}[-\tau s]$, where Q_0 represents the initial discharge (i.e., at abscissa s=0) and τ is a parameter that regulates the discharge decay. In the simulation we choose $Q_0 = 300\ \mathrm{m}^3/\mathrm{s}$ and $\tau = 1.37 \cdot 10^{-5}\ \mathrm{m}^{-1}$ (that is, an equivalent transmission loss of 1.2 m^3/s km). The exceeding bank velocity u_{sb} for a bankfull discharge, satisfies the following differential equation (Ikeda et al., 1981)

$$\frac{\mathrm{d}u_{sb}}{\mathrm{d}s} + 2C_f \frac{U_0}{H} = bU_0 \left(\frac{Fr^2 + A + A_s - 1}{H} C_f k - \frac{\mathrm{d}k}{\mathrm{d}s} \right) \quad , \tag{1}$$

where U_0 and H are the mean velocity and the water depth of the uniform flow, Fr is the Froude number, C_f (0.0024) is a dimensionless friction factor; A and A_s (both fixed equal to 8.5) are constants that account for the bed slope and for the convective transport of downstream momentum respectively (Edwards and Smith, 2002; Camporeale et al., 2004), k is the local curvature, and b is the river half-width, assumed to vary in the downstream direction according to the relation proposed by Hey and Thorne (1986), $b = 0.5aQ^{c}$ (a=3.74, c=0.5). In the numerical simulation, the time is discretized in time intervals Δt and the algorithm consists of the following four steps in each interval. Firstly, the exceeding bank velocity u_{sb} is evaluated by numerical integration of Eq. (1). Secondly, the relationship $v = E\, u_{sb}$ is used to obtain the bank erosion, where v is the normal-to-the-curve migration rate and E (equal to $3 \cdot 10^{-5}$) is the local erodibility; this relation has frequently been used (Howard and Knudson, 1984; Stølum, 1996; Sun et al., 1996) and experimentally verified (Beck, 1984; Beck et al., 1984; Pizzuto and Meckelnburg, 1989). Thirdly, the points of the river are then moved along the normal coordinate according to the scheme proposed by Sun et al., (1996). Finally, the bed slope and the discharge are updated according to the new river sinuosity. Other numerical details are reported elsewhere (Perona et al., in preparation). The results of these analyses are shown in Figures 5a-c. Figure 5a reports a meandering pattern generated by the model starting from a straight line of length L=80 km which is perturbed with additive white noise with zero mean and unit variance. It should be noted that

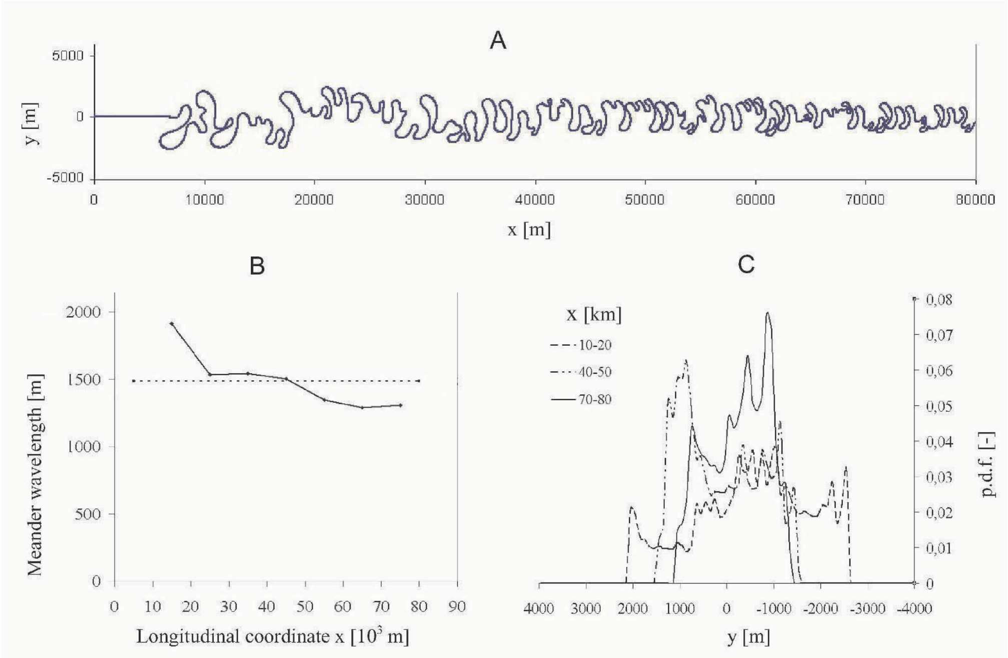

Figures 5a-c. (a) Example of a meandering pattern obtained after 5300 years of evolution starting from a noised straight line. (b) Longitudinal variation of the meandering wavelength and (c) the pdf of the transversal coordinate of the points occupied by the river on the floodplain. The characteristic reduction of the meandering belt width can be noted.

some cutoffs had already occurred. The effect produced by the decrease in discharge is a significant reduction of the amplitude and the wavelength of the meanders. Figure 5b shows the decrease of meander wavelength averaged in non-overlapping spatial windows (window width equal to 10 km). Figure 5c shows the time-averaged frequency density function of the transversal coordinate (y) of the points occupied by the meandering river after the initial transient; the amplitude of the function gives a reasonable estimation of the width of the meandering belt: the effect of the decreasing streamflow is that in the different river segments there is a reduction in the width of the "migration belt" of the river within the floodplain. It is important to recall that, at the statistical steady state, the only mechanism controlling the river spread is the effect of cutoffs (see, for example Perona et al., 2002). Such a highly nonlinear mechanism plays a fundamental role in driving the dynamics toward a probable critical self-organized statistical steady state in which the river shows geometrical characteristics that are statistically constant confirming the mechanism of self- confinement already hypothesized by Stølum (1996) and Liverpool and Edwards (1995).

These results seem to be coherent with field observations conducted on sub-humid and semi-arid regions (Clark and Davies, 1998; Tooth, 2000a-b; Hooke and Mant, 2002) and confirm some peculiar geometrical characteristics of dryland rivers.

4. Riparian vegetation

4.1. GEOMETRY AND SOME ECOLOGICAL CHARACTERISTICS

The patterns of riparian vegetation are greatly influenced by the local hydrological conditions. Unlike humid regions, seasonally arid and semiarid environments exhibit visually well-defined and easily distinguishable patterns of riparian vegetation that can be interpreted easily, by means of, for example, the quadrant analysis or other methods (Trodd and Dougill, 1998; Hooke and Mant, 2002). Riparian vegetation generally exhibits characteristic patterns (Figure 6) organised along the banks of the watercourse (see, for example Malanson, 1993). Sparse vegetation is considered to be mainly the result of heavy erosion during floods, however this effect can be enhanced by other concomitant disturbances (e.g., deep groundwater level, severe local aridity) from which vegetation may take many years to recover (Nanson et al., 2002). Conversely, regularly distributed vegetation is typical of conditions with more regular and sufficient water availability.

Riparian vegetation species are usually *phreatophytes*, i.e. species with a tangled root system that is directly connected to the groundwater table (Robinson, 1958; Graf, 2002). Grass and shrub communities generally prevail among riparian floodplain species and their zonation along valley floors can vary considerably, as is the case in Mediterranean regions (Hooke and Mant, 2002). Analyses of the sources of water used by these species carried out in the San Pedro River (Arizona, U.S.A.) show that grasslands basically rely on recent precipitation, while mesquite shrubs obtain water from deeper zones in the soil profile and are therefore more sensitive to groundwater changes (Scott at al., 2000). Other field observations have shown significant differences in vegetation species due to the geographical location of sites and the local climate (Hupp and Osterkamp, 1985; Wainwright et al., 2002). Hancock et al. (1996), for instance, argued that arid catchments exhibit riparian vegetation with more complex structure, survival ability and competitive strategy than upland vegetation which, is instead more inclined to tolerate water stress. This agrees with predictions made by the Competitor-Stress tolerator-Ruderal (C-S-R) model proposed by Grime (1979) and interesting examples have been found in some sites across the western U.S.A. (Kauffman et al., 1983, Tucker Shulz et al., 1990; Hancock et al., 1996).

The dynamics of riparian vegetation in drylands seems to be predominantly influenced by the competition (or cooperation) between different communities classified as native dominant, pioneering, invader or opportunistic. Their main characteristics are briefly outlined in the

Figure 6. Riparian vegetation along the slowly disappearing Sandover River, Central Australia (from Tooth, 2000b).

Table I. Example of a classification of plant species according to their behaviour and adaptability.

Characteristics	Species	Soil type
Pionering	*Salix Caprea, Cottonwood, Malaleuca argentea, etc*	riparian floodplain, water shelf
Invaders	*Tamarix Ramossis*ima, *Artemisia Tridentata*), *Rosa Woodsii, etc*	riparian floodplain, river bed
Opportunistic	*Teatrees*	sandy, mod. gravel bars
Native dominant	*Reichardia picroides,Phlomis fructicosa, Dianthus vultaria*	cultivated, very arid lands
	Artemisia barberia, Inula viscosa Lygeum spartum	dry rocky hillslops, even. degradated

following (see also Table I), but it should be noted that this classification is not closely connected to any particular species, since in some cases these could potentially belong to either one or another class, depending on the geographical and climatic conditions.

The native dominant species become well established locally and organized in a cooperative co-existence, with a yearly life cycle that is characterized by seasonal growth. Depending on flood frequency, the season of flood occurrence, flood intensity, and land use, such species can be found rather close to the watercourses (Hughes, 1990). The density of dominant species can vary in space (along rivers and within them as partial invaders) and time (invasions of river beds can be destroyed by even moderate floods), while the hydrological characteristics of floods seems to have a remarkable effect on the evolution of this type of vegetation (Hooke and Mant, 2002).

The pioneering species (see, Malanson (1993) and Hancock et al. (1996) for a more detailed classification) show (i) a rapid growth rate, (ii) enough flexibility and adaptation to form reclined habits (this is called ‘f-strategy’ and is adopted by trees when strong external forces are applied (see, for example Mosbrugger, 1990)), (iii) recruitment and encroachment, that mostly occur in the bed of the river, and (iv) a good group strategy. Therefore pioneering species have the typical characteristics that are necessary for efficient rooting. *Malaleuca Argentea*, for instance, spends 90% of the time in low stage of an ephemeral river in tropical environments and has a multiple stem form (which ensures that at least a part of the tree remains intact during severe flood events), modified bark (thick and multi-layered as a protection against traveling debris), modified crown and root development to adapt to extreme variation in water supply, and adventitious buds, which allow for rapid recovering after damages (Fielding et al., 1997).

The invader species are often associated with exotic species imported from other sites that in some cases are even geographically distant. Because of their water tolerance these plant communities sometimes have a competitive advantage over native species (Graf, 2002). This quality makes them the ideal candidates for sites where streamflow diversion, whether natural or anthropic, can be particularly severe. Examples found in literature include the case of Bishop Creek (Nevada), where the invasion of sagebrush (*Artemisia Tridentata*) and *Rosa Woodsii* produced a consequent reduction of the native riparian vegetation (Smith et al., 1991) or Southwestern Australia, where the invasion of *Tamarix* was clearly induced by river regulation (Griffin et al., 1989; Tooth, 2000a).

Opportunistic species, such as *teatrees*, grow in the periods subsequent to infrequent floods; their stems are sufficiently flexible to allow them to survive moderate inundation and damage during floods; they are able to live in highly stressed channel-bed habitats and are likely to co-exist with local species (Tooth and Nanson, 2000).

4.2. VEGETATION EFFECT ON ROUGHNESS AND SEDIMENT TRANSPORT

It is commonly recognized that the presence of vegetation greatly affects local channel roughness (Graeme and Dunkerlay, 1993; Nanson et al., 2002) as well as the mechanisms of erosion and sediment deposition (Ashworth, 1996; Huang and Nanson, 1997, Hooke and Mant, 2002). Nanson et al. (2002), showed that channel morphogenesis is driven by the important role of vegetation due to its impact on the interaction between flow and sediment transport. However, sedimentation is not necessarily high in all vegetated reaches since it depends on the cover density, which is in turn influenced by many other variables. For example, Hooke and Mant (2002) observed that, in some drylands in Spain, the mechanism of flow-vegetation interaction depends also on species, age, position (i.e. transversal or longitudinal and elevation above the river bed), zonation, and season: these factors play a crucial role on vegetation influence and on the hydrological dynamics of river channel and riparian zone. A quantitative assessment based on field campaign measurements and calculation of the dependence of hydraulic roughness on density and average diameter of woody vegetation were proposed by McKenney et al. (1995); their analyses were made on groups of trees of different age and indicated that, in the case of adult

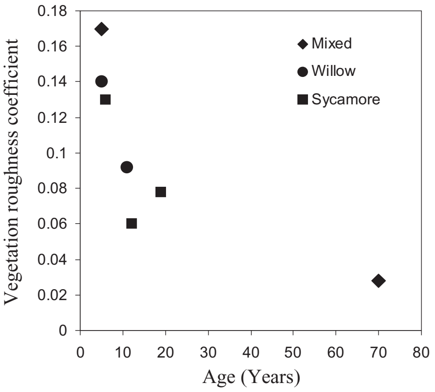

Figure 7. Graph of roughness values versus age for vegetation groups. The vegetation becomes less effective in providing flow resistance with age (after McKenney at al.,1995).

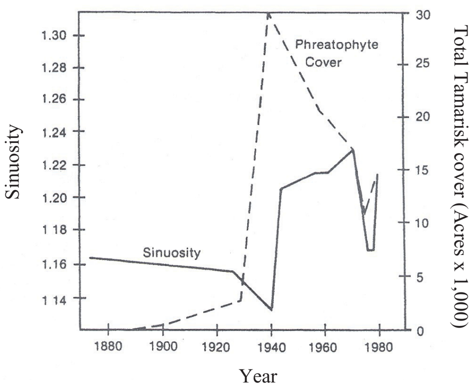

Figure 8. Gila River, Arizona. Relationship between density, coverage and channel sinuosity; this latter occurred mainly during flood periods, thus explaining the lag with vegetation changes (after Graf, 1981).

vegetation, flow resistance decreases with the age (see Figure 7). This result is particularly interesting because young and dense vegetation can significantly contribute to flow resistance; in low-energy zones, this favours the formation of sedimentation sites with an effect on the stabilization of the river morphology. An example of these dynamics is reported in Salinas et al. (2002), who investigated the role of highly developed root systems in river bank stabilization in a semi-arid region of Spain. This effect was discussed also by Hooke and Mant (2002), and explains why in many cases the stabilizing effect is associated with a gradual channel narrowing (Tooth, 2000b) or a reduction in channel sinuosity (Graf, 1981) (see Figure 8), thus showing the clear active role (in the sense explained in Figure 1) of the riparian ecosystem. An example of the opposite influence of vegetation concerns the channel invasion of phreatophytes leaving little space for water flow. Because of the frequent water deficit and the high spatial-temporal variability of precipitation typical of drylands, plants can colonize the river bed and develop a relatively dense vegetation. Despite the different effect of the various vegetation types (Hooke and Mant, 2002) on the channel hydraulics, the bed colonization increases the frequency of bankfull discharge as well as that of overbank floods, which, in turn, remove part of the vegetation and consequently change the fluvial morphology (Graf, 1980; Thornes, 1994; Tooth, 2000b). This uprooting mechanism is considered to be responsible for channel widening and lateral erosion. Moreover, the return period of floods plays an important role; in fact, flash floods can be more destructive than useful for the growth of young vegetation, while moderate floods significantly recharge the ground, providing soil moisture which is used by vegetation during the growing season (Hooke and Mant, 2002).

After heavy floods have occurred, the active role of vegetation becomes fundamental for channel recovery (Hooke and Mant, 2002) or can lead to the formation of intriguing shapes such as anabranching channels. This type of channel would represent the optimal equilibrium configuration to carry water and sediments, and is therefore also important for apportion and distribution of nutrients along rivers (Nanson et al., 2002).

4.3. ROLE OF SOME SOIL CHARACTERISTICS

The role of riparian vegetation, whether active or passive, is fundamental as it provides nutrients to the ecotone and affects the water quality. Vegetation also controls algae proliferation as it offers shadow to the river. The passive effect given by both bed and bank vegetation encourages the local deposition of fine material (Salinas et al., 2000) rich in organic matter and nutrients

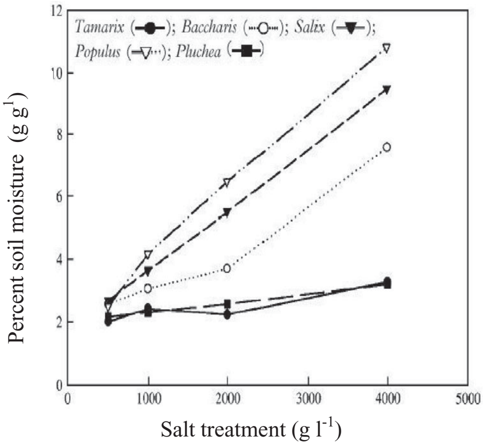

Figure 9. Average percent of soil moisture in root zones of riparian plants grown on four salinity treatments (after Vandersande et al., 2001).

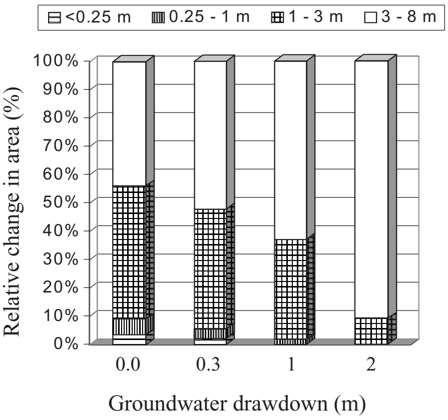

Figure 10. Relative change in extent of four depth-to-groundwater zones of the San Pedro river floodplain, for four hypothetical groundwater decline scenarios (after Stromberg et al., 1996).

(Jacobson, 2000). These apportions of material, thanks to the combined contribution of the fertility of fine sediments and the post-mortem role of wood debris, are important for the soil enrichment of new habitats (Forbes, 1902). The way fine sediments augment fertility is closely related to the silt layer that influences soil moisture dynamics and, in turn, decomposition and nutrient cycling (Chapter 8). Moreover, silt layers act as hydraulic barriers: in conditions of overbank flow moisture is stored on the floodplain (Higgins et al., 1997), thus providing a microhabitat, which is favourable for blue-green algae, fungi, lower plants and invertebrates. It has been also found that high values, i.e. peaks, in vegetation density correspond to peaks in soil silt and nutrient contents (Jacobson et al., 2000). Some connections have emerged from interesting observations monitored in the Namib desert (Namibia, Africa) by Jacobson et al. (2000), between the soil moisture regime and the related soil properties. While sands can become dry at depths of tens of cm, several centimetres of silt can maintain subsurface soil moisture levels of some percent (by weight) for several months or weeks after a flood (Jacobson et al., 2000).

Another factor considered as important to the biological activity of some vegetation species is the soil salinity, which usually increases downstream. This increase in salinity can be attributed to the combined effect of leaching and evaporation. The ability to spread under such conditions is a characteristic of some riparian tree species and is sometimes enhanced by their distribution, morphology and productivity (Jolly et al., 1993; Bush and Smith, 1995). As an example, Vandersande et al. (2001) compared the effects of both salt and water stress between native and invasive species in the Colorado River (Arizona, U.S.A) and found that invaders have a greater stress tolerance and competitive ability to extract water under increasing soil salinity than native species (Figure 9). The reduction in the mean flow discharge and the consequent increase in salinity have therefore been used to explain the absence or the disappearance of some species (i.e., the *Faidherbia albidia* in some riparian sites of ephemeral rivers in the Namib desert), with the successive replacement by halophytic (Jacobson et al., 2000) or phreatophytic species wherever the dieback and decline of dominant riparian species have occurred (Jolly et al., 1993; Bush and Smith, 1995; Jolly, 1996; Vandersande et al., 2001). Thus, soil salinity is an important factor characterising the current evolution of the ecotone and can be used to predict environmental changes resulting from natural or anthropogenic diversions of river flow (Jolly, 1996; Rozin and Schick, 1996; Jacobson et al., 2000; O'Connor, 2001).

4.4. ROLE OF GROUNDWATER

Because riparian vegetation relies heavily on groundwater (Figure 10, see also Malanson, 1993; Stromberg et al., 1996; Higgins, 1997), an accurate knowledge of groundwater dynamics is therefore necessary. Dryland sediments generally have a higher porosity than in wet regions, thus causing groundwater processes near rivers to be strongly dependent on the stratigraphy. In some riparian zones groundwater is recharged mostly by infiltration into the alluvium and groundwater flow from the river to the nearby area (Malanson, 1993; Stromberg, 1993; Carter Johnson et al., 1995; Stromberg et al., 1996). In the absence of major unconfined aquifers, the water table decreases away from the river. Figure 10 shows the results of the experiments made by Stromberg et al. (1996) where four zones (with depth-to-groundwater ranging from 0.25 – 8 m) respond markedly to different scenarios of groundwater drawdown. This picture represents in a sense the draining capacity of arid environments and, thus it suggests that there is only a limited lateral zone where roots are still able to uptake water. Water uptake is the main mechanism controlling vegetation survival in drylands. Smith et al. (1991), for example, showed some interesting differences in water use for species in uplands or in riparian areas. Only riparian vegetation, which grows along the river banks, uses groundwater. The access to groundwater resources allows riparian vegetation to survive longer in dry periods. This has important effects on the impact of anthropogenic disturbances to the natural river flow as indicated for example by O'Connor (2001) in a study on the effects of dam construction on downstream vegetation in small catchments in the Northern Province (South Africa): during low flow periods the reduced soil water availability may not be sufficient to meet the high evaporative demands of the atmosphere under typical late summer climatic conditions, leading to changes in vegetation patterns. Smith et al. (1991), for instance, investigated the effects of stream diversion consequent to the construction of hydroelectric plants on the Bishop Creek (Nevada) and showed that, in the diverted reaches, the reduction of the groundwater table increases the frequency and the level of water stress in vegetation. As a consequence, changes in the physiological behavior (e.g. of reduced leaf size, reduced leaf area per unit length and increased leaf thickness) were observed for all species. These effects were more pronounced for juvenils, indicating that in the early stages of life plants are particularly vulnerable to extreme drought conditions. It was concluded that these changes are typical of adaptations of broad leaf vegetation to water deficit (Smith et al., 1991). Streamflow diversion and the elimination of high flows can have important effects on aquifer recharge, leading to the depletion of groundwater, with a negative impact on plant communities in the riparian zone (Stromberg, 2001).

4.5. CONCEPTUAL MODELS OF RIVER-VEGETATION INTERACTION

Conceptual models of river-vegetation dynamics aim to understand and, consequently, describe the interactions between fluvial processes and riparian vegetation as well as their impact on the geomorphological modifications occurring at time scales ranging from years to several decades. These models concentrate qualitatively on some aspects of the passive and active role of vegetation in fluvial geomorphology described in Section 2. Their mathematical formalization allows for numerical or analytical solutions, which provide quantitative predictions. Conceptual models are of fundamental importance from both a speculative and applicative point of view. These models allow the analysis of the behavior of riparian vegetation (in terms of percentage cover, species richness, degree of connectivity, number of exotic plants, and natural regeneration) in relation to environmental changes and to identify zones that need restoration. For example, Rozin and Shick (1996) used models to analyse the effects of grazing in Israel; Salinas et al. (2000) compared the effect of different anthropogenic disturbances and their relative effects in the South-eastern Iberian Penisula. Their observations suggested that water channelling and modern agriculture can alter or even eliminate natural vegetation, while the effects of mining and sewage are quite limited in space and time (paradoxically the disturbed zones can give rise to heophyte communities that harbour important species of birds).

After the works by Wolman and Gerson (1978) and Stromberg (1993) dealing with the description of the complex vegetation-fluvial dynamics in semi-arid and arid ecosystems in the U.S.A., some new contributions have been made recently to the modelling of river-vegetation interaction in humid regions (McKenney et al., 1995), in Mediterranean areas (Brookes et al., 2000; Hooke and Mant, 2002) and in Australia (Tooth and Nanson, 2000; Tooth, 2000b). The observations proposed by Wolman and Gerson (1978), and also discussed by Hooke and Mant (2002), support the hypothesis that significant changes in vegetation would take place only during a limited number of high and infrequent flow events, and that only small adjustments occur in between these events. The model does not lead to any equilibrium state for ephemeral streams, but illustrates the effects caused by flows of different magnitudes. Hooke and Mant (2002) noticed that these models describe too extreme conditions for some sub-humid and semi-arid environments such as parts of the Mediterranean basin where vegetation is present in significant quantities and non-aquatic vegetation can be found in channels. In this case vegetation has a significant impact on flood propagation (Hooke and Mant, 2002). While Brooks et al. (2000) aimed to modelling such an effect, McKenney et al. (1995) suggested a more detailed analysis and explained the progressive decrease in the geomorphic threshold for bar erosion after germination of a vegetation band.

Tooth and Nanson (2000) suggested an interesting interpretative model for river anabranching mechanisms in the presence of *teatrees*. On the basis of their observations the formation of anabranching channels would occur in three phases (Figure 11 a-c) and would be driven by the interactions between vegetation growth and sedimentation. The chaotic growth of vegetation on the channel bed in ephemeral channels induces flow separation which influences the local patterns of velocity, bed shear, erosion, deposition and accumulation of sediment in the lee of the obstacles, thus forming lemniscate forms that show clues of self-similarity (Figure 11a). In the second step (Figure 11b), lemniscate shapes of sediment deposits, which concentrate the flow giving rise to stable vegetated sand deposits over which local clusters of vegetation aligned along the stream. Finally (Figure 11c), the clusters of vegetation coalesce and form longitudinal ridges so that the stream is concentrated in relatively narrow channels that are free of vegetation. Strong floods can damage these structures and the cycle starts again (Nanson et al., 2002). Reaches disturbed by the interplay between flooding and dry periods are characterized by more intriguing dynamics of vegetation interacting with erosion and deposition processes. This would explain the formation of vegetation islands in high-energy zones (or riffles), i.e. where channel movement is dominated by avulsion (Graf, 1981; McKenney et al., 1995; Tooth and Nanson, 2000).

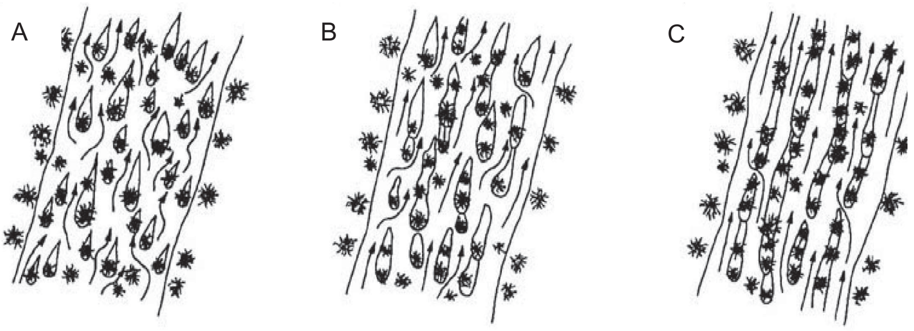

Figures 11a-c.The three basic steps of the conceptual model for river anabranching formation proposed by Tooth & Nanson (2000).

5. Conclusions

This chapter concentrated on the importance of riparian vegetation in dryland river morphodynamics. Due to the variety of hydrological and geomorphological characteristics of arid and semiarid regions and to the difficulties involved in carrying out reliable measurements, it is not yet clear whether a general classification of the main features of dryland rivers and riparian vegetation can be made. Most of the existing literature on this topic remarks that river dynamics and vegetation evolution in drylands are closely linked and it is not possible to study them separately. This calls for cooperation within the science community to develop an interdisciplinary eco-hydrological and eco-hydraulic approach to the study of the effect of the interactions between fluvial processes and riparian vegetation. An example of a possible quantitative framework for the study of fluvial-vegetation dynamics is suggested in this chapter by our study on the effect of transmission losses on the dynamics of meandering rivers.

The review of existing studies on river- riparian vegetation interactions suggests two fundamental directions for future research in this field. On the one hand, there is the need for more detailed and extensive analyses of real cases of riparian environments, with measurements of hydrological, hydraulic, ecological, and geomorphological quantities. On the other hand, new qualitative and quantitative conceptual models need to be developed, which are able to connect and organize the experimental observations. These models should describe the complex river-riparian vegetation system as a whole, and lead to a better understanding, prediction, and control of its response to external forcing. These models could be subsequently used also to assess river system sensitivity to environmental change as well as to test future management strategies (Cummins, 1993; Halse and Jensen, 1993; Zalewski et al., 1998; Zalewski, 2000; Stromberg, 2001).

Acknowledgments

The authors thank the Cassa di Risparmio di Cuneo (CRC) Foundation for the financial support.

6. References

Ashworth, P. J. (1996). Mid-Channel bar growth and its relationship to local flow strength and direction. Earth Surface Processes and Landforms, 21, 103-123.

Beck, S. (1984). Mathematical modeling of meander interaction. In River Meandering, Proceedings of the Conference, Rivers'83, Elliot CM (ed.). ASCE: New York, 932-941.

Beck S, Melfi D.A. and Yalamanchili K. (1984): Lateral migration of the Genesses River, New York, in Conference Rivers' 83, New Orleans, Lousiana, October 24-26, 1983, editor: Elliott C. M. (published by ASCE, New York.

Blondeaux, P. and Seminara, G. (1985). A unified bar-bend theory of river meanders. Journal of Fluid Mechanics, 157, 449-470.

Brookes, C.J., Hooke, J. M. and Mant, J. (2000). Modelling vegetation interactions with channel flow in river valley of the Mediterranean region. Catena, 40, 93-118.

Bull, W. B. (1997). Discontinuous ephemeral streams. Geomorphology, 19, 227-276.

Busch, D.E. and Smith, S.D (1995), Mechanism associated with decline of woody species in riparian ecosystem of the southwestern U.S. Ecological Monographs, edited by E.S.A., 65, 347-370.

Camporeale, C., Perona, P., Porporato, A. and Ridolfi, L. (2004). Hierarchy of models for meandering rivers and related morphodynamic processes. Journal of Fluid Mechanics, submitted.

Carter Johnson, W., Dixon, M. D., Simons, R., Jenson, S., and Larson, K. (1995). Mapping the response of riparian vegetation to possible flow reductions in the Snake River, Idaho. Geomorphology, 13, 159-173.

Chebaane, M., Salas, J. and Boes, D. C. (1995). Product periodic autoregressive processes for modeling intermittent monthly streamflows. Water Resources Researches, 31(6), 1513-1518.

Clark, P.B. and Davies S.M.A. (1998), The application of regime theory to wadi channels in desert conditions. International Conference on River Regime, edited by W.R. White, John Wiley & Sons.

Cummins K.W. (1993). Riparian stream linkages: In-stream issues. In Ecology and management of riparian zones in Australia, S.E. Bunn, B.J. Pusey, P.Price editors, LWRRDC Occasional Paper Series No: 05/93.

Darby, S. E. (1999). Effect of riparian vegetation on flow resistance and flood potential. Journal of Hydraulics Engineering ASCE, 125 (5), 443-454.

Dunkerley, D. L. and Brown, K. J. (2002). Oblique vegetation banding in the Australian arid zone: implication for theories of pattern evolution and maintenance. Journal of Arid Environments, 51, 163-181.

Edwards, B. F. and Smith, D. H. (2002). River meandering dynamics. Physical Review E, 65, 1-12.

Farquharson, F. A. K., Meigh, J. R. and Sutcliffe, J.V. (1992). Regional flood frequency analysis in arid and semi-arid areas. Journal of Hydrology, 138, 487-501.

Fielding C.R., Alexander J. and Newman-Sutherland E., (1997). Preservation of in situ, arborescent vegetation and fluvial bar construction in the Burdekin River of north Qeensland, Australia. Palaeogeography, Palaeoclimatology, Palaeoecology. 135(1997) 123-144.

Flügel, W. A. (1995). River salination due to dryland agricolture in the Western Cape Province, Republic of South Africa. Environment International, 21(5), 679-686.

Forbes, R. H. (1902). The river-irrigating waters of Arizona-their character and effects. University of Arizona Agricultural Experiment Station, Bulletin,44, 143-214.

Friedman, J. M. and Lee, V. J. (2002). Extreme floods, channel change, and riparian forests along ephemeral streams. Ecological Monograph, edited by E.S.A., 72(3), 409-425.

Graeme, D. and Dunkerley, D.L. 1993. Hydraulic resistance by the river red gum, Eucalyptus camaldulensis, in ephemeral desert streams. Australian Geographical Studies, 31, 141-154

Graf, W. L. (1980). Riparian management: a flood control perspective. Journal of Soil and Water Conservation, 7, 158-161.

Graf, W. L. (1981). Channel instability in a braided, sand bed river. Water Resources Researches, 17(4), 1087-1094.

Graf, W. L. (2002). Fluvial processes in dryland rivers. Caldwell: Blackburn Press.

Griffin, G. F., Stafford Smith, D. M., Morton, S. R., Allan, G. E. and Masters, K. A. (1989). Status and implications of the invasion of Tamarisk (Tamarix aphylla) on the Finke River, Northern Territory, Australia. Journal of Environmental Management, 29, 297-315.

Grime, J. P. (1979). Primary strategy in plants. Transaction of the Botanical Society of Edinburg, 43, 151-160.

Halse, S.A. and Jensen, A. (1993). Riparian zone management in WA and SA: Policy and Practice. In Ecology and management of riparian zones in Australia, S.E. Bunn, B.J. Pusey, P.Price editors, LWRRDC Occasional Paper Series No: 05/93.

Hancock, C.N., Ladd, P.G. and Froend, R.H. (1996). Biodiversity and management of riparian vegetation in Western Australia. Forest Ecology and Management, 85, 239-250.

Hey, R. D. and Thorne, C. R. (1986). Stable Channels with mobile gravel beds. Journal of Hydraulics Engineering ASCE, 112 (8), 671-689.

Higgins, S.I, Rogers, K.H. and Kemper, J. (1997). A description of the functional vegetation pattern of a semi-arid floodplain, South Africa. Plant Ecology 129, 95-101

Hooke J. and Mant, J., (2002). Morpho-dynamics of ephemeral streams. In Dryland River: Hydrology and Geomorphology of Semi-arid Channels. Edited by Bull, L. J. and Kirby, M. J., John Wiley and Sons, Ltd.

Howard, A.D. and Knudson, T.R. (1984). Sufficient conditions for river meandering: a simulation approach. Water Resources Research, 20(11), 1659-1667.

Huang, H.Q. and Nanson, G.C. (1997). Vegetation and channel variation; a case study of four small streams in southeastern Australia. Geomorphology, 18, 237-249.

Hughes, M. R. (1990). The influence of flooding regimes on forest distribution and composition in the Tana river floodplain, Kenya. Journal of Applied Ecology, 27, 475-491.

Hupp, C. R. and Osterkamp, W. R. (1985). Bottomland vegetation distribution along Passage Creek, Virginia, in relation to fluvial landforms. Ecology, 66(3), 670-681.

Ikeda, S., Parker, G. and Sawai, K, (1981). Bend theory of river meanders. Part 1. Linear development. Journal of Fluid Mechanics, 112, 363-377.

Jacobson P.J, Jacobson K.M, Angermeier P.L. and Cherry D.S (2000), Hydrological influences on soil properties along ephemeral rivers in the Namib Desert. Journal of Arid Environment, 45, 21-34.

Johannesson, H. and Parker, G. (1989). Linear theory of river meanders. In Water Resour. Monogr, S. Ikeda , G. Parker (eds),. 12, 181-213.

Jolly, I.D., Walker, G.R. and Thorburn, P.G. (1993). Salt accumulation in semi-arid floodplain soils with implications for forest health. Journal of Hydrology, 150, 589-614.

Jolly, I. D. (1996). The effects of river management on the hydrology and hydroecology of arid and semi-arid floodplains. In Floodplain Processes, edited by Anderson, M, Walling, E., Bates, P., John Wiley & Sons Ltd.

Kauffman J.B., Krueger W.C. and Vavra M. (1983). Effects of late season cattle grazing on riparian plant communities. Journal of Range Management, 36(6), 685-691.

Knighton, A. D. and Nanson, G. C. (1994). Flow transmission along an arid zone anastomosing river, Cooper Creek, Australia. Hydrological Processes, 8, 137-154.

Knighton, A. D. and Nanson, G. C. (1997). Distinctiveness, diversity and uniqueness in arid zone river systems. In: Arid Zone Geomorphology: Process, Form and Change in Drylands. D.S.G. Thomas Eds., John Wiley & Sons, Chichester, 185-203.

Knighton, A.D. and Nanson, G.C. (2000). Waterhole form and process in the anastomosing channel system of Cooper Creek, Australia. Geomorphology, 35, 101-117.

Kouwen, N. and Li, R. M. (1980). Biomechanics of vegetative channel linings. Journal of Hydraulics Div. ASCE, 106 (6), 713-728.

Lancaster, S.T. and Bras, R.L. (2002). A simple model of river meandering and its comparison to natural channels. Hydrological Processes, 16, 1-26.

Laronne, J.B. and Reid, I. (1993). Very high rates of bedload sediment transport by ephemeral desert river. Nature, 366, 148-150.

Langbein, W. B. and Shumm, S. A. (1958). Yield of sediment in relation to mean annual precipitation. Transactions of the American Geophysical Union, 39, 1076-1084.

Le Houerou, H. N. (1982) The Arid Bioclimates in the Mediterranean Isoclimatic Zone. Ecologia Mediterranea, T.VIII, Fasc. 1/2, 103-114.

Lekach, J., Amit, R., Grodek, T. and Schick, A. (1998). Fluvio-pedogenic processes in an ephemeral stream channel, Nahal Yael, Southern Negev, Israel. Geomorphology, 23, 353-369.

Leopold, L. and Wolman, M.G. (1960). River Meanders. Geol. Society American Bullettin, 71, 769-794.

Lewin, J. (1989). Floods in fluvial geomorphology. In: Floods: Hydrological, Sedimentological and Geomorphological Implications. Edited by K. Beven and P. Carling. Wiley, Chichester.

Liverpool, T.B. and Edward, S.F. (1995). Dynamics of meandering river. Physical Review Letters, 75, 3016-3020.

Lopez-Bermudez, F., Conesa-Garcia, C. and Alonso-Sarria, F. (2002). Floods: Magnitudo and Frequency in Ephemeral Streams of the Spanish Mediterranean Region. In Dryland Rivers: Hydrology and Geomorphology of Semi-arid Channels. Edited by L.J. Bull and M.J. Kirkby. John Wiley & Sons.

Malanson, G.P. (1993). Riparian Landscapes, Cambridge Studies in Ecology.

Masterman, R. and Thorne, C. R. (1992). Predicting influence of bank vegetation on channel capacity. Journal of Hydraulics Engineering ASCE, 118 (7), 1052-1058.

McKenney, R. Jacobson, R. B. and Wertheimer, R. C. (1995). Woody vegetation and channel morphogenesis in low-gradient, gravel-bed streams in the Ozark Plateaus, Missouri and Arkansas. Geomorphology, 13, 175-198.

McMahon, T. A. (1979). Hydrological characteristics of arid zones. Proceedings of the Canberra Symposium – The Hydrology of Areas of Low Precipitation. IAHS-IASH Publication No. 128, 105-123.

Millar, R.G. (2000). Influence of bank vegetation on alluvial channel patterns. Water Resources Researches 36 (4), 1109-1118.

Mosbrugger, V. (1990). The tree habit an land plants. Lecture notes in earth sciences, 28, Springer, Berlin

Nash, D. J. (2001). Arid Geomorphology. Progress in Physical Geography, 25(3), 409-427.

Nanson, G. C., Tooth, S. and Knighton, D. (2002). A global perspective on dryland rivers: perceptions, misconceptions and distinctions. In Dryland River: Hydrology and Geomorphology of Semi-arid Channels. Edited by Bull, L. J. and Kirby, M. J., John Wiley and Sons, Ltd.

O'Connor, T. G., (2001). Effect of small catchment dams on downstream vegetation of a seasonal river in semi-arid African savanna. Journal of Applied Ecology, 38, 1314-1325.

Park, C.C. (1977). World-wide variations in hydraulic geometry exponents of stream channels: an analysis and some observations. Journal of Hydrology, 33, 133-146.

Perona, P., Porporato, A. and Ridolfi, L. (2002). River dynamics after cutoff: a discussion of different approaches. Proceedings of the River Flow 2002 IAHR International Conference on Fluvial Hydraulics, Edited by Bousmar, D, Zech, Y, Vol. 2, 715-721.

Perona, P., Camporeale, C. and Ridolfi, L. In preparation

Pettit, N. E., Froend, R. H. and Davies, P. M. (2001). Identifying the natural flow regime and the relationship with riparian vegetation for two contrasting Australian rivers. Regulated rivers: Research & Management, 17, 201-215.

Pizzuto, J. E. and Meckelnburg, T. S. (1989) Evaluation of a linear bank erosion equation, Water Resources Research, 25, 1005-13.

Puckridge, J. T., Walker, K. F. and Costello, J. F. (2000). Hydrological persistence and the ecology of dryland rivers. Regulated Rivers: Research and Management, 16, 285-402.

Reid, I. and Laronne, J.B, (1995). Bedload sediment transport in ephemeral stream and comparison with seasonal and perennial counterparts. Water Resources Research, 31, 773-781

Reid, I., Laronne, J.B. and Powell, D.M. (1998). Flash Flood and bedload dynamics of desert gravel-bed steams. Hydrological Processes, 12, 543-557.

Robinson, T.W. (1958). Phreatophytes. U.S. Geological Survey Water-Supply,, 1423, 521-560.

Rozin, U. and Shick, A. P. (1996). Land use, change, conservation measures and stream channel response in the Mediterranean/semi-arid transition zone: Nahal Hoga, Southern Coastal Plain, Israel. Proceedings Exeter Symposium, Erosion and Sediment Yield: global and regional perspectives, IAHS Publication No. 234, 427-444.

Salinas, M.J., Blanca, G. and Romero, A.T. (2000). Evaluating riparian vegetation in semi-arid Mediterranean watercourses in south-eastern Iberina Penisola. Environmental Conservation, 27, 24-35.

Scott, R.L., Shuttleworth, W.J., Goodrich, D.C. and Maddock III, T. (2000). The water use of two dominant vegetation communities in a semiarid riparian ecosystem. Agricultural and Forest Meteorology, 105, 241-256.

Smith,S.D., Wellington, A. B., Nachlinger, J. L. and Fox, A. (1991). Functional response of riparian vegetation to streamflow diversion in the eastern Sierra Nevada. Ecological Applications, 1 (1), 89-97.

Smith, M. A., Dodd, J. L., Skinner, Q. D. and Rodgers, J. D. (1993). Dynamics of vegetation along and adjacent to an ephemeral channel. Journal of Range Management, 46(1), 56-64.

Stølum, H. H. (1996). River meandering as a self-organization process. Science, 271, 1710-1713.

Stromberg, J.C. (1993). Instream flow models for mixed deciduous riparian vegetation within a semiarid region. Regulated Rivers: Research e Management, 8, 225-235

Stromberg, J. C., Tiller, R. and Ricther, B. (1996). Effects of Groundwater decline on riparian vegetation of semiarid regions: the San Pedro, Arizona. Ecological Applications, 6(1), 113-131.

Stromberg, J. C. (2001). Restoration of riparian vegetation in the south-western United States: importance of flow regimes and fluvial dynamism. Journal of Arid Environments, 49, 17-34.

Sun, T., Meakin, P. and Jøssang, T. (1996). A simulation model for meandering rivers. Water Resources Research, 32(9), 2937-2954.

Thornes, J.B. (1994). Channel processes, evolution and history. In: Geomorphology of Desert Environments Abrahams, A.D., Parson A.J. (eds), Chapman & Hall, London, 288-317.

Tooth, S., (2000a). Process, form and change in dryland rivers: a review of recent research. Earth-Science Review, 51, 67-107.

Tooth, S. (2000b). Downstream changes in dryland river channels: the Northern Plains of arid central Australia. Geomorphology, 34, 33-54.

Tooth, S. and Nanson, G. C. (2000). The role of vegetation in the formation of anabranching channels in an ephemeral river, Northern plains, arid central Australia. Hydrological processes, 14, 3099-3117.

Trodd, N. M. and Dougill, A. J. (1998). Monitoring vegetation dynamics in semi-arid Africa rangelands: use and limitation of Earth observation data to characterize vegetation structure. Applied Geography, 18 (4), 315-330.

Tucker Schulz T. and Leininger W.C. (1990). Differences on riparian vegetation structure between grazed areas and exclosures. Journal of Range Management, 43(4), 295-299.

Vandersande, M. W., Glenn, E. P. and Walworth, J. L. (2001). Tolerance of five riparian plants from the lower Colorado River to salinity drought and inundation. Journal of Arid Environments, 49, 147-159.

Wainwright, J., Parson, A.J., Schlesinger, W.H. and Abrahams. A.D. (2002). Hydrology-vegetation interactions in areas of discontinuous flow on a semi-arid bajada, Southern New Mexico. Journal of Arid Environments, 51, 319-338.

Wende, R. and Nanson, G. C., (1998). Anabranching rivers: ridge-form alluvial channels in tropical northern Australia. Geomorphology, 22, 205-224.

Wolman, M.G. and Gerson, R. (1978). Relative scales of time and effectiveness of climate in watershed geomorphology. Earth Surface Processes and Landforms, 3, 189-208.

Zalewski, M., Bis, B., Lapinska, M., Frankiewicz, P. and Puchalski, W. (1998). The importance of the riparian ecotone and river hydraulics for sustainable basin-scale restoration scenarios. Acquatic Conservation: Marine and Freshwater Ecosystems, 8, 287-307.

Zalewski, M. (2000). Ecohydrology – the scientific background to use ecosystem properties as management tools toward sustainability of water resources. Ecological Engineering, 16, 1-8.

Zolezzi, G. and Seminara, G. (2001). Downstream and upstream influence in river meandering. Part 1. General theory and application to overdeepening. Journal of Fluid Mechanics, 438, 183-211.

PART III

ECOHYDROLOGIC CONTROLS ON NUTRIENT CYCLING

Crucially located on the earth surface at the interface between atmosphere and biosphere, soils are the stage where important exchanges of water, organic matter, nutrients, and gases take place at time scales ranging between a few seconds to several centuries. The overall result of these dynamics is the cycling of nutrients within the soil-plant-atmosphere continuum, the storage of carbon in standing biomass, litter, and soil, as well as the release of CO_2 (soil and plant respiration) and other gases to the atmosphere. Thus, the study of nutrient and carbon cycling in terrestrial ecosystems is relevant to the understanding of vegetation dynamics (e.g., response to environmental stress and to different levels of nutrient availability) as well as to the assessment of carbon and nutrient storages and fluxes. Significant efforts have been invested by the scientific community over the last two decades in the study and modelling of fundamental properties of nitrogen and carbon dynamics at the daily, annual, and multi-decadal time scale.

This part focuses on the hydrologic controls on nutrient dynamics in different water-limited ecosystems. Chapter 11 analyzes the coupling between water and nitrogen cycles, and discusses some unresolved issues in the understanding of nitrogen and carbon dynamics in arid and semiarid environments. The controls exerted by water and nitrogen on the productivity of semiarid grasslands and shrublands are investigated in Chapter 12 at different spatial and temporal scales. Chapter 13 presents a thorough review of the effects of water availability on the cycling of nutrients in dry tropical forests. The controls of soil moisture on biogenic emissions of nitrogen oxides from arid and semiarid soils are discussed in Chapter 14.

Chapter 11

MODELING OF CARBON AND NITROGEN CYCLING IN ARID AND SEMIARID ECOSYSTEMS

Stefano MANZONI[1], Amilcare PORPORATO[1] and Paolo D'ODORICO[2]

[1] Department of Civil and Environmental Engineering, Duke University, 127 Hudson Hall, Durham, NC 27708, USA - e-mail: amilcare@duke.edu
[2] Department of Environmental Sciences, University of Virginia, 291 McCormick Rd., Charlottesville, VA 22903-4123, USA -e-mail: paolo@virginia.edu

1. Introduction

In this Chapter we present a general discussion of the dynamics of soil nutrient cycles with special attentions to the interaction with hydrological processes in semi-arid systems, and with emphasis on modeling issues. We will present an analytical approach developed by the authors and co-workers to model the propagation of hydrologic fluctuation through the various components of the soil biogeochemical cycles of arid and semiarid ecosystems. We do not attempt to provide here a complete review of the subject (see Chapters 12-14, and 18 for related discussion on soil nutrient cycles in drylands) but rather focus on interaction between hydrological and ecological processes and outline some open problems and future directions for research.

The impact of hydrological and meteorological processes on carbon and nitrogen cycles takes place through an intricate series of linkages and feedbacks at various levels. Figure 1 provides a schematic representation of the main components of the nitrogen cycle in soils. It is clear the existence of an internal cycle, which involves only soil and plants through nitrogen uptake and production of soil organic matter (SOM) and dominates the nitrogen turnover at the daily-to-seasonal time scales. The other external fluxes, such as wet and dry deposition and the biological fixation, become important only in the long-term balance.

Hydrometeorologic fluctuations act as an external forcing to the soil-plant system, causing a propagation of temporal variability at different scales (e.g., Noy-Meir, 1973; Cui and Caldwell, 1997; Porporato et al., 2003; D'Odorico et al., 2003; Schimel and Bennet, 2004). In particular, in arid and semi-arid ecosystems the intermittent nature of the hydrologic forcing often translates into propagation of pulses in the soil-plant nutrient cycles (Noy-Meir, 1973; Austin et al., 2004; Schwinning and Sala, 2004). The complexity of the temporal dynamics of soil nutrient cycles is further increased by spatial heterogeneities due to micro-topography, spatial distribution of soil properties and plants, soil water content, temperature, and solar irradiance. All these forms of fluctuation in soil nutrient availability have important effects on vegetation composition and structure in drylands, as evidenced by occurrences of grassland-to-shrubland conversion and desertification (Archer, 1989; Schlesinger et al., 1990; 1996; Schlesinger and Pilmanis, 1998; see Chapter 18).

P. D'Odorico and A. Porporato (eds.), Dryland Ecohydrology, 183–199.

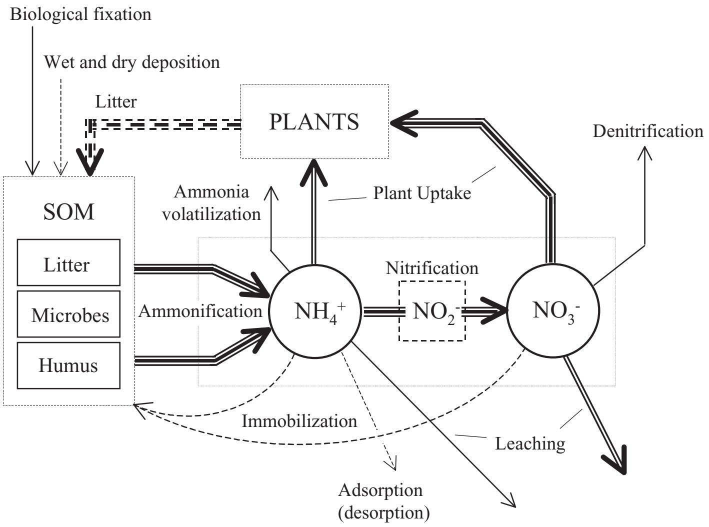

Figure 1: Schematic representation of the soil nitrogen cycle (the dimension of the arrows indicates the relative importance of the various fluxes in the cycle; the continuous lines refer to processes wherein the impact of soil moisture is relevant). Modified after Porporato et al. (2003a).

2. The soil carbon and nitrogen cycles

Plants assimilate carbon from the atmosphere through photosynthesis; part of it is used by vegetation as a source of energy and then directly released by respiration, while the remaining part is assimilated by vegetation and later transferred as litter and plant residues to the soil, where it becomes part of soil organic matter (SOM). SOM is a complex and varied mixture of organic substances, which can be divided into three main components: plant residues, microbial biomass, and humus (e.g., Porporato et al., 2003). Soil organic matter typically contains about 5% nitrogen, while inorganic nitrogen is usually not more than 1 to 2% of the total nitrogen in the soil; aridisols sometimes contain only mere traces of this nutrient.

SOM decomposition and mineralization involve an enzymatic oxidation of carbohydrates that produces mineral compounds (e.g., ammonium) and carbon dioxide (soil respiration). While part of the carbon is lost as soil respiration and the simpler compounds are metabolized by soil microbes, the most complex ones are not metabolized but, along with other compounds polymerized by soil microbes, are combined to form the so-called humic substances, or resistant humus. Other less-resistant (non-humic) substances are also formed. Humic substances are very stable and contribute to maintain high organic levels in soils, preventing a rapid nutrient loss from the soil via leaching or denitrification (e.g., Brady and Weil, 1996).

In soils of mature natural ecosystems in equilibrium, the release of carbon as CO_2 is generally balanced in the long term by the input of plant residues; however, the carbon and nitrogen content are subject to fluctuations at the interannual, seasonal, and daily time scales. The decomposition process is regulated by the SOM carbon-to-nitrogen (C/N) ratio, by the inorganic nitrogen availability, and by the environmental conditions. The complex interplay between these two factors determine the direction of nitrogen fluxes between the organic (SOM) and inorganic (ammonium and nitrate) pools (Figure 1). In particular, the most favourable conditions for mineralization are found around 20-30° C (e.g., McCarron et al., 2003), while mineralization practically ceases outside the temperature range 5-50° C. A decline in mineralization rates is also observed with increasing soil acidity (e.g., Brady and Weil, 1996). The influence of soil moisture on mineralization is due mainly to the balance between aeration, which diminishes with soil moisture, and the occurrence of favourable humid conditions for microbial biomass (Figure 2; see also McCarron et al., 2003). At high soil moisture levels, anoxic conditions prevent bacteria to perform the aerobic oxidation necessary for decomposition. The reason for the reduction of the decomposition rate at low soil moisture levels rate is twofold (Stark and Firestone, 1995; Fenchel et al., 1998). Firstly, a lack of substrate supply due to the reduced water content reduces microbial activity; as the pores within solid matrices dry and the water film coating the surfaces becomes thinner, diffusion paths become more tortuous and the rate of substrate diffusion to microbial cells declines. Secondly, low water contents induce low soil water potentials, which lower intracellular water potential and in turn reduce hydration and activity of soil microorganisms. Interestingly, the water stress of soil microbes has similar characteristics to plant water stress (Chapter 4, see also Porporato et al., 2001).

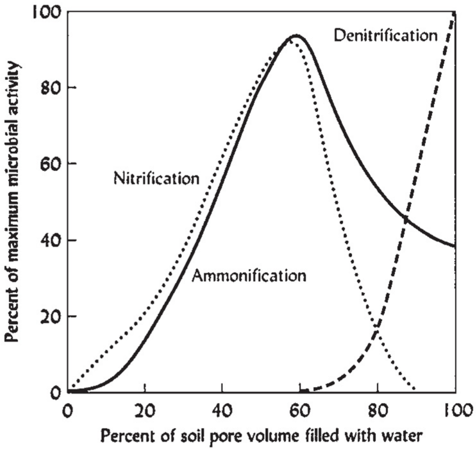

Figure 2: Rate of microbial activity related to the various phases of nitrogen transformation as a function of soil water content; after Brady and Weil (1996).

Growth activity of various soil microorganisms as a function of water potential is shown in Figure 3. In arid and semi-arid systems, the decomposing microorganisms tend to be quite diverse with a wide range of adaptation to water stress and plant competition for nutrients (e.g., Kaye and Hart, 1997).

Although it is an essential nutrient for plants, nitrogen is found in the soil mostly in the form of organic compounds that prevent leaching losses but leave nitrogen largely unavailable to vegetation (this view has been challenged recently, as explained below in Section 5.3 and in Schimel and Bennet, 2004). Plants almost only uptake mineral nitrogen, in form of ammonium (NH_4^+) and nitrate (NO_3^-), which are made available through SOM decomposition and mineralization. For this reason, the nitrogen cycle is intimately linked to the carbon cycle.

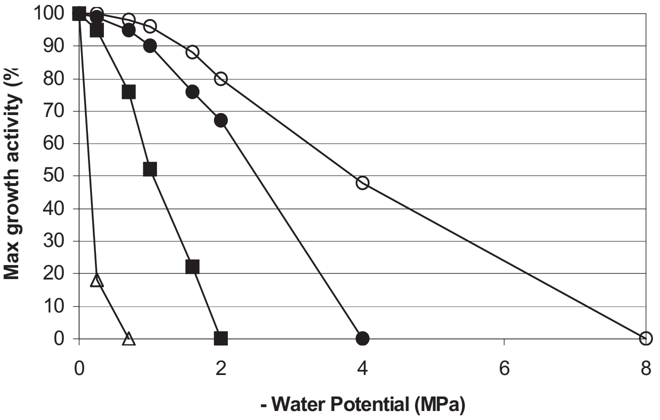

Figure 3. Effects of soil water potential on the activity of different soil microorganisms expressed as percentage of maximum growth activity: Fungivourous nematode (open triangles), gram-bacteria (closed squares), G. graminis (closed circles), F. roseum (open circles);redrawn from Freckman (1986).

Soil organic matter decomposition yields ammonium and nitrate (ammonification and nitrification); approximately 1.5-3.5% of the organic nitrogen of a soil mineralizes annually. When the conditions are favorable nitrification is quite rapid. In hot and dry environments, sudden water availability can cause a flush of soil nitrate production (e.g., Cui and Caldwell, 1997; Gebauer and Ehleringer, 2000; Fierer and Schimel, 2002; D'Odorico et al., 2003), which may greatly influence the growth patterns of natural vegetation (see Figure 5 below).

Mineralization rates depend also on the composition of plant residues and, in particular, on their C/N ratio. The growth of microbial colonies often takes place with fixed proportion of carbon and nitrogen so that their C/N ratio remains practically constant, although it may also present some seasonal variability due to internal population shifts in response to plant litter production (e.g., Corre et al., 2002). As a consequence, if the nitrogen content of the organic matter being decomposed is high, mineralization proceeds unrestricted and mineral components in excess are released into the soil. On the contrary, when the litter is nitrogen poor, microbes can use some of the mineral nitrogen through the process of immobilization (Aber et al., 1990; Mary et al., 1996). If mineral nitrogen is not available, then mineralization may be halted.

Nitrate is easily soluble in water and, although this facilitates its uptake by plants, it also makes it prone to losses by leaching at high soil moisture levels. Differently, the positive charge of ammonium ions attracts them to the negatively charged surfaces of clays and humus, thus partially protecting them from leaching. Plant nitrogen requirements are met by two different mechanisms of root uptake: either passively through the soil solution during the transpiration process or actively by a diffusive flux driven by concentration gradients produced by the plant itself (e.g., Wild, 1988; Engels and Marschner, 1995; Larcher, 1995). Recent developments have advocated a more important role of uptake of organic nitrogen by plants than what used to be expected in the past (Neff, 2003; Schimel and Bennett, 2004).

3. Modeling the carbon and nitrogen cycles

Different studies in the literature have investigated the effect of climate and hydrologic conditions, at different time scales, on SOM and nutrients (e.g., Pastor and Post, 1986; Parton et al., 1987; Jenkinson, 1990; Hunt et al., 1991; Aber and Driscoll, 1997; Moorhead et al., 1999; Gusman and Marino, 1999; Birkinshaw and Ewen, 2000; Baisden and Amundson, 2003), pointing out the importance of mathematical modeling in the analysis of the soil-nutrient system. A quantitative prediction of carbon and nitrogen dynamics is relevant to the understanding of vegetation response to disturbances, environmental stress and different scenarios of water, CO_2, and nutrient availability (e.g., McMurtrie et al., 2000). Because some changes in soil organic matter take place at decade-to-century timescales, process-based models need to be used to make projections of how carbon (C) and nitrogen (N) fluxes (and stocks) are expected to change in terrestrial ecosystems under different climate and disturbance scenarios. In general, most models lump the C-N dynamics into a number of pools and describe the fluxes among them as empirical functions of substrate availability and environmental variables (e.g., soil temperature, water content and pH); on the contrary, few models consider the composition of SOM as a continuum (Bosatta and Agren, 1985). In the discrete models, mass balance equations - more or less explicitly formulated – relate the changes in N and C stocks in each pool to the inputs and outputs associated with these fluxes.

It would be impossible to provide here a complete review of all the numerous models proposed in the literature. In this section, we describe with some detail the biogeochemical model proposed by Porporato et al. (2003). This model was developed to study in particular how the variability of hydroclimatic variables propagates to the different soil C and N pools through the nonlinear dynamics of the soil biogeochemical processes (see also D'Odorico et al. 2003 and Manzoni et al. 2004).

The carbon and nitrogen cycles are modeled using five different pools, one for each main component of the system. SOM is divided into three compartments, representing litter, humus, and microbial biomass, as shown in Figure 4. The general structure is in agreement with the recommendation of Bolker et al. (1998), who suggested using at least a fast and slow decomposing pool to model SOM. The nitrogen pools are defined through their C/N ratios as in Parton et al. (1987; 1988), Mueller et al. (1998), and Katterer and Andren (2001). Two additional pools account for inorganic nitrogen (i.e., ammonium and nitrate).

Once plant residues enter the litter pool, they move partially to humus and partially to the biomass pool, losing a respired fraction during the decomposition process (e.g. Molina and Smith, 1998). Differently from the models based on linear decomposition kinetics, such as for instance the CENTURY (Parton et al. 1987; 1988) and NCSOIL models (Molina et al., 1983), decomposition is explicitly modeled as a function of microbial biomass. The model needs eight state variables, each expressed as mass per unit volume of soil (e.g., g/m^{-3}). Six variables describe carbon and nitrogen concentrations in the three SOM pools, and one variable expresses the soil mineral nitrogen:

C_l, carbon concentration in the litter pool;
C_h, carbon concentration in the humus pool;
C_b, carbon concentration in the biomass pool;
N_l, organic nitrogen concentration in the litter pool;
N_h, organic nitrogen concentration in the humus pool;
N_b, organic nitrogen concentration in the biomass pool;
N^+, mineral nitrogen concentration in the soil (ammonium);
N^-, mineral nitrogen concentration in the soil (nitrate)

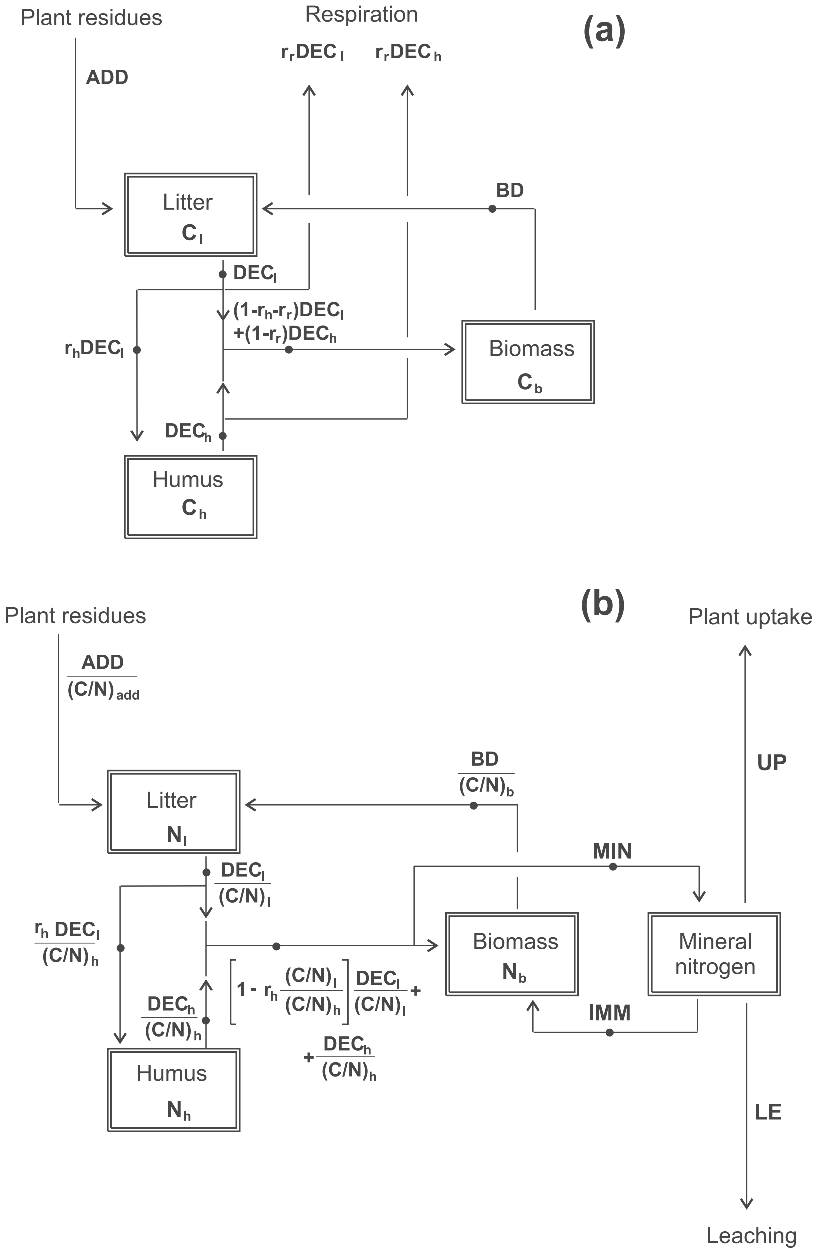

Figure 4. Schematic representation of the main components of the model. a) Soil carbon cycle; b) soil nitrogen cycle. For simplicity, a single mineral nitrogen pool, including ammonium (N^+) and nitrate (N^-) has been represented.

The temporal dynamics of such variables are controlled by a system of eight coupled differential equations describing the balance of carbon and nitrogen in the various pools and the fluxes among them, in terms of mass per unit volume per unit time (e.g., g m^{-3} d^{-1}). Since many of the fluxes are controlled by environmental fluctuations, their modeling explicitly accounts for soil moisture and temperature conditions. The system of first order nonlinear differential equations is

$$\begin{aligned}
\frac{dC_l}{dt} &= ADD + BD - DEC_l \\
\frac{dN_l}{dt} &= \frac{ADD}{(C/N)_{add}} + \frac{BD}{(C/N)_{bio}} - \frac{DEC_l}{(C/N)_l} \\
\frac{dC_h}{dt} &= r_h DEC_l - DEC_h \\
\frac{dN_h}{dt} &= r_h \frac{DEC_l}{(C/N)_l} - \frac{DEC_h}{(C/N)_h} \\
\frac{dC_b}{dt} &= (1 - r_h - r_r) DEC_l + (1 - r_r) DEC_h - BD \\
\frac{dN_b}{dt} &= \left[1 - r_h \frac{(C/N)_l}{(C/N)_h}\right] \frac{DEC_l}{(C/N)_l} + \frac{DEC_h}{(C/N)_h} - \Phi \\
\frac{dN^+}{dt} &= \Phi - NIT - UP^+ \\
\frac{dN^-}{dt} &= NIT - LE - UP^-
\end{aligned} \tag{1}$$

The first six equations represent the balances of litter (*l* subscript), humus (*h* subscript) and biomass (*b* subscript) pools, while the last two are the balance equations for the mineral nitrogen, i.e. in the form of ammonium (superscript +) and nitrate (superscript -). A brief description of the terms is given next. For a more detailed discussion of the rationale and modeling assumptions reference is made to Porporato et al. (2003).

The term *ADD* in the first two equations is the external input into the system (Figure 4), representing the rate at which carbon in plant residues (i.e., mainly leaves and dead roots) is added into the soil and made available to the microbial colonies. Here *ADD* is assumed to be constant in time. In the case of deciduous vegetation *ADD* would have a well-defined seasonality, or it could be determined by the frequency of fire occurrences, in fire dependent ecosystems (e.g., Ojima et al., 1994). The term *BD* is the rate at which carbon returns to the litter pool due to the death of microbial biomass. Porporato et al. (2003) simply used a linear dependence on the amount of microbial biomass, i.e., $BD = k_d C_b$.

The rate of litter carbon decompositions due to microbial activity, DEC_l , is modeled using first order kinetics with respect to both the substrate concentration (e.g., Hansen et al., 1995; Gusman and Marino, 1999; Birkinshaw and Ewen, 2000), and the microbial biomass (Blagodatsky and Richter, 1998). In this way, the role of exoenzymes, whose production can be related to the active biomass, is implicitly kept into account (Schimel and Weintraub, 2003).

$$DEC_l = \varphi \, k_l f(s,T) C_l C_b \tag{2}$$

The coefficient φ is a non-dimensional factor accounting for a possible reduction of the decomposition rate when the litter is very poor in nitrogen and immobilization is not sufficient to integrate the nitrogen required by microbial biomass (see for details Porporato et al. 2003). The constant k_l defines the rate of decomposition for the litter pool as a weighted average of the decomposition rates of the different organic compounds in the plant residues. Its average value is usually much higher than the corresponding value for humus, k_h.

The factor $f(s,T)$ is of particular interest here as it describes soil moisture (s) and soil temperature (T) effects on decomposition. Following Cabon et al. (1991) and Gusman and Marino (1999), the soil moisture control on aerobic microbial activity and decomposition is modeled via a linear increase - from $s=s_b$ to a maximum value at field capacity - and a hyperbolic decrease between field capacity and soil saturation. The parameter s_b represents a sort of 'wilting' point for soil microbial biomass. Although this parameter is either not considered explicitly or is assumed to be equal to the corresponding plant wilting point its role in soil nutrient dynamics is very important. In particular, its relationship with the plant wilting point (i.e., the soil moisture level at which transpiration and passive nitrogen uptake cease) provides a way to account for the impact of water stress on the competition for nutrients between plants and soil microbial biomass (Kaye and Hart, 1997). In terms of soil water potential, s_b ranges between -0.8 and -8 MPa, depending on biomass composition, with higher values for bacteria and lower values for fungi (Freckman 1986, see also Figure 2). The corresponding values in terms of soil water content depend on soil type and are easily obtainable through the water retention curves (see Chapter 2).

The dependence of microbial activity on soil temperature can be described by a quadratic relation (Ratkowsky et al. 1982; Katterer and Andren, 2001), with a minimum survival temperature for microbial biomass (about -5°C, according to Hunt et al., 1991) and an optimum temperature that, on account of the adaptation of microbial colonies to a specific site, can be taken as the maximum soil temperature measured in the field (Katterer and Andren, 2001), except for hot environments, where high temperature possibly becomes a limiting factor.

The second equation of the system (1) represents the nitrogen balance in the litter pool. This is similar to that of carbon, with each term divided by the C/N ratio of its respective pool. C/N_{add} is the C/N ratio of added plant residues, whose variability may cause pronounced changes in the C/N ratio of the litter pool and on the Mineralization Immobilization Turnover (MIT) (Berg and Ekbohm, 1983; Aber et al., 1990; Mary et al., 1996).

The balance equation for carbon in the humus pool has a single input flux, represented by the fraction r_h of the decomposed litter undergoing humification. It is also assumed that the products of the humification process from litter have the same characteristics, and thus the same C/N ratio, as the soil humus. As a consequence, the value of $(C/N)_h$ remains constant in time.

The input of carbon in the biomass pool is represented by the fraction of organic matter incorporated by the microorganisms from litter and humus decomposition. The constant r_r ($0 \le r_r \le 1 - r_h$) defines the fraction of decomposed organic carbon that goes into respiration, usually estimated to be in the interval 0.6-0.8 (Brady and Weil 1996).

The nitrogen balance of the microbial biomass, the fifth equation of (1), has an additional term, Φ, that accounts for litter net mineralization (MIN, see figure 4), which occurs when decomposition of N-rich litter results in N surplus for the microbial biomass, or net immobilization (IMM), when the biomass needs to assimilate inorganic nitrogen (i.e., the net flux of nitrogen mineralization is negative). The modeling of this critical term of the nitrogen balance, and its role in the dynamic behaviour of the system (1), are discussed in detail in Porporato et al. (2003) and Manzoni et al. (2004).

The last equations describe the balance of mineral nitrogen, in which mineralization is the only input, while plant uptake, leaching, and possibly net immobilization are the losses. Leaching is simply modeled as proportional to the deep infiltration losses through a solubility coefficient (Porporato et al., 2003). The uptake flux involves a passive and an active process, which can be regarded as additive processes (Wild, 1988). The passive uptake is assumed to be proportional to the plant transpiration rate, and to the nitrogen concentration in the soil solution. Plants try to compensate the nitrogen deficit with the active mechanism of uptake only if the passive uptake is lower than a given plant demand. Following Porporato et al. (2003), when the diffusion of nitrogen ions through the soil is limiting, plant N demand cannot be satisfied and the active uptake is assumed to be proportional to the nitrogen concentration in the soil through a diffusion coefficient; otherwise (i.e., when N diffusion is not limiting) active uptake is simply the difference between the demand and the passive uptake.

4. Application to a semiarid ecosystem: the Nylsvley Savanna in South Africa

D'Odorico et al. (2003) present an application of this model to the broad-leaved savanna located in the Nylsvley region (South Africa). The broad-leaved sites at Nylsvley are generally found on nutrient-poor, acidic soils, while fine-leaved savannas are typically observed on more fertile grounds (Scholes and Walker, 1993). Both in the fertile and in the unfertile sites, soils are sandy and about 1 m deep, though most of the organic matter and nutrients are concentrated in the top 80 cm.

Nitrogen may represent a limiting factor for productivity in the broad-leaved savanna (Vitousek and Howarth, 1991), where the release of mineral nitrogen from decomposition of litter and plant residues is quite slow (average turnover time of about 5 years; Scholes and Walker, 1993). Most of the decomposition is due to soil microbes (compared to fire oxidation and termites) and is mostly controlled by soil water content. Inorganic nitrogen is present in the soil as nitrate (about 1.0 gN m^{-3}), while ammonium is found in much smaller concentrations, indicating an almost instantaneous nitrification. This suggests that the nitrogen cycle is limited by the slow rate of decomposition (i.e., by the availability of substrate for nitrification), while the process of nitrification does not exert any constraint.

Figure 5 shows examples of model-generated time series reported by D'Odorico et al. (2003) for some of the state variables relevant to the carbon and nitrogen cycles. Depending on the inertia of the various pools and on the degree of dependence on soil moisture, the random fluctuations imposed by precipitation are filtered by the temporal dynamics of the state variables in a very interesting manner. Some variables (e.g., NO_3^-) preserve much of the high-frequency variability imposed by the random forcing of precipitation, while some others (C_h, C_l, and C_b) show smoother fluctuations (Figure 5).

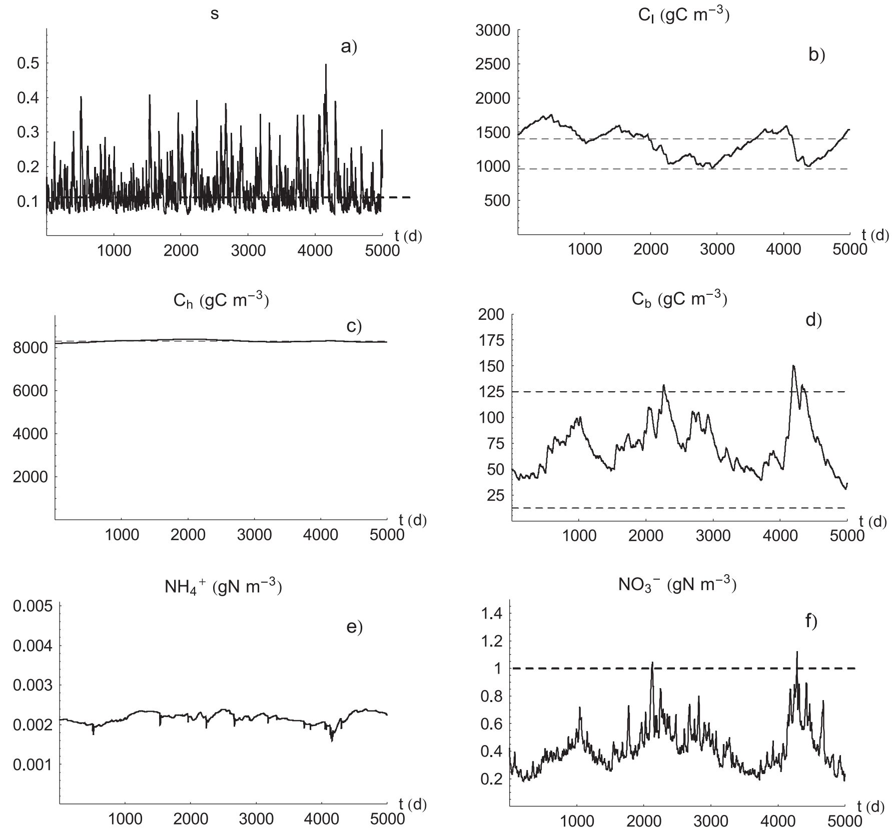

Figure 5. Temporal dynamics of soil moisture (a), carbon biomass (b), nitrate (c), litter decomposition (d), nitrate uptake (e), and nitrate leaching (f) simulated during a few growing seasons at Nylsvley. After D'Odorico et al. (2003).

Nitrate dynamics are the final product of a number of intertwined processes in which both high- and low-frequency components interact. In particular, the high-frequency component of NO$_3^-$ fluctuations (period of days to weeks) can be linked to the direct dependence of mineralization and nitrification on soil moisture (Figure 5), which transfers the random fluctuations of the rainfall forcing to the budget of NO$_3^-$. On the other hand, the low-frequency variability (period of seasons to years) resembles the one of organic matter (in particular of microbial biomass; e.g., Figure 5d) and depends on the inertia imposed on the dynamics by the dimension of the soil carbon and nitrogen pools. Notice that the same low frequency component also characterizes the litter dynamics, which is negatively correlated to C$_b$ as the growth of one of these pools occurs at the expenses of the other one.

A closer inspection of the time series of soil moisture and nitrate reveals that such a phenomenon is due to the presence of sudden flushes of nitrate; following a prolonged wet period after a drought (see Figure 6). Initially, the dry soil hinders decomposition and favors soil organic matter (SOM) accumulation, then the subsequent wet period elicits biomass growth and enhances mineralization (e.g., Cui and Caldwell, 1997; Scholes and Walker., 1997; Fierer and Schimel, 2002). Episodic changes in nitrate levels greatly influence plant growth, because plants response to increased availability of nitrogen tends to be very quick (e.g., Brady and Weil, 1996). These pulses of nitrate are therefore of considerable importance for dryland ecosystems where rainfall events are very intermittent (Noy-Meir, 1973). This suggests that some semiarid ecosystems can be limited both by water and nitrogen at different times. The daily temporal resolution is fundamental to capture the impact of soil moisture on nutrient dynamics.

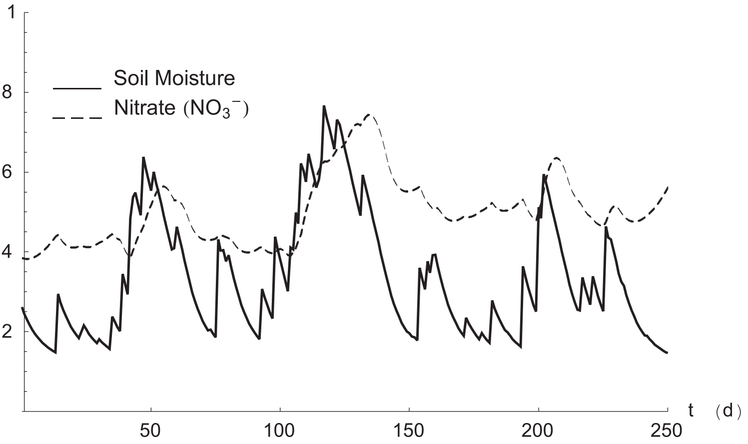

Figure 6. Response of the soil nitrate pool to fluctuations in the soil water content. After D'Odorico et al. (2003).

5. Current Challenges in the study of soil C and N cycles

The previous results provide an example of how external hydroclimatic fluctuations induce a hierarchy of responses in the nonlinear dynamical system of the soil carbon and nitrogen cycles. Many aspects of these dynamics are still not completely understood. The following topics indicate new exciting avenues of further research in dryland biogeochemistry.

5.1. IMPACT AND PROPAGATION OF EXTREME HYDRO-CLIMATIC EVENTS IN SOIL BIOGEOCHEMISTRY

Previous assessments of ecosystem response to climate change focused primarily on changes in the mean climatic states. There is now growing consensus that an increase in frequency and intensity of extreme hydro-climatic events will represent one of the most potent features of global climate change with huge social and biotic impacts (e.g., Easterling et al. 2000; Allen and Ingram, 2002; Ackerly, 2003). Thus, a better understanding of the temporal scales involved in the response of soil-plant system to extreme hydro-climatic events (e.g., droughts and intense storms) is necessary. Recent investigations have started analysing the impact of changes in frequency and amount of rainfall events of soil biogeochemistry and plant productivity (see Chapter 3; see also Knapp et al., 2002; D'Odorico et al., 2000; Porporato et al., 2004) showing effects that are even more important that those due to mere shifts in mean annual rainfall values.

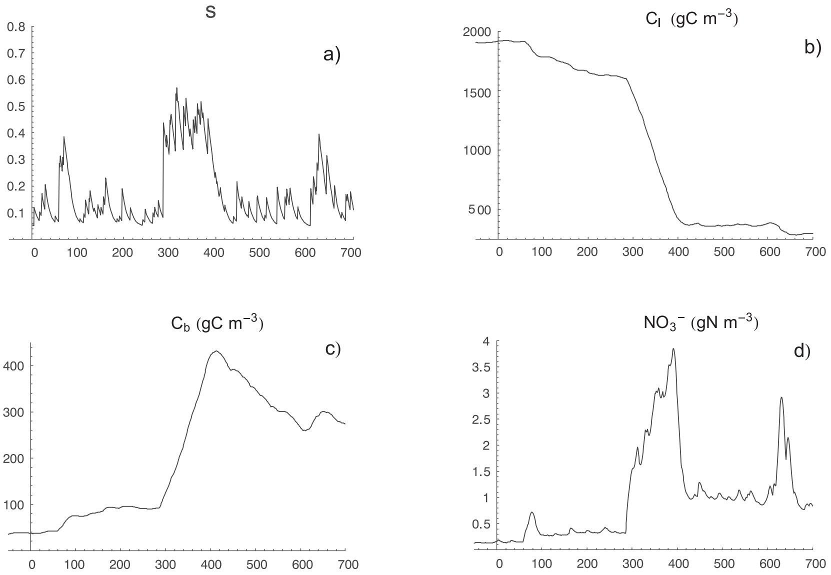

Figure 7. Effect of a prolonged wet period on the soil organic matter and nitrate dynamics. After D'Odorico et al. (2003).

An example of the importance of the temporal stochastic characterization of the hydrologic fluctuation in soil biogeochemistry is given in the model results of Figure 7. An exceptionally long wet period is shown to cause a dramatic increase of microbial biomass activity and nitrate with a consequent decrease of the substrate pools (C_l and, not shown, C_h). The high nitrate concentration is soon depleted by plant uptake and leaching and, in the long run, the event has dramatic consequences on the ecosystem in terms of nitrogen availability.

5.2. COMPETITION BETWEEN MICROBIAL BIOMASS AND PLANTS FOR MINERAL NITROGEN AND RESPONSE TO NUTRIENT AND WATER LIMITATIONS

Environmental fluctuations have an impact on the competition between microbial biomass and plants for mineral nitrogen through their different response to nutrient and water limitation. This is an area of intense research with interesting new developments.

It was traditionally assumed that plants could access only inorganic forms of nitrogen made available via the mineralization of soil organic matter and that soil microorganisms are superior competitors for this (Jackson et al., 1989; Schimel et al., 1989; Zak et al., 1990). Ultimately, however, plants are superior competitors in the longer term because of the less rapid cell turnover that allows them to retain more nitrogen (e.g., Kaye and Hart, 1997). Hydro-climatic fluctuations (e.g., freeze-thaw and drying-rewetting events) tend to disrupt microbial cells providing plants with a competitive opportunity on a reduced microbial population and an increased N availability from microbial-cell lysis. Moreover, spatio-temporal differences related to microbial and root turnover further determine the success in nitrogen competition (Kaye and Hart, 1997).

Drying-rewetting events were shown to induce significant changes in microbial C and N dynamics with effects lasting for months after the stress events (e.g., Fierer and Schimel, 2002). In particular, rewetting and drying increased the total amount of available N due to osmotic shocks in bacteria and subsequent rapid release of cytoplasmic solutes. However, when these cycles were repeated for long time, different forms of adaptation of soil microorganisms were also noticed, involving osmoregulatory measures during dry periods to compensate the low soil water potential and maintain biologic activity. The long term implications of these cycles are not completely clear.

A detailed investigation of root-microbial interaction and competition for nutrients, water, and energy must also account for the similar but not identical response of plants and soil microorganisms (fungi and bacteria) to water deficit (see also Schwinning and Sala, 2004). Even slight competitive advantage in resistance to water stress can, in fact, play a key role in the entire dynamics of arid ecosystems (see Figures 2 and 3 and the discussion on plant water stress in Chapter 4).

5.3. BIOAVAILABLE DISSOLVED ORGANIC NITROGEN IN ARIDISOILS

The picture of soil biogeochemical cycling is further complicated by a recent change in the way the decomposition and uptake of soil nutrients are understood. In the traditional view of the terrestrial nitrogen cycle, plant nitrogen uptake follows in a rigid sequence nitrogen mineralization assuming that plants use only inorganic nitrogen for their nutrition. However, over the last decade it became increasingly clear that the depolymerization of N-containing polymers by soil microbes releases organic N-containing monomers that may be used by either plants or microbes (Neff, 2003; Schimel and Bennett, 2004).

This paradigmatic shift has actually important implications in arid and semi-arid ecosystems characterized by nitrogen-poor soils. Fluxes and plant uptake of dissolved organic nitrogen might be responsible for yet unexplained pathways of import and export of nutrient into and from ecosystems, while the uptake of some forms of organic nitrogen by plants could contribute to reduce the competitive advantage of soil microbes on plants (e.g. Kaye and Hart, 1997).

5.4. NUTRIENT UPTAKE, FOLIAR NITROGEN CONTENT, AND PHOTOSYNTHESIS

The existence of a significant dependence of photosynthesis on foliar nitrogen concentration (e.g., Heitholt et al. 1991; Ciompi et al. 1996) adds a further important link between soil biogeochemistry and plant dynamics. In particular, foliar nitrogen has been found to be related to the availability of the rubisco enzyme for the carboxylation reaction in photosynthesis (Field and Mooney 1986). Low nitrogen availability in the soil may cause a reduction of foliar nitrogen and photosynthesis, resulting in slow growth and possibly higher C/N in plant tissues. This, in turn, modifies the decomposition dynamics of the litter pool, introducing further complex feedbacks between the soil water balance and soil-plant biogeochemistry. For example, this positive feedback toward high carbon content in the soil and in plant tissues has been shown to be one of the major mechanisms regulating the primary production of grasslands subject to seasonal fires (Seastedt et al., 1991; Ojima et al., 1994). At the leaf scale, Baldocchi and Meyers (1998) investigated the feedback between foliar nitrogen and photosynthesis by linking the parameters of a commonly used photosynthesis model (e.g., Farquar et al. 1980; Ball et al. 1987; Collatz et al., 1991) to the foliar nitrogen content. However, the long-term consequences of the interaction between nitrogen uptake, photosynthesis and litter dynamics are still largely unexplored.

5.5. SOIL TEXTURE, PORE SCALE HETEROGENEITY, AND NUTRIENT DYNAMICS

Most of the current SOM and nutrient cycle models use vertically averaged carbon and nitrogen concentrations as state variables (e.g., Parton et al., 1987; Mueller et al., 1998; Katterer and Andren, 2001; Porporato et al., 2003; Parton et al., 1998). Although this allows us to capture the most important aspects of the soil nutrient dynamics, a more refined spatial description of the nonlinear interactions among the different components of the soil is necessary to describe the rapid fluctuations in nutrient cycles in ecosystems where strong hydroclimatic forcing and sharp differences between the surface and deep soil layers are present (e.g., Kemp et al., 2003). Similarly, the lateral variability at the scale of few meters (e.g., of the single plant) is expected to play a role in the producing the so-called 'oases of fertility' in arid ecosystems (e.g., Schlesinger et al. 1996; Schlesinger and Pilmanis, 1998), and even the pore-scale spatial heterogeneity has recently been recognized to be central in the MIT turnover and microbe-plant competition (Schimel and Bennett, 2004). In summary, the modeling of these complex interactions and feedbacks between soil matrix and organic matter dynamics (e.g., feedbacks between microorganisms and microfauna, roots, chemical properties, and soil texture; see Sollins et al., 1996; Six et al., 2004) at various spatial scales is a next step for a better understanding of the nutrient cycles in soils.

6. Conclusions

Soil biogeochemistry in semiarid ecosystems is heavily controlled by the hydrometeorological forcing (e.g., temperature and especially moisture fluctuations). For this reason water and nutrient cycles are intimately coupled and affect the above ground and below ground ecosystem dynamics in a complex network of interactions and feedbacks.

The difficulties in experimental observation of belowground processes the uncertainties in modeling complex nonlinear systems with biological components, and the temporal and spatial variability make it a field that calls for synergetic use of modeling exercises and field experiments. Both the prediction of ecosystem responses to climate change and the assessment of their stability to climatic and/or anthropogenic perturbations require an understanding of soil-plant biogeochemistry. However, some of the problems are still open, such as the long-term consequences of competition for nutrients between soil microbes and plants or the feedback of SOM dynamics on hydrological processes (e.g., soil hydraulic conductivity, albedo etc.), and stand as challenging but promising research topic.

7. Acknowledgements

We acknowledge support from the Office of Science, Biological and Environmental Research Program, U.S. Department of Energy, through the Great Plains Regional Center of the National Institute for Global Environmental Change under cooperative agreement DEFC02-03ER63613, and NSF-Hydrology Program (grant #EAR-0236621).

8. References

Aber J.D., J.M. Melillo, and C.A. McClaugherty. 1990. Predicting long-term patterns of mass loss, nitrogen dynamics, and soil organic matter formation from initial fine litter chemistry in temperate forest ecosystems. Can. J. Bot. 68: 2201-2208.

Aber J.D. and C.T. Driscoll. 1997. Effects of land use, climate, vegetation, and N deposition on N cycling an C storage in northern hardwood forests. Global Biogeochem. Cycles 11(4): 639-648.

Ackerly D. 2003. Canopy Gaps to Climate Change - Extreme Events, Ecology and Evolution. New Phytol. 160 (1): 2-4.

Allen M.R. and W.J. Ingram. 2002. Constraints on future changes in climate and the hydrologic cycle. Nature 419(6903): 224+.

Archer S. 1989. Have Southern Texas savannas been converted to woodlands in recent hystory? Am. Nat. 134(4): 545-561.

Austin A.T., L. Yahdjian, J.M. Stark, J. Belnap, A. Porporato, U. Norton, D.A. Ravetta, S.M. Schaeffer. 2004. Water pulses and biogeochemical cycles in arid and semiarid ecosystems. Oecologia 141: 221-235.

Baisden W.T. and R. Amundson. 2003. An analytical approach to ecosystem biogeochemistry modeling. Ecol. Appl. 13(3):649-663.

Baldocchi D. and T. Meyers. 1998. On using eco-physiological, micrometeorological and biogeochemical theory to evaluate carbon dioxide, water vapor and trace gas fluxes over vegetation: a perspective. Agric. Forest Meteor. 90:1-25.

Ball J.T., I.E. Woodrow, and J.A. Berry. 1987. A model predicting stomatal conductance and its contribution to the control of photosynthesis under different environmental conditions. In: Progress in Photosynthesis Research, ed. J. Biggins. Martinus-Nijhoff Publishers, Dordrecht, The Netherlands. 221-224.

Berg B. and G. Ekbohm. 1983. Nitrogen immobilization in decomposing needle litter at variable carbon:nitrgen ratios. Ecology 64(1): 63-67.

Birkinshaw S.J. and J. Ewen. 2000. Nitrogen transformation component for SHETRAN catchment nitrate transport modelling. J. Hydrol. 230: 1-17.

Blagodatsky S.A. and O. Richter. 1998. Microbial growth in soil and nitrogen turnover: a theoretical model considering the activity state of microorganisms. Soil Biol. Biochem. 30(13): 1743-1755.

Bolker B.J., S.W. Pakala and W. J. Parton. 1998. Linear analysis of soil decomposition: insights from the century model. Ecol. Appl. 425-439.

Bosatta E. and G.I. Agren. 1985. Theoretical Analysis of decomposition of heterogeneous substrates. Soil Biol. Biochem. 17(5): 601-610.

Brady N.C. and R.R. Weil. 1996. The Nature and Properties of Soil. 11th ed. Upper Saddle River, New Jersey, Prentice Hall.

Cabon F., G. Girard, and E. Ledoux. 1991. Modelling of the nitrogen cycle in farm land areas. Fertilizer Res.. 27: 161-169.

Ciompi S., E. Gentili, L. Guidi, and G.F. Soldatini. 1996. The effect of nitrogen deficiency on leaf gas exchange and chlorophyll fluorescence parameters in sunflower. Plant Science 118: 177-184.

Collatz G.J., J.T. Ball, C. Grivet, and J.A. Berry. 1991. Physiological and environmental regulation of stomatal conductance, photosynthesis and transpiration: a model that includes a laminar boundary layer. Agric. Forest Meteor. 54:107-136.

Corre M.D., R.R. Schnabel, and W.L. Stout. 2002. Spatial and seasonal variation of gross nitrogen transformations and microbial biomass in a Northeastern US grassland. Soil Biol. Biochem. 34: 445-457.

Cui M. and M.M.Caldwell. 1997. A large ephemeral release of nitrogen upon wetting soil and corresponding root responses in the field. Plant and Soil 191: 291-299.

D'Odorico P., L. Ridolfi, A. Porporato, and I. Rodriguez-Iturbe. 2000. Preferential states of seasonal soil moisture: impact of climatic fluctuations. Water Resour. Res. 36(8): 2209-2220.

D'Odorico P., F. Laio, A. Porporato, and I. Rodriguez-Iturbe. 2003. Hydrologic control on soil carbon and nitrogen cycles II a case study. Adv. Water Res. 26: 59-70.

Easterling D.R., G.A. Meehl, and C. Parmesan, S.A. Changnon, T.R Karl, and L.O. Mearns. 2000. Climate Extremes: Observations, Modeling, and Impacts. Science 289 (5487): 2068-2074.

Engels C. and H. Marschner. 1995. Plant uptake and utilization of nitrogen. In: Nitrogen Fertilization in the environment. P.E. Bacon, ed. Marcel Dekker Inc. New York.

Farquhar G.D., S. von Caemmerer, and J.A. Berry. 1980. A biochemical model of photosynthetic CO_2 assimilation in leaves of C_3 species. Planta 149:78-90.

Fenchel T. G.M. King, and T.H. Blackburn. 1998. Bacterial biogeochemistry: the ecophysiology of mineral cycling. San Diego: Academic Press.

Field C. and H. Mooney. 1986. The photosynthesis-nitrogen relationship in wild plants. In: On the Economy of Plant Form and Function. T.J. Givinish, ed. Cambridge University Press, New York. 25-55.

Fierer N. and J.P. Schimel. 2002. Effects of drying-rewetting frequency on soil carbon and nitrogen transformation. Soil Biol. Biochem. 34: 777-787.

Freckman D.W.. 1986. The ecology of dehydration in soil organisms. 157-168. In: Membranes, Metabolism and Dry Organisms. A.C. Leopold, ed. Cornell University Press. Ithaca.

Gebauer R.L.E. and J.R. Ehleringer. 2000. Water and nitrogen uptake patterns following moisture pulses in a cold desert community. Ecology 81(5): 1415-1424.

Gusman A.J. and M.A. Marino. 1999. Analytical modeling of nitrogen dynamics in soils and ground water. J. Irrig. Drainage Eng. 125(6): 330-337.

Hansen S., H.E. Jensen, and M.J. Shaffer. 1995. Developments in modeling nitrogen transformation in soils. In: Nitrogen Fertilization in the Environment. P.E. Bacon, ed. Marcel Dekker Inc. New York.

Heitholt J.J., R.C. Johnson, and D.M. Ferris. 1991. Stomatal limitation to carbon-dioxide assimilation in nitrogen-stressed and drought-stressed wheat. Crop Science 31: 135-139.

Hunt H.W., M.J. Trlica, E.F. Redente, J.C. Moore, J.K. Detling, T.G.F. Kittel, D.E. Walter, M.C. Fowler, D.A. Klein, and E.T. Elliott. 1991. Simulation model for the effects of climate change on temperate grasslands ecosystems. Ecological Modeling 53: 205-246.

Jackson L.E., J.P. Schimel, and M.K. Firestone. 1989. Short-term partitioning of ammonium and nitrate between plants and microbes in an annual grassland. Soil Biol. Biochem. 21(3): 409-415.

Jenkinson D.S. 1990. The turnover of organic carbon and nitrogen in soil. Phil. Trans. R. Soc. B 329(1255): 361-368.

Katterer T. and O. Andren. 2001. The ICBM family of analitically solved models of soil carbon, nitrogen and microbial biomass dynamics - description and application examples. Ecol. Model. 136: 191-207.

Kaye J.P. and S.C. Hart. 1997. Competition for nitrogen between plants and soil microorganisms. Trends Ecol. Evol. 12: 139-143.

Kemp P.R., J.F. Reynolds, R.A. Virginia, and W.G. Whitford. 2003. Decomposition of leaf and root litter of Chihuahuan desert shrubs: effectsof three years of summer drought. J. Arid Environ. 53: 21-39.

Knapp A.K., P.A. Fay, J.M. Blair, S.L. Collins, M.D. Smith, J.D. Carlisle, C.W. Harper, B.T. Danner, M.S. Lett, and J.K. McCarron. 2002. Rainfall Variability, Carbon Cycling, And Plant Species Diversity In A Mesic Grassland. Science 298(5601): 2202-2205.

Larcher W. 1995. Physiological plant ecology. Springer Verlag. New York.

Manzoni S., A. Porporato, P. D'Odorico, F. Laio, and I. Rodriguez-Iturbe. 2004. Soil nutrient cycles as a nonlinear dynamical system. Nonlinear Proc. Geophys. 11: 589-598.

Mary B., S. Recous, D. Darwis, and D. Robin. 1996. Interactions between decomposition of plant residues and nitrogen cycling in soil. Plant Soil 181: 71-82.

McCarron J.K., A.K. Knapp, and J.M. Blair. 2003. Soil C and N responses to woody plant expansion in a mesic grassland. Plant Soil 257:183-192.

McMurtrie R., E.B. Medlyn, and R.C. Dewar. 2001. Increased understanding of nutrient immobilization in soil organic matter is critical for predicting the carbon sink strength of forest ecosystems over the next 100 years. Tree Physiol. 21: 831-839.

Molina J.A. and P. Smith. 1998. Modeling carbon and nitrogen processes in soils. Adv. Agron.62: 253-298.

Molina J.A.E., C.E. Clapp, M.J. Shaffer, F.W. Chichester, and W.E. Larson. 1983. NCSOIL, a model of nitrogen and carbon transformations in soils: description, calibration and behavior. Soil Sci. Soc. Am. J. 47: 85-91.

Moorhead D.L., W.S. Currie, E.B. Rastetter, W.J. Parton, and M.E. Harmon. 1999. Climate and litter quality controls on decomposition: an analysis of modeling approaches. Global Biogeochem. Cycles 13(2): 575-589.

Mueller T., J. Magid, L.S. Jensen, H. Svendsen, and N.E. Nielsen. 1998. Soil C and N turnover after incorporation of chopped maize, barley straw and blue grass in the field: evaluation of the DAISY soil-organic-matter submodel. Ecol. Model. 111: 1-15.

Neff J.C., F.S. Chapin III, and P.M. Vitousek. 2003. Breaks in the cycle: dissolved organic nitrogen in terrestrial ecosystems. Front. Ecol. Environ. 1(4): 205-211.

Noy-Meir I. 1973. Desert ecosystems: environment and producers. Ann. Rev. Ecol. Sys. 4: 25-51.

Ojima D.S., D.S. Schimel, W.J. Parton, and C.E. Owensby. 1994. Long- and short-term effects of fire on nitrogen cycling in tallgrass prairie. Biogeochemistry 24: 67-84.

Parton W.J., D.S. Schimel, C.V. Cole, and D.S. Ojima. 1987. Analysis of factors controlling soil organic matter levels in Great Plains grasslands. Soil Sci. Soc. Am. J. 51:1173-1179.

Parton W.J., J.W.B. Stewart, and C.V. Cole. 1988. Dynamics of C, N, P and S in grasslands soil: a model. Biogeochemistry 5:109-131.

Parton W.J., M. Hartman, D. Ojima, and D. Schimel. 1998. DAYCENT and its land surface submodel: description and testing, Global Planet. Change 19: 35–48.

Pastor J. and W.M. Post. 1986. Influence of climate, soil moisture, and succession on forest carbon and nitrogen cycles. Biogeochemistry 2:3-27.

Porporato A., F. Laio, L. Ridolfi, and I. Rodriguez-Iturbe. 2001. Plants in water-controlled ecosystems. Active role in hydrological processes and response to water stress. III Vegetation water stress. Adv. Water Res. 24(7): 725-744.

Porporato A., P. D 'Odorico, F. Laio, and I. Rodriguez-Iturbe. 2003. Hydrologic controls on Soil carbon and nitrogen cycle I: Modelling scheme. Adv. Water Res. 26: 45-58.

Porporato A., E. Daly, I. Rodriguez-Iturbe. 2004. Soil water balance and ecosystem response to climate change. Am. Nat. 164 (5): 625-632.

Ratkowsky D.A., J. Olley, T.A. McMeekin, and A. Ball. 1982. Relationship between temperature and growth rate of bacterial cultures. J. Bacteriol. 149(1): 1-5.

Schimel J.P., L.E. Jackson, and M.K. Firestone. 1989. Spatial and temporal effects on plant-microbial competition for inorganic nitrogen in a California annual grassland. Soil Biol. Biochem. 21(8): 1059-1066.

Schimel J.P. and M.N. Weintraub. 2003. The implications of exoenzyme activity on microbial carbon and nitrogen limitation in soil: a theoretical model. Soil Biology & Biochemistry 35(4): 549-563.

Schimel J.P. and J. Bennett. 2004. Nitrogen mineralization: challenges of a changing paradigm. Ecology 85(3):591-602.

Schwinning S. and O.E. Sala. 2004. Hierarchy of responses to resource pulses in arid and semiarid ecosystems. Oecologia 141: 211-220.

Schlesinger W.H., J.F. Reynolds, G.L. Cunningham, L.F. Huenneke, W.M. Jarrell, R.A. Virginia, and W.G. Whitford. 1990. Biological feedbacks in global desertification. Science 247(4946): 1043-1048.

Schlesinger W.H., J.A. Raikes, A.E. Hartley, and A.E. Cross. 1996. On the spatial pattern of soil nutrients in desert ecosystems. Ecology 77(2): 364-374.

Schlesinger W.H. and A.M. Pilmanis. 1998. Plant-soil interactions in deserts. Biogeochemistry 42: 169-187.

Scholes R.J. and B.H. Walker. 1993. An African savanna. Cambridge University Press.

Seastedt T.R., J.M. Briggs, and D.J. Gibson. 1991. Controls of nitrogen limitation in tallgrass prairie. Oecololgia 87: 72-79.

Six J., H. Bossuyt, S. Degryze, and K. Denef. 2004. A history of research on the link between (micro)aggregates, soil biota, and soil organic matter dynamics. Soil Tillage Research 79: 7-31.

Sollins P., P. Homann, and B.A. Caldwell. 1996. stabilization and destabilization of soil organic matter: mechanisms and controls. Geoderma 74: 65-105.

Stark J.M. and M.K. Firestone. 1995. Mechanisms for soil moisture effects on activity of nitrifying bacteria. Appl. Environ. Biology 61: 218-221.

Vitousek P.M. and R. Howarth. 1991. Nitrogen limitation on land and in the sea - How can it occur., Biogeochemistry 13(2): 87-115.

Wild A. (editor). 1988. Russell's soil condition and plant growth. 11th ed. Longman Group, Essex, UK.

Zak D.R., P.M. Groffman, K.S. Pregitzer, S. Christensen, and J.M. Tiedje. 1990. The vernal dam: plant-microbe competition for nitrogen in North American hardwood forests. Ecology 71(2): 651-656.

Chapter 12

INTERACTIONS OF WATER AND NITROGEN ON PRIMARY PRODUCTIVITY ACROSS SPATIAL AND TEMPORAL SCALES IN GRASSLAND AND SHRUBLAND ECOSYSTEMS

Howard E. EPSTEIN, José M. PARUELO[2], Gervasio PIÑEIRO[2], Ingrid C. BURKE[3],
William K. LAUENROTH[3], and John E. BARRETT[4]

[1] *Department of Environmental Sciences, University of Virginia, Charlottesville, VA 22904-4123, USA - e-mail:* hee2b@virginia.edu
[2] *Facultad de Agronomía, Universidad de Buenos Aires, Ciudad de Buenos Aires, Argentina - e-mails:* paruelo@agro.uba.ar, pineiro@ifeva.edu.ar
[3] *Department of Forest, Range and Watershed Stewardship, Colorado State University, Fort Collins, CO 80523, USA - e-mails:* indy@cnr.colostate.edu, Billl@cnr.colostate.edu
[4] *Department of Environmental Studies, Dartmouth College, Hanover, NH 03755, USA - e-mail:* John.E.Barrett@dartmouth.edu

1. The driving influence of water on spatial patterns of global and regional scale primary productivity in grasslands and shrublands

Soil moisture, and hence precipitation, exerts a dominant control on net primary productivity (NPP; the rate of carbon accumulation by autotrophs) in semiarid to sub-humid ecosystems, such as grasslands and shrublands. At the global scale, mean annual precipitation has been shown to account for >50% of the variance in aboveground net primary production (ANPP) in grassland ecosystems (Lauenroth 1979, Le Houérou et al. 1988). Within specific regions, numerous investigators have demonstrated strong positive relationships between mean annual precipitation and primary productivity (or some surrogate variable) for various ecosystems globally, including the Great Plains grasslands (Sala et al. 1988, Epstein et al. 2002), the Patagonian steppe (Austin and Sala 2002, Jobbágy et al. 2002), African grasslands and savannas (Breman and de Wit 1983, McNaughton et al. 1993, Scanlon et al. 2002) and grasslands and shrublands of Inner Mongolia and northeastern China (Gao and Yu 1998, Yu et al. in press). Environmental factors other than precipitation, yet directly related to soil moisture, such as temperature and soil texture, have also been shown to be important regional-scale controls over primary productivity in grasslands and shrublands (Noy-Meir 1973, Sala et al. 1988, Epstein et al. 1996, 1997, Lane et al. 1998, Jobbágy et al. 2002).

2. Moisture controls on the interannual variability in primary productivity for grasslands and shrublands

Interannual variability in net primary productivity for grasslands and shrublands is also substantially controlled by precipitation and soil moisture. Growing season rainfall explained 43% of the interannual variance in forage production for a northeastern Colorado shortgrass steppe ecosystem over a 52-year period (Lauenroth and Sala 1992), and annual precipitation explained 37% of net primary production for a northeastern Kansas tallgrass prairie, from a 19-year dataset (Briggs and Knapp 1995). Using irrigation treatments over an 8-year period, Knapp et al. (2001) found that 81% of ANPP was explained by the annual water inputs, also for tallgrass prairie in Kansas.

P. D'Odorico and A. Porporato (eds.), Dryland Ecohydrology, 201–216.

Lauenroth and Sala (1992) noted that the interannual response of ANPP to changes in precipitation (in this case for a shortgrass steppe ecosystem of northeastern Colorado) was less than the spatial response for an equivalent precipitation change (e.g. Sala et al. 1988) (Figure 1), suggesting that at a given site, there were constraints on productivity responses to changing moisture. This idea was examined further for temperate grasslands globally using ANPP field data, and for grasslands along a mean annual precipitation gradient in the U.S. Great Plains, using remote sensing data (Paruelo et al. 1999b). Both the field data and the remote sensing data (which used the Normalized Difference Vegetation Index [NDVI] as a surrogate for ANPP) demonstrated that the temporal responses of ANPP to changes in moisture availability were constrained relative to spatial patterns at both the dry and wet extremes of the precipitation gradient (Figure 2).

The explanation for these findings was related to both vegetation and biogeochemical constraints on ecosystem response to fluctuating moisture conditions (see also Chapters 2, 3, and 11). At the dry end of the precipitation gradient (approximately <400 mm yr^{-1}), the plant community is dominated, as would be expected, by drought-resistant species. These species have traits such as high allocation of tissue to belowground structures (e.g. roots and rhizomes) rather than leaves, low leaf area relative to leaf mass, and low stomatal conductance to restrain water loss. These plant traits, coincident with drought-tolerance, are the same traits that would constrain the rates of photosynthesis and growth of these plants in response to variable moisture (Tilman 1988, Keddy 1992, Grime 1977).

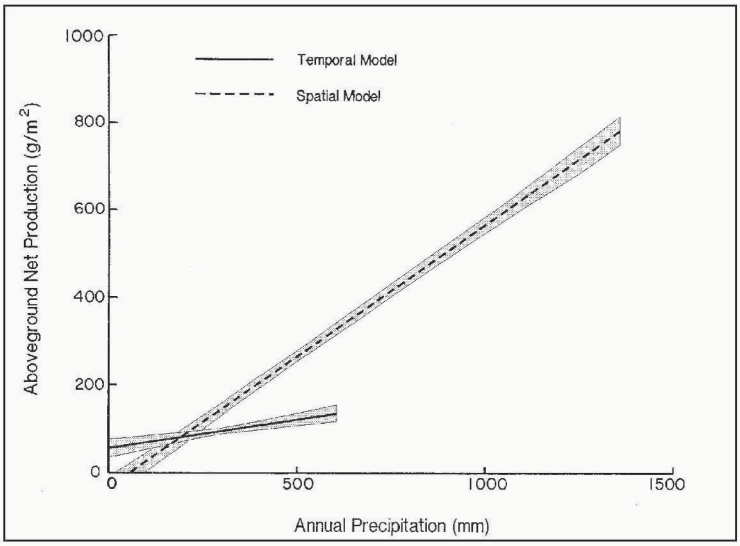

Figure 1. Temporal and spatial response of aboveground net primary production (g m^{-2}) to changes in annual precipitation (from Lauenroth and Sala 1992).

At the wet end of the precipitation gradient (approximately >800 mm yr^{-1}), primary productivity also does not respond substantively to interannual variability in precipitation (Hooper and Johnson 1999, Paruelo et al. 1999b). These constraints in the vegetation response to moisture, however, may not be related to plant traits (as is hypothesized for the drier end of the gradient). The dominant plant species at the wet end of the mean annual precipitation gradient (typically tallgrasses) tend to have greater plasticity in their photosynthetic and growth-related properties than do the drought-tolerant species. Paruelo et al. (1999a) illustrate this for grass species that dominate in different portions of the typical mean annual precipitation gradient for grassland regions. In a greenhouse experiment using species from grasslands of both North and South America, they showed that the magnitude of plant response to drought, in characteristics such as relative growth rate, transpiration, tiller production and leaf expansion, increased from arid to sub-humid ecosystems (Figure 3).

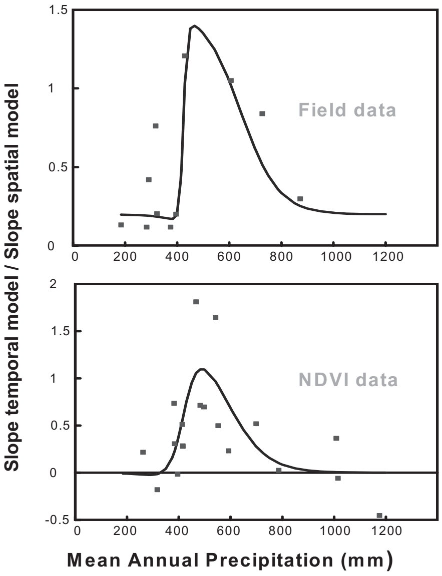

Figure 2. Temporal response of aboveground net primary productivity (from field data and represented by the normalized difference vegetation index [NDVI]) to interannual precipitation variability, along a spatial gradient of increasing mean annual preciption (from Paruelo et al. 1999b). Points represent the slopes of the regression between MAP and either ANPP (top) or NDVI (bottom) for specific sites (temporal relationship) normalized by the slope of the spatial relationship between MAP and either ANPP (0.64) or NDVI (0.48). Lines are double logistic functions fitted to the data.

At the wet end of the precipitation gradient (approximately >800 mm yr^{-1}), primary productivity also does not respond substantively to interannual variability in precipitation (Hooper and Johnson 1999, Paruelo et al. 1999b). These constraints in the vegetation response to moisture, however, may not be related to plant traits (as is hypothesized for the drier end of the gradient). The dominant plant species at the wet end of the mean annual precipitation gradient (typically tallgrasses) tend to have greater plasticity in their photosynthetic and growth-related properties than do the drought-tolerant species. Paruelo et al. (1999a) illustrate this for grass species that dominate in different portions of the typical mean annual precipitation gradient for grassland regions. In a greenhouse experiment using species from grasslands of both North and South America, they showed that the magnitude of plant response to drought, in characteristics such as relative growth rate, transpiration, tiller production and leaf expansion, increased from arid to sub-humid ecosystems (Figure 3).

In the absence of vegetation-related constraints to primary productivity responses, an alternative explanation was proposed related to biogeochemical properties of these systems, with a particular emphasis on nitrogen (Breman and de Wit 1983, Burke et al. 1997, see next section).

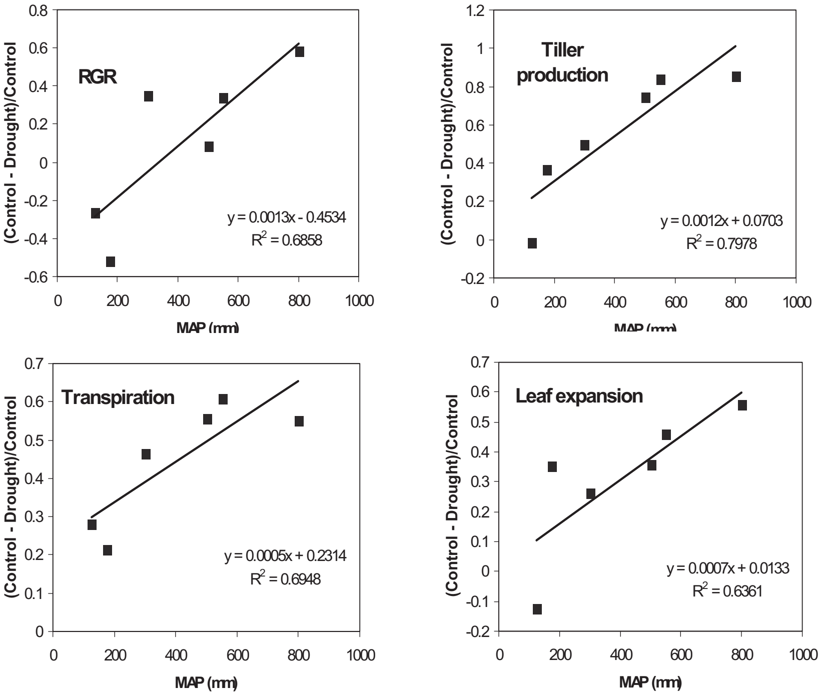

Figure 3. Responses of relative growth rate (RGR), tiller production, transpiration and leaf expansion to drought conditions along a spatial gradient of mean annual precipitation. The y-axis represents the response of the particular function to drought (control – drought) normalized by the rate of the function under control conditions, i.e. the relative response of the function to drought. The species analyzed are dominant at the mean annual precipitation level indicated on the x-axis in South American (SA) and North American (NA) grasslands. The species included in the analysis are Stipa humilis (SA), Poa ligularis (SA), Festuca pallescens (SA), Hilaria jamessii (NA), and Stipa viridula (NA). Reconstructed from Paruelo et al. (1999a).

3. The relationship between soil water and soil nitrogen availability at the regional scale and the relative limitations of these factors to primary productivity

While soil moisture clearly exerts a strong positive effect on net primary productivity in grasslands and shrublands, water also positively influences plant-available nitrogen in soils (e.g. Drury et al. 2003, Paul et al. 2003; see also Chapter 11); this in turn can stimulate primary productivity across a variety of ecosystems, as demonstrated in numerous experimental studies (see Hooper and Johnson 1999 for a comprehensive list) and in simulation modeling (Schimel et al. 1997b). Burke et al. (1997) found that mean annual precipitation explained 94% of the spatial variability in simulated net nitrogen (N) mineralization (the rate at which plant-available forms of nitrogen accumulate in soils), using the CENTURY model (Parton et al. 1987) for sites with constant mean annual temperature in the U.S. Great Plains. They also found that 40% of the interannual variability in simulated net N mineralization could be explained by annual rainfall.

One field study in Patagonian grasslands, shrublands and forests found that mean annual precipitation was positively associated with, and explained 96% of the variability in, soil ammonium (NH_4^+) levels (Austin and Sala 2002). Not surprisingly, ANPP was also strongly and positively related to total inorganic soil nitrogen in that study. Other field studies, however, conducted in the Great Plains to evaluate the relationships among interannual variability in precipitation, nitrogen availability and productivity across a transect from semiarid to sub-humid sites have been much less conclusive (Barrett et al. 2002), suggesting that net nitrogen mineralization rates may not vary systematically across precipitation gradients. In general it is very difficult to assess nitrogen availability across regional and landscape spatial gradients (Zak et al. 1994, Hook and Burke 2000, Barrett et al. 2002). As net primary production, soil organic matter and soil microbial biomass all increase with increasing precipitation, so does the nitrogen immobilization potential of the soil (Barrett and Burke 2000, 2002). Thus net nitrogen mineralization, or perhaps our ability to estimate it, may not necessarily change across these moisture gradients.

So, it is rather apparent that water has a strong positive relationship with primary productivity in semiarid to sub-humid ecosystems. Water may also have a positive relationship with net nitrogen mineralization and plant-available soil N. However some field studies have shown otherwise for regional moisture gradients (Barrett and Burke 2000, Barrett et al. 2002) and have suggested that while gross N mineralization might increase along precipitation gradients, N immobilization by decomposers might increase as well. Since several studies have found that ANPP is more responsive than net N mineralization to spatial increases in precipitation (Seagle and McNaughton 1993, Burke et al. 1997, Austin and Sala 2002, Barrett et al. 2002), this suggests that nitrogen may become more limiting to grassland and shrubland ecosystems as water availability is augmented. There are several pieces of evidence supporting this idea that N limitation increases with available water in grasslands and shrublands.

First, there are more data demonstrating nitrogen limitations to primary productivity in tallgrass prairie ecosystems (e.g. Owensby et al. 1970, Risser and Parton 1982, Knapp and Seastedt 1986, Tilman 1987, Seastedt et al. 1991, Benning and Seastedt 1995, Turner et al. 1997) than there are in shortgrass steppe or desert ecosystems (Ettershank et al. 1978, Lauenroth et al. 1978, Dodd and Lauenroth 1979, Horn and Redente 1998). Tallgrass prairie in the Great Plains of the U.S. typically receives approximately 50-100% more annual rainfall than shortgrass steppe (Paruelo et al. 1995). Additionally, N amendments to shortgrass steppe ecosystems showed greater responses under wetter conditions (Dodd and Lauenroth 1979), whereas tallgrass prairie exhibited large responses to N additions in all but the driest years (Owensby et al. 1970).

Second, there is evidence that plant nitrogen-use efficiency increases with increasing water availability in the U.S. Great Plains (Schimel et al. 1991, Vinton et al. 1993, Vinton and Burke 1995, Murphy et al. 2002) and in the Sahel and savannas of West and Central Africa (Breman and de Wit 1983), suggesting increased N limitations to plant productivity (Vitousek 1982) with increasing soil moisture. Oyarzabal et al. (submitted) analyzed 12 grass species from areas differing in mean annual precipitation and found that N conservation within plants [as indicated by N resorption efficiency from leaves, defined as (N in green leaves – N in senescent leaves) / N in green leaves] increased significantly across an annual rainfall gradient (Figure 4) (see Austin and Sala 2002 however for opposing results). So, if the efficiency of nitrogen-use increases along a precipitation gradient then N availability need not increase to the same extent as water availability, and the increase in ANPP will still occur. Therefore there is some information supporting the idea that vegetation constraints limit primary productivity responses to moisture changes in drier areas and that resources (possibly nitrogen) exhibit greater limitations to primary productivity as water limitations decline.

4. Examining the hypothesis that nitrogen limitation in grasslands and shrublands increases as water limitation declines

It has been assumed that as annual precipitation increases in dryland ecosystems, so will plant demand for nitrogen (Seagle and McNaughton 1983, Hooper and Johnson 1999). N availability may or may not increase with mean annual precipitation, yet if any increase in N availability does not meet the increasing plant demand for nitrogen (Seagle and McNaughton 1993, Burke et al. 1997, Barrett et al. 2002), then nitrogen will become more limiting as precipitation increases.

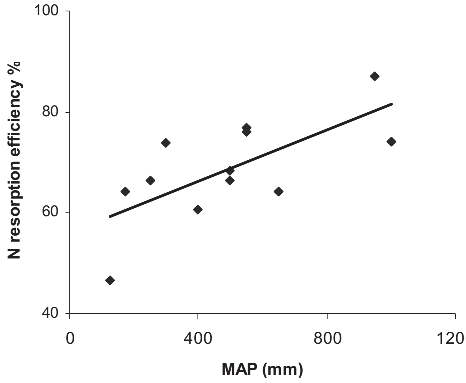

Figure 4. Relationship between the nitrogen resorption efficiency % [defined as (N in green leaves – N in senescent leaves) / N in green leaves] and the mean annual precipitation where the species is dominant for 12 grasses of North and South America. (Redrawn from Oyarzabal et al. submitted).

Hooper and Johnson (1999) used a meta-analytical approach to test this hypothesis that nitrogen limitation increases with increasing soil moisture in dryland ecosystems. In their analysis of over 50 studies of nitrogen fertilization experiments in grasslands and shrublands globally, they found that neither the relative response nor the maximum response of ANPP to N fertilization increased with increasing moisture. Fertilizer-use efficiency, and hence an absolute response, did however increase significantly with spatial and temporal increases in moisture. Their conclusions were that water and nitrogen co-limit ANPP along spatial and temporal gradients of moisture, and there is likely no switch from water-limited to nitrogen-limited systems as moisture increases.

Two alternative hypotheses that arise from these results are: 1) ANPP, plant N demand and N availability all increase similarly along moisture gradients (this is the scenario proposed by Hooper and Johnson 1999) or 2) plant N demand and N availability vary similarly along moisture gradients, yet increase to a lesser extent than does ANPP with increasing precipitation. The latter of the two hypotheses, with regard to changes in N availability along precipitation gradients, is better supported by the published data, as mentioned above (Seagle and McNaughton 1993, Burke et al. 1997, Austin and Sala 2002, Barrett et al. 2002). In addition, nitrogen-use efficiency has been shown to increase (i.e. relative plant N demand decreases) with increasing precipitation (Breman and de Wit 1983, Schimel et al. 1991, Vinton et al. 1993, Vinton and Burke 1995, Murphy et al. 2002). The relative lack of response to N additions in sub-humid grasslands along the precipitation gradient implies that the demonstrated increase in N-use efficiency with increasing moisture may not be the result of nitrogen limitation, but rather could be inherent in the structure and function of the taller vegetation.

Hooper and Johnson (1999) found several other intriguing results in their analysis. The first is that, with few exceptions, nitrogen was equally or more limiting than water in terms of the relative response of ANPP across the entire precipitation gradient, and secondly, the relative responses of ANPP to water, nitrogen, and water plus nitrogen were all greatest at moderate levels of mean annual precipitation (~500 mm yr^{-1}) (Figure 5). This at the very least corroborates the Paruelo et al. (1999b) findings of greatest response to moisture at intermediate levels of annual precipitation, and also suggests a constraint to productivity in addition to water and nitrogen in dry areas (vegetation properties, for example). However the nature of the constraint at the sub-humid end of the gradient remains puzzling, as it appears not to be nitrogen.

Light limitation and grazing may explain the response of ANPP to soil moisture variability in subhumid ecosystems. At the wettest extreme of the precipitation gradient, light could constrain the ANPP response to both water and nitrogen. Altesor et al. (in press) found, for tallgrass prairies of Uruguay, that the ANPP in ungrazed sites was less than ANPP in grazed sites, even though quantities of soil nitrogen and water were greater under ungrazed conditions. When standing dead biomass was experimentally removed, effectively increasing the within-canopy light level, the ungrazed sites produced more than both grazed sites and intact grazing exclosures.

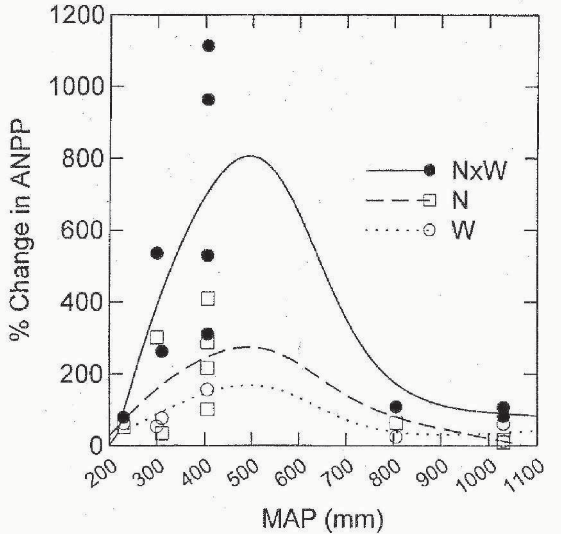

Figure 5. Relative response of aboveground net primary production (ANPP) to additions of water, nitrogen and water plus nitrogen, along a gradient of mean annual precipitation (MAP) (from Hooper and Johnson 1999). Points represent the relative response of ANNP from a variety of water addition and N fertilization studies conducted in grasslands receiving differing levels of annual precipitation. Curves are fitted by a distance weighted least squares procedure for nitrogen and water additions (N x W), nitrogen additions only (N) and water additions only (W).

Grazing can also obscure water and nitrogen relationships at the regional scale, because herbivores may consume the greatest proportions of ANPP at the wet extreme of the precipitation gradient (Oesterheld et al. 1992). Piñeiro et al. (submitted) showed using simulation modeling that the reduction in N mineralization induced by grazing increases from the dry to the wet end of the precipitation gradient (Figure 6), thereby modifying water and nitrogen relationships. Hence both light and grazing could be constraining ANPP responses to water and nitrogen at the wet extreme of the precipitation gradient.

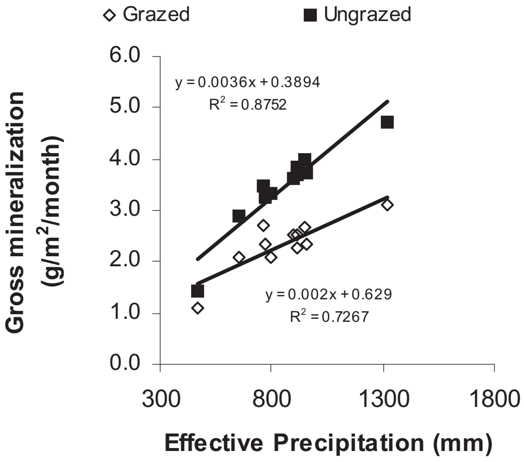

Figure 6. Changes in gross nitrogen mineralization rates for heavily grazed and ungrazed sites over 400 years along a precipitation gradient in South America, as simulated by the CENTURY model (Parton et al., 1987) (from Piñeiro et al. submitted).

So clearly, this is not the final say in the matter, and several questions beg for further examination. Do water and nitrogen co-limit productivity in dryland ecosystems across the range of annual precipitation values? Is nitrogen equally as limiting as (or even more limiting than) water in arid and semi-arid grasslands and shrublands? What does constrain ecosystem response to changes in water and nitrogen availability in sub-humid grasslands and shrublands? Figure 7 summarizes the available evidence into a new conceptual framework describing the relative importance of different types of constraints on the response of ANPP along a precipitation gradient.

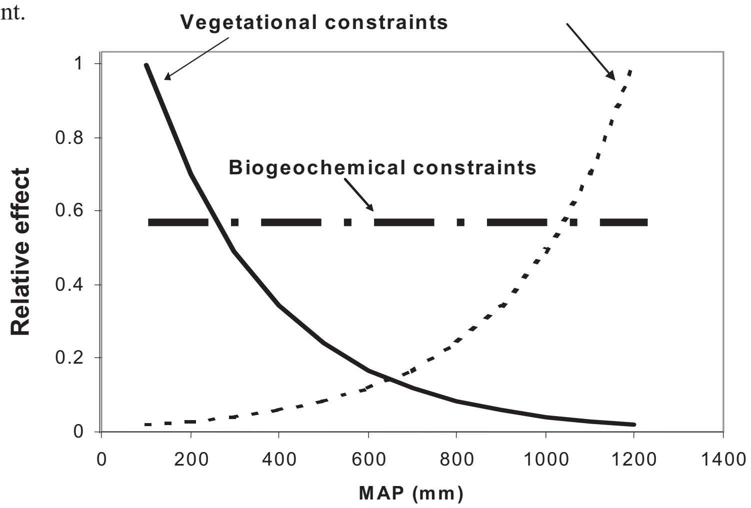

Figure 7. Conceptual diagram of the relative effects of the proposed constraints on primary productivity along a gradient of mean annual precipitation (MAP). While plant properties constrain the productivity response to water in dry ecosystems, the evidence suggests that nitrogen limitation does not vary along a precipitation gradient. A resource other than available nitrogen is likely constraining the productivity response to water in subhumid ecosystems (e.g. light).

5. Landscape-scale relationships between water and nitrogen

In order to assess the co-limitation of water and nitrogen to primary productivity in grasslands and shrublands, we can attempt to examine the relationships between water and nitrogen across topographic, soil texture and disturbance gradients within a landscape. Topography affects water redistribution, which modifies soil moisture (see Chapter 7) and is an important control of the spatial and interannual variability in net primary production at the landscape scale (Schimel et al. 1985, Briggs et al. 1989, Milchunas et al. 1989, Knapp et al. 1993, Briggs and Knapp 1995, Singh et al. 1998). As an example, lowland topographic positions in tallgrass prairie in northeastern Kansas generally have greater aboveground net primary productivity than upland topographic positions (Briggs and Knapp 1995), likely due to greater soil moisture (Knapp et al. 1993). The responses of both total ANPP and grass ANPP were controlled to a greater extent by precipitation (both total and growing season) in upland tallgrass prairie compared to lowland tallgrass prairie (Briggs and Knapp 1995), and interannual variability in ANPP was greater in the upland sites relative to the lowland sites (Knapp et al. 2001). These results suggest that rainfall exhibits a greater limitation to productivity at the dry uplands sites compared to wetter lowland sites, at the landscape scale.

In addition to controlling net primary production, topography (through its effects on soil moisture and other ecosystem properties) can influence rates of gross and net nitrogen mineralization (e.g. Schimel and Parton 1986, Burke et al. 1989, Verchot et al. 2002). However, while it seems reasonable that landscape-scale gradients of water availability and nitrogen availability should be spatially correlated (and controlled largely by topography), this is frequently not the observed pattern; several studies have shown that whereas soil moisture increases from upper to lower slope positions, the same is not always true for nitrogen availability. Hook and Burke (2000) found that, for the shortgrass steppe, net N mineralization rates were not significantly related to topography. Results from Turner et al. (1997) for the tallgrass prairie showed that net N mineralization rates were substantially greater in the drier uplands than the wetter lowlands. Many additional studies demonstrate that direct effects of soil texture, soil organic matter, fire and grazing on net N mineralization rates are often greater than those of topographically-driven soil moisture (Burke 1989, Turner et al. 1997, Tracy and Frank 1998, Augustine and Frank 2001, Delin and Linden 2002).

Landscape-scale topographic gradients therefore may not be very conducive for studying the relative limitations of water and nitrogen on primary productivity in dryland ecosystems. Nitrogen fertilization experiments conducted across topographic gradients of soil moisture may have highly variable initial conditions with respect to levels of soil organic and inorganic N, and net N mineralization rates; and given the current state of the science, these pools of nitrogen and net N mineralization rates are not necessarily predictable across topographic moisture gradients. Either spatially extensive (encompassing a wide range of initial conditions) or very controlled experiments would need to be done to assess the relative limitations of water and nitrogen to primary productivity across landscape-scale moisture gradients.

Grazing and fire are recurrent disturbances in dryland ecosystems and both have a strong influence on water and nitrogen dynamics across landscapes; the effects of these particular disturbances on N and water availability are not always easily predictable. For example, grazing has been shown to either increase (Frank & Evans 1997) or decrease (Verchot et al., 2002) N mineralization rates at Yellowstone National Park depending on the age of the grazing exclosures. Fire can increase N availability in the first few months after the disturbance (Laterra et al. 2001) yet decrease overall soil N content after several years of recurrent fires (Oesterheld et al., 1999). Spatial heterogeneity of grazing may contribute to nutrient patchiness through positive feedbacks on nutrient cycling in heavily grazed locations (McNaughton et al 1997). Interactions among disturbances and landscape features therefore provide additional complexity to the analysis of nitrogen and water interactions. As an example, grazing could reverse the expected patterns of plant nitrogen content generated by water availability along a topographic sequence. In the Mesopotamic Pampa of Argentina the nitrogen content of both litter and aboveground biomass generally increases from uplands to lowlands in ungrazed areas, however grazing has been shown to alter this pattern (Figure 8, G. Piñeiro et al. unpublished data).

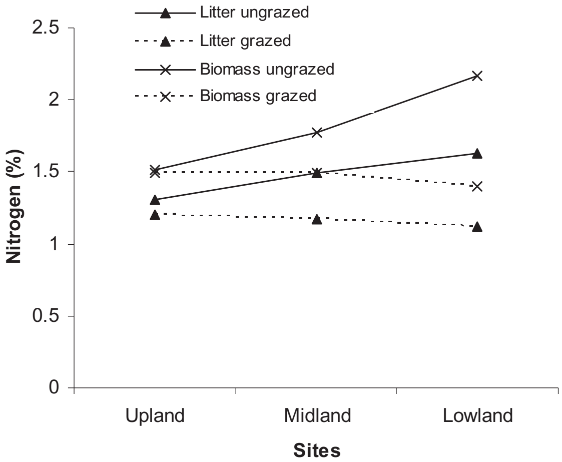

Figure 8. Changes in nitrogen content of litter and aboveground plant biomass in grazed and ungrazed grassland plots across a topographic gradient, at El Palmar National Park, Argentina.

6. Fine temporal scale relationships between water and nitrogen – pulses of resources and the relative limitations of water and nitrogen on plant growth

One other approach for addressing the relative limitations of these plant resources is to examine how water and nitrogen vary over fine temporal scales at a given site, and how individual plants may be limited temporally by either water or nitrogen. The logistics and costs involved with taking frequent *in situ* measurements of either gross or net nitrogen mineralization limit the data available for determining how plant-available N varies over fine temporal scales (e.g. hours, days, weeks) in response to variable soil moisture. Fluxes of NO and N_2O from soils, however, have been measured more frequently, and the data suggest pulse accelerations of nitrogen cycling processes with temporal increases in soil water content (e.g. Parton et al. 1988, Davidson et al. 1993, Hutchinson et al. 1993, Epstein et al. 1998, Martin et al. 1998, Smart et al. 1999).

Laboratory incubation studies examining the effects of soil moisture on nitrogen mineralization do show strong positive effects of soil water content on nitrogen mineralization rates across the range of unsaturated conditions; the relationships found between soil water content and nitrogen mineralization are generally non-linear and may have threshold values, where the nature of the relationship changes (Linn and Doran 1984, Low et al. 1997, Drury et al. 2003, Paul et al. 2003). Simulation models typically use first-order kinetics to describe nitrogen mineralization, where the decay rate terms (which act on dead organic matter pools) are functions of soil temperature, soil moisture, dead organic matter C:N ratio and microbial biomass (Herlihy 1979, Cabrera and Kissel 1988, Parton et al. 1988, Das 1995, Vigil et al. 2002, Porporato et al. 2003).

Applying these concepts to the field, of course, is difficult. Grassland and shrubland ecosystems are characterized by low annual rainfall with a high frequency of low precipitation events (< 10mm) and frequent dry periods lasting several days or longer (Sala and Launroth 1982, Sala et al. 1992). How this temporal variability in moisture relates to the temporal variability in plant-available nitrogen is still extremely unclear. At the seasonal scale, rainfall and soil water status may dictate the seasonality of nitrogen mineralization rates (Jamieson et al. 1999), however at finer temporal scales the relationship is more complex. Schimel and Parton (1986) suggested that additional small rainfall events in shortgrass steppe ecosystems would not increase the total N mineralized, however some studies in the Great Basin of the U.S. have found that not only did rainfall events temporarily stimulate nitrate production (Cui and Caldwell 1997a), but plants were also able to capitalize on the pulses of available nitrogen following small precipitation episodes (Cui and Caldwell 1997b, Ivans et al. 2003).

So, small rainfall events in dryland ecosystems may stimulate the mineralization of nitrogen during brief periods when water is not directly limiting for photosynthesis. Other than event size, additional attributes of temporal precipitation patterns will influence water-nitrogen interactions as well. The length of the dry period between rainfall events may affect nutrient pulses during wetting, as a substantial portion of microorganisms may dessicate and die during these dry periods, entering a labile pool of soil organic matter (Bottner 1985, Kieft et al. 1987, Olfs et al. 2004). The frequency of drying and rewetting cycles can also influence the cumulative quantities of net nitrogen mineralized and nitrified (Fierer and Schimel 2002, Olfs et al. 2004, Burke et al. unpublished data).

7. Limitations of water and nitrogen across temporal scales

The co-limitation of water and nitrogen with respect to photosynthesis and plant growth has been demonstrated by field studies (Klages and Ryerson 1965, Smika et al. 1965, Lauenroth et al. 1978, Hamerlynck et al. 2004), laboratory experiments (Heitholt et al. 1991, Ciompi et al. 1996), and ecophysiological and ecosystem models (Peri et al. 2003 and Friend 1995, respectively). One interesting aspect of the relationship between these two resources is the timeframe of their limitations in arid to sub-humid ecosystems, which is related to the nature of their storage mechanisms. Water in plants and near-surface soils has a relatively short residence time (although certain plant types such as succulents can increase the duration of residence), and therefore the degree of water limitation can vary substantially over fine temporal scales, especially in dryland ecosystems. Deeply-rooted plants in dry ecosystems, however, can tap into soil reservoirs with high water content including groundwater, thereby reducing the variability of water limitations and at times eliminating water stress completely, when precipitation is low (Soriano and Sala 1983, Sala et al. 1989, Knoop and Walker 1985, Dodd et al. 1998). Nitrogen, on the other hand, can have relatively long residence times in plant tissue, and therefore nitrogen limitations to plant productivity may be less variable than water limitations (Schimel et al. 1997a). In addition, plants may take up excess nitrogen during periods when it is not the limiting resource for use under future conditions (Chapin et al. 1986, Seastesdt and Knapp 1993). Soil organic matter represents an even longer-term storage pool for nitrogen.

Therefore changes in water limitations in dryland ecosystems most often occur over fine temporal scales (e.g. minutes to days – with the exception of very deep-rooted plants), whereas nitrogen limitations have a more historical nature, resulting from the integration of plant-soil processes that occurred under prior conditions (e.g. days to years). Given the complexity of these dynamics, the effect of the co-limitation of water and nitrogen on primary productivity in dryland ecosystems, where precipitation is relatively low yet variable across many time scales (at least minutes through years), is still a subject worthy of extensive research.

8. Summary

At the regional scale, it has been thought that water limitations to primary production decrease, and nitrogen limitations to primary production increase, with increasing mean annual precipitation in dryland ecosystems. Hooper and Johnson (1999), in a comprehensive review of fertilization experiments across precipitation levels, found that the relative response of primary productivity to N fertilization does not increase with increasing precipitation, suggesting that sub-humid ecosystems are no more N-limited than semiarid ecosystems. They reasoned that if net primary productivity, N availability and plant nitrogen demand all increase similarly along precipitation gradients, then the relative response of plants to N fertilization will not vary along these gradients.

Since the Hooper and Johnson study in 1999, however, several studies have added to the evidence that N-availability either does not vary or increases to a lesser extent than net primary productivity along precipitation gradients (Austin and Sala 2002, Barrett and Burke 2002, Barrett et al. 2002); this begs for an alternative explanation of why the NPP response to N fertilization does not vary along precipitation gradients. One potential explanation is that plant nitrogen demand either does not vary or increases to a lesser extent than NPP along these gradients, an idea already supported by greater C:N ratios in wetter areas along moisture gradients (e.g. Murphy et al. 2002). Greater nitrogen-use efficiencies, in general, might not necessarily be indicative of nitrogen limitation, but may indicate less of a demand for nitrogen by plants.

Both Paruelo et al. (1999b) and Hooper and Johnson (1999) found that primary productivity responses to changes in water and N were greatest at intermediate levels of mean annual precipitation (~400-700 mm yr^{-1}), areas that are likely to be composed of a mixture of shorter and taller plant species. These results also suggest constraints to primary productivity responses at lower and higher levels of annual precipitation; structural and functional properties of the vegetation may be the culprits at both ends of gradient, although more work is clearly necessary here. The interactions between water and nitrogen over space and time, and their effects on plant productivity, are quite complex, and past research efforts have only scratched the surface of underlying mechanisms.

9. Acknowledgements

H.E. Epstein's contribution was funded in part by the NSF award EAR-0236621.

10. Literature Cited

Altesor, A. I., M. Oesterheld, E. Leoni, F. Lezama, and C. Rodríguez. Effect of grazing exclosure on community structure and productivity of a temperate grassland. Journal of Vegetation Science in press.

Augustine, D.J., and D.A. Frank. 2001. Effects of migratory grazers on spatial heterogeneity of soil nitrogen properties in a grassland ecosystems. Ecology 82:3149-3162.

Austin, A.T., and O.E. Sala. 2002. Carbon and nitrogen dynamics across a natural precipitation gradient in Patagonia, Argentina. Journal of Vegetation Science 13:351-360.

Barrett, J.E., and I.C. Burke. 2000. N immobilization in grassland soils: control by soil organic matter. Soil Biology and Biochemistry 32:1707-1716.

Barrett, J.E., and I.C. Burke. 2002. Nitrogen retention in semiarid ecosystems across a soil organic matter gradient. Ecological Applications 12:878-890.

Barrett, J.E., R.L. McCulley, D.R. Lane, I.C. Burke, and W.K. Lauenroth. 2002. Influence of annual and seasonal climate variability on plant production and N mineralization in central U.S. grasslands. Journal of Vegetation Science 13:383-394.

Benning, T.L., and T.R. Seastedt. 1995, Landscape-level interactions between topoedaphic features and nitrogen limitation in tallgrass prairie. Landscape Ecology 10:337-348.

Bottner, P. 1985. Response of microbial biomass to alternate wet and dry conditions in a soil incubated with C-14-labelled and N-15-labelled plant material. Soil Biology and Biochemistry 17:329-337.

Breman, H., and C.T. de Wit. Rangeland productivity and exploitation in the Sahel. Science 221:1341-1343.

Briggs, J.M., and A.K. Knapp. 1995. Interannual variability in primary production in tallgrass prairie: climate, soil moisture, topographic positions, and fire as determinants of aboveground biomass. American Journal of Botany 82:1024-1030.

Briggs, J.M., T.R. Seastedt, and D.J. Gibson. 1989. Comparative analysis of temporal and spatial variability in aboveground production in a deciduous forest and prairie. Holarctic Ecology 12:130-136.

Burke, I.C. 1989. Control of nitrogen mineralization in a sagebrush steppe landscape. Ecology 70:1115-1126.

Burke, I.C., W.K. Lauenroth, and W.J. Parton. 1997. Regional and temporal variation in net primary production and nitrogen mineralization in grasslands. Ecology 78:1330-1340.

Cabrera, M.L., and D.E. Kissel. 1988. Evaluation of a method to predict nitrogen mineralized from soil organic matter under field conditions. Soil Science Society of America Journal 52:1027-1031.

Chapin, F.S. III, P.M. Vitousek, and K. Van Cleve. 1986. The nature of nutrient limitation in plant communities. American Naturalist 127:48-58.

Ciompi, S., E. Gentili, L. Guidi, and G.F. Soldatini. 1996. The effect of nitrogen deficiency on leaf gas exchange and chlorophyll fluorescence parameters in sunflower. Plant Science 118:177-184.

Cui, M.Y., and M.M. Caldwell. 1997a. A large ephemeral release of nitrogen upon wetting of dry soil and corresponding root responses in the field. Plant and Soil 191:291-299.

Cui, M.Y., and M.M. Caldwell. 1997b. Growth and nitrogen uptake by *Agropyron desertorum* and *Pseudoroegneria spicata* when exposed to nitrate pulses of different duration. Australian Journal of Plant Physiology 24:637-642.

Das, B.S., G.J. Kluttenberg, and G.M. Pierzynski. 1995. Temperature dependence of nitrogen mineralization rate constant: A theoretical approach. Soil Science 159:294-300.

Davidson, E.A., P.A. Matson, P.M. Vitousek, R. Riley, K. Dunkin, G. García Méndez, and J.M. Maass. 1993. Processes regulating soil emissions for NO and N_2O seasonally in dry tropical forest. Ecology 74:130-139.

Delin, S., and B. Linden. 2002. Relations between net nitrogen mineralization and soil characteristics within an arable field. Acta Agriculturae Scandinavica Section B-Soil and Plant Science 52:78-85.

Dodd, J.L., and W.K. Lauenroth. 1979. Analysis of the response of a grassland ecosystem to stress. Pages 43-58 in N.R. French, editor. Perspectives in grassland ecology. Ecological Studies 32. Springer-Verlag, New York, New York, USA.

Dodd, M.B., W.K. Lauenroth, and J.M. Welker. 1998. Differential water resource use by herbaceous and woody plant life-forms in a shortgrass steppe community. Oecologia 117:504-512.

Drury, C.F., T.Q. Zhang, B.D. Kang. 2003. The non-limiting and least limiting water ranges for soil nitrogen mineralization. Soil Science Society of America Journal 67:1388-1404.

Epstein, H.E., I.C. Burke, and W.K. Lauenroth. 2002. Regional patterns of decomposition and primary production rates in the U.S. Great Plains. Ecology 83:320-327.

Epstein, H.E., I.C. Burke, A.R. Mosier and G.L. Hutchinson. 1998. Plant functional type effects on trace gas fluxes in the shortgrass steppe. Biogeochemistry 42:145-168.

Epstein, H.E., W.K. Lauenroth and I.C. Burke. 1997. Effects of temperature and soil texture on ANPP in the U.S. Great Plains. Ecology 78:2628-2631.

Epstein, H.E., W.K. Lauenroth, I.C. Burke and D.P. Coffin. 1996. Ecological responses of dominant grasses along two climatic gradients in the Great Plains of the United States. Journal of Vegetation Science 7:777-788.

Ettershank, G., J. Ettershank, M. Bryan, and W.G. Whitford. 1978. Effects of nitrogen fertilization on primary production in a Chihuahuan Desert ecosystem. Journal of Arid Environments 1:135-139.

Fierer, N., and J.P. Schimel. 2002. Effects of drying-rewetting frequency on soil carbon and nitrogen transformations. Soil Biology and Biochemistry 34:777-787.

Frank, D.A., and R.D. Evans. 1997. Effects of native grazers on grassland N cycling in Yellowstone Nation al Park. Ecology 78:2238-2248.

Friend, A.D. 1995. PGEN – an integrated model of leaf photosynthesis, transpiration, and conductance. Ecological Modelling 77:233-255.

Gao, Q., and M. Yu. 1998. A model of regional vegetation dynamics and its application to the study of Northeast China Transect (NECT) responses to global change. Global Biogeochemical Cycles 12:329-344.

Grime, J.P. 1977. Evidence for the existence of three primary strategies in plants and its relevance to ecological and evolutionary theory. American Naturalist 111:1169-1194.

Hamerlynck, E.P., T.E. Huxman, J.R. McAuliffe, and S.D. Smith. 2004. Carbon isotope discrimination and foliar nutrient status of *Larrea tridentata* (creosote bush) in contrasting Mojave Desert soils. Oecologia 138:210-215.

Heitholt, J.J., R.C. Johnson, and D.M. Ferris. 1991. Stomatal limitation to carbon-dioxide assimilation in nitrogen-stressed and drought-stressed wheat. Crop Science 31:135-139.

Herlihy, M. 1979. Nitrogen mineralization in soils of varying texture, moisture and organic matter. Plant and Soil 53:255-267.

Hook, P.B., and I.C. Burke. 2000. Biogeochemistry in a shortgrass landscape: Control by topography, soil texture, and microclimate. Ecology 81:2686-2703.

Hooper, D.U., and L. Johnson. 1999. Nitrogen limitation in dryland ecosystems: Responses to geographical and temporal variations in precipitation. Biogeochemistry 46:247-293.

Horn, B.E., and E.F. Redente. 1998. Soil nitrogen and plant cover of an old-field on the shortgrass steppe in southeastern Colorado. Arid Soil Research and Rehabilitation 12:193-206.

Hutchinson, G.L., W.D. Guenzi, and G.P. Livingston. 1993. Soil-water controls on aerobic soil emissions of gaseous nitrogen-oxides. Soil Biology and Biochemistry 25:1-9.

Ivans, C.Y., A.J. Leffler, U. Spaulding, J.M. Stark, R.J. Ryel, and M.M. Caldwell. 2003. Root responses and nitrogen acquisition by *Artemisia tridentata* and *Agropyron desertorum* following small summer rainfall events. Oecologia 134:317-324.

Jamieson, N., R. Monaghan, D. Barraclough. 1999. Seasonal trends of gross N mineralization in a natural calcareous grassland. Global Change Biology 5:423-431.

Jobbágy, E.G., O.E. Sala, and J.M. Paruelo. 2002. Patterns and controls of primary production in the Patagonian Steppe: a remote sensing approach. Ecology 83:307-319.

Keddy, P.A. 1992. Assembly and response rules: two goals for predictive community ecology. Journal of Vegetation Science 3:157-164.

Kieft, K.L., E. Soroker, and M.K. Firestone. 1987. Microbial biomass response to a rapid increase in water potential when dry soil is wetted. Soil Biology and Biochemistry 19:119-126.

Klages, M.G., and D.E. Ryerson. 1965. Effect of nitrogen and irrigation on yield and botanical composition of western Montana range. Agronomy Journal 57:78-81.

Knapp, A.K., J.M. Briggs, and J.K. Koelliker. 2001. Frequency and extent of water limitation to primary production in a mesic temperate grassland. Ecosystem 4:19-28.

Knapp, A.K., J.T. Fahnestock, S.P. Hamburg, L.B. Statland, T.R. Seastedt, and D.S. Schimel. 1993. Landscape patterns in soil-water relations and primary production in tallgrass prairie. Ecology 74:549-560.

Knapp, A.K., and T.R. Seastedt. 1986. Detritus accumulation limits production of tallgrass prairie. BioScience 36:662-668.

Knoop, W.T., and B.H. Walker. 1985. Interactions of woody and herbaceous vegetation in a southern African savanna. Journal of Ecology 73:235-253.

Lane, D.R., D.P. Coffin, and W.K. Lauenroth. 1998. Effects of soil texture and precipitation on above-ground net primary productivity and vegetation structure across the Central Grassland Region of the United States. Journal of Vegetation Science 9:239-250.

Lauenroth, W.K. 1979. Grassland primary production: North American grasslands in perspective. Pages 3-24 in N. French, editor. Perspectives in grassland ecology. Springer-Verlag, New York, New York, USA.

Lauenroth, W.K., and I.C. Burke. 1995. Great Plains, climate variability. Pages 237-249 in W.A. Nierenberg, editor. Encyclopedia of environmental biology, Volume 2. Academic Press, San Diego, California, USA.

Lauenroth, W.K., J.L. Dodd, and P.L. Sims. 1978. The effects of water- and nitrogen-induced stresses on plant community structure in a semiarid grassland. Oecologia 36:211-222.

Lauenroth, W.K., and O.E. Sala. 1992. Long-term forage production of North American shortgrass steppe. Ecological Applications 2:237-403.

Le Houérou, H.N., R.L. Bingham, and W. Skerbek. 1988. Relationship between the variability of primary production and the variability of annual precipitation in world arid lands. Journal of Arid Environments 7:1-35.

Linn, D.M., and J.W. Doran. 1984. Effect of water-filled pore space on carbon dioxide and nitrous oxide production in tilled and nontilled soils. Soil Society of America Journal 48:1267-1272.

Low, A.P., J.M. Stark, and L.M. Dudley. 1997. Effects of soil osmotic potential on nitrification, ammonification, N-assimilation, and nitrous oxide production. Soil Science 162:16-27.

McNaughton, S., F. Banyikwa, and M. McNaughton. 1997. Promotion of the cycling of diet-enhancing nutrients by African grazers. Science 278:1798-1800.

McNaughton, S.J., O.E. Sala, and M. Oesterheld. 1993. Comparative ecology of African and South American arid to subhumid ecosystems. Pages 548-567 in P. Goldblatt, editor. Biological relationships between Africa and South America. Yale University Press, New Haven, Connecticut, USA.

Martin, R.E., M.C. Scholes, A.R. Mosier, D.S. Ojima, E.A. Holland, and W.J. Parton. 1998. Controls on annual emissions of nitric oxide from soils of the Colorado shortgrass steppe. Global Biogeochemical Cycles 12:81-91.

Milchunas, D.G., W.K. Lauenroth, P.L. Chapman, and M.K. Kazempour. 1989. Effects of grazing, topography, and precipitation on the structure of a semiarid grassland. Vegetatio 80:11-23.

Murphy, K.L., I.C. Burke, M.A. Vinton, W.K. Lauenroth, M.R. Aguiar, D.A. Wedin, R.A. Virginia., and P.N. Lowe. 2002. Regional analysis of litter quality in the central grassland region of North America. Journal of Vegetation Science 13:395-402.

Noy-Meir, I. 1973. Desert ecosystems: environment and producers. Annual Review of Ecology and Systematics 4:25-41.

Oesterheld, M., O.E. Sala and S.J. McNaughton. 1992. Effect of animal husbandry on herbivore-carrying capacity at a regional scale. Nature 356:234-236.

Olfs, H.W., A. Neu, and W. Werner. 2004. Soil N transformations after application of N-15-labeled biomass in incubation experiments with repeated soil drying and rewetting. Journal of Plant Nutrition and Soil Science 167:147-152.

Oyarzábal, M., J.M. Paruelo, F. Del Pino, M. Oesterheld, and W.K. Lauenroth. Structural and functional plant traits of C_3 and C_4 grasses across a precipitation gradient. Plant Ecology (submitted).

Owensby, C.E., R.M. Hyde, and K.L. Anderson. 1970. Effects of clipping and supplemental nitrogen and water on loamy upland bluestem range. Journal of Range Management 23:341-346.

Parton, W.J., A.R. Mosier, and D.S. Schimel. 1988. Rates and pathways of nitrous oxide production in a shortgrass steppe. Biogeochemistry 6:45-58.

Parton, W.J., D.S. Schimel, C.V. Cole, and D.S. Ojima. 1987. Analysis of factors controlling soil organic matter levels in Great Plains grasslands. Soil Science Society of America Journal 51:1173-1179.

Paruelo J.M., F. Del Pino, W.K. Lauenroth, M. Oesterheld, and J. Loretti. 1999a. Vegetational constraints over grassland precipitation use efficiency: response of the relative growth rate of grasses to drought. ESA Abstracts, 84th Annual Meeting, Spokane, WA. p.291

Paruelo, J.M. W.K. Lauenroth, I.C. Burke, and O.E. Sala. 1999b. Grassland precipitation-use efficiency varies across a resource gradient. Ecosystems 2:64-68.

Paruelo, J.M., W.K. Lauenroth, H.E. Epstein, I.C. Burke, M.R. Aguiar and O.E. Sala. 1995. Regional climatic similarities in the temperate zones of North and South America. Journal of Biogeography 22:915-925.

Paul, K.I., P.J. Polglase, A.M. O'Connell, J.C. Carlyle, P.J. Smethurst, P.K. Khanna. 2003. Defining the relationship between soil water content and net nitrogen mineralization. European Journal of Soil Science 54:39-47.

Peri, P.L., D.J. Moot, and D.L. McNeil. 2003. An integrated model for predicting maximum net photosynthetic rate of cocksfoot (Dactylis glomerata) leaves in silvopastoral systems. Agroforestry Systems 58:173-183.

Picote L.I., G. Quaglia, F.O. Garcia, and P. Laterra. 2003. Biological and chemical response of a grassland soil to burning. Journal of Range Management 56:291-297.

Piñeiro, G., J. M. Paruelo, and M. Oesterheld. Long-term domestic herbivores grazing impacts on carbon and nitrogen cycling in South American grasslands. Global Change Biology (submitted).

Porporato, A., P. D'Odorico, F. Laio, and I. Rodriguez-Iturbe. 2003. Hydrologic controls on soil carbon and nitrogen cycles. I. Modeling scheme. Advances in Water Resources 26:45-58.

Risser, P.G., and W.J. Parton. 1982. Ecosystem analysis of the tallgrass prairie: nitrogen cycle. Ecology 63:1342-1351.

Sala, O.E., R.A. Golluscio, W.K. Lauenroth, and A. Soriano. 1989. Resource partitioning between shrubs and grasses in the Patagonian steppe. Oecologia 81:501-505.

Sala, O.E., and W.K. Lauenroth. 1982. Small rainfall events: an ecological role in semiarid regions. Oecologia 53:301-304.

Sala, O.E., W.K. Lauenroth, and W.J. Parton. 1992. Long-term soil water dynamics in the shortgrass steppe. Ecology 73:1175-1181.

Sala, O.E., W.J. Parton, L.A. Joyce, and W.K. Lauenroth. 1988. Primary production of the central grassland region of the United States. Ecology 69:40-45.

Scanlon, T.M., J.D. Albertson, K.K. Caylor, and C.A. Williams. 2002. Determining land surface fractional cover from NDVI and rainfall time series for a savanna ecosystem. Remote Sensing of Environment 82:376-388.

Schimel, D.S., B.H. Braswell, and W.J. Parton. 1997. Equilibration of the terrestrial water, nitrogen, and carbon cycles. Proceedings of the National Academy of Sciences of the United States of America 94:8280-8283.

Schimel, D.S., T.G.F. Kittel, A.K. Knapp, T.R. Seastedt, W.J. Parton, and V.B. Brown. 1991. Physiological interactions along resource gradients in a tallgrass prairie. Ecology 72:672-684.

Schimel, D.S., and W.J. Parton. 1986. Microclimate controls of nitrogen mineralization and nitrification in shortgrass steppe soils. Plant and Soil 93:347-357.

Schimel, D.S., M.A. Stillwell, and R.G. Woodmansee. 1985. Biogeochemistry of C, N, and P in a soil catena of the shortgrass steppe. Ecology 66:276-282.

Schimel, D.S., VEMAP Participants, and B.H. Braswell. 1997b. Continental scale variability in ecosystem processes: models, data, and the role of disturbance. Ecological Monographs 67:251-271.

Seastedt, T.R., J.M. Briggs, and D.J. Gibson. 1991. Controls of nitrogen limitation in tallgrass prairie. Oecologia 87:72-79.

Seastedt, T.R., and A.K. Knapp. 1993. Consequences of nonequilibrium resource availability across multiple time scales: The transient maxim hypothesis. American Naturalist 141:621-633.

Seagle, S.W., and S.J. McNaughton. 1993. Simulated effects of precipitation and nitrogen on Serengeti grassland productivity. Biogeochemistry 22: 157-178.

Singh, J.S., D.G. Milchunas, and W.K. Lauenroth. 1998. Soil water dynamics and vegetation patterns in a semiarid grassland. Plant Ecology 134:77-89.

Smart, D.R., J.M. Stark, and V. Diego. 1999. Resource limitation to nitric oxide emissions from a sagebrush-steppe ecosystem. Beiogeochemistry 47:63-86.

Smika, D.E., H.J. Haas, and J.F. Power. 1965. Effects of moisture and nitrogen fertilizer on growth and water use by native grass. Agronomy Journal 57:483-486.

Soriano, A., and O.E. Sala. 1983. Ecological strategies in a Patagonian arid steppe. Vegetatio 56:9-15.

Tilman, D. 1987. Secondary succession and the pattern of plant dominance along experimental nitrogen gradients. Ecological Monographs 57:189-214.

Tilman, D. 1988. Plant strategies and the dynamics and structure of plant communities. Princeton University Press, Princeton, NJ, USA.

Tracy, B.F., and D.A. Frank. 1998. Herbivore influence on soil microbial biomass and nitrogen mineralization in a northern grassland ecosystem: Yellowstone National Park. Oecologia 114:556-562.

Turner, C.L., J.M. Blair, R.J. Schartz, and J.C. Neel. 1997. Soil N and plant responses to fire, topography, and supplemental N in tallgrass prairie. Ecology 78:1832-1843.

Verchot, L.V., P.M. Groffman, and D.A. Frank. 2002. Landscape versus ungulate control of gross mineralization and gross nitrification in semi-arid grasslands of Yellowstone National Park. Soil Biology and Biochemistry 34:1691-1699.

Vigil, M.F., B. Eghball, M.L. Cabrera, B.R. Jakubowski, and J.G. Davis. 2002. Accounting for seasonal nitrogen mineralization: An overview. Journal of Soil and Water Conservation 57:464-469.

Vinton, M.A., and I.C. Burke. 1995. Interactions between individual plant species and soil nutrient status in shortgrass steppe. Ecology 76:1116-1133.

Vinton, M.A., D.C. Hartnett, E.J. Finck, and J.M. Briggs. 1993. Interactive effects of fire, bison (*Bison-bison*) grazing and plant community composition in tallgrass prairie. American Midland Naturalist 129:10-18.

Vitousek, P.M. 1982. Nutrient cycling and nutrient use efficiency. American Midland Naturalist 119:553-572.

Wedin, D. A. 1995. Species, nitrogen, and grassland dynamics: the constraints of stuff. Pages 253-262 in C. Jones and J. H. Lawton, editors. Linking species and ecosystems. Champan & Hall.

Yu, M., J.E. Ellis, Q. Gao, and H.E. Epstein. Regional analysis of climate, primary production, and livestock density in Inner Mongolia Autonomous Region, China. Journal of Environmental Quality, in press.

Zak, D.R., D. Tilman, R.R. Parmenter, C.W. Rice, F.M. Fisher, J. Vose, D. Milchunas, and C.W. Martin. 1994. Plant production and soil microorganisms in late-successional ecosystems: a continental study. Ecology 75:2333-2347.

Chapter 13

INTERACTIONS BETWEEN WATER AVAILABILITY AND NUTRIENT CYCLING IN DRY TROPICAL FORESTS

Larissa READ[1] and Deborah LAWRENCE[2]

[1] *Intermountain Support Office, National Park Service, 12795 W. Alameda Parkway, Lakewood, CO, 80228 and Department of Environmental Sciences, University of Virginia, P.O. Box 400123, Charlottesville, VA, 22904-4123, USA – email: larissa_read@nps.gov*

[2] *Department of Environmental Sciences, University of Virginia, P.O. Box 400123, Charlottesville, VA, 22904-4123, USA – email: lawrence@virginia.edu*

1. An overview of dry tropical forest ecology

1.1. GENERAL CHARACTERISTICS OF DRY TROPICAL FOREST

Current scientific and public attention on various aspects of global change has highlighted the complex relationship between climatic events and ecological function in terrestrial ecosystems. Dry tropical forests, which cover more area and are more suitable for human habitation than wet tropical forests, provide an excellent example of this interaction because they display structure and function that are closely linked to sporadic rainfall. As the distribution of dry tropical forest across the globe appears to be increasing (Brown and Lugo 1990; Cairns et al. 2000) in response to the interactions of global change and human disturbance, an understanding of the complexity of dry tropical forest ecosystems has become increasingly important.

Dry tropical forests are defined by marked seasonality and interannual variability in precipitation, which ranges from 250-2000 mm/year and limits forest growth, structure, and function (Murphy and Lugo 1986a). These forests are frost-free and have a mean annual biotemperature greater than 17°C. Dry tropical forests often have two distinct dry periods, one major and one minor, which correspond to periods of high litterfall (Murphy and Lugo 1986a). The ecology of dry tropical forest is especially complex because many biological activities, such as growth, phenology, and nutrient cycling, are tightly coupled with patterns in precipitation (Borchert 1994; Murphy and Lugo 1986a).For more detail than we can provide, see the in-depth review of dry tropical forest ecology compiled by Mooney, Bullock, and Medina (1995).

Forest structure and productivity in dry tropical forests are limited by the drought conditions that occur for several to many months of the year. Net primary productivity is 50-75% of that of wet tropical forest (Murphy and Lugo 1986a). Estimates of biomass are 80-320 tons per hectare (Mg/ha) in dry tropical forest and 270-1190 Mg/ha in the wet tropics. This trend is evident even within dry tropical systems, as biomass in dry tropical forest generally increases with increasing precipitation (Brown and Lugo 1982; Read and Lawrence 2003a). Although above-ground biomass in dry tropical forest is lower than in the wet tropics, belowground root biomass can comprise up to half of total forest biomass (Murphy and Lugo 1986b). This substantial below-ground biomass affects ecosystem processes by storing organic matter and nutrients.

The vegetation in dry tropical forest is less diverse than in the wet tropics (Gentry 1995), and mean canopy height, basal area, and leaf area are about half that found in the wet tropics (Murphy and Lugo 1986a). Litterfall, leaf flush and flowering often occur during the dry season, despite the stress induced by the severe water deficit (Daubenmire 1972; Bullock and Sollis-Magallanes 1990; Borchert 1994). Reproduction through coppicing is common in dry tropical forest because regeneration through seed production is uncertain in dry climates and fire is more

P. D'Odorico and A. Porporato (eds.), Dryland Ecohydrology, 217–232.

prevalent (Kauffman 1991); likewise, the dry climate is less likely to cause decay in coppiced trees (Ewel 1980). Tree coppicing has marked effects on dry tropical forest structure. For example, in their study of Guanica Forest, Puerto Rico, Murphy and Lugo (1986b) found that 57% of trees were of coppice origin in a site that not been grazed or logged in more than 50 years. Coppicing can also result in clumped vegetation and scattered leaf area (Ewel 1980), which are also common features of dry tropical forest structure.

1.2. THE GLOBAL DISTRIBUTION OF DRY TROPICAL FORESTS

Dry tropical forests cover 42% of closed tropical forested areas, compared to 33% covered by moist forest, and only 25% by wet tropical forest (Brown and Lugo 1982). Dry tropical forests are found on the continents of Asia, Africa, North and South America, and Australia. The historic distribution of dry tropical forest is hard to discern because disturbed dry tropical forest may have become scrub woodlands and savannas (Murphy and Lugo 1986a). However, it is generally believed that dry tropical forest once covered a larger area than presently occurs. Pennington et al. (2000) present a unique study of Neotropical dry tropical forest biogeography based on taxonomy and distribution of dry tropical species. They suggest that a closed seasonally dry tropical forest covered a larger area that is now occupied by only fragmented dry tropical forest. These forests served as refugia for drought-tolerant, dry tropical species during cooler, drier periods, out of which the current patchy distribution of dry tropical forest developed at the end of the Ice Age (Pennington et al. 2000). The future distribution of dry tropical forest will likely be determined by both natural and anthropogenic change. Current climate models predict that different regions of the world will respond differently to climate change. Longer dry seasons may occur in South America, while Asia, India, and Africa may experience shorter dry seasons (Silver 1998). The impacts of global climate change remain to be seen, and many climate models do not agree on the rate of change or future distribution of dry tropical forest, but it is indisputable that human activity is altering the structure and function of these forests.

1.3. HUMAN IMPACTS ON DRY TROPICAL FOREST

Both in the past and in modern times, dry tropical forests have provided favorable living conditions for humans because of their moderate climate and fertile soils, and major urban centers have historically been located in the dry tropics rather than in moister life zones (Murphy and Lugo 1986a). Relatively small statured, dry tropical forests are easier to clear for agriculture and pasture than wet tropical forest, and their soils tend to be more fertile due to reduced leaching of nutrients (Murphy and Lugo 1986a). In addition, dry tropical forests are cleared for habitation and fuel wood. The most direct effect of human use of dry tropical forest is the disturbance of mature forest and the creation of secondary forests. In the late 1980s, secondary forest comprised about 40% of closed tropical forests worldwide, and new secondary forest was being created at a rate of about 9 million ha/yr (Brown and Lugo 1990). At present, secondary forests represent approximately 60% of tropical forests worldwide (ITTO). In their study of land-use change in an area covering about one-quarter of the landmass of Mexico, Cairns et al. (2000) found that over a 15-year period, there was a 64% increase in the area of agricultural systems. In addition, the area of closed forest declined by 26%, and open forest area declined by 31%. They estimated that these changes released about 20% of the region's 1977 carbon (C) pool (Cairns et al. 2000).

The indirect effects of land conversion are numerous. Belowground biomass is augmented by forest cutting, which leaves relictual roots in the soil (see Murphy and Lugo 1986b). Logged areas have a higher fuel load than undisturbed areas, and are therefore more susceptible to fire during periods of drought (Silver 1998). Fire activity in dry tropical forest has therefore been exacerbated by human activity (Murphy and Lugo 1986a), both from increased habitation and from use of fire as a method of clearing land.

In addition to changes caused directly by human activity, the predicted effects of climate change on tropical forests are severe because of their role in the global C cycle. Tropical forests store an estimated 46% of the terrestrial C pool (Brown and Lugo 1982) and over half of the Earth's aboveground C (Saugier et al. 2001). Although dry tropical forests store only 22% of the global organic matter pool, less than that stored in wet tropical forests (Brown and Lugo 1982), dry tropical forests store more belowground C than wet tropical forest, especially at depths greater than 1 meter (Murphy and Lugo 1986a; Silver 1998). The C storage of tropical forests may decline with climate change. First, increased fire frequency may reduce aboveground C. Second, changes in the length of the dry season might alter the structure or composition of the vegetation. Changes in seasonal rainfall will also affect soil microbial dynamics with potential effects on belowground C (Silver 1998).

2. Nutrient cycling in dry tropical forests

2.1 ECOSYSTEM PROCESSES

Nutrient cycling in dry tropical forest is largely driven by the low and temporally variable precipitation that these ecosystems receive. In general, nutrients accumulate in the soil during the dry period because of reduced leaching, low rates of decomposition, minimal microbial turnover, and little plant uptake. During the wet season, nutrient cycling resumes as nutrients are released from the soil, litter, and microbes, and become available to the plant community (Jaramillo and Sanford 1995).

2.1.1 Litter nutrient cycling

As in most forests, leaf litter is the main pathway for movement of organic matter, phosphorus (P), nitrogen (N), calcium (Ca), potassium (K) and magnesium (Mg) from vegetation to the soil (Vitousek 1982). However, in dry tropical forests, root biomass is much greater than in wetter forests. As a consequence, roots may provide a significant source of belowground litter nutrients (Cuevas 1995, Jaramillo and Sanford 1995). One of the fundamental trade-offs governing nutrient cycling through the litter, and through the entire plant-soil system, is whether vegetation is deciduous or evergreen in response to drought. The structure and physiology associated with leaves, stems and roots of deciduous vs. evergreen trees have cascading effects on ecosystem processes. The leaves of deciduous species tend to be less tough and to have higher nutrient concentrations than those of evergreen species (Medina 1984; Mooney et al 1984), making their tissues decompose much more rapidly. The physiological adaptations for deciduous or evergreen leaves are linked with stem and root characteristics (Holbrook et al 1995) that affect the timing and depth of nutrient uptake from seasonally dry soils. The hydraulic properties of narrower, shorter vessels found in dry forest trees (Barajas-Morales 1985) may reduce the rate of nutrient uptake due to lower conductance efficiency (Holbrook et al 1995). In addition, these structural properties make the wood of dry tropical forest denser than that of wet forests (Barajas-Morales 1987), reducing the turnover time of nutrients associated with coarse woody debris.

In evaluating litter nutrient dynamics, Jaramillo and Sanford (1995) have stated that dry tropical forests tend not to be nutrient limited. However, they and others have suggested that P may limit productivity (Vitousek 1982, 1984; Murphy and Lugo 1986a, 1986b, but see Campo et al. 2001). Vitousek (1984) used an analysis of the ratio of litter mass to its nutrient content (nutrient use efficiency, NUE) as a way of comparing nutrient use in forests. Forests on nutrient-poor substrates exhibit higher NUE, which may be reflected in production of equivalent biomass using fewer nutrients, as well as higher resorption of foliar nutrients prior to litterfall (Vitousek 1982, 1984; Boerner 1984). Tropical forests display lower nitrogen use efficiency (N-UE) compared to phosphorus use efficiency (P-UE), suggesting that P is limiting in these forests (Vitousek 1984). In addition, P-UE in dry tropical forests are among the highest reported for the tropics (Vitousek 1984; Lugo and Murphy 1986; Singh 1989; Read and Lawrence 2003b).

Phosphorus availability is low in the tropics for several reasons: the soils tend to be highly weathered (Babbar and Richter 1991), atmospheric inputs are negligible (Campo et al. 2001), P is easily leached from soils, and it may be tightly adsorbed to the clay oxides found in many tropical soils (Vitousek 1984) or bound to calcium in limestone-derived soils (Lugo and Murphy 1986, Tiessen et al 1983). Drought conditions in dry tropical forests exacerbate the situation by preventing P and other nutrients from dissolving into the soil solution, and also by limiting the ability of plants to take up available nutrients from the soil (Lugo and Murphy 1986).

Tropical forest vegetation responds to low P availability by conserving litter P through foliar resorption (Chapin 1980; Vitousek 1982; Lugo and Murphy 1986; Murphy and Lugo 1986a). Resorption may be an especially important mechanism in the dry tropics, where nutrient cycling is so tightly coupled with precipitation patterns. For example, P resorption was high in Guanica Forest, Puerto Rico, where retranslocation accounted for 65% of the P requirement (Murphy and Lugo 1986a). In their study of nutrient resorption in 90 different dry tropical tree species in India, Lal et al. (2001a, 2001b) found that foliar P resorption was higher than both N and K resorption, although species also had a significant effect. In the Southern Yucatan, an investigation of nutrient resorption proficiency, or the absolute level to which nutrients are reduced in senesced leaves (sensu Killingbeck 1996), showed that P proficiency was highest in older and drier sites but N proficiency did not vary with age or annual precipitation regime (Read and Lawrence 2003b). If resorption proficiency is correlated with the degree of nutrient limitation, these results suggest that phosphorus limitation may develop with forest age, as the same soil P pool is used to produce ever larger trees. This successional development of P limitation in dry forests may ultimately be caused by water limitation, through a depression of soil biological activity (Cuevas 1995). Drought inhibits plant and microbial access to more tightly bound P in the soil. Even with the greater plant biomass of older forests, root exploration and microbial activity will ultimately be regulated by soil moisture.

2.1.2 Soils and decomposition

Like litter nutrient cycling, nutrient cycling in the soils of dry tropical forest is generally limited by water availability. Decomposition and mineralization rates are low during the dry season, both due to dry conditions on the forest floor and a decrease in microbial activity associated with low soil moisture (Ewel 1976; Arnason and Lambert 1982; Singh et al. 1989; Garcia-Mendez et al. 1991; Cuevas 1995). In a study of litter decomposition in Guatemala, Ewel (1976) found that soil type affected the rate at which various nutrients and minerals were lost, likely due to differences in soil water content. However, although water availability is a critical determinant of many processes in dry tropical forests, it is not necessarily the primary driver of all forest processes. For example, Harmon et al. (1995) found that woody debris from different tree species in the Yucatan decomposed at different rates due to the quality of the wood itself, rather than climatic conditions.

The most dramatic difference between the soils of wet and dry tropical forests is the preponderance of roots in the latter. The mean proportion of total biomass in roots is estimated at 27-34% for dry forests compared with a mean of 11-16% for wet forests (Holbrook et al. 1995, Jaramillo and Sanford 1995). Because the surface soils dry out periodically, roots are found at greater depth (Kummerow et al 1990), further from the nutrient inputs of aboveground litter. This situation may exacerbate nutrient limitation as the organs for uptake are spatially segregated from a readily available nutrient source. Upon wetting, however, fine root proliferation is rapid (Cuevas 1995) and may minimize any lag between aboveground inputs and uptake by roots. Limited data suggest that fine root production (Holbrook et al 1995) and nutrient content (Jamarillo and Sanford 1995) are higher in dry tropical forests than in temperate or wet tropical forests, and that they can decompose as rapidly as leaves (Srivastava et al 1986). Additionally, the prevalence of coppicing as a growth form in dry tropical forests can result in a larger proportion of belowground biomass than in other tropical forests due to greater root production

(Murphy and Lugo 1986b). Roots, and fine roots in particular, function as an important nutrient source as well as playing a fundamental role in water and nutrient uptake.

2.1.3 Microbial activity

Microbial activity in dry tropical forests is substantially moderated by water availability. Singh et al. (1989) suggest that microbes act as a sink for nutrients during dry periods when microbes have access to water that is unavailable to plants, and release these nutrients during wet periods. Microbe-regulated nutrient turnover in the wet season may also be enhanced by grazers in the soil fauna, which make dead microbial cells and materials available for plant uptake (Singh et al. 1989). Little or no net nitrification occurred during the dry period, but high nitrification rates were observed during the wet period. In addition, microbial biomass decreased and soil nutrient pools declined during the wet season as N mineralization increased, suggesting that microbial N is an important source for plants (Singh et al. 1989). Srivastava (1992) found that the highest microbial mass of C, N, and P occurred during the dry season, and the lowest levels during the wet season. Campo et al. (1998) found comparable results in a soil wetting experiment in Chamela, where soluble P and microbial P were higher in the dry season than in the wet season. The initial pulse of soil nutrients detected at the beginning of the rainy season is likely due to microbial biomass turnover, which can support the rapid initial growth of vegetation at that time (Singh et al. 1989; Srivastava 1992; Campo et al. 1998). Jamarillo and Sanford (1995) suggest that nutrient release-immobilization cycles are important not only at the onset of the wet season, but throughout the wet (growing) season, when periodic dry spells occur. In dry tropical forests, the role of above- and below-ground litter, soils, and microbes in nutrient storage and cycling is moderated to a great extent by water availability. The relative contribution of microbes, roots, and aboveground litter to plant nutrient uptake is an important avenue for future research (Jaramillo and Sanford 1995).

2.2 EFFECTS OF NATURAL DISTURBANCE ON NUTRIENT CYCLING

2.2.1 Hurricanes and abnormal climatic events

Hurricanes are a recurrent climatic event in parts of the dry tropics, and affect both forest structure and distribution of nutrients. Hurricanes move large amounts of organic matter to the soil over a short time period due to litterfall, woody debris, and root death. Hurricanes also alter nutrient cycling over a longer time frame because of increased runoff and reduced plant uptake (Silver 1998). Damage to dry tropical forest structure from rain and high winds during hurricanes can be substantial. For example, Arnason and Lambert (1982) report that about 900 kg litter / ha fell at their site in Belize during Hurricane Greta in October 1978. Hurricane Gilbert, which struck the Yucatan in September 1988, did not immediately cause tree mortality in the northeastern region of the peninsula, although all the trees were damaged or defoliated (Whigham et al. 1991). However, after a year and a half, almost 13% of trees had died. Immediately after the hurricane, coarse woody debris increased from 31 Mg/ha to 47 Mg/ha, and standing stocks of N, Ca, Mg, and K in coarse woody debris increased up to 36%, while that for P and manganese increased 57%. Additionally, canopy growth occurred at the highest rates recorded during the five previous years of study, probably due to nutrients from the downed debris that became available to vegetation, as well as increased light levels from opened canopy. Interestingly, natural fire had a more devastating effect than the hurricane, by consuming much of the post-hurricane litter and killing 85% of trees at one site (Whigham et al. 1991).

Although not as extreme as the effect of hurricanes, abnormal drought and precipitation patterns can play an important role in the ecosystem processes of dry tropical forests. For example, during the extreme drought caused by the 1997 El Nino Southern Oscillation (ENSO), deciduous trees in Guanacaste, Costa Rica did not shed their leaves, which were young at the time (Borchert et al. 2002). However, leaf turnover occurred several months earlier than normal once the rainy season began, and leaves were shed again during the next regular dry season (Borchert et al. 2002). Since litterfall is one of the primary pathways for nutrient cycling in dry tropical forests, and litter decomposition is tightly coupled with seasonal water availability, climatic events such as abnormal drought can have profound effects on the nutrient cycle in dry tropical forests as a whole.

2.2.2 *Typical climatic processes*

In addition to precipitation, other aspects of the weather patterns in dry tropical forest have important ramifications for nutrient cycling. For example, dry season winds move litter into microsites, causing patchy litter accumulation that results in irregular nutrient distribution during the wet season (Roy and Singh 1994). At the beginning of the wet season, throughfall nutrient levels are highest, likely due to rainfall enrichment from atmospheric deposition, photodegradation of plant material, and insect activity during the dry season (Kauffman et al. 1993; Campo et al. 2001; Maass et al. 2002). In the heavy rains and high winds of the wet season, fragmentation of branches can also result in nutrient-enriched leachate transferred to the soil (Maass et al. 2002). Due to the critical link between precipitation and nutrient cycling in dry tropical forests, natural disturbances on both the small and large scale can have dramatic impacts on forest structure and function due to their effect on nutrient availability, accumulation, and transfer.

2.3 EFFECTS OF HUMAN DISTURBANCE ON NUTRIENT CYCLING

The limited literature available suggests that nutrient cycling in *secondary* dry tropical forest is generally water- and perhaps P-limited as in mature dry tropical forest. Soil nutrient dynamics are altered dramatically during logging, slash burning and crop installation, or clearing for pasture (Buschbacher et al. 1988; Kauffman et al. 1993; Ellingson et al. 2000; Giardina et al. 2000). Likewise, timber or fuel wood extraction results in the redistribution and removal of biomass and nutrients (Murphy and Lugo 1986a; Brown and Lugo 1990).

Recovery of dry tropical forest from disturbance is thought to be faster than in the wet tropics, likely due to coppicing (Murphy and Lugo 1986a). The rate and trajectory of recovery in secondary dry tropical forests is impacted to a large extent by the type and degree of disturbance, its impact on nutrient levels in the substrate, and water availability (Ewel 1980; Brown and Lugo 1990; Read and Lawrence 2003a). Recovery of mature forest biomass following clearing in dry tropical forest takes at least 50 years (Brown and Lugo 1990; Read and Lawrence 2003a) although species composition can recover more rapidly (Perez-Salicrup 2004). Litter production in young secondary forests is high, reaching mature forest levels after 12-25 years (Brown and Lugo 1990; Lawrence and Foster 2002).

The current literature on human disturbance in tropical forest is substantial, but the primary focus of the research has been on wet and moist regions. Many of the impacts of human activity on nutrient cycling in the dry tropics are similar to those reported in other areas of the tropics. We refer readers to a review by Chazdon (2003) and additional works with more of a focus on nutrient dynamics (Uhl and Jordan 1984; Vitousek 1984; Buschbacher et al. 1988; Uhl et al 1988; Brown and Lugo 1990; Hughes et al. 1992; Lugo 1992; Kauffman et al. 1993; Zimmerman et al 1995; Fearnside and Guimaraes 1996; Tucker et al 1998; Hughes et al 1999; Hughes et al 2000; Moran et al 2000, Pascarella et al 2000; Steininger 2000; Giardina et al. 2000; Lawrence and Schlesinger 2001; Hughes et al 2002).

3. The role of water in dry tropical forest ecosystems

3.1 THE EFFECTS OF VARIABLE PRECIPITATION ON PRODUCTION

The role of water in dry tropical forests is not limited to its direct impact on nutrient cycling. At both large and small scales, water regulates and modifies forest structure and function, causing secondary effects on nutrient cycling. In dry forests receiving up to 1500 mm in annual rainfall, litter production was positively correlated with total rainfall (Martinez-Yrizar 1995). Beyond 1500 mm, there was no relationship. Seasonal and interannual variability in precipitation can be substantial—for example, the coefficient of variation for annual rainfall in temperate zones is about 15%, compared to 30% in the tropics—and extreme years may be more important than average years in regulating dry tropical forest structure and function (Murphy and Lugo 1986a; Whigham et al. 1990). Interannual variability in precipitation is often caused by storms that occur in normally dry months (Martinez-Yrizar and Sarukhan 1990). It may also be related to hurricanes and prolonged dry seasons associated with ENSO. Variable precipitation affects forest structure by moderating the distribution of resources within and available to vegetation. In the northeastern Yucatan Peninsula, variation in annual rainfall (almost 600 mm over a 4-year period) was correlated with annual differences in tree growth and litter production (Whigham et al. 1990). Litter production was negatively correlated with precipitation in a given year, and basal area increased significantly with total precipitation in the current and previous years. The basal area response was more pronounced than the litter response (Whigham et al. 1990). In this case, water availability affected nutrient cycling through plant uptake and biomass storage, rather than through litter production and litterfall.

Litterfall and debris accumulation, however, can also be strongly influenced by the spatial and temporal scale of water availability. Litterfall increases dramatically during the dry season, but decreases rapidly with the onset of the rainy season (see studies on seasonality of litterfall in Lambert et al. 1980; Arnason and Lambert 1982; Lugo and Murphy 1986; Martinez-Yrizar and Sarukhan 1990; Singh 1992; Read and Lawrence 2003b). In Chamela, Mexico, the rate of litterfall was highest at the beginning of the dry season at a hill site, but peak litterfall was delayed by several months at a lower-elevation valley site (Martinez-Yrizar and Sarukhan 1990). The two sites exhibited different time-lags between maximum rainfall and maximum litterfall; a lag of four months was found on the hill site, but the valley site exhibited a six-month time lag. Spatial differences in the litterfall time-lag were likely due to the timing of soil water draw-down, rather than differences in other possible triggers such as photoperiod or temperature (Martinez-Yrizar and Sarukhan 1990).

The effect of precipitation on organic matter production and storage is evident across a range of tropical life zones (Brown and Lugo 1982,Martinez-Yrizar 1995). In the seasonally dry tropical forests of Guanacaste, Costa Rica, tree ring chronologies indicate that species responses to variation in monthly and annual rainfall were stronger than their responses to variation in temperature. This phenomenon was attributed to differences in the ability of individual species to tap available soil water (Enquist and Leffler 2001). Fine root production tracks seasonal patterns of precipitation, apparently cued by soil moisture (Cuevas 1995). Secondary production also varies systematically with precipitation. In India, the abundance of soil and litter fauna was highest during the months of greatest precipitation (Singh and Shukla 1977). Although microbial biomass may decline with either too much or too little precipitation, soil respiration, an integrated measure of soil biological activity, tends to increase with precipitation in dry forests (Cuevas 1995).

3.2 THE EFFECTS OF WATER AVAILABILITY ON NUTRIENT CYCLING

3.2.1 Effects of water availability at various spatial scales

The effects of water availability on plant uptake and nutrient cycling can be seen at both large and small scales. In their study of the effects of site heterogeneity on nutrient cycling, Roy and Singh (1994) found that troughs on the forest floor had faster decomposition rates and greater litter mass, microbial biomass, nutrient levels, and fine root biomass compared to flats. Troughs contained more herbaceous shoot biomass, which in turn reduced leaching and allowed for tree root development due to higher nutrient availability in these patchy microsites (Roy and Singh 1994). At the landscape scale, topography may also contribute to systematic differences in soil water and nutrient availability between the seasonally inundated Bajo forests and upland forests interwoven across the southern Yucatan (Lawrence, unpublished data). On a much larger scale, regional differences in annual precipitation in the Yucatan Peninsula resulted in substantial differences in litter nutrient quality. Trees in the wettest sites produced litter almost twice as rich in N and P as the litter of drier sites (Read and Lawrence 2003b). Precipitation, integrated over the annual cycle, affects the total amount of nutrients cycling in the system. The total amount of precipitation is not the only predictor of nutrient dynamics in dry systems. In addition to the initial soil wetting at the end of the dry season, Jaramillo and Sanford (1995) suggest that the timing and duration of dry periods within the wet season may have a profound impact on nutrient fluxes.

3.2.2 Phenological effects of water availability on deciduous trees

Water availability also has direct effects on forest function through its impact on phenology, which is tied to nutrient cycling because litter is the main pathway for nutrient return to the soil in the tropics. Soil water content is an important determinant of litter production and decomposition, because water stress is one of the main factors affecting leaf abscission (Lambert et al. 1980; Martinez-Yrizar and Sarukhan 1990; Borchert 1994). Leaf flush and flower development in dry tropical forests usually begins during the dry season (Murphy and Lugo 1986a; Borchert 1994). Since leaf flush often occurs before the rainy season starts (Borchert 1994), it is likely fed by nutrients that were previously resorbed (Singh et al. 1989; Lal et al. 2001b). During the dry season, plants use the little available water, likely conserved through reduced transpiration, to rehydrate stem tissues to support leaf flush (Borchert 1994). The specific allocation of these resources may allow vegetation to respond to available water first by increasing photosynthetic area, and then through storage. For example, in India, Lal et al. (2001b) found that leaf area peaked before or at the beginning of the rainy season, but leaf mass continued to rise for several months.

Plant growth is governed to a large extent by the water transport capability of individual species, and thus water availability impacts individual plant function as well. In a study of a dozen dry tropical tree species in Costa Rica, Brodribb et al. (2002) found that while evergreen species showed only a moderate increase in stem-specific conductivity at the onset of the rainy season, the responses in deciduous species ranged from negligible to nine-fold increases. Photosynthetic rates were variable among all the species during the dry season, but within two months of the first rainfall, all but one species exhibited similar photosynthetic rates (Brodribb et al. 2002). Additionally, the authors found a stronger relationship between water transport and photosynthetic measures in the dry season than in the wet season. This study highlights the importance of individual species responses to water availability, and the effect that species traits have on overall forest function in the dry tropics.

3.2.3 Effects of other vegetation on water-nutrient interactions in trees

Competition for water among vegetation, especially during the dry season, also has a significant impact on ecosystem function in dry tropical forests. Lianas and palms are structurally and functionally different than deciduous dry forest trees, and their role in dry forest ecology has only begun to be studied. Lianas are woody-stemmed climbing plants that compete with their host trees for water (Perez-Salicrup and Barker 2000). They are common in disturbed areas because of their ability to respond to canopy openings, but they also play an important role in mature forest (Dewalt et al. 2000). To understand the impact of lianas on the water status of mature dry tropical forest trees in Bolivia, leaf water potential was measured in trees with lianas intact and also in those with lianas removed in an area twice the crown radius of the host tree (Perez-Salicrup and Barker 2000). The water potential in liana-cut trees was significantly less negative than those with lianas intact, a pattern which developed within one day of cutting and lasted until the onset of the rainy season. Liana-cut trees showed higher circumference growth rates than did control trees, which the authors suggested might be attributable to true growth, expansion due to access to water, or increased access to radiation (Perez-Salicrup and Barker 2000). The results highlight the importance of lianas in reducing water availability to trees in mature dry tropical forests. Given the prevalence of lianas in secondary forests as well (Dewalt et al. 2000, Read and Lawrence 2003a), this work may also have important implications for understanding recovery of dry tropical forests following disturbance.

Likewise, palm trees are found in both secondary and mature dry tropical forest, and their resistance to fire enhances their prevalence in disturbed or burned sites (Tomlinson 1979; Arnason and Lambert 1982; Read and Lawrence 2003a). Since palm leaves decompose more slowly and have a different nutrient balance than deciduous trees, their impact on forest floor biomass and soil recovery can be substantial (Arnason and Lambert 1982). A study from Belize highlights influence of vegetation type on nutrient cycling in dry tropical forests. At a site dominated by Cohune palm, Arnason and Lambert (1982) report a litterfall rate of 4.3 Mg/ha/yr, compared to a nearby deciduous site, where litter fell at almost three times that rate (Arnason and Lambert 1982). However, accumulation on the forest floor at the palm site was almost 44 Mg/ha, compared to 7 Mg/ha at the deciduous site. Due to the extremely high level of N in the Cohune palm litter, N storage (in above-ground biomass and litter on the forest floor) at the Cohune site was almost 1200 Mg/ha, compared to 270 Mg N/ha at the deciduous site. Although litter N concentrations were high at the palm site, a slow decomposition rate resulted in soil N levels that were slightly lower than those found at the deciduous site (Arnason and Lambert 1982). In the southern Yucatan, an 18-year old secondary forest dominated by palms had over twice the basal area but only 75% of the aboveground biomass of a near by 15-year old secondary forest with no palms (Read and Lawrence 2003a). The ecohydrological effects of lianas and palms on deciduous vegetation in dry tropical forests have not yet been well-documented. However, because of their impact on the uptake, storage, and return of water and nutrients, they constitute an important albeit overlooked component of ecosystem function in the dry tropics.

4. Case studies

Dry tropical forests have not received the scientific or public attention that is prevalent for the wet tropics. However, there are several systems, especially in the Neotropics, that have been studied closely. These studies explore nutrient cycling in response to spatial and temporal variability in precipitation and water availability in general. See Table 1 for a comparison of these sites and several other selected studies that are discussed in the text.

4.1 CHAMELA, MEXICO (748 mm/yr)

The dry tropical forests of Chamela, Mexico receive low rainfall, and the vegetation is leafless for more than 5 months of the year (Martinez-Yrizar et al. 1992). As part of their study of mature dry tropical forest on a hill site and a valley site, which differed in slope, soil quality, and vegetation, Martinez-Yrizar and Sarukhan. (1990) found higher annual litterfall at the valley site (6.6 Mg/ha/yr) compared to the hill site (4.0 Mg/ha/yr). During the dry season, 75% of the canopy at the valley site becomes leafless, while 95% of the hill site canopy sheds its leaves. Soil organic matter at the valley site was lower than at the hill site (5.2% vs. 6.8%) (Martinez-Yrizar and Sarukhan 1990), suggesting more rapid decomposition and mineralization in the valley site. The hill site also experienced significant variation in total litterfall between years, suggesting that it is more susceptible to drought-related stress (Martinez-Yrizar and Sarukhan 1990). In a study at a nearby site, Maass et al. (2002) found significant differences in the mass of standing dead wood in three plots along an elevation gradient, but no differences in mass of dead wood on the forest floor. In these forests, the effect of elevation on soil moisture produced differences in litter and dead phytomass production.

In contrast to some other dry tropical forests, the Chamela forest may not be P-limited (Campo et al. 2001). Phosphorus turnover on the forest floor is slightly faster than the turnover rate of organic matter, and the concentration of P in litter is higher than seen for other forests (Campo et al. 2001). The total annual return of P to the forest floor from litterfall (3.9 kg/ha) was considered high, but annual P return from litter in mature forests of southeastern Mexico averaged 5.8 kg/ha (Read and Lawrence 2003b). In a comprehensive six-year study of P inputs, outputs, and fluxes, the authors found that P inputs averaged 0.16 kg/ha/yr, while outputs averaged 0.06 kg/ha/yr. In contrast to P cycling, outputs of Ca, K, and Mg were higher than inputs, and these nutrients accumulated in dry years but were lost in wet years (Campo et al. 2000). The authors suggest that these observations point to high retention of P in this system, low P loss, and a lack of P limitation, a condition which may be supported by rapid plant uptake (Campo et al. 2001).

4.2 GUANICA, PUERTO RICO (860 mm/yr)

In Guanica, Puerto Rico, the forest was heavily disturbed during the past, but had been protected for the past 50 years from cutting and grazing. The study site is unique because it contained an especially high stem density for mature forest—12,000 stems/ha, of which only 12% were greater than 5 m in height. Additionally, almost 50% of the total live biomass occurred belowground, likely due to the prevalence of coppiced stems and relictual roots in the soil (Murphy and Lugo 1986b).

The unique mature forest structure at Guanica contributed to its low annual litter production of 4.8 t/yr (Lugo and Murphy 1986). The annual return of nutrients through leaf and wood litter was relatively low for dry tropical forests, cycling 49 kgN/ha/yr and 0.79kgP/ha/yr. The authors estimate that 65% of the required P is retranslocated, compared to 30% of the required N, suggesting that P is cycled more efficiently in this forest. High P-UE (6067) compared to N-UE (98) and high levels of phosphorus-binding Ca in the soil also indicate the importance of P conservation in this system (Lugo and Murphy 1986). Guanica forest soils were slightly basic at pH 7.8, and had relatively high levels of nutrients (0.57 mgP/g and 1.13 % N) near the surface), due in part to reduced leaching because of low rainfall. Likewise, litter decomposition at the Guanica site was relatively slow; 95% of litter inputs would decompose within 7.3 years.

This work emphasizes the interaction of natural and anthropogenic effects on nutrient cycling in dry tropical forest. Relictual roots and coppiced stems resulting from human and hurricane disturbance have created a forest with high stem density, small stature, low production and slow nutrient turnover. Although this forest has been protected from extensive human disturbance for more than half a century (Murphy and Lugo 1986b), ecosystem processes such as nutrient cycling and development of forest structure continue to be moderated by anthropogenic as well as natural causes.

Table 1. Characteristics of selected tropical dry forest ecosystems, arranged in order of increasing annual precipitation.

Region	**Country**	**Rain (mm/yr)**	**Dry Season**	**Mean Canopy Height**	**Basal Area (m^2/ha)**	**Above-Ground Biomass (AGB)**	**Litterfall Return**	**Litter [P]**	**Litter [N]**	**Soil -OM**	**Soil type**	**Studies**
Chamela	Mexico	680	Nov-Jun	6-10m	25.6 (>3cm)	85 Mg/ha live AGB, 112 Mg/ha total AGB	6.6 Mg/ha/yr Valley site, 3.9 Mg/ha/yr Hill site	0.11%		2.9% in top 20	Shallow young sandy loam, pH 6.2	Maass et al. 2002, Campo et al. 2000, Campo et al. 1998, Ellingson et al. 2000, Martinez-Yrizar & Sarukhan 1990, Martinez-Yrizar et al. 1992, Campo et al. 2001.
Uttar Pradesh	India	800	Nov-Feb Mar-Jun				3.9 Mg/ha/yr	0.70%	1.12%		coarse sandy loam, ultisol, pH 6.3	Roy & Singh 1995; Srivastava 1992; Singh 1992; Singh et al. 1989; Roy & Singh 1994; Lal et al. 2001a, 2001b
Guanica Forest	Puerto Rico	860	Jan-Mar		19.8 (>2.5cm), 21.2 (all)	44.9 Mg/haABG, 45 Mg/ha roots/BGB	4.8 Mg/ha/yr	0.30 mg/g	1.34%	0-5 23%, 5-15 18%	clay, pH 7.8	Lugo & Murphy 1986, Murphy & Lugo 1986a
Quintana Roo	Mexico	1110	Feb-Apr	10-20m	24.7		5.3 Mg/ha/yr			51.5%	Shallow weathered limestone, pH 7.1	Whigham et al. 1991, Whigham et al. 1990, Harmon et al. 1995
Southern Yucatan Peninsula Region	Mexico	900-1400	Jan-Jun	10-15m	31-45	118-163 Mg/ha	12-15 Mg/ha/yr	0.44-0.87 mg/g	1.1-1.2%	0-15 11-22%	shallow, calcareous, pH 7.6	Lawrence & Foster 2002, Read & Lawrence 2003 & in press, Turner et al. 2001, Klepeis 2000,
Indian Church	Belize	1720	Jan-May	20m		63 Mg/ha total AGB decid, 226 Mg/ha total AGB palm site	12.6 Mg/ha/yr decid, 4.3 Mg/ha/yr palm site	0.01% decid	1% decid	0-12 cm 20%(decid) 14% (palm)	karst limestone	Arnason & Lambert 1982, Lambert et al. 1980
Murcielagos Farm	Guatemala	2000	Jun-Oct	>15m		137 Mg/ha live AGB	9.0 Mg/ha/yr	0.06%	1.88%			Ewel 1976

4.3 THE SOUTHERN YUCATAN PENINSULA, MEXICO (900-1400 mm/yr)

Despite a clear precipitation effect, biomass and litter nutrient dynamics were more profoundly influenced by forest age than by annual precipitation in successional forests of the Southern Yucatan Peninsula (Lawrence and Foster 2002; Read and Lawrence 2003a; Read and Lawrence 2003b). This study spanned 120 km and included a rainfall gradient from ca. 900 to ca.1400 mm/yr. The secondary forests ranged in age from 2-25 years since abandonment of maize agriculture. Mature forests had never been farmed but had experienced sporadic logging activity, and the entire region had been a Mayan stronghold until ca. 700-900 AD.

Litter P concentrations increased with increasing precipitation, but declined with forest age, suggesting that P is less conserved in areas where water is more available and in younger forests. Furthermore, older sites and drier sites exhibited higher P resorption proficiency, suggesting that these stands realized greater foliar conservation of P (Read and Lawrence 2003b). In contrast, litter N did not display strong regional or successional trends in either absolute concentration or resorption proficiency. Both litter P and N were significantly reduced during periods of peak litterfall, and were highest during the wet season. This pattern was exhibited most strongly for P in the wettest region. Both mature and secondary forests exhibited the same seasonal pattern of litter production, but a higher proportion of total litter fell during the dry season in mature forests (Lawrence, unpublished data). Monthly litterfall was much less variable over the course of the year in younger forests. Older secondary forests (12-25 years old) demonstrated similar levels of litter production as mature forests, despite significantly lower aboveground biomass (Lawrence and Foster 2002).

Aboveground biomass increased from 25 Mg/ha in the youngest stands to 136 Mg/ha in mature stands (Read and Lawrence 2003a). Contrary to expectations, basal area and aboveground biomass in the southern-most, wettest region were not much greater than those of two drier study areas within the region. However, biomass in the southernmost study region consisted of fewer, larger trees of greater basal area and biomass. Lower than expected biomass in this area was attributed to at least two factors, one natural and one anthropogenic. Higher precipitation may encourage greater litter production rather than biomass storage. Alternatively, the forest structure (fewer, larger trees) may be a result of heavy logging in the region half a century ago, with persistent effects on biomass (Klepeis 2004; Lawrence and Foster 2002; Read and Lawrence 2003a). As in the Guanica Forest, work in the Southern Yucatan highlights the interaction between anthropogenic factors and constraints imposed by nutrient and water availability, in determining dry forest ecosystem structure and function.

4.4 BELIZE (1720 mm/yr)

In a mature dry tropical forest of Belize, Lambert et al. (1980) investigated seasonal changes in vegetation and soil nutrients over a one-year period at a broadleaf deciduous site. Total annual litterfall was 12.6 Mg/ha, with litterfall returning 156 kgN/ha/yr, 9 kgP/ha/yr, and 373 kgCa/ha/yr. Litter decomposition occurred at a relatively high rate for dry tropical forests (95% of litter would decompose in 1.7 years) (Lambert et al. 1980). The carbonate-rich soil was slightly acidic (pH 6.8) during the dry season, and slightly basic (pH 7.2) during the wet season. Soil organic matter was highest during two distinct time periods, one towards the end of the wet season during a period of slightly higher litterfall, and one at the end of the dry season as slower decomposition rates resulted in organic matter accumulation (Lambert et al. 1980). Organic matter concentrations were high in the upper soil profile: 20% in the top 12cm, and 15% in the 12-24cm layer. Concentrations of exchangeable soil cations dropped at the start of the wet season because of leaching, but increased again during the wet season due to increased decomposition that is greater than plant uptake (Lambert et al. 1980). During the dry season, as plants continued to take up cations, soil reserves declined. In their study of nutrient content of various components of vegetation, the authors found the highest nutrient concentrations in lianas, and high concentrations in sapling leaves and tree wood (Lambert et al. 1980). This study again highlights the tight coupling between nutrient cycling and seasonal rainfall patterns.

5. Conclusion

Dry tropical forests experience low annual rainfall with high seasonal and interannual variability. As such, many important biological processes are tied to precipitation patterns, including leaf production, litterfall, and fruiting and flowering. In some dry tropical forests, there are two pronounced periods of drought, resulting in two episodes of litterfall, one major and one minor. Nutrient cycling in dry tropical forests is also tightly coupled to precipitation patterns. For example, during the dry season, leaching rates are reduced and decomposition slows, and nutrients are stored on the forest floor, or in microbial biomass. When the rainy season returns, the rate of decomposition and mineralization increases and nutrients are released from microbes, becoming available for plant uptake as soil moisture levels increase. Dry conditions also prevent plants from accessing phosphorus, the limiting nutrient in most dry tropical forests, by reducing its dissolution into the soil, and by reducing the ability of plants to take it up.

Although the total biomass stored in dry tropical forest is less than in its wet counterparts, a greater amount of this biomass is stored belowground. This organic matter storage may play an important role in the response of dry tropical forest ecosystems to continuing global change. In addition, mature dry tropical forests are being converted to secondary forest at an unprecedented rate, because they are more suitable for human habitation, pasture land, and agriculture than wetter life zones. Therefore, the need for a comprehensive understanding of the ecosystem processes governing dry tropical forests is becoming increasingly important in light of their growing areal extent and human population levels in the face of global change.

6. References

Arnason, J.T. and J.D.H. Lambert. 1982. Nitrogen cycling in the seasonally dry forest zone of Belize, Central America. Plant and Soil, 67: 333-342.

Barajas-Morales, J. 1985. Wood structural differences between trees of two tropical forests in Mexico. IAWA Bulletin 6: 355-364.

Barajas-Morales, J. 1987. Wood specific gravity in species from two tropical forests in Mexico. IAWA Bulletin 8: 143-148.

Boerner, R.E.J. 1984. Foliar nutrient dynamics and nutrient use efficiency of four deciduous tree species in relation to site fertility. Journal of Applied Ecology 21: 1029-1040.

Borchert, R. 1994. Soil and stem water storage determine phenology and distribution of tropical dry forest trees. Ecology 75: 1437-1449.

Borchert, R., G. Rivera, and W. Hagnauer. 2002. Modification of vegetative phenology in a tropical semi-deciduous forest by abnormal drought and rain. Biotropica 34: 27-39.

Brodribb, T.J., N.M. Holbrook, and M.V. Gutierrez. 2002. Hydraulic and photosynthetic co-ordination in seasonal dry tropical forest trees. Plant, Cell and Environment 15: 1435-1444.

Brown, S. and A.E. Lugo. 1982. The storage and production of organic matter in tropical forests and their role in the global carbon cycle. Biotropica 14: 161-187.

Brown, S. and A.E. Lugo. 1990. Tropical secondary forests. Journal of Tropical Ecology 6: 1-32.

Bullock, S. H., and J. A. Solis-Magallanes. 1990. Phenology of canopy trees of a tropical deciduous forest in Mexico. Biotropica 22: 22-35.

Buschbacher, R., C. Uhl, and E.A.S. Serrao. 1988. Abandoned pastures in eastern Amazonia II: Nutrient stocks in the soil and vegetation. Journal of Ecology 76: 682-699.

Cairns, M.A., P.K. Haggerty, R. Alvarez, B.H.J. DeJong, and I. Olmsted. 2000. Tropical Mexico's recent land-use change: A region's contribution to the global carbon cycle. Ecological Applications 10: 1426-1441.

Campo, J., V.J. Jaramillo, and J. Manuel Maass. 1998. Pulses of soil phosphorus availability in a Mexican tropical dry forest: effects of seasonality and level of wetting. Oecologia 115: 167-172.

Campo, J., M. Maass, V.J. Jaramillo, A. Martinez-Yrizar, and J. Sarukhan. 2001. Phosphorus cycling in a Mexican tropical dry forest ecosystem. Biogeochemistry 53: 161-179.

Campo, J., J. Manuel Maass, V.J. Jaramillo, and A. Martinez-Yrizar. 2000. Calcium, potassium, and magnesium cycling in a Mexican tropical dry forest ecosystem. Biogeochemistry 49: 21-36.

Chapin, F.S. 1980. The mineral nutrition of wild plants. Annual Review of Ecology and Systematics 11: 233-260.

Chazdon, R. 2003. Tropical forest recovery: legacies of human impact and natural disturbance. Perspectives in Plant Ecology, Evolution and Systematics 6: 51-71.

Cuevas. E. 1995. Biology of the belowground system of tropical dry forests. in Seasonally Dry Tropical Forests. Eds. H. A. Mooney, S. H. Bullock, and E. Medina: 362-383. Cambridge University Press, Cambridge.

Daubenmire, R. 1972. Phenology and other characteristics of tropical semi-deciduous forest in northeastern Costa Rica. Journal of Ecology 60: 147-170.

Dewalt, S.J., S.A. Schnitzer, and J.S. Denslow. 2000. Density and diversity of lianas along a chronosequence in a central Panamanian lowland forest. Journal of Tropical Ecology 16: 1-19.

Ellingson, L.J., J.B. Kauffman, D.L. Cummings, R.L. Sanford Jr., and V.J. Jaramillo. 2000. Soil N dynamics associated with deforestation, biomass burning, and pasture conversion in a Mexican dry tropical forest. Forest Ecology and Management 137: 41-51.

Enquist, B.J. and A. J. Leffler. 2001. Long-term tree ring chronologies from sympatric tropical dry-forest trees: individualistic responses to climatic variation. Journal of Tropical Ecology 17: 41-60.

Ewel, J.J. 1976. Litter fall and leaf decomposition in a tropical forest succession in eastern Guatemala. Journal of Ecology 64: 293-307.

Ewel, J. 1980. Tropical Succession: Manifold routes to maturity. Biotropica 12: 2-7.

Fearnside, P. M., and W. M. Guimaraes. 1996. Carbon uptake by secondary forests in Brazilian Amazonia. Forest Ecology and Management 80: 35-46.

Garcia-Mendez, G., J. M. Maass, P. A. Matson, and P. M. Vitousek. 1991. Nitrogen transformations and nitrous oxide flux in a tropical deciduous forest in Mexico. Oecologia 88: 362-366.

Gentry, A. H. 1988. Changes in plant community diversity and floristic composition on environmental and geographic gradients. Annals of the Missouri Botanical Gardens 75:1-34.

Giardina, C.P., R.L. Sanford Jr., I.C. Dockersmith, and V.J. Jaramillo. 2000. The effects of slash burning on ecosystem nutrients during the land preparation phase of shifting cultivation. Plant and Soil 220: 247-260.

Harmon, M.E., D.F. Whigham, J. Sexton, and I. Olmstead. 1995. Decomposition and mass of woody detritus in the dry tropical forests of the northeastern Yucatan Peninsula, Mexico. Biotropica 27: 305-316.

Holbrook, N. M., J. L. Whitbeck, and H. A. Mooney. 1995. Drought responses of neotropical dry forest trees. In Seasonally Dry Tropical Forests. Eds. H. A. Mooney, S. H. Bullock, and E. Medina. Cambridge University Press, Cambridge: 243-276.

Hughes, R. F., J. B. Kauffman, and V. J. Jaramillo. 1999. Biomass, carbon, and nutrient dynamics of secondary forests in a humid tropical region of Mexico. Ecology 80: 1892-1907.

Hughes, R.F., J.B. Kauffman, and V.J. Jaramillo. 2000. Ecosystem-scale impacts of deforestation and land use in a humid tropical region of Mexico. Ecological Applications 10: 515-527.

Hughes, R. F., J. B. Kauffman, and D. L. Cummings. 2002. Dynamics of aboveground and soil carbon and nitrogen stocks and cycling of available nitrogen along a land-use gradient in Rondonia, Brazil. Ecosystems 5: 244-259.

Jaramillo, V. J., and R. L. Sanford. 1995. Nutrient cycling in tropical deciduous forests. In Seasonally Dry Tropical Forests. Eds. H. A. Mooney, S. H. Bullock, and E. Medina. Cambridge University Press, Cambridge: 346-361.

Kauffman, J. B., 1991. Survival by sprouting following fire in tropical forests of the eastern Amazon. Biotropica 23: 219-224.

Kauffman, J.B., R.L. Sanford, Jr., D.L. Cummings, I.H. Salcedo, and E.V.S.B. Sampaio. 1993. Biomass and nutrient dynamics associated with slash fires in neotropical dry forests. Ecology 74: 140-151.

Klepeis, P. 2004. Forest extraction to Theme Parks: The Modern History of Land Change in the Region. In Integrated Land-Change Science and Tropical Deforestation in the Southern Yucatan: Final Frontiers: pp. 39-62, Eds. B.L. Turner II., J. Geoghegan, and D.R. Foster. Oxford, Oxford University Press.

Killingbeck, K.T. 1996. Nutrients in senesced leaves: Keys to the search for potential resorption and resorption proficiency. Ecology 77: 1716-1729.

Kummerow, J., J. Castellanos, M. Maass, and A. Larigauderie. 1990. Production of fine roots and the seasonality of their growth in a Mexican deciduous dry forest. Vegetatio 90: 73-80.

Lal, C.B., C. Annapurna, A.S. Raghubanshi, and J.S. Singh. 2001a. Effect of leaf habit and soil type on nutrient resorption and conservation in woody species of a dry tropical environment. Canadian Journal of Botany 79: 1066-1075.

Lal, C.B., C. Annapurna, A.S. Raghubanshi, and J.S. Singh. 2001b. Foliar demand and resource economy of nutrients in dry tropical forest species. Journal of Vegetation Science 12: 5-14.

Lambert, J.D.H., J.T. Arnason, and J.L. Gale. 1980. Leaf litter and changing nutrient levels in a seasonally dry tropical hardwood forest, Belize, C.A. Plant and Soil 55: 429-443.

Lawrence, D. and D. R. Foster. 2002. Changes in forest biomass, litter dynamics and soils following shifting cultivation in southern Mexico: an overview. Interciencia 27: 400-408.

Lawrence, D. and W.H. Schlesinger. 2001. Changes in soil phosphorus during 200 years of shifting cultivation in Indonesia. Ecology 82: 2769-2780.

Lugo, A.E. 1992. Comparison of tropical tree plantations with secondary forests of similar age. Ecological Monographs 62: 1-41.

Lugo, A.E. and P.G. Murphy. 1986. Nutrient dynamics of a Puerto Rican subtropical dry forest. Journal of Tropical Ecology 2: 55-72.

Maass, J.M., A. Martinez-Yrizar, C. Patino, and J. Sarukhan. 2002. Distribution and annual net accumulation of above-ground dead photomass and its influence on throughfall quality in a Mexican tropical deciduous forest ecosystem. Journal of Tropical Ecology 18: 821-834.

Martinex-Yrizar, A. 1995. Biomass distribution and primary productivity of tropical dry forests. In Seasonally Dry Tropical Forests. Eds. H. A. Mooney, S. H. Bullock, and E. Medina. Cambridge University Press, Cambridge: 326-345.

Martinez-Yrizar, A. and J. Sarukhan. 1990. Litterfall patterns in a tropical deciduous forest in Mexico over a five-year period. Journal of Tropical Ecology 6: 433-444.

Martinez-Yrizar, A., J. Sarukhan, A. Perez-Jimenez, E. Rincon, J.M. Maass, A. Solis-Magallanes, and L. Cervantes. 1992. Above-ground phytomass of a tropical deciduous forest on the coast of Jalisco, Mexico. Journal of Tropical Ecology 8: 87-96.

Medina, E. 1984. Adaptations of tropical trees to moisture stress. In Tropical Rain Forest Ecosystems: structure and function, ed. F. B. Golley: 225-237. Elsevier, New York.

Mooney, H. A., S. H. Bullock, and E. Medina. 1995. Seasonally Dry Tropical Forests. Cambridge University Press, Cambridge.

Mooney, H. A., C. Field, and C. Vazquez-Yanes. 1984. Photosynthetic characteristics of wet tropical forest plants. In Physiological Ecology of Plants of the Wet Tropics, ed. E. Medina, H. A. Mooney and C. Vazquez-Yanes: 129-138. Dr. W. Junk, The Hague.

Moran, E. F., E. S. Brondizio, J. M. Tucker, M. C. de Silva-Forsberg, S. McCracken, and I. Falesi. 2000. Effects of soil fertility and land-use on forest succession in Amazonia. Forest Ecology and Management 139: 93-108.

Murphy, P.G. and A.E. Lugo. 1986a. Ecology of tropical dry forest. Annual Review of Ecology and Systematics 17: 67-88.

Murphy, P.G. and A.E. Lugo. 1986b. Structure and biomass of a subtropical forest in Puerto Rico. Biotropica 18: 89-96.

Pascarella, J. B., T. M. Aide, M. I Serrano, and J. K. Zimmerman. 2000. Land-use history and forest regeneration in the Cayey Mountains, Puerto Rico. Ecosystems 3: 217-228.

Pennington, R.T., D.E. Prado, and C.A. Pendry. 2000. Neotropical seasonally dry forests and Quaternary vegetation changes. Journal of Biogeography 27: 261-273.

Perez-Salicrup, D.R. 2004. Forest types and their implications. In Integrated Land-Change Science and Tropical Deforestation in the Southern Yucatan: Final Frontiers: pp. 63-80, Eds. B.L. Turner II., J. Geoghegan, and D.R. Foster. Oxford, Oxford University Press.

Perez-Salicrup, D.R. and M.G. Baker. 2000. Effect of liana cutting on water potential and growth of adult Senna multijuga (Caesalpinioideae) trees in a Bolivian tropical forest. Oecologia 124: 469-475.

Read, L. and D. Lawrence. 2003a. Recovery of Biomass Following Shifting Cultivation in Dry Tropical Forests of the Yucatan. Ecological Applications 13: 85-97.

Read, L. and D. Lawrence. 2003b. Litter nutrient dynamics during succession in dry tropical forests of the Yucatan: Regional and seasonal effects. Ecosystems 6: 747-761.

Roy, S. and J.S. Singh. 1994. Consequences of habitat heterogeneity for availability of nutrients in a dry tropical forest. Journal of Ecology 82: 503-509.

Roy, S. and J.S. Singh. 1995. Seasonal and spatial dynamics of plant-available N and P pools and N-mineralization in relation to fine roots in a dry tropical forest habitat. Soil Biology and Biogeochemistry 27: 33-40.

Saugier, B., J. Roy, and H. A. Mooney. 2001. Estimations of global terrestrial productivity: converging toward a single number? Pages 543-557 in J. Roy, B. Saugier, and H. A. Mooney, editors. Terrestrial Global Productivity. Academic Press, San Diego, CA.

Silver, W.L. 1998. The potential effects of elevated CO_2 and climate change on tropical forest soils and biogeochemical cycling. Climatic Change 39: 337-361.

Singh, K. P. 1989. Mineral nutrients in tropical dry deciduous forest and savanna ecosystems oin India. In Mineral Nutrients in Tropical Forest and Savanna Ecosystems, Ed. J. Proctor: 153-168. Blackwell Scientific Publications. Oxford.

Singh, K. P. and A. N. Shukla 1977. Soil respiration in relation to mesofaunal and mycofloral populations during rapid course decomposition on the floor of a tropical dry deciduous forest. Revue d'Ecologie et de Biologie du Sol 14: 363-370.

Singh, Lalji. 1992. Dry matter and nutrient inputs through litter fall in a dry tropical forest of India. Vegatatio 98: 129-40.

Singh, J.S., A.S. Raghubanshi, R.S. Singh, and S.C. Srivastava. 1989. Microbial biomass acts as a source of plant nutrients in a dry tropical forest and savanna. Nature 338: 499-500.

Srivastava, S.K. 1992. Microbial C, N, and P in dry tropical soils: Seasonal changes and influence of soil moisture. Soil Biology and Biogeochemistry 24: 711-714.

Srivastava, S.K., K. P. Singh, and R. S. Upadhyay. 1986. Fine root growth dynamics in teak (Tectona grandis Linn. f.). Canadian Journal of Forest Research 16: 360-364.

Steininger, M. K. 2000 Secondary forest structure and biomass following short and extended land-use in central and southern Amazonia. Journal of Tropical Ecology 16: 689-708.

Tiessen, H., J.W.B. Stewart, and J.O. Moir. 1983. Changes in organic and inorganic phosphorus composition of two grassland soils and their particle size fractions during 60-90 years of cultivation. Journal of Soil Science 34:815-823.

Tomlinson, P.B. 1979. Systematics and ecology of the Palmae. Annual Review of Ecology and Systematics 10: 85-107.

Uhl, C., and C.F. Jordan. 1984. Succession and nutrient dynamics following forest cutting and burning in Amazonia. Ecology 65: 1476-1490.

Uhl, C., R. Buschbacher, R., and E. A. S. Serrao. 1988. Abandoned pastures in eastern Amazonia. I. Patterns of plant succession. Journal of Ecology 76: 663-681.

Vitousek, P. 1982. Nutrient cycling and nutrient use efficiency. The American Naturalist 119: 553-572.

Vitousek, P. 1984. Litterfall, nutrient cycling, and nutrient limitation in tropical forests.Ecology 65: 285-298.

Whigham, D.F., P. Zugasty Towle, E. Cabrera Cano, J. O’Neill, and E. Ley. 1990. The effect of annual variation in precipitation on growth and litter production in a tropical dry forest in the Yucatan of Mexico. Tropical Ecology 31: 23-34.

Whigham, D.F., I. Olmsted, E. Cabrera Cano, and M.E. Harmon. 1991. The impact of Hurricane Gilbert on trees, litterfall, and woody debris in a dry tropical forest in the Northeastern Yucatan Peninsula. Biotropica 23: 434-441.

Zimmerman, J. K., T. M. Aide, M. Rosario, M. Serrano, and L. Herrera. 1995. Effects of land management and a recent hurrican on forest structure and composition in the Luquillo Experimental Forest, Puerto Rico. Forest Ecology and Management 77: 65-76.

Chapter 14

BIOGENIC EMISSIONS OF NITRIC OXIDE AND NITROUS OXIDE FROM ARID AND SEMI-ARID LAND

Franz X. MEIXNER[1,2] and Wen X. YANG[1,3,†]

[1] *Biogeochemistry Department, Max Planck Institute for Chemistry, J.J.v. Becherweg 27, D-55128 Mainz, Germany - e-mail: meixner@mpch-mainz.mpg.de*
[2] *Department of Physics, University of Zimbabwe, Mount Pleasant, P.O.Box MP 167, Harare, Zimbabwe*
[3] *Laboratory of Material Cycling in Pedosphere, Institute of Soil Science, Academia Sinica, P.O.Box 821, Nanjing 210008, P.R. China*
[†] *on 25 February, 2002, Dr. WenXing Yang untimely passed away in the age of 42.*

1. Introduction

Carbonaceous trace gases in the atmosphere, like carbon monoxide, methane, volatile organic compounds, are oxidized by hydroxyl and other radicals through various catalytic cycles (Crutzen, 1987). Nitrogen oxide (NO) and nitrogen dioxide (NO_2) are the key catalysts in these cycles and their ambient concentrations determine whether ozone is generated or destroyed in the troposphere (Chameides et al., 1992). A mixing ratio of NO_x (= NO+NO_2) of only ≈30 pptv establishes a critical threshold between ozone destruction (<30 pptv) and generation (>30 pptv). Ozone is usually generated in polluted, industrialized regions, where ambient levels of nitrogen oxides are high, and it is destroyed in remote parts of the globe. The present evolution of sources of nitrogen oxides in non-industrialized regions triggers a potential increase of global tropospheric ozone concentrations and thus attracts scientific attention. Nitrous oxide (N_2O) is important because it absorbs the outgoing infrared radiation (like other radiatively effective trace gases, e.g., CO_2, H_2O, methane). It contributes by approximately 5% to the anthropogenic greenhouse effect. N_2O is chemically inert in the troposphere. However, once transported into the stratosphere, it contributes to the destruction of the ozone layer, which protects terrestrial life from incoming solar ultra-violet radiation. Fossil-fuel combustion in power stations and in car engines is still the most important (and best documented) global source of nitrogen oxides. The corresponding global source strength was estimated to be 21 Tg a^{-1} (in terms of mass of nitrogen) by Kasibhatla et al. (1993); the corresponding, most recent estimate by IPCC (2001) is 33 Tg a^{-1}. The strongest global sources for N_2O are natural soils (6 Tg a^{-1}), followed by N_2O emissions from agricultural (fertilized) soils (4.2 Tg a^{-1}), and other anthropogenic sources (IPCC, 2001). Nitrification and denitrification processes in soils give rise to strong NO and N_2O emissions. There is continuous interest to quantify worldwide biogenic sources of these trace gases (e.g. Hutchinson et al., 1993; IPCC, 2001). A global inventory of NO emissions from soils, based on field measurements worldwide, has been provided by Davidson and Kingerlee (1997). Their estimate of the global NO soil source strength is 21Tg a^{-1} (with an error margin of 4 to 10 Tg a^{-1}), while the most recent IPCC (2001) estimate is 5.6 Tg a^{-1}. Stratifying soil sources according to major biomes, it turned out, that the combined biomes "tropical savanna/woodlands" and "chaparral/thorn forests" contribute more than half to the global source (Davidson and Kingerlee, 1997). However, the uncertainties in the NO emission data for these strata are very large. Emissions from semi-arid and arid lands, which are part of these biomes, particularly contribute to the high error margins, simply because a very small number of corresponding measurements is available (both in the laboratory and in the field). Before we try to re-compile and to up-date the data base of NO and N_2O emissions from semi-arid and arid lands, we like to describe processes and controlling

P. D'Odorico and A. Porporato (eds.), Dryland Ecohydrology, 233–255.

factors of these emissions, (a) in general, and (b) under the specific conditions of semi-arid, arid, and hyper-arid landscapes.

2. Biogenic emission of NO and N_2O from soils and plants – general aspects

Nitric oxide (NO) and nitrous oxide (N_2O) are produced and consumed within soils. Generally, soils contribute to the global budgets of NO and N_2O as sources (Table 1) and their contribution as sinks is likely but considered to be small (c.f. Meixner and Eugster, 1999). As plants are concerned, there are no mechanisms known for biogenic emission or uptake of N_2O. Wildt et al. (1996) observed biogenic emission of NO from several higher plant species. However, the plants' contribution to the global atmospheric budget of nitrogen oxides is presumably less than 4% (see Table 1). Generally, there is (stomatal) uptake of nitrogen dioxide (NO_2). Stomatal uptake of NO is thought to occur in polluted environments (cf. Meixner, 1994), but - due to the low solubility of NO - this uptake is expected to be low. The values in Table 1 are are estimated with uncertainty due to a number reasons (Conrad, 1996). The fluxes of NO and N_2O are reliably measured by a variety of techniques, ranging from small-scale soil- and/or leaf enclosures to tower-based and airborne micrometeorological techniques (c.f. Matson and Harriss, 1995). It is by far not trivial, however, to estimate atmospheric budgets from local NO and N_2O flux measurements (Andreae and Schimel, 1989). NO and N_2O fluxes are controlled by a diversity of abiological and microbiological processes which themselves depend on environmental conditions. Thus, fluxes are highly variable with respect to time and space. Most of observed uncertainties and problems with NO and N_2O flux data can be traced to this fact. However, the mentioned problems are not necessarily solved by integration of fluxes over larger areas and longer time periods, since—according to Conrad (1996)—"each individual flux event is caused by deterministic processes that change in a non-linear way, even when conditions change slightly".

Table 1. Contribution of soils (NO and N_2O) and plants (NO) to the global cycles of nitric and nitrous oxides (after Meixner and Eugster, 1999).

trace gas	ambient conc. [ppb]	lifetime [days]	total budget [Tg a^{-1}]	annual increase [%]	contribution of soils or plants as source [%]	contribution of soils or plants as sink [%]
N_2O (soils)	310	60000	15	0.2–0.3	70	?
NO (soils)	< 0.1–20	1	60	?	20	?
NO (plants)					< 4	?

2.1. SOIL-AIR EXCHANGE OF NO AND N_2O: PROCESSES

Soil processes can be classified into chemical (abiotic) and microbial (biotic) processes. Abiotic formation of NO (and N_2O) in soils is imporant in acid soils (e.g. Davidson, 1992). However, microorganisms are considered to be responsible for most NO and N_2O production and consumption processes in soils. In their oxidative and reductive metabolisms, these trace gases act as growth substrates and/or co-metabolites; or they are considered to be stoichiometric and other products (see comprehensive review by Conrad, 1996). In principle, all microbial processes, which involve oxidative or reductive transformation of nitrogen involving its +2 valence state, were identified as both, biogenic sources or sinks for NO and N_2O (Conrad, 1996). Nevertheless, it is widely accepted that microbial nitrification and denitrification constitute the principal processes. In this context, it is important to keep in mind, that the production and consumption and hence exchange of NO and N_2O between soils and atmosphere is predominantly controlled at the microscopic scale, i.e., at the level of the metabolism of microorganisms. However, for the study of biogenic emissions from whole landscape patterns (topographically and/or climatologically stratified), higher scales of organization and control must be considered (Meixner and Eugster, 1999). Therefore, (a) processes and (b) controls of biogenic NO and N_2O emission from soils (of at least plot to ecosystem scales) are considered next.

2.1.1. Chemodenitrification

Chemical oxidation of NO by O_2 is limited by the requirement of unrealistically high NO mixing ratios in soil air (Conrad, 1996). Abiotic formation of NO in soils can be of importance in acid soils ($pH<5$) with high nitrite (NO_2^-) concentrations: under these conditions HNO_2 undergoes self-decomposition and reacts with soil organic matter. Addition of NO_2^- to both, sterile and nonsterile soils has been observed to stimulate NO and N_2O emissions (Davidson, 1992). Recently, it has been argued, that burning of tropical ecosystems may decouple different nitrogen cycling processes in soils due to microbial sterilization (e.g. Weitz, et al., 1998). Therefore, soil NO emissions, observed immediately after typical “slash and burn” activities, require abiotic (chemodenitrification) NO production processes (Kirkman, 2001). Laboratory work on gamma irradiated Brazilian pasture soils (50 kGy day^{-1}) indicated abiotic NO production to be responsible for up to 50% of the total NO production (Trebs, 2001).

2.1.2. Denitrification

Denitrification is the bacterial respiratory reduction of nitrate (NO_3^-) and nitrite (NO_2^-) to N_2O, NO, and N_2. Because of the gaseous products, this process is commonly associated with the loss of soil nitrogen to the atmosphere. Denitrifying bacteria can grow in anaerobic environments due to their capability to use and reduce oxidised forms of soil nitrogen when oxygen is limited. The latter conditions occur at high soil water content or large respiration and oxygen consumption rates. The presence of readily oxidizable organic carbon is a requirement for most denitrifying bacteria (heterotrophs). A broad diversity of bacterial groups is capable of this metabolic pathway (Conrad, 1996). Therefore, denitrifiers are present in almost all natural and cultivated soil. It is generally accepted that NO and N_2O are obligatory intermediates in the denitrification sequence. This fact suggests that denitrifiers not only can produce but also consume NO and N_2O. The rates of NO and N_2O production (or consumption) and the overall denitrification rate are strongly affected by numerous parameters entering the complex reaction scheme. One parameter for instance, oxygen availability, is in turn regulated by various factors, e.g., soil water content, soil texture, activity of plant roots, and microbial respiration (see Chapters 3 and 11).

2.1.3. Nitrification

Nitrification involves the biological oxidation of nitrogen compounds, typically the oxidation of soil ammonium (NH_4^+) to NO_3^- (with NO_2^- as an intermediate), but there are also bacteria which oxidize NH_4^+ to NO_2^- and NO_2^- to NO_3^-. The capacity for nitrification is restricted to a few genera of strictly aerobic, mainly chemoautotrophic bacteria, which require only CO_2, H_2O, O_2, and either NH_4^+ or NO_2^- for growth. Nitrifying bacteria produce NO and N_2O as a by-product of NH_4^+ oxidation. It is unknown which biochemical pathway is the most important one for NO production; the N_2O production, however, occurs most likely via reduction of NO_2^- by NH_4^+ oxidizers. Using NO_2^- as an electron acceptor, nitrifiers can sustain oxidation of NH_4^+ even at low O_2 partial pressures. Overall nitrification rates will increase in well-aerated soils and at soil pH > 4–5.Under these conditions the nitrification rate is predominantly controlled by the availability of NH_4^+. The yield of NO typically ranges between 0.1% to 10% of the NH_4^+ oxidized (Veldkamp and Keller, 1997).

2.1.4. Nitrification vs. denitrification

It has been shown that NO production may be dominated by nitrification in a particular soil and by denitrification in another one (Conrad, 1996). It is still a difficult task to assess the importance of nitrification versus denitrification for the exchange of NO and N_2O. Results of most recent studies are still contradictory: in many field situations it is difficult to ascribe NO (and N_2O) production to one of both processes, because nitrifying and denitrifying bacteria might act simultaneously due microsite heterogenities within the same soil profile (cf. Ludwig et al., 2001).

2.1.5. Transport processes in soil, canopy and surface boundary layers

Commonly, molecular diffusion accomplishes the transport of NO and N_2O in soil pores (see Chapter 2); some laboratory studies, however, demonstrated the importance of convective transfer (Rudolph et al., 1996; Rudolph and Conrad, 1996). NO and N_2O diffusion coefficients in water are several orders of magnitude lower than in air; therefore, water-filled pores form strong barriers to the emission of NO and N_2O into the atmosphere. The soil water content also impacts strongly the diffusion of O_2 into the soil and consequently the microbial activity (Skopp et al., 1990). Thus, denitrifier activity will benefit from high soil water contents, but NO and N_2O diffusional removal will be the limiting factor. This situation enhances the probability of NO and N_2O being reconsumed by denitrifiers; consequently, emission of NO and N_2O to the atmosphere deviates significantly from the production of NO and/or N_2O in the soil (cf. Skiba et al., 1997). Chemistry, plant physiology and turbulent transport determine the further fate of NO once emitted from soil. In (dense) canopies, NO is rapidly oxidized by ozone (O_3) to nitrogen dioxide (NO_2). NO_2 uptake by plants (and soil) is much more effective than NO uptake (Meixner, 1994). As a result, only a fraction of NO emitted from soils reaches the atmospheric boundary layer and the free troposphere. This effect is usually termed the "canopy reduction factor" (CRF). Due to the fast and reversible conversion of NO to NO_2 in the presence of ozone and sunlight, NO_x, i.e. the sum of NO and NO_2, is the more suitable quantity for the description of the fate of soil derived NO. CRF-values are frequently given as that fraction of soil derived NO, which escapes a vegetation canopy in the form of NO_x (i.e. 100×(1-CRF) is the percental "loss" of NO_x in the canopy). For (dense tropical) forests, current estimates of the CRF are around 0.55 (Meixner et al., 2002).

2.2. SOIL-AIR EXCHANGE OF NO AND N_2O: INFLUENCING FACTORS

Any environmental factor that regulates the processes of NO and N_2O production and consumption in soils potentially affects the exchange of NO and N_2O between soil and the atmosphere. We will confine the following sub-sections to those factors, which have been identified as major controllers within a wide range of field situations. Under more specific environmental conditions (e.g. Meixner, 1994), other variables like soil pH, concentration and composition of organic C, soil texture, plant cover, as well as some cultivation practices (tillage, burning) might be of importance. Though correlation of soil parameters with observed NO and N_2O fluxes will depend on the vertical distribution of the relevant processes within the soil column, there is broad evidence that primary production and consumption zones for NO are located within a very shallow layer at the soil surface (0.01 to 0.1 m, e.g. Rudolph et al., 1996, Yang and Meixner, 1997). For N_2O, however, the situation is more complex; commonly it is assumed, that the major contribution to N_2O fluxes arises from (well) below 0.5 m, since major production zones of N_2O might be at the ground water level. However, Neftel et al. (2000) reported experimental evidence for a N_2O scale length of 0.007–0.03 m soil depth only.

2.2.1. Nitrogen availability and fertilization

It is evident, that all biological processes controlling nitrogen and carbon availability are of fundamental importance for NO and N_2O emission fluxes. Here, special emphasis is given to the pool size of soil NH_4^+ and NO_3^- serving as substrates for nitrifying and denitrifying bacteria.

Recently, some sophisticated ecosystem models became available, which describe local, regional, and global NO and N_2O emission patterns (monthly and diel) on the basis of carbon availability, gross nitrogen mineralization, denitrification, nitrification, decomposition, and soil carbon–nitrogen fluxes (e.g. Potter et al., 1993, 1996; Parton et al. 1998; Li et al., 2000; Parton et al., 2001). Field and laboratory studies have demonstrated numerous correlations between fluxes of N_2O and NO and NO_3^- or NH_4^+ concentrations in soil. Studies, however, were very site specific, and there is hardly a consistent trend to be recognized (e.g. Ludwig et al., 2001). The importance of nitrogen availability direcly links to fertilizers which strongly affect the exchange of NO and N_2O. A strong stimulation of NO emission by addition of N fertilizers has been noticed at uncultivated as well as agricultural sites. Input of nitrogen by (a) excreta of grazing animals or (b) wet (dry) deposition of NO_3^- (HNO_3, HNO_2, NO_2) and NH_4^+ (NH_3) resulted in enhanced levels of the NO and N_2O release over grasslands (Thornton et al., 1998) and forests (Butterbach-Bahl et al., 1997). Independently of fertilizer type and land use, a rapid increase of NO emissions is observed within one or two days after fertilization (nitrogen input, wet/dry deposition). Maximum emission rates are typically approached within 1–2 days, and pre-fertilization levels might be reached again within a few days or several weeks. Presently, the global mean of released NO is approximately 0.5% of the applied fertilzer nitrogen. For the most recent review and a very comprehensive global compilation of fertilizer induced emissions of NO and N_2O, the reader is referred to Bowman et al. (2000a, 2000b).

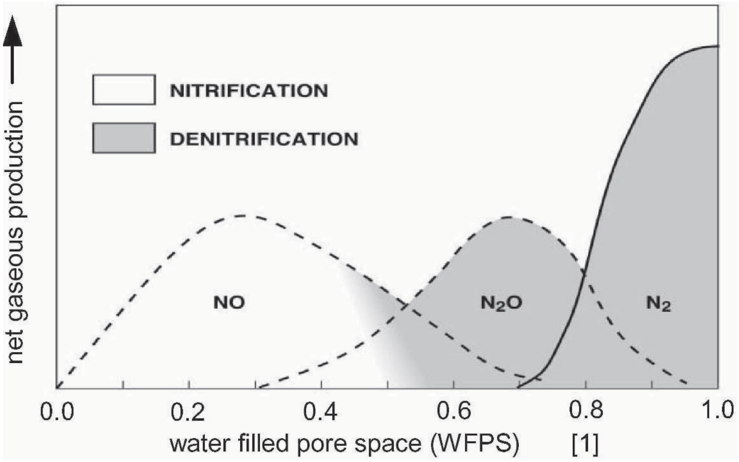

Fig. 1: The relationship between percent water-filled pore space (WFPS) of soil and the relative fluxes of nitrogen trace gases (Kirkman (2001), adapted from Davidson, 1991).

2.2.2. Soil moisture content

Nitrification and denitrification are intimately related to the soil water content for two important reasons: (a) the substrate supply for soil microorganisms (e.g., NH_4^+ for nitrifying bacteria) is accomplished by diffusion of the substrates in soil water films, and (b) water in soil pores is the dominant controller of gaseous diffusion in soils. The ratio of volumetric soil water content to total porosity of the soil, which is termed the water-filled pore space (WFPS), is commonly considered to be a suitable expression of the soil water content, since WFPS is largely comparable among soils of different texture (see Chapters 2 and 3 for the definitions of soil water content). In the context of NO and N_2O sources and source partition, Davidson and Schimel (1995) have suggested, that (a) if WFPS < 60%, nitrification is more important than denitrification and the N_2O:NO emission ratio is < 1, while (b) if WFPS > 60%, denitrification overrides nitrification and N_2O:NO > 1. N_2 may be the dominant end product of denitrification under completely anaerobic conditions. The relationship between WFPS of soil and the relative fluxes of nitrogen trace gases is shown in Figure 1, which is adapted from Davidson (1991). Most of the current ecosystem models make use of this conceptual relationship: the shape of relative NO, N_2O, and N_2 emissions curves, as a result of two opposing processes, namely the substrate diffusion limit (towards low WFPS) and the O_2 diffusion limit (towards high WFPS), is a more general issue of soil water content vs. soil microbial activity (Skopp et al., 1990).

2.2.3. Soil temperature

The dominance of soil microbial processes in the production of NO and N_2O anticipates a marked influence of soil temperature on NO and N_2O emission rates. Most studies have only demonstrated the increase of NO emissions with increasing soil temperatures. This is in line with the fact that rates of chemical and/or enzymatic processes generally increase exponentially with temperature, as long as other factors (substrate or moisture availability) are not limiting. A convincing example obtained from laboratory studies on actual field samples is presented in Fig. 2. Doubling of NO emission rates was often observed when soil temperatures increased by 10°C (commonly dubbed as $Q_{10} = 2$). Valente and Thornton (1993) reported an average $Q_{10} = 5$ with a considerable variation between different ecosystems. Further restrictions to the validity of a uniform temperature response concern the emission of NO at more elevated temperatures and soil water contents (see *3.1*). It should be noted that soil temperature often cannot explain seasonal variations of NO fluxes (cf. Ludwig et al., 2001). It seems to be more appropriate that soil temperature modulates short-term variations of the NO and N_2O exchange, whereas the magnitude of the biogenic emissions is predominantly controlled by other factors, especially soil moisture (see Otter et al., 1999; Gut et al., 2002; Kirkman et al., 2002).

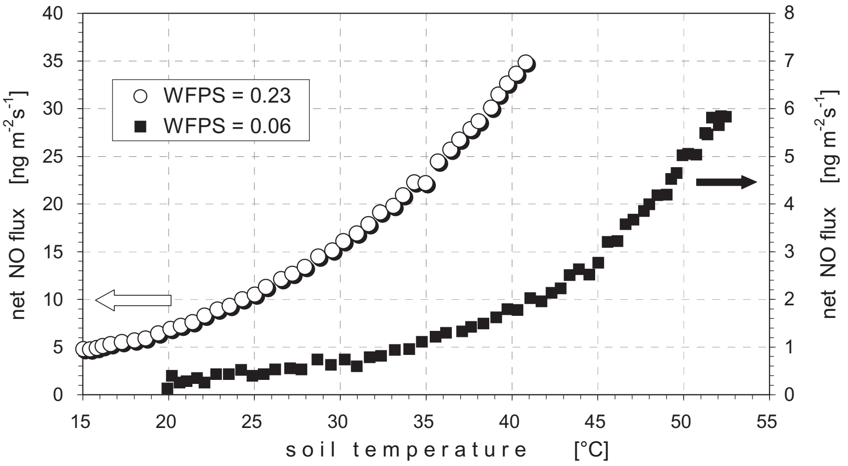

Figure 2: The relationship between (near surface) soil temperature and the net flux of nitric oxide (NO) from a bare soil taken from a semi-arid grassland site (results of laboratory experiments on a soil sample taken on 14 December 1994 at the Marondera Grassland Research Station, Mashona-land-East, Zimbabwe).

2.2.4. Atmospheric concentrations of NO and N_2O

Trace gas production and consumption processes occur simultaneously in the soil. Consequently, bi-directional fluxes of NO and N_2O have been observed under laboratory and field conditions. Within aggregated soils, soil crumbs may be considered as units of trace gas metabolism, in nonaggregated soils, sand grains covered with a microbial biofilm may play that role. Particularly, surfaces near soil crumbs are usually heterogeneous with regard to their aerobic–anaerobic metabolism. Even (generally well) aerated upland soils contain anoxic microniches. Then, the ambient NO (and N_2O) concentration determines whether a given soil acts as source or as sink for NO (and N_2O). The equilibrium concentration at which the rate of NO (N_2O) production equals the rate of NO (N_2O) consumption (i.e., at which the apparent net flux equals zero) is commonly termed NO (N_2O) compensation concentration (or "compensation point"). Whether compensation points are of major importance for the exchange of NO and N_2O on a larger (regional, global) scale, is currently not clear. There are only a few reports of NO (N_2O) compensation concentrations, and their range is extremely wide (< 1 ppbv to several hundreds of ppb). In most studies, the average ambient air concentration of NO (or N_2O) was found to be well below the compensation concentration. Consequently, the mean net flux was directed from the surface to the atmosphere (mean net emission).

3. Biogenic emissions of NO and N_2O from semi-arid and arid soils

More than one third of the global land area are deserts and drylands (see Chapter 1): semi-arid, arid and hyper-arid land constitute respectively 17.7 %, 12.1 %, and 7.5 % of planet Earth's total land area of 13049 million hectares (Harrison and Pearce, 2000). In this review of recent literature on NO and N_2O emissions from natural and semi-natural soils of semi-arid and arid regions studies on agricultural fields (fertilizer effects) have not been included. The reader is referred to the extensive work of Bowman et al. (2000a, 2000b), who made a global compilation of 846 N_2O emission and 99 NO emission measurements in agricultural fields; however, a subset of only 8 measurements remains for regions with an annual rainfall less than 450 mm. With respect to natural and semi-natural soils, we have used the global inventory by Davidson and Kingerlee (1997) as a starting point. When stratifying all data (field and laboratory measurements) according to the Koppen-Geiger climate classification scheme (cf. Strahler and Strahler, 1999), only 17 NO and N_2O flux measurements have been identified for BW (desert) and BS (steppe) climates (for NO: 3 (BW), 8 (BS); for N_2O: 2 (BW); 4 (BS)). We enlarged this rather small database by (a) addition of some results from our laboratory studies on semi-arid and desert soils (see below), and (b) consideration of all data obtained in transition regions (e.g. Cwa/BSh, Csa/Bsk). Our compilation is presented in Table 2. To facilitate comparison between NO and N_2O fluxes, all data are given in terms of mass of nitrogen (N). NO and N_2O fluxes are listed for "dry soil" and "wet soil" conditions. Whenever possible, the column "wet soil" contains those NO and N_2O fluxes, which have been found at respective optimum soil moisture conditions (Section.2.2.2, Fig.1). Low and very low NO and N_2O fluxes are generally observed from dry arid and dry/hot semi-arid soils (< 1.5 ng $m^{-2}s^{-1}$). This low number might be compared to the 10 to 100-fold NO and N_2O fluxes emitted from temperate grasslands and forests (NO), as well as from rainforests soils (N_2O) (cf. Davidson and Kingerlee, 1997; Verchot et al., 1999; Ludwig et al., 2001). However, semi-arid and arid soils, which are generally believed to be (a) nutrient poor, (b) nitrogen limited, and (c) of low microbiological activity due to water and starvation stress, release considerable amounts of NO and N_2O, as soon as they are wetted (e.g. even by low and/or sporadic rainfall). The ratio of fluxes from wet to those from dry soils ranges between 1.5–325 and 2.3–23 for NO and N_2O, respectively. It should be mentioned, that emissions (at least of NO) from semi-arid soils at the onset of the rainy season could have an "explosive" character (Meixner et al. 1997, Otter et al. 1999). For Chihuanan desert soils, Hartley and Schlesinger (2000) reported a 10-fold increase of biogenic NO emission within only 10 min after a 20 mm artificial rainfall.

Table 2 : Compilation of recent literature concerning field and laboratory measurements of NO and N_2O fluxes from semi-arid, arid, and hyper-arid soils (Harris et al (1996) have not reported NO fluxes under dry soil conditions; data of Aranibar et al. (2004) have been used to calculate the corresponding wet/dry ratio).

location	description	mean flux dry	/ wet	flux meas. method	wet/dry ratio	geographic position lat. / long.	eleva-tion	annual precip.	annual air temp.	climate (Koppen-Geiger)	reference
		[ng $m^{-2}s^{-1}$]			[1]		[m a.s.l.]	[mm]	[°C]		
fluxes of nitric oxide (NO) :											
New Mexico,USA	Chihuahua desert, grassland	0,06	3,6	chamber (field)	65	32.6166° N 106.6666° W	1250	230	27,5	BWk	Hartley & Schlesinger 2000
New Mexico,USA	Chihuahua desert, Creosotebush	0,06	18	chamber (field)	325	32.6166° N 106.6666° W	1250	230	27,5	BWk	Hartley & Schlesinger 2000
Israel	Negev desert	3,2	29	chamber (laboratory)	9,3	30.8500° N 34.7800° E	470	100	18,5	BWh	this work
Namibia	Savanna, Kalahari sands (Oshivelo)	1,5	30	aircraft gradient	20	18.7000° S 17.2000° E	1102	358	22,4	BWh	Harris et al. 1996
Namibia	Namib desert, gravel desert	0,3	3,6	chamber (laboratory)	12	23.1117° S 15.0219° E	670	23	21,1	BWh	this work
Namibia	Namib desert, dune	0,3	7,0	chamber (laboratory)	23	23.3407° S 15.0230° E	464	23	21,1	BWh	this work
Namibia	Namib desert, interdunal plane	0,3	3,1	chamber (laboratory)	10	23.3410° S 15.0210° E	434	23	21,1	BWh	this work
Botswana	Kalahari sands (Tshane)	1,5	5,0	chamber (laboratory)	3,3	24.1600° S 21.8900° E	1118	296	20,6	BWh	Aranibar et al. 2004
China	Gobi desert Inner Mongolia	0,5	20	chamber (laboratory)	40	49.2333° N 119.7166° E	614	352	-1,6	BWk / BSk	this work
Colorado, USA	Shortgrass steppe	2,0	23	chamber (field)	12	40.8166° N 104.7666° W	1650	322	8,6	Bsk	Epstein et al. 1998
Colorado, USA	Shortgrass steppe, sandy loam	4,7	28	chamber (field)	5,8	40.8166° N 104.7666° W	1650	322	8,6	Bsk	Martin et al. 1998
Colorado, USA	Shortgrass steppe, sandy clay loam	2,3	9,3	chamber (field)	4,0	40.8166° N 104.7666° W	1650	322	8,6	Bsk	Martin et al. 1998
Colorado, USA	Shortgrass steppe, clay loam	2,5	17	chamber (field)	7,0	40.8166° N 104.7666° W	1650	322	8,6	Bsk	Martin et al. 1998
Colorado, USA	Grassland	0,2	1,2	chamber (field)	6,0	40.0166° N 105.2833° W	1885	478	10,7	Bsk / H	Parrish et al. 1987

Table 2 :Compilation of NO and N_2O fluxes from semi-arid, arid, and hyper-arid soils (cont'd).(For the Niger site, Le Roux et al. (1995) have not given any NO fluxes under dry soil conditions; half of their NO flux detection limit has been used here, since no detectable NO fluxes have been observed there under dry soil conditions).

location	**description**	**mean flux dry / wet [ng $m^{-2}s^{-1}$]**		**flux meas. method**	**wet/dry ratio [1]**	**geographic position lat. / long.**	**eleva- tion [m a.s.l.]**	**annual precip. [mm]**	**annual air temp. [°C]**	**climate (Koppen- Geiger)**	**reference**
fluxes of nitric oxide (NO) :											
Niger	Savanna, topical, dry	0,1	5,7	chamber (field)	57	13.5000° N 3.0000° E	305	540	29,0	BSh	Le Roux et al. 1995
Zimbabwe	Kalahari sands (Victoria Falls)	0,5	22	chamber (laboratory)	44	18.1000° S 25.8500° E	1061	659	20,9	BSh	this work
Botswana	Kalahari sands (Pandamatenga)	1,5	10	chamber (laboratory)	6,7	18.6600° S 25.5000° E	950	659	20,9	BSh	Aranibar et al. 2004
Botswana	Kalahari sands (Maun)	1,5	36	chamber (laboratory)	24	19.9200° S 23.5900° E	945	452	22,4	BSh	Aranibar et al. 2004
Botswana	Kalahari sands (Okwa)	1,5	61	chamber (laboratory)	41	22.4100° S 21.7100° E	1131	439	21,2	BSh	Aranibar et al. 2004
South Africa	Savanna, nutrient poor	1,3	8,0	chamber (laboratory)	6,2	24.6500° S 28.7000° E	1250	625	19,0	BSh	Otter et al. 1999
South Africa	Savanna, nutrient rich	0,9	5,5	chamber (laboratory)	6,1	24.6500° S 28.7000° E	1250	625	19,0	BSh	Otter et al. 1999
South Africa	Savanna (Nylsvley)	1,9	20	chamber (field)	10	24.6500° S 28.7000° E	1250	625	19,0	BSh	Scholes et al. 1997
Spain (Andalusia)	arable land, non-fertilized	2,0	109	chamber (field)	55	37.0000° N 5.6000° W	20	585	18,5	BSh / Csa	Slemr & Seiler 1984
Venezula	managed natural savanna	1,9	12	chamber (field)	6,1	8.8833° N 67.3166° W	500	1300	27,6	Aw / BSh	Cardenas et al. 1993
California, USA	Grassland, unburned	4,0	11	chamber (field)	2,8	34.2000° N 117.7667° W	366	420	16,8	Csa / Bsk	Levine et al. 1988
California, USA	Grassland, burned	2,4	16	chamber (field)	6,5	34.2000° N 117.7667° W	366	420	16,8	Csa / Bsk	Levine et al. 1988
California, USA	Chaparral, unburned	10	15	chamber (field)	1,5	34.2000° N 117.7667° W	366	420	16,8	Csa / Bsk	Levine et al. 1988
California, USA	Chaparral, burned	8,8	45	chamber (field)	5,1	34.2000° N 117.7667° W	366	420	16,8	Csa / Bsk	Levine et al. 1988
California, USA	Chaparral, burned	15	23	chamber (field)	1,5	34.2000° N 117.7667° W	366	420	16,8	Csa / Bsk	Anderson & Poth 1989

Table 2 :Compilation of recent literature concerning field and laboratory measurements of NO and N_2O fluxes from semi-arid, arid, and hyper-arid soils (cont'd).

location	description	mean flux dry / wet		flux meas. method	wet/dry ratio	geographic position lat. / long.	eleva-tion	annual precip.	annual air temp.	climate (Koppen-Geiger)	reference
		dry	wet								
		[ng $m^{-2}s^{-1}$]			[1]		[m a.s.l.]	[mm]	[°C]		
fluxes of nitric oxide (NO) :											
Zambia	Kalahari sands (Mongu)	1,5	13	chamber (laboratory)	8,7	23.2500° E 117.7667° W	1053	979	22,6	Cwa / BSh	Aranibar et al. 2004
Zimbabwe	Savanna, period. flooded	2,2	142	chamber (laboratory)	65	31.4666° E 117.7667° W	1630	800	15,4	Cwa / BSh	this work
Zimbabwe	Savanna, sheep grazing	0,5	33	chamber (laboratory)	66	31.4666° E 117.7667° W	1630	800	15,4	Cwa / BSh	this work
Zimbabwe	Savanna, cattle grazing	0,5	51	chamber (laboratory)	102	31.4666° E 117.7667° W	1630	800	15,4	Cwa / BSh	this work
Zimbabwe	Miombo, burned	2,0	90	chamber (laboratory)	45	31.4666° E 117.7667° W	1630	800	15,4	Cwa / BSh	this work
Zimbabwe	Miombo (Marondera)	0,5	1,5	chamber (field)	3,0	31.4666° E	1630	800	15,4	Cwa / BSh	Meixner et al. 1997
Zimbabwe	grassland (Marondera)	1,8	5,6	chamber (laboratory)	3,1	18.1833° S 31.4666° E	1630	800	15,4	Cwa / BSh	this work
Zimbabwe	grassland (Marondera)	0,5	4,4	chamber (field)	8,8	18.1833° S 31.4666° E	1630	800	15,4	Cwa / BSh	Meixner et al. 1997
Zimbabwe	agricultural soil, fallow	0,2	5,3	chamber (field)	27	18.1833° S 31.4666° E	1630	800	15,4	Cwa / BSh	Meixner et al. 1997
Zimbabwe	Savanna, maize unfertilized	0,6	3,5	chamber (laboratory)	5,8	18.1833° S 31.4666° E	1630	800	15,4	Cwa / BSh	this work
Zimbabwe	Savanna, ground-nut unfertilized	1,8	9,0	chamber (laboratory)	5,0	18.1833° S 31.4666° E	1630	800	15,4	Cwa / BSh	this work
Zimbabwe	Savanna, ground-nut unfertilized	0,5	27	chamber (field)	54	18.1833° S 31.4666° E	1630	800	15,4	Cwa / BSh	Meixner et al. 1997
Zimbabwe	Savanna, ground-nut fertilized	2,7	16	chamber (laboratory)	5,8	18.1833° S 31.4666° E	1630	800	15,4	Cwa / BSh	this work
Zimbabwe	Savanna, ground-nut fertilized	0,5	8,5	chamber (field)	17	18.1833° S 31.4666° E	1630	800	15,4	Cwa / BSh	Meixner et al. 1997
South Africa	Savanna (Krueger National)	1,4	28	chamber (field)	20	31.2333° S 25.2500° E	600	740	21,0	Cwa / BSh	Levine et al. 1996, Parsons et al. 1996

Table 2 :Compilation of recent literature concerning field and laboratory measurements of NO and N_2O fluxes from semi-arid, arid, and hyper-arid soils (cont'd).

location	description	mean flux dry	mean flux wet	flux meas. method	wet/dry ratio	geographic position lat. / long.	eleva-tion	annual precip.	annual air temp.	climate (Koppen-Geiger)[C]	reference
		[ng $m^{-2}s^{-1}$]			[1]		[m a.s.l.]	[mm]	[°C]		
fluxes of nitrous oxide (N_2O) :											
Nevada, USA	Mojave desert	0,3	N/A	chamber (field)	N/A	36.8166° N 115.9166° W	968	140	20,2	BWk	Billings et al. 2002
Arizona, USA	Sonoran desert	0,5	4,3	chamber (field)	8,6	32.2500° N 110.9666° W	648	305	17,3	BWk	Guilbault & Matthias 1998
Colorado, USA	Shortgrass steppe	0,2	2,9	chamber (field)	13	40.8166° N 104.7666° W	1650	322	8,6	Bsk	Epstein et al. 1998
Colorado, USA	Shortgrass steppe, non-fertilized	0,2	1,1	chamber (field)	5,0	40.8166° N 104.7666° W	1650	350	8,6	Bsk	Mosier et al 1996
South Africa	Savanna (Krueger National)	1,0	N/A	chamber (field)	N/A	31.2333° S 25.2500° E	600	740	21,0	BSh / Aw	Levine et al. 1996
Spain (Andalusia)	arable land, non-fertilized	4,2	9,7	chamber (field)	2,3	37.0000° N 5.6000° W	20	585	18,5	BSh / Csa	Slemr et al. 1984
Washington, USA	shrub-steppe	0,4	8,5	chamber (field)	23	46.4550° N 119.4231° W	200	220	10,5	Csb / H	Mummey et al. 1997
Canada	fallow, black soil zone	0,4	4,6	chamber (field)	11	53.0166° N 105.7500° W	350	395	2,2	Dfc / Bsk	Corre et al. 1996

[C] The used shorthand code of letters are those of the Koppel-Geiger climate classification system (see Strahler and Strahler, 1999). *First letter*: A=tropical climates; B=dry climates, C=warm temperature climates, D=snow climates; H=highland climates. *Second Letter*: S=steppe climates (semi-arid); W=desert climates (arid); f=sufficient precipitation in all months; s=dry season in summer of the respective hemisphere; w=dry season in winter of the respective hemisphere. *Third Letter*: a=warmest month over 22 °C; b=warmest month under 22 °C; c=fewer than 4 months with means over 10 °C; h=dry and hot (mean annual temperature over 18 °C); k=dry and cold (mean annual temperature under 18 °C).

3.1 THE ROLE OF SOIL MOISTURE AND SOIL TEMPERATURE

As already mentioned above, field data do not allow to easily seperate the effects of soil moisture and soil temperature on biogenic NO and N_2O fluxes. Only few authors have performed a comprehensive analyses of their field data (Slemr and Seiler, 1984; Cardenas et al., 1993; Parsons

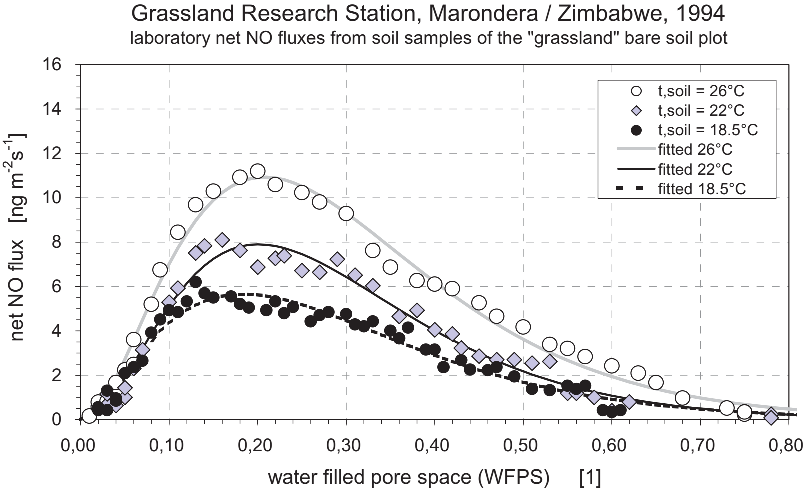

Figure 3a: The dependence of net NO flux from soil moisture (WFPS) and soil temperature for a semi-arid, unfertilzed savanna grassland soil (results of laboratory experiments on a soil sample taken on 14 December, 1994 at the Mariner Grassland Research Station, Mashonaland-East, Zimbabwe).

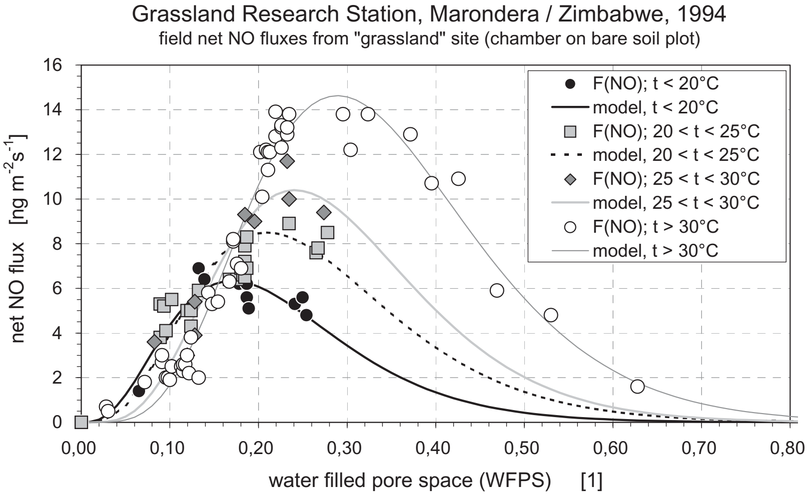

Figure 3b: Net NO flux as dependent on soil moisture (WFPS) and soil temperature at bare soil plot of a semi-arid, unfertilized savanna grassland site (results of field experiments using dynamic soil chambers; September–December 1994, Marondera Grassland Research Station, Mashonaland-East, Zimbabwe; see Meixner et al., 1997).

et al., 1996; Scholes et al., 1997; Epstein et al., 1998; Martin et al., 1998; Pilegaard et al., 1999; Hartley and Schlesinger, 2000). However, laboratory investigations on soil samples offer the unique chance to study responses of one factor, while the other is held constant (Yang and Meixner, 1997; Otter et al., 1999; van Dijk and Meixner, 2001; Aranibar et al., 2004). Corresponding laboratory results on soil samples from a semi-arid, unfertilized grassland site in Zimbabwe are presented in Figure 3a. A characteristic optimum curve for the response of the net NO flux to soil moisture and an exponential increase with soil temperature ($Q_{10} \approx 2$; see 2.2.3.) is observed. Optimum soil moistures ($WPPS_{opt}$) are around 0.20 with a tendency to slightly decrease with decreasing soil temperature. Kirkman et al. (2001) used these laboratory results for the first countrywide estimate of spatio-temporal soil emissions in southern African (Zimbabwe).

Soil samples (0–5 cm) at Marondera were taken exactly from those soil plots, which have been enclosed by the steel frames of the dynamic chambers used during field measurements. Results of the field experiments (see Meixner et al., 1997) have been classified according to measured WFPS and ranges of measured soil temperatures at –5 cm ($t_{soil} < 20°C$, $20 < t_{soil} < 25°C$, $25 < t_{soil} < 30°C$, and $t_{soil} > 30°C$). While there is larger scatter of the field data and low data coverage for WFPS > 0.3 and $t_{soil} < 30°C$, differences between laboratory and field data are small, as already reported earlier (Yang and Meixner, 1997; Ludwig et al., 2001). There is a significant increase of $WFPS_{opt}$ with increasing soil temperature.

An algorithm has to be developed to fit the laboratory as well as the field data. The net NO flux, F_{NO} (in ng $m^{-2}s^{-1}$) is described by

$$F_{NO}(WFPS) = a\ WFPS^b \exp(-c\ WFPS)$$

where WFPS is the water filled pore space. The parameters a, b, and c are related to observed values by

$$a = F_{NO}(WFPS_{opt}) / [WFPS_{opt}{}^b \exp(-b)]$$
$$b = \ln[F_{NO}(WFPS_{opt}) / F_{NO}(WFPS_{upp})] / [\ln(WFPS_{opt}/WFPS_{upp}) + WFPS_{upp}/WFPS_{opt} - 1]$$
$$c = -b / WFPS_{opt}$$

where $WFPS_{opt}$ is the soil moisture at which the maximum net NO flux is observed; $F_{NO}(WFPS_{opt})$ equals $\max[F_{NO}(WFPS)]$; and $WFPS_{upp}$ is the soil moisture at which $F_{NO}(WFPS) = F_{NO}(WFPS_{upp}) \approx 0$ for $WFPS > WFPS_{opt}$. Numerical values of the parameters a, b, and c can be determined by minimizing the sum product of the difference between measured and fitted data points.

We applied this algorithm also to the results of laboratory studies on soil samples that have been taken in the Namib desert (Gobabeb Research Station, 23.34°S, 15.02°E). Results are shown in Figure 4. To our knowledge, these are the first results of net NO fluxes from a hyper-arid region. Compared to the results obtained with semi-arid soils (Fig. 3a), net NO emissions are lower, and –at comparable soil temperatures– $WFPS_{opt}$ of Gobabeb desert soils are approximately two third of the semi-arid Marondera soils. Since the work of Linn and Doran (1984), $WFPS_{opt}$ of approximately 0.6 is often be quoted for a number of microbial processes. However, this value is definitely not applicable with respect to the emission of NO from semi-arid and arid soils (see also Cárdenas et al. (1993), Parsons et al. (1996), Yang and Meixner (1997), Scholes et al. (1997), Epstein et al. (1998), Martin et al. (1998), Otter et al. (1999), Hartley and Schlesinger (2000), and Aranibar et al. (2004)). Very low values for $WFPS_{opt}$ (< 0.15) might be typical for hot arid regions: similar and even lower values have been found for the Chihahuan desert (Hartley and Schlesinger, 2000) and for the southern part of the Kalahari transect (Aranibar et al., 2004). As already pointed out by Aranibar et al. (2004), these low $WFPS_{opt}$ values indicate that even relatively dry soils can emit considerable amounts of NO. Nevertheless, NO emissions from desert soils are at the very low end of those observed globally, since emission rates decrease strongly with aridity.

It is well known that addition of water to dry soils typically produces strong increases not only of NO, but also of N_2O emission (e.g. Davidson, 1992; Meixner and Eugster, 1999). It seems, that this increase is caused by a “dormant” water-stressed microbial community. As soon as the first water drops are supplied to the desiccated soil, this microbial community “wakes up”. It is fed by

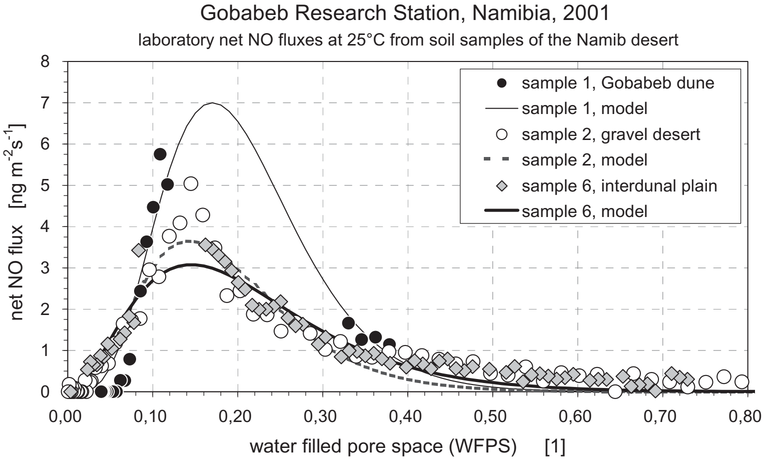

Figure 4: The dependence of net NO flux from soil moisture (WFPS) and soil temperature for hyper-arid desert soils (results of laboratory experiments on soil samples taken on 14 December, 1994 at the Gobabeb Research Station, Namib, Namibia).

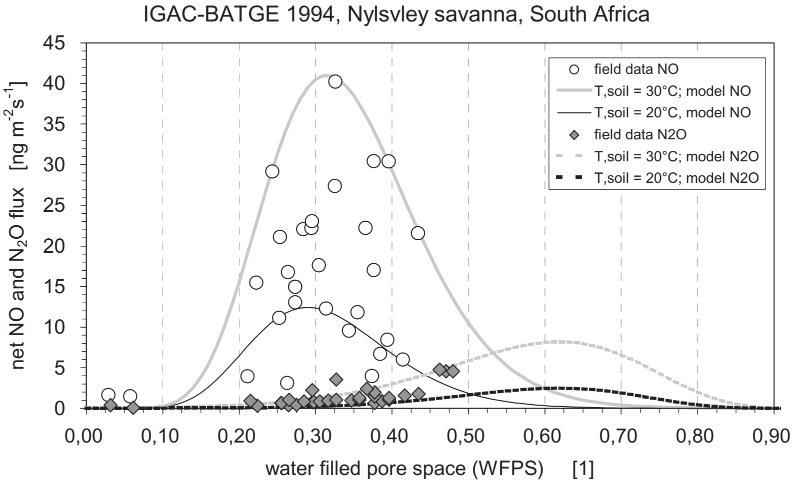

Figure 5: The dependence of net NO and net N_2O fluxes from soil moisture (WFPS) and soil temperature for semi-arid svanna soils (results of field experiments 12-30 November, 1994 at Nylsvley Nature Reserve, South Africa).

nutrients (nitrate and or ammonium), which have accumulated during the dry season (semi-arid regions) or longer dry periods between infrequent/sporadic rainfalls (deserts). Indeed, nitrifying bacteria (e.g. autotrophic nitrifiers) and persistent denitrifying enzymes have been found (a) to be well adapted to survive extreme drought and starvation stresses and (b) to become very active within minutes after wetting (Davidson, 1992). In turn, since soil microbes in semi-arid ecosystems have a strong sensitivity to water deficit, they experience water stress earlier than starvation due to the depletion of soil mineral nitrogen (D'Odorico et al., 2003). For a mechanistic description of wetting and drying effects on nutrient cycles see Chapter 11.

The relationship between WFPS and relative fluxes of NO, N_2O, and N_2 shown in Fig. 1 suggests that low N_2O fluxes are to be expected for semi-arid and arid soils. Indeed, whenever detected at all, N_2O fluxes are low in these enviroments. Data in Table 2 show that there is a strong tendency for much higher NO than N_2O fluxes under "wet soil" conditions. Out of the few studies with NO and N_2O fluxes having been measured simultaneously in semi-arid regions, the results of Scholes et al. (1997) have been selected for presentation in Figure 5. This data set was obtained during subsequent wetting experiments on nutrient-poor and nutrient-rich soils of the Nylsvley Nature Reserve (South Africa). Since soil temperatures between 21and 32°C have been reported for this experiment, t_{soil} = 20 and 30°C have been used to calculate enveloping curves in Figure 5 by the new algorithm. The highest WFPS observed was 0.48, where N_2O fluxes still have not started to decrease. A value of $WFPS_{opt}$ = 0.62 has arbitrarily been chosen for the calculation of the N_2O flux, this value being in accordance with the results of Parsons et al. (1996) and Davidson (1992). Under actual conditions at Nylsvley, the ratio of N_2O and NO fluxes was on the average 0.09. This result led Scholes et al. (1997) to the conclusion, that undisturbed and unfertilized semi-arid savanna soils are unlikely to make a major contribution to global N_2O emissions.

3.1. PRODUCTION AND CONSUMPTION OF NO UNDER SEMI-ARID CONDITIONS

During the laboratory studies on savanna grassland soil samples from Marondera (c.f. Fig. 3a), a selection of soil samples (grassland and Miombo woodland plots (both unfertilized); unfertilized

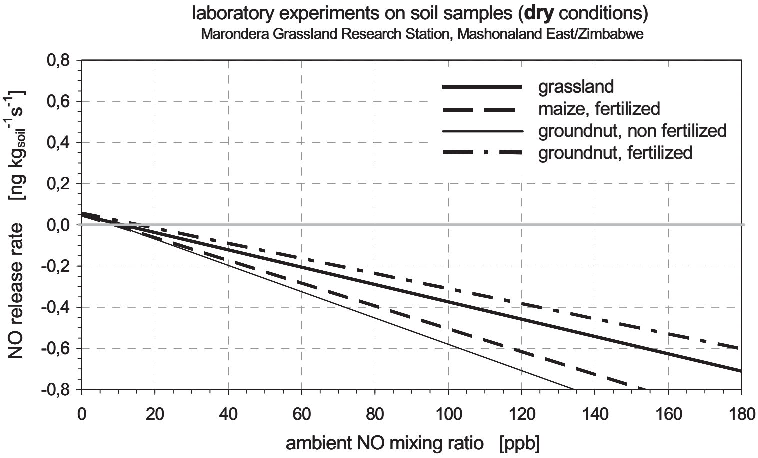

Figure 6a: Results of NO fumigation experiments on different soil samples under "dry soil conditions" (i.e. volumetric soil water content < 3 %). NO release rates are measured in ng of nitrogen per kg of soil and per sec. Soil samples have been taken on 14 December 1994 at the Marondera Grassland Research Station, Mashonaland-East, Zimbabwe.

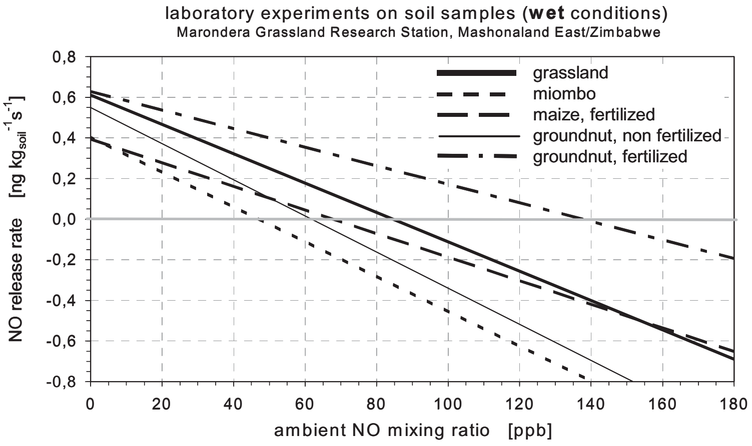

Figure 6b: Same as Figure 6a, but for "wet soil conditions" (i.e. volumetric soil water content = 13 %).

and fertilized maize and groundnut plots) have been fumigated with known NO concentrations. Corresponding NO release rates versus NO concentration in the headspace of the dynamic soil chamber are plotted in Figures 6a ("dry soil conditions") and 6b ("wet soil conditions"). The intercepts of the individual lines with the y-axis are equivalent to the NO production rates of the different soils at natural conditions. The intercepts with the x-axis are equivalent to the corresponding NO compensation concentrations (see Section 2.2.4), and NO consumption rates are calculated from the slope of the lines (see Remde et al., 1993; Yang et al., 1996). NO production and consumption rates, as well as NO compensation concentrations are much lower under dry soil than under wet soil conditions, elucidating again a "dormant" water-stressed microbial community, which "wakes up" after the first water is supplied to the desiccated soils. The observed ambient NO concentrations at the Marondera site are typically well below 1 ppb (Meixner et al. 1997). Nevertheless, these semi-arid soils are -at least in the wet season- definitely a source for atmospheric NO. However, during the dry season, when wide spread savanna fires cause massive pyrogenic NO emissions and consequently higher ambient NO concentrations, soils may also act as temporary sinks of NO.

3.2. SOIL TEXTURE: A CONTROLLING FACTOR FOR NO AND N_2O EMISSION FROM SEMI-ARID, ARID, AND HYPER-ARID LANDS?

There is evidence from a recent modelling study (Ridolfi et al., 2003) that N_2O emissions from fine-textured soils typically exceed those from coarser soils, while the opposite is the case for NO emissions (see Chapters 3 and 11). Moreover, NO emissions from clayey soils might be very low, while N_2O emissions become significant. From a soil physical/chemical point of view these results are very plausible with respect to NO fluxes, since coarser (sandy) soils (below field capacity) reveal higher rates of diffusion than fine-textured (clayey) soils. Furthermore, in sandier soils the importance of advective transport increases, which has the potential to increase the soil-atmosphere exchange severalfold over that by molecular diffusion (Martin et al., 1998). Consequently, NO has a higher chance to escape from sandier soils before it is biologically consumed and/or takes part in any reactions (Scholes et al., 1997). The escape efficiency by physical pathways is more important for NO than for N_2O because the chemical reactivity of NO is much higher. However, during a 2-year, large-scale study in the Colorado shortgrass steppe, Martin et al. (1998) observed highest average NO fluxes from sandy loam soils and lowest fluxes from clay loam soils. Admittedly, the trend of increasing NO fluxes with increasing sand content was statistically not significant. There is, however, increasing evidence that there is a textural influences on the optimum water filled pore space ($WFPS_{opt}$) for NO emission.

Table 3. Optimum water filled pore space ($WPFS_t$) for NO emission from semi-arid, arid, and hyper-arid soils.

location	biome	sand [%]	silt [%]	clay [%]	bulk density [kg m^{-3}]	$WFPS_{opt}$ [1]	Reference
New Mexico, U.S.A.	Chihuahuan desert, shrubland	71	NA	8	1580	< 0.15	Hartley & Schlesinger 2000
New Mexico, U.S.A.	Chihuahuan desert, grassland	69	NA	10	1580	< 0.10	Hartley & Schlesinger 2000
New Mexico, USA.	Chihuahuan desert, playa	18	NA	51	1580	0.38	Hartley & Schlesinger 2000
China	Gobi desert / Inner Mongolia	NA	NA	NA	1290	0.25	this work
Namibia	Namib desert, gravel	NA	NA	NA	1390	0.12	this work
Namibia	Namib desert, dune	NA	NA	NA	1330	0.14	this work
Namibia	Namib desert, interdunal	NA	NA	NA	1390	0.12	this work
Zambia	Kalahari sands (Mongu)	98	2	1	1260	0.14	Aranibar et al. 2004
Botswana	Kalahari sands (Pandamatenga)	97	2	1	1580	0.23	Aranibar et al. 2004
Botswana	Kalahari sands (Okwa)	96	2	2	1530	0.10	Aranibar et al. 2004
Botswana	Kalahari sands (Maun)	96	1	3	1600	0.17	Aranibar et al. 2004
Zimbabwe	savanna, grassland	87	3	10	1430	0.16	Meixner et al. 1997
S. Africa	savanna (Nylsvley)	88	NA	4	1560	0.26	Scholes et al. 1997
S. Africa	savanna, biennial burned	85	5	10	1600	0.20	Parsons et al. 1996
S. Africa	savanna, fire exclusion	83	7	11	1600	0.22	Parsons et al. 1996
S. Africa	savanna, thornveld	36	8	56	1700	0.35	Parsons et al. 1996
S. Africa	savanna, nutrient poor	74	6	20	1560	0.28	Otter et al. 1999
S. Africa	savanna, nutrient rich	71	7	22	1560	0.40	Otter et al. 1999
S. Africa	savanna, floodplain	34	12	54	1100	0.51	Otter et al. 1999
Spain	agricultural, non-fertilized	89	4	7	1630	0.15	Slemr & Seiler 1984
Venezuela	Savanna	70	13	17	1500	0.41	Cardenas et al. 1993
Colorado, U.S.A.	shortgrass steppe	72	15	13	1400	0.35	Martin et al. 1998
Colorado, U.S.A.	shortgrass steppe	42	18	30	1300	0.66	Martin et al. 1998

For a total of 35 soil samples from the Brazilian tropics, van Dijk (2001) found a clear relationship between increasing $WFPS_{opt}$ and increasing clay content . Studying NO fluxes under semi-arid field conditions, Otter et al. (1999) detected $WFPS_{opt}$ values between 0.3 and 0.4 for sandy soils, while for a clayey floodplain soil $WFPS_{opt}$ was 0.6. Table 3 contains those results for NO fluxes from semi-arid, arid, and hyperarid soils where soil texture data and/or $WFPS_{opt}$ values have been reported too. For clay contents > 30 %, corresponding $WFPS_{opt}$ values for NO emission are higher than 0.35. Lowest $WFPS_{opt}$ (< 0.15) have been observed for arid and hyper-arid soils with clay contents less than 10%. This leads us to the hypothesis, that arid and hyper-arid lands will emit NO after very low-intensity rainfalls. But also dew fall and/or deposition of fog droplets (as occurring in the Namib desert) might add enough moisture to the first millimetres of the surface to trigger temporarily limited NO emission.

3.3. NITRIFICATION VS. DENITRIFICATION: OBSERVATIONS FROM SEMIARID AND ARID LANDS

Generally, if nitrification is dominating NO and N_2O fluxes from soils, than the major controllers are soil moisture, O_2 and NH_4^+ availability (see Chapter 11). If denitrification is dominating, soil moisture and the availability of reduced C and terminal electron acceptors (O_2, NO_3^-, NO_2^-) are most important (Smart et al., 1999). The limiting factors for any biological activity in semi-arid and arid systems are known: soil moisture and nitrogen availability (in that order; D'Odorico et al., 2003). Nitrogen availability in semi-arid and arid ecosystems depends considerably on the area and time (Fisher et al., 1987). This is especially true for the surface soil layers where NO production and NO consumption processes are located (Conrad, 1996). It is no surprise, that early reports about the dominance of nitrification vs. denitrification for NO and N_2O emissions from semi-arid and arid soils have been somewhat contradicting and rely on the choice of the site, such as wet tropical savannas or semi-arid / arid regions (Smart et al., 1999). Addition of NO_3^- (NH_4^+) led to higher (lower) NO fluxes in wet tropical systems. Consequently denitrification has been accounted for the dominant process. In warm (hot) semi-arid and arid regions, addition of NH_4^+ (NO_3^-) led to higher (lower) NO fluxes, respectively. Therefore, nitrification has been claimed to be the more important process. Considering, that nitrification is a highly aerobic process, there is growing evidence that arid soils are characterized by high nitrification activities due to their warm, dry and aerobic nature (Smart et al. 1999). Indeed, Martin et al. (1998) clearly state that nitrification is the dominant process for both NO and N_2O emissions from shortgrass steppe. According to Parsons et al. (1996), Scholes et al. (1997), Otter et al. (1999), and Aranibar et al. (2004) this holds (at least) for NO emissions from semi-arid and arid southern African savannas and deserts. Hartley and Schlesinger (2000) state, that in (semi-) deserts, with a short wet season, corresponding NO fluxes from nitrifying bacteria could be extremely high (see Table 2) because soil NH_4^+ accumulates by mineralization of organic nitrogen (e.g. from litterfall of shrubs) (Fisher et al., 1987). Finally, it should be mentioned, that in semi-arid, particularly in arid soils, where generally low nutrient pools are prevailing, high microbial metabolism and high turnover rates of (few) nutrients might be major factors of observed NO fluxes (Le Roux et al., 1995). Davidson (1992) has specifically addressed the (small) NO_2^- pool of these soils, but also the potentially high (and at least temporarily) nitrogen flux through this pool.

3.4. NITROGEN INPUTS TO SEMI-ARID AND ARID ECOSYSTEMS

Input of plant available nitrogen to semi-arid and arid systems is caused by two major processes: (a) biogenic fixation of atmospheric molecular nitrogen (N_2) and (b) to deposition of nitrogen compounds from the atmosphere (see also Chapter 11). For arid areas, N_2 fixation is a desirable process only when nitrogen is the major limiting nutrient; overall costs are high (Aranibar et al., 2004). Nitrogen fixating legumes (Fabaceae) are also dominant in the driest regions of the Kalahari sands. Cyanobacteria, also capable of fixing atmospheric N_2, are widely distributed in semi-arid and arid soils. An estimate of nitrogen inputs by N_2 fixation of soil crusts is difficult, corresponding values range from a few grams to 100 kg $ha^{-1}a^{-1}$. Scholes et al. (2003) have estimated biological N_2 fixation at southern African fine leafed and broad-leafed semi-arid sites to 18 and 5 kg $ha^{-1}a^{-1}$, respectively. Deposition of nitrogen compounds from the atmosphere to semi-arid and arid lands can occur in the form of (a) wet deposition (i.e. in-cloud and below-cloud scavenging) of soluble gases (HNO_3, HNO_2, NH_3) and aerosol particles (NO_3^-, NO_2^-, NH_4^+), (b) dry deposition of gases NO, NO_2, HNO_3, HNO_2, NH_3 and PAN (peroxyacetylnitrate), (c) dry deposition of aerosol particles (NO_3^-, NO_2^-, NH_4^+), and (d) deposition during the dew forming process (see Meixner, 1994). Since most semi-arid and arid areas are (very) remote, atmospheric input from the industrialized, polluted regions is thought to be generally small; nitrogen inputs through dry and wet deposition of 3 and < 2 kg $ha^{-1}a^{-1}$ were reported for Sonoran desert and Utah semi-arid sites, respectively (Guilbault and Matthias, 1998; Smart at al. 1999). Galy-Lacaux et al. (2003) estimated 2 kg $ha^{-1}a^{-1}$ as total nitrogen deposition to West African semi-arid and arid ecosystems (65% by dry, 35% by wet deposition). However, there is a very particular situation for large-scale nitrogen deposition in southern Africa. Pyrogenic and anthropogenic emissions of NH_3, NO and NO_2 are dispersed into a well-mixed, persistent, atmospheric boundary layer, which is typically capped by a strong temperature inversion (see Chapters 11 and 16 for a discussion of fire effects on nitrogen cycling and fire regimes). This leads to considerable accumulation of nitrogen containing gaseous and particulate pollutants in the atmospheric boundary layer; here NO and NO_2 will be transformed to HNO_3 and/or aerosol NO_3^- within a few days. Within very persistent anti-cyclons (see Garstang et al., 1996), air of the atmospheric boundary layer is frequently cycling over southern Africa, transporting pollution (and products) from industrialized (burning) regions to the remote semi-desert and desert areas. This specific situation enhances dry deposition of nitrogen compounds also at remote semi-arid and arid ecosystems. In particular, HNO_3 and NH_3 are deposited, since their dry deposition rates are at least one order of magnitude higher than that of NO_2 (see Meixner, 1994). Scholes et al. (2003) have estimated corresponding average inputs of 8 and 7–21 kg $ha^{-1}a^{-1}$ by wet and dry deposition processes, respectively.

3.5. GLOBAL IMPORTANCE OF NO AND N_2O EMISSIONS FROM NATURAL SEMI-ARID AND ARID SOILS

According to Davidson and Kingerlee (1997), who stratified worldwide NO emissions according to major biomes, the categories “chaparral/thorn forest” and “tropical savanna/woodland” comprise more than half of the total global NO soil source (21 Tg a^{-1}). It is most likely, that humid tropical savannas contribute most to this figure. According to Otter et al. (1999), large NO emissions from tropical savannas are determined by the length of long, hot and wet summers, providing optimal conditions for biogenic production of NO (and N_2O) in the soil. However, towards sub-tropical semi-arid, and particularly for arid regions, this determinant may become less important. Scholes et al. (1997) state that NO fluxes from sub-tropical savannas generally exceed those from sub-tropical forest soils. Concerning N_2O fluxes, they consider (a) N_2O fluxes from tropical forest soils (warm and wet) to be the globally most important, and (b) N_2O fluxes from sub-tropical savannas to be always lower than those from corresponding forest soils. The argument is based on the fact that denitrification benefits from the carbon-rich and somewhat wetter soils in the forests. The undoubtedly large effect of the first rains to the “wetting” pulse of the NO emission from semi-arid and arid African soils is thought to contribute little to the global NOx budget. However, Scholes et al. (1997) consider this pulse to be an important contributor to episodes of high ambient ozone in southern Africa.

Despite the few additional results from desert and semi-desert soils presented in this paper, the statement of Davidson and Kingerlee (1997) is still valid.These biomes still constitute a major gap in our knowledge, but are probably very significant for the global NOx budget. They emphasize that, despite the fact that deserts have low plant productivity in general, inorganic nitrogen can accumulate in desert and semi-desert soils during (long) dry periods. During regular or short wet periods, microbial activity will peak and lead to substantial NO emissions, which are additionally favoured by mostly sandy soils with high porosity (see 3.3.).

Due to the fact, that biogenic N_2O emission is favoured by denitrification processes at high soil moisture contents ($WFPS_{opt} \approx 0.6$), N_2O fluxes from semi-arid soils are expected to be low. Those from desert soils are very low, if detectable at all. Indeed, based on field measurements, there is broad consensus that the contribution of biogenic N_2O emissions from these (unfertilized) ecosystems does not contribute much to the global N_2O budget (e.g. Scholes et al., 1997; Billings et al., 2002).

Effects of land-use changes on N_2O fluxes have been reported for semi-arid shortgrass steppe of the Great Plains of central North America (Mosier et al., 1996), which comprise approximately 19% of the global temperate grasslands. Conversion of grasslands to croplands led to 8-fold higher N_2O emissions for about 18 months following tillage. Still 25-50% higher N_2O emissions from tilled soils are observed even after 3 years. Reversion of cultivated soils back to grasslands will bring N_2O emissions from tilled soils down to those of native state in a period longer than 8 but shorter than 50 years. Guilbault and Matthias (1998) focussed the practice to change low-latitude desert ecosystems by fertilization and irrigation for agricultural, recreational, and landscaping purposes. The conversion of a natural Sonoran desert soil into a golf course (by regular irrigation with secondary sewage effluents) resulted in a considerable increase of N_2O fluxes. Information about the effects of (long-term) land use change on soil biogenic NO emissions are hardly available. There is only the suggestion of Hartley and Schlesinger (2000) that NO fluxes from Chihuahuan desert soils may have declined with the conversion of grassland to shrubland. However, it can be assumed that future land use changes of natural semi-arid and arid lands will (a) either include irrigation and fertilization (which will presumably cause higher NO emissions), or (b) will lead to degradation (e.g. through overgrazing and salinization, which will cause generally lower NO emission. Chapter 18 discusses in detail the main factors contributing to land degradation and desertification. According to Harrison and Pearce (2000), approximately 20 % of the world's susceptible dryland soils (1.035×10^9 ha) were degraded at the end of the 1990s (either by water and wind erosion or by chemical and physical deterioration); partitions to region constitute 7.7, 7.6, 9.6, 30.9, 35.8, and 8.4 % for North America, South America, Europe, Africa, Asia, and Australasia, respectively. Prominent and very important targets in this respect are the arid and semi-arid lands of Africa, East and Central Asia (Chuluun and Oijma, 2002). Particularly the latter deserve future attention, since virtually no measurements of soil NO and N_2O emissions are known for these regions.

Acknowledgements

The authors want to express their gratitude to Grant Kirkman and Sabine Seitz for taking soil samples in Namibia; to Ivonne Trebs, Faraidon Ashuri, and Grant Kirkman for their laboratory work on the Namibian soil samples; and to Dominique Serça, Franz J. Nathaus, Lackson T. Marufu, Edson Makina, and Thomas Fickinger for their support during the field experiment at the Grassland Research Station Marondera. Many thanks also to Jorn v. Jouanne for his valuable comments and his help to edit this paper. The research visit of WenXing Yang in Mainz has been supported through the partnership agreement between the Max Planck Society and the Chinese Academy of Science.

4. References

Anderson, I.C., Poth, M.A., Semiannual losses of nitrogen as NO and N_2O from unbumed and bumed chaparral, Global Biogeochemical Cycles, **3**, 1989, 121-135.

Andreae, M.O., Schimel, D.S., Exchange of trace gases between terrestrial ecosystems and the atmosphere, 1989, 346 p., Dahlem Konferenzen, Chichester, New York, John Wiley & Sons Ltd.

Aranibar, J.N., Otter, L., Macko, S.A., Feral, C.J.W., Epstein, H.E., Dowty, P., Eckardt, F., Shugart, H.H., Swap, R.J., Nitrogen cycling in the soil-plant system along a precipitation gradient in the Kalahari sands, Global Change Biology, **10**, 2004, 359-373.

Billings, S.A., Achaeffer, S.M., Evans, R.D., Trace N gas losses and N mineralization in Mojave desert soils exposed to elevated CO_2, Soil Biology and Biochemistry, **34**, 2002, 1777-1784.

Bouwman, A.F., Boumans, L.J.M., Batjes, N.H., Emissions of N_2O and NO from fertilized fields: Summary of available measurement data, Global Biogeochemical Cycles, **16**(4), 2002a, 1058, doi:10.1029/2001GB001811.

Bouwman, A.F., Boumans, L.J.M., Batjes, N.H., Modeling global annual N_2O and NO emissions from fertilized fields, Global Biogeochemical Cycles, **16**(4), 2002b, 1080, doi:10.1029/2001GB001812.

Butterbach-Bahl, K., Gasche, R., Breuer, L., Papen, H., Fluxes of NO and N_2O from temperate forest soils: impact of forest type, N deposition and of liming on the NO and N_2O emissions, Nutrient Cycling in Agroecosystems, **48**, 1997, 79-90.

Cárdenas, L., Rondón, A., Johansson, C., Sanhueza, E., Effects of soil moisture, temperature, and inorganic nitrogen on nitric oxide emission from acidic tropical savannah soils, Journal of Geophysical Research, **98** (D8), 1993, 14,783-14,790.

Chameides, W.L., Fehsenfeld, F., Rodgers, M.O., Cardelino, C., Martinez, J., Parrish, D., Lonneman, W., Lawson, D.R., Rasmussen, R.A., Zimmerman, P., Greenberg, J., Middleton, P., Wang, T., Ozone precursor relationships in the ambient atmosphere, Journal of Geophysical Research, **92**, 1992, 6037-6055.

Chuluun, T., Ojima, D., Land use change and carbon cycle in arid and semi-arid lands of East and central Asia, Science in China (Series C), **45**, 2002, 45-54.

Conrad, R., Soil microorganisms as controllers of atmospheric trace gases (H_2, CO, CH_4, OCS, N_2O, and NO). Microbiological Reviews, **60**, 1996, 609–640.

Corre, M.D., van Kessel, C., Pennock, D.J., Landscape and seasonal patterns of nitrous oxide emissions in a semiarid region. Soil Science Society of America Journal, **60**, 1996, 1806–1815.

Crutzen, P.J., Role of the tropics in atmospheric chemistry, in: The Geophysiology of Amazonia, Dickinson, R.E. (ed.), 1987, pp. 107-132, John Wiley & Sons, New York.

Davidson, E.A., Fluxes of nitrous oxide and nitric oxide from terrestrial ecosystems. In: Microbial production and consumption of greenhouse gases: Methane, nitrogen oxides, and halomethanes, Rogers, J.E. and Whitman, W.B. (eds), 1991, pp. 219–235. American Society for Microbiology, Washington, D.C.

Davidson, E.A., Sources of nitric oxide and nitrous oxide following wetting of dry soil, Soil Science Society of America Journal, **56**, 1992, 95-102.

Davidson, E.A., Kingerlee, W., A global inventory of nitric oxide emissions from soils, Nutrient Cycling in Agroecosystems, **48**, 1997, 37–50.

Davidson, E.A., Schimel, J.P., Microbial processes of production and consumption of nitric oxide, nitrous oxide and methane, in: Biogenic trace gases: measuring emissions from soil and water, P.A. Matson and R.C. Harriss (eds.), 1995, pp. 327–357. Oxford: Blackwell Scientific Publications Ltd.

van Dijk, S.M., PhD Thesis, 2001, Nitric oxide emissions from soils: effects of deforestation, 131 pp., University of Utrecht, Utrecht, The Netherlands, Universal press, Veenendal, The Netherlands (ISBN 90-393-2741-6).

D'Odorico, P., Laio, F., Porporato, A., Rodriguez-Iturbe, I., Hydrologic controls on soil carbon and nitrogen cycles. II. A case study, Advances in Water Resources, **26**, 2003, 59-70.

Epstein, H.E., Burke, I.C., Mosier, A.R., Hutchinson, G.L., Plant functional type effects on trace gas fluxes in the shortgrass steppe, Biogeochemistry, **42**, 1998, 145-168.

Fisher, F.M., Parker, L.W., Anderson, J.P., Whitford, W.G., Nitrogen Mineralization in a desert soil: Interacting effects of soil moisture and nitrogen fertilizer, Soil Science Society of America Journal, **51**, 1987,1033-1041.

Galy-Lacaux, C., Al Ourabi, H., Lacaux, J.P., Pont, V., Galloway, J., Mphepya, J., Pienaar, K., Sigha, L., Yoboue, V., Dry and wet atmospheric nitrogen deposition in Africa, IGACtivities Newsletter, **27**, 2003, 6-11.

Garstang, M., Tyson, P.D., Swap, R., Edwards, M., Kallberg, P., Linesay, J.A., Horizontal and vertical transport of air over southern Africa, Journal of Geophysical Research, **101**, 1996, 23,721-23,736.

Guilbault, M.R., Matthias, A.D., Emissions of N_2O from Sonoran Desert and effluent-irrigated grass ecosystems, Journal of Arid Environments, **38**, 1998, 87-98.

Gut, A., van Dijk, S., Scheibe, M., Rummel, U., Kirkman, G.A., Welling, M., Meixner, F.X., Andreae, M.O., NO emission from an Amazonian rain forest soil: Continuous measurements of NO flux and soil concentration, Journal of Geophysical Research, **107**(D20), 2002, 8050, doi:10.1029/2001JD000521.

Harris, G.W., Wienhold, F.G., Zenker, T., Airbome observations of strong biogenic NO_X emissions from the Namibian savanna at the end of the dry season, Journal of Geophysical Research, **101**, 1996, 23,107-23,712.

Harrison, P., Pearce, F., Deserts and Drylands, AAAS Atlas of Population and Environment, 2000, pp. 131-134, University of California Press, Berkeley, USA.

Hartley, A.E., Schlesinger, W.H., Environmental controls on nitric oxide emission from northern Chihuahuan desert soils, Biogeochemistry, **50**, 2000, 279-300.

Hutchinson, G.L., Livingston, G.P., Brams, E.A., Nitric and nitrous oxide evolution from managed subtropical grassland, in Oremland, R.S. (ed), Biogeochemistry of Global Change: Radiatively Active Trace Gases, 1993, pp. 290-316. New York: Chapman & Hall.

IPCC, Climate Change 2001: The Scientific Basis, Contribution of Working Group I to the Third Assessment Report of the Intergovernment Panel on Climate Change (IPCC), Houghton, J.T., Ding, Y., Griggs, D.J., Noguer, M., van der Linden, P.J., Xiaosa, D. (eds.), chap. 4: Atmospheric Chemistry and Greenhouse Gases, 2001, pp.239–287, Cambridge University Press, Cambridge, New York.

Kasibhatla, P.S., Levy II, H., Moxim, W.J., Global NO_X, HNO_3, PAN, and NO_Y distributions from fossil fuel combustion emissions: A model study, Journal of Geophysical Research, **98**(D4), 1993, 7165-7180.

Kirkman, G.A., The surface exchange of trace gases in the tropics and savannas, PhD Thesis, 2001, 140 pp., Johannes Gutenberg University, Mainz, Germany.

Kirkman, G.A., Yang, W.X., Meixner, F.X., Biogenic nitric oxide emissions up-scaling: an approach to Zimbabwe, Global Biogeochemical Cycles, **15**(4), 2001, 1005-1020.

Kirkman, G.A., Gut, A., Ammann, C., Gatti, L.V., Cordova, A.M., Moura, M.A.L, Andreae, M.O., Meixner F.X., Surface exchange of nitrogen dioxide, nitric oxide and ozone at a cattle pasture in Rondonia, Brazil, Journal of Geophysical Research, **107**(D20), 2002, 8083, doi:10.1029/2001JD000523.

Le Roux, X., Abbadie, L., Lensi, R., Serça, D., Emission of nitrogen monoxide from African tropical ecosystems: Control of emission by soil characteristics in humid and dry savannas of West Africa, Journal of Geophysical Research, **100**(D11), 1995, 23,133-23,142.

Levine, J.S., Cofer III, W.R., Sebacher, D.I., Winstead, E.L., Sebacher, S., Boston, P.J., The effects of fire on biogenic soil emissions of nitric oxide and nitrous oxide, Global Biogeochemical Cycles, **2**, 1988, 445-449.

Levine, J.S., Winstead, E.L., Parsons, D.A.B., Scholes, M.C., Scholes, R.B., Cofer III, W.R., Cahoon Jr., D.R., Sebacher, D.I., Biogenic soil emission of nitric oxide (NO) and nitrous oxide (N_2O) from savannas in South Africa: The impact of wetting and burning, Journal of Geophysical Research, **101**, 1996, 23,689-23,698.

Levine, J.S., Winstaed, E.I., Sebacher, D.I., Biogenic soil emissions of nitric oxide (NO) and nitrous oxide (N_2O) from savannas in South Africa: The irnpact of wetting and burning, Journal of Geophysical Research, **101**, 1996, 23689-23698.

Li, C., Aber, J.D., Stange, F., Butterbach-Bahl, K., Papen, H., A process-oriented model of N_2O and NO emissions from forest soils, 1 Model development, Journal of Geophysical Research, **105**, 2000, 4369–4384.

Linn, D.M., Doran, J.W., Effect of water-filled pore space on carbon dioxide and nitrous oxide production in tilled and nontilled soils, Soil Science Society of America Journal, **48**, 1984, 1267–1272

Ludwig, J., Meixner, F.X., Vogel, B., Forstner, J, Processes, influencing factors, and modelling of nitric oxide surface exchange—an overview, Biogeochemistry, **52**(3), 2001, 225-257.

Martin, R.E., Scholes, M.C., Mosier, A.R., Ojima, D.S., Holland, E.A., Parton, W.J., Controls on annual emissions of nitric oxide from soils of the Colorado shortgrass steppe, Global Biogeochemical Cycles, **12**(1), 1998, 81-91.

Matson, P.A., Harriss, R.C., Biogenic trace gases: measuring emissions from soil and water, 1995, 394 pp. Oxford: Blackwell Scientific Publications Ltd.

Meixner, F.X., Surface exchange of odd nitrogen oxides, Nova Acta Leopoldina NF 70, Nr. **288**, 1994, 299-348.

Meixner, F.X., Eugster, W., Effects of landscape pattern and topography on emissions and transport, in: Integrating Hydrology, Ecosystem Dynamics, and Biogeochemistry in Complex Landscapes, Tenhunen, J.D., Kabat, P. (eds.), 1999, pp. 147 - 175, Dahlem Workshop Report, Chichester: John Wiley & Sons Ltd.

Meixner, F.X., Fickinger, Th., Marufu, L., Serca, D. Nathaus, F.J., Makina, E., Mukurumbira, L., Andreae, M.O., Preliminary results on nitric oxide emission from a southern African savanna ecosystem, Nutrient Cycling in Agroecosystems, **48**, 1997, 123-138.

Meixner, F.X., Ammann, A., Rummel, U., Gut, A., Andreae, M.O., The rain forest canopy reduction effect on NOx emissions, Proceedings of the 7th Scientific Conference of the International Global Atmospheric Chemistry Project (IGAC), 2002, 18-25 September 2002, Creta Maris, Hersonissos, Crete, Greece.

Mosier, A.R., Parton, W.J., Valentine, D.W., Ojima, D.S., Schimel, D.S., Delgado, J.A., CH_4 and N_2O fluxes in the Colorado shortgrass steppe: 1. Impact of landscape and nitrogen addition, Global Biogeochemical Cycles, **10**(3), 1996, 387-399.

Mummey, D.L., Smith, J.L., Bolton, Jr., H., Small-scale spatial and temporal variability of N_2O flux from a shrub-steppe ecosystem, Soil Biology and Biochemistry, **29**(11/12), 1997, 1699-1706.

Neftel, A., Blatter, A., Schmid, M., Lehmann, B., Tarakanov, S.V., An experimental determination of the scale length of N_2O in the soil of a grassland, Journal of Geophysical Research, **105**(D10), 2000, 12,095-12,103.

Otter, L.B., Yang, W.X., Scholes, M.C., Meixner, F.X., Nitric oxide emissions from a Southern African savanna, Journal of Geophysical Research, **104** (D15), 1999, 18,471-18,485.

Parrish, D.D., Williams, E.J., Fahey, D.W., Liu, S.C., Fehsenfeld, F.C., Measurement of nitrogen oxide fluxes from soils: intercomparison of enclosure and gradient measurement techniques, Journal of Geophysical Research, **92**, 1987, 2165-2171.

Parsons, D.A.B., Scholes, M.C., Scholes, R.J., Levine, J.S., Biogenic NO emissions from savanna soils as a function of fire regime, soil type, soil nitrogen and water status, Journal of Geophysical Research, **101**, 1996, 23683-23688.

Parton, W.J., Hartman, M.D., Ojima, D., Schimel, D., DAYCENT and its land surface submodel: description and testing, Global Planetary Change, **19**,1998, 35–48.

Parton, W.J., Holland, E., Del Grosso, S., Hartman, M.D., Martin, R., Arvin R. Mosier, Ojima, D.S., Schimel, D.S., Generalized model for NOx and N_2O emissions from soils, Global Biogeochemical Cycles, **106** (D15), 2001, 17,403-17,419.

Pilegaard, K., Hummelshoj, P., Jensen, N.O., Nitric oxide emission from a Norway spruce forest floor, Journal of Geophysical Research, **104**(D3), 1999, 3433-3445.

Potter, C.S., Matson, P.A., Vitousek, P.M., Davidson, E.A., Process modeling of controls on nitrogen trace gas emissions from soils worldwide, Journal of Geophysical Research, **101**, 1996, 1361–1377.

Potter, C.S., Randerson, J.T., Field, C.B., Matson, P.A., Vitousek, P.M., Mooney, H.A., Klooster, S.A., Terrestrial ecosystem production: A process model based on global satellite and surface data, Global Biogeochemical Cycles, **7**, 1993, 811–841

Remde, A., Ludwig, J., Meixner, F.X., Conrad, R., A study to explain the emission of nitric oxide from a marsh soil, Journal of Atmospheric Chemistry, **17**, 1993, 249-275.

Ridolfi, L., D'Odorico, P., Porporato, A., Rodriguez-Iturbe, I., The influence of stochastic soilmoisture dynamics on gaseous emissions of NO, N_2O, and N_2, Hydrological Sciences –Journal des Sciences Hydrologiques, **48**(5), 2003, 781-798.

Rudolph, J., Conrad, R., Flux between soil and atmosphere, vertical concentration profiles in soil, and turnover of nitric oxide: 2. Experiments with naturally layered soil cores. Journal of Atmospheric Chemistry, **23**, 1996, 275–300.

Rudolph, J., Rothfuss, F., Conrad, R., Flux between soil and atmosphere, vertical concentration profiles in soil, and turnover of nitric oxide: 1. Measurements on a model soil core. Journal of Atmospheric Chemistry, **23**, 1996, 253–273.

Scholes, M.C., Martin, R., Scholes, R.J., Parsons, D., Winstead, E., NO and N_2O emissions from savanna soils following the first simulated rains of the season, Nutrient Cycling in Agroecosystems, **48**, 1997, 115-122.

Scholes, M.C., Otter, L.B., Lowman, G., Terrestrial ecology and the interaction with trace gas fluxes, First Open Science Conference of iLEAPS (Integrated Land Ecosystem – Atmosphere Processes Study), 29 September – 03 October, 2003, Helsinki, Finland, http://www.atm.helsinki.fi/ILEAPS/index.php?page=fosc

Skiba, U., Fowler, D., Smith, K.A., Nitric oxide emissions from agricultural soils in temperate and tropical climates: Sources, control and mitigation options, Nutrient Cycling in Agroecosystems, **48**, 1997, 139–153.

Skopp, J., Jawson, M.D., Doran, J.W., Steady-state aerobic microbial activity as a function of soil water content, Soil Science Society of America Journal, **54**, 1990, 1619–1625.

Slemr, F., Seiler, W., Field measurements of NO and NO_2 emissions from fertilized and unfertilized soils, Journal of Atmospheric Chemistry, **2**, 1984, 1–24.

Slemr, F., Conrad, R., Seiler, W., Nitrous oxide emissions from fertilized and unfertilized soils in a subtropical region (Andalusia, Spain), Journal of Atmospheric Chemistry, **1**, 1984, 159–169.

Smart, D.R., Stark, J.M., Diego, V., Resource limitations to nitric oxide emissions from a sagebrush-steppe ecosystem, Biogeochemistry, **47**, 1999, 63-86.

Strahler, A.H., Strahler, A.N., Introducing Physical Geography, 2nd edition, pp. 155-196, 1999, John Wiley & Sons, Inc., New York.

Thornton, F.C., Shurpall, N.J., Bock, B.R., Reddy, K.C., N_2O and NO emission from poultry litter and urea applications to Bermuda grass, Atmospheric Environment, **32**, 1998, 1623–1630.

Trebs, I., Primärregenwälder und brandgerodete Gebiete in Brasilien.Untersuchungen zur Freisetzung und Aufnahme von Stickstoffmonoxid (NO) an Bodenproben im Labormassstab, MSc thesis No. 58/00, 2001, Hochschule für Technik, Wirtschaft und Kultur, Leipzig,Germany.

Valente, R.J., Thornton, F.C., Emissions of NO from soil at a rural site in Central Tennessee. Journal of Geophysical Research, **98**, 1993, 16,745–16,753.

van Dijk, S.M., Meixner, F.X., Production and consumption of NO in forest and pasture soils from the Amazon basin: A laboratory study. Water, Air and Soil Pollution: Focus, **1**, 2001, 119-130

Veldkamp, E., Keller, M., Fertilizer induced nitric oxide emissions from agricultural soils, Nutrient Cycling in Agroecosystems, **48**, 1997, 69–77.

Verchot, L.V., Davidson, E.A., Cattanio, J.H., Ackerman, I.L., Erickson, H.E., Keller, M., Land use change and biogeochemical controls of nitrogen oxide emissions from soils in eastern Amazonia, Global Biogeochemical Cycles, **13**, 1999, 31–46.

Weitz, A.M., Veldkamp, E., Keller, M., Neff, J., Crill, P.M., Nitrous oxide, nitric oxide, and methane fluxes from soils following clearing and burning of tropical secondary forest, Journal of Geophysical Research, **103**, 1998, 28,047–28,058.

Wildt, J., Kley, D., Rockel, A., Rockel, P., Segschneider, H.J., Emission of NO from several higher plant species, Journal of Geophysical Research, **102**, 1996, 5919–5927.

Yang, W.X., Meixner, F.X., Welling, M., Laboratory studies on the release of nitric oxide from a grassland soil (Marondera, Zimbabwe), Annales Geophysicae, **14**(S II), 1996, C 72.

Yang, W.X., Meixner, F.X., Laboratory studies on the release of nitric oxide from sub-tropical grassland soils: The effect of soil temperature and moisture, in: Gaseous Nitrogen Emissions from Grasslands, Jarvis, S.C., Pain, B.F. (eds.), 1997, pp. 67-70, CAB International, Wallingford, New York.

PART IV

DISTURBANCES AND PATTERNS IN ARID AND SEMIARID ECOSYSTEMS

Ecological theories define disturbances as processes causing consumption or removal of live biomass at timescales shorter than those of biomass accumulation. These disturbances have important impacts on the dynamics of arid and semiarid ecosystems in that they affect the composition and structure of dryland vegetation. In the Introduction we have described how soil texture and rainfall regimes affect the dominance and codominance of grasses and trees or shrubs. This picture is completed in this fourth part of the monograph by the analysis of disturbances and their effects on vegetation structure and composition in water-limited ecosystems. For example, grazing favors woody shrubs by limiting the accumulation of grass biomass. Conversely, fires, browsing, and wood harvesting limit the competitive advantage of woody vegetation by damaging shrubs and tree seedlings.

The observed spatial and temporal patterns of dryland vegetation are the result of plant competition and disturbance regime. Finding the relation between patterns and the underlying ecohydrological processes is a crucial step towards an integrated understanding of the role of local competition and landscape-scale controls (e.g., topography, fires, and grazing) in the dynamics of arid and semiarid ecosystems.

The chapters included in this part focus on vegetation patterns and disturbance regimes, and on their relation to the ecohydrological processes addressed in the previous Chapters. Processes controlling the emergence of vegetation patterns are discussed in Chapter 15 along with theories of pattern formation and methods for the analysis of the spatial structure of vegetation. Chapter 16 presents a comparative analysis of fire dynamics and of their ecohydrological controls in a number of arid and semiarid environments around the world. The active role played by termites in the local soil water balance is discussed in Chapter 17 through a quantitative analysis of the ecohydrological relevance of termite nests. The effects of livestock grazing and anthropogenic disturbances are presented in the last chapter in a review of current research on desertification. This last chapter provides also a synthesis of ecohydrologic processes affecting the stability of dryland ecosystems.

Chapter 15

PATTERN AND PROCESS IN SAVANNA ECOSYSTEMS

Kelly K. CAYLOR[1] and Herman H. SHUGART[2]

[1] *Department of Civil and Environmental Engineering, Princeton University, Princeton, NJ 08540 USA. email: kcaylor@princeton.edu*
[2] *Department of Environmental Sciences, University of Virginia, Charlottesville, VA 22903 USA. email: hhs@virginia.edu*

1. Introduction

The spatial pattern of vegetation is both a cause and effect of variation in resource availability in semiarid ecosystems. At landscape to regional scales, climatic and geologic constraints on soil moisture and nutrient availability are primary determinants of vegetation structural pattern in semiarid ecosystems. Similarly, at local to landscape scales, the patchy vegetation structural mosaic serves to redistribute the availability of soil moisture and nutrients in ways that have important consequences for structural dynamics and community composition.

The investigation of vegetation organization as a means to understand underlying patterns in the environment originates in the first ecological writings and continues throughout the history of the discipline. Theophrastus (3rd Century BC) observed the distribution of deciduousness and evergreenness with respect to climate (Hort, 1916; Morton, 1981) and experimentally transplanted plants to areas outside their natural range to determine if they would grow (or flower). The pioneering work of the early American ecologist, Henry Chandler Cowles (Cowles, 1899) documented the succession of vegetation as the cause of spatial variation in composition observed across dune formations of different ages. In this work, Cowles anticipated both the individualistic nature of the response of plant species to their environments (e.g. Gleason, 1927) and the “continuum concept” of species distribution along environmental gradients (McIntosh, 1967; Austin, 1985). Indeed, the historical foundation of plant ecology in biogeography (Humboldt, 1807) is itself an indication of the critical interactions between the large-scale spatial organization of the physical environment and the distribution of vegetation in the landscape. These same relationships were observed 3 millennia earlier by Theophrastus, who noted the positive relationship between altitude and latitude with respect to their climates and vegetation.

Today as in the past, relationships observed between environmental conditions and plant occurrences are fundamental to the study of plant ecology (Greig-Smith, 1979; Grime 1979; Tilman 1982; Weiher and Keddy, 1999). The concept that ecological processes are evident in vegetation patterns was formalized by Watt (1947), and this paradigm has often been used to investigate the relationships between the spatial structure of vegetation and the nature of competition, disturbance, and resource heterogeneity across a range of ecosystems. Even still, many outstanding issues in plant ecology are directly related to our incomplete understanding of the dynamics and persistence of spatial patterns (Levin, 1992). These include:

1) the relationship between competition/facilitation, spatial pattern, and the persistence of biodiversity;
2) the relative importance of biotic and abiotic factors in structuring vegetation communities;
3) the role of both current and former plant patterns in determining the spatial distribution of resource availability; and

P. D’Odorico and A. Porporato (eds.), Dryland Ecohydrology, 259–281.

4) the time and space scales over which various disturbances affect spatial pattern and the consequences of spatial disturbances on long-term stability of vegetation communities.

Semi-arid ecosystems (most notably savannas), exhibit a number of characteristics relevant to the investigation of these unresolved issues in spatial ecology. A most striking characteristic of savannas is their pronounced functional diversity in the form of tree/grass coexistence. The maintenance of this functional diversity is directly tied to question (1) above. Though extensive in distribution, savannas exhibit a high degree of small-scale spatial heterogeneity and maintain strong interactions between biotic and abiotic determinants of both soil moisture (see Chapter 7) and nitrogen availability. These factors make savannas ideally suited to address questions (2) and (3). In addition, disturbances such as fire and herbivory are ubiquitous in savanna vegetation and the importance of these disturbances is at the core of question (4).

The ecological relevance of savannas has encouraged many studies and theories regarding the nature of spatial patterns and the consequences of pattern on the dynamics of savanna vegetation. In this chapter, we will summarize the methods used to assess spatial pattern in savannas and the conceptual frameworks employed to integrate pattern and process in savanna ecosystems. Where possible, we will connect these methods and concepts with results from our own investigations on the nature and consequences of pattern in the Kalahari savannas of southern Africa. Although our examples are drawn mostly from savannas and our own results are specifically from southern African savannas only, many of the methods and concepts are equally applicable to other semi-arid vegetation communities.

2. Southern African Savannas

Savanna ecosystems vary systematically along gradients of available moisture and available soil nutrients (Scholes and Walker, 1993) and they are profoundly influenced by wildfire, by grazing animals, and by human modification to both fire and grazing regimes (Walker and Noy-Meir, 1982). Savannas are not a narrow “transition” vegetation between conditions that favor grasses and conditions that favor trees (Jeltsch, 1998). Rather, they occupy a substantial part of natural gradient of soil moisture and nutrients as well as a considerable portion of the arable land in Africa. In southern Africa, tropical savannas are extensive but varied, ranging from partially-closed woodlands to sparsely-covered scrublands (Scholes *et al*., 2002). Many tropical savannas are found in semi-arid climates where a constantly changing distribution of soil moisture is supplied by predominately convective storms that vary considerably in both frequency and depth (Sala and Laurenroth, 1982; McCown and Williams, 1990; Hutley *et al.,* 2001).

The Kalahari Transect (KT) provides a unique opportunity to investigate vegetation pattern in semi-arid savanna ecosystems across a number of spatial scales. The distribution of Kalahari sands occupies a third of southern Africa (Scholes and Parsons, 1997). The KT is one of a number of IGBP transects designated throughout the world (Koch *et al*., 1995), and spans a latitudinal rainfall gradient varying from 250 mm/year in the south to 1000 mm/year in the north. Although low frequency periodicities in annual rainfall have been observed for most of southern Africa (Tyson, 1986), rainfall events in the Kalahari are largely convective, and locations throughout the Kalahari Transect experience large variability in inter-annual rainfall amounts. The coefficient of variability in annual rainfall for the 20th century ranges from a minimum of 16% in the north to over 40% at the transect’s southern extreme. The large gradient in both the mean and variation of annual rainfall results in dramatic changes in vegetation structure across the study sites (Scholes, *et al*., 2002; Caylor *et al.*, 2003; Privette *et al*., 2003), and vegetation type ranges from partially closed woodlands in the north to open shrub land in the south. Throughout the KT, the mixed life-form composition characteristic of savanna communities is maintained. The consistency in geomorphology over the entire region -

primarily deep Kalahari sands (Thomas and Shaw, 1991) - allows for an analysis of vegetation structure and ecosystem processes independent of soil type. These structural changes, coupled with the regional rainfall gradient lead to changes in the relative contribution of trees and grasses to vegetation productivity across the transect (Dowty *et al*., 2000; Caylor *et al*., 2004).

3. A conceptual organization of spatial pattern and process in savannas

The persistence and extensive distribution of savannas has spawned a number of theoretical models of tree-grass coexistence. These differ in their underlying assumptions about the importance of soil moisture and nutrient limitation and the ways in which trees and grasses access and use soil moisture and nutrients. Initial dynamic models of tree-grass coexistence assumed that soil moisture is horizontally homogeneous (Eagleson and Segarra, 1985), and that competition for soil moisture is sufficient to explain observed patterns of vegetation in semi-arid systems (Yeaton and Cody, 1976; Phillips and MacMahon, 1981). Walter (1971) postulated a niche-differentiation model to explain a balance of trees and grasses at equilibrium. This model was based on tree and grass roots using different soil different layers for their water supplies - trees having deep roots and grasses having shallower roots. Due to a lack of direct evidence of a two-tiered layering of root structure in many savanna environments (Seghieri, 1995; Mordelet *et al*., 1997; Hipondoka *et al*., 2003), the importance of vertical niche-differentiation as a means of stabilizing savanna dynamics has been questioned. Accordingly, the Walter model has been modified in a number of ways to better approximate field observations (Eagleson and Segarra, 1985; Scholes and Archer, 1997).

As an alternative to vertical variation in soil moisture access, the role of horizontal heterogeneity in maintaining savanna vegetation structure has been increasingly explored. A striking characteristic of savanna vegetation (and semi-arid vegetation in general) is the pronounced patchiness exhibited across scales ranging from tens of meters to tens of kilometers. A particular challenge in understanding the importance of this patchy structure is that the characterization of horizontal spatial pattern depends strongly on the manner in which the pattern itself is conceptualized. The differences in these conceptualizations and how they affect the interpretation of spatial pattern is the focus of this chapter. To this end, we define three "types" of vegetation pattern: (1) Individual-based; (2) Patch-based; and (3) Intensity-based. Figure 1 provides a summary of these three types of pattern characterization for a single representation of hypothetical vegetation structure, and Table 1 provides a summary of the ways in which these conceptualizations are manifested in analyses of semi-arid ecosystems. Before discussing the methods used to describe and analyze these various types of spatial patterns, we will briefly distinguish how observations of patterns and process are coupled to develop conceptual models of pattern dynamics in semi-arid ecosystems.

4. Links between pattern and process

Any observation of spatial pattern is associated with a distinct conceptual framework that determines how pattern is characterized, as well as how pattern is used to inform dynamics of vegetation structure (Table 1). The basis of all vegetation pattern is the distribution of individual plants. The individual-based distribution of plants may be described along a single dimension as a transect, or within a two-

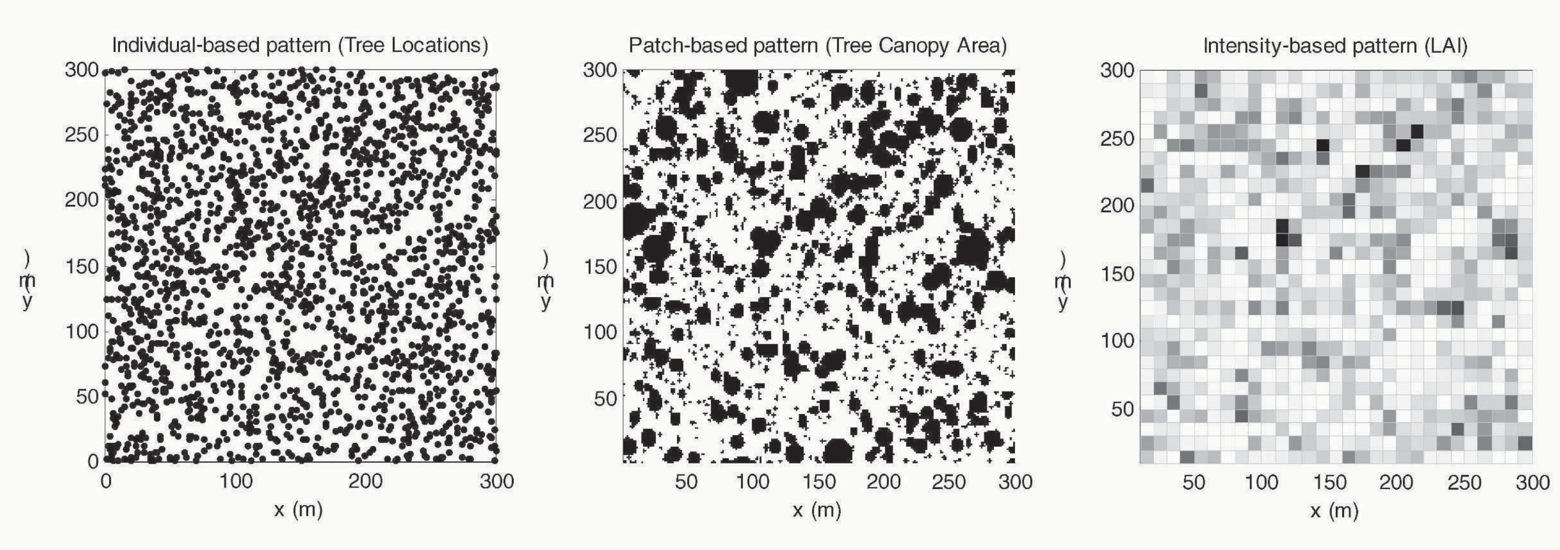

Figure 1. *Three different views of vegetation pattern for a single hypothetical dataset of savanna vegetation structure. The individual-based pattern depicts the location of each tree in a 300 x 300 meter area. The patch-based pattern displays the projected canopy area of the canopy trees, and the intensity-based pattern depicts leaf area index aggregated to a 10-meter grid. The individual-based distribution provides the most information on competition and spacing, while the patch and intensity-based patterns provide greater information on the scale of landscape patchiness, and heterogeneity*

Table 1 Summary of pattern observations and conceptualizations commonly employed in savanna vegetation. Citations to recent articles employing each method are provided, as well as references to example figures and analysis provided in this chapter.

Observations of savanna spatial pattern

Vegetation pattern as...	*Pattern is described by…*	*Analysis techniques*	*Recent examples for semi-arid vegetation*
… a discrete distribution of individuals *(cf. Figure 1a)*	Mapped plant positions within a study area	1 – Nearest neighbor 2 – K-function *[Figures 2 & 3]* 3 – Fourier analysis	1– Miriti *et al*., 2001 2 – Caylor *et al*., 2003; Schenk *et al*., 2003; Barot *et al*., 1999 3 – Couteron, 2001
… a continuous distribution of landscape components or patches *(cf. Figure 1b)*	Spatially contiguous field-based or remotely-sensed observations of landscape patches	1 – Change detection *[Figure 4]* 2 – Patch size distribution *[Figure 5]* 3 – Scaling analysis *[Figure 6]*	1 – Archer *et al*., 1998; Hudak & Wessman, 2001 2 – Li and Archer, 1997 3 – Ludwig *et al*., 2000
… a continuous distribution of intensity *(cf. Figure 1c)*	Spatially contiguous field-based or remotely-sensed observations of vegetation intensity (e.g. NDVI, LAI)	1 – Autocovariance & autocorrelation 2 – Fractal dimension *[Figure 8]* 3 – Scale analysis *[Figure 9]*	1 – Pearson, 2002 2 – Chen *et al*., 2002 3 – Caylor *et al*., in review; Qi and Wu, 1996

Conceptualizations of savanna spatial pattern

Vegetation pattern as...	*Relevant spatial conceptualization is…*	*Modeling techniques*	*Recent examples for semi-arid vegetation*
… a spatially interactive distribution of individuals	The spatial location of each individual	1 – Individual-based models 2 – Spatial moment-closure models	1 – Higgins *et al*., 2000; Simioni *et al.,* 2000 2 – Bolker & Pacala, 1999
… a non-spatially interactive mosaic of patches	The relative abundance of each "patch" component	1 – Non-spatial patch models *[Figure 7]* 2 – Markov transition models	1 – Breshears & Barnes, 1999; Caylor *et al*., in press 2 – Bestelmeyer *et al*., 2003
… a spatially interactive mosaic of patches	The spatial location of each individual patch	1 – Cellular automata 2 – Interactive landscape models	1 – Van Wijk & Rodriguez-Iturbe, 2001 2 – Couteron & Lejeune, 2001; Boone *et al*., 2002; Ludwig *et al*., 1999

dimensional plot, three-dimensional canopy space, and even four-dimensional time series of change. Studies that attempt to characterize the density of individuals as well as the distances between individuals focus on this most basic of vegetation pattern description. Individual-based models of vegetation originated with forestry models in the mid-1960's. The initial models were well ahead of the digital computers of the time. They featured explicit 3-dimesional canopy interactions among trees, for example (see Shugart 1998 for review). In the early 1970's, simplifications in the competition algorithms under the rubric of "gap models" (Shugart and West 1980) allowed for an expansion of these applications into a large number of natural vegetation types (mostly forests). The consideration of forest "gaps" indicates the importance of mortality and regeneration in individual-based models, and therefore a key consideration in these models is the coupled spatial and demographic structure of the vegetation pattern. Unfortunately, the radical differences in scale of resource exploitation in the competition algorithm among plants of very different sizes (trees and grasses), as well as lack of a clear characteristic "gap size" has limited the development of individual-based models in savannas (Menaut *et al*., 1990). For savanna ecosystems the first such model was developed for West African palm savanna (Gignoux et al*.* 1995, Simioni *et al*. 2000). This model, called the LAMPTO model for its geographical location simulated the interactions among trees but treated the grasses as a homogeneous collection of leaf biomass. Peters (2002) has developed an individual-based grass-shrub model that is based on an earlier model of interaction of small alpine plants (Humphries *et al*. 2002, derived in turn from the ZELIG forest model of Urban *et al*. (1991)). Jeltsch *et al.* (1996) and Higgins *et al.* (2000) also presented cellular automata models of individual tree growth and demographics. These models contain greater detail regarding woody vegetation demography, but reduced emphasis on biophysical fluxes of carbon, nitrogen and water. All of these models emphasize the spatial distribution of individual trees, with reduced emphasis on the spatial organization of grasses. The challenge of "scaling-up" individual-based models to landscape-scale representations of vegetation structural pattern and structural change is an important and ongoing research task (Bolker and Pacala, 1999).

In many cases, the absence of clear scaling rules for individual-interactions makes it difficult to predict changes in vegetation structure and pattern at landscape scales. In addition, the presence of distinctly "patchy" structure in such varied ecosystems as semi-arid woodlands (Whittaker et al., 1979), annual grasslands (Wu and Levin, 1994) and rocky-intertidal marine communities (Levin and Paine, 1974) has fostered the development of a patch-based mosaic theory of vegetation dynamics (Levin et al., 1993). The division of a landscape into discrete land cover types is an obvious example of a patch-based pattern description, while the conceptualization of a savanna into "tree" and "grass" patches is another. In most patch-based descriptions of spatial pattern, information regarding the exact location (and size) of individual organisms is eliminated in favor of a more conceptually tractable description of the overall landscape organization. The applications of patch-based pattern to understand the dynamics of savanna vegetation include both spatially interactive and non-spatial mosaic models, as well as stochastic Markov-transition models. Patch-based models incorporate spatial processes either through spatially-explicit landscape-scale spatial heterogeneity (Coughenour, 1992) or grid-based cell automata (Gignoux *et al.,* 1995; Jeltsch *et al.,* 1998; Wijk and Rodriguez-Iturbe, 2002). These spatially-interactive mosaic models have proven to be particularly useful in diagnosing the dynamics of banded semi-arid vegetation mosaics, such as "tiger bush" (Lefever and Lejeune, 1997; Lejeune and Tlidi, 1999), where limited soil moisture and sloping terrain lead to the formation of alternating bands of bare soil and vegetation that organize in response to anisotropic gradients of soil moisture availability. Non-spatial patch models include classic "equilibrium-based" models that focus on competition for soil moisture (e.g. Walker *et al.*, 1981), as well as more modern biogeochemical models that include nutrient cycling and disturbance (Daly *et al.*, 2000). The use of pseudo-spatial patch models that allow various degree of interaction between landscape components (Breshears and Barnes, 1999; Caylor *et al.*, in press) have proven particularly adept at examining the dynamic balance between structural pattern, vegetation dynamics and resource availability in savanna ecosystems. Markov-transition models describe the savanna landscape as a series of discrete states, with transition probabilities associated with the conversion of each state into any other (Shugart, 1998). These models have been applied in rangeland management (Bestelmeyer *et al.*, 2003), but generally lack the mechanistic detail to accommodate changes in environmental factors without extensive parameterization.

A third way of expressing the structure of vegetation communities is the description of spatial pattern as the spatially-explicit intensity of a continuous variable such as biomass or leaf area. This intensity-based pattern description is often associated with remotely-sensed data, and is rapidly emerging as the most common representation of vegetation pattern over large areas. The incorporation of these intensity-based patterns into a conceptualization of savanna dynamics is most difficult, since the abstraction of savanna pattern as a continuous distribution of leaf area or biomass eliminates most of the demographic and structural information necessary to predict vegetation change. The availability of remotely-sensed data has allowed to large-scale estimates of vegetation productivity (Prince and Goward, 1995), and recent Dynamic Global Vegetation Models (DGVM's) include modules that simulate the behavior of different life forms of plants and apply these in regional scale patches for global simulations of vegetation dynamics (Potter et al. 1993, Woodward et al. 1995, Delire et al. 2003). The same approach can be used to represent the productivity of different life forms of savanna plants using remote sensing products that estimate intensities off grass, trees, shrubs, and bare ground at smaller scales. Development of canopy productivity models in semi-arid ecosystems (Hanan *et al.*, 1997; Dowty *et al.*, 2000) has allowed for smaller-scale estimate of vegetation production derived from either field-based or remotely-sensed intensity-based observations of canopy structure (Caylor and Shugart, 2004; Caylor *et al.*, 2004). The relationships between environmental variability and vegetation function derived from these small-scale canopy production models can be incorporated into larger-scale simulations of regional production to yield estimates of changes in tree/grass production associated with climatic variability (Hély *et al.*, 2003a) or regional fuel load production and biomass burning (Hély *et al.*, 2003b). This multi-scale approach of nesting biophysical canopy production models into large scale landscape productivity models should be extended into the patch-based and individual-based approaches in order to simulate multi-year changes in structural pattern and composition (Shugart, 2000; Shugart *et al.*, in prep). The difficulty encountered integrating these various approaches (i.e. combining canopy production models with individual-based demographic models) highlights the conceptual challenges facing a synthesis of pattern and process in semi-arid ecosystems.

Of the three types of pattern descriptions (individual, patch, and intensity), the individual-based description requires the greatest amount of field-data collection, while the patch- and intensity-based descriptions are highly sensitive to the spatial resolution of observation. Each conceptualization leads to distinctly different approaches for predicting the nature of spatial pattern and structural dynamics in savanna ecosystems. While no single method is appropriate or practical in all instances, certain methods are better suited to address certain questions than others. In addition, as the spatial scale of observation increases, the abstraction of vegetation spatial pattern tends to become greater so that there exist correlations between each of these conceptualizations and the scale at which they are applied. It is our strong belief that any synthesis regarding the important role that spatial ecology plays in savanna ecosystems depends on a proper appreciation of the diversity of strengths, weaknesses, and assumptions that underlie the observation and application of each of these three conceptualizations of spatial pattern, as well as the development of methods that integrate patterns observed across the various spatial scales and conceptual frameworks.

5. Spatial pattern as a distribution of individuals

A primary method of vegetation pattern analysis is the assessment of the distribution of individuals within a study area. The locations of plants are usually mapped so that the data are a series of zero-dimension point locations which exist in a plane (e.g. Figure 1a). Of particular interest in this type of analysis is the relative amount of aggregation or dispersion between individuals. In general, the significance of the observed pattern is derived from statistical inferences regarding the expected distribution of points, which is assumed to be generated according to a poisson process acting within the region considered (Diggle, 1983). The deviation between the observed distribution and the poisson process allows for the classification of spatial pattern as a continuum moving from highly aggregated communities to regularly spaced or hyper-dispersed communities, with random distribution patterns (i.e. showing no effect of either pattern) occupying the middle of the continuum (Ripley, 1976). The presence of a particular pattern is often associated with the operation of ecosystem-specific processes that serve to structure the community in a non-random manner (Dale, 1999).

The occurrence of hyper-dispersed (also termed "uniform" or "regularly spaced") community patterns has been explained as the result of density-dependent mortality associated with competition for a homogeneously distributed resource (Beals, 1968). In contrast, the observation of clumping in savanna ecosystems has been associated with high rates of disturbance or the presence of nurse sites for seedling establishment (Raffaele and Veblen, 1998). In particular, it has been hypothesized that clumping in savanna communities is a response to high fire disturbance (see Chapter 16 for a more complete analysis of fire regimes), as vegetation in the centers of clumps tends to persist after a fire (Gignoux *et al.,* 1995). It is important to realize that regardless of the particular pattern found, the observation of pattern itself cannot elucidate the process of cause without appropriate experimental manipulation of the community under investigation (Cale *et al.,* 1989). Regardless, the observation of a particular pattern serves to establish the presence of non-random structuring mechanisms within a community and to indicate the direction in which experimental investigations should proceed.

5.1. INDIVIDUAL-BASED OBSERVATIONS

5.1.1. Nearest Neighbor methods

The low-density and seemingly uniform spacing of woody vegetation in many arid systems has fostered the hypothesis that individuals in savanna communities exhibit a high degree of competitive exclusion. Consequently, there have been a variety of studies investigating the spatial pattern of woody vegetation, many of these focusing on the interaction between species pairs using nearest neighbor techniques (Pielou, 1962). Work in the Mojave and Sonoran deserts (Yeaton and Cody, 1976; Yeaton *et al.,* 1977) shows size-dependent species dispersion patterns between *Yucca schidigera*, *Opuntia acanthocarpa* and *O. ramosissima*. Cody (1986) found that levels of positive and negative associations in nearest-neighbor distance were species dependent for a range of woody shrubs in a diverse Mojave Desert community. These patterns were attributed to differences in root system structure and germination requirements. In southern Africa, Smith and Goodman (1987) explored spacing relationships between *Acacia nilotica* and *Euclea divinorum* in the Mkuzi Game Reserve, South Africa. Their work showed a clear size-dependent nearest-neighbor exclusion pattern in mature *Acacia* individuals and understory *Euclea*, supporting the hypothesis of density-dependent spatial regulation of water-limited savanna systems.

5.1.2. Second moment analysis

In addition to nearest-neighbor analysis the spatial pattern of a community can be examined across a range of spatial scales, and therefore provide a more comprehensive picture of vegetation pattern at a site (Clark and Evans, 1954; Ripley, 1977). Phillips and MacMahon (1981) found numerous instances of aggregated dispersion patterns for saplings of 11 different species in 9 different sites across the same region, with little tendency for larger individuals to form aggregated dispersion patterns. The tendency for individuals to change from aggregated to random and occasionally uniform distributions with increasing size (and decreasing density) was taken as evidence of density-dependent mortality associated with the homogeneous distribution of soil moisture in a moisture-limited environment. Skarpe (1991) investigated the dispersion of *Acacia erioloba* and *Acacia mellifera* in both mono-specific and mixed plots near Naojane, Botswana, and found a tendency for saplings of both species to exhibit aggregated distributions. Mature individuals in her plots exhibited a random spatial distribution. More recently, Jeltsh *et al.* (1999) used aerial photography to examine vegetation patterns in the Kalahari Gemsbok Park in southern Botswana. They found patterns that were generally aggregated at four out of six study sites, and random at the other two. Both Skarpe and Jeltsch's sites were located in the southern portion of the Kalahari Desert.

The interpretation of spatial pattern in a particular vegetation community necessarily depends on an understanding of how the observed pattern differs from the null hypothesis of complete spatial randomness. When individuals are distributed according to a Poisson process, the expected number of individuals within some distance t of any particular individual is $K(t)=\rho\pi t^2$, where ρ is the density of individuals. This K-function can be further transformed into an L-function such that $L(t)=K(t)-\rho\pi t^2=0$. Since the L-function, $L(t)$, is only valid for individuals distributed under an ideal Poisson process, it is necessary to compare observed results at a field site with the results of multiple simulated calculations using the same density of individuals distributed randomly in an identically sized sample area. The use of sufficient simulations allows for minimum and maximum confidence intervals ($L_{min}(t)$ and $L_{max}(t)$, respectively) to be put on the expected values of $L(t)$ for any distance within the plot. Values of $L_{obs}(t)$ calculated for the actual distribution of individuals sampled in the field plot can then be compared to these thresholds to determine the significance of observed distribution patterns in the sampled data. Since the analysis is essentially a measure of the deviation between the number of observed events and the expected deviation under complete spatial randomness, values greater than $L_{max}(t)$ indicate significantly clumped or aggregated patterns within the plot, and values less than $L_{min}(t)$ indicate significantly uniform or hyper-dispersed patterns. Values of $L_{obs}(t)$ falling between $L_{max}(t)$ and $L_{min}(t)$ indicate random distributions. Using this technique, it is possible to determine the character of spatial pattern within each site. Furthermore, subsets of community data based on vegetation characteristics can be analyzed to examine the distribution patterns peculiar to that population. Care should be taken when forming these subsets, as pattern may be the result of interactions between events not contained within the subset itself. For example, $L(t)$ functions for small size-classes of individuals (e.g. saplings and seedlings) can be difficult to interpret independently of the distribution of large individuals, due to the high possibility of asymmetric effects between large and small individuals (Keddy, 1989).

Figure 2 provides an example of the L-function results for a single site along the Kalahari Transect, while Figure 3 provides a summary of individual-based spatial pattern across the entire transect. The lack of uniform spacing in large individuals across the range of sites calls into question the idea of density-dependent processes as a means for determining vegetation structure in these systems. The high degree of aggregation in the spatial distribution of small individuals suggests that distribution of suitable regeneration sites and subsequent patterns of establishment may be critical phenomena in determining the spatial pattern of vegetation (Higgins *et al., 2000*).

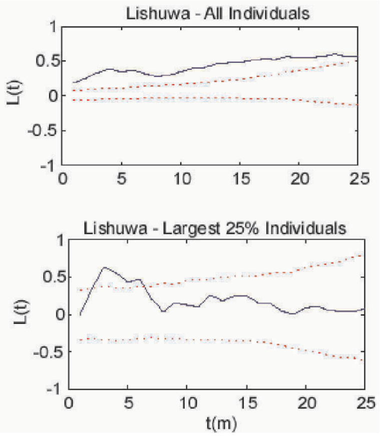

Figure 2. Individual-based pattern of distribution for all trees and the largest 25% trees at the northern-most Kalahari Transect site derived from second moment analysis as presented in Caylor et al. (2003). The L(t) function represents the departure of pattern from the hypothesis of complete spatial randomness, with L(t)>0 indicating aggregation, L(t)<0 indicating hyper-dispersion and L(t)=0 representing a purely random distribution. Dashed lines represent the 95% confidence intervals for a series of monte carlo simulations. At all distances, the distribution of the entire community is observed to be significantly aggregated, while the distribution of large individuals is observed to be predominately random, with some significant aggregation observed at spatial scales of 3-7 meters. These results suggest that the smaller individuals are causing the highly aggregated pattern observed for all individuals.

5.2. SPATIAL PATTERN AS A DISTRIBUTION OF PATCHES

In contrast to the view of savanna vegetation as the distribution of individual plants, it can be convenient to define savanna landscapes into a finite number of elements or patches. Typically, distinctions are made between tree cover, grass cover, and bare soil so that the landscape can simply be described as the fraction of each component present. More complex patches can be defined when data permit – often patches with small trees or mature tree patches with grass are considered independently. The complexity of patch definition is usually associated with the detail included in the field survey, with the most detailed approaches converging on individual-based techniques described above.

5.2.1. Patch-based observations

In many semi-arid ecosystems the primary patch-based distinctions made are between woody canopy vegetation and non-woody canopy portions of the landscape. An underlying assumption of any patch-based pattern analysis is that the patch definitions (e.g. “tree patches” and “non-tree patches”) are an ecologically meaningful description of savanna landscapes. The significance of this portioning is supported by the many studies that have investigated the effect of tree canopies on various components of soil water balance and nutrient availability. Observed effects of tree canopies include an increase in soil moisture storage and drainage under tree canopies (Joffre and Rambal, 1993); an increase in soil temperature, soil drying time and soil water deficit between tree canopies (Breshears *et al.,* 1997; Breshears *et al.*, 1998); and strong contrasts in light availability, temperature and soil moisture between the under-canopy and between-canopy environment (Belsky *et al.*, 1989; Belsky *et al.*, 1993). More recently, Jackson and Wallace (1999) described as much as a 40% reduction in bare soil evaporation under tree canopies in a Kenyan agro-forestry plantation and Smit and Rethman (2000) report increased infiltration and evapotranspiration of experimentally thinned plots of Mopane woodland (*Hardwikia mopane*). The difference between soil moisture under and between tree canopies has been used to explain observed patterns of herbaceous productivity of humid West African savannas (Menaut and Cesar, 1979; Mordelet and Menaut, 1995).

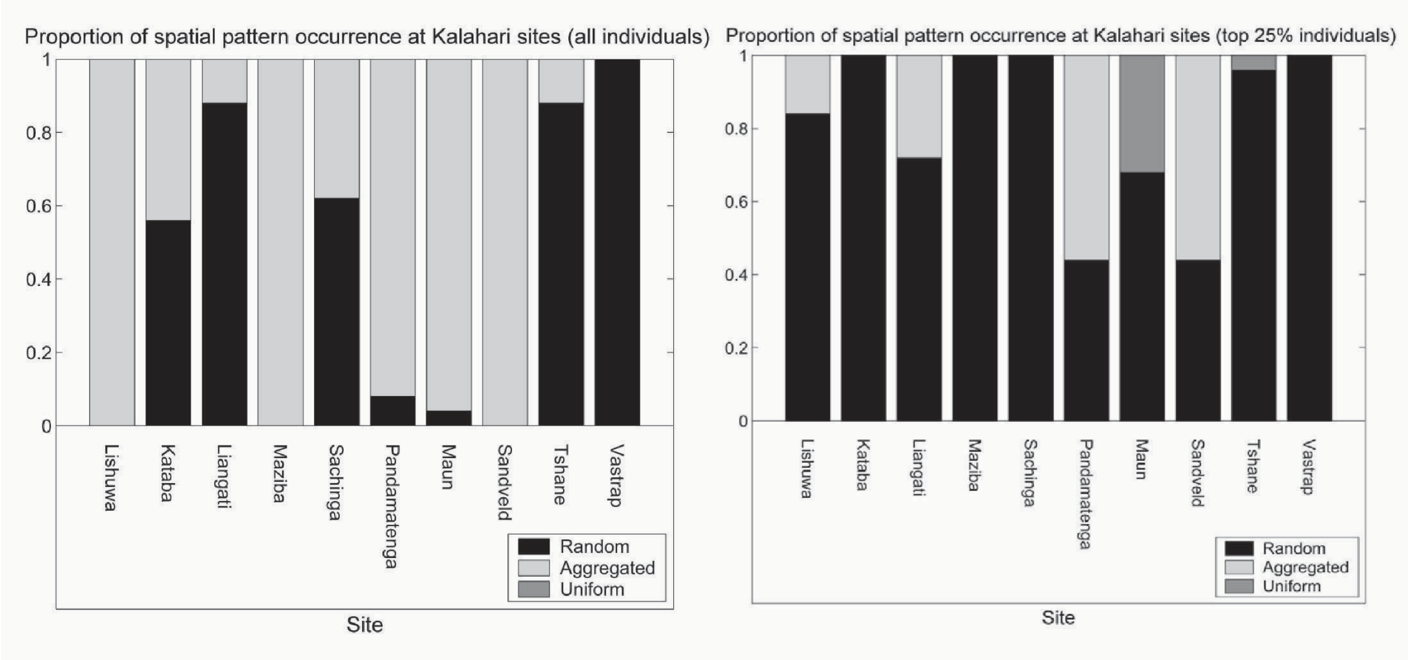

Figure 3. *Individual-based pattern of distribution for all individuals and large trees at each of the 10 sites across the Kalahari Transect derived from second moment analysis as presented in Caylor et al. (2003). At most sites, the distribution of large individuals is observed to be more random than the distribution of all individuals, which is predominately aggregated. Some aggregation of large trees occurs at four out of ten sites, and uniform distributions are only observed in large individuals at two out of ten sites.*

Tree canopy-related soil moisture changes have been shown to impact seedling germination of southern African woody vegetation (Keya, 1997; Wilson and Witkowsk*,* 1998) and woody species distribution patterns (Smith and Grant, 1986; Smith and Goodman, 1987). However, the effect of tree canopies is not always consistent; observed differences in canopy microclimate led to higher productivity of grass under trees in a low-rainfall savanna, but a lower relative productivity of under-canopy grasses in a high-rainfall savanna (Belsky *et al.*, 1993). Similar patterns were observed by Ludwig *et al*. (2001), who found that the effect of tree canopies on herbaceous productivity was determined by a balance of tradeoffs between facilitation and competition, with varying outcomes dependent on annual rainfall.

Patch-based approaches offer a distinct benefit over individual-based approaches by allowing for the incorporation of remotely-sensed data such as aerial photography. Such data are usually the greatest source of historical vegetation patterns in remote regions (Dunn *et al*., 1990). Kadmon and Harari-Kremer (1999) demonstrate the viability of image texture derived from aerial photography as a means for characterizing vegetation structure, particularly in heterogeneous environments. In open savannas, tree canopies can often be distinguished from the grass/bare soil background, so that a binary image of "tree patches" and "bare soil/grass patches" can be generated (e.g. Figure 1b). Such images allow for analysis of canopy cluster size, fraction of tree cover, and – when time series of data are present - rates of woody cover change. Archer *et al* (1998) use aerial photos to document 40+ years of woody vegetation change in southern Texan savannas. Their analysis of the aerial photography includes measurements of canopy patch density, size and spacing. In southern Africa, Hudak and Wessman (1998) use historical aerial photographs to estimate historical woody plant distribution in savanna regions of South Africa.

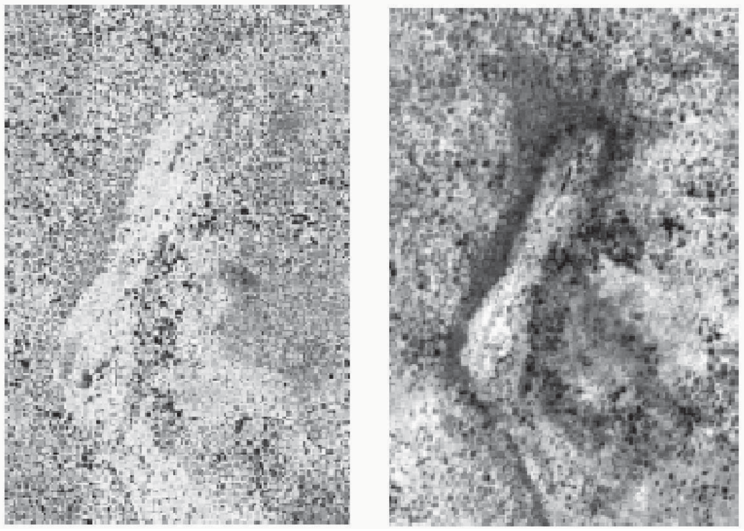

Figure 4. An example of observed change in vegetation in the Kalahari savannas as presented in Dowty et al. (2000). A comparison of declassified satellite (CORONA) data from 1967 (A) and an aerial photograph from 1995 (B) for a location in the Caprivi Strip region of Namibia show an expansion of vegetation along the edges of a shallow depression. Overall change in estimated woody cover is 27% over the 28-year period. In both images, the resolution is sufficient to discern individual tree canopies.

As a supplement to sparse aerial photography, satellite photographs from the recently declassified Corona project can also be used to infer historical patterns of vegetation structure

(Shugart *et al.*, 2001). Corona photographs meet three important criteria in regards to vegetation pattern observation and change detection: They have high resolution, are regional in extent, and are old enough to extract historical rates of change. In certain cases, individual trees and shrubs can be identified using Corona imagery taken in the 1960s, making it an excellent potential tool for exploring vegetation pattern and change in vegetation structure in semi-arid ecosystems. The suitability of Corona imagery for vegetation analysis in the KT region has been examined using two strips of Corona film taken in September of 1967 (Dowty *et al.*, 2000). The strips are sequential negatives taken by the forward facing camera on the KH-4B platform during Corona flight 120, which was launched on the 15th of September, 1967. This was the first flight to carry the KH-4B camera which had 2 meter ground resolution, and therefore the mission's acquisition represents the earliest available sub-5m resolution photos of the Earth's surface from space (McDonald, 1997). Figure 4 demonstrates the utility of the Corona data for analyzing vegetation change in semi-arid regions. Both the Corona image and an aerial photograph taken in 1995 are sufficiently detailed to discern individual trees. The observation of a 27% increase in woody cover between the 1967 Corona image and the 1995 aerial photograph is almost identical to the observed change in woody cover found in other regions of southern Africa over a similar time period (Hudak and Wessman, 2001).

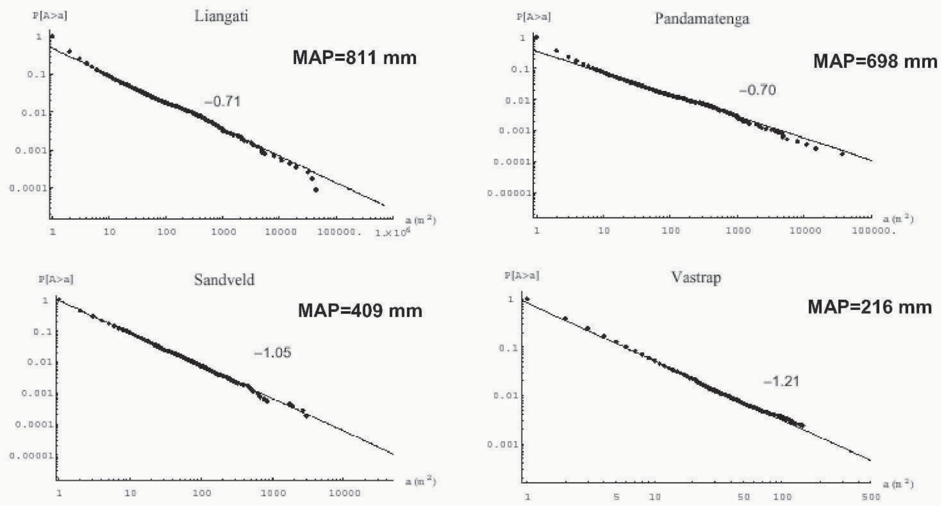

Figure 5. Probability distribution of the size of vegetation canopy cluster sizes. The size distribution at each site follows a power law probability distribution ($P[A\geq a] \propto a^{\beta}$). The slopes of the fitting lines are: (β=-0.71) Liangati; (β=-0.70) Pandamatenga; (β=-1.05) Sandveld; and (β=-1.21) Vastrap. As mean annual rainfall decreases, the slopes decrease indicating a decrease in the maximum cluster size observed at each site (note changes in the x-axis scale).

The application of fractal geometry to spatial analysis has extended descriptions of landscape patchiness described by classical Euclidean analysis of points, polygons and lines into the description of spatial configurations that are irregular, fragmented and disjointed. At the core of fractal geometry is the concept of scale-independence or self-similarity of patterns (Mandelbrot, 1983), such that observations of pattern at one scale inform the description of pattern at other scales through distinct scaling laws. Such patterns are often found in natural systems (Brown *et al.*, 2002), and can be easily demonstrated such diverse areas as the organization of stream networks (Rodriguez-Iturbe, 1997) mountain terrain (Dietler and Zhang, 1992), and plant morphology (Niklas, 1994). The application of fractal analysis to patterns of vegetation structure has proceeded through a variety of methods (see Li, 2000 for a recent review). These include scaling properties of area-perimeter relationships in patch sizes (Krummel *et al.*, 1987), patch size distributions (Li and Archer, 1997), and the spatial autocorrelation of landscape pattern (Burrough, 1981).

Satellite-based assessments of the fractal patterns evident in savanna vegetation structural pattern can be achieved using recently available high-resolution commercial sensors. As example, we have used 1-m panchromatic data from the IKONOS satellite to determine the scaling properties of the size distribution of vegetation canopy clusters at four sites along the KT. The contrast between the bright, uniform sandy soils and dark vegetation canopies found across the Kalahari Transect makes the extraction of canopy features possible using simple binary threshold algorithms. In this case, we use the method described by Otsu (1979), which generates a black and white (binary) image from a grayscale image by minimizing the intraclass variance of the thresholded black and white pixels. The resulting binary matrix of vegetation canopies is then transformed into discrete clusters using 8-pixel adjacency to find contiguous vegetation canopies. The distribution of cluster sizes (Figure 5) is seen to follow a site-specific power law probability distribution, suggesting that the spatial structure of vegetation is scale invariant.

Any use of remote sensing data must contain a determination of what types of pattern (and change in pattern) can be detected based on observations at a given resolution. Woody vegetation dynamics are dependent on a number of factors (Skarpe, 1992), and the detection of change requires high-resolution spatial data over substantial time scales (Fransen *et al*., 1998; Skarpe, 1991;Whiteman and Brown, 1998). These issues are particularly problematic in savanna ecosystems, where the small-scale interactions between individual organisms exert a strong control on the overall system dynamics and patterns of vegetation structure (Barot *et al.*, 1999). Therefore, in any discussion of remotely-sensed spatial patterns, it is critical to note that analysis techniques can only capture spatial pattern across a range of finite scales (namely the minimum scale of resolution). In order to demonstrate the critical role of spatial resolution in describing structural pattern, high-resolution data sets can be successively aggregated and parameters of vegetation structure can be repeatedly estimated. Using a simple unsupervised classification scheme with a 95% convergence threshold, we have derived estimates of woody vegetation cover in a 100 km area of savanna in the Caprivi Strip region of Namibia over a range of resolutions (5 to 1000 meters). As expected, our results demonstrate that estimates of percent tree cover exhibit a high degree of sensitivity to underlying data resolution, particularly at fine scales (Figure 6). In particular, where the sensor resolution is not sufficient to discern individual tree canopies, the effect appears to be an under-estimation of total woody vegetation cover.

5.3. SPATIAL PATTERN AS A DISTRIBUTION OF INTENSITY

The previous section discussed a number of patch-based descriptions that have been employed to conceptualize the pattern and important pattern-related processes that occur in savanna ecosystems. In many types of ecosystems these descriptions are often both a useful conceptual abstraction and an appropriate characterization of the overall landscape pattern. Indeed, the use of patch-based descriptions of savannas has led to substantial theoretical synthesis of savanna dynamics (Breshears and Barnes 1999). Unfortunately, the fine-scale structural heterogeneity present in savannas implies that many savanna landscapes exist not as distinct patches, but instead as surfaces of continuous variation. As such, the overall landscape pattern cannot be easily described using methods that presume the existence of clearly defined homogeneous units (i.e. “tree patches” and “grass patches”). In a recent study of northern Australian savannas, Pearson (2002) demonstrates that the treatment of savanna landscapes as homogenous units over-simplifies the complexity of their spatial structure, even in highly disturbed savannas. Furthermore, such over-simplification may lead to a reduced ability to monitor current and future changes in landscape health and quantify structural change.

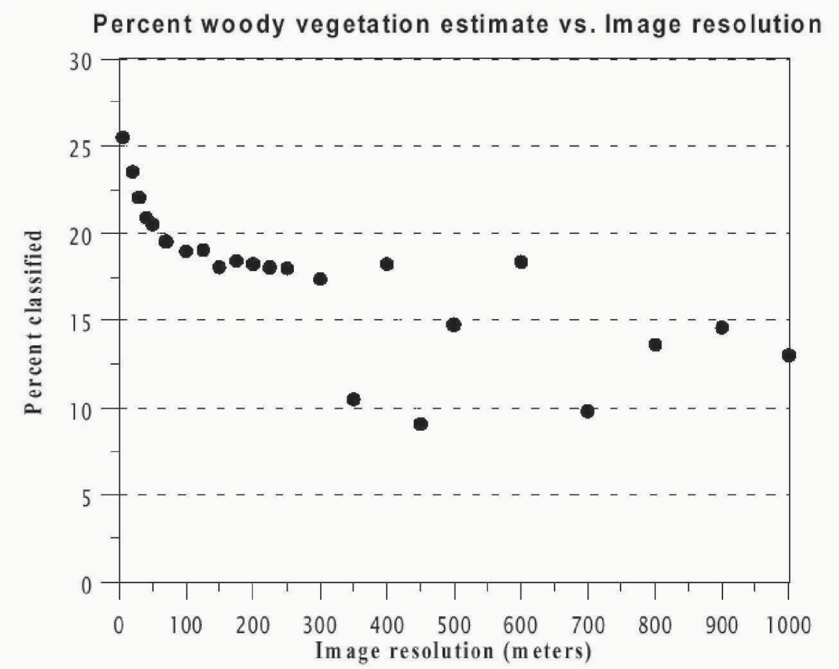

Figure 6. Effect of image resolution on percent woody cover estimation of declassified CORONA satellite data using a three-level unsupervised classification algorithm (adapted from Dowty et al., 2000). Increases in image resolution initially lead to lower estimates of total percent tree cover. At intermediate resolutions, the estimate of tree cover is highly variable with shifts in image resolution.

The introduction of multi-spectral remotely-sensed data has provided an additional incentive to define an "intensity-based" analysis of spatial pattern. Remote sensing data products such as the 18-year record of normalized difference vegetation index (NDVI) and emerging data sets such as the MODIS Leaf Area Index (LAI) product provide an aggregated sampling of the relative abundance of vegetation at a specific resolution. In contrast to the individual-based analysis of plant distributions or the patch-based segregation of the landscape into distinct spatial units, these data describe the continuous variation of a spatially extensive variable at discrete spatial scales (e.g. Figure 1c). When the resolution of the remotely-sensed data is sufficient to resolve individual plants, the distinction between "individual", "patch" and "intensity"-based pattern descriptions are blurred, although a passive sensor is never capable of re-creating the underlying individual-based data when the spatial extent of individuals overlaps. The use of spectral un-mixing approaches allows for patch-based inferences of pixel composition that can be derived from time series of intensity data (e.g. Scanlon *et al.*, 2002). The use of radar-based observations for the delineation of individual tree canopies (Treuhaft *et al.*, 2002; Weishampel *et al.*, 1994), suggest that these intensity-based and individual-based approaches may exhibit greater overlap in the near future.

5.3.1. Intensity-based Observations

The use of intensity-based observations of vegetation structure requires spatial statistics to quantify patterns within the image data (*Stein et al.*, 1998). Spatial autocorrelation in image data can often be associated with physical properties of vegetation such as tree density and height (Bruniquel-Pinel *and* Gastellu-Etchegorry, 1998; Wulder and Boots, 1998). In addition to autocorrelation techniques, the semi-variogram can be used to estimate the scale and range of variation in an image (St-Onge and Cavayas, 1995). To some extent, all measures of landscape variability are dependent upon the spatial resolution of measurement (Qi and Wu, 1996) and the methods of aggregation between resolutions (Bian and Butler, 1999).

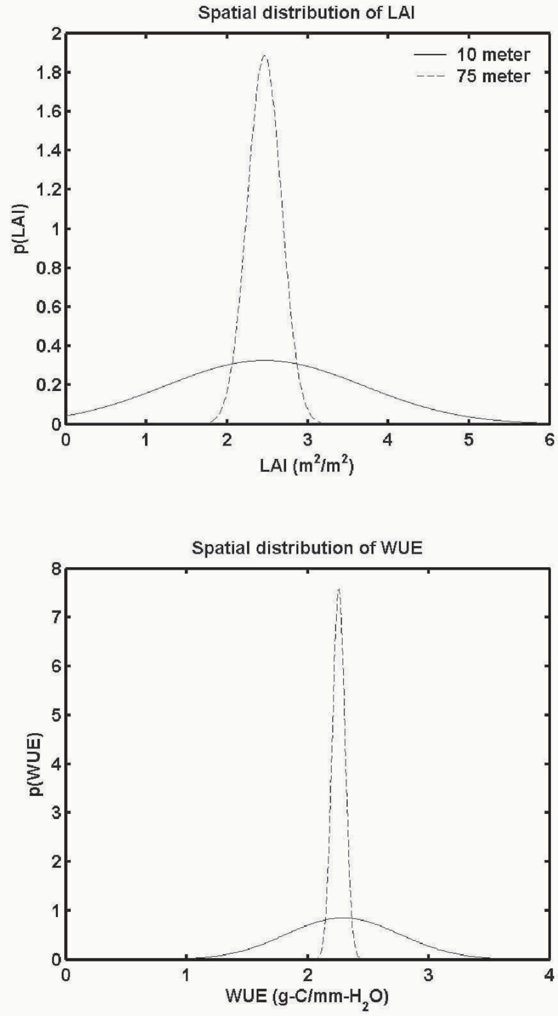

Figure 7. Effect of pattern resolution on simulation of processes in a non–spatially interactive savanna mosaic. The normalized distribution of tree leaf area (A) is provided at both 10 and 75-meter resolution (100m^2 and 5625m^2 pixels respectively) for a woodland site in western Zambia. The resulting distribution of simulated annual water use efficiency at each scale are also provided (B). Increases in the size of patch used for structural parameterization lead to rapid reductions in the range and variability of a key component of vegetation performance. The elimination of "extremes" in the distribution of water use efficiency and vegetation structure leads to an inability to discern demographic processes such as regeneration and mortality, which underlie the patchy mosaic structure.

Therefore, the accurate characterization of vegetation structural change depends not only on the presence of historical data, but also on an understanding of scale effects in heterogeneous tree/grass savanna mosaics (Figure 7). Characterization of vegetation structure using radar sensors has been performed in both forested areas (Sun and Ranson, 1998) and semi arid rangelands (Musick *et al*., 1998).

The fractal dimension, D, can be used to characterize the complexity of autocorrelation in image data across spatial scales. Because of the non-rectifiable nature of fractal patterns, the fractal dimension exceeds the topological dimension, d, but is less than $d+1$, so that in the case of 2-dimensional spatial pattern, $2<D<3$. Larger fractal dimensions are characteristic of patterns that exhibit short-range variation, and smaller fractal dimensions imply long-range variation. In practice, the fractal dimension can be derived from the slope of the semivariogram in a doubly logarithmic plot (Burrough, 1983; Lam and Cola, 1993; Chen *et al.*, 2002). Although patterns that exhibit self-similarity maintain the same fractal dimension across all scales, structured patterns such as those found in characteristic semi-arid vegetation mosaics yield scale-dependent measures of fractal dimension. Therefore, estimates of fractal dimension must be performed across a range of scales (Palmer, 1988). The scale-dependent fractal nature of spatial patterns in savanna ecosystems has been analyzed using the Corona data described above. Figure 8 displays the estimated fractal dimension of three different landscape types estimated at a range of scales. The three landscape types – pastoral, or undisturbed vegetation; township or settlement vegetation; and agricultural vegetation vary in their fractal dimension at high spatial resolutions, but converge as the resolution of the image is reduced. The undisturbed vegetation pattern exhibits the greatest fractal dimension, indicating that natural savanna vegetation is dominated by short-range variation characterized by the patchy distribution of individuals. The agricultural landscape is made up of a mosaic of small agricultural fields, which have a longer range of variation, and therefore the lowest fractal dimension.

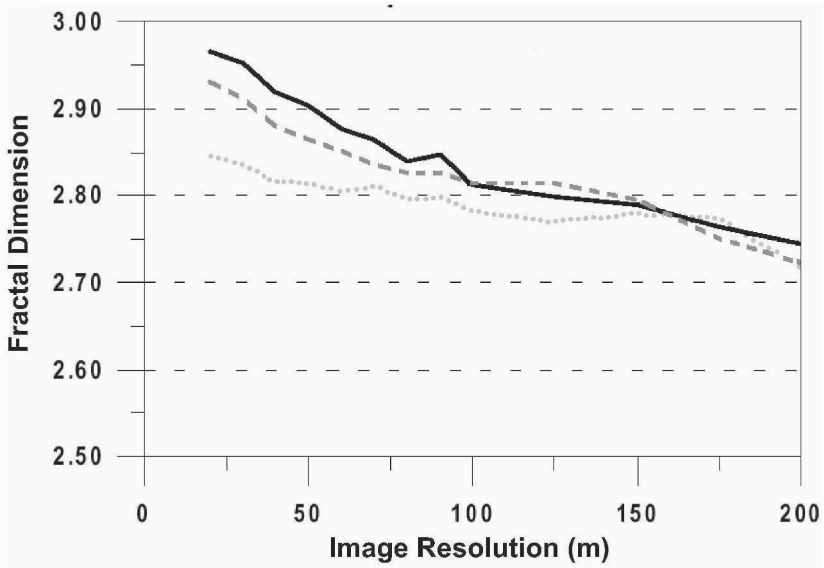

Figure 8. Landscape fractal dimension derived from semivariogram analysis as a function of image resolution and landcover type (adapted from Dowty et al., 2000). Pastoral (undisturbed) savanna vegetation [—] exhibits a greater fractal dimension at higher resolutions than either township [--] or agricultural [··] landscape mosaics. At coarser resolutions (>100m), the difference between the fractal dimension of landscape types is eliminated.

The availability of large-scale multi-resolution data sets of biophysical surface parameters has led to a number of insights into the scaling behavior of parameter fields across a wide range of spatial scales (Justice *et al.*, 1989; Townshend and Justice, 1990; Smith *et al.,* 1992). Although studies of land-atmosphere interaction have demonstrated that the scaling of biological parameters will both be altered by and contribute to the formation of observed scaling patterns in physical parameters, few studies have investigated the scaling properties of vegetation structure directly (e.g., Sole and Manrubia, 1995; Chen *et al.*, 2002). High-resolution satellite imagery has been used to address the scaling properties of the variance in NDVI at scales ranging from 16-m^2 to 90,000 m^2 at four savanna and woodland locations across a large regional moisture gradient. Preliminary analyses of spatial patterns of NDVI show a change in scaling regime between the patch and the landscape scales. This is evidenced by log-log plots of the variance of NDVI as a function of the scale over which NDVI is averaged (Figure 9). A deviation in the expected linear decrease indicates a change in dominant pattern generating process. In the case of study sites on the Kalahari Transect there is a break in the linearity of the log variance curve that occurs at systematically larger scales as one transitions from the drier to the wetter end of the Transect. This change in breakpoint appears to be a consequence of plant canopy processes controlling pattern at small scales and other landscape processes then controlling pattern at larger scales. This implies that satellite data collection systems with differing resolutions might monitor the consequences of different processes and that for particular resolutions the same sensors might detect the consequences of different processes in different parts of the same region.

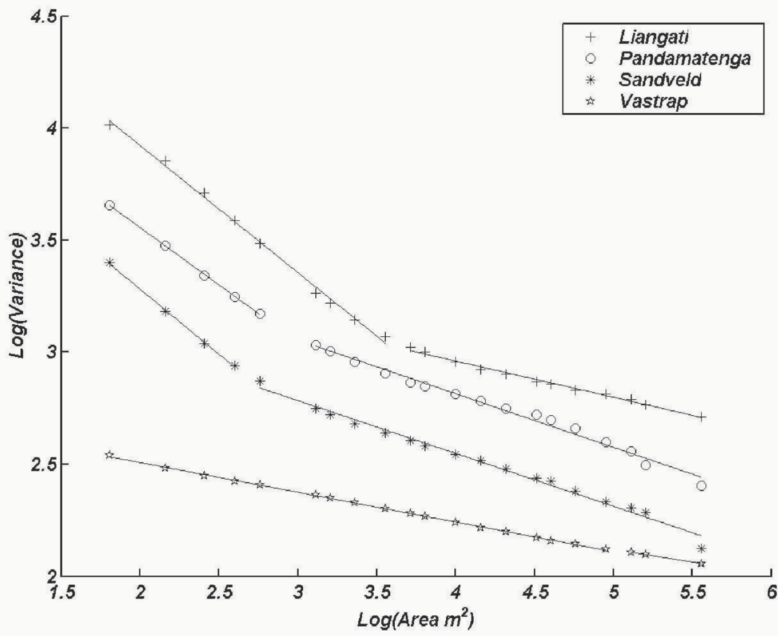

Figure 9 - Realization of the multi-scale nature of savanna ecosystems, depicting the variance of the NDVI field as a function of the area over which the field is averaged. The threshold scales between the distinct patch and landscape regimes are: (3600 m^2) Liangati; (576 m^2) Pandamatenga; and (400 m^2) Sandveld. No threshold scale is observed for the southernmost site, Vastrap. It is likely that the minimum scale of 16 m2 is insufficient to resolve the individual-patch scale pattern at the southernmost site, where vegetation is sparse and consists of small shrubs and isolated grass clumps.

6. Conclusions

In this review we have compared various conceptualizations used to both observe and simulate spatial pattern in semi-arid ecosystems. A series of examples using field-based as well as both historical and recent satellite imagery has demonstrated the diversity of these approaches for measuring and interpreting spatial pattern in southern African savannas. These results contribute to the growing evidence of a multi-scale organization of vegetation in southern African savannas. Although the overall pattern of vegetation cover for the KT savanna is determined by mean annual rainfall and nutrient availability, small-scale patterns of vegetation structure are highly organized by internal processes, which operate at local scales. This conclusion has significant implications for 1) understanding how changes in global climate affect savanna ecosystems, 2) understanding how changes in savanna ecosystems affect the entire Earth system, and 3) monitoring vegetation at different resolutions in time and space, a central issue in the interpretation of remotely-sensed data collection.

Advancement in our understanding of the dynamics of semi-arid ecosystems depends on our capacity to understand how spatial patterns arise from (and modify) ecosystem processes. However, our ability to unravel the importance of multi-scale determinants of vegetation structure depends on the manner by which vegetation structural pattern is characterized in semi-arid ecosystems. In particular, the strong control that vegetation exerts on water availability and the subsequent impact of soil moisture on energy and nutrient cycles implies that key spatial processes occur at the scale of individual tree canopies. However, the observed scaling of patchy structure in savanna ecosystems as well as the presence of large-scale disturbances such as herbivory and fire suggest that these individual-based determinants of structure and function are hierarchically embedded within a suite of organizing processes operating across a wide range of temporal and spatial scales. In this chapter we have attempted to highlight the fact that any observation of spatial pattern necessarily includes assumptions regarding the importance of various pattern-forming mechanisms, and methods of pattern observation vary across time and space scales. Therefore, we suggest approaches that successfully integrate the information and assumptions contained in the diversity of pattern conceptualizations (i.e. individual stem maps at tens of meters to regional distribution of LAI over thousands of kilometers) will lead to new insight into the multi-scale patterns and processes that govern the dynamics of semi-arid vegetation.

7. Acknowledgements

K.K. Caylor's research was supported by a NASA Earth System Science Fellowship while at the University of Virginia, and the Clayton Postdoctoral Fellowship at Princeton University, as well as the National Center for Earth-surface Dynamics (EAR-0120914). Additional funding was provided through the following NASA grants - NAG5-7956, NAG5-7266, NAG5-7862 and NAG5-9357. Figures 2 and 3 are reprinted from Journal of Arid Environments, Volume 54, Caylor et al., "Tree spacing along the Kalahari Transect in southern Africa", 281-296, 2003, with permission from Elsevier.

8. References

Archer, S., C. Scifres, C. R. Bassham and R. Maggio (1988). Autogenic succession in a subtropical savanna: Conversion of grassland to thorn woodland. Ecological Monographs 58(2): 111-127.

Austin, M. P. (1985). Continuum concept, ordination methods, and niche theory. Annual Review of Ecology and Systematics 16: 38-61.

Barot, S., J. Gignoux and J. C. Menaut (1999). Demography of a savanna palm tree: Predictions from comprehensive spatial pattern analyses. Ecology 80(6): 1987-2005.

Beals, E. W. (1968). Spatial pattern of shrubs on a desert plain in Ethiopia. Ecology 49(4): 744-746.

Belsky, A. J., R. G. Amundson, J. M. Duxbury, S. J. Riha, A. R. Ali and S. M. Mwonga (1989). The effects of trees on their physical, chemical and biological environments in a semi-arid savanna in Kenya. Journal of Applied Ecology 26(3): 1005-1024.

Belsky, A. J., S. M. Mwonga, R. G. Amundson, J. M. Duxbury and A. R. Ali (1993). Comparative effects of isolated trees on their undercanopy environments in high and low-rainfall savannas. Journal of Applied Ecology 30(1): 143-155.

Bian, L. and R. Butler (1999). Comparing effects of aggrgation methods on statistical and spatial properties of simulated spatial data. Phtogrammetric Engineering and Remote Sensing 65(1): 73-84.

Bolker, B. M. and S. W. Pacala (1999). Spatial moment equations for plant competition: Understanding spatial strategies and the advantages of short dispersal. American Naturalist 153(6): 575-602.

Boone, R. B., M. B. Coughenour, K. A. Galvin and J. E. Ellis (2002). Addressing management questions for Ngorongoro Conservation Area, Tanzania, using the SAVANNA modelling system. African Journal of Ecology 40(2): 138-150.

Breshears, D.D. and F.J. Barnes (1999). Interrelationships between plant functional types and soil moisture heterogeneity for semiarid landscapes within the grassland/forest continuum: a unified conceptual model. Landscape Ecology 14:465-478.

Breshears, D., J. Nyhan, C. Heil and B. Wilcox (1998). Effects of woody plants on microclimate in a semiarid woodland: Soil temperature and evaporation in canopy and intercanopy patches. International Journal of Plant Sciences 159(6): 1010-1017.

Bestelmeyer, B.T. J.R. Brown, K.M. Havastad, R. Alexander, G. Chavez, J. Herrick (2003) Development and use of state-and-transition models for rangelands. Journal of Range Management 56(2):114-126.

Breshears, D. D., O. B. Myers, S. R. Johnson, C. W. mEyer and S. N. Martens (1997). Differential use of spatially heterogeneous soil moisture by two semiarid woody species: Pinus edulis and Juniperus monosperma. Journal of Ecology 85(3): 289-299.

Brown, J.H., V.K. Gupta, B.L. Li, B.T. Milne, C. Restrepo and G.B. West (2002). The fractal nature of nature: power laws, ecological complexity and biodiversity. Philosophical Transactions of the Royal Society of London: Series B. 357: 619-626.

Bruniquel-Pinel, V. and J. P. Gastellu-Etchegorry (1998). Sensitivity of texture of high resolution images of forest to biophysical and acquisition parameters. Remote Sensing of Environment 65: 61-85.

Burrough, P.A. (1981). Fractal dimensions of landscapes and other environmental data. Nature 294:241-243.

Burrough, P.A. (1983). Multiscale sources of spatial variation in soil: I. Application of fractal concepts to nested levels of soil variations. Journal of Soil Science 34:577-597.

Cale, W. G., G. M. Henebry and J. A. Yeakley (1989). Inferring process from pattern in natural communities. Bioscience 39(9): 600-605.

Caylor, K. K., P. R. Dowty, H. H. Shugart and S. Ringrose (2004). Relationship between small-scale structural variability and simulated vegetation productivity across a regional moisture gradient in southern Africa. Global Change Biology 10(3):374-382.

Caylor, K. K., H. H. Shugart (2004). Simulated productivity of heterogeneous patches in Southern African savanna landscapes using a canopy productivity model. Landscape Ecology 19(4): 401-415.

Caylor, K. K., H. H. Shugart and I. Rodriguez-Iturbe (in press). Tree canopy effects on simulated water balance in southern African savannas. Ecosystems.

Caylor, K. K., H. H. Shugart and T. M. Smith (2003). Tree spacing along the Kalahari Transect. Journal of Arid Environments 54(2): 281-296.

Chen, Y.F., F.H. Yu and M. Dong (2002) Scale-dependent spatial heterogeneity of vegetation Mu Us sandy land, a semi-arid area of China. Plant Ecology 162:135-142.

Clark, P. J. and F. C. Evans (1954). "Distance to nearest neighbor as a measure of spatial relationships in populations." Ecology **35**(4): 445-453.

Cody, M. L. (1986). Spacing patterns in Mojave Desert plant communities: near-neighbor analysis. Journal of Arid Environments 11: 199-217.

Coughenour, M.B. (1992). Spatial modeling and landscape characterization of an African pastoral ecosystem: a prototype model and its potential use for monitoring drought. In: D.H. McKenzie, D.E. Hyatt and V.J. McDonald (eds.), Ecological Indicators, Vol 1, p. 787-810, Elsevier Applied Science, London and New York.

Couteron, P. (2001) Using spectral analysis to confront distributions of individual species with an overall periodic pattern in semi-arid vegetation. Plant Ecology 156(2):229-243.

Couteron, P. and O. Lejeune (2001). Periodic spotted patterns in semi-arid vegetation explained by a propagation-inhibition model. Journal of Ecology 89(4):616-628.

Cowles, H. C. (1899). The ecological relations of the vegetation on the sand dunes of Lake Michigan. Botanical Gazette 27: 95.

Dale, M. R. T. (1999). Spatial Pattern Analysis in Plant Ecology. Cambridge, Cambridge University Press.

Daly, C., D. Bachelet, J. M. Lenihan, R. P. Neilson, W. Parton and D. Ojima (2000). Dynamic simulation of tree-grass interactions for global change studies. Ecological Applications 10(2): 449-469

Delire C, Foley JA, Thompson S. 2003. Evaluating the carbon cycle of a coupled atmosphere-biosphere model. Global Biogeochemical Cycles 17 (1): art. no. 1012.

Dietler, G. and Y.C. Zhang (1992) Fractal aspects of the swiss landscape. Physica A. 191(1-4):213—219.

Diggle, P.J. (1983) Statistical Analysis of Spatial Point Patterns. London: Academic Press

Dowty, P., K. K. Caylor, H. H. Shugart and W. R. Emanuel (2000). Approaches for the estimation of primary productivity and vegetation structure in the Kalahari region. Towards Sustainable Natural Resource Management in the Kalahari Region. S. Ringrose and R. Chanda. Gaborone, Botswana, University of Botswana.

Dunn, C. P., D. M. Sharpe, G. R. Guntenspergen, F. Stearns and Z. Yang (1990). Methods for analyzing temporal changes in landscape pattern. Quantitative Methods in Landscape Ecology. M. G. Turner and R. H. Gardner. New York, Springer-Verlag.

Eagleson, P. S. and R. I. Segarra (1985). Water-limited equilibrium of savanna vegetation systems. Water Resources Research 21(10): 1483-1493.

Gignoux, J., I. R. Noble and J. C. Menaut (1995). Modelling tree community dynamics in savannas: effects of competition with grasses and impact of disturbance. Functioning and dynamics of natural and perturbed ecosystems. D. Bellan-Santini, G. Bonin and C. Emig. Paris, Lavoisier Intercept Ltd**:** 219-230.

Gleason, H. A. (1927). Further views on the succession concept. Ecology 8(3): 299-326.

Greig-Smith, P. (1979). Pattern in vegetation. Journal of Ecology 67(3): 775-779.

Grime, J. P. (1979). Plant strategies and vegetation processes. Chichester ; New York, Wiley.

Hély, C., P. R. Dowty, S. Alleaume, K. K. Caylor, S. Korontzi, R. J. Swap, H. H. Shugart and C. O. Justice (2003a). Regional fuel load for two climatically contrasting years in southern Africa. Journal of Geophysical Research - Atmospheres 108(D13): 8475-8491.

Hély, C., K. K. Caylor, S. Alleaume, R. J. Swap and H. H. Shugart (2003b). Release of gaseous and particulate carbonaceous compounds from biomass burning during the SAFARI 2000 dry season field campaign. Journal of Geophysical Research - Atmospheres 108(D13): 8740-8750.

Higgins, S. I., W. J. Bond and W. S. W. Tollope (2000). Fire, resprouting and variability: a recipe for grass-tree coexistence in savanna. Journal of Ecology 88(2): 213-229.

Hipondoka, M.H.T, J.N. Aranibar, C. Chirara, M. Lihavha, S.A. Macko. 2003. Vertical distribution of grass and tree roots in arid ecosystems of Southern Africa: niche differentiation of competition? Journal of Arid Environments. 54:319-325.

Hort, A. (1916) Enquiry into plants and minor works on odours and weather signs. By Theophrastus and translated by Sir Albert Hort, vols. I and II. Heinemann, London.

Hudak, A.T. and C.A. Wessman (2001). Textural analysis of high resolution imagery to quantify bush encroachment in Madikwe Game Reserve, South Africa, 1955-1996. International Journal of Remote Sensing, 22(14) 2731-2740.

Hudak, A.T., and C.A. Wessman. (1998). Textural Analysis of Historical Aerial Photography to Characterize Woody Plant Encroachment in South African Savanna. Remote sensing of environment, 66(3):317.

Humboldt, A. von. (1807). Ideen zu einer Geographie der Pflanzen. F.G. Cotta, Tübingen (reprinted in 1963 by Wissenschaftl. Buchges, Darmstadt).

Humphries HC, D.P. Coffin DP, W.K. Lauenroth. 1996. An individual-based model of alpine plant distributions. Ecological Modeling 84:99-126.

Hutley, L. B., A. P. O'Grady, and D. Eamus. 2001. Monsoonal influences on evapotranspiration of savanna vegetation of northern Australia. Oecologia 126:434-443.

Jackson, N. A. and J. S. Wallace (1999). Soil evaporation measurements in an agroforestry system in Kenya. Agricultural and Forest Meteorology 94: 203-215.

Jeltsch, F., S. Milton, W. R. J. Dean and N. v. Rooyen (1996). Tree spacing and coexistence in semiarid savannas. Journal of Ecology 84(4): 583-595.

Jeltsch, F., S. J. Milton, W. R. J. Dean, N. van Rooyen and K. A. Moloney (1998). Modelling the impact of small-scale heterogeneities on tree- grass coexistence in semi-arid savannas. Journal of Ecology 86(5): 780-793.

Jeltsch, F., K. Moloney and S. J. Milton (1999). Detecting process from snapshot pattern: lessons from tree spacing in the southern Kalahari. Oikos 85(3): 451-466.

Joffre, R. and S. Rambal (1993). How tree cover influences the water balance of Mediterranean rangelands. Ecology 74(2): 570-582.

Justice, C. O., J. R. G. Townshend and B. J. Choudhury (1989). Comparison of AVHRR and SMMR data for monitoring vegetation phenology on a continental scale. International Journal of Remote Sensing 10(10): 1607-1632.

Kadmon, R., and R. Harari-Kremer. (1999). Studying long-term vegetation dynamics using digital processing of historical aerial photographs. Remote Sensing of Environment, 6 8:164-176.

Keddy, P. A. (1989). Competition. New York, Chapman and Hall.

Keya, G. A. (1997). Environmental triggers of germination and phenological events in an arid savannah region of northern Kenya. Journal of Arid Environments 37(1): 91-106.

Koch, G. W., P. M. Vitousek, W. L. Steffen and B. H. Walker (1995). Terrestrial transects for global change research. Vegetatio 121: 53-65.

Krummel, J.R., R.H. Garder, G. Sugihara, R.V. O'Neill and P.R. Coleman (1987). Landscape patterns in disturbed environment. Oikos 48: 321-324.

Lam, N.S., and L.D. Cola. (1993). Fractal measurement. In: N. S. Lam and L. D. Cola (Ed.), Fractals in Geography, pp. New Jersey: Prentice Hall.

Lefever, R. and O. Lejeune (1997). On the origin of tiger bush. Bulletin of Mathematical Biology 59(2): 263-294.

Lejeune, O. and M. Tlidi (1999). A model for the explanation of vegetation stripes (tiger bush). Journal of Vegetation Science 10: 201-208.

Levin, S. A., 1992. The problem of pattern and scale in ecology: The Robert H. MacArthur Award Lecture. Ecology, 73(6): 1943-1967.

Levin, S.A., T. Powell and J.H. Steele, editors (1993) Patch dynamics. Springer-Verlag, New York, New York. USA.

Li, B.L. (2000). Fractal geometry applications in description and analysis of patch patterns and patch dynamics. Ecological Modelling. 132:33-50.

Li, B.-L. and S. Archer (1997). Weighted mean patch size: A robust index for quantifying landscape structure. Ecological Modelling 102(2-3): 353-361.

Ludwig, F., H. de Kroon, H. H. T. Prins and F. Berendse (2001). Effects of nutrients and shade on tree-grass interactions in an East African savanna. Journal of Vegetation Science 12(4): 579-588.

Ludwig, J. A., D. J. Tongway and S. G. Marsden (1999). Stripes, strands or stipples: modelling the influence of three landscape banding patterns on resource capture and productivity in semi-arid woodlands, Australia. Catena 37: 257-273.

Ludwig, J. A., J. A. Wiens and D. J. Tongway (2000). A scaling rule for landscape patches and how it applies to conserving soil resources in savannas. Ecosystems 3(1): 84-97.

Mandelbrot, B. (1982). The Fractal Geometry of Nature. W.H. Freeman & Company. 468 pp.

McCown, R. L. and J. Williams (1990). The water environment and implications for productivity. Journal of Biogeography 17(4/5): 513-520.

McDonald, R., Ed. (1997). Corona: Between the Sun and the Earth. Baltimore, MD, American Society for Programmetry and Remote Sensing.

McIntosh, R. P. (1967). Continuum Concept of Vegetation. Botanical Review 33(2): 130.

Menaut, J. C. and J. Cesar (1979). Structure and primary productivity of Lamto savannas, Ivory Coast. Ecology 60(6): 1197-1210.

Miriti, M.N., S.J. Wright and H.F. Howe. The effects of neighbors on the demography of a dominant desert shrub (Ambrosia dumosa). Ecological Monographs 71(4):491-509.

Mordelet, P. and J. C. Menaut (1995). Influence of Trees on Aboveground Production Dynamics of Grasses in a Humid Savanna. Journal of Vegetation Science 6(2): 223-228.

Mordelet, P., J. C. Menaut and A. Mariotti (1997). Tree and grass rooting patterns in an African humid savanna. Journal of Vegetation Science 8(1): 65-70.

Morton, A.G. (1981) History of Botanical Science. Academic Press, London.

Musick, H.B., G.S. Schaber, and C.S. Breed. (1998). AIRSAR Studies of Woody Shrub Density in Semiarid Rangeland: Jornada del Muerto, New Mexico. Remote sensing of environment, 66(1):29.

Niklas, K. J. (1994). Plant allometry : the scaling of form and process. Chicago, University of Chicago Press.

Ojima, D. (ed.). 1992. Modeling the Earth System. UCAR/Office for Interdisciplinary Earth Studies, Boulder, Colorado.

Otsu, N. (1979). A threshold selection method from gray-level histograms. IEEE Trans. System, Man, and Cybernetics 9(1): 62-66.

Pacala, S. W. and D. H. Deutschman (1995). Details that matter: The spatial distribution of individual trees maintains forest ecosystem function. Oikos 74(3): 357-365.

Palmer, A.R., and A.F. van Rooyen. (1998). Detecting Vegetation Change in the Southern Kalahari Using Landsat TM. Journal of arid environments, 39(2):143.

Pearson, D. (2002). The application of local measures of spatial autocorrelation for describing pattern in north Australian landscapes. Journal of Environmental Management 64(1): 85-95.

Peters, D.P.C. 2002. Plant species dominance at a grassland-shrubland ecotone: an individual-based gap dynamics model of herbaceous and woody species. Ecological Modeling 152: 5-32.

Pielou, E. C. (1962). The use of plant-to-neighbor distance for the detection of competition. Journal of Ecology 50: 357-367.

Phillips, D. L. and J. A. MacMahon (1981). Competition and spacing patterns in desert shrubs. Journal of Ecology 69(1): 97-115.

Potter, C.S., J.T. Randerson, C.B. Field, P.A. Matson, P.M. Vitousek, H.A. Mooney and S.A. Klooster. 1993. Terrestrial ecosystem production – a process model based on global satellite and surface date. Global Biochemical Cycles 7:811-841.

Privette, J., Y. Tian, G. Roberts, R. J. Scholes, Y. Wang, K. K. Caylor, P. Frost and M. Mukelabai (2004). Structural characteristics and relationships of Kalahari woodlands and savannas. Global Change Biology 10(3):281-291.

Qi, Y. and J. Wu (1996). Effects of changing spatial resolution on the results of landscape pattern analysis using spatial autocorrelation indicies. Landscape Ecology 11(1): 39-49.

Raffaele, E. and T. T. Veblen (1998). Facilitation by nurse shrubs of resprouting behavior in a post-fire Shrubland in northern Patagonia, Argentina. Journal of vegetation science 9(5): 693.

Ripley, B.D. (1976) The second order analysis of stationary point processes. Journal of Applied Probability, 13, 255-266.

Ripley, B. D. (1977). Modelling spatial patterns. Journal of the Royal Statistical Society, Series B (Methodological) 39(2): 172-212.

Rodriguez-Iturbe, I. and A. Rinaldo (1997). Fractal river basins: Chance and self-organization. New York, Cambridge University Press.

Sala, O. E. and W. K. Laurenroth (1982). Small rainfall events: an ecological role in semiarid regions. Oecologia 53: 301-304.

Scanlon, T. M., J. D. Albertson, K. K. Caylor and C. Williams (2002). Determining land surface fractional cover from NDVI and rainfall time series for a savanna ecosystem. Remote Sensing of Environment 82(2-3): 376-388.

Schenk, H.J., C. Holzapfel, J.G. Hamilton and B.E. Mahall (2003). Spatial ecology of a small desert shrub on adjacent geological substrates. Journal of Ecology 91:383-395.

Scholes, R. J. and S. R. Archer (1997). Tree-grass interactions in Savannas. Annual Review of Ecology and Systematics. **28:** 517-544.

Scholes, R. J., P. R. Dowty, K. K. Caylor, D. A. B. Parsons, P. G. H. Frost and H. H. Shugart (2002). Trends in savanna structure and composition on an aridity gradient in the Kalahari. Journal of Vegetation Science 13(3): 419-428.

Scholes, R. J. and D. A. B. Parsons, Eds. (1997). The Kalahari Transect: Research on Global Change and Sustainable Development in Southern Africa, IGBP Report 42. Stockholm, IGBP Secretariat.

Scholes, R. J. and B. H. Walker (1993). An African Savanna: Synthesis of the Nylsvley Study. Cambridge, Cambridge University Press.

Seghieri, J. (1995). The rooting patterns of woody and herbaceous plants in a savanna; are they complementary or in competition? African journal of ecology. Nairobi 33(4): 358-365.

Shugart, H.H., K.K. Caylor, C. Hély, R.J. Swap, P.R. Dowty. (in prep) Dynamic change in the woodland and savannah ecosystems of sub-tropical Africa.

Shugart, H. H., N. H. F. French, E. S. Kasischke, J. J. Slawski, C. W. Dull, R. A. Shuchman and J. Mwangi (2001). "Detection of vegetation change using reconnaissance imagery." Global Change Biology 7(3): 247-252.

Shugart, H. H., L. L. Bourgeau-Chavez and E. S. Kasischke (2000). "Determination of stand properties in boreal and temperate forests using high-resolution photography and satellite imagery." Forest Science 46(4): 478.\

Shugart, H. H. (2000). Importance of structure in the longer-term dynamics of landscapes. Journal of geophysical research 105(D15): 20065-20075.

Shugart, H. H. (1998). Terrestrial Ecosystems in Changing Environments. New York, Cambridge University Press.

Shugart, H.H., and D.C. West. 1980. Forest succession models. BioScience 30:308-313.

Simioni, G., X. LeRoux, J. Gignoux and H. Sinoquet (2000). Treegrass: a 3D, process-based model for simulating plant interactions in tree-grass ecosystems. Ecological Modelling 131(1): 47-63.

Skarpe, C. (1991). Spatial patterns and dynamics of woody vegetation in an arid savanna. Journal of vegetation science 2(4): 565-572.

Skarpe, C. (1992). Dynamics of savanna ecosystems. Journal of Vegetation Science 3(3).

Smit, G. N. and N. F. G. Rethman (2000). The influence of tree thinning on the soil water in a semi-arid savanna of southern Africa. Journal of Arid Environment 44: 41-59.

Smith, T. M., J. F. Weishampel, H. H. Shugart and G. B. Bonan (1992). The response of terrestrial C storage to climate change: modeling C dynamics at varying temporal and spatial scales. Water, Air, & Soil Pollution 64(1-2): 307-326.

Smith, T. M. and P. S. Goodman (1987). "Successional dynamics in an Acacia nilotica - Euclea divinorum savannah in southern Africa." Journal of Ecology **75**(3): 603-610.

Smith, T. M. and K. Grant (1986). The role of competition in the spacing of trees in a Burkea africana - Terminalia sericea savanna. Biotropica 18(3): 219-223.

Sole, R. V. and S. C. Manrubia (1995). Are rainforests self-organized in a critical state? Journal of Theoretical Biology 173: 31-40.

Stein, A., W. G. M. Bastiaanssen and A. Saldana (1998). Integrating spatial statistics and remote sensing. International journal of remote sensing 19(9): 1793.

St-Onge, B. A. and F. Cavayas (1995). Estimating forest stand structure from high resolution imagery using the directional variogram. International Journal of Remote Sensing 16(11): 1999-2021.

Sun, G. and K. J. Ranson (1998). Radar modelling of forest spatial patterns. International journal of remote sensing 19(9): 1769.

Thomas, D. S. G. and P. A. Shaw (1991). The Kalahari Environment. Cambridge, Cambridge University Press.

Tilman, D. (1982). Resource competition and community structure. Princeton, N.J., Princeton University Press.

Townshend, J. R. G. and C. O. Justice (1986). Analysis of the dynamics of African vegetation using the normalized difference vegetation index. International Journal of Remote Sensing 7(11): 1435-1445.

Treuhaft RN, Asner GP, Law BE, Van Tuyl S (2002). Forest leaf area density profiles from the quantitative fusion of radar and hyperspectral data, Journal of Geophysical Research - Atmospheres 107:(D21).

Tyson, P. D. (1986). Climatic Change and Variability in Southern Africa. Cape Town, Oxford University Press.

Urban, D.L., G.B. Bonan, T.M. Smith and H.H. Shugart. 1991. Spatial applications of gap models. Forest Ecology and Management 42:95-110.

Walker, B. H. and I. Noy-Meir (1982). Aspects of the Stability and Resilience of Savanna Ecosystems. Ecology of Tropical Savannas. B. J. Huntley and B. H. Walker. Berlin, Springer-Verlag**:** 556-590.

Walter, H. (1971). Natural savannas. Ecology of Tropical and Subtropical Vegetation. J. H. Burnett. Edinburgh, Oliver and Boyd.

Watt, A. S. (1947). Pattern and process in the plant community. Journal of Ecology 35(1/2): 1-22.

Weishampel, J. F., G. Sun, K. J. Ranson, K. D. LeJeune and H. H. Shugart (1994). Forest textural properties from simulated microwave backscatter: The influence of spatial resolution. Remote Sensing of Environment 47(2): 120-131.

Whiteman, G. and J. R. Brown (1998). Assessment of a method for mapping woody plant density in a grassland matrix. Journal of Arid Environments 38: 269-282.

Whittaker, R. H., L. E. Gilbert and J. H. Connell (1979). Analysis of two-phase pattern in a mesquite grassland, Texas. Journal of Ecology 67(3): 935-952.

Wijk, M. T. v. and I. Rodriguez-Iturbe. 2002. Tree-grass compeition in space and time: Insights from a simple cellular automata model based on ecohydrological dynamics. Water Resources Research 38(9): 1179-1193.

Wilson, T. B. and E. T. F. Witkowski (1998). Water requirements for germination and early seedling establishment in four African savanna woody plant species. Journal of arid environments 38(4): 541-550.

Woodward, F.I., T.M. Smith and W.R. Emanuel. 1995. A global land primary productivity and phytogeography model. Global Biogeochemical Cycles 9:471-490.

Wu, J. and Levin, S. A., 1994. A spatial patch dynamic modeling approach to pattern and process in an annual grassland. Ecological Monographs, 64(4): 447-464.

Wulder, M. and B. Boots (1998). Local spatial autocorrelation characteristics of remotely sensed imagery associated with the Getis statistic. International Journal of Remote Sensing 19(11).

Yeaton, R. I. and M. L. Cody (1976). Competition and spacing in plant communities: the northern Mohave desert. Journal of Ecology 64(2): 689-696.

Yeaton, R. I., J. Travis and E. Gilinsky (1977). Competition and spacing in plant communities: The Arizona upland association. Journal of Ecology 65(2): 587-595.

Chapter 16

FIRE REGIMES IN DRYLAND LANDSCAPES

Christelle HÉLY[1] and Samuel ALLEAUME[2]

[1] *Centre Européen de Recherche et d'Enseignement des Géosciences de l'Environnement, Europôle de l'Arbois, B.P. 80, 13545 Aix-en-Provence cedex 04, FRANCE - e-mail: hely@cerege.fr*

[2] *Centre d'Etudes Biologiques de Chizé, B.P. 14, 79360 Beauvoir sur Niort, FRANCE - e-mail: alleaume@cebc.cnrs.fr*

1. Introduction

Dryland regions are climatically defined through low annual precipitation, with in general dry season periods that can span over several months and take place once or twice a year. A combination of climate and soil characteristics defines the range of likely vegetation composition from grasslands and savannas to dry forests (van Wilgen and Scholes 1997). As these climatic and vegetation characteristics are suitable to recurrent fires, several authors consider such ecosystems as pyrophytic vegetations (Trabaud 1991, Scholes 1997, van Wilgen and Scholes 1997, Mistry 1998, Trollope and Everson 1999, Roques et al. 2001). Fire affects ecosystem dynamics in terms of species selection, regeneration, structure, nutrient cycling, and mortality. While this chapter is devoted to fire regimes, the effects of fires on soil moisture dynamics, infiltration and runoff production are discussed in Chapter 3; the effect on soil nutrient cycling and soil gas emissions are briefly analysed in Chapters 11 and 14. Additional discussion on the role of fire dynamics on different biomes, e.g. grasslands, shrublands, dry forests and savannas, can be found in Chapters 12, 13, and 15.

The concept of fire regime includes several features, related to space and time, characterizing fires typically occurring in a given regional ecosystem such as the fire extent, the frequency, the cycle, the season of burning and the fire behaviour (Whelan 1995).

While these pyrophytic ecosystems are distributed on all continents, this chapter will focus on few ecosystems selected from Africa, southern America, and Europe.

In the southern African region dominated by the savanna biome, where annual precipitation is less than about 600 mm, semi-arid vegetation presents woody species (trees and shrubs) with small and thin broadleaves. In particular, vegetation in Namibia and Botswana is dominated by *Acacia* species and "sweet" or palatable grasses for livestock, i.e. grass with low fiber content and winter sequestration of nutrients in their leaves (Scholes 1997). On the contrary, where rainfall is higher than 600 mm, vegetation is characterized by large broadleaved trees species and "sour" grasses having higher fiber content. In Zambia and Tanzania, forests are mainly represented by Miombo characterized by *Brachystegia* and *Isoberlina* species.

In the tropical climate region of the South American continent, cerrado (a complex vegetation mosaic of savannas, grasslands, and dry forests (Kauffman et al. 1994, Mistry 1998)) is representative of dryland ecosystems and it is widely present in Brazil and Chile. Cerrado results from frequent and successive fires induced naturally by climate but also by anthropogenic activities related to deforestation of the Amazon basin.

In the European Mediterranean region, the typical shrubland ecosystems are the garrigue and maquis, which are similar to the chaparral vegetation in California. Garrigue and maquis differ from their species composition, which reflects differences in soil characteristics and stress tolerance. Those two ecosystems are known in the vegetation succession as transitional stages between grassland and forests mainly dominated by pines and oaks (Trabaud 1989, Vernet 1997, De las Heras et al. 2002). Their dynamics is linked to disturbances such as fires, and they have

P. D'Odorico and A. Porporato (eds.), Dryland Ecohydrology, 283–301.

been selected for agricultural and management perspectives and maintained in Mediterranean landscapes for thousands years (Carcaillet et al. 1997, Vernet 1997, Figueiral and Terral 2002, Quilès et al. 2002, Wick et al. 2003).

Thus, the current vegetation composition and structure, such as the openness, of these pyrophytic ecosystems is the result of past and present climates, soil type, and also disturbances such as fires, spreading over these systems with variability in time and space. This chapter will first provide general information about the fire environment and of the combustion process. The different variables characterizing the fire regime will be discussed along with their assessment at different spatial scales. Finally, different fire regimes typical of pyrogenic dryland ecosystems will be described.

2. Fire in its environment

Fire-related processes are controlled by the physics and chemistry of combustion (Whelan 1995). However, a fire starts, spreads, and dies also as the result of three environmental factors, namely vegetation, climate, and topography, which interact together to constitute the natural environment of fire. These three factors and their interactions have already been partially presented in the first section of this book (Sections 2-7). In this chapter, interactions are analysed from the point of view of fire processes.

2.1 COMBUSTION

Energy, initially stored in vegetation during the photosynthesis process, is released during fire as heat when materials such as leaves, grass, or wood are combined with oxygen to form carbon dioxide, water vapour, and other substances (Brown and Davis 1973, Whelan 1995). Three stages in the process of combustion can be recognized in a vegetation fire in relation to the basic principles of combustion physics (Trollope 1984a). These are (i) preheating, in which the fuel just ahead of the fire front is heated, dried, and partly pyrolysed; (ii) flaming combustion, which results from the ignition of the flammable hydrocarbon gases; (iii) glowing combustion, during which the remaining charcoal burns as a solid, with oxidation taking place on the surface, without flame, and leaving a small amount of residual ash. To start, combustion requires the « activation energy » of an external energy source, such as lightning for the dominant natural source, or a human induced source. In the heating process, the fuel moisture is first evaporated (fuel temperatures > 100°C), then cellulose is thermally broken down (pyrolysis), and its breakdown products are volatilised (> 200°C), and ignited to form a visible flame (300 - 400°C) (Johnson 1992). The modes of heat transfer responsible for fire spread from the flaming front are convection and radiation (Figure 1, top). Conduction does not contribute significantly to fire spread because wood and soil are such poor heat conductors. To maintain a solid visible flame, the fire front must be constantly moving to recruit adjacent unburned fuels (Johnson 1992). The moving fire front provides the pilot flame to ignite the unburned vegetation. The flaming combustion ends when most of the volatile compounds have burned. The remaining carbon will eventually burn during the glowing phase. A fire can therefore be considered as a chain reaction, with the initial ignition source providing the activation energy that permits ignition and self-sustainability of a fire (Alexander 1982). The difference between flaming and glowing combustion are of interest to ecologists because they can have different ecological effects (Johnson 1992). For instance, flaming combustion is primarily responsible for plant death and glowing combustion for duff consumption and seedbed preparation.

The combustion process in vegetation fires takes place in a physical environment represented by the vegetation, the climate or weather, and the topography. We will now present these different factors and see how they interact.

2.2 TOPOGRAPHY

Among the abiotic factors, topography presents changes that only occur at the geological temporal scales and therefore it is considered for a given area as a constant and fixed factor in the fire environment. Topography directly and indirectly affects fire ignition and propagation. Hilltops are more affected by lightning than bottom hills or flat terrains. Mid and upper slopes present drier soil conditions and drier vegetation composition due to better water drainage. These dryer conditions favour fire ignition because the combustion of dry vegetation involves less water evaporation and requires less energy before flame occurrence. During the flaming combustion phase, the fire front propagation is facilitated towards uphill direction because the radiation energy released by the flame enhances the pre-heating stage of the adjacent fuel that lies uphill near the flame (Figure 1 bottom). For the same reason, uphill fire will propagate faster than fire spreading on flat or downhill directions.

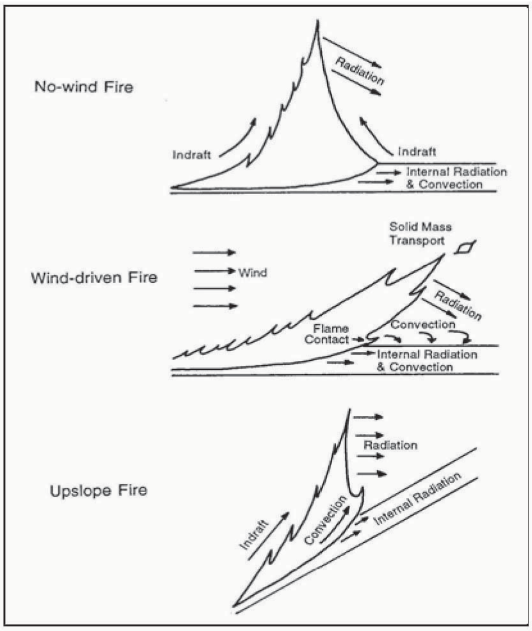

Figure 1. Idealized flaming front with modes of heat transfer. The similar influence of wind and topography on fire behaviour is illustrated in these fire profiles. Both slope and wind bring the flame closer to the adjacent, unburned fuel, so enhancing the pre-heating and increasing the rate of spread (figures from Alexander (1982) Source: Canadian Forest Service, used with permission).

2.3 CLIMATE and WEATHER

Precipitation, temperature, and wind conditions affect the fire at different spatial and temporal scales, through climate at longer term and weather at short term. For a given region, climate, and particularly annual rainfall, determines the main characteristics of dryland landscapes and fire regime. Indeed, climate determines vegetation types, fire season, and fire frequency.

Weather, and especially precipitation, is the most fluctuating factor from days to years in the fire environment (Shroeder and Buck 1970, Trabaud 1991). On a yearly basis, water availability (mostly fed by precipitation) determines the quantity of vegetation and fuel production (van Wilgen and Scholes 1997, Hély et al. 2003b). On a daily basis, weather defines the quality of fuel (moisture content), the fire hazard (dry and windy air), and the fire behaviour. Moisture content in live vegetation changes over the season as the result of plant phenology. Physiological processes, such as stomata closure, prevent vegetation from heating and drying up to a certain stress level at which vegetation dies. Conversely, dead vegetation reacts passively to changes in humidity, and loss of moisture content is faster in thin material than in coarse debris (Burgan and Rothermel 1984, Johnson 1992). Both topography and wind are significant factors for fire spread (Figure 1, middle). Finally, lightning is often associated with first rainfall and thunderstorms at the end of dry seasons, as it provides the perfect natural ignition source for fire triggering.

According to several authors, climate and weather are the most significant factors in determining fire occurrence and fire spread (Bessie and Johnson 1995), though other authors demonstrated that vegetation has to be considered as well (Agee 1997, Hély et al. 2001).

2.4 VEGETATION

Vegetation is the biotic factor providing fuel, and it is characterized in terms of quantity, quality, and spatial arrangement. As previously mentioned, the amount of vegetation is directly related to precipitation quantity, with maximum production for the years with very high precipitation amounts (van Wilgen and Scholes 1997, Hély et al. 2003b). Vegetation growth takes place during the rainy seasons, and as soon as the rain season ends vegetation starts to dry. After few weeks of dry season, vegetation may be dry enough (particularly grasses) to sustain a fire if the minimum fuel load has been reached. In southern African savannas, this minimum fuel load has been estimated at approximately 250-300g/m^2 (van Wilgen and Scholes 1997, Hély et al. 2003a). The size of vegetation particles is also very important as fine debris burn more easily than coarse debris. Therefore, fuels have been classified into diameter classes according to the time lag necessary to loose 2/3 of their saturated moisture content (Brown et al. 1982). One-hour time lag fuel (1-H fuel) is representative of particles whose diameter is less than 0.65 cm and which require only one hour to dry and loose 2/3 of their water content. In the same way, there are 10- and 100-H time lag fuels, which present diameters between 0.65 and 2.5 cm and between 2.5 and 7.6 cm, respectively (Burgan and Rothermel 1984). All grasses, fine woody debris such as small twigs, and litter debris are included in the 1-H time lag class. The 10-H time lag class includes branches of larger diameter, while the 100-H time lag class takes into account small diameter boles and branches less than 8 cm in diameter. Depending on the ecosystem type, larger trunks may not be considered as fuel during the fire front propagation as these pieces are too big and usually still too moist to ignite quickly. However, in many case, if the fire front spreads slowly, or in areas burning against the wind or in the back fire perimeter zone, the residence time of flame can be long enough to ignite these boles that will burn for several hours or days after the fire is over. In such conditions, these large boles and trunks will be completely consumed, leaving only characteristic white ashes on the location of the consumed woody piece. Fuel quality refers both to moisture content and to the chemical composition of vegetation. Indeed, the presence of essential oils and waxes enhance fuel ignition and combustion. Spatial arrangement includes both fuel density and fuel patchiness. The density, which is related to the fuel size and the number of particles, determines the fuel compactness and therefore influences the fire propagation at the local scale. On a larger scale, the patchiness of vegetation types defines the vegetation mosaic, which influences fire propagation through the landscape. This pre-existing patchiness is created by previous fires. This fact suggests the existence of complex interactions and feedbacks between fire and vegetation.

2.5 HUMAN ACTIVITIES

In most dryland regions, anthropogenic activities based on fire use are superimposed over the natural fire environment to create the actual fire environment. Humans are a source of fire ignition caused by their agricultural and hunting activities, or due to accidents. Humans also affect the fire environment through their agricultural and management practices, by changing the fuel availability in terms of quantity, quality, spatial arrangement, and landscape composition. These anthropogenic effects will be further discussed in section 5 through examples from southern African, southern American, and Mediterranean systems.

3. The fire regime and its components

The term fire regime is becoming widely used in the fire ecology literature but it appears to be gaining two denotations: the description of a particular fire or the characterization of fires typically occurring in a given regional ecosystem (Whelan 1995). According to several authors, the second specification should be preferred. The fire regime includes several features related to space and time. Spatial components include the type of fire and its extent, while temporal components relate to the fire frequency, the fire cycle, and the season of burning. Finally the fire behaviour combines both time and space as it includes the fire spread and its intensity. Fire severity is sometimes included in the fire regime definition as the impacts of these above-mentioned variables on the ecosystem in terms of regeneration and resilience. However, in this present chapter, fire severity will not be included in the fire regime definition.

3.1 FIRE TYPE

Fire type describes globally the layer in the vertical structure of the vegetation where the fire spreads. In most dryland regions, the main fuel types are grass, litter, and small shrub layers, with light fuel loads, which generally induce surface fires, running above ground. In regions characterized by Mediterranean vegetation, the vertical fuel structure is more complex as the dominating vegetation layer is composed of shrubs and small trees. In such case, fires can more easily encounter extreme conditions in terms of heavy fuel loads associated with strong winds and low relative humidity. These conditions allow the flame to reach the canopy layer and fire will spread as a crown fire in the tree canopy (Valette 1990, Trabaud 1991). Ground fires, spreading very slowly in deep organic layers of soil, usually without flaming combustion, and over long periods are unusual in dryland regions and restricted to areas such as the Okavango delta and similar landscapes where long-term water presence prevents trees but may favour peatland build up. Fires may be also classified into head fires that burn downwind and/or upslope, and backfires, which burn upwind and/or down slope.

3.2 FIRE EXTENT AND SHAPE

Fire extent is the surface (usually expressed in hectares) burned by a fire. It mainly depends on the stand fuel quality and quantity as well as on the connectivity between stands, and the total heterogeneity of the landscape. To analyse the fire extent patterns in order to reconstruct fire history (linking fire cycle and area), it is necessary to select a landscape size that is larger than the largest fire extent that has ever occurred. Fire extent also depends on the weather conditions taking place over the area when the fire is spreading. Among the weather variables, wind is the most important one in terms of extent and shape. Slope and wind have a synergic effect on burned area when wind blows upwards. Under no-wind conditions in a homogeneous area, the burned scar starting from a point source ignition has a circular perimeter, whereas under windy conditions the fire perimeter has an elliptical shape with the ratio width over length being negatively proportional to the wind speed (Figure 2). Fire breaks (roads, humid areas, lakes and rivers) will influence fire extent and fire shape. Fire extent is the most commonly used and reported variable to describe fire regime for economical and political purposes. However, to better understand the consequences and impacts of fires in a given region, all variables describing fire regime should be taken into account. For instance, large areas burned in grassland savannas will have less ecological and economical consequences than the same areas burned in woody Mediterranean vegetation.

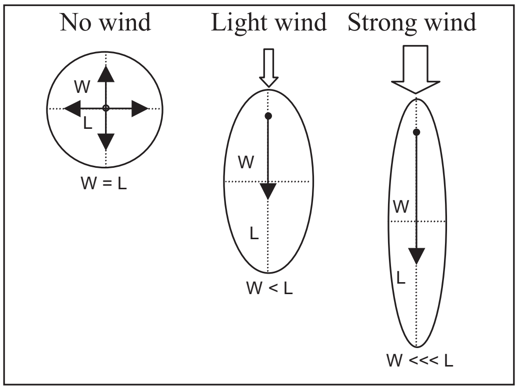

Figure 2. Fire shapes ignited from a point source (·) under different wind conditions in homogeneous fuel bed. Arrows show main direction of the fire front. W is for width, L for length, and r for the ratio W/L, this ratio ranging from 1 under no wind condition to almost 0 under violent winds (from Alexander 1982, Source: Canadian Forest Service, used with permission).

3.3 FIRE FREQUENCY and FIRE CYCLE

The fire frequency for a given area represents the number of fires during a given time unit. Fire cycle is the inverse of fire frequency. Fire cycle is also called fire return or period. For a heterogeneous landscape, the landscape frequency is the sum of the frequencies of each subunit weighted by their area. As an example, Mozambique is one of the southern African countries with high fire incidence. Barbosa *et al.* (1999) estimates that between 18 % and 38 % of the total area of the country is burned annually. Therefore a mean fire cycle in Mozambique may range between 2.5 and 5 years.

Fire frequency depends mainly on two factors: the time required to build up a load of available fuel since the last fire, and the number of potential ignitions. In natural conditions, these ignitions depend on the variability caused by weather during the fire season each year (Whelan 1995). As fire frequency depends on fuel production, it is influenced in African regions by total rainfall (Figure 3) and its inter annual variability (Hély et al. 2003b). Anthropogenic activities may also affect fire frequency through controlled or accidental ignitions, as well as land cover and land use managements. Nevertheless, from the vegetation type classification, average fire frequency can be estimated and positively related to the amount of tree cover and negatively to the total amount of precipitation in African ecosystems. For instance, infertile moist Miombo grasslands, named *Dambo* in Zambia, may burn every year due to heavy rainfall and important grass fuel load. Semi arid grassland and open savannas in Namibia may burn every five years due to high inter annual variability in precipitation, with several consecutive years during which precipitation amounts may not be high enough to produce the minimum fuel load needed to sustain fire spread. As tree cover increases, fuel load is heavier and composition more diverse (tree leaves, twigs, and shrubs) but at the same time the relative humidity also increases, leading to decreasing likelihood of fire ignition and spread. A shift in fire frequency may in turn drastically affect vegetation composition and ecosystem functioning.

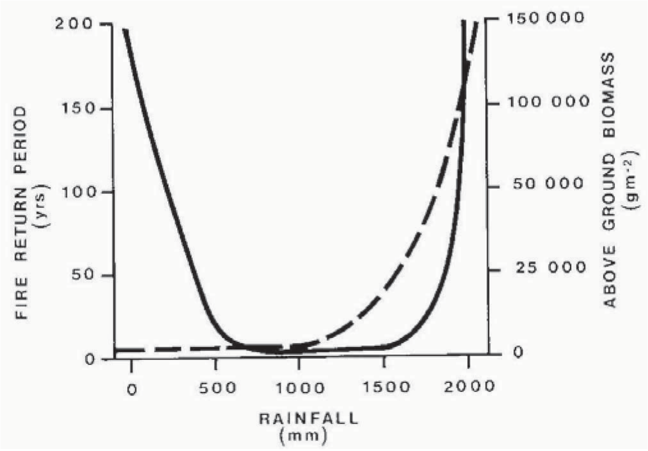

Figure 3. The relationship between rainfall, fuel accumulation (----), and fire frequency (—) in southern African region (van Wilgen and Scholes 1997).

3.4 FIRE SEASON

The fire season describes the season when most fires occur. Fire season is usually related to climate characteristics such as dry seasons in arid regions and to drought periods in more humid regions. However, this natural fire season pattern can be modified by anthropogenic activities. In dryland landscapes, according to the definition mentioned in the beginning of this chapter, fire season corresponds with the dry seasons in terms of number of dry periods where monthly precipitation is less than 50 mm. The length of the fire season is shorter than the length of the dry season because in the early dry season the fuel is still too wet to ignite and to sustain a flame. For instance, natural African fire season is shifted towards the end of the dry season, when lightning, associated with convective storms, reaches extensive areas of vegetation that are dry enough to ignite (Booysen and Tainton 1984, Stott 2000). However, the effective fire season starts few weeks only after the beginning of the dry season due to human ignitions, and it spans all over the dry season due to land management (Stott 2000).

3.5 FIRE BEHAVIOR

The fire behaviour describes the fire propagation mainly in terms of intensity (amount of energy release in kW/m (kJ/s/m)) and rate of spread (rate of energy release that is estimated by the rate of forward movement of the fire front in m/s) (Trollope 1984a). The fire behaviour depends mainly upon weather conditions (wind, air humidity, dew depositing, and air temperature), and fuel load availability and characteristics. Both intensity and rate of spread are usually reported for the fire front line, but both variables can be reported for the flanks and the back of the fire. Backfire intensity is released at the fire perimeter located behind the ignition source point from which fire spreads against the wind and/or downwards the hill. Fire behaviour is one of the fire regime variables, in association with fire season and fire frequency, which is used for land use management through prescribed fires. Such controlled fires are usually applied to reduce fire risk and enhance regeneration.

4. Tools for fire regime analysis

To take into account the aforementioned components of the fire regime characteristic of a given ecosystem type, it is necessary to analyse each of them at the stand and landscape scales.

4.1 GROUND SURVEY AT THE STAND LEVEL

This spatial scale is relevant to analyse the fire type, fire frequency, and fire behaviour. Charcoals trapped in humus, or deposited at the bottom of small surrounding lakes are indicators of past fire events, and provide valuable information for calculation of fire frequency (Carcaillet et al. 1997, Quilès et al. 2002, Thevenon et al. 2003, Wick et al. 2003). When woody vegetation is present (especially trees) fire type can be inferred by looking at the scorch height on the trunks, and at the humus consumption if the last fire was quite recent. Fire scars on trunks reveal also some information about fire frequency and fire behaviour. Indeed, scars generally occur, under windy conditions, on the leeward side of the trunk due to vortex creation that increases the residence time of the flame near the front and enhances hot temperature on that particular side (Gutsell and Johnson 1996). Fire scars reflect therefore the occurrence of fire intensities that are high enough to injure trees, but not enough to kill them. The main wind direction occurring during a fire can be determined when several trees in the burned stand present fire scars in the same direction. One may date the fire that created fire scars by using dendrochronological approaches based on tree ring counting on a transversal trunk section and calibrated series. A main fire event is likely to have occurred when fire scars on different trees within the stand present the same estimated date. Fire frequency is reconstructed through the presence of successive fire scars on a given tree, or on different trees. Variables representative of fire behaviour such as fire intensity, rate of spread and fuel consumption are generally better analysed during experimental prescribed fires. Indeed, pre-fire measurements need to be done in order to estimate fuel load and fuel moisture content before the fire occurs. The instantaneous rate of spread can be then calculated by recording the time the flame spends to reach from one point to another, and repeated instantaneous measurements are averaged over the total length of the fire. Flame length can be related to scorch height on trunks and is measured on different locations to estimate the fire intensity (Alexander 1982).

In National Parks or private properties, managers use prescribed fires during particular periods and for specific targeted objectives (understorey cleaning in forested stands to avoid “ladder fuel” accumulation, early dry season burning to enhance grass regeneration and greenness). They can also use fire behaviour models to estimate potential fire behaviour through the course of the dry season to be aware of risks if fire ignition would occur.

4.2 REMOTE SURVEY AT THE LANDSCAPE LEVEL

Fire cycle, burned areas, and fire shapes need to be analysed at the landscape level in order to provide realistic estimates of the fire regime. Remote sensing approaches (drawing, aerial photography, and more recently satellite images) are relevant techniques to capture spatial and temporal information of vegetation fires. Remote sensing contributes to fire regime studies with: (1) the location of active fires, (2) the assessment of post fire burned area, and (3) of the fire behaviour.

Active fire detection using remote sensing techniques relies on measuring the thermal emission from the combustion process itself (Stroppiana *et al.* 2000). Methods have been developed according to the Plank radiation law (Figure 4): a high temperature body emits radiation more strongly in the shorter wavelength range (shortwave and middle infra-red) than it does at longer infrared wavelength (Stephens and Matson, 1989). The Earth surface at 300°K reaches a maximum emittance at 9.5-µm (thermal infrared), while a burning grass at about 800ºK reaches its maximum emittance at 3.5-µm (Kennedy et al, 1994). Most of detection algorithms have been based on this difference between a shortwave channel very sensitive to hot spots and a longer wave channel relatively insensitive (Figure 4). Main sensors used for active fire detection include the Advanced Along Track Scanning Radiometer (AVHRR) (Giglio *et al.* 1999, Stroppiana *et al.* 2000), the European Space Agency (ESA) Along Track Scanning Radiometer (ATSR, Arino and Rosaz 1999), and the Moderate resolution Imaging Spectroradiometer (MODIS, Justice *et al.* 2002). More recent techniques such as contextual algorithms have been developed to improve the accuracy of fire detection from remote sensing imagery in a global context using a relative threshold based on the statistics of neighbouring pixels (Giglio *et al*, 1999). Such methods are efficient to detect fire occurrence on large areas and they contribute to estimate fire frequency and fire season (Dwyer et al. 2000). However, the timing and spatial extent of burning may not be estimated reliably from active fire detection, as the satellite may not overpass when burning occurs, and clouds may preclude active fire detection (Justice et al. 2002). Moreover, a very small hot spot may saturate the entire pixel, inducing an overestimation of the real burned area. Others methods have been developed for burned area estimation.

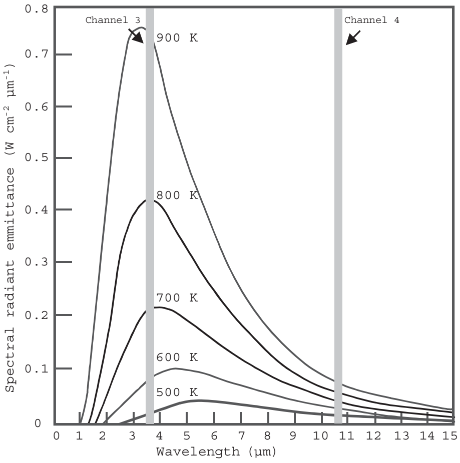

Figure 4. Emittance of a black body at different temperatures according to the Planck radiation Law. A temperature increase produces a greater increase in emitted radiation in shortest infrared wavelengths than it does at longer infrared wavelengths (AVHRR channels3 and 4,respectively). Figure modified from Weaver et al. 1995.

Burned areas are characterized by deposits of charcoals and ashes, by the removal of vegetation, and by the alteration of the vegetation structure (Peirera 1999, Roy et al. 1999). These alterations modify the surface reflectance of such areas (Figure 5), which can be detected from remote sensing (Barbosa et al. 1999, Dwyer et al. 2000, Roy et al. 2002). Several indexes have been used to discriminate between burned and unburned surfaces such as the Normalized Difference Vegetation Index (NDVI) (Salvador et al. 2000), the burn scar index (Roy et al. 1999), the burned area index (Chuvieco et al. 2002), and the normalized burn index (Alleaume et al. in Press)). Recent methods (Roy et al. (2002)) are based on a multi-temporal, multi-threshold approach model of surface reflectance against recent observations of the surface. As soon as fires spread in open dryland areas characterized by a dominant grass layer, the burned area may quickly disappear under windy conditions removing completely ashes, or when the regeneration process starts soon after the fire has occurred. In closed canopy forests, the detection of burned areas is even more difficult when fires are surface fires, because canopies are not affected by fire. When fires affect both grass and trees, due to the scorched foliage, burned areas usually are longer visible than in open grasslands and savannas.

Remote sensing or airborne data are therefore useful to map fire extents and to reconstruct fire map history over dry seasons, and over successive years. They may also provide information on fire spread for fires burning during several consecutive days if the return time is short enough and the residence time over each pixel is long enough. They also improve ground surveys, from which information on each burned area is usually integrated into a Geographic Information System to assist land managers.

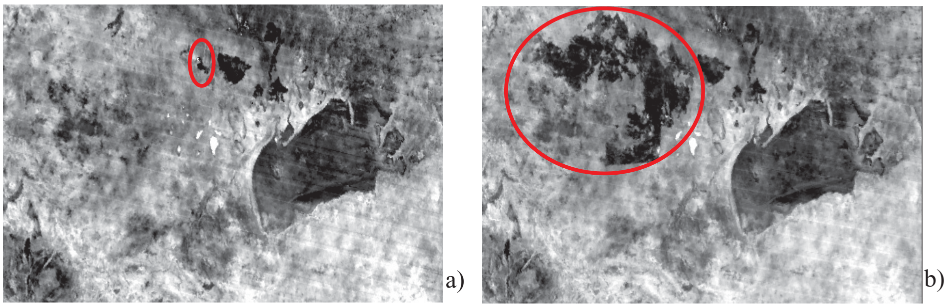

Figure 5. Burned area spreading over Etosha National Park (3000 km^2) in late August 2000. The bean area on the right represents the salt pan of Etosha while the fire is on the northern left region. a) August 24th, b) September 5th 2000.

5. Examples of fire regimes in dryland regions

5.1 SOUTHERN AFRICAN SAVANNAS

It is impossible to determine the beginning of the interactions between man and fire in South African forests and savannas (Granger 1984), however we notice that anthropogenic fires may have been a feature of these ecosystems for the last 150 000 to 180 000 years (Early Stone Age). For a long period, the seasonality of anthropogenic fires was modulated by the life style of both nomadic and sedentary populations. During the Stone Age, nomadic people used fire as a tool to manipulate the environment by opening and maintaining grasslands in a state attractive to the large herds of animals that were hunted, and to possibly induce flushes of edible herbs. As these populations followed the natural phenological cycle of vegetation, there was a lag in fire seasonality between neighbouring regions associated with this migration (Granger 1984). However, because of their low density, these Stone Age populations had probably only a minimal impact, and fire regime was mostly natural (lightning and rock falls ignition sources). Conversely, sedentary populations had a more important impact on vegetation and fire regime. Farmers appeared and settled in this region during the Iron Age. These populations turned to pastoralism and made additional use of fire to clear patches of fertile forest soil for timber exploitation (hut and stockade constructions), food cooking, and to plant crops (Granger 1984, van Wilgen and Scholes 1997, Trollope and Everson 1999). Thus, over approximately the past 4 000 years, man has strongly exploited and disturbed (i.e. burned) these ecosystems, leading to the removal of forest vegetation and to the increase in savanna vegetation (Granger 1984, Vincens et al. 2003). During this period, the anthropogenic contribution to the fire regime has become increasingly more important. Over the last two centuries, fire use regulation in southern African countries has slowly evolved through several stages, including allowance, interdiction, and the use of fire as a management tool in the last few decades. In subsistence agriculture, people use fire throughout the dry season to prepare new fields to cultivate crops such as manioc (*Manihot escultenta* Crantz), which is the basic food for several millions of people. Thus, before cultivating manioc, the people in Zambia practice *Chitemene*, which consists in cutting down and burning all the trees and branches in the middle of a Miombo forested stand and using ashes as a fertilizing bed for crops in the subsequent years before moving to another stand (Holden 1993). They also use fire to favour grass regeneration for livestock feeding. In Namibia or Botswana, where farmers with high number of livestock in semi-arid region practice extensive grazing within very large properties, fire is considered as a competitor of grazing during the dry season (Figure 6). Thus, farmers have attempted to apply fire exclusion in their properties for several consecutive years. However, by increasing the resulting fire frequency, farmers have induced a change in vegetation composition and structure. Less palatable grass species have become dominant over palatable species, and shrub cover has expanded. This phenomenon is known as the "bush encroachment" (Shackleton and Scholes 2000, Hudak and Wessman 2001, Roques et al. 2001, Skowno and Bond 2003). The change in vegetation structure reduced the walking trail allowed to grazing livestock searching for food, and increased woody biomass and total fuel. Therefore, due to the fire exclusion policy, those farms became for a few years extremely susceptible to burning in case of ignition. National Parks such as Etosha national park in Namibia or Kruger national park in South Africa conducted studies on this type of fire management and concluded that fire was necessary for ecosystem dynamics and conservation (Siegfried 1981, Scholes and Walker 1993). Frost (1984) showed that fire regimes can be schematically represented as particular combinations of fire frequency, intensity and seasonality (Figure 7). However, all combinations are not equally likely to occur in nature. Therefore, nowadays, except for National Parks and reserves where the managed fire regime tends to emulate natural fire regime, the majority of African savannas and forests present anthropogenically dominated fire regimes. The major components of the fire regime for each type of the vegetation in the southern hemisphere of the African continent (i.e. from deciduous forest to savannas and grasslands) have been summarized by van Wilgen and Scholes (1997) and are reported and completed in Table 1.

Figure 6. Fire spreading in a semi-arid Namibian savanna with open canopy layer and "sweet grasses".

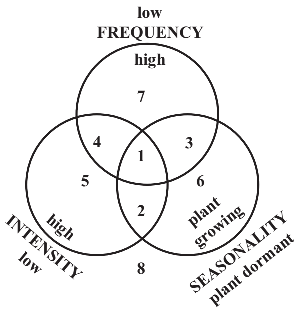

Figure 7. Diagram illustrating possible combinations of fire frequency, intensity and seasonality giving rise to different fire regimes (from Frost, (1984)). Regimes numbered in approximate order of severity to the organisms. Not all combinations are equally likely to occur in nature. Within the South African region, combination 2 probably applies to forest, 7 (or possibly 4) to moist savannas and grasslands, and 8 to arid grass and shrublands.

Table 1. Components of the current fire regimes for African savannas and related vegetation type in. Kruger National Park (KNP) and, Etosha national Park (ENP).

Vegetation type	*Fire type and season*	*Fire frequency*	*Fire behaviour*	*Sources*
Dry/deciduous forests	Surface or crown fires. Dry winter season generally June to September.	20-100 yr intervals	Variable. Fire intensity typically low if only litter is consumed, can be very high if stem wood ignite	No fire-related literature exists (van Wilgen and Scholes 1997)
Moist infertile savannas	Surface fires in grass layers. Restricted to dry winter when grasses cured and dormant. Trees may be scorched but low flammable tree foliage. Frequent back fires.	1-6 yr intervals (mean of 2-3 yr in KNP).	Intensities <100 to 6000 kW/m. Back fires more intense. Woody species more affected by head fires as heat energy release occurs at levels near terminal buds	(Trollope 1984b, Frost et al. 1985, Trollope and Potgieter 1985, Trollope 1993, van Wilgen and Scholes 1997)
Arid fertile savannas	Surface fires in grass layers. Restricted to dry winter when grasses cured and dormant Frequent back fires.	2-11 yr intervals (mean of 4-8 yr in KNP, 3-10 yr in ENP). Lightning ignition dominates in National Parks	Intensities <100 to 4000 kW/m. Lower than in moist savannas due to lower fuel load	(Siegfried 1981, Trollope 1984b, Frost et al. 1985, 1993, van Wilgen and Scholes 1997)
Infertile grasslands	Surface fire only. Restricted to dry winter.	2-4 yr intervals. Annual fires are possible (mean of 3 yr in the natal Drakensberg, South Africa).	Intensities: 1000 -3000 kW/m	(van Wilgen et al. 1990, van Wilgen and Scholes 1997)
Fertile grasslands	Surface fire only. Restricted to dry winter.	4-10 yr intervals, with the lower frequencies in the more arid areas.	No data	No fire-related literature exists (van Wilgen and Scholes 1997)

5.2 SOUTHERN AMERICAN CERRADO

Cerrado comprises several physiognomic forms, which constitute a biological gradient: grasslands (campo limpo), open shrub savanna (campo sujo), woody savannas (cerradao), and dry deciduous forests (riparian forests) (Santos et al. 2003). Cerrado sustains surface fires all over the landscape mosaic, but the fire frequency varies according to the openness of the stands (Coutihno 1990, Pivello and Coutihno 1996). For instance, fire is naturally infrequent in closed canopy dry forests and occurs only during abnormally low rainfall years, or if ignited by human activities such as those currently related to deforestation (Uhl and Kauffman 1990, Nepstad et al. 1997, Cavelier et al. 1998, Cochrane et al. 1999). In such cases, the fire only consumes the litter and grass layers, but because of the typically thin tree bark, it still kills roughly 95% of the stems (invested by the fire) larger than 1 cm in diameter at breast height. Only large, thicker barked trees survive. By exposing the mineral soil, the ground surface temperature increases, and the soil dries out, inducing further stress in the surviving individuals. After the fire, combustible fuels of all sizes fall from standing dead trees and tree mortality continues for at least 2 years. Thus, this first fire changes the forest functioning and increases the forest susceptibility to burn in the near future (Cochrane et al. 1999). The opening of the canopy (50 to 70% cover) allows greater solar heating and air movement to dry out the forest fuels. Successive fires change forest composition from non-tolerant fire species to more tolerant ones. They also slowly open the forest canopy by killing trees and favouring grass growth (Cochrane and Schulze 1998), transforming the forest into a savanna stand even more susceptible to frequent fires with higher intensities (Cochrane and Schulze 1999). Grasslands are the most open stands and present the highest fire frequencies from 1 to 3 years (San Jose and Farinas 1983, Sanaiotti and Magnusson 1995). The “bush encroachment” phenomenon occurs also in cerrados (San Jose and Farinas 1983, Moreira 2000). Such shifts from forest to savannas and grasslands and the reverse occurred several times in the past (i.e., back to the Pleistocene and Holocene) as a result of climate change (Kellman 1975, Meave and Kellman 1994, Desjardins et al. 1996, Cavelier et al. 1998). In such shifts, riparian forest may have played an important transitional stage with a high tree species diversity and relatively small individuals as a result of frequent disturbances such as fires (Meave and Kellman 1994). Nowadays, this shift from forest towards grassland results mainly from human activities superimposed to the current climate change conditions (Uhl and Kauffman 1990, Nepstad et al. 1997, Cavelier et al. 1998). The unknown effects depend on the speed of this change as several species may be unable to adapt their resistance against fire and could disappear in the near future (Kauffman et al. 1993, Nepstad et al. 1997, Nepstad et al. 2001). To illustrate the impact of land use management on current fire regime in the Brazilian cerrado from the State of Parà, Cochrane and Schulze (1998) estimated that over the next 25 years 90 % of the currently unburned areas will be impacted by fires at least three times (Figure 8). The disappearance of unburned areas will be likely associated with the extinction of several species in these ecosystems (Cochrane and Schulze 1998). The different components of fire regimes in cerrado mosaics have been compiled from literature review and are presented in Table 2.

Table 2. Components of the current fire regimes for South American cerrado and related vegetation types.

Vegetation type	*Fire type and season*	*Fire frequency*	*Fire behaviour*	*Sources*
Amazonian Rain forest (riparian forest)	Surface to crown fires. Naturally during extreme droughts.	Past: 20-100 yr intervals. Currently 40-60 yr in Belize and Venezuela. Mainly due to deforestation with associated dryness of microclimate.	Variable. Fire intensity typically very low as only litter consumed during the first fire. Increasing intensity during successive facilitated burns.	(Uhl and Kauffman 1990, Kellman and Tackaberry 1993, Kellman and Meave 1997)
Cerradao (medium - tall woodlands with closed canopy dry/deciduous forests) *Cerrado (savanna woodlands of low trees or shrubs)*	Surface fires in grass layers. Canopies of trees scorched but do not contribute to combustion. Large fires during dry winter season (May to September, maximum in August). Lightning fires frequent during wet season creating small burned areas.	50-60 yr intervals down to 3-4 yr for severe fires in Emas National Park and Chapada dos Veadeiros National Park (Brazil).	No fire-related literature exists.	(Coutihno 1990, Kellman and Meave 1997, Ramos-Neto and Pivello 2000)
Campo sujo – open savanna with scattered trees or shrubs	Surface fires with high fire activity induced by lightning in Belize. Dry winter season.	1- 10 years with mean interval of 2-3 yr when used as pasture management.	Low intensities probably like in African fertile arid savannas (<100 to 4000 kW/m).	(Kellman 1975, Coutihno 1990)
Campo limpo - Grasslands	Surface fire only.	1-3 yr intervals. Frequent annual fires.		(Uhl and Kauffman 1990)

5.3 MEDITERRANEAN VEGETATION

The garrigue ecosystem has been present in the European Mediterranean region since the last glaciation (Carcaillet et al. 1997, Carrion et al. 1999, Willcox 1999, Brewer et al. 2002). It results from the successive fires that burned the widespread forests of Oaks (*Quercus ilex, Q. suber,* and *Q. coccifera*) and Pines (*Pinus halepensis*). Garrigue was originally featured from natural wildfires, and then mainly related to intensive human activities starting 7 000 years BP for agricultural and pastoral purposes (Trabaud et al. 1993). A new wave of intensification in the fire use started with the beginning of the historical period (750 BC until today). Today, lightning fires represent only about 2% of the area burned annually in the Mediterranean Basin (0-6%, depending on the country (Trabaud et al. 1993)). Fire ignition sources are therefore mainly accidental or voluntary activities as compared to lightning, and these human fire ignitions are responsible for the high number of small fires as compared to past periods (Lloret and Mari 2001). Essential oils and waxes are representative chemical components found on different but common species such as thymus (*Thymus vulgaris*), rosmarinus (*Rosmarinus officinalis*), and pines. Moreover, sclerophyll leaves and needles, which have been first selected for drought resistance, reinforce the fire hazard and fire propagation over wide areas during summer when very dry and hot air masses associated with strong winds dominate the region. Less than a century ago, the garrigue was used and managed on a yearly basis to feed goats and sheeps from spring to fall.

Vegetation removal by animals was reducing both the fuel load and the fire hazard associated with breaking the continuum in spatial arrangement of fuel. In the second half of 20th century, agricultural practices have shifted and such land management has disappeared. The main direct effect of such abandon has been the fuel load accumulation from the ground surface to the shrub and small tree crowns, inducing an overall average fire frequency of 15 to 20 years. However, several stages of vegetation can be distinguished based on the composition and the structure of the vegetation inducing different fire regimes (see Table 3 for details). All these vegetation types present the same fire season from late spring (June) to early fall (September) based on the Mediterranean dry period climate. Several studies have shown that all these vegetation types present the particular pattern of post-fire regeneration known as "autosuccession" where post-fire vegetation composition is generally the same as the pre-fire composition (Odion and Davis 2000). This is explained by the fact that vegetation is maintained by fire resistant species (*Quercus suber* and its very thick bark of cork), fire-induced seed germination (*Pinus halepensis* and its serotinous cones), obligate postfire shrub seedling regeneration, and resprouting from geophytes and fire resistant ligotubers (*Q. coccifera Q. suber*, and *Q. ilex*, *Pistacia lentiscus*) (Trabaud 1989). *Quercus coccifera* garrigue is subject to frequent burns preventing other tree species to settle and therefore fire in such case is recognized as a blocking succession disturbance. If fire interval increases, the succession will succeed to start again and the forest stage will succeed to the *Q. coccifera* shrubland stage. In forested stages, oaks stand succeed to pines. In pine forests, if fire intervals are shorter than the time necessary for pines to produce fertile cones then the postfire stage will go back to a Garrigue stage.

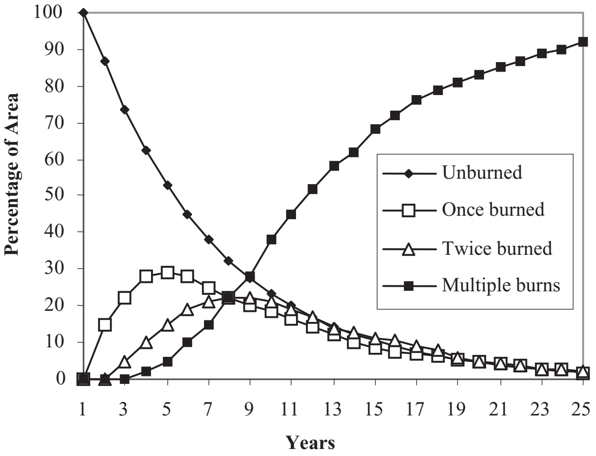

Figure 8. Projected 25-year change in forest type near Tailândia, Parà (Brazil), under the current fire regime. Unburned forests are present within the fire affected matrix. The multiple burns class lumps together all forests burned three or more times (From Cochrane and Schulze (1998)).

Table 3. Components of the current fire regimes for Mediterranean garrigue and related vegetation types.

Vegetation type	*Fire type and season*	*Fire frequency*	*Fire behaviour*	*Sources*
Garrigue	"Crown" fires in the unique shrub layer; Dry summer season from late spring (June) to early fall (September).	5-7 yr intervals down to 2-3 yr in *Q. coccifera* garrigue.	Intensity: variable (low intensity in early spring fires and very intense later), only qualitative assessment of intensity related to temperature rather than to energy release.	(Rego et al. 1993, Trabaud et al. 1993)
Maquis	"Crown" fires in the unique shrub layer; Dry summer season.	10-20 yr intervals, up to 40 yr in Californian chaparral.	Intensity: variable (low intensity in early spring fires and very intense later), only qualitative assessment of intensity.	(Trabaud et al. 1993, Odion and Davis 2000, Mouillot et al. 2002)
Coniferous forest (Pinus sp.)	Surface and crown fires depending on meteorological conditions (strong wind). Dry summer season.	30-70 yr intervals.	Intensities: up to 15 000 kW/m with strong wind and drought.	(Trabaud 1989, Trabaud et al. 1993, Lloret and Mari 2001, Mouillot et al. 2002)
Deciduous forest (Quercus sp.)	Surface and crown fires depending on meteorology (strong wind). Dry summer season	30-50 yr intervals down to 5-25 yr in *Q. suber* and *Q. ilex* forests.	Intensities: up to 15 000 kW/m with strong wind and drought.	(Trabaud et al. 1993, Trabaud and Galtié 1996)

6. Conclusion

Fire regimes of dryland systems are highly influenced by the water components. Indeed, it has been shown that dryland fuels are directly related to climate through precipitation for the fuel production and relative humidity and moisture content for fuel flammability. The driest lands, receiving sparse and scarce rainfall, present longer fire returns due to slower rates of fuel production and accumulation than moister lands. The fire event retroactively influences the hydrology. Indeed, the vegetation removal decreases the interception and the evapotranspiration, whereas it increases the surface runoff. Indirectly, fire can also influence the erosion processes. These physical changes are associated to chemistry modification. Indeed, during the fire event nutrients stocked in vegetation are released in the atmosphere and on the ground. Therefore successive frequent fires may irreversibly change the biogeochemistry of soil and water reservoirs.

Dryland systems are in general dominated by grass and shrub layers, sustaining surface fires with low intensity and variable rate of spread, and producing few amounts of ashes and charcoals as compared to denser tree canopies. Therefore, fire events in dryland systems leave short lasting scars that need to be detected quickly after the fire has occurred in order to properly estimate fire regime components. Remote sensing technology is efficient for such task but needs better spatial and temporal cover and resolution.

7. References

Agee, J. K. (1997). The severe weather wildfire - too hot to handle? Northwest Science 71:153-156.

Alexander, M. E. (1982). Calculating and interpreting forest fire intensities. Canadian Journal of Botany 60:349-357.

Alleaume, S., C. Hély, J. Le Roux, S. Korontzi, R. J. Swap, H. H. Shugart, and C. O. Justice. in Press. Using MODIS to evaluate heterogeneity of biomass burning and emissions in Southern African savannas: Etosha National Park Case Study. International Journal of Remote Sensing.

Barbosa, P. M., D. Stroppiana, J. M. Grégoire, and J. M. C. Pereira. (1999). An assessment of vegetation fire in Africa (1981-1991): Burned areas, burned biomass, and atmospheric emissions. Global Biogeochemical Cycles 13:933-950.

Bessie, W. C., and E. A. Johnson. (1995). The relative importance of fuels and weather on fire behavior in subalpine forest. Ecology 76:747-762.

Booysen, P. d. V., and N. M. Tainton, editors. (1984). Ecological effects of fire in South African ecosystems. Springer-Verlag, Berlin.

Brewer, S., R. Cheddadi, J. L. de Beaulieu, M. Reille, and D. contributors (2002). The spread of deciduous Quercus throughout Europe since the lasi glacial period. Forest Ecology and management 156:27-48.

Brown, A. A., and K. P. Davis (1973). Forest fire: control and use. McGraw-Hill book company, New York.

Brown, J. K., R. D. Oberheu, and C. M. Johnston (1982). Handbook for inventoring surface fuels and biomass in the interior West. General Technical Report INT-129, US Forest Service.

Burgan, R. E., and R. C. Rothermel (1984). BEHAVE: fire behavior prediction and fuel modeling system--FUEL subsystem. General technical report INT-167, U. S. Department of agriculture, Forest service, Ogden, UT. Intermountain forest and range experiment station.

Carcaillet, C., H. N. Barakat, C. Panaiotis, and R. Loisel (1997). Fire and late-Holocene expansion of Quercus ilex and Pinus pinaster on Corsica. Journal of Vegetation Science 8:85-94.

Carrion, J. S., M. Munuera, C. Navarro, F. Burjachs, M. Dupré, and M. J. Walker (1999). The palaeooceological potential of pollen records in caves: the case of Mediterranean Spain. Quaternary Science Reviews 18:1061-1073.

Cavelier, J., T. M. Aide, C. Santos, A. M. Eusse, and J. M. Dupuy (1998). The savannization of moist forests in the Sierra Nevada de Santa Marta, Colombia. Journal of Biogeography 25:901-912.

Chuvieco, E., M. P. Martin, and A. Palacios (2002). Assessment of different spectral indices in the red-near-infrared-spectral domain for burned land discrimination. International Journal of Remote Sensing 23:5103-5110.

Cochrane, M., and M. D. Schulze (1999). Fire as a recurrent event in tropical forests of the eastern Amazon: Effects on forest structure, biomass, and species composition. Biotropica 31:2-16.

Cochrane, M. A., A. Alencar, M. D. Schulze, C. M. J. Sousa, D. C. Nepstad, P. Lefebvre, and E. A. Davidson (1999). Positive feedbacks in the fire dynamic of closed canopy tropical forests. Science 284:1832-1835.

Cochrane, M. A., and M. D. Schulze (1998). Forest fires in the Brazilian Amazon. Conservation Biology 12:948-950.

Coutihno, L. M. 1990. Fire in the ecology of the Brazilian cerrado. Pages 82-105 in J. G. Goldammer, editor. Fire in the tropical biota: ecosystem processes and global challenges. Springer-Verlag, Berlin.

De las Heras, J., J. J. Martinez-Sanchez, A. I. Gonzales-Ochoa, P. Ferrandis, and J. M. Herranz. (2002). Establishment of Pinus halepensis Mill. saplings following fire: effects of competition with shrub species. Acta Oecologica 23:91-97.

Desjardins, T., A. Carneiro Filho, A. Mariotti, A. Chauvel, and C. Girardin (1996). Changes of the forest-savanna boundary in Brazilian Amazonia during the Holocene revealed by stable isotope ratios of soil organic carbon. Oecologia 108:749-756.

Dwyer, E., S. Pinnock, J. M. Gregoire, and J. M. C. Pereira (2000). Global spatial and temporal distribution of vegetation fire as determined from satellite observations. International Journal of Remote Sensing 21:1289-1302.

Figueiral, I., and J. F. Terral (2002). Late Quaternary refugia of mediterranean taxa in the Portuguese Estremadura: charcoal based paleovegetation and climatic reconstruction. Quaternary Science Reviews 21:549-558.

Frost, P. G. H. (1984). The responses and survival of organisms in fire-prone environments. Pages 274-309 in P. d. V. Booysen and N. M. Tainton, editors. Ecological effects of fire in South African ecosystems. Springer-Verlag, Berlin.

Frost, P. G. H., J. C. Menaut, B. Walker, E. Medina, O. T. Solbrig, and M. Swift. (1985). Responses of savannas to stress and disturbance. Meeting report 10, The International Union of biological Sciences, Harare.

Granger, J. E. (1984). Fire in forest. Pages 179-197 in P. d. V. Booysen and N. M. Tainton, editors. Ecological effects of fire in South African ecosystems. Springer-Verlag, Berlin.

Gutsell, S. L., and E. A. Johnson. (1996). How fire scars are formed: coupling a disturbance process to its ecological effect. Canadian Journal of Forest Research 26:166-174.

Hély, C., S. Alleaume, R. J. Swap, H. H. Shugart, and C. O. Justice (2003a). SAFARI-2000 characterization of fuels, fire behavior, combustion completeness, and emissions from experimental burns in infertile grass savannas in western Zambia. Journal of Arid Environments 54:381-394.

Hély, C., P. R. Dowty, S. Alleaume, K. Caylor, S. Korontzi, R. J. Swap, H. H. Shugart, and C. O. Justice. (2003b). Regional fuel load for two climatically contrasting years in southern Africa. Journal of Geophysical Research 108:8475.

Hély, C., M. D. Flannigan, Y. Bergeron, and D. McRae. (2001). Role of vegetation and weather on fire behavior in the Canadian mixedwood boreal forest using two fire behavior prediction systems. Canadian Journal of Foreast Research 31:430-441.

Holden, S. T. (1993). Peasant household modelling: Farming systems evolution and sustainability in northern Zambia. Agricultural economics 9:241-267.

Hudak, A. T., and C. A. Wessman. (2001). Textural analysis of high resolution imagery to quantify bush encroachment in Madikwe game reserve, South Africa, 1955-1996. International Journal of Remote Sensing 22:2731-2740.

Johnson, E. A. (1992). Fire and vegetation dynamics: studies from the North American boreal forest. Cambridge University Press, Cambridge.

Kauffman, B. J., R. L. Sanford, D. L. Cummings, I. H. Salcedo, and E. V. S. B. Sampaio. (1993). Biomass and nutrient dynamics associated with slash fore in neotropical dry forests. Ecology 74:140-151.

Kauffman, J. B., D. L. Cummings, and D. E. Ward. (1994). Relationships of fire, biomass and nutrient dynamics along a vegetation gradient in the Brazilian Cerrado. Journal of Ecology 82:519-531.

Kellman, M. (1975). Evidence for Late Glacial Age fire in a tropical montane savanna. Journal of Biogeography 2:57-63.

Kellman, M., and J. Meave. (1997). Fire in the tropical galerry forests of Belize. Journal of Biogeography 24:23-34.

Kellman, M., and R. Tackaberry. (1993). Disturbance and tree species coexistence in tropical riparian forest fragments. Global Ecology and Biogeography letters 3:1-9.

Lloret, F., and G. Mari. (2001). A comparison of the medieval and the current fire regimes in managed pine forests of Catalonia (NE Spain). Forest Ecology and management 141:155-163.

Meave, J., and M. Kellman. (1994). Maintenance of rain forest diversity in riparian forests of tropical savannas : implications for species conservation during Pleistocene drought. Journal of Biogeography 21:121-135.

Mistry, J. (1998). Corticolous lichens as potential bioindicators of fire history: a study in the cerrado of the Districto federal, central Brazil. Journal of Biogeography 25:409-441.

Moreira, A. G. (2000). Effects of fire protection on savanna structure in Central Brazil. Journal of Biogeography 27:1021-1029.

Mouillot, F., S. Rambal, and R. Joffre. (2002). Simulating climate change impacts on fire frequency and vegetation dynamics in a mediterranean-type ecosystem. Global Change Biology 8:423-437.

Nepstad, D., G. Carvalho, A. C. Barros, A. Alencar, J. P. Capobianco, J. Bishop, P. Moutinho, P. Lefebvre, U. L. J. Silva, and E. Prins. (2001). Road paving, fire regime feedbacks, and the future of Amoazon forests. Forest Ecology and management 154:395-407.

Nepstad, D., C. A. Klink, C. Uhl, I. C. Vieira, P. Lefebvre, M. Pedlowski, E. Matricardi, G. Negreiros, I. F. Brown, E. Amaral, A. Homma, and R. Walker. (1997). Land-use in Amazonia and the Cerrado of Brazil. Ciencia e Cultura 49:73-86.

Odion, D., and F. W. Davis. (2000). Fire, soil heating, and the formation of vegetation patterns in chaparral. Ecological Monographs 70:149-169.

Pivello, V. R., and L. M. Coutihno. (1996). A qualitative successional model to assist in the management of Brazilian cerrados. Forest Ecology and management 87:127-138.

Quilès, D., V. Rohr, K. Joly, S. Lhuillier, P. Ogereau, A. Martin, F. Bazile, and J. L. Vernet. (2002). Les feux préhistoriques holocènes en montagne sub-méditerranéenne : premiers résultats sur le Causse Méjean (Lozère, France). Comptes Rendus Palevol 1:59-65.

Ramos-Neto, M. B., and V. R. Pivello. (2000). Lightning fires in a Brazilian savanna National Park : Rethinking management strategies. Environmental management 26:675-684.

Rego, F., J. Pereiras, and L. Trabaud. (1993). Modelling community dynamics of a Quercus coccifera L. garrigue in relation to fire using Markov chains. Ecological Modelling 66:251-260.

Roques, K. G., T. G. O'Connor, and A. R. Watkinson. (2001). Dynamics of shrub encroachment in an African savanna: relative influences of fire, herbivory, rainfall and density dependence. Journal of Applied Ecology 38:268-280.

Roy, D. P., L. Giglio, J. D. Kendall, and C. O. Justice. (1999). Multi-temporal active-fire based burn scar detection algorithm. International Journal of Remote Sensing 20:1031-1038.

Roy, D. P., P. E. Lewis, and C. O. Justice. (2002). Burned area mapping using multi-temporal moderate spatial resolution data - a bi-directional reflectance model-based expectation approach. Remote Sensing of Environment 83:263-286.

San Jose, J. J., and M. R. Farinas. (1983). Changes in tree density and species composition in a protected Trachypogon savanna, Venezuela. Ecology 64:447-453.

Sanaiotti, T. M., and W. E. Magnusson. (1995). Effects of annual fires and the production od fleshy fruits eaten by birds in a Brazilian Amazonian savanna. Journal of Tropical Ecology 11:53-65.

Santos, A. J. B., G. T. D. A. Silva, H. S. Miranda, A. C. Miranda, and J. Lloyd. (2003). Effects of fire on surface carbon, energy and water vapor fluxes over campo sujo savanna in central Brazil. Functional Ecology 17:711-719.

Scholes, R. J. (1997). Savanna. Pages 258-277 in R. M. Cowling, D. M. Richardson, and S. M. Pierce, editors. Vegetation of southern Africa. Cambridge University Press, Cambridge.

Scholes, R. J., and B. H. Walker, editors. (1993). An African Savanna: Synthesis of the Nylsvley Study. Cambridge Univ. Press, New York.

Shackleton, C. M., and R. J. Scholes. (2000). Impact of fire frequency on woody community structure and soil nutrients in the Kruger National Park. Koedoe 43:75-81.

Shroeder, M. J., and C. C. Buck. (1970). Fire weather: a guide for application of meteorological information to forest fire control operations. Agriculture Handbook 360, USDA, Forest Service, Boise, Idaho.

Siegfried, W. R. (1981). The incidence of veld-fire in the Etosha national Park, 1970-1979. Madoqua 12:225-230.

Skowno, A. L., and W. J. Bond. (2003). Bird community composition in an actively managed savanna reserve, importance of vegetation structure and vegetation composition. Biodiversity and Conservation 12:2279-2294.

Stott, P. (2000). Combustion in tropical biomass fires: a critical review. Progress in Physical Geography 24:355-377.

Thevenon, F., D. Williamson, A. Vincens, O. Merdaci, G. Buchet, and M. Taieb. (2003). A late-Holocene charcoal record from Lake Masoko, SW Tanzania: climatic and anthropologic implications. Holocene 13:785-792.

Trabaud, L. (1991). Comment se propagent les incendies de végétation. La Recherche 234:908-912.

Trabaud, L. V. (1989). Les effets du regime des feux : Exemples pris dans le bassin méditerranéen. CIHEAM - Options Méditerranéennes 3:89-94.

Trabaud, L. V., N. L. Christensen, and A. M. Gill. (1993). Historical biogeography of fire in temperate and mediterranean ecosystems. Pages 277-295 in P. J. Crutzen and J. G. Goldammer, editors. Fire in the environment: the ecological, atmospheric, and climatic importance of vegetation fires. John Wiley & Sons, Chichester.

Trabaud, L. V., and J.-F. Galtié. (1996). Effects of fire frequency on plant communities and landscape pattren in the massif des Aspres (southern France). Landscape Ecology 11:215-224.

Trollope, W. S. W. (1984a). Fire behavior. Pages 200-217 in V. Booysen, Tainton, N., M., editor. Ecological effects of fire in South African Ecosystems. Ecological Studies, Berlin.

Trollope, W. S. W. (1984b). Fire in Savanna. Pages 151-175 in P. d. V. Booysen and N. M. Tainton, editors. Ecological effects of fire in South African Ecosystems. Springer-verlag, Berlin.

Trollope, W. S. W. (1993). Fire regime of the Kruger national Park for the period 1980-1992. Koedoe 36:45-52.

Trollope, W. S. W., and C. S. Everson. (1999). Veld burning. Pages 217-243 in N. M. Tainton, editor. Veld management in South Africa. University of Natal Press, Pietermaritzburg.

Trollope, W. S. W., and A. L. F. Potgieter. (1985). Fire behavior in the Kruger National Park. J grassland Society Southern Africa 3:148-152.

Uhl, C., and J. B. Kauffman. (1990). Deforestation, fire susceptibility, and potential tree responses to fire in the Eastern Amazon. Ecology 71:437-449.

Valette, J. C. (1990). Inflammabilités des espèces forestières méditerranéennes- Conséquences sur la combustibilité des formations forestières. Revue forestière française XLII:76-92.

van Wilgen, B. W., C. S. Everson, and W. S. W. Trollope. (1990). Fire management in Southern Africa: some examples of current objectives, practices, and problems. Pages 179-215 in J. G. Goldammer, editor. Fire in the tropical biota: ecosystem processes and global challenges. Springer-verlag, Berlin.

van Wilgen, B. W., and R. J. Scholes. (1997). The vegetation and fire regimes of southern hemisphere Africa. Pages 27-46 in B. W. Van Wilgen, M. O. Andreae, J. G. Goldammer, and J. A. Lindesay, editors. Fire in the southern African savannas: Ecological and atmospheric perspectives. Witwatersrand University press, Johannesburg.

Vernet, J.-L. (1997). L'Homme et la forêt méditerranéenne: de la Préhistoire à nos jours. éditions errance, Paris.

Vincens, A., D. Williamson, F. Thevenon, M. Taieb, G. Buchet, M. Decobert, and N. Thouveny. (2003). Pollen-based vegetation changes in southern Tanzania during the last 4200 years: climate change and/or human impact. Palaeogeography, Palaeoclimatology, Palaeoecology 198:321-334.

Weaver, J. F., J. F. W. Purdom, and T. L. Schneider. (1995). Observing forest fires with the GOES-8, 3.9 um imaging channel. Weather and Forecasting 10:803-808.

Whelan, R. J. (1995). The ecology of fire. Cambrige University Press, Cambridge.

Wick, L., G. Lemcke, and M. Sturm. (2003). Evidence of Lateglacial and Holocene climatic change and human impact in eastern Anatolia: high-resolution pollen, charcoal, isotopic and geochemical records from the laminated sediments of Lake Van, Turkey. Holocene 13:665-675.

Willcox, G. (1999). Charcoal analysis and Holocene vegetaton history in southern Syria. Quaternary Science Reviews 18:711-716.

Chapter 17

TERMITES AS MEDIATORS OF THE WATER ECONOMY OF ARID SAVANNA ECOSYSTEMS

J. Scott TURNER

Department of Environmental & Forest Biology, SUNY College of Environmental Science & Forestry, Syracuse, NY 13159, USA – email jsturner@mailbox.syr.edu

1. Introduction

Large termite mounds, constructed by colonies of various species of macrotermitine termites (Isoptera, Termitidae, Macrotermitinae), are dominant features of the arid and semi-arid savannas of southern Africa. These mounds can populate a savanna in very high densities, generally one to four colonies per hectare, containing biomass of termites and symbiotic fungi that exceeds the typical biomass of vertebrate and non-termite arthropod herbivores in these systems. Termites' construction of nest and mound turns over savanna soils at substantial rates, and, like other central-place foragers, they convey significant quantities of inorganic and organic matter into their nests, concentrating it there. In short, macrotermitine termites are "ecosystem engineers", structuring and controlling to a large extent the flows of energy and matter through tropical savannas (Dangerfield et al. 1998).

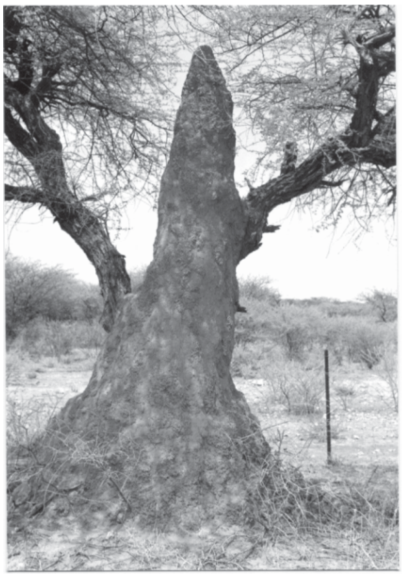

Figure 1. A representative mound of Macrotermes michaelseni *in northern Namibia, built up around an* Acacia mellifera *tree.*

This chapter concerns one aspect of these termites' engineering activities: their possible roles as mediators of the water economy in arid savannas. It is inspired by an observation made in the course of ongoing research on respiratory gas exchange in nests of *Macrotermes michaelseni* (formerly *M mossambicus*), in northern Namibia (Turner 2000; 2001). These termites' habitat is

P. D'Odorico and A. Porporato (eds.), Dryland Ecohydrology, 303–313.

designated as mixed mopane/acacia savanna, which is characterized by a mixture of grasses, geophytes and patchy assemblages of broad-leaf (commonly *Colophospermum mopane*) and narrow-leafed (commonly *Acacia* spp) trees (Ruelle et al. 1975). As in most tropical savannas, rainfalls in northern Namibia are strongly seasonal, with intense summer rains interspersed with strenuous winter drought. During winter, most trees there either drop their leaves or allow them to die on the branch. A few trees, however, retain green vegetation throughout the year. Invariably, these trees are associated with termite mounds (Figure 1), suggesting that termite colonies provide a local source of water that sustains the trees well into the dry season. How termites provide this water has broad implications for ecosystem function in dry tropical savannas.

2. Water balance in arid savannas

The water relations of arid savannas have been extensively documented elsewhere and in other chapters in this volume (Chapters 2-4), so only a few salient points will be made here.

Tropical savannas experience strongly seasonal rainfalls (see Chapter 15 for a discussion on precipitation patterns in tropical savannas), which arise from a combination of convective disturbances and frontal storms. In southern Africa, annual rainfalls are generally higher in the east and decline toward the west, reflecting a longitudinal shift in the relative importance of frontal vs. convective storms. Toward the east, frontal storms predominate, fed by inputs of water vapor from the Indian Ocean. The influence of frontal systems diminishes to the west, leaving convective disturbances as the most common source of rainfalls. This brings with it a strong interannual and spatial variation of rainfall. Thus, dryer savanna habitats must cope not only with annual and frequent multiyear droughts, but with significant spatial droughts as well.

The surface water balance in tropical savannas is dominated by evapotranspiration and infiltration, while runoffs generally are minuscule (Nicholson et al. 1997). Evapotranspiration is by far the dominant surface flux, which varies through the year between rainfall equivalents of 70 mm mo^{-1} in summer to roughly 15 mm mo^{-1} during winter. Rainfall exceeds evapotranspiration during summer, while the reverse is true in winter. Consequently, there is a net storage of water in soils during summer, which may then be tapped by plants or animals into the dry season. Once these stores are exhausted, production of above-ground biomass declines and standing biomass dies and dries. The dry and dead vegetation represents a store of fixed water in cellulose that can be a significant source of metabolic water for herbivores like termites.

3. Natural history and colonial physiology of *Macrotermes* colonies

The termite fauna of arid savannas is dominated by the fungus-cultivating Macrotermitinae (Termitidae). The macrotermitine termites are characterized by large body size (2-3 times heavier than other types of termites), large colony populations (1-2 million workers per colony, one to two orders of magnitude more populous than other types of termite colonies), and cultivation of symbiotic fungi (*Termitomyces* spp) in the nest, on specialized structures called fungus combs (Batra and Batra 1979; Thomas 1987; van der Westhuizen and Eicker 1990; Veivers et al. 1991). The fungi and fungus combs are part of an extracorporeal digestive system for the colony, in which raw cellulose forage is digested into more readily digestible sugars and oligosaccharides (Martin and Martin 1978). The fungi also provide fixed nitrogen and other nutrients (Rouland-Lefevre 2000). Together, the termites and fungi comprise a superorganismal metabolism rivalling that of many ungulate herbivores. Metabolic rates of *Macrotermes jeaneli* colonies, for example, have been estimated at about 55 watts, similar to that of a small goat: some estimates put the figure as high as 210 watts (Darlington et al. 1997). This metabolic effervescence helps make *Macrotermes* the dominant component of the termite fauna in many African savannas (Dangerfield et al. 1998; Deshmukh 1989).

The colony's high collective metabolism requires a considerable rate of respiratory gas exchange, which is regulated by the mound superstructure (Figure 2; Turner 2001). The mound is essentially an organ of extended physiology, a device to capture wind energy for powering ventilation of the nest (Turner 2000b). It is also an adaptive structure, its architecture being adjusted by the termites to balance ventilation with the colony's respiratory demands. This confers upon the nest environment a considerable degree of homeostasis, regulating nest concentrations of oxygen and carbon dioxide, and importantly, water vapor (Turner 2001).

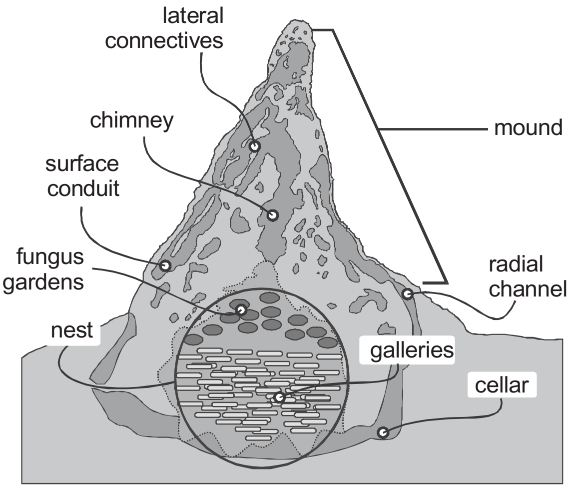

Figure 2. Cross section through a mound and nest of Macrotermes michaelseni*, showing locations of nest and fungus garden, and basic layout of the network of ventilatory tunnels. From Turner (2001).*

4. Water balance of *Macrotermes* colonies

The air in an active *Macrotermes* nest is much more humid than the atmosphere. During the summer, when the colony is most active, water vapor partial pressures (pH_2O) in a *M michaelseni* nest are on average 3.4 kPa, typically 2.6 kPa above atmospheric humidity (Table 1). In winter, humidity is lower, primarily because temperatures within the nest are cooler then. There is also a slight daily variation in humidity, again due mostly to daily variations of temperature within the nest. Nest humidity appears to be actively regulated, and is comparatively steady with respect to variations of atmospheric humidity, more so in the active summer season than the more dormant winter (Turner 2001). This tendency to nest homeostasis has significant consequences for soil water in and around the nest.

Table 1. Humidity and humidity gradients (expressed as water vapor pressure) driving evaporation in colonies of Macrotermes michaelseni in northern Namibia. Values are reported as mean (standard deviation): sample size. After Turner (2001).

Humidity (kPa)	Winter	Summer	Morning	Afternoon
Nest	2.58 (0.29)	3.40 (0.43)	2.99 (0.50)	3.08 (0.65)
Environment	0.35 (0.21)	0.83 (0.56)	0.65 (0.51)	0.55 (0.47)
dpH_2O (nest - env)	+2.23 (0.23)	+2.57 (0.47)	+2.34 (0.37)	+2.53 (0.46)

The high nest humidity drives a considerable rate of water vapor loss from the nest. Darlington et al (1997) estimated average evaporation rates equivalent to 5 liters per day (1,825 l y^{-1}) from the nests of *M jeaneli,* with some nests evaporating nearly 13 l water d^{-1} (4,750 l y^{-1}). Weir (1973) reported similar rates of evaporation from the mounds of *M subhyalinus* (12 l d^{-1}, or 4,380 l y^{-1}), although he suggested that evaporation in large colonies can amount to as much as 25,000 kg water per annum. Weir (1973) and Darlington et al. (1997) made their measurements at different times of the year, so it is unclear whether these rates are reflective of sustained rates of evaporation through the year. It is likely that they are, however. In nests of *M michaelseni*, for example, the pH_2O differences driving evaporation do not vary appreciably between summer and winter (Turner 2001; Table 1). Average rates of air turnover within *M michaelseni* nests also do not differ significantly between summer and winter (Turner 2001). Because evaporation rate is the product of water vapor partial pressure difference and the nest-to-atmosphere vapour conductance, the absence of a discernible seasonal difference in either suggests evaporation rate will not differ appreciably between summer and winter.

5. Sources of water for termite nests

To maintain a specific nest humidity, evaporation from the nest must be offset by inputs of liquid water into the nest. There are three likely sources of such water: water released from metabolism, matric water wicked in from superficial or deep soils, and water brought up actively from deep soil horizons.

By any estimation, metabolic water accounts for a small proportion of the nest's total water inputs (Darlington et al. 1997). A colony's rate of metabolic water generation can be calculated from its metabolic rate: for typical oxidative respiration, metabolic water is generated at a rate of about 25 μg per joule energy consumed. Metabolic rates for *Macrotermes* colonies have been estimated to range from about 50 to 200 watts (Darlington et al. 1997). For a colony metabolic rate on the high end of that range (200 W), this corresponds to a generation of roughly 190 kg metabolic water per year, or about 10% of the colony's annual evaporation: actual inputs are probably smaller. Preformed water in soil must therefore make up the other 90% of water inputs to the nest.

How soil water gets into the nest has long been a matter of controversy (Lee and Foster 1991; Lobry de Bruyn and Conacher 1990). In 1947, Milne suggested that capillary action in the nest's soil matrix wicks in water from deeper soils. He suggested this might explain the high concentrations of carbonate minerals often found in mound soils, but offered no evidence for or against his inference. However, Watson (1969; 1971) followed movements of soil water below mounds of *M bellicosus* and *Odontotermes badius,* in what was then Rhodesia, (traced using ^{51}Cr tracers injected into soil water), and could not show the upward movement of water that (Milne 1947) had predicted. The enrichment of minerals in the nest that Milne sought to explain could therefore not be the result of wicking. More likely, the distribution of minerals arose through differential leaching: poor leaching in soils directly below mounds in juxtaposition with strongly leached soils in the intervening spaces between mounds (Watson 1969). On the other hand, termite colonies transport immense quantities of coarse-grained soils outward and upward from the nest (Pomeroy 1976), which leave behind in the nest a fabric of fine-grained silts and clays (Arshad 1981). These are molded together by salivary glues that tend to readily mineralize (Mermut et al. 1984). Water could conceivably be wicked into the nest by the very strong matric potentials that characterize fine-grained soils like clays (Campbell 1977). Wicking of water into the nest in this way is a double-edged sword, however. Strong matric forces might draw water in, but also hold the water tightly, making it unavailable for the nest occupants. In any event, the many reports of moist soils within nests, and the tendency of colony-associated trees to stay green through periods of drought (Turner, personal observation, Konaté et al. 1999) indicate that termite mounds and colonies are, if anything, at higher water potentials than surrounding soils. Weir

(1972; 1973) and Watson (1969) have also suggested that the extent of mineral accumulations observed in mound soils would require periods of continuous occupancy of mounds for centuries. Mound re-occupancy does occur among the macrotermites, albeit rarely (<10% of extant colonies; Pomeroy 1976). Nevertheless, continuous occupancy of nests for centuries by subsequent generations of termite colonies is not unheard of. For example, a peculiar landform in the winter-rainfall regions of the Karoo in South Africa, known in the vernacular as *heuweltjies* (Afrikaans for "little hill"), arises from just such a pattern of ongoing colonization of a particular patch of ground by a species of harvester termite, *Microhodotermes viator* (Lovegrove 1991; Moore and Picker 1991). It remains unclear what effects termite colonies might have on the movements of matric water in soils: the macrotermitine termites colonize such a wide diversity of soils and climatic regimes that no generalizations can safely be drawn at present.

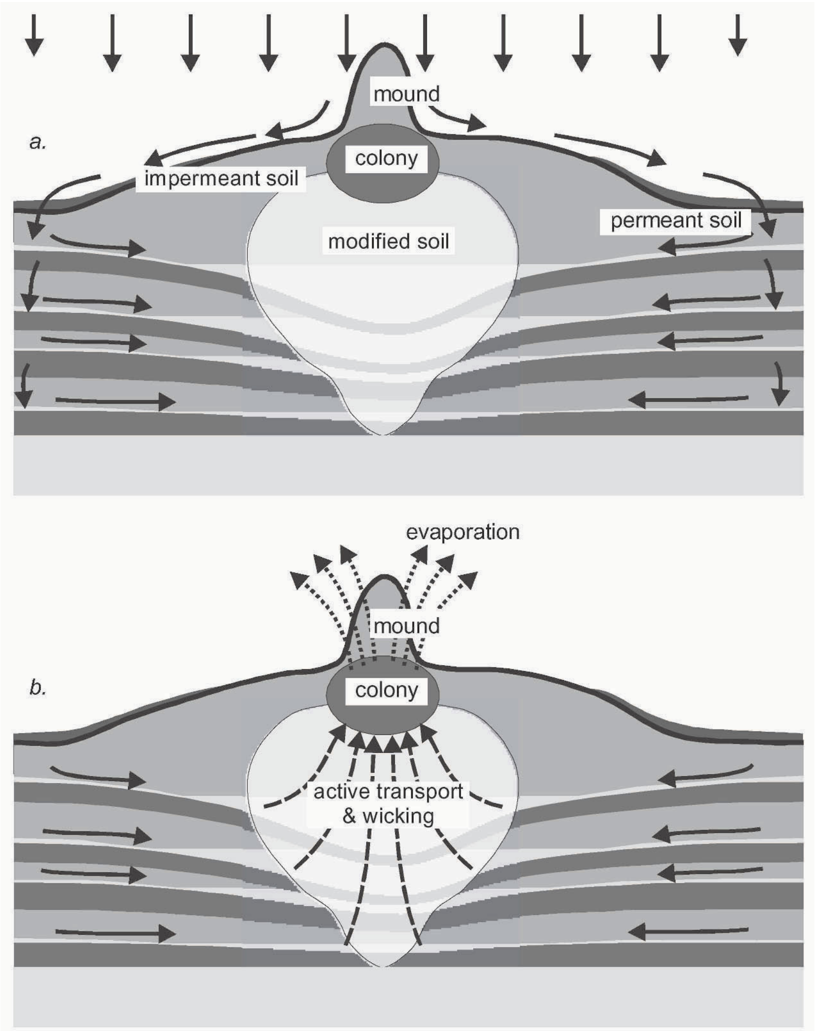

Figure 3. Scheme of pedology and hydrology of soils around a Macrotermes bellicosus *colony, after Boyer (1975).* a. *Patterns of runoff and percolation of rainfalls and their catchment as perched water tables (light shading) by impermeant layers in the soil (dark shading).* b. *Patterns of soil water movement and evaporation that maintains a particular humidity within the nest.*

Termites also construct extensive underground networks of tunnels and cavities, and it is likely that the resultant changes in soil hydrology will affect movement of water through the nest. The construction of a mound involves translocating several cubic meters of soil from deep horizons to the surface (Pomeroy 1976), and this must open commensurate void space and macropores in the soil below the mound. A typical mound of *M michaelseni*, for example, occupies a volume of 5-7 m^3, of which roughly 80% is soil excavated from deep soils and brought up into the mound (Turner 2000a). Because soils within mounds tend to be compacted compared to surrounding soil, the actual subterranean void space is probably more capacious (Arshad 1981). The mound is also a dynamic structure, with roughly a cubic meter of soil per year being transported up to replace soil lost from the mound through erosion (Pomeroy 1976). Finally, foraging tunnels around colonies of *Macrotermes* can radiate for 50 m or more into surrounding soils, and these also involve a substantial upward transport of soil. All this activity increases the volume of soil macropores, which enhances rates of infiltration and retention of rainfalls around the mound (Mando 1997; Mando et al. 1996), as is the case for soils in the Chihuahuan desert of North America, where termites generally enhance infiltration and water retention (Elkins et al. 1986).

At the nest itself, however, the local enrichment of clays and other fine-grained soils (Arshad 1981, Holt and Lepage 2000) makes soils there relatively impermeable. For example, a nest of *M michaelseni* is typically surrounded by an impermeant clay barrier that protects it from periodic flooding (Dangerfield et al. 1997) and from aardvark attack (Turner, personal observation). Soils below *Macrotermes* nests also show a remarkably low leach rates (Watson 1969), suggesting an enhancement of runoff, rather than infiltration, at the mound itself.

The overall picture suggests that *Macrotermes* nests impart a complex hydrology to savanna soils. The most comprehensive assessment of this comes from the work of Boyer (1973; 1975a; b), who showed extensive and widespread effects of nests of *Macrotermes bellicosus* and *M natalensis* on pedology and hydrology of savannas in the Central African Republic. Below the nest, there is a zone of extensive modification of soils that can extend to depths of 10-12 meters (Figure 3). From this zone, termites draw soil for mound construction. The continual disturbance of the soil there, along with biogenic deposition of calcite, forms impermeable depressions below the mound into which perched water tables can drain (Figure 3). Above and around the nest proper, the relatively impermeant layers of soil there promote runoff, eroding the relatively friable surface layers of the mound onto a broad, comparatively impermeant, outwash pediment that can radiate ten to twenty meters from the mound. In soils beyond the outwash pediment, infiltration is enhanced by the colony's extensive networks of foraging tunnels there, charging both perched and permanent reservoirs of ground water. These ultimately drain back to the impermeable depressions below the colony.

Water may also be brought into the nest through a peculiar form of active transport. Termites are known to bring soil up into the nest and mound from considerable depths, so that soils in the nest and mound soils often differ considerably from the ambient surface soils (Watson 1972; 1974; 1977). For example, soils in northern Namibia commonly comprise coarse iron-rich sands overlaying a calcite base: it is not uncommon to see chalky-white mounds emerging from these reddish sandy soils (Turner, personal observation). Termites' tendencies to bring soils up from deep horizons has led some to suggest mounds could serve as useful probes for detecting mineral-rich ores below the surface. For example, *Macrotermes* mounds in the Kalahari are enriched in zinc, drawn presumably from zinc-rich horizons that lay several meters below the surface (Watson 1970; 1972; West 1970). There are also many anecdotal reports of mound soils being enriched in gold, brought up from deep alluvial deposits (Gleeson and Poulin 1989). If the soil carried up by termites from deep horizons is damp, this amounts to a form of active water transport: movement of water against a water potential difference, driven by the colony's metabolism. This, rather than wicking, might account for a considerable rate of water movement into the nest and mound. Its magnitude is completely unknown.

Whatever its magnitude, active transport of water into the nest can be undertaken at surprisingly little cost to the colony, and might be a major effector in the regulation of nest humidity. The energy cost, Q (J) of transporting water into the mound from deep reservoirs can be estimated from gravity potential (Ψ_g; J kg^{-1}), itself the product of gravitational acceleration, g (9.8 m s^{-2}) and the height, h (m), the water is lifted:

$$\Psi_g = g\,h \tag{1}$$

and the mass, M (kg), lifted:

$$Q = M\,\Psi_g \tag{2}$$

The cost of transporting, say, 1800 kg of water up 5 m into a mound (equivalent to the estimated annual evaporation from colonies of *M jeaneli*; Darlington et al. 1997), requires an expenditure of roughly 88 kJ. Spread over a year, this amounts to a power demand of only 2.8 mW. Upward transport of soil is about as cheap. Densities of silica sands and clays range from 1800 kg m^{-3} (bulk density) to 2600 kg m^{-3} (density of the parent rock). Assuming termites transport roughly a cubic meter of soil into the mound each year (Pomeroy 1976), this amounts to lifting roughly 1800-2600 kg into the mound annually. If the soil is lifted on average 5 m upwards, the work done raising this quantity of soil by 5 m amounts to 88-127 kJ, or roughly 4 mW. Even if one assumes an extremely low conversion efficiency of muscle work to transport work of, say 1%, these rates correspond to metabolic expenditures of roughly 600 mW, roughly 1% of the estimated 55-210 W metabolic rate for *M jeanelli* colonies (Darlington et al. 1997).

6. Termites as homeostatic water gatherers in savanna ecosystems

Irrespective of the mechanistic details, evaporation from *Macrotermes* mounds is sustained by what seems to be a substantial water input from surrounding soils. During the rainy season, rainfalls shed from the mound and relatively impermeant soils surrounding it charge perched and permanent water tables in the more permeable soils between mounds. These form a reservoir that the colony can then tap during dry periods, using a combination of passive and active transports of water into the nest, ensuring a relatively steady evaporative flux through the year. In short, a *Macrotermes* colony can act as a “water gatherer”, a physiological system that draws water from a broad expanse of soil centripetally to the colony. In this sense, a termite colony is physiologically akin to a tree, with an extensive system of conduits for the centripetal transport of water.

If water gathering by termites is driven by the demands of nest homeostasis, it would confer upon the colony a certain independence from seasonal, interannual and spatial variation in the hydric environment (Figure 4). In wetter environments, for example, a specific nest humidity can be achieved by a combination of a mound’s high evaporative conductance and rapid translocation of wet soil from the nest to the mound surface. The same humidity in dryer environments can be maintained through a combination of building mounds with low evaporative conductance, limited transport of damp soil to the surface, and more intense transport of soil water into the nest. Because *Macrotermes* colonies can bring more metabolic power to these tasks than can other termites, they are able to colonize dryer habitats than any other termite species. In sub-Saharan Africa, for example, *Macrotermes* spp come to dominate termite biomass as habitats become dryer and dryer (Figure 5; Deshmukh 1989).

Nest homeostasis regulates more than nest humidity, though, and this poses challenges for balancing regulation of various nest properties against one another. For example, maintaining the colony’s fungal symbionts requires that CO_2 concentrations within the nest be kept within narrow limits (Batra and Batra 1979). Nitrogen fixation within termite nests also is compromised by high oxygen concentrations (Curtis and Waller 1996). Finally, colony temperatures are also steady

(Korb and Linsenmair 1998a; b; 2000), although this derives largely from damping by the capacious thermal sink of the soil rather than active regulation. Thus, nest homeostasis involves managing fluxes of a variety of materials - oxygen, carbon dioxide, water vapor - and energy, and regulation of one may conflict with regulation of others. For example, a colony in a dry environment that maintains humidity by reducing the mound's gas conductance might be faced with a compromised ventilatory exchange of the CO_2 or oxygen upon which the colony's fungal symbionts depend. Conversely, a mound that is sufficiently porous to support the proper exchange rates of oxygen and carbon dioxide will also support high rates of water vapor flux, and along with it, the risk of nest desiccation.

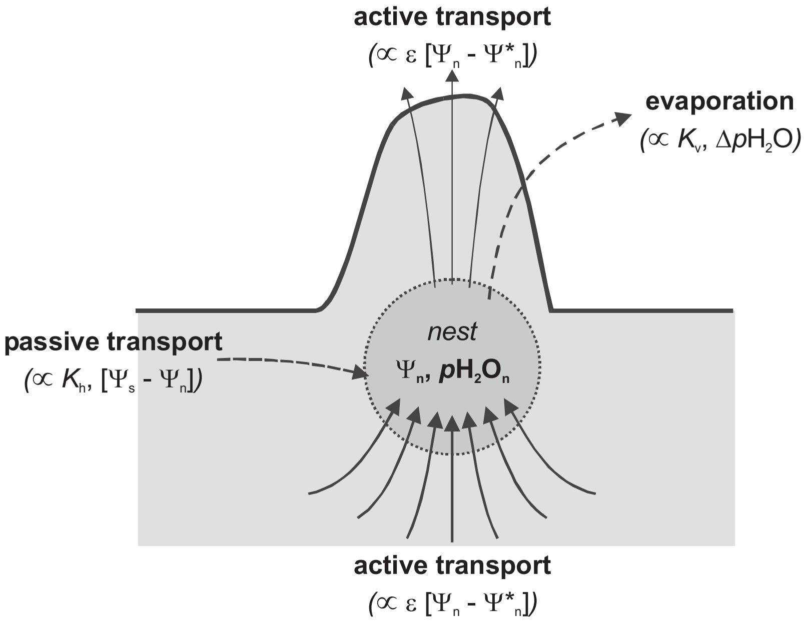

Figure 4. Scheme of managing water balance in a Macrotermes nest. The nest's water balance is geared to regulating nest humidity (pH_2O_n) *and water potential* (Ψ_n)*. Evaporation is proportional to the mound's vapor conductance* (K_v)*, which the termites manage by altering mound architecture, and the water vapor partial pressure difference between nest and atmosphere* (ΔpH_2O)*. Water can be transferred into the nest from perched water tables in soils, driven by the difference in water potential between nest and soil* ($\Psi_s - \Psi_n$)*, and limited by the soils' hydraulic conductance* (K_h)*. Water can be conveyed actively into the nest from deep soils, or to the surface from the nest by transport on damp soil. This will be regulated by an error signal (*ε*), which reflects the difference between actual nest humidity* (Ψ_n) *and a "target" nest humidity* (Ψ^*_n).

Such tradeoffs between multiple exchanges usually arise when sources and sinks of the various materials are linked. In the case of the respiratory gases, carbon dioxide, oxygen and metabolic water vapor, all are linked by the stoichiometry of respiration, and anything which affects the exchange of one similarly affects exchange of the others. Such tradeoffs can be avoided by uncoupling the links between the various fluxes. This, in a roundabout way, is the rationale for drinking of liquid water by animals. There is no inherent reason why animals need to drink - the kangaroo rat is the quintessential example of an animal that balances its water budget with metabolic water inputs alone - but not drinking means tying water balance inextricably to the stoichiometry of respiration, and elaborate mechanisms of water conservation and retention are necessary for this to work. Most animals avoid the problem by coupling water vapor flux to both metabolic water and an external source, namely drunk liquid water. Through access to an additional capacious source, high water flux rates can be maintained without simultaneously disrupting flux rates of oxygen and carbon dioxide, and hence their concentrations within the body. Water gathering by termites is the superorganismal equivalent of drinking, coupling high evaporative fluxes to the relatively capacious source of soil water, enabling the simultaneous regulation of all the respiratory gases. Plants, of course, make similar tradeoffs, and like termite colonies, resolve the conflicts by decoupling water flux rates from gas flux at the leaf (see Chapter 4 for more details on plant physiology).

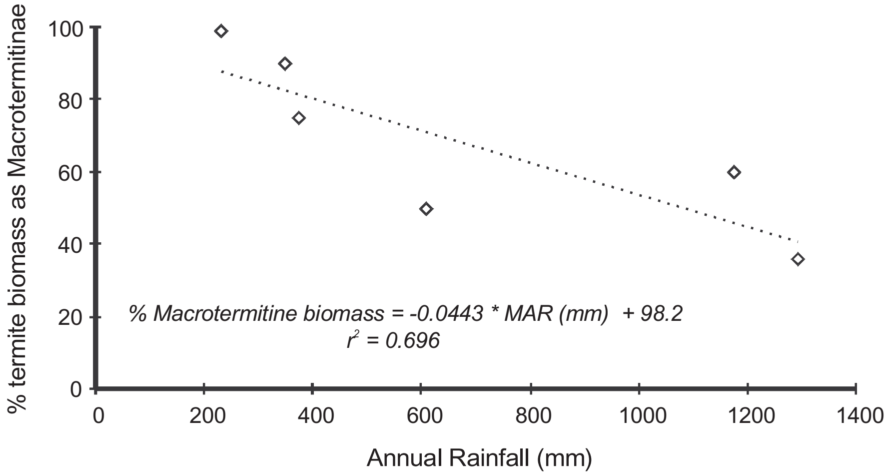

Figure 5. Proportion of termite biomass that is represented by Macrotermitinae in savannas with various annual rainfalls. After Deshmukh (1989).

What impact water gathering has on savanna systems will depend, of course, upon how rare is the resource of soil water. In wetter savannas, “drinking” by termite colonies is unlikely to have much impact on the soil water balance, and hence the availability of soil water to other organisms. Certainly, wetter environments support a higher diversity of other termites, and termites there have lesser impacts on differential soil leaching and other functions that depend upon rainfall. In environments where the inputs of rainfall are less, and the desiccating forces greater, the draw on soil water by macrotermitine termites will be proportionally greater, with larger consequences for the soil’s hydric environment and the organisms that depend upon it. Substantial ecological consequences might follow, exemplified by the observation that inspired this paper. Northern Namibia hosts some of the dryer savannas in Africa, with annual rainfalls averaging about 250-450 mm. Trees in this environment associated with termite mounds would appear to have a clear competitive advantage over trees that are not (Konaté et al. 1999). What other ecological consequences might follow in an ecosystems dominated by such a powerful draw on scarce soil water? Questions abound, but very few answers are at hand.

Water gathering also has implications for our understanding and ability to predict climate in tropical savanna systems. Climate models depend strongly upon measurements that assume some degree of homogeneity to the flux processes upon which climate depends. For example, expected transpiration is often calculated from a variant of the Penman equation, which estimates evaporation from air temperature, local humidity, ground cover and so forth (Campbell 1977; Nicholson et al. 1997). Increasingly, these parameters are sensed remotely from various satellite platforms, with resolutions typically in the km^2 range, and the results validated against commensurably homogeneous habitats on the ground, like agricultural fields. Despite the great strides in remote sensing, however, none are capable of resolving the kind of hydrological patchiness that *Macrotermes* nests in a habitat might impart. Let us assume, for the sake of argument, that a *Macrotermes* mound evaporates roughly 5 liters of water per day (Darlington et al. 1997). This water leaves the soil through the "footprint" of the mound's basal area, estimated to average roughly 4 m^2 (Turner 2000a), yielding a focal water flux density of 1.25 kg m^{-2} d^{-1}, or about 457 kg m^{-2} y^{-1}. This is numerically identical to a "rainfall equivalent" of 457 mm y^{-1}. Throughout the year, this amounts to a monthly evaporation from the mound's footprint that is equivalent to 38.1 mm rainfall. Contrast this with estimates of monthly evapotranspiration from a semi-arid savanna, which range from roughly 75 mm mo^{-1} in summer to less than 20 mm mo^{-1} in winter (Nicholson et al 1997). Notice that a conservative estimate of the mound's annual evaporation have been used: Weir's (1973) more extravagant estimate of 25,000 kg of water evaporated annually from nests of *M subhyalinus* in Tanzania corresponds to an evapotranspiration rate of more than 500 mm mo^{-1}, roughly equivalent to the *annual* evapotranspiration estimated from climate measurements (Nicholson et al. 1997). This suggests that the development and validation of microclimate models would have to account for the extreme patchiness associated with the presence of termite mounds.

7. Acknowledgements

I wish to thank two anonymous reviewers who provided many perceptive comments. Original research reported here was supported by a grant from the Earthwatch Institute.

8. Literature Cited

Arshad M. A. 1981. Physical and chemical properties of termite mounds of two species of *Macrotermes* (Isoptera, Termitidae) and the surrounding soils of the semiarid savanna of Kenya. Soil Science 132, 161-174.

Batra L. R. and Batra S. W. T. 1979. Termite-fungus mutualism. *In* Insect-fungus Symbiosis. Nutrition, Mutualism and Commensalism, Ed L R Batra. pp 117-163. John Wiley and Sons, New York.

Boyer P. 1973. Action de certains termites constructeurs sur l'évolution des sols tropicaux I. Annales des Sciences Naturelles Zoologie Paris sér. 12 15, 329-498.

Boyer P. 1975a. Action de certains termites constructeurs sur l'évolution des sols tropicaux II. Etude particuliére de trois termitieres de *Bellicositermes* et de leur action sur les sols tropicaux. Annales des Sciences Naturelles Zoologie Paris sér. 12 17, 273-446.

Boyer P. 1975b. Action de certains termites constructeurs sur l'évolution des sols tropicaux III. Les différents aspects de l'action de *Bellicositermes* sur les sols tropicaux. Annales des Sciences Naturelles Zoologie Paris sér. 12 17, 447-504.

Campbell G. S. 1977. An Introduction to Environmental Biophysics. Springer Verlag, New York. 159 p.

Curtis A. D. and Waller D. A. 1996. The effects of decreased pO_2 and increased pCO_2 on nitrogen fixation rates in termites. Journal of Insect Physiology 42, 867-872.

Dangerfield J. M., McCarthy T. S. and Ellery W. N. 1998. The mound-building termite *Macrotermes michaelseni* as an ecosystem engineer. Journal of Tropical Ecology 14, 507-520.

Darlington J. P. E. C., Zimmerman P. R., Greenberg J., Westberg C. and Bakwin P. 1997. Production of metabolic gases by nests of the termite *Macrotermes jeaneli* in Kenya. Journal of Tropical Ecology 13, 491-510.

Deshmukh I. 1989. How important are termites in the production ecology of African savannas? Sociobiology 15, 155-168.

Elkins N. Z., Sabol G. V., Ward T. J. and Whitford W. G. 1986. The influence of subterranean termites on the hydrological characteristics of a Chihuahuan desert ecosystem. Oecologia 86, 521-528.

Holt J. A. and Lepage M. 2000. Termites and soil properties. *In* Termites: Evolution, Sociality, Symbioses, Ecology, Eds T Abe, D E Bignell and M Higashi. pp 389-407. Kluwer Academic Publishers, Dordrecht.

Konaté S., Le Roux X., Tessier D. and Lepage M. 1999. Influence of large termitaria on soil characteristics, soil water regime, and tree leaf shedding pattern in a west African savanna. Plant and Soil 206, 47-60.

Korb J. and Linsenmair K. E. 1998a. The effects of temperature on the architecture and distribution of *Macrotermes bellicosus* (Isoptera, Macrotermitinae) mounds in different habitats of a west African Guinea savanna. Insectes Sociaux 45, 51-65.

Korb J. and Linsenmair K. E. 1998b. Experimental heating of *Macrotermes bellicosus*(Isoptera, Macrotermitinae) mounds: What role does microclimate play in influencing mound architecture? Insectes Sociaux 45, 335-342.

Korb J. and Linsenmair K. E. 2000. Ventilation of termite mounds: New results require a new model. Behavioral Ecology 11, 486-494.

Lee K. E. and Foster R. C. 1991. Soil fauna and soil structure. Australian Journal of Soil Research 29, 745-775.

Lobry de Bruyn L. A. and Conacher A. J. 1990. The role of termites and ants in soil modification: A review. Australian Journal of Soil Research 28, 55-93.

Lovegrove B. G. 1991. Mima-like mounds (*heuweltjies*) of South Africa: The topographical, ecological and economic impact of burrowing animals. Symposia of the Zoological Society of London 63, 183-198.

Mando A. 1997. The impact of termites and mulch on the water balance of crusted Sahelian soil. Soil Technology 11, 121-138.

Mando A., Stroosnijder L. and Brussaard L. 1996. Effects of termites on filtration into crusted soil. Geoderma 74, 107-113.

Martin M. M. and Martin J. S. 1978. Cellulose digestion in the midgut of the fungus-growing termite *Macrotermes natalensis*: the role of acquired digestive enzymes. Science 199, 1453-1455.

Mermut A. R., Arshad M. A. and St Arnaud R. J. 1984. Micropedological study of termite mounds of three species of *Macrotermes* in Kenya. Soil Science Society of America Journal 48, 613-620.

Milne G. 1947. A soil reconnaissance journey through parts of Tanganyika Territory, December 1935 to February 1936. Journal of Ecology 35, 192-265.

Moore J. M. and Picker M. D. 1991. *Heuweltjies*(earth mounds) in the Clanwilliam District, Cape Province, South Africa: 4000-year-old termite nests. Oecologia 86, 424-432.

Nicholson S. E., Kim J., Ba M. B. and Lare A. R. 1997. The mean surface water balance over Africa and its interannual variability. Journal of Climate 10, 2981-3002.

Pomeroy D. E. 1976. Studies on a population of large termite mounds in Uganda. Ecological Entomology 1, 49-61.

Rouland-Lefevre C. 2000. Symbiosis with fungi. *In* Termites: Evolution, Sociality, Symbioses, Ecology, Eds T. Abe, D. E. Bignell and M. Higashi. pp 289-306. Kluwer Academic Publishers, Dordrecht.

Ruelle J. E., Coaton W. G. H. and Sheasby J. L. 1975 National survey of the Isoptera of southern Africa 8. The genus *Macrotermes* Holmgren (Termitidae: Macrotermitinae). Cimbebasia 3A, 73-94.

Thomas R. J. 1987. Distribution of *Termitomyces* and other fungi in the nests and major workers of several Nigerian Macrotermitinae. Soil Biology and Biochemistry 19, 335-341.

Turner J. S. 2000a. Architecture and morphogenesis in the mound of *Macrotermes michaelseni* (Sjostedt) (Isoptera: Termitidae, Macrotermitinae) in northern Namibia. Cimbebasia 16, 143-175.

Turner J. S. 2000b. The Extended Organism. The Physiology of Animal-Built Structures. Harvard University Press, Cambridge, MA.

Turner J. S. 2001. On the mound of *Macrotermes michaelseni* as an organ of respiratory gas exchange. Physiological and Biochemical Zoology 74, 798-822.

van der Westhuizen G. C. A. and Eicker A. 1990. Species of *Termitomyces* occurring in South Africa. Mycological Research 94, 923-937.

Veivers P. C., Mühlemann R., Slaytor M., Leuthold R. H. and Bignell D. E. 1991. Digestion, diet and polyethism in two fungus-growing termites: *Macrotermes subhyalinus* Rambur and *M. michaelseni* Sjøstedt. Journal of Insect Physiology 37, 675-682.

Watson J. P. 1969. Water movement in two termite mounds in Rhodesia. Journal of Ecology 57, 441-451.

Watson J. P. 1970. Contribution of termites to development of zinc anomaly in Kalahari sand. Transactions of the Institution of Mineralogy and Metallurgy, (Series B) 79.

Watson J. P. 1971. Comparison of chromium^{51}-versenate and tritiated water movement in a termite mound and soil. Soil Science 111, 188-191.

Watson J. P. 1972. The distribution of gold in termite mounds and soils at a gold anomaly in Kalahari sand. Journal of Soil Science 113, 317-321.

Watson J. P. 1974. Calcium carbonate in termite mounds. Nature 247, 74.

Watson J. P. 1977. The use of mounds of the termite *Macrotermes falciger* (Gerstäcker) as a soil amendment. Journal of Soil Science 28, 664-672.

Weir J. S. 1973. Air flow, evaporation and mineral accumulation in mounds of *Macrotermes subhyalinus*. Journal of Animal Ecology 42, 509-520.

Weir J. S. 1972. Mechanisms of mineral accumulation in *Macrotermes* mounds in Africa. *In* Abstracts of the 14th International Congress of Entomology, Canberra, Australia, 1972. pp 196.

West W. F. 1970. The Bulawayo Symposium Papers: no 2. Termite prospecting. Chamber of Mines Journal 30, 32-35.

Chapter 18

UNDERSTANDING GLOBAL DESERTIFICATION: BIOPHYSICAL AND SOCIOECONOMIC DIMENSIONS OF HYDROLOGY

Fernando T. MAESTRE[1,2], James F. REYNOLDS[1,3], Elisabeth HUBER-SANNWALD[4],
Jeff HERRICK[5], and Mark STAFFORD SMITH[6]

[1]Department of Biology, Phytotron Bldg., Box 90340, Duke University, Durham NC 27708-90340, USA-e-mail: maestre@duke.edu
[2]Unidad de Biodiversidad y Conservación, E.S.C.E.T., Universidad Rey Juan Carlos, C/ Tulipán s/n, 28933 Móstoles, SPAIN
[3]Division of Environmental Science and Policy, Nicholas School of the Environment and Earth Science, Duke University, Durham, NC 27708-90340, USA –e-mail: james.f.reynolds@duke.edu
[4]Departamento de Ingeniería Ambiental y Manejo de Recursos Naturales, Instituto Potosino de Investigación Científica y Tecnológica (IPICYT), Apdo. Postal 3-74 Tangamanga 78231, San Luis Potosí, SLP, MEXICO
[5]USDA-ARS Jornada Experimental Range MSC 3JER, Box 30003, NMSU, Las Cruces NM 88003-8003, USA
[6]Desert Knowledge Cooperative Research Centre, PO Box 2111, Alice Springs, NT 0871, AUSTRALIA

1. Introduction

Drylands are regions of the globe where the index of aridity (IA)—defined as the ratio of mean annual precipitation (P) to mean annual potential evapotranspiration (PET)—is less than 0.65 (see Chapters 1 and 8). If we restrict IA to the range of 0.05 to 0.65, drylands consist of *arid*, *semiarid*, and *dry sub-humid* regions, which together cover approximately 5.2 billion hectares or 40% of the land area of the world (Table 1). This definition *excludes* hyper-arid regions of the globe where IA < 0.05, such as the Atacama, Arabian, and Sahara deserts (ca. 0.98 billion hectares or 7.5% of global land area). Based on human land use, ca. 88% of drylands are classified as rangeland, with the remaining 12% used in agricultural production (3% irrigated cropland, 9% rainfed; Table 1). Combined, Asia and Africa contain 64% of all global drylands, dwarfing the amount of dryland area on other continents. In terms of importance, however, these numbers can be somewhat misleading. While Europe contains only ca. 5% of the world's drylands, this represents over 32% of its landmass and is home to 25% of its population. Similarly, Australia contains about 10% of the world's drylands but they cover over 75% of the continent and are home to 25% of its population.

Some of the highest densities of the world's human populations are located in the drylands of India, China, and Europe (White et al., 2003). In addition, drylands contain the fastest growing human populations on Earth; thus, it is not surprising that these areas are facing enormous environmental problems and challenges (Clarke et al., 2002). Among them, land degradation—commonly referred to as desertification—is perhaps the most important environmental issue (Le Houérou, 1996; Darkoh, 1998; Dregne, 1996; Kassas, 1995; Reynolds, 2001). Nevertheless, in spite of its importance, desertification remains a controversial topic: scientists and policy-makers from diverse disciplines and perspectives are engaged in ongoing debates ranging from defining land degradation to estimating the amount of total land affected (Reynolds, 2001; Thomas, 1997; Reynolds and Stafford Smith, 2002a).

P. D'Odorico and A. Porporato (eds.), Dryland Ecohydrology, 315–332.

In this chapter we review some of the key concerns and challenges associated with desertification in drylands, emphasizing the role of hydrological processes. First, we briefly review the extent, causes and consequences of desertification, elucidating some of the underlying issues on this topic that make research and exchange of dialogue so challenging. Second, we discuss the importance of ecohydrological feedbacks and linkages in desertification, focusing on both biophysical and socioeconomic aspects. Hydrological processes lie at the heart of desertification in drylands (Sharma, 1998), and thus are key to understanding both the causes and consequences of land degradation. Importantly, these processes must be viewed in the context of "shared water" between society and nature in order to avoid future human water shortages and undesirable environmental impacts, particularly in developing countries dealing with desertification. Third, we present an overview of the Dahlem Desertification Paradigm (DDP), a new approach to desertification designed to facilitate directed research effort and progress, and briefly describe an international network designed to facilitate debate and solicit input to refine and improve the DDP. Lastly, we introduce a stepwise model of grazing-induced land degradation, which highlights interactions between hydrological, ecological, and socioeconomic processes with management and restoration options, and briefly discuss future research needs.

Table 1. Amounts and distribution of drylands of the world, and global totals of drylands considered to be degraded, subdivided into three dominant types of human land-use categories: irrigated agricultural cropland, rainfed agricultural cropland, and rangelands. Compiled from UNEP (1992) and Grainger (1992). T = total amount of dryland area (millions of hectares), and D = total amount of degraded dryland area (millions of hectares).

	IRRIGATED CROPLAND			**RAINFED CROPLAND**			**RANGELANDS**			**TOTALS**		
Continent	**T**	*D*	*(%)*	**T**	D	*(%)*	**T**	*D*	*(%)*	**T**	*D*	*(%)*
Africa	**10.4**	*1.9*	*18*	**79.8**	*48.9*	*61*	**1,342.4**	*995.1*	*74*	**1,432.6**	1,045.9	*73*
Asia	**92**	*31.81*	*35*	**218.2**	*122.3*	*56*	**1,571.2**	*1,187.6*	*76*	**1,881.4**	1,341.7	*71*
Australia	**1.9**	*0.25*	*13*	**42.2**	*14.3*	*34*	**657.2**	*361.4*	*55*	**701.3**	375.9	*54*
Europe	**11.9**	*1.91*	*16*	**22.1**	*11.9*	*54*	**111.6**	*80.5*	*72*	**145.6**	94.31	*65*
N. America	**20.9**	*5.86*	*28*	**74.2**	*11.6*	*16*	**483.1**	*411.2*	*85*	**578.2**	428.7	*74*
S. America	**8.4**	*1.42*	*17*	**21.4**	*6.6*	*31*	**390.9**	*297.8*	*76*	**420.7**	305.82	*73*
TOTALS	**145.5**	*43.15*	*30*	**457.7**	*215.6*	*47*	**4,556.4**	*3,333.5*	*73*	**5,159.6**	3,592.2	*70*

2. Desertification: a global concern

2.1. BACKGROUND

Many definitions of desertification have been proposed (see review in Reynolds, 2001). We favor the definition stemming from the United Nations Convention to Combat Desertification (CCD) (UNCCD, 1994): "land degradation in arid, semi-arid and dry subhumid areas resulting from various factors, including climatic variations and human activities". This definition makes it clear that desertification is about biophysical and socioeconomic linkages and how they affect human welfare. It also emphasizes that land degradation is not equated to soil degradation per se. Hence, it is essential in any elaboration of what constitutes land degradation, to make it clear that whilst *biophysical* components of ecosystems and their properties are involved (e.g., soil erosion and the loss of vegetation), the interpretation of change as 'loss' is dependent upon the integration of these components within the context of the *socio-economic* activities of human beings (often via a generic use of the term 'productivity'). We further propose a model for understanding and predicting conditions of arid land degradation in the context of the balance between natural and social systems (Figure 1).

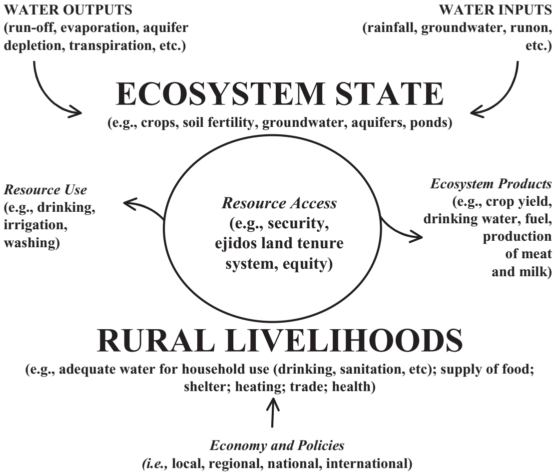

Figure 1. Illustration of social and biophysical factors in a rural community in a developing country. The cores of the biophysical and socioeconomic systems are shown as the 'state of the ecosystem' and 'rural livelihood', respectively, whereas hydrological processes are highlighted to show how the biophysical-socioeconomic systems are closely linked and constantly changing. From Huber-Sannwald et al. (2005).

Desertification is caused by a relatively large number of factors, which vary from region to region, and that often act in concert with one another in varying degrees. In a worldwide review of the causes of desertification, Geist and Lambin (2004) identified four major categories of proximal causal agents: 1) increased aridity; 2) agricultural impacts, including livestock production and crop production; 3) wood extraction, and other economic plant removal; and 4) infrastructure extension, which could be separated into irrigation, roads, settlements, and extractive industry (e.g., mining, oil, gas). Their study showed that: i) only about 10% of the case studies were driven by a single cause (with about 5% due to increased aridity and 5% to agricultural impacts); ii) about 30% of the case studies were attributable (primarily) to increased aridity and agricultural impacts; and iii) the remaining cases were combinations of three or all of the proximal causal factors. These results clearly highlight the complexity of desertification, and the need for integrative approaches that consider both its biophysical and socio-economic dimensions, which we discuss in more detail below.

2.2. EXTENT OF DESERTIFICATION

The extent of global desertification is routinely reported by international agencies to be as high as 70% of all drylands (UNCCD, 2000). However, such estimates must be considered with caution. Obtaining accurate, logical estimates on the amount of drylands that have been "desertified" is not a trivial task, especially given the lack of agreement as to the meaning of land degradation (Reynolds and Stafford Smith, 2002a). Thus, the multitude of global estimates of the extent of desertification are a product of subjective opinions, qualitative assessments, and data of varying authenticity and consistency (Verstraete, 1986; Hellden, 1991; Mainguet, 1991; Thomas and Middleton, 1994; Nicholson et al., 1998).

The CCD definition of desertification (see Section 2.1) is not amenable to easy quantification as a single number or as a synthetic index. Another confounding problem is how changes that occur over short-term temporal scales (e.g., decrease in plant cover) are often cited as evidence of desertification, ignoring the fact that drylands are highly variable over time and that a temporary loss of vegetation cover due to a short-term drought is not necessarily related to a permanent loss indicative of desertification (Tucker et al., 1998; Tucker and Nicholson, 1998; Nicholson et al., 1998; Reynolds, 2001). For a detail discussion of these topics, see Thomas (1997) and Reynolds (2001).

2.3. IMPORTANCE OF MULTIPLE CAUSAL AGENTS

A crucial, but often overlooked, fact is that desertification is usually promoted by two or more causal agents (see Geist and Lambin, 2004). However, most estimates of desertification are derived from either *biophysical* factors (e.g. soil erosion, plant cover) or *socioeconomic* factors (e.g., low production, economic stress, poverty, emigration), but rarely both (Stafford Smith and Reynolds, 2002). This complicates quantitative estimates of the process since most studies focus only on single variables, or on a set of related variables, either biophysical *or* socioeconomic. When assessments are made without good knowledge of the underlying causes, it brings into question the validity of the variables or sets of variables being used in the assessment.

In recent years there has been a concerted effort to categorize and map various forms of land degradation, but these efforts failed to include a detailed identification of the critical biophysical *and* socioeconomic variables that cause the observed dynamics (Stafford Smith and Reynolds, 2002). This problem lies at the base of the confusion about how much 'desertification' there really is (see Batterbury et al., 2002). Much of this confusion could be eliminated by focusing on a small number of critical variables that contribute to an understanding of the *cause*, rather than *effect*, of desertification (Stafford Smith and Reynolds, 2002). Of course, this is all the more problematic when we try to account for the differences in causal factors driving desertification in different regions of the world and at different times: approaches developed to estimate desertification in one region may not be effective in others. The failure to recognize these issues has led to the disparities of estimates of desertification in the literature and is responsible for many of the disagreements alluded to above (Stafford Smith and Pickup, 1993; Stafford Smith and Reynolds, 2002).

2.4. CONSEQUENCES

Regardless of the specific amount of area affected, desertification has serious biophysical and socioeconomic consequences. The list of socioeconomic consequences is large, and includes, for example, loss of social capital, an increase in household debt, loss of local customs and traditional environmental knowledge, emigration, and so forth (Zaman, 1997; Fredickson et al., 1998; Latchininsky and Gapparov, 1996; Pamo, 1998; Bollig and Schulte, 1999; Stafford Smith and Reynolds, 2003). From the biophysical point of view the list is equally large, and includes, for example, factors such as the loss of soil and plant cover, a decrease in soil fertility and in biodiversity, a reduction of infiltration in rainfall, and the modification of local climate (Schlesinger et al., 1999; Sharma, 1998; Maestre and Cortina, 2004; Whitford, 1993; Von Handenberger et al., 2001; Reynolds, 2001; Rosenfeld et al., 2001).

However, care must be taken when applying general statements regarding the consequences of desertification to specific situations. For instance, while there is an established view that biodiversity decreases with desertification, a number of recent studies have shown that shrub encroachment into former grasslands in the southwestern United States, a form of desertification (Schlesinger et al., 1990), results in an *increase* in the species richness of birds (Pidgeon et al., 2001), mammals (Whitford, 1997) and ants (Bestelmeyer, 2005). In another example, based on the preliminary results of relatively simple models used over 30 years ago, it has long been conjectured that desertification is responsible for alteration of regional climates. Recent studies challenge this view: while land degradation is accompanied by changes in land-surface properties, which have the potential to influence energy and water balances, Xue and Fennessy (2002) argue that atmosphere–biosphere interactions are much more complex than the situations considered by these simple models, and that other key processes, including interactions between soil moisture, soil texture and structure, albedo and evaporation, are also involved in the alteration of regional climate (see Chapter 6). Improvements in surface models and more realistic changes in land-surface conditions will help improve our understanding of the mechanisms of land–atmosphere interaction and the role of desertification in climate feedbacks (Xue and Fennessy, 2002 Asner and Heidebrecht, 2005).

3. Hydrology and desertification: importance and feedbacks

By definition, drylands are areas where precipitation is so scarce that water is the main factor controlling biological processes (Whitford, 2002). A sound understanding of hydrology is thus essential in order to develop robust management strategies that address both the causes and consequences of land degradation in drylands. In this section, we briefly review some of the unique attributes and processes of drylands and their effects on hydrological functioning and visa versa.

3.1. BIOPHYSICAL LINKS

Rainfall size and frequency—and antecedent soil moisture—is a key driver of plant performance in arid and semi-arid areas (Reynolds et al., 2004). Once rainfall reaches the soil surface, its redistribution is influenced by topography (Puigdefábregas et al., 1999; see also Chapter 7), characteristics of bare soil surfaces (Eldridge et al., 2000; Maestre et al., 2002; see also Chapter 3), and by ecosystem structural attributes such as the number, width and spatial pattern of discrete plant patches (Ludwig and Tongway, 1995). With regard to the latter, in many dryland regions of the world vegetation occurs as a two-phase mosaic, consisting of vegetated patches within a matrix of bare soil (Valentin et al., 1999). The maintenance of these vegetated patches and thus, the overall functioning of the ecosystem, is dependent upon inputs of rainfall and the redistribution of water, sediments and nutrients from bare soil to these discrete patches (Noy-Meir, 1973; Aguiar and Sala, 1999;Reynolds et al., 1997). Such dynamics in two-phase mosaics have been aptly characterized as a series of "sources" (areas of loss) and "sinks" (areas of accumulation), reflecting a myriad of complex interactions between climate, topography, vegetation and soil surface properties.

Because drylands are highly sensitive, any type of disturbance—ranging from *natural* (e.g., reduction in total precipitation, shifts in rainfall seasonality) to *anthropogenic* (roads, plowing, overgrazing, etc.)—that negatively impact key structural components (e.g. plant cover) may initiate a 'cascading' effect on other components and processes, leading to a progressive deterioration of the ecological structure and functioning, and thus promoting desertification processes (Aguiar and Sala, 1999; Von Handerberg et al., 2001; Seguieri and Galle, 1998; Puigdefábregas et al., 1999; Reynolds et al., 1997; Reynolds and Stafford Smith, 2002b).

3.2. SOCIOECONOMIC LINKS

From a socioeconomic point of view, hydrology in drylands is also of paramount importance considering that local and regional water availability affects all aspects of economic prosperity and sustainable development. Hydrology is a major determinant of plant and livestock yield, and thus human impacts—intentional and otherwise—on basic hydrological processes such as infiltration and runoff carry significant implications (Li et al., 2000; Abu-Awwad and Kharabsheh, 2000; Droppelman and Berliner, 2003). This is an especially acute concern in developing countries where the welfare of people is more directly dependent upon the hydrological functioning of local agro-ecosystems (Sharma, 1998). Any disruption in these hydrological processes, which leads to a reduction in water availability, will reduce the capacity of the land to support plant growth and animal production. During early stages of desertification such losses are compensated by the social resilience of the local human populations, especially in developing countries, or by economical inputs from government (Vogel and Smith, 2002). However, when certain thresholds are crossed, social resilience or government subsidies may not be enough to compensate for the loss of productivity. This in turn fuels a multitude of socioeconomic changes, ranging from modifications in trade promoted by lower agricultural production to the migration of large populations of human beings (Fernández et al., 2002).

Many countries are facing increasingly severe reductions in water availability (United Nations, 2003). Whereas drought is a contributing factor, the key long-term drivers are increasing human population growth, extensive land cover change, and rural development. While developed countries are not immune, these drivers are largely characteristic of developing countries, which often fall below sustainable levels of water availability for *both* human populations and natural ecosystems (United Nations, 1997). Although most countries and international programs are logically focused on the human problems of alleviating hunger and poverty associated with limited water, there is a recent, growing concern for the impacts of human appropriation of water on natural ecosystems (Wallace et al., 2003).

Understanding the balance and the complex of feedbacks of “shared water” between society and nature is required to avoid future human water shortages and undesirable environmental impacts (Wallace et al., 2003). This is particularly relevant for developing countries dealing with desertification. In Figure 1, Huber-Sannwald et al. (2005) present an illustration of the numerous connections (direct and indirect) between the *biophysical* (shown as the ‘state of the ecosystem’) and *socioeconomic* (represented as ‘rural livelihoods’) dimensions in a typical rural dryland systems. Within this framework several hydrological functions are depicted, which are crucial elements of both the natural ecosystem (e.g., rainfall, run-off , evaporation) and socioeconomic system (e.g., drinking water, profit from crop yield, water for sanitation). When portrayed in the context of the many feedbacks, linkages, and causal pathways between the biophysical and socioeconomic dimensions, it is evident that hydrology is a fundamental component of the social structure of rural communities.

3.3. FEEDBACK LOOPS

Links between desertification and hydrological processes in drylands are often self-reinforced through complex feedback loops. For instance, Rosenfeld et al. (2001) reported a feedback loop between rainfall and desert dust. Using aircraft and satellite observations, they have shown that small droplets dominate clouds derived from desert dust, and that this leads to a reduced rainfall due to little coalescence of these droplets (see Chapters 8 and 9). The reduction of rainfall promoted by the formation of these desert dust-clouds reduces soil water availability, which in turn raises more dust, thus providing a possible positive feedback to further decrease precipitation and foster desertification in drylands. This feedback loop is initiated by human activities (see Chapter 9), such as overgrazing and cultivation, which tend to expose and disrupt the topsoil, enhancing dust emission from the soil surface (Tegen and Fung, 1995).

Another example of a possible desertification loop is provided by studies evaluating the spatial pattern of the tussock grass *Stipa tenacissima* in semiarid Mediterranean steppes (Figure 2). The two-phase mosaic patterns of vegetation in these areas resemble those of the “tiger bush” vegetation typical of arid and semiarid areas worldwide (Valentin et al., 1999), and are determined by topography and the associated water fluxes (Puigdefábregas and Sánchez, 1996). On moderate slopes, *S. tenacissima* tussocks tend to be aligned parallel to the contours; this maximizes their ability to trap and store water and sediment and gives the appearance of a regular pattern (Puigdefábregas et al., 1999; Webster and Maestre, 2004). As the gradient steepens, the amount of water, nutrients and sediments transported during runoff events increases up to levels that may exceed the ability of existing tussocks to retain them. Under these circumstances, vegetated patches tend to become broken, and stripes develop downslope (Puigdefábregas et al., 1999). As a consequence of this change in the spatial configuration of vegetation, a greater proportion of resources are exported from the system, the quality of the soil in places once occupied by patches drops, and the overall resilience of the system against further runoff events is reduced, fostering erosion and degradation processes (Ludwig and Tongway, 1995). Degradation processes that destroy or modify the number and width of *S. tenacissima* tussocks, such as grazing and fiber cropping, often result in an increased distance between remaining tussocks (Maestre and Cortina, 2004). Such increased distance is negatively related to infiltration at the plot scale (Figure 3), and thus favors the generation of runoff and soil loss. The increase of runoff in the bare ground areas prevent their re-colonization by the tussocks, thus providing a possible feedback to further increase water and sediment loss, and thus desertification.

These examples illustrate how the study of feedbacks between hydrological, ecological and human processes is an essential focus in the integrative discipline of ecohydrology (Eagleson, 2002). This is especially important for studying desertification processes in drylands. Disturbances to the hydrological cycle that result in detrimental changes in ecosystem processes can potentially have severe consequences. For example, a disturbance that triggers gully formation and sediment transport has the potential to self-propagate at remarkably large spatial scales, the result of which is to reshape vast landscapes in semiarid and arid regions (Huber-Sannwald et al., 2005).

4. The Dahlem Desertification Paradigm (DDP): A new look at desertification

4.1. BACKGROUND

Traditional approaches to study desertification in drylands have focused on either the human or the natural dimensions of the problem. Yet, as noted above, desertification encompasses both biophysical and socioeconomic issues and partial approaches are not comprehensive enough to provide an adequate framing of the relevant questions (Reynolds and Stafford Smith, 2002b). In fact, partial approaches have been identified as a major obstacle to improve our abilities to understand and model this complex phenomenon, and to provide land managers and stakeholders with appropriate tools to mitigate their negative effects (Reynolds and Stafford Smith, 2002a). While many useful conceptual, methodological and technological advances have been developed in recent years to improve the assessment and understanding of desertification processes (e.g., Tongway, 1995; de Soyza et al., 1998; Prince et al., 1998; Puigdefábregas and Mendizábal, 1998; Oxley and Lemon, 2003), a comprehensive conceptual framework that embraced both the natural and human dimensions of desertification was lacking.

To fill this gap, an initiative involving the Global Change and Terrestrial Ecosystems (GCTE) and Land Use and Cover Change (LUCC) programs of the International Geosphere-Biosphere Programme (IGBP) was formulated. The intent of this initiative was to bring together researchers from the various global change programs, representing both natural and human-influenced systems, with the objective of stimulating, developing, and refining new ideas to bear on desertification as an important global change concern. Over the course of multiple meetings, conferences and brain-storming sessions, the Dahlem Desertification Paradigm (DDP) evolved from this activity (Reynolds and Stafford Smith, 2002b). In general, many of the constituent ideas contained within the DDP are not necessarily new, but rather, the DDP brings together much of the previous work on this difficult topic in a way that reveals new insights and ultimately may serve as a framework to identify the causes, consequences and extent of desertification.

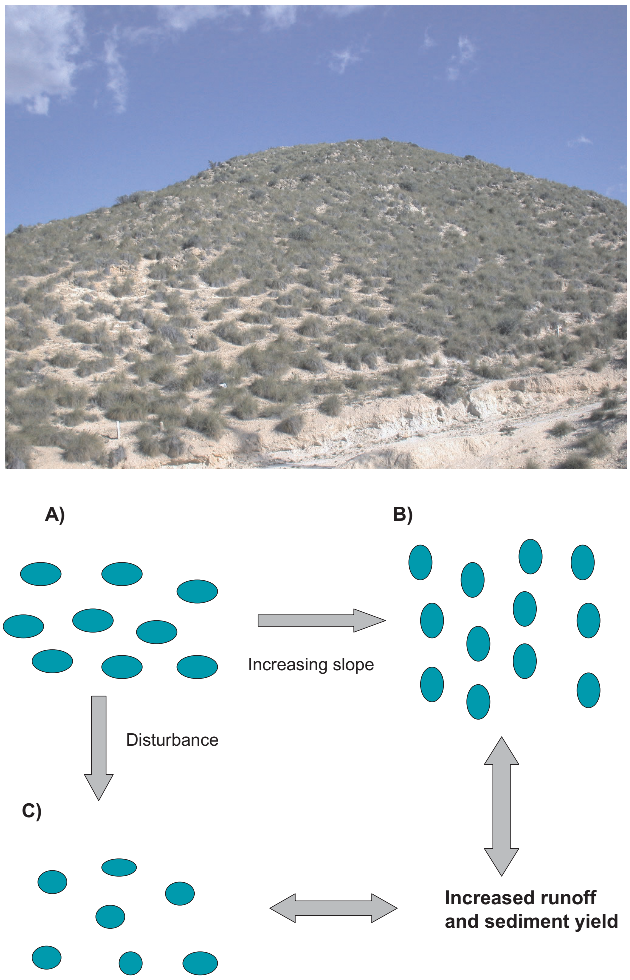

Figure 2. A possible desertification feedback between changes in plant spatial patterns and increased erosion in semiarid Mediterranean steppes dominated by the perennial tussock grass Stipa tenacissima *(upper graph). On moderate slopes,* S. tenacissima *tussocks tend to be aligned parallel to the contours (A). As the gradient steepens, the amount of water, nutrients and sediments transported during runoff events increases up to levels that may exceed the ability of existing tussocks to retain them, and stripes develop downslope (B). Degradation processes that destroy or modify the number and width of* S. tenacissima *tussocks, such as grazing and fiber cropping, may result in an increased distance between remaining tussocks (C). In both cases, the increase of runoff in the bare ground areas prevent their re-colonization by the tussocks, thus providing a possible feedback to further increase water and sediment loss, and thus desertification. Based on Puigdefábregas and Sánchez (1996) and Maestre and Cortina (2004).*

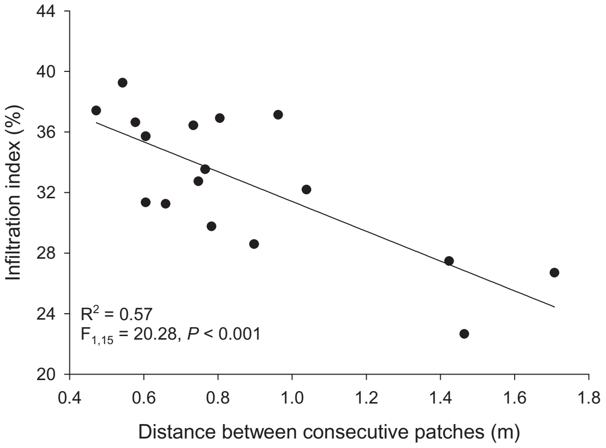

Figure 3. Relationship between the distance between consecutive perennial plant patches and the infiltration index (a surrogate of infiltration rate) in sixteen Stipa tenacissima *steppes located along a degradation gradient in SE Spain. From data reported in Maestre and Cortina (2004).*

4.2. THE DDP

The DDP, presented in detail in Reynolds and Stafford-Smith (2002b), is unique in two ways: i) it attempts to capture the multitude of interrelationships within human-environment systems that cause desertification, within a *single*, synthetic framework; and ii) it is testable, which ensures that it can be revised and improved upon as a *dynamic* framework. The DDP consists on nine assertions (Table 2), which embrace a hierarchical view of desertification in drylands and highlight key linkages between socioeconomic and biophysical systems at different temporal and spatial scales. In general, the DDP can be summarized as follows:

- that an integrated approach to desertification, which simultaneously considers both biophysical and socioeconomic attributes in dryland systems, is essential (assertions #1, #7);
- that the biophysical and socioeconomic attributes that govern or cause land degradation in any particular dryland region are invariably '*slow'* (e.g., soil nutrients) relative to those that are of immediate concern to human welfare (e.g., crop yields, the '*fast'* variables). It is necessary to distinguish these in order to identify the *causes* of land degradation from its *effects* (assertion #2);
- that socio-ecological systems in drylands of the world are *not static* (assertions #3, #6);
- that while change is inevitable, there does exist a *constrained set of ways* in which these socio-ecological systems function, thereby allowing us to understand and manage them (assertion #9);
- that restoring degraded socio-ecological systems to a sustainable state requires outside intervention (assertion #4);
- that socio-ecological systems in drylands of the world are hierarchical (assertion #8). Hence, scale-related concerns abound and desertification itself is a regionally-emergent property of localized degradation (assertion #5).

Table 2. The nine assertions of the Dahlem Desertification Paradigm, and some of their implications. From Stafford Smith and Reynolds (2002).

Assertions	Implications
Assertion 1. Desertification Always Involves Human and Environmental Drivers	Always expect to include both socioeconomic and biophysical variables in any monitoring or intervention scheme
Assertion 2. 'Slow' Variables are Critical Determinants of System Dynamics	Identify and manage for the small set of 'slow' variables that drive the 'fast' ecological goods and services that matter at any given scale
Assertion 3. Thresholds are Crucial, and May Change Over Time	Identify thresholds in the change variables at which there are significant increases in the costs of recovery, and quantify these costs, seeking ways to manage the thresholds to increase resilience
Assertion 4. The Costs of Intervention Rises Non-linearly with Increasing Degradation	Intervene early where possible, and invest to reduce the transaction costs of increasing scales of intervention
Assertion 5. Desertification is a Regionally Emergent Property of Local Degradation	Take care to define precisely the spatial and temporal extent of and processes resulting in any given measure of local degradation. But don't try to probe desertification beyond a measure of generalized impact at higher scales
Assertion 6. Coupled Human-Environment Systems Change over Time	Understand and manage the circumstances in which the human and environmental sub-systems become 'de-coupled'
Assertion 7. The Development of Appropriate Local Environmental Knowledge (LEK) must be Accelerated	Create better partnerships between LEK development and conventional scientific research, employing good experimental design, effective adaptive feedback and monitoring
Assertion 8. Systems are Hierarchically Nested (Manage the Hierarchy!)	Recognize and manage the fact that changes at one level affect others; create flexible but linked institutions across the hierarchical levels, and ensure processes are managed through scale-matched institutions
Assertion 9. A Limited Suite of Processes and Variables at Any Scale Makes the Problem Tractable	Analyze the types of syndromes at different scales, and seek the investment levers which will best control their effects – awareness and regulation where the drivers are natural, changed policy and institutions where the drivers are social

4.3. ARID*NET* RESEARCH NETWORK

The joint GCTE-LUCC initiative on desertification that gave birth to the DDP is embodied within the ARID*net* (Assessment, Research, and Integration of Desertification) research network (http://www.biology.duke.edu/aridnet/). The general objective of this network is to foster the exchange of ideas by facilitating practical, field-level interactions between researchers and stakeholders. ARID*net* is organized into three geographical nodes (Figure 4) and is pursuing four specific tasks:

1) Paradigm-building: By conducting workshops and symposia in different parts of the world, the goal of ARID*net* is to facilitate the development and refinement of the contents of the DDP via the joint participation of the international community of desertification researchers, stakeholders, and policy-makers;

2) Case studies: Working Groups (WG) are being formed to develop case studies based on existing data and specific stakeholders. The WGs are designed to represent a wide range of biophysical-socioeconomic land degradation issues throughout the world. Recently, the first case study was completed in La Amapola, a small rural community located in the surroundings of San Luis Potosí, in the Central Plateau of Mexico (Huber-Sannwald et al. 2005). New studies will be evaluated in forthcoming months;

3) Synthesis. The case studies will be synthesized into a quantitative assessment of what really matters in desertification. This synthesis will especially focus on those interactions between key biophysical and socioeconomic variables; and

4) Network-building. An important goal of ARID*net* is to recruit, and foster the participation, of a diversity of researchers from different fields and countries in the activities of the network.

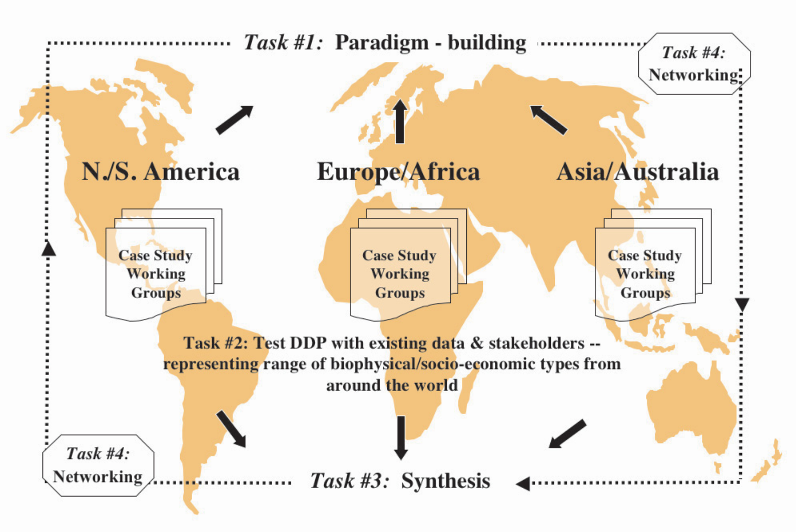

*Figure 4. ARID*net *is organized into three nodes, with four tasks. The development and maintenance of the ARID*net *website (http://www.biology.duke.edu/aridnet/) is currently underway to support these tasks.*

5. Concluding remarks

5.1. STEPWISE MODEL OF LAND DEGRADATION INCORPORATING HYDROLOGY

The DDP (Table 2) suggests that the process of chronic land degradation is directional, i.e. that it increases in severity, surpassing numerous thresholds along the way involving both biophysical (e.g., ecology, hydrology) and socioeconomic (income, hunger, customs, etc) variables, eventually reaching an irreversible (potentially) set of conditions. In this section we present a final example (modified from Reynolds 2001) that includes the ideas underlying the DDP and that focuses on a hypothetical instance of land degradation of rangelands in which grazing-induced desertification is a stepwise phenomena, and the potential for recovery *at any given step* is related to the function of the affected component. Some of the key processes and variables involved in this conceptual model are summarized in Table 3. The human dimensions component emphasizes management options and that part of the ecosystem specifically targeted for management.

Table 3. Proposed stepwise degradation of landscape, driven mainly by overgrazing, illustrating key biophysical and socioeconomic factors involved. Symptoms characterize the state of plant and animal assemblages; management options refer to actions to improve the condition of the landscape; and management "target" refers to where management could be focused. A system threshold (see Assertion #3, Table 2) may be somewhere between steps 2-4. Based on conceptual model for stepwise degradation of arid and semiarid rangelands by Milton et al. (1994) as modified by Reynolds (2001).

Step	**Biophysical Factors**		**Socioeconomic Factors**	
No.	**Ecological**	**Hydrological**	**Management Options**	**Management Targets**
0	Biomass and composition of vegetation varies with weather; Adequate drinking water	Hydrologically functional landscape; High infiltration, low runoff	Adaptive management Education/Out-reach Education at household level is crucial	Household Community
1	Herbivory reduces palatable plants and modifies plant demography; Increase in exotic or undesirable species	The proportion of bare soil increases	Strict grazing controls (rotation schemes, intensity, type of animals, etc.)	Secondary producers
2	Plant species that fail to recruit are lost, as are their specialized predators and symbionts reduced primary and secondary productivity	Formation of erosion cells	Manage vegetation (e.g., seeding, plant removal); removal of livestock; culling abundant herbivores	Primary and secondary producers
3	Biomass and productivity of vegetation fluctuates as ephemerals benefit from lost of perennial cover; Perennial biomass reduced (short-lived plants and instability increase), resident birds decrease; dominant vegetation: annual weeds, exotic perennials	Signs of hydrologic dysfunctionality; Changes in surface albedo and soil moisture; Formation of erosion gullies	Manage soil cover (e.g., mulching, erosion barriers, roughen soil surface)	Physical environment
4	Denudation of all vegetation cover; changes in ecosystem structure and function; Inadequate drinking water	Hydrologically dysfunctional landscape; lots of bare soil; Accelerated wind erosion; Aridification; Soil salinization, large gullies, low infiltration	Only large amounts of external funding could have any impact (Assertion #4, Table 2)	Physical environment

At step zero, the landscape is hydrologically functional, that is, it is characterized by high infiltration rates, low runoff, no erosion, high vegetative cover and so forth. As Reid et al. (1999) note, a fully functional landscape is one in which only very small part of the water and nutrients that enter the system are subsequently lost. Runoff is redistributed within the system but not lost. In contrast, a significant portion of water and other resources are lost in a dysfunctional landscape because the patches of vegetation are too spotty or low in number to trap surface runoff (see Section 3.1). The type of management that might be used at this step is mostly linked to educational activities. Annual changes in biomass and composition of vegetation vary as a function of natural climatic cycles and stochastic events (e.g, fire, drought, diseases). An understanding of the relationships between these processes can be used effectively as a management tool and thus we believe education is a crucial factor at this stage since the farmer or rancher is able to exert formable control over the landscape *prior* to it becoming highly degraded. For example, a rancher can change livestock densities (secondary producers) depending upon range conditions (see Vogel and Smith, 2002 for a number of examples of how management at this level can be highly effective, requiring no outside intervention).

The first step of ecological degradation concerns a decline in the native plant populations since those species are the ones most frequently defoliated by grazers, whereas toxic or distasteful plants (generally unaffected by grazers) are able to establish. The type of management that might be used at this step (shifting or varying the grazing season, stocking intensity, animal type) is a function of the type of objective (e.g., game viewing, meat production) and vegetation type (annual or perennial grassland, shrubland, savanna). The second step in land degradation involves a decrease in plant and animal productivity and signs of telling signs of changing hydrology. The challenge for resource managers is to identify threshold conditions in the local area with high potential to lead to formation of phenomena as erosion cells, rapid deep drainage losses, excessive lateral-flow, and so forth. For example, Pickup (1985) describes how erosion cells initially form once the vegetation in a particular area is denuded: high impact of rainfall tends to scour the soil surface, leading to the movement of water and sediment out of the bare area, and into adjacent ones. One started, such changes led to conditions that tend to facilitate further changes. Reversal of degradation at this stage is usually not cost-effective, particularly in regions where it might involve removal of domestic livestock, culling of other abundant herbivores, and manipulating the vegetation (reseeding, herbicide treatments, bush-cutting, etc.).

The third step involves processes associated with the reduction of perennial plant vegetation cover and an increase in ephemeral and weedy species. This includes accelerated wind and water erosion and various land surface impacts, such as increased albedo, surface temperatures, reduced soil moisture storage, and cloudiness. Once a rangeland reaches this condition, conditions are not suitable for the rancher to make profits and restoration necessarily must focus on the physical environment, e.g., reducing erosion, increasing water infiltration, protecting the soil surface from sun and frost, and creating microsites suitable for the establishment of perennial seedlings. This is costly, and requires outside intervention. Whisenant (1999) describe a number of examples of restoration approaches (ranging from low- to high-tech) that address this level of degradation. Their probability of success is highly variable and strongly coupled to abiotic conditions (Maestre et al., 2003). However, it can be improved by incorporating recent advances in our knowledge of dryland ecosystem structure, functioning and dynamics into restoration actions (Tongway and Ludwig, 1996; Ludwig and Tongway, 1996; Maestre et al., 2001; Maestre and Cortina, 2004).

The final step in the degradation process is characterized by a complete loss of vegetation cover, accelerated erosion, and soil salinization: a true 'human-made' desert that is hydrologically dysfunctional. Such rangelands are usually abandoned due to the high costs of—and low probably of successful—restoration and rehabilitation.

Whereas viewing land degradation as a directional process is an oversimplification, it is useful for showing how different factors are involved at different stages of degradation and how the various assertions of the Dahlem Desertification Paradigm (DDP) can be linked to real-world examples. Furthermore, this example also points out that rational decision-making based on an integrated view of the problem is necessary.

5.2. RESEARCH NEEDS

In this chapter we have emphasized that both biophysical components and the socioeconomic activities of human beings are necessarily involved in desertification processes, both as causal agents and as actors suffering its consequences. For example, in Figure 1 we identify some key components of hydrology in dryland systems that depicts some of the key interrelationships between the biophysical and socioeconomic dimensions in rural dryland communities. The simplified, stepwise model of land degradation (as depicted in Figure 5) highlights the enormous degree of complexity and importance of desertification (Puigdefábregas, 1998; Reynolds and Stafford Smith, 2002b; Geist and Lambin, 2004). As a coupled biophysical and socioeconomic process, researchers and policy-makers are increasingly sensitive to the necessity of examining both dimensions *simultaneously*. To do so requires multi-scaled, multidisciplinary approaches.

Although it is an enormous challenge—involving the building the bridges to improve communication among scientists across disciplines and establishing multidisciplinary collaborations—the potential rewards are equally large: this will undoubtedly advance our understanding of this complex, problematic phenomenon.

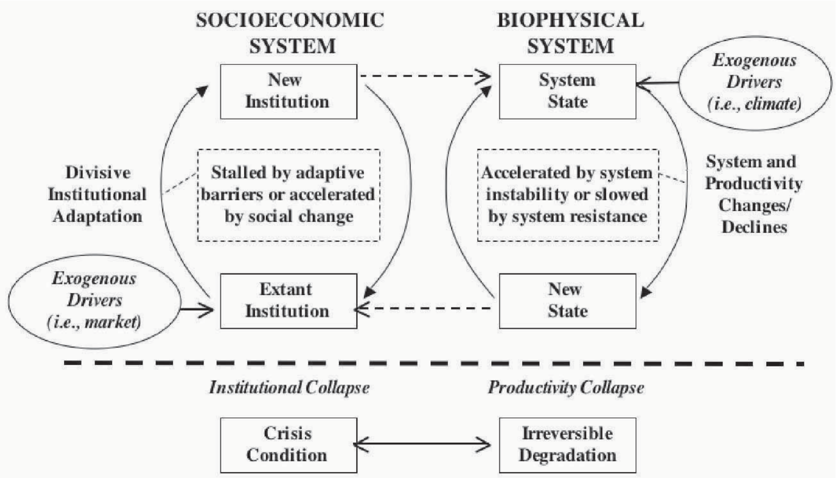

Figure 5. Balance between natural and social systems is key to understanding land degradation in drylands. We suggest that the systems are not static and that, even under conditions of dramatic change and uncertainty, sustainable land use is possible when environmental change and institutional adaptation are synchronous, that is, when the rate of change and spatial overlap in the human and environmental systems are matched. Accelerated environmental change and decelerated and uncoordinated community adaptation can together lead to social crisis and irreversible environmental degradation (Modified from Robbins et al. 2002).

There is an enormous body of empirical evidence and case studies on the drivers and consequences of desertification. However, not surprisingly the overwhelming majority of these focus on either the natural or social sciences. In the long-term, we are confident that this will change. For example, the new Global Land Project (GLP; Details at: http://www.nrel.colostate.edu/projects/glp.colostate.edu/), a joint research project for land systems of the IGBP and the International Human Dimensions Programme, emphasizes the study of coupled human-environment systems. The aforementioned ARID*net* project (Section 4.3) is an excellent example of such interdisciplinary collaboration. While surprisingly few quantitative syntheses of desertification data (e.g., Geist, 2004; Geist and Lambin, 2004) have been previously conducted, these new programs (and others) will undoubtedly stimulate future syntheses to identify the causal drivers of desertification, to evaluate the effectiveness of the different actions taken to combat it, and to identify areas in need of further research.

Our brief overview outlining the role of hydrological processes on desertification suggests that future studies should pay particular attention to the feedbacks between hydrological processes and both ecosystem structure and human activities, especially in those cases when feedbacks are amplifying those processes leading to desertification. Understanding these feedbacks is of crucial importance in order to establish appropriate management measures to reverse them, and thus should be a core topic for future research in the area.

5.3. FUTURE DIRECTIONS

In this chapter we have described the Dahlem Desertification Paradigm (DDP) as a tool to aid in developing a synthetic framework for tackling the enormous problem of dryland degradation (Section 4.2). Undoubtedly, we must recognize the simultaneous roles of—and complex feedbacks between—the meteorological, ecological, and human dimensions of land degradation and recognize that in the past, a failure to do so slowed progress.

There is an immediate need at all levels (local, regional, national, international) for policy decisions on how to identify, prevent and/or adapt to desertification and land degradation in general. It is essential to move beyond isolated studies of various parts of the desertification problem and to work through the causal links of dryland land degradation, from climate dynamics to ecological impacts to policy response strategies, and to span a wide range of temporal and spatial scales, from small geographical units to larger regions. The DDP is able to incorporate our state-of-the-art knowledge about the detection, prevention and consequences of desertification and is flexible enough to embrace specific concerns—such as hydrology in this chapter—enabling us to better understand linkages and interactions between biophysical and socioeconomic issues. Through rigorous testing and refinement (Section 4.3), it is our hope that the DDP framework will continue to evolve by incorporating new ideas and approaches in order to explore the full suite of quantitative as well as qualitative interactions between the various elements of the problem.

Although the DDP is new, an international network (Section 4.3; Figure 4) is facilitating research to refine and test its core principles via multiple case studies throughout the world. These case studies will be selected from a wide range of biophysical and socioeconomic conditions and, in time, will help advance our understanding of desertification. It will be particularly useful to bring new ideas to the long-standing debate and controversies surrounding desertification (e.g., Section 2.2). Ultimately, it is the job of researchers to assist policy-makers and land managers to develop useful and straightforward—but at the same time, powerful and robust—tools that can be readily employed to deal with the complex topic of desertification in drylands.

6. Acknowledgements

This research was supported, in part, by National Science Foundation under Grant No. 0234186 (ARID*net*) and the Center for Integrated Study of the Human Dimensions of Global Change, through a cooperative agreement between the National Science Foundation (SBR-9521914) and Carnegie Mellon University. FTM acknowledges support via a Fulbright fellowship from the Spanish Ministry of Education and Science, funded by Secretaría de Estado de Universidades and Fondo Social Europeo. JFR acknowledges partial support by the research award (Humboldt-Forschungspreis) of the Humboldt Foundation (Bonn). Financial support to distribute free copies of the book, *Global Desertification: Do Humans Cause Deserts?* (Reynolds and Stafford Smith, eds., Berlin: Dahlem Workshop Report 88, 2002, Dahlem University Press) to colleagues in developing countries is provided by GCTE, LUCC, CIS-HDGC, and Environment Australia. We thank all of our colleagues for access to their work and for their contributions to these ideas.

7. References

Abu-Awwad A.M., and A. A. Kharabsheh. 2000. Influence of supplemental irrigation and soil surface furrowing on barley yield in arid areas affected by surface crust. J. Arid Environ. 46: 227-237.

Aguiar M.R., and O.E. Sala. 1999. Patch structure, dynamics and implications for the functioning of arid ecosystems. Trends Ecol. Evol. 14: 273-277.

Asner G.P., and K.B. Heidebrecht. 2005. Desertification alters regional ecosystem-climate interactions. Global Change Biol. 11: 182-194.

Batterbury S.P.J., R.H. Behnke, P.M. Döll, J.E. Ellis, P.A. Harou, T.J.P. Lynam, A. Mtimet, S.E. Nicholson, J.A. Obando, and J.B. Thornes. 2002. Responding to desertification at the national scale: detection, explanation, and responses. In: Global Desertification: Do Humans Cause Deserts?, J.F. Reynolds and D.M. Stafford Smith, eds. Dahlem University Press, Berlin, 357-386.

Bestelmeyer B.T. 2005. Does desertification diminish biodiversity? Enhancement of ant diversity by shrub invasion in south-western USA. Divers. Distrib. 11: 45-55

Bollig M, and A. Schulte. 1999. Environmental change and pastoral perceptions: Degradation and indigenous knowledge in two African pastoral communities. Human Ecol. 27:493-514.

Clarke R., R. Lamb, and D.R. Ward (eds.). 2002. Global Environmental Outlook 3. Past, present and future perspectives. London: Earthscan publications.

Darkoh M.B.K. 1998. The nature, causes and consequences of desertification in the drylands of Africa. Land Degrad. Devel. 9:1-20

de Soyza A, W.G. Whitford, J.E. Herrick, J.W. Van Zee, and K.M. Havstad. 1998. Early warning indicators of desertification: examples of tests in the Chihuahuan Desert. J. Arid Environ. 39: 101-112.

Dregne H.E. 1996. Desertification: challenges ahead. Ann. Arid Zone 35: 305-311.

Droppelmann K., and P. Berliner. 2003. Runoff agroforestry-a technique to secure the livelihood of pastoralists in the Middle East. J. Arid Environ. 54: 571-577.

Eagleson, P.S. 2002. Ecohydrology. Darwinian Expression of Vegetation Form and Function. Cambridge: Cambridge University Press.

Eldridge D.J., E. Zaady, and M. Shachak. 2000. Infiltration through three contrasting biological soil crusts in patterned landscapes in the Negev, Israel. Catena 40: 323-336.

Fernández R.J., E.R.M. Archer, A.J. Ash, H. Dowlatabadi, P.H.Y. Hiernaus, J.F. Reynolds, C.H. Vogel, B.H. Walker, and T. Wiegand. 2002. Degradation and recovery in socioecological systems: a view from the household/farm level. In: Global Desertification: Do Humans Cause Deserts?, J.F. Reynolds and D.M. Stafford Smith, eds. Dahlem University Press, Berlin, 297-324.

Fredrickson E., K.M. Havstad, R. Estell, and P. Hyder. 1998. Perspectives on desertification: South-western United States. J Arid Environ. 39: 191-207.

Geist H.J. 2004. The Causes and Progression of Desertification. Burlington: Ashgate.

Geist H.J., and E.F. Lambin. 2004. Dynamic causal patterns of desertification. BioScience 54: 817-829.

Grainger A. 1992. Characterization and assessment of desertification processes. In: Desertified Grasslands: Their Biology and Management, Linnean Society Symposium Series, No. 13, ed. G.P. Chapman. Academic Press, London, 17-33.

Hellden U. 1991. Desertification −time for an assessment? Ambio 20: 372–383.

Huber-Sannwald E., F.T. Maestre, J. Herrick, and J.F. Reynolds. 2005. In Press. Applying a new desertification paradigm linking biophysical and socioeconomic elements: the Amapola, Mexico case study. Hydrol. Proc. (in press).

Kassas M. 1995. Desertification: a general review. J Arid Environ 30: 115-128.

Latchininsky A., and F.A. Gapparov. 1996. Consequences of the Aral sea's drying up on the regional locust situation. Secheresse 7: 109-113.

Le Houérou H.N. 1996. Climate change, drought and desertification. J. Arid Environ. 34: 133-185.

Li, X.Y., J.D. Gong, and X.H. Wei. 2000. In-situ rainwater harvesting and gravel mulch combination for corn production in the dry semi-arid region of China. J. Arid Environ. 46: 371-382.

Ludwig J.A., and D.J. Tongway. 1995. Spatial organization of landscapes and its function in semi-arid woodlands, Australia. Landscape Ecol. 10: 51-63.

Ludwig, J.A., and D.J. Tongway. 1996. Rehabilitation of semiarid landscapes in Australia. II. Restoring vegetation patches. Restor. Ecol. 4: 398-406.

Maestre F.T., S. Bautista, J. Cortina, and J. Bellot. 2001. Potential for using facilitation by grasses to establish shrubs on a semiarid degraded steppe. Ecol Appl 11: 1641-1655 .

Maestre F.T., and J. Cortina. 2004. Insights into Ecosystem Composition and Function in a Sequence of Degraded Semiarid Steppes. Restor. Ecol. 12: 494-502.

Maestre F.T., J. Cortina, S. Bautista, J. Bellot, and R. Vallejo. 2003. Small-scale environmental heterogeneity and spatiotemporal dynamics of seedling establishment in a semiarid degraded ecosystem. Ecosystems 6: 630-643.

Maestre F.T., M.T. Huesca, E. Zaady, S. Bautista, and J. Cortina. 2002. Infiltration, penetration resistence and microphytic crust composition in contrasted microsites within a Mediterranean semi-arid steppe. Soil Biol. Biochem. 34: 895-898.

Mainguet M. 1991. Desertification, natural background and human mismanagement. Berlin: Springer-Verlag.

Middleton N.J., and D.S.G. Thomas (eds.). 1997. World Atlas of Desertification. New York: U.N. Environment Programme, Edward Arnold.

Milton S.J., W.R.J. Dean, M.A. Duplessis, and W.R. Siegfried. 1994. A conceptual model of arid rangeland degradation - The escalating cost of declining productivity. BioScience 44: 70-76.

Nicholson, S.E., C.J. Tucker, and M.B. Ba. 1998. Desertification, drought and surface vegetation: an example from the West African Sahel. Bull. Am. Meteorol. Soc. 79:815–829

Noy-Meir I. 1973. Desert ecosystems: environment and producers. Ann. Rev. Ecol. System. 4: 25-51.

Oxley T., and M. Lemon M. 2003. From social-enquiry to decision support tools: towards an integrative method in the Mediterranean rural environment. J. Arid Environ. 54: 595-617.

Pamo E.T. 1998. Herders and wildgame behaviour as a strategy against desertification in northern Cameroon. J. Arid Environ. 39:179-190.

Pickup G. 1985. The erosion cell - a geomorphic approach to landscape classification in range assessment. Aust. Rangeland J. 7: 114-21.

Pidgeon A.M., N.E. Mathews, R. Benoit, and E.V. Nordheim. 2001. Response of avian communities to historic habitat change in the northern Chihuahuan Desert. Cons. Biol. 15: 1772-1788.

Prince S.D., E.B. de Colstoun, and L.L. Kravitz. 1998. Evidence from rain-use efficiencies does not indicate extensive Sahelian desertification. Global Change Biol. 4:359-374.

Puigdefábregas J. 1998. Ecological impacts of global change on drylands and their implications for desertification. Land Degrad. Devel. 9: 393–406.

Puigdefábregas J., and Sánchez G. 1996. Geomorphological implications of vegetation patchiness on semi-arid slopes. In: Advances in Hillslope Processes, volume 2, eds. M.G. Anderson and S.M. Brooks, John Willey and Sons, London, 1027-1060.

Puigdefábregas J., A. Solé-Benet, L. Gutiérrez, G. Del Barrio, and M. Boer. 1999. Scales and processes of water and sediment redistribution in drylands: results from the Rambla Honda field site in Southeast Spain. Earth-Sci. Rev. 48: 39-70.

Puigdefábregas J., and T. Mendizábal. 1998. Perspectives on desertification: western Mediterranean. J. Arid Environ. 39: 209-224.

Reid K.D., B.P. Wilcox, D.D. Breshears, and L. MacDonald. 1999. Runoff and erosion in a pinon-juniper woodland: Influence of vegetation patches. Soil Sci. Soc. Am. J. 63:1869-1879.

Reynolds J.F., P.R. Kemp, K. Ogle, and R.J. Fernández. 2004. Modifying the "pulse-reserve" paradigm for deserts of North America: precipitation pulses, soil water, and plant responses. Oecologia 141: 194-210.

Reynolds J.F. 2001. Desertification. In: Encyclopedia of Biodiversity, Volume 2, ed. S. Levin. Academic Press, San Diego, 61-78.

Reynolds, J.F., and D. M. Stafford Smith. 2002a. Do humans cause deserts? In: Global Desertification: Do Humans Cause Deserts?, J.F. Reynolds and D.M. Stafford Smith, eds. Dahlem University Press, Berlin, 1-21.

Reynolds, J.F., and D. M. Stafford Smith, editors. 2002b. Global Desertification: Do Humans Cause Deserts? Berlin: Dahlem University Press.

Reynolds, J.F., D.M. Stafford Smith, and E.F. Lambin. 2003. ARIDnet: Seeking novel approaches to desertification and land degradation. IGBP Global Change Newsletter 54: 5-9 (PDF available at: http://www.igbp.kva.se).

Reynolds, J.F., R.A. Virginia, and W.H. Schlesinger. 1997. Defining functional types for models of desertification. In: Plant Functional Types: Their Relevance to Ecosystem Properties and Global Change, T.M. Smith, H.H. Shugart, and F.I. Woodward, eds. Cambridge University Press, Cambridge, 194-214.

Robbins, P.F., N. Abel, H. Jiang, M. Mortimore, M. Mulligan, G.S. Okin, D.M. Stafford Smith, and B.L. Turner II. 2002. Desertification at the community scale: Sustaining dynamic human-environment systems. In: Global Desertification: Do Humans Cause Deserts?, J.F. Reynolds and D.M. Stafford Smith, eds. Dahlem University Press, Berlin, 325-356.

Rosenfeld D., Y. Rudich, and R. Lahav. 2001. Desert dust suppressing precipitation: A possible desertification feedback loop. Proc. Natl. Acad. Sciences USA 98:5975-5980.

Schlesinger W.H., A.D. Abrahams, A.J. Parsons, and J. Wainwright. 1999. Nutrient losses in runoff from grassland and shrubland habitats in Southern New Mexico: I. rainfall simulation experiments. Biogeochemistry 45: 21-34.

Schlesinger W.H., J.F. Reynolds, G.L. Cunningham, L.F. Huenneke, W.M. Jarrell, R.A. Virginia, and W.G. Whitford. 1990. Biological feedbacks in global desertification. Science 247: 1043-1048.

Seghieri J., and S. Galle. 1999. Run-on contribution to a Sahelian two-phase mosaic system: Soil water regime and vegetation life cycles. Acta. Oecol. 20: 209-217.

Sharma K.D. 1998. The hydrological indicators of desertification. J. Arid Environ. 39:121-132.

Stafford Smith D.M., and G. Pickup. 1993. Out of Africa, looking in: understanding vegetation change. In: Range Ecology at Disequilibrium: New Models of Natural Variability and Pastoral Adaptation in African Savannas R.H. Behnke, I. Scoones, and C. Kerven (eds.). Overseas Development Institute and International Institute for Environment and Development, London, 196-244.

Stafford Smith D. M., and J. F. Reynolds. 2002. The Dahlem Desertification Paradigm: A new approach to an old problem. In: Global Desertification: Do Humans Cause Deserts?, J.F. Reynolds and D.M. Stafford Smith, eds. Dahlem University Press, Berlin, 403-424.

Stafford Smith D.M., and J.F. Reynolds. 2003. The interactive role of human and environmental dimensions in the desertification debate. Ann. Arid Zone 42: 255-270.

Tegen I., and I. Fung. 1995. Contribution to the atmospheric mineral aerosol load from land surface modification. J Geophys. Res. 100:18707–18726.

Thomas D.S.G. 1997. Science and the desertification debate. J. Arid Environ. 37:599-608.

Thomas D.S.G., and N.J. Middleton. 1994. Desertification: exploding the myth. Chichester: John Wiley and Sons.

Tongway D.J. 1995. Monitoring soil productive potential. Environ. Monit. Assessment 37: 303–318.

Tongway D.J., and J.A. Ludwig. 1996. Rehabilitation of semiarid landscapes in Australia. I. Restoring productive soil patches. Restor. Ecol. 4: 388-397.

Tucker C.J., H.E. Dregne, and W.W. Newcomb. 1998. Expansion and contraction of the Sahara desert from 1980 to 1990. Science 253: 299–301.

Tucker C.J., and S.E. Nicholson. 1998. Variations in the size of the Sahara desert from 1980 to 1997. Ambio 28:587 591.

United Nations. 1997. Report of the Secretary General: Comprehensive Assessment of the Freshwater Resources of the World. New York: United Nations.

United Nations. 2003. Water for People, Water for Life. World Water Development Report. Barcelona: UNESCO Publishing.

UNCCD. 1994. United Nations Convention to Combat Desertification, Intergovernmental Negotiating Committee For a Convention to Combat Desertification, Elaboration of an International Convention to Combat Desertification in Countries Experiencing Serious Drought and/or Desertification, Particularly in Africa. U.N. Doc. A/AC.241/27, 33 I.L.M. 1328. New York: United Nations.

UNCCD. 2000. Fact Sheet 2: The Causes of Desertification. United Nations Secretariat of the Convention to Combat Desertification http://www.unccd.int/publicinfo/factsheets/showFS. php?number=2 [Geo-2-171].

UNEP. 1992. United Nations Environmental Programme, World Atlas of Desertification. Editorial commentary by N. Middleton and D.S.G. Thomas. London: Edward Arnold Publishers.

Valentin C., J.M. d Herbes, and J. Poesen. 1999. Soil and water components of banded vegetation patterns. Catena 37: 1-24.

Verstraete M.M. 1986. Defining desertification: a review. Clim. Change 9:5 18.

Vogel C.H., and J. Smith. 2002. Building social resilience in arid ecosystems. In: Reynolds JF, Stafford Smith DM (eds) Global Desertification: Do Humans Cause Deserts? Dahlem University Press, Berlin, pp 149-166

von Hardenberg J., E. Meron, M. Shachak, and Y. Zarmi. 2001. Diversity of vegetation patterns and desertification. Phys. Rev. Lett. 87: 198101-1-198101-4.

Wallace J.S., M.C. Acreman, and C.A. Sullivan. 2003. The sharing of water between society and ecosystems: from conflict to catchment-based co-management. Philos. Trans. R. Soc. Lond. B - 358:2011-2026.

Webster R., and F.T. Maestre. 2004. Spatial analysis of semi-arid patchy vegetation by the cumulative distribution of patch boundary spacings and transition probabilities. Environ. Ecol. Stat. 11: 257-281.

Whisenant S.G. 1999. Repairing damaged wildlands. Cambridge: Cambridge University Press.

White R., D. Tunstall, and N. Henninger. 2003. An Ecosystem Approach to Drylands: Building Support for New Development Policies. World Resources Institute, EarthTrends Publication Series. Available online: http://earthtrends.wri.org/features/view_feature.cfm?fid=37andtheme=39.

Whitford W.G. 1993. Animal feedbacks in desertification: An overview. Rev. Chil. Hist. Nat. 66: 243-251.

Whitford W.G. 1997. Desertification and animal biodiversity in the desert grasslands of north America. J. Arid Environ. 37: 709-720.

Whitford W. G. 2002. Ecology of desert systems. London: Academic Press.

Xue, Y., and M. J. Fennessy. 2002. Under what conditions does land cover change impact regional climate? In: Global Desertification: Do Humans Cause Deserts?, J.F. Reynolds and D.M. Stafford Smith, eds. Dahlem University Press, Berlin, 59-74.

Zaman S. 1997. Effects of rainfall and grazing on vegetation yield and cover of two arid rangelands in Kuwait. Environ. Cons. 24: 344-350.

Contributors

John D. Albertson, Department of Civil and Environmental Engineering, Duke University, Hudson Hall, Durham, NC 27708, USA (john.albertson@duke.edu).

Samuel Alleaume, Centre d'Etudes Biologiques de Chizé, B.P. 14, 79360 Beauvoir sur Niort, FRANCE (alleaume@cebc.cnrs.fr).

John E. Barrett, Department of Environmental Studies, Dartmouth College, Hanover, NH 03755, USA (John.E.Barrett@dartmouth.edu).

Ingrid C. Burke, Department of Forest, Range and Watershed Stewardship, Colorado State University, Fort Collins, CO 80523, USA (indy@cnr.colostate.edu).

Carlo Camporeale, Dipartimento di Idraulica, Trasporti ed Infrastrutture Civili, Politecnico di Torino, Corso Duca degli Abruzzi, 24, 10129, Turin, Italy (carlo.camporeale@polito.it).

Kelly K. Caylor, Department of Civil and Environmental Engineering, Princeton University, Princeton, NJ 08540 USA. email: kcaylor@princeton.edu.

Justin F. Costelloe, Department of Civil and Environmental Engineering and CRC for Catchment Hniversity, Coupure links 6ydrology, University of Melbourne, Victoria, Australia.

Wim M. Cornelis, International Centre for Eremology, Department of Soil Management and Soil Care, Ghent U53,B-9000 Ghent, Belgium (wim.cornelis@UGent.be).

Paolo D'odorico, Department of Environmental Sciences, University of Virginia, 291 McCormick Road, Charlottesville, VA 22903-4123, USA (paolo@virginia.edu).

Howard E. Epstein, Department of Environmental Sciences, University of Virginia, 291 McCormick Road, Charlottesville, VA 22903-4123, USA (hee2b@virginia.edu)

Andrew S. Goudie, School of Geography and the Environment, University of Oxford, Mansfield Road, Oxford, OX1 3TB, United Kingdom (andrew.goudie@stx.ox.ac.uk).

Rodger Grayson, Department of Civil and Environmental Engineering and CRC for Catchment Hydrology, University of Melbourne, Victoria, Australia (rodger@civenv.unimelb.edu.au).

Christelle Hély, Centre Européen de Recherche et d'Enseignement des Géosciences de l'Environnement, Europôle de l'Arbois, B.P. 80, 13545 Aix-en- Provence Cedex 04, France (hely@cerege.fr).

Feff Herrick, USDA-ARS Jornada Experimental Range MSC 3JER, Box 30003 NMSU Las Cruces, NM 88003-8003, USA (jherrick@nmsu.edu).

Jan W. Hopmans, Hydrology, Department of Land, Air and Water Resources, 123 Veihmeyer Hall, University of California, Davis, CA, 95616, USA (jwhopmans@ucdavis.edu).

Elisabeth Huber-Sannwald, Dpto. Ingenieria Ambiental y Manejo de Recursos Naturales, Instituto Potosino de Investigacion Cientifica y Tecnologica (IPICYT), Apdo. Postal 3-74 Tangamanga 78231, San Luis Potosi, SLP, Mexico (ehs@ipicyt.edu.mx).

Durga D. Kandel, Department of Civil and Environmental Engineering and CRC for Catchment Hydrology, University of Melbourne, Victoria, Australia (ddkandel@civenv.unimelb.edu.au).

William K. Lauenroth, Department of Forest, Range and Watershed Stewardship, Colorado State University, Fort Collins, CO 80523, USA (Billl@cnr.colostate.edu).

Deborah Lawrence, Department of Environmental Sciences, University of Virginia, 291 McCormick Road, Charlottesville, VA 22903-4123, USA (lawrence@virginia.edu).

LEONARDO LOMBARDINI, Department of Horticultural Sciences, Texas A&M University, TAMU 2133, College Station, TX 77843, USA (l-lombardini@tamu.edu).

FERNANDO T. MAESTRE, Unidad de Biodiversidad y Conservacion, E.S.C.E.T., Universidad Rey Juan Carlos, C/ Tulipan s/n, Mostoles, Spain (maestre@duke.edu).

STAFANO MANZONI, Department of Civil and Environmental Engineering, Duke University, Hudson Hall, Durham, NC 27708, USA (stefano.manzoni@duke.edu).

FRANZ X. MEIXNER, Biogeochemistry Department, Max Planck Institute for Chemistry, J.J.v. Becherweg 27, D-55128 Mainz, Germany (meixner@mpch-mainz.mpg.de).

NICOLA MONTALDO, Dipartimento di Ingegneria Idraulica, Ambientale, e del Rilevamento, Politecnico di Milano, Piazza Leonardo da Vinci 32, 20133 Milano, Italy (Nicola.Montaldo@polimi.it).

JOSÉ M. PARUELO, Facultad de Agronomía, Universidad de Buenos Aires, Ciudad de Buenos Aires, Argentina (paruelo@agro.uba.ar).

PAOLO PERONA, Institute of Hydromechanics and Water Resources Management, ETH Hönggerberg, W. Pauli Strasse 15, 8093, Zurich, Switzerland (perona@ihw.baug.ethz.ch).

GERVASIO PINEIRO, Facultad de Agronomía, Universidad de Buenos Aires, Ciudad de Buenos Aires, Argentina (pineiro@ifeva.edu.ar).

AMILCARE PORPORATO, Department of Civil and Environmental Engineering, Duke University, Hudson Hall, Durham, NC 27708, USA (amilcare@duke.edu).

LARISSA READ, Intermountain Support Office, National Park Service, 12795 W. Alameda Parkway, Lakewood, CO, 80228 (larissa_read@nps.gov).

JAMES F. REYNOLDS, Division of Environmental Science and Policy, Nicholas School of the Environment and Earth Science, Duke University, Durham, NC 27708-90340, USA (james.f.reynolds@duke.edu).

LUCA RIDOLFI, Dipartimento di Idraulica, Trasporti ed Infrastrutture Civili, Politecnico di Torino, Corso Duca degli Abruzzi, 24, 10129, Turin, Italy (ridolfi@polito.it).

TODD M. SCANLON, Department of Environmental Sciences, University of Virginia, 291 McCormick Road, Charlottesville, VA 22903-4123, USA (tms2v@virginia.edu).

HERMAN H. SHUGART, Department of Environmental Sciences, University of Virginia, 291 McCormick Road, Charlottesville, VA 22903-4123, USA (hhs@virginia.edu).

MARK STAFFORD SMITH, Desert Knowledge Cooperative Research Centre, P.O. Box 2111, Alice Springs, NT 0871, Australia (mark.staffordsmith@csiro.au).

J. SCOTT TURNER, Department of Environmental & Forest Biology, SUNY College of Environmental Science & Forestry, Syracuse, NY 13159, USA (jsturner@mailbox.syr.edu).

YONGKANG XUE, Department of Geography, Department of Atmospheric and Oceanic Sciences, University of California, Los Angeles, CA 90095-1524, USA (yxue@geog.ucla.edu).

WEN X. YANG, Laboratory of Material Cycling in Pedosphere, Institute of Soil Science, Academia Sinica, P.O.Box 821, Nanjing 210008, P.R. China.

JEFFREY P. WALKER, Department of Civil and Environmental Engineering and CRC for Catchment Hydrology, University of Melbourne, Victoria, Australia (j.walker@civenv.unimelb.edu.au).

ANDREW W. WESTERN, Department of Civil and Environmental Engineering and CRC for Catchment Hydrology, University of Melbourne, Victoria, Australia (western@civenv.unimelb.edu.au).

CHRISTOPHER A. WILLIAMS, Natural Resource Ecology Laboratory, Colorado State University, Campus Delivery 1499, Fort Collins CO, 80523, USA (caw@nrel.colostate.edu).

DAVID J. WILSON, Department of Civil and Environmental Engineering and CRC for Catchment Hydrology, University of Melbourne, Victoria, Australia.

Index

Aboveground Net Primary Production (ANPP), 201-209
Abrasion,142, 144-146
Abscisic acid (ABA), 42, **52**-54
Acclimation, 47
Adaptation, 22, **47**, 49, 53, **57-59**, 62-63, 166, 174, 185, 190
  - morphological, 6, **58-59**, 62-63, 219
  - physiological, **59-60**, 62-63
Adhesion, 149
Adsorbed-layer bonding, 149
Aerobic
  - oxidation, **191**
  - microbial activity, 190, 235, 239, 250
Aerodynamics roughness, **146**
Aerosols, 87, **101-102**, **144**
Afforestation, 36
Aggregates, 145-146, **148**, 150, 155
Agriculture, 35, 86, **88**, 143, 218, 228-229, 292
Agro-ecosystem, 320
Albedo, **86-87**, 90-99, 103, 120
Ammonium, 22, **184-191**, 205, 235, 246
Anabranching, 166, 172, **175**
Anaerobic conditions, 235, 238-239
Anthropogenic disturbances, 5, 86, 88-89, 161, 173-174, 218, 226, 228, 233, **257**, 283, 286-289, 292-293
Aridity, **3-4**, 77, 88, **129-130**, 133-135
  - index, 3, 113, **315**
Arroyos, 166
Ashes, 56, 284, 286, 291-292

Bank, 111, 162-163, 166-169, 171
  - erosion, 162, 169
  - full discharge, 168, 171
Bare soil, 99, 121, 238, 244, **264-267**, 271
Bedload transport, 167
Bioavailable dissolved organic N, **197**
Biogeochemical cycles, **181, 183, 255**
Biosphere, 86, 90-92, 98
Boundary layer, 59, 91, 98, 101, 146-147, 236, 251
Braiding, 166
Budyko, **33-34**, 38
Burned area, **290-292**
Bush encroachment, 137, 293, 295

C_3, **61-62**, 77,135
C_4, **61-62**, 77,135
CO_2, 18, **53, 55-56**, 62, 69-71, **77-78**, 233, 310
CAM, 54, **61-62**
Capillarity, 149
Carbon
  - assimilation, 25, 34, **53**-55, 58-59, 61
  - cycle, 67, **183-189**
Carboxylation, 54, 61-**62**, 195
Catchment, **35-36, 111-115**, 117, 119, 125, 170, 174
Cavitation, **49-50**, 54
Cellular automata models, 264
Cerrados, **8**, 283, **295-296**
Chaparral vegetation, 37, 56, 233, 241, 251, 298
Chemodenitrification, **235**
Chlororplast, 55, 61-62
Climate, **2-5,** 6-9, 35, 39-42, **85-103**, **129-136**, 141-142, 218
  - change, 93, 129, 193, 218-219
  - fluctuations, 5, **42**
  - variability, 42
Cloudiness, 96
Cluster size distribution, 269-271
Codominance, 7
Coexistence, 6, 8, 260-261
Cohesion, 147-149, 154
Combustion, 233, **284**-287, 296
Community composition, 259
Competition, **8**, 50, 100, 164, 170, 185, **194**-196, 224, 259, 261, **264**-265
Conductance (stomatal) , 31, 33-**34**, **51-53, 69-70**, 202, 309-310
Contact angle, 15, 37
Continentality, 129-130
Coppicing, 217-218, 220-222
Crop, 13-28, 34, 47, 142-147, 155-156, 222, 292
Cytoplasm, 60

Dahlem desertification, **321-325**
Darcy's law, **16**, 18-19
Decomposition, 184-187, **190**-192, **220**, 222, 224-229, 237
Deflation, 131, 136, **144**-151
Deforestation, **26, 86**, 283, 295-296
Dehydration, 47, 50, 52-53, 58-60
Denitrification, 184, **233-237**, **250-251**
Deposition (dry/wet), 237, **249-251**
Desert, 2-5, 57, **86-90**, 93, **100-103, 129-137**, 142-144, 172-173, 239-252, 266
Desertification, 86-89, 94-96, 101, 137, **315-328**
Diffusion, 17-20, 53-54, 69-70, 185, 191, 236-238, 248
Dispersion, 19
  - (species), 265-267
Disturbance, **5-9**, 36, 42, 174, 209, **221-222**, 224-226, **257**, 259-260, 283-298, 319, 321-322

Dominance, **6-8**
Downward siphoning, **37**
Drought, **3-5, 47**
  - agricultural, 5
  - avoiders, 47
  - endurers, 47
  - indices, 3
  - hydrological, **4**
  - meteorological, **3**
  - resistors, 47
  - societal, **5**
  - stress: *see* Water stress
Dry
Drylands, **1-8,** 141, 161, 239, **315-316**, 317-328
  - deposition *see* Deposition
  - season, 3, 161, 218-229, 286-293
  - tropical forests, **217-229**
Dunes, 89, **130**, 135-136, 142
Dust, **87**, 90, 101-103, 130, 135-137, 141-145, 155, 320
  - storm, 90, 135, 143-144

Ecohydrology, **1**
Eddy covariance, 72-73
El Nino Southern Oscillation (ENSO), 68, **137**, 221, 223
Elastic adjustment, 59
Embolism, 49
Emigration, 318
Encroachment, 89, 170, 293
Entrainment, 145, 147, 150-151
Ephemeral channels, 164, 166, 173, 175
Equilibrium-base models, 264
Erodibility, 145-151, 155-156, 162-163, 168-169
Erosion, 36-37, 130-132, **141-156**, 162-163, 166-176, 316, 318
Erosivity, 137, **145-147**, 152
Evaporation, 14-15, 21, **32-34**, **69-71**, 86, 90-91, 97-98, 102-103, 109-110, 151-152, 164, 267, 285, 306
Evapotranspiration, 3, 31-**33**, 34, **70-72**, **76-77**, 99, 109-113, 267, 312
  - potential, 2, 32, **70**, 129, 315
Extreme events, 56, 166, 174, **193**, **221**, 223, 243, 296

Facilitation, 259, 269
Feedback, 9, **85-103**, 195, 209, 316, 319, **320-321**, 322-324, 328
Fertilization, 206-207, 209, 212, 237, 252
Field capacity, **38**, 111, 117-118, **190**, 248
Fire, 7-9, **37**, **56**, 189, 209, 218-219, 248-251, 260, 265, **283-298**
  - behavior, 289
  - cycle, 287-288
  - extent, 287
  - frequency, 288
  - intensity, 289-290
  - regime, 283-298
  - scars, **290**
  - season, **289**, 292, 297
  - spread, 284-289, 292
Flaming combustion, 284-285
Flood, 132-133, 161-167, 169-175
Floodplain, 111-112, 114, 126, 167-169
Foliar nitrogen content, **195**
Fractal analysis, 263, 270-**274**
Fractional cover, **69**, 79-80
Fruit, 48, 50-51
Fuel
  - load, 7, 56, 218, **284**, 298
Functional type
  see Plant functional type
Fungi, 190, 195, **304**

Gaps, 264
Garrigue, 296-298
Geophytes, 297, 304
Germination, 48, 56, 266-267, 297
Glaciation, 135-136
Global change, 321
Global Circulation Model (GCM), 86, 91-95, 100-101
Glowing combustion, 284
Glycophytes, 58
Government, 320
Grasslands, 2, 5, 93, 95, **201-212**, 239, 252, 283, 291-296
Grazing, 2, 5, 36, 89, 207-210, 226, 257, 293, 321, 322, **325-327**
Greenness, 78, 93, 122
Groundwater, 13-14, 109, 114, 132-**133**, 161, 163-164, 169, **173-174**
Guard cells, 52-53, 70
Gully formation, 321

Halophytes, 57-58
Heterogeneity, 35-37, **195-196**, 209, 259-264, 271, 287
Hillslope, 109-114, 119-120
Holding capacity, 7, 120
Holocene, 100, 131-137, 295
Homeostasis, 305, 309-310
Human impacts, 319
Humic substances, 184
Humus, 184, 186-187, 189-190, 290
Hurricanes, 144, **221**
Hydraulic resistance, 53, 162
Hydraulic conductivity
  - saturated, 35, 38
  - unsaturated, **16**-18, 38
Hydraulic lift, 37

Hydrologic fluctuations *see* Rainfall fluctuation
Hydrolysis, 50
Hydrophytes, 47
Hydrophobicity, 36-37
Hypoxia, 58

Ignition, **284-290**, 292-296
IKONOS satellite, 271
Immobilization, 184, 186, 190-191, 205
Infiltration, 13-20, 32-33, **35-36**, 38, 70, 76, 109-111, 164-167, 191, 308, 318-319, 321, 326
  - capacity, 35-36
  - excess runoff, 35
  - index 323
Interannual climate fluctuations, 42
Interannual variability, 4, 87, 201-205, 209, 217, 223
International Geosphere-Biosphere Programme (IGBP), 321
Intertropical Convergence Zone (ITCZ), 92, 101
Inverse texture effect, 40-41
Irradiance, 54, **56**
Isotope, **53-54**, 134

Karst, 133

Lake, 4, 111-114, **130-132**, 136-137
Land
  - conversion, 218
  - degradation, 89-103, 141, 315, **316**-328
  - managers, 321, 328
  - surface models, 31, 34, **91**
  - use, **315-316**, 321
Latent heat flux, 55, 69, 72, 85-86, 90-91, 97-99
Leaching, 5-7, 13-14, 184-186, 191-194, 218-219
Leaf
  - Area Index (LAI), 91, 98-99, 120, 262, 272
  - biomass, 69, 264
  - expansion, 50-51, 203-204
  - nitrogen *see* Foliar nitrogen
  - temperature, 54-55
Light, 55-57, 59, 207, 267
Lightning, 56, 284-286, 289, 294-296
Litter, 36, 184, **186-195**, **210, 219-**228, 286-287, 294-296
Litterfall, 217, 221-**223**, 225-229
Livestock, 317, 318, 326-327
Loess, 131, 135-136, 143
Logging, 222, 228

Macrotermes, **303-312**
Magnesium, 218
Markov-transition models, 263-264
Masophyll, 50, 55, 61-62
Meandering, 166, **167-169**
Mediterranean steppe, 320, 322
Mesophytes, 47
Metabolism, 54-57, 62, 234-235, 304-306
Microbial
  - activity, **185**, 190, 220-221, 236-238, 251
  - biomass, **184-190**, **194**, 205, 221, 223-224
Mineralization, **184-186,** 190-195, 204-205, 208-211, 220-221, 237
Miombo woodland, 242, 247-248, 288

NDVI, 78, 202-203, 272, 275, 291
Neotropical dry forest, *see also* Dry Forest, 218
Net Ecosystem Exchange (NEE), 71, 78
Net Primary Productivity (NPP), 201, 203-204, 209, 211-212
Net radiation, 68-73, 86, 90-**91**, 98, 101-102
Niche, 6, 261
Nitrate, 22-26, 28, 185-194, 235
Nitrification, **184, 186,** 191-192, 221, **234-237**, **250**
North Atlantic Oscillation (NAO), 137
Nutrient
  - availability, 25, 183, 222-224, 267
  - cycle, 183, 195-196, 222
  - uptake, 13-14, **19-27**, 37, 119, 121, **195**

Organic matter, 145, **183-196**, 209-212, 219-229
Osmotic adjustment, 58-61
Overbank flow, 163, 171
Overgrazing, 35-36, 89, 101, 141, 319-320
Ozone, 233, 236, 251

Palaeoclimate, 293
Palatable grass, 293
Palynology, 133
Panchromatic data, 271
Patch-based models, 264
Patches (tree), 263-271, 319, 321, 323
Permanent wilting point *see* Wilting point
Permeability, 18
pH, 52-53, 58, 226-229
Phenology, 3, 224
Photoinhibition, 56-57
Phosphorus, 219-229
  - availability, 220
  - use efficiency, 219
Photosynthesis, 34, **53-56**, 60-62, 69-72, 77, 90, **195**, 211
Photosystem, 55-57
Phreatophytes, 169, 171
Plant functional type, 6-8, 71, 78

Plant available nitrogen, 204, 211, 250
Plant residues, 170-171
Pleistocene, 135-136
Pliocene, 135
Pluvial lakes, 131-132
Policy-makers, 315, 324, 327-328
Pollen, 133-134
Potential evapotranspiration, *see* Evapotranspiration
Priestley-Taylor, 70
Probability distribution
  - of soil moisture, 38-42
  - of wind speed, *see* Weibull distribution
  - of vegetation cluster size, 270-271
Pyrophytic ecosystems, 283-284

Quaternary, 132, 136

Radiative forcing, 144
Rain shadow, 2, 130, 135
Rainfall
  - fluctuations, 42
  - regime, 2-5, 39-43, 164, 319-320
Recovery (post disturbance), 222, 225
Recruitment, 41, 164, 170
Reforestation, 36
Rehabilitation, 327
Relief, 111
Remote sensing, 78, 116, 122, 202, 263-272, **290-291**
Resistance (stomatal), 32, 91, 93, 98-99
Resorption, 205-206, 219-220, 228
Respiration, 18, 20, **55**, 62-71, 184-185, 190, 235, 310
Respiratory gas exchange, 303-305
Restoration, **327**
Reverse flow, 37
Richards equation, **18**, 33, 38
Riparian vegetation, 161-176
Root
  - biomass, 219, 224
  - density, 21, 26
  - uptake: *see also* Uptake, 23-24, 186
  - zone, 5, 21-26, 33, 37-42, 69, 74-80, 115-125
Rubisco, 55-56, 61-62
Runoff, **35-37**, 90, 95-97, 110-111, 164, 307-308, 321-322, 326
Rural development, 320

Sagebrush, 48, 171
Salinity, 21, 24, 48, **57-**60, 62, 172-173, 326-327
Salt, **57-58**, 87, 173
Saturation, 14-19, 35
  - excess runoff, 35, 110
Scaling behavior, 274
Seasonality, 2, 16, 217, 292-294
Secondary forest, 218, 222, 225, 228
Seed, 48-51, 56
Sensible heat flux, **68-74, 85**, 90-91, 97-98
Signaling, 51-52
Shortgrass steppe, 41, 201-211, 240, 248-252
Shrub encroachment, *see also*Bush encroachment, 318
Shrubland, 2, 201-212, 283, 327
Shoot, 47-53, 55, 69
Slash burning, 222
Social resilence, 320
Society, 5, 316, 320
Sodicity, 58
Soil
  - aridisols, 5-6
  - degradation, *see also* Land degradation, **316**
  - drying, 51, **74**
  - erosion: *see* Erosion
  - mollisols, 5-6
  - moisture, 31-47
  - Organic Matter (SOM) *see* Organic Matter
  - palaeosols, 130-131, 133
  - permeability, *see* Permeability
  - properties, 5, 14, 40-41, 111-113, 120, 145
  - storage capacity, 38
  - ultisols, 6
  - texture, 6
Solar radiation, 55-56, 59
Stakeholders, 321, 324-325
Stochastic modeling, 32, 34-42, 147, 163-164, 194, 264
Stomata, 32-34, 49-55, 59-62, 69-70, 91-93, 99
Storm
  - depth, 4, 38, 40, 42
  - dust *see* Dust storm
  - frequency, 4, 39-42
Stress
  - resistance, 47
  - tolerance, 47, 173
  - water, 5-6, 24, 33-35, **40-41**, **47-63**, 80, 173-174, 185, 194-195
Surface roughness, 86, 91, 145-146, **152-153**
Surface tension, 15, 37, 149
Suspension, 144, 155

Tallgrass praire, 201-209
Temperature, 2, 25-26
  - stress, 24-25, **54**-56, 58-59, 68-70, 86-90, 95, 102, 129-137, 185, 190, **238**, **244-247**, 267, 285-290, 295, 305
Tensiometer, 15
Termites, 303-312
Thermohaline circulation, 137
Threshold shear velocity, 145-153
Thornthwaite, 33

Tiger bush, 264, 320
Topography, **110-120**, 209, 284-**285**
Trace gases, 86, **233-234**, 237
Transpiration, *see also* Evapotranspiration, 2-6, 20-23, 31-**33**, 34-38, 48-59, 69-73, **74-79,** 109-110, 186, 190-191, 203-204, 311
Turgor, **48-61**

Uptake, *see also* Root uptake, 190-192, 194-195, 219-221

Vadose zone, 13-19
Vegetation
- composition, 7, 77, 283-284, 288, 293, 297
- structure, 8, 79-81, 260, 276, 291-293

Velocity profile, 146-147
Ventilatory gas exchange, 305, 310

Walker circulation, 93
Water availability, 3-6, 15, 24, 32-33, **51-54**, 61, 125-126, 162, 186, 205, 209-210, 217-229, 276, 285, 319-320
Water content, *see also* Soil moisture, **14**-25, **31-39**, 48-49, 149-152, 185, 193, 210-211, 235-238
Water deficit, 2, 5, 35, **48-59**, 247
Water holes, 36
Water level, 4, 169
Water potential, 14-18, 33-37, 47-52, 57-61, 185-186, 195, 225, 306, 308-310
- gravitational, 14-16, 48
- matric, 15-16, 19-21, 34, 149-151, 306
- osmotic, **15**, 20, 24-25, **57**, **60**
- pressure, 14-15, 48
- total, 14-16

Water relations, 6-8, 34, **47-51**
Water repellency, 37
Water retention curves, **14-19, 149-150**, 190
Water stress, 5-6, 24, 31-34, **35**, 40-42, **47-61**, 173-174, 185, 194-195, 211, 245-248
Water Use Efficiency (WUE), 25, 53, 61, 70, **77-78**, 273
Weibull distribution, 147
Wet bonding, 149
Wet season, **6**, 72-73, 219-229
Wilting point, **34-35,** 71, 75-76, 111, 117-119, **125**, 190
Wind erosion, 130, **141-156**
Wood extraction, 317
Woody debris, 219-221

Xerophytes, 47, 53
Xylem, 20, 48-55, 58